The Petrography and Mineralogy of the C29/30 Candle Lake Kimberlite, Saskatchewan, Canada

by
John M^c^Bride

Supervisor: Dr. Roger H. Mitchell

Department of Geology
Lakehead University
Thunder Bay, Ontario
Canada
December, 2009

Abstract

Petrography and mineralogy of the C29/30 Candle Lake kimberlite (Saskatchewan, Canada) was studied to understand the characteristics of the kimberlite. Using standard optical microscopy three units where distinguished; pyroclastic kimberlite; resedimented volcaniclastic kimberlite and a crystal tuff kimberlite unit. Each kimberlite unit has been classified based on textural relationships between magmaclasts and the interstitial matrix, as well as phenocrysts, macrocrysts and minor mineral phases within the magmaclasts. Pyroclastic kimberlites are characterized by carbonate or serpentine interclast matrix supporting amoeboid magmaclasts with protruding macrocrysts and phenocrysts of pseudomorphed olivines. Resedimented units have a serpentine-carbonated interclast matrix that is poorly defined against rounded and fractured magmaclasts. The crystal tuff unit is distinguished by fine-grained (<700 μm) clast supported pyrocrysts of pseudomorphed olivine as well as magmaclasts with thin selvages (<100 μm). The interclast matrix is a serpentine-carbonate mixture.

The mineralogy of the C29/30 is typical of an archetype kimberlite. The minerals analyzed include spinels, serpentine, olivine, carbonates, phlogopite, perovskite, apatite, garnets, ilmenite and magnetite. Three types of spinels where identified; type [1] spinels occur enclosed within macrocrysts and phenocrysts with a TIMAC composition; type [2] spinels nucleate along the edges of the macrocrysts and phenocrysts and have a TIMAC core and QUM rim composition; type [3] spinels occur as isolated grains within the matrix and are dominantly QUM in composition but can have a TIMAC core. Atoll spinels are observed in type [2] and type [3] spinels with magnetite rims. The compositions of the spinels are identical to trend T1 spinels from Wesselton. However; they are unlike spinels from Smeaton 169 kimberlite which is also from the Fort à la Corne field which indicates kimberlite within the same kimberlite field may not have the same source.

The eruption was shallow and excavated Mannville sandstones, Paleozoic limestone and any Colorado mudstone if present. The eruption style was probably dry-phreatomagmatic. This is supported by the shallow bowl shape of the kimberlite body with a depth to width ratio of 1:5.

The C29/30 kimberlite is similar to other Fort à la Corne kimberlites by textural and mineralogical comparison.

Acknowledgments

There are many people who have helped me though this project. I would first like to thank Dr. Mitchell for supporting me throughout this project. Many thanks to Anne Hammond for the numerous hours she has spent preparing samples and Al MacKenzie for all the time spent on the SEM. A special thanks to the rest of the geology students and my family, for without them I could not have accomplished this. Most importantly thank you Sarah for loving me even though I love rocks.

Table of Contents

List of Figures

List of Tables

Chapter 1: Introduction

1.1 Objectives:

The objective of this work is to examine the petrography and mineralogical characteristics of clasts in the pyroclastic units of the C29/30 Candle Lake kimberlite, Saskatchewan, Canada. Textures and composition of the components, including the major mineral assemblages with emphasis on spinel group minerals, will be compared to those of hypabyssal kimberlite and tuffistic kimberlite in order to identify any differences or similarities between the different varieties of kimberlite.

There are limited petrographic and mineralogical data for Fort à la Corne type kimberlite, and specifically no data for the Candle Lake kimberlite. This study will examine the volcanic clasts of this "Prairie-type" kimberlite (type 2) with comparisons to type-1 and type-3 kimberlites (see below).

1.2 Location:

The C29/30 Candle Lake kimberlite, owned by Vaaldiam Resources Ltd. is located about 90km north-east of Prince Albert, Saskatchewan (Figure 1.2.1). The property consists of two claim groups; the more northerly consist of eighteen claim blocks totaling 8495hm of land enclosing the C29/30 kimberlite (Great Western Diamand Corp., 2007). The Candle Lake Kimberlite Group is approximately 40km north of the Star Kimberlite within the Fort à la Corne Group. The Candle Lake Kimberlite Group lies along the same trend as the Fort à la Corne Group as well as the Weirdale Group, Birchbark Lake Group, Foxford Group and the Snowden Group; these groups comprise one of the largest kimberlite fields in the world (Zonneveld et al. 2004).

1.3 Regional Geology:

The Candle Lake Diamond Project is situated approximately in central Saskatchewan; geologically this places the occurrence in Phanerozoic sediments on the eastern edge of the North American Interior platform (Zonneveld et al. 2004). The Phanerozoic sediments overlie Archean and Proterozoic basement rocks (Figure 1.3.1). The Archean basement is assumed to be present by extrapolation from deeper drill holes in the surrounding area (Great Western Diamand Corp., 2007). U/Pb age determinations have been performed on zircons from

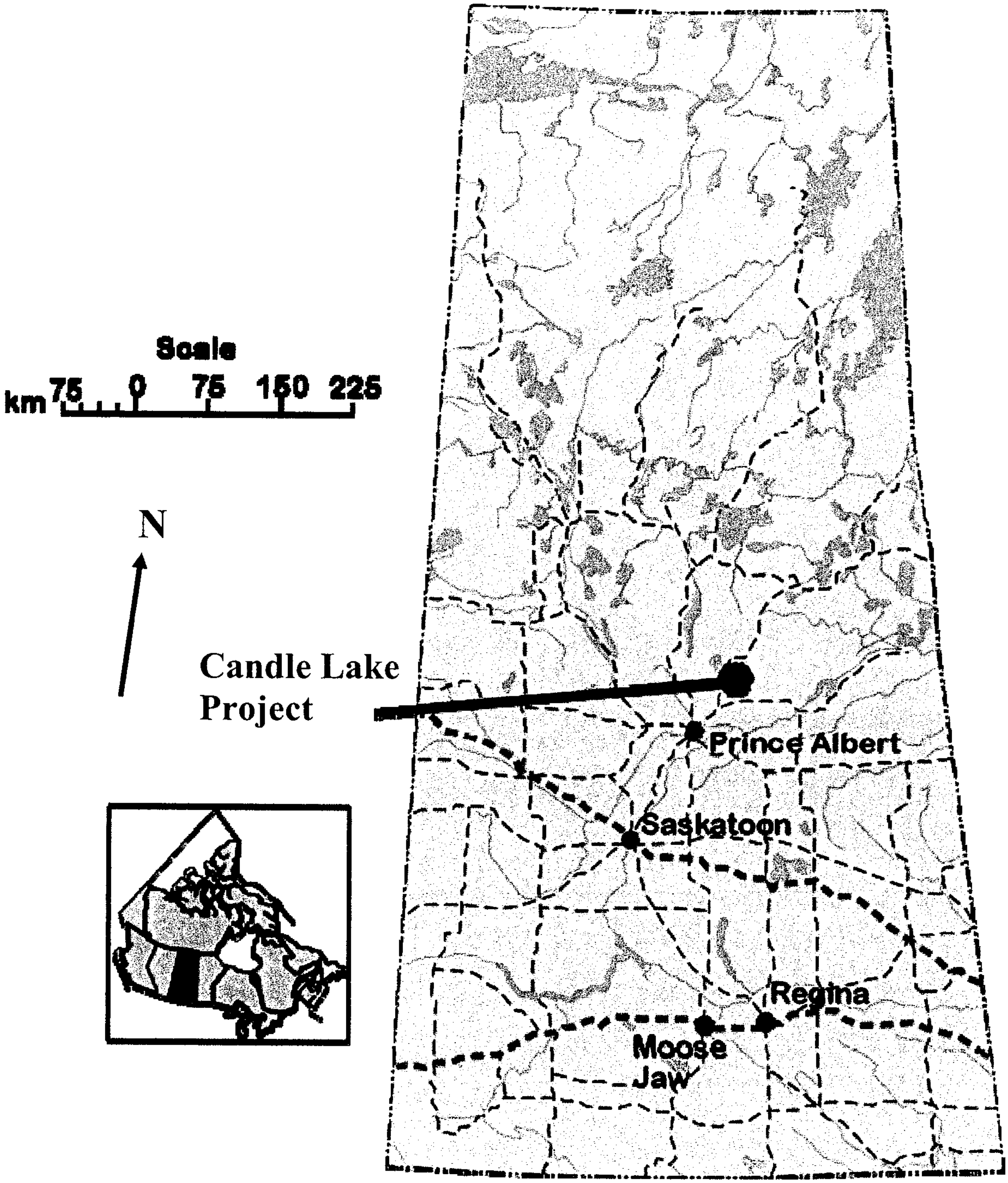

Figure 1.2.1 Location Map of the Candle Lake Diamond Project in Saskatchewan Canada (Modified from the Natural Resource of Canada, 2001).

xenoliths and give ages of 1.85Ga (Ansdell 2005). Above the Archean-Proterozoic basement there are four hundred metres of Paleozoic clastic and carbonate rock sequences. These are present as angular xenoliths in kimberlite drill cores. Above the Paleozoic sequence there is an unconformity within the Mesozoic sequence that is host to the kimberlite intrusions. The Mesozoic sequence is divided into two groups, the Mannville Group and the Colorado Group; both of Albian age. These units record transgressive successions from coastal plain fluvial and deltaic to offshore and proximal offshore sediments (Zonneveld et al. 2004).

The Mannville Group is divided into two formations, the Cantuar Formations and the Pense Formation.

The Cantuar Formation is of variable thickness ranging from absent to hundreds of metres thick. It is interpreted as a variable marginal marine to continental lacustrine depositional setting. The lithologies of the formation are a heterolithic planar laminated to blocky shales, ripple laminated siltstones and graded to cross-stratified coarse-medium-fine grained sandstones. Fossil remains found in the formations, such as Cylindrichnus, Trichinchnus, Oyroliths and Planoliles, suggest brackish conditions and transition from fluvial to deltaic environments (Zonneveld et al. 2004).

The Pense Formation abruptly overlies the Cantuar Formation producing a regional unconformity. The lithology of the formation is fine-medium grained high bioturbidity sandstone with minor dark grey to black silty shales. Fossil evidence which includes Zoophycos, Teichichnus and Palaeophycus support an offshore transition to lower shore face environments (Zonneveld et al. 2004).

The Colorado Group overlies the Pense Formation producing an unconformity. Because the Pense Formation is not laterally continuous, this results in the Colorado Group overlying the Cantuar Formation in some locations. The Colorado Group is divided into an upper and lower group. The upper group consists of the Fish Scale Formation and the Belle Fourche Formation but does not host the C29/30 kimberlite. The lower Colorado Group, however; does host kimberlite including the C29/30 occurrence. The lower Colorado Group is composed of three formations the Joli Fou, the Viking and the Westgate.

The Joli Fou Formation is the oldest of the Colorado Group and is a heterolithic succession, dominated by black silty shales with minor siltstones and sandstones. Fossil evidence such as Palaeophycus, Scalarituta, Zoophycos and Thalassiance along with a high mud to sand ratio suggests a proximal offshore to offshore transitional environment (Zonnveld et al. 2004).

The Viking Formation together with the Westgate Formation are dominated by laminated black silty shales with minor siltstones and very fine grained sandstones. These formations are interpreted as distal offshore environments (Zonneveld et al. 2004).

The Upper Colorado Group is of no consequence relative to the Candle Lake kimberlite because glacial erosion has removed overlying formations younger than the Lower Colorado Group and deposited eighty to a hundred and fifteen metres of thick unconsolidated glacial till and glacial fluvial outwash (Zonneveld et al. 2004).

The C29/30 Candle Lake kimberlite is situated 30km north of the main Fort à la Corne kimberlite field which includes: Smeaton; Foxford; Snowden and the Star Kimberlite (Figure 1.3.2).

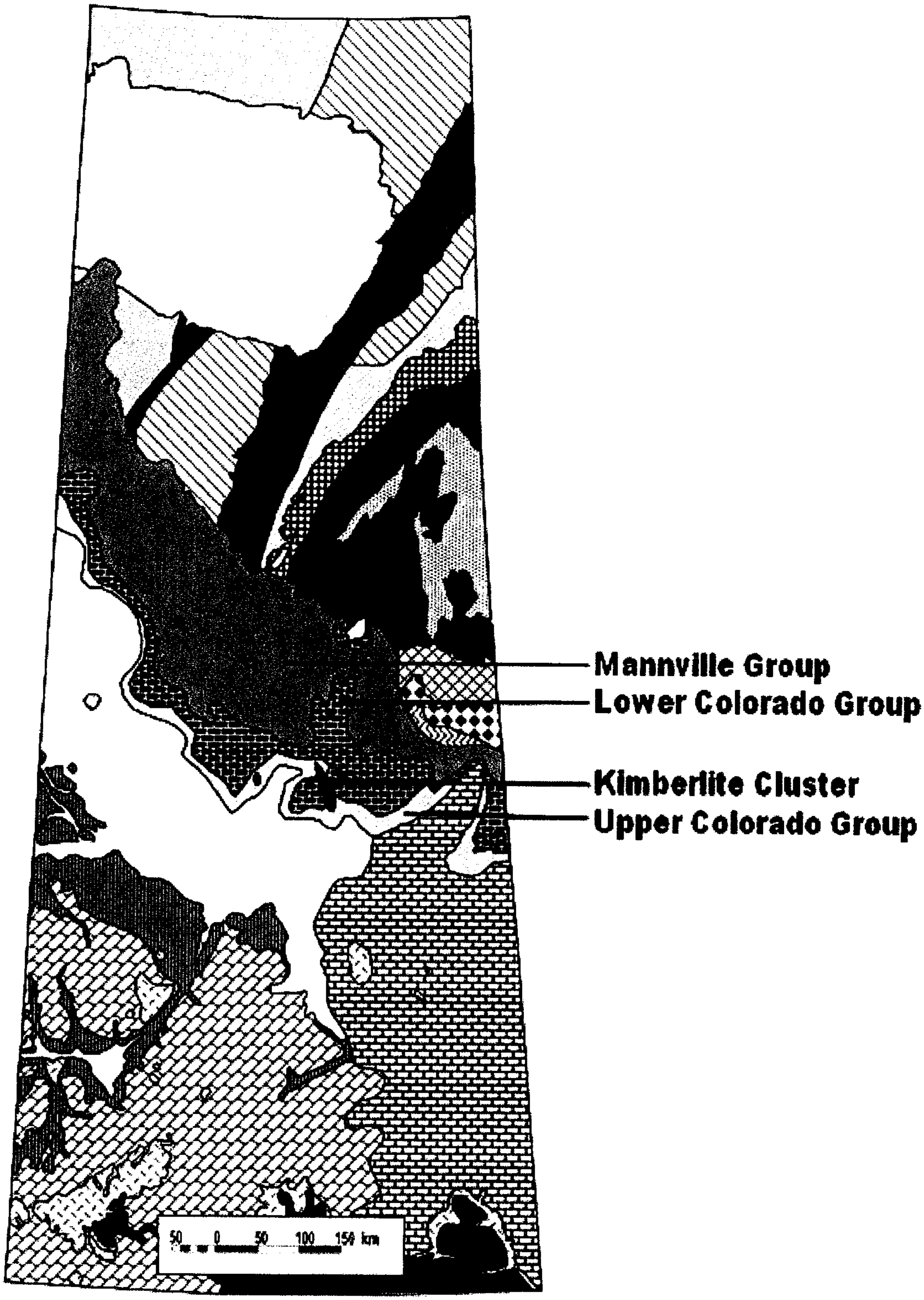

Figure 1.3.1 Geological Map of Saskatchewan (Modified from the Geological Survey of Canada, 2002).

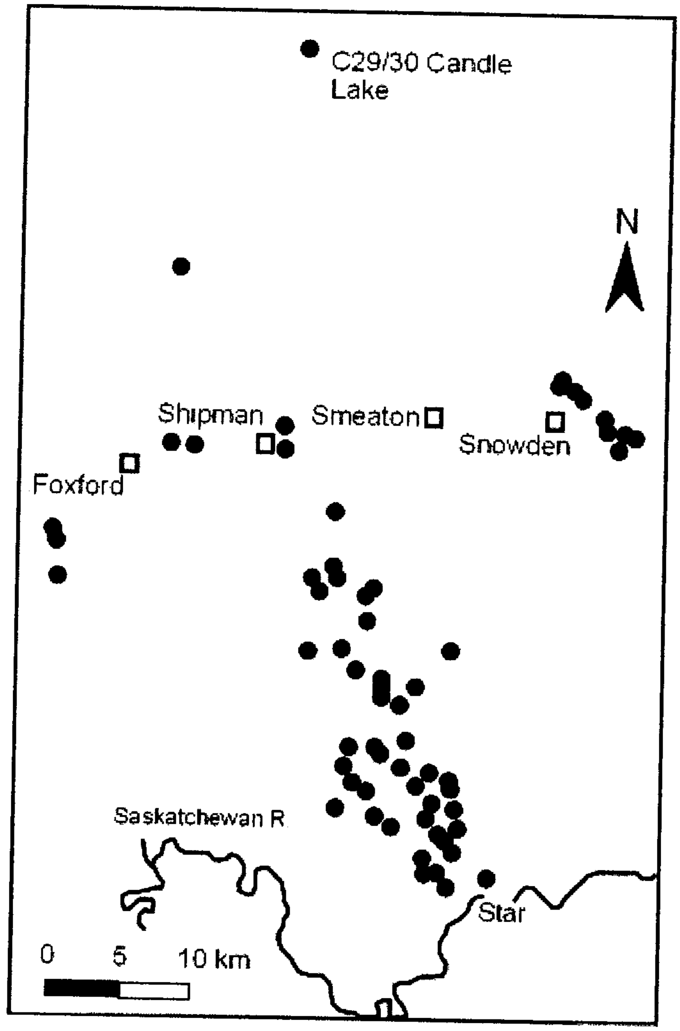

Figure 1.3.2: Location map of the C29/30 Candle Lake kimberlite relative to the rest of the Fort à la Corne kimberlites (Scott Smith, 2008a). Black circles represent kimberlite occurrences, hollow squares represent town locations.

1.4 Terminology:

Existing volcanologic and sedimentary nomenclature are insufficient to describe and classify kimberlite for all three types of pipes (refer to chapter 2), without implying a genetic interpretation. Furthermore terminology used for kimberlites does not follow internationally recognized volcanologic nomenclature resulting in further problems. For example the use of the term lapilli, as a volcanological term describes a grain size between 2-64mm. However, in reference to kimberlite, lapilli are a specific lithologic type of volcanic clast (Zonnveld et al. 2004). This overlap of terms has been modified by Field and Scott Smith (1998) who redefined the kimberlite clast term, lapilli, as magmaclasts (see below). The continued evolution of kimberlite nomenclature will help explain and define kimberlite features uniformly for all three types of kimberlite pipes beyond standard volcanologic and sedimentary terms. Nomenclature used in this thesis is as defined below.

Table 1.4.1: Comparative Terminology

Past Terminology (Mitchell, 1995)	**Present Terminology**
Lapilli – serpentinized olivine set in a fine-grained primary altered monticellite, melilite, phlogopite, opaque minerals and perovskite matrix with cryptocrystalline interstitial calcite and serpentine. The selvage varies from thin-to-amoeboid in shape.	Magmaclast (general use) or Pyromagmaclast (more specific)– a physically distinct piece or fragment of magma comprising former melt plus any entrained solids (xenoliths, xenocrysts, macrocrysts, phenocrysts) and trapped volatile-rich fluids. Kimberlite magmaclasts are commonly smooth-surfaced and fluidal in shape which indicates a low viscosity melt and thus shaped by surface tension (Scott-Smith et al. 2008a).
Pyroclasts or Free Olivine Grains– melt free crystals that are liberated during eruption and may or may not be genetically related.	Pyrocrysts – are discrete crystals liberated from the magma by pyroclastic processes. Olivine is the most common pyrocryst due to pyroclastic kimberlite having olivine in high abundance. However, grains liberated from magmaclasts by resedimentation are not included as pyrocrysts (Scott-Smith et al. 2008a).
Xenocrysts – a single grain inclusion in an igneous rock which is not genetically related.	No change.
Macrocrysts – are grains derived from the mantle and range is size from 0.5mm to 20mm. They are rounded-to-anhedral, polycrystalline and show deformation.	No change.
Phenocrysts – a grain crystallized from the kimberlite magma, ranging is size from 0.5mm to 1.5mm, subhedral-to-euhedral and monocrystalline.	No change.

Clement and Skinner (1985) have defined the following units in a kimberlite pipe which will be used here as a guideline for terminology. These are: hypabyssal-facies kimberlite; diatreme-facies kimberlite or tuffistic kimberlite (which will be used in this work), and crater-facies kimberlite which includes pyroclastic and epiclastic material.

Because of the varieties of volcaniclastic kimberlites that make up the crater-facies unit, Field and Scott-Smith (1999) have divided this unit into, pyroclastic kimberlite, resedimented volcaniclastic kimberlite and epiclastic kimberlite.

Pyroclastic kimberlites are composed of components that formed during volcanic eruptions and were deposited by primary pyroclastic processes. The main components include magmaclasts and pyrocrysts set in an interclast serpentine or carbonate cement.

Resedimented volcaniclastic kimberlites are deposits that have been moved and reworked which results in a change of the primary pyroclastic textures. There is commonly a large mixture of extraneous material and abrasion of preexisting clasts.

Epiclastic kimberlites are rocks formed by the consolidation of fragments of preexisting rocks derived from surface processes such as weathering, physical abrasion and gravitational collapse.

1.5 Analytical Techniques:

Quantitative X-ray Spectrometry:

Samples were analyzed on a JEOL 5900 scanning electron microscope equipped with an Oxford X-ray energy dispersion system with a resolution of 139 eV. An acceleration voltage of 20 kV, with a beam current of 0.475 nA and a beam width of less than 0.2 μm was used. The system was calibrated against a nickel standard; for a count time of 30 seconds the acquisition rate gave 2900 to 3100 cps.

The instrument was standardized relative to each mineral analyzed. The standard count time was for thirty seconds at 2000x magnification, except when standardizing for fluorine and phosphorus, which was standardized with a count time of three hundred seconds.

Spinels were standardized using; Ilmenite (Fe, Ti), Chromite (Al, Cr, Mg), Mn-Hortonolite (Mn) and Wollastonite (Ca).

Serpentine was standardized using; Jadeite (Na), GL 12 Orthoclase (Al), P140 Olivine (Mg, Fe,Si) and Wollastonite (Ca). H_2O was calculated by subtracting the total cation formula from the ideal anion formula including the OH group. The difference was assumed to be the H_2O content.

Phlogopite was standardized using; Jadeite (Na), Wollastonite (Ca), Periclase (Mg), Apatite BM1926 665 (F, P), Mn-Hortonolite (Mn) GL 12 Orthoclase (Si, Al, K), Ilmenite (Fe, Ti), Barite (Ba) and Chromite (Cr).

Carbonates were standardized using; Wollastonite (Ca), Periclase (Mg), Strontium titanate (Sr) and Barite (Ba). A raster beam was used for analyses to minimize carbonate decomposition.

Olivines were standardized using; Mn-Hortonolite (Mn), Wollastonite (Ca) and P140 Olivine (Si, Mg, Fe).

Apatite was standardized using; LaF_3 (La), CeF_3 (Ce), PrF_3 (Pr), NdF_3 (Nd), SmF_3 (Sm), Strontium titanate (Sr), Apatite Bm1926 665 (Ca, P) and CaF_2 (F). Fluorine was corrected to oxygen equivalent.

Perovskite was standardized using; LaF_3 (La), CeF_3 (Ce), PrF_3 (Pr), NdF_3 (Nd), Nb metal (Nb), Barite (Ba), Strontium titanate (Sr), Jadeite (Na), Wollastonite (Ca) and GL ilmenite (Ti, Fe).

Garnet, magnetite and ilmenite where standardized together using, Ilmenite (Ti, Fe), Mn-Hortonolite (Mn), DJ35 (Si, Al, Mg), Chromite (Cr), Wollastonite (Ca).

Due to the limited abundance of garnet, magnetite and ilmenite in thin section, heavy mineral separations were performed in order to concentrate these minerals. The samples were crushed and sieved, grains between 100 and 200Φ (0.1475-0.2500 mm) were collected. The sieved portion was then placed in a tetrabromoethane solution which has a density of 3.21. Minerals with a higher density than tetrabromoethane such as garnet, magnetite and ilmenite settled out and were collected for grain mounts.

FeO and Fe_2O_3 were recalculated from analyzed FeO total value using Droops (1987) method for spinel, garnet, ilmenite and magnetite.

Representation of Spinel Compositions:

Spinel compositions are represented in an eight component system due to the extensive solid solution between end members. These end members include; $MgCr_2O_4$ (magnesiochromite), $FeCr_2O_4$ (chromite), $MgAl_2O_4$ (spinel), $FeAl_2O_4$ (hercynite),

Mg_2TiO_4 (qandilite), Fe_2TiO_4 (ulvöspinel), $MgFe_2O_4$ (magnesioferrite), and Fe_3O_4 (magnetite) (Mitchell 1986). They are commonly represented in a six component Johnson spinel prism (Irvine 1965). Two types of prisms are used; "oxidized" prisms and "reduced" prisms. The "oxidized" prisms are used with iron to represent recalculated Fe^{2+} and Fe^{3+}, however, this method does not include Mg_2TiO_4 or Fe_2TiO_4. The "reduced" prism does not accurately represent Fe_3O_4 or $MgFe_2O_4$ but it does incorporate all major elements within the prism (Mitchell 1986). This study uses a "reduced" prism in order to represent the variation in Mg_2TiO_4 and Fe_2TiO_4 components.

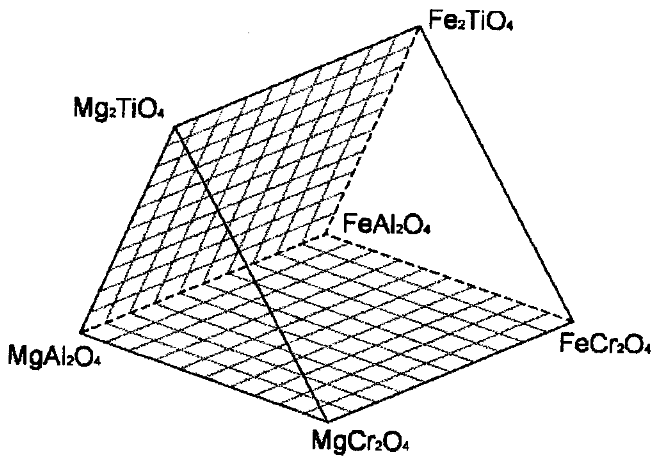

Figure 1.5.1: Reduced spinel prism modeled from Irvine (1965).

To create the spinel prism Corel Bryce 5 software was used. This software permits three dimensional modeling and manipulation along the X, Y and Z planes. A skeleton frame for the prism was created on a XYZ axis with an origin (0,0,0) at the $MgAl_2O_4$ corner.

The X axis is along the $MgAl_2O_4$ – $MgCr_2O_4$ axis. The Y axis is along the Mg_2TiO_4 and mid $MgAl_2O_4$ – $MgCr_2O_4$ axis. The Z axis is along the $MgAl_2O_4$ – $FeAl_2O_4$ axis. The XYZ axis is shown in Figure 1.5.2.

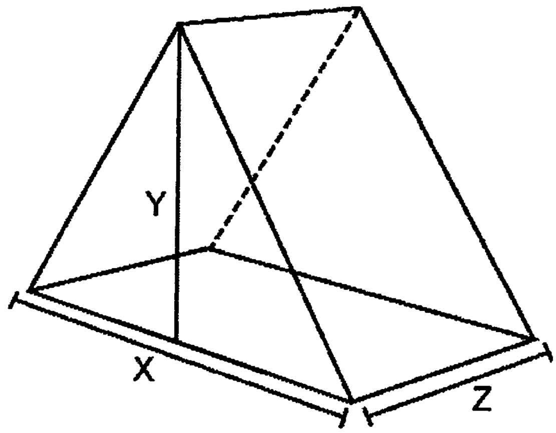

Figure 1.5.2. XYZ axis shown on a prism.

To convert the cation ratios needed to plot on a spinel prism into XYZ space the following calculations are performed. Z is unchanged and is equal to Fe_T^{2+} / (Mg + Fe_T^{2+}).

Y is [Ti / (Ti + Cr + Al)] x √(3/4), this correction factor is to scale for the height of an equilateral triangle with side lengths of 1, set in the XYZ axis (Figure 1.5.3).

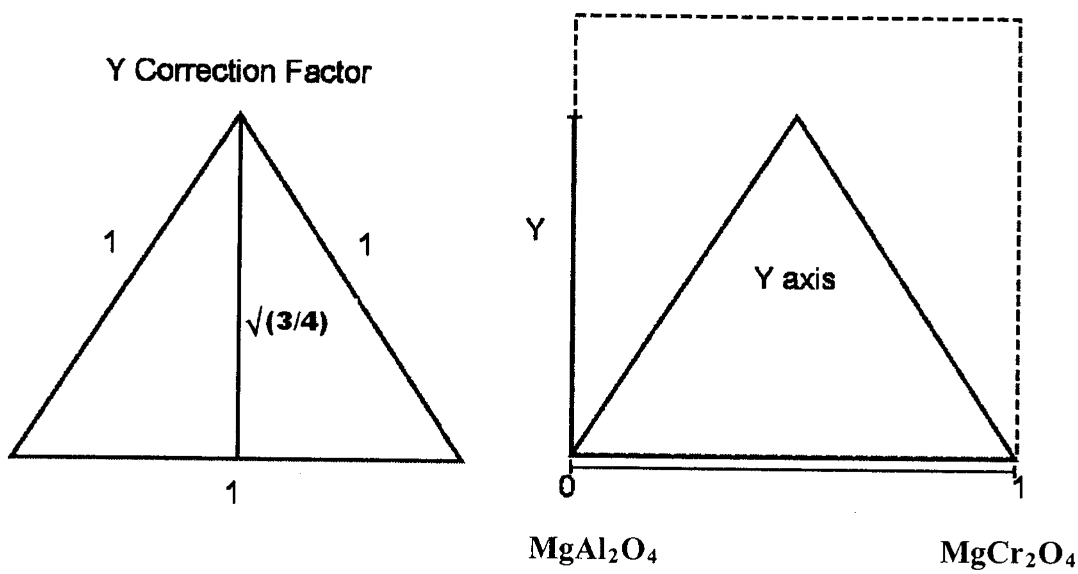

Figure 1.5.3. a) Equilateral triangle with height correction. b) Y axis shown on two dimensional plane.

X is [Cr / (Cr + Al)] x [1 – (Ti / (Ti + Cr + Al))] + [½ Ti / (Ti + Cr + Al)]
The term [1 – (Ti / (Ti + Cr + Al))] is a correction for the width of the triangle as a function of increasing Y value, and is labeled A in Figure 1.5.4. The term [½ Ti / (Ti + Cr

+ Al)] is a correction for the offset of the triangles edge from the Y axis and is labeled B in Figure 1.5.4.

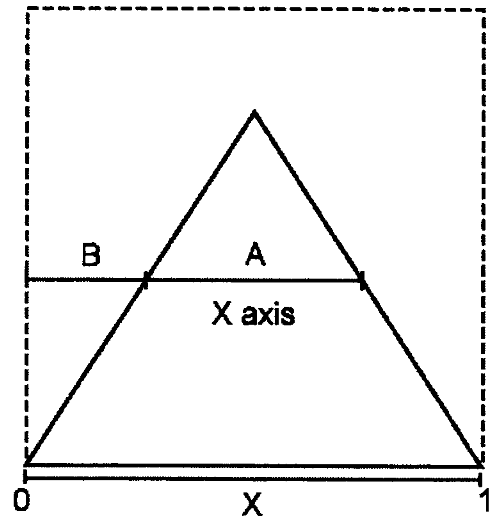

$MgAl_2O_4$ **$MgCr_2O_4$**

Figure 1.5.4. X axis shown on a two dimensional plane. A is the width factor correction and B is the offset factor correction. A and B are both dependent on Ti / (Ti + Cr + Al).

This computerized plotting procedure using Corel Bryce 5 software has been checked against standard graphical methods and found to give identical positions compared to these methods.

Chapter 2: Kimberlite Emplacement Models

2.1 Styles of Kimberlite Emplacement:

Three types of kimberlite pipes have been distinguished by Field and Scott-Smith (1998) based on unique characteristics of the pipe shape and the internal geology. The pipes are classified as: type 1 or "South African-type"; type 2 or "Prairie-type" and type 3 or "Lac de Gras-type". The morphology of a kimberlite pipe is directly related to the style of emplacement and the geological environment in which the magma intrudes. These two factors control the pipe shape, the internal geology, and ultimately which type of kimberlite pipe is formed.

2.2 Type 1 Pipes:

Type 1 kimberlite pipes are primarily recognized in South Africa as deep (up to 3km) carrot-shaped bodies that taper inward with increased depth and are approximately circular in cross-section. The sides of the pipe dip inward between 80°-85° (Mitchell 1986). Three facies are recognized, if erosional processes have not occurred (Figure 2.1.1).

The lower-most zone is made up of the irregular root zone and feeder dykes. It is composed of hypabyssal kimberlite. The hypabyssal kimberlite has an igneous texture, with irregular-shaped carbonate and serpentine segregations (Mitchell 1986).

The intermediate zone is unique to type 1 kimberlite pipes and is called the diatreme. This section of the pipe is composed mainly of tuffistic kimberlite or tuffistic kimberlite breccia (>15% xenoliths). The xenoliths are dominantly wall rock and show little thermal or chemical alteration (this is distinct from xenoliths in hypabyssal kimberlite).

The tuffistic kimberlite is dominantly composed of globular magmaclasts supported in a serpentine and chlorite groundmass. Magmaclasts are spherical-to-elliptical and range in size from 1-10mm. They are dominated by a single "kernel" (core grain) of pseudomorphosed olivine, phlogopite or other macrocrysts. The matrix is composed of fine grained euhedral olivine, phlogpite phenocrysts, spinels, perovskite, diopside and is replaced by serpentine and calcite.

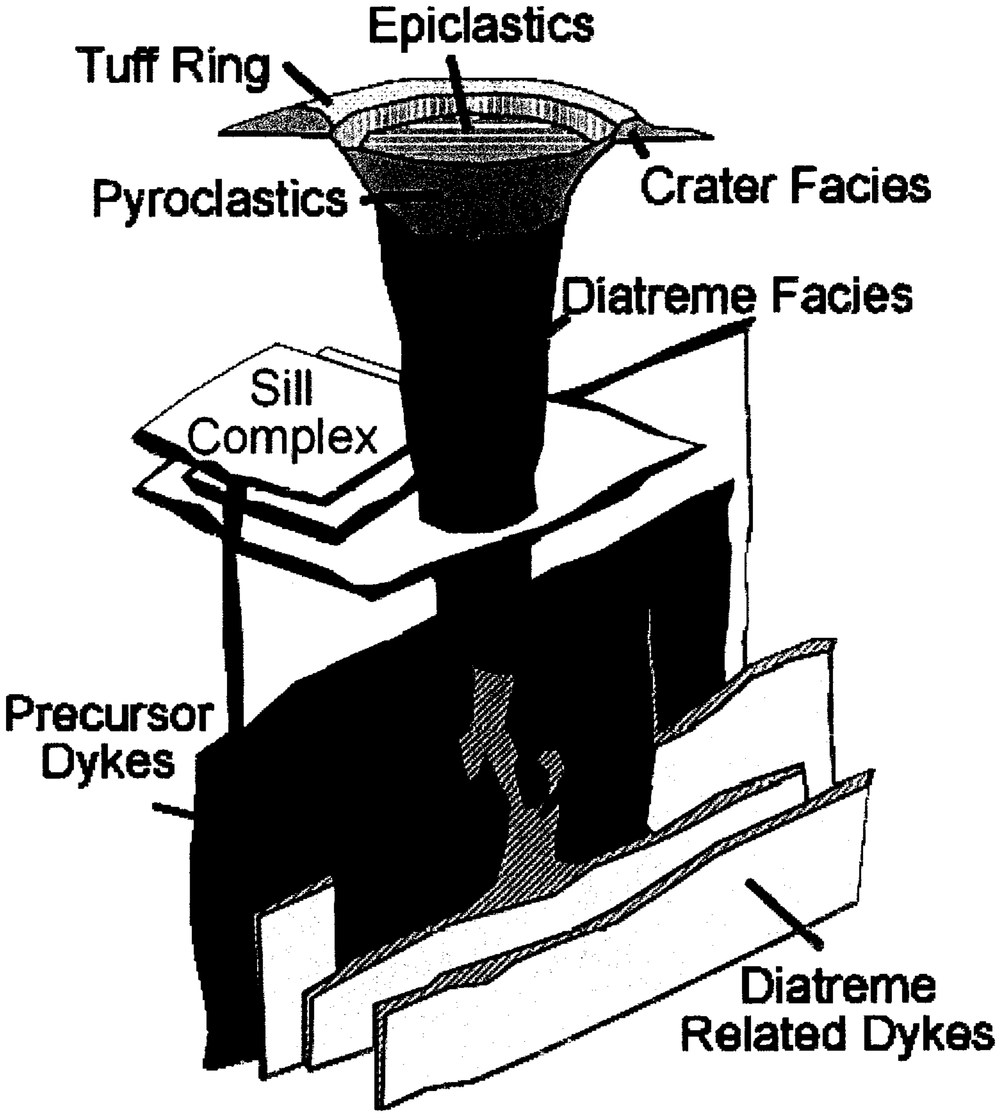

Figure 2.2.1: Type 1 – South African pipe model with pyroclastics at the surface overlying a steep carrot-shaped diatreme underlain by an irregular root zone and feeder dykes (Modified from Mitchell 1986).

The uppermost facies is the crater zone. It is infilled with epiclastics and resedimented volcaniclastic kimberlite up to a depth of 700m. This facies is rarely preserved due to erosion. The crater zone is dominated by pyroclastic kimberlite and lesser resedimented volcaniclastic kimberlite and is well-bedded, normally-graded with an average grain size from ash to lapilli. The magmaclasts are commonly less than 2mm. Xenoliths and xenocrysts are rare but quartz is commonly present in the resedimented units. The matrix is dominated by serpentine with rare carbonates.

2.3 Type 2 Pipes:

Type 2 kimberlite pipes were first discovered in central Saskatchewan Canada in 1988 and termed "Prairie-type" kimberlites. They have a shallow bowl shape, with a basin 50-1500m in diameter, with the bowl extending to a depth of less than 500m. The feeder pipe is thin and simple relative to type 1 pipes.

The infill is dominantly pyroclastic kimberlite which is produced by near-surface magmatic eruptions, which include fire fountain, air-fall and column collapse processes (Scott-Smith 2008a,b, Leckie et al., 1997). The pyroclastic kimberlite consists mainly of pyrocryst olivines due to the low viscosity of the magma. Pyromagmaclasts are also a component and are amoeboid in shape (also reflecting the low viscosity) with partially-altered olivine macrocrysts and phenocrysts. Also present are vesicles infilled by carbonates. The matrix of the magmaclast is composed of serpentine, carbonates or both. The overall groundmass between clasts is dominated by serpentine but carbonates can be present. Epiclastic kimberlite occurs as resedimented volcanic kimberlite but is less common than pyroclastic kimberlite. The magmaclasts are rarely flattened, welded or molded which suggests that they were solid prior to deposition.

2.4 Type 3 Pipes:

Type 3 kimberlite pipes are characteristic of the "Lac de Gras" region in northern Canada such as the Ekati mine (Masun, 1999). Type 3 pipes have a steep sided crater wall with a depth greater than 500m. Figure 2.4.1 (after Scott-Smith 2008a) compares the shape and infill of type 1, 2 and 3 kimberlite pipes. The infill of type 3 is dominated by resedimented volcaniclastic kimberlite but minor graded pyroclastic kimberlite is also present.

The constituents of the resedimented volcaniclastic kimberlite are similar to those of the "Prairie-type" kimberlite but carbonates are the dominant groundmass component. Xenoliths and xenocrysts are abundant and coarse grained. Due to the dominance of resedimented volcaniclastic kimberlite, macrocrysts, magmaclasts and country rock are set in a mud-rich matrix. Primary pyroclastic kimberlite is poorly preserved due to the degree of resedimentation, because of the high rate of resedimentation it is suggested that the pyroclastic kimberlite is derived from the eruption of adjacent pipes (Scott-Smith 2008a).

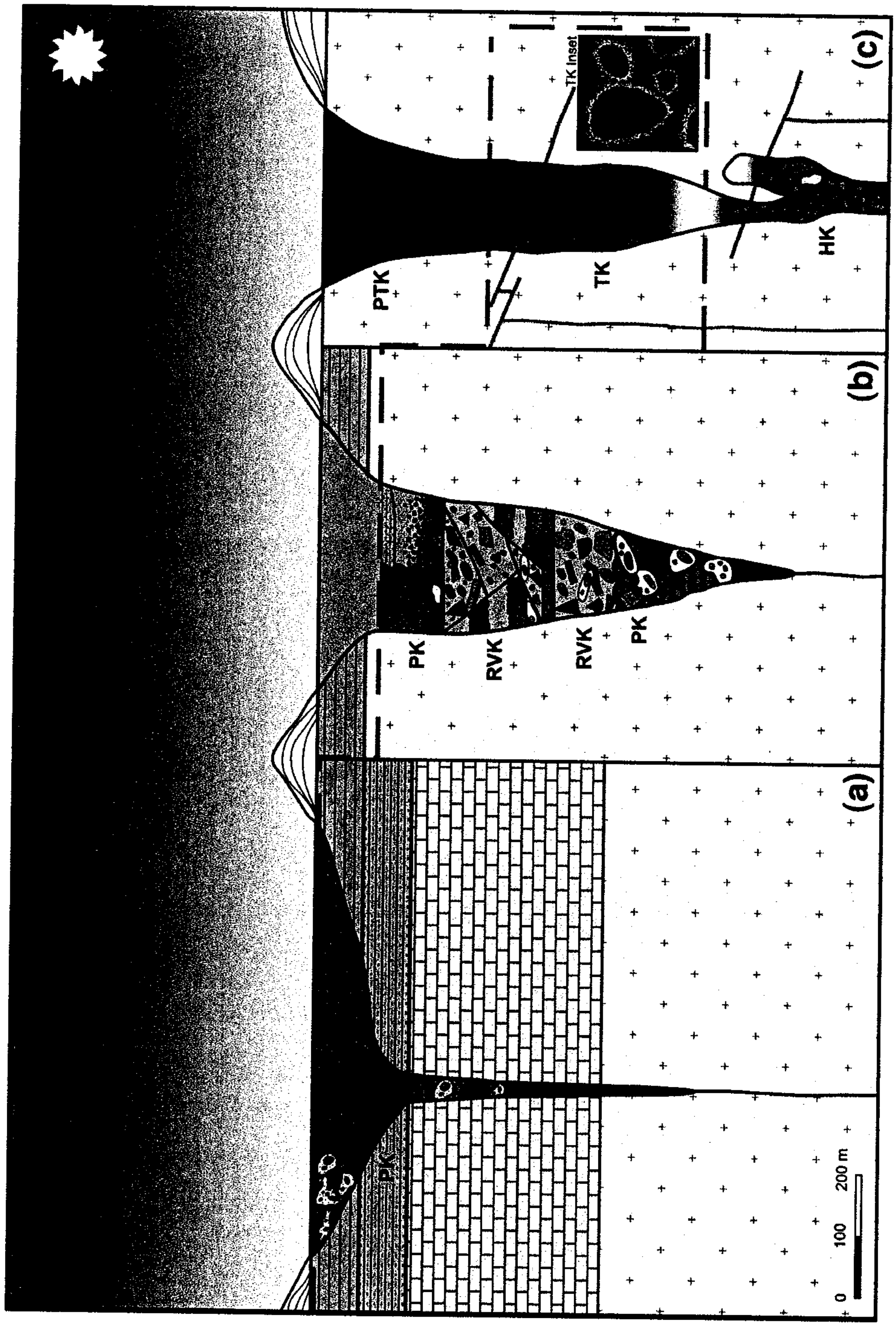

Figure 2.4.1 The three types of pipe models with correlating infilling. (a) is type 2 with a shallow bowl shape and pyroclastic kimberlite infill. (b) is type 3 with a steep carrot shape infilled with resedimented volcanic kimberlite and pyroclastic kimberlite. (c) is type 1 a steep carrot shaped pipe with a irregular hypabyssal zone infilled with pyroclastic kimberlite at surface, tuffistic kimberlite in the diatreme and hypabyssal kimberlite in the root zone (Scott Smith 2008a).

Chapter 3: Fort à la Corne Kimberlite

3.1 Fort à la Corne Kimberlite:

Uranerz Exploration and Mining Limited discovered the first kimberlite body in the Fort à la Corne kimberlite field in 1989. Now over seventy kimberlite bodies comprise one of the largest kimberlite fields in the world and extend over a zone 45km long and 30km wide in a North-North-West to South-South-East direction. The Star kimberlite is hosted in Phanerozoic sediments.

3.2 Age Determination:

There have been five ages determined for kimberlite from the Fort à la Corne field. These include: Rb-Sr ages of 94-96Ma (error not given); Rb-Sr age of 96 ± 1Ma ; U-Pb (perovskite) at 99.8 ± 1Ma; and 101.1 ± 2.2Ma, U-Pb (perovskite) at 99.8 ± 2.4Ma and 99.5 ± 1.8Ma (Scott Smith, 2008a). The age range determined by the various techniques suggests a period of magmatism occurring over a 7Ma period from 94-101Ma. The fossil records for the formation correlate with this time and support the age determined by radiometric techniques.

3.3 Shape:

The Fort à la Corne kimberlite bodies are sub-circular, bowl-shaped with no carrot-shaped diatreme, tuffistic kimberlite or hypabyssal kimberlite infilling (Figure 2.1.2). The "Prairie-type" kimberlite is, typically, 80-200ha in size (about 2000m in diameter), but the shape can be more complex.

Based on drill core data they extend from 160m to 500m in depth. The wall contact to the surrounding sediments varies from 5° to 55°. The bodies are not symmetrical and the margins have a dip from 0° to 60° (Scott-Smith, 2008a).

3.4 Constituents of Pyroclastic Kimberlite:

There are two main types of kimberlite infill in the Fort à la Corne kimberlite. These include pyroclastic kimberlite and resedimented volcaniclastic kimberlite. Each of these two types of infill are divided into three main components: magmaclasts; pyrocrysts; and interclastic material (Scott-Smith, 2008a).

A general description of each component for pyroclastic kimberlite is as described below by Scott-Smith (2008a).

The magmaclasts are pyroclastic in origin and are amoeboid in shape-to-curviplanar in shape and less commonly spherical-to-elliptical. There are commonly phenocrysts protruding from the clast matrix. The magmaclasts are commonly less than 10mm in size but can be up to 50mm in diameter.

Macrocrysts and phenocrysts can be partially-to-completely pseudomorphed but are commonly fresh. The magmaclasts enclose several macrocrysts and phenocrysts, if they are large enough, but commonly enclose a single olivine grain with a thin selvage.
The selvage or "magma melt" (matrix) primarily crystallized monticellite, phlogopite, perovskite and spinels (atoll structures are common) set in a cryptocrystalline serpentine and less common carbonate interstitial material. Spherical vesicles are present but not abundant.

There is minor to no flattening of the magmaclast or welding which suggest crystallization of the clasts prior to deposition. The amoeboid shape and relative paucity of vesicles is suggestive of a low viscosity magma which is consistent with the high MgO and volatile content in the magma.

Pyrocrysts of pseudomorphed olivine are commonly smaller than 10mm. They are typically replaced by serpentine, carbonate, magnetite and sulphides. Most grains have not been modified after deposition.

Interclastic material is similar to a residual fluids found crystallized in a hypabyssal kimberlite and is dominated by serpentine, carbonate and minor magnetite. It occurs in voids between magmaclasts and macrocrysts.

3.5 Constituents of Resedimented Volcaniclastic Kimberlite:

Resedimented volcaniclastic kimberlite is not common and is characterized by an increase in the extent of brittle fracturing, abrasion or replacement textures. Pyroclastic recycling is observed in samples examined by Scott-Smith (2008a).

Magmaclasts are sub-spherical-to-ovoid-to-fractured in habit. There is an increase in magnetite replacement relative to pyroclastic kimberlite.

Pyrocrysts can be more intensely fractured but are otherwise similar to those of the pyroclastic kimberlite.

Interclastic material is a non-magmatic fine-grained matrix and is all a cryptocrystalline grey-to-brown coloured material containing perovskite, spinel and mica.

Other phenocrysts and macrocrysts include phlogopite which is commonly found as laths that are 20mm in size; these occur in both magmaclasts and as single grains.

Mantle-derived xenocrysts include garnet, ilmenite, and chrome diopside (very minor). The garnet grains commonly have a thick kelyphitic rim surrounding the grain and even complete replacement is observed. Mantle xenocrysts occur in both magmaclasts and as microxenoliths. Country rock xenoliths and xenocrysts are typically uncommon but some units consist of up to 80% xenolithic material.

3.6 Structure

Most of the kimberlites are loosely-packed, clast-supported and commonly have been well-sorted with normally-graded bedding structures. The beds have an average thickness of 2m but can be up to 12m. Most grains that are less than 0.5mm in size are suspected to have been removed by wind-willowing and sorting. Sorting is also preserved laterally from the vent, where the grains become finer away from the vent (Scott-Smith, 2008a).

The kimberlite beds dip between 0° to 80° but on average the dip is less than 30°. There is a lack of bomb textures and sag structures, suggesting gravity deposition (Scott-Smith, 2008a).

Chapter 4: Candle Lake Kimberlite

4.1 Candle Lake Kimberlite:

Exploration around the Candle Lake area has consisted of several geophysical surveys including: airborne and ground magnetics; electro magnetic (EM); gravity; and IP-Resistivity. The C29/30 kimberlite body was defined by a ground magnetic survey as two discrete bodies; one magnetic and the other non-magnetic. However, the boundaries between the magnetic high and low have not been identified in the drill core.

As of March 2007, Great Western Diamond Corporation has drilled 46 diamond drill holes and 11 reverse core holes intersecting 1611.66m of kimberlite. The C29/30 kimberlite body is buried below 100-150m of glacial overburden. Based on drill hole and geophysical data the body has an NW-SE trend, and extends a length of 1700m with a width of 400m and a maximum depth of 150m (Figure 4.1.1).

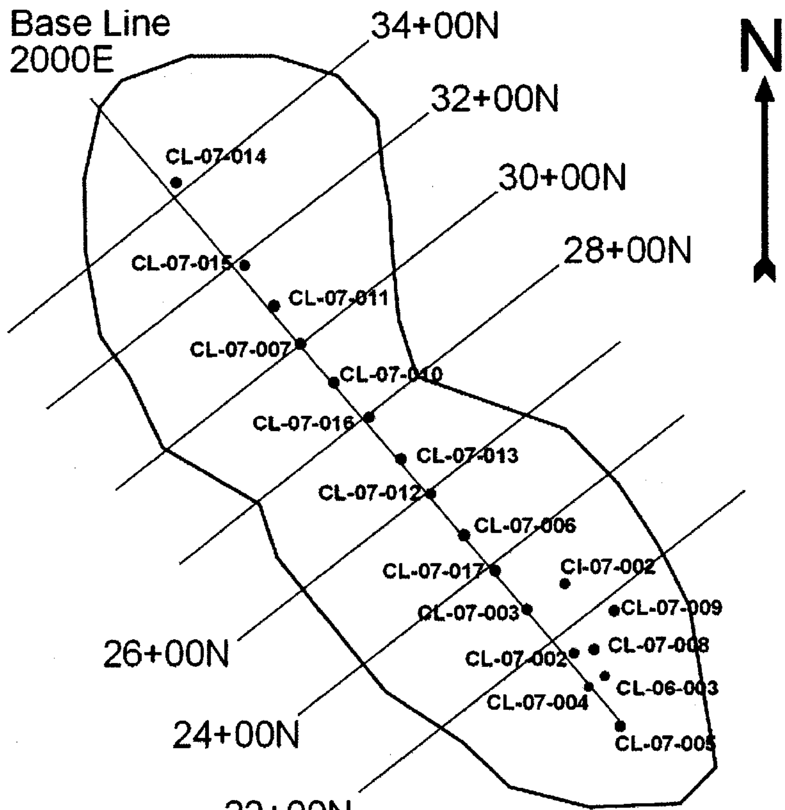

Figure 4.1.1 2007 and CL-06-003 drill hole locations for the Candle Lake C29/30 kimberlite (Great Western Diamond Corp., 2007).

Three distinct kimberlites phases have been recognized by Great Western Diamond Corporation on the basis of their interpretation of the drill core material.

Kimberlite 1:

Dark green, massive, uniformly fine-to-medium grained and poorly-sorted volcaniclastic kimberlite. This contains more country rock xenoliths (3-5%), mostly limestone, relative to the other two units. The pyrocrysts are visually estimated at 50% by volume of the kimberlite and are dominantly medium-grained macrocrysts which have been serpentinized. Magmaclasts are medium-grained (2mm in size) and are less abundant then the pyrocrysts. Indicator minerals include garnet (with a kelyphitized rim), ilmenite and clinopyroxene (typically very minor to absent). The interclast matrix supporting the clasts is composed of dark green serpentine.

Kimberlite 2:

A dark green-to-grey bedded volcaniclastic kimberlite. There are alternate beds up to 10cm thick with carbonate groundmass or serpentine groundmass, with minor normal grading. The beds are clast-supported. The pyrocrysts are visually estimated at 60% volume, dominated by mostly serpentinized olivine. Magmaclasts are medium-grained and are less abundant then the pyrocrysts. Indicator minerals include garnet and rare ilmenite. Country rock xenoliths (1-2%) are dominantly limestone but some brown shales are present.

Kimberlite 3:

A pale green volcaniclastic kimberlite that is bedded and varies in grain size from very fine grained to medium grained. Pyrocrysts of olivine are estimated at 40% volume, but can be in graded beds that comprise up to 50% volume of the finer-grained material. The magmaclasts are less abundant compared to kimberlites 1 and 2. The groundmass is composed of serpentine with minor carbonate and is clast-supported. Mantle xenoliths include garnet with a kelyphytic rim and minor magnetite (most probably secondary alteration). Country rock xenoliths comprise less than 1% volume of the rock unit.

The three kimberlite types defined by Great Western Diamond Corporation cannot be recognized as pyroclastic kimberlites or resedimented volcaniclastic kimberlite on the basis of macroscopic observations alone. Thus, it is evident that detailed petrographic work is needed to reclassify the Candle Lake kimberlites.

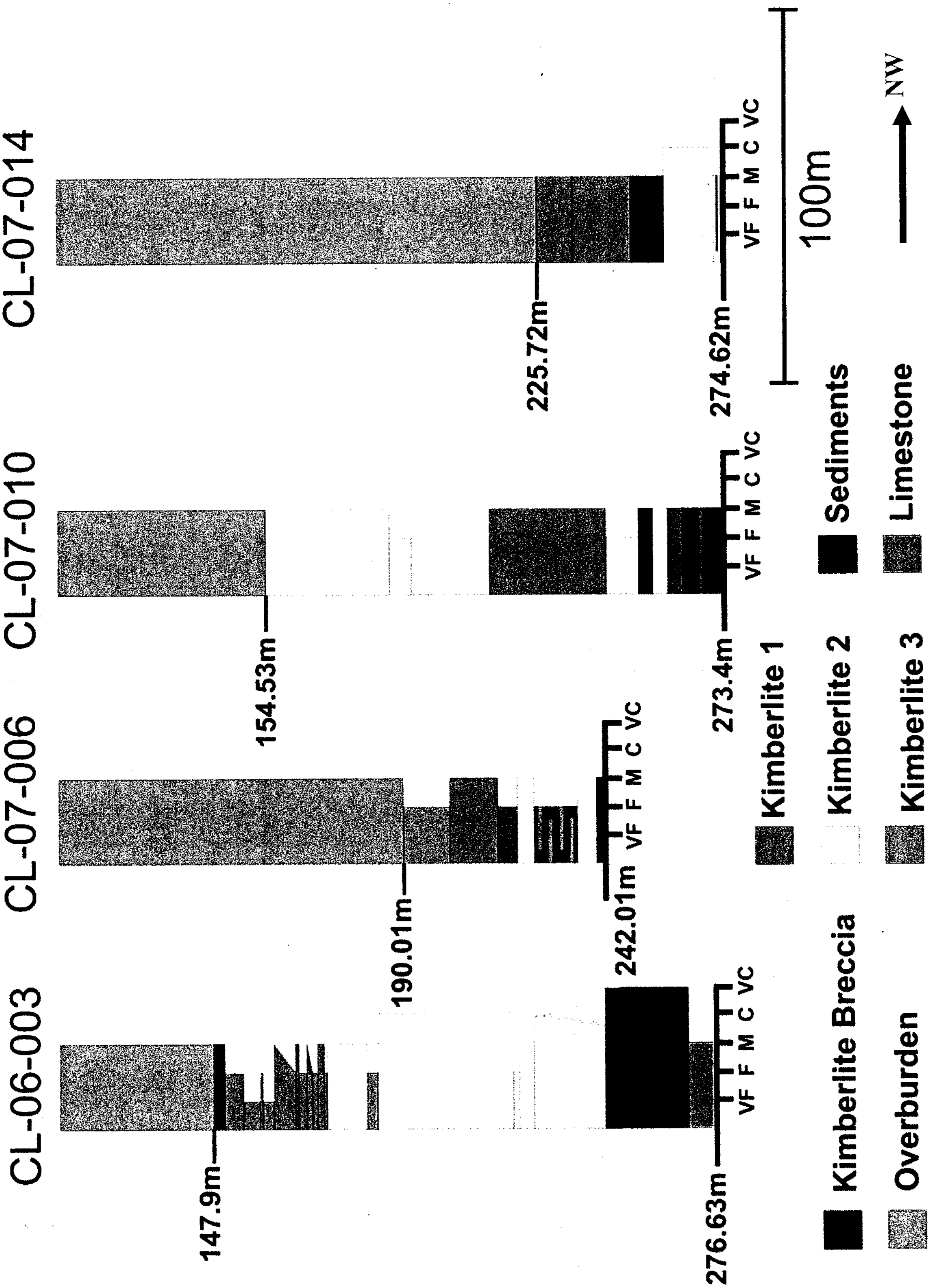

Figure 4.1.2: Cross sectional view of drill holes CL-06-003, CL-07-006, CL-07-010 and CL-07-014. The drill holes are divided into kimberlite units based on Great Western Diamond Corp. interpretations of the C29/30 kimberlite.

Chapter 5: Candle Lake Kimberlite Units

5.1 Introduction:

Kimberlite from Candle Lake has been divided into three types on the basis of optical petrography and BSE-imagery. The dominant type is a well-preserved pyroclastic kimberlite that is matrix-supported and contains well-defined amoeboid magmaclasts. The second type is a resedimented pyroclastic kimberlite, which is a pyroclastic kimberlite unit that has been remobilized by wave, tidal or slumping activity. The magmaclasts in resedimented pyroclastic kimberlite are rounded-to-fractured and poorly-preserved. The third unit is a lapilli tuff which is very-well sorted and clast-dominated. It is not recognized as a continuous unit through the drill core and is limited to only one sample.

5.2.1 Pyroclastic Kimberlite Description:

Fourteen of thirty samples investigated are interpreted as pyroclastic kimberlite. This type of kimberlite is very well-preserved, moderately-to-poorly sorted, and matrix supported (Figure 5.2.1). Welding and bomb-sag textures (a bomb-sag texture is the disruption of bedding caused by the impact of falling clasts) are absent. Lack of welding suggests crystallization of the clast before deposition. The ratio of pseudomorphed macrocrysts and pyrocrysts to magmaclasts is on average 2:1. There are two types of interclast matrix that occur in the pyroclastic kimberlite. The principal variety of interclast matrix is cryptocrystalline, light-to-dark green, and composed dominantly of an intimate intergrowth serpentine-calcite-chlorite (Figure 5.2.4). The other is a homogenous, intergrown calcite (Figure 5.2.1).

Late-forming secondary phases include minor, thin calcite veins cross-cutting the samples with no preferred orientation. Also present in low abundance are angular xenoliths up to 3 cm in size, consisting of carbonate, mudstone and granite. Garnet xenocrysts are also present and have kelyphite rims.

5.2.2 Macrocrysts vs. Phenocrysts:

Macrocrysts are distinguished from phenocrysts on the basis of grain size, habit and replacement. Macrocrysts range in size from 700 μm to 10 mm and are rounded-to-oval with minor internal fracturing (Figure 5.2.1, 5.2.2). phenocrysts are on average 300 μm in size, rounded to subhedral in habit, and are replaced by zoned serpentine. Macrocrysts and phenocrysts of pseudomorphed olivine are the dominant clast. The internal fractures are filled by calcite. The olivine is replaced by two-to-three sequences of light green serpentine (see serpentine, section 6.2). Iron nickel sulphides occur in trace amounts as very thin, short veins within the serpentine. The cores of the macrocrysts are replaced by angular calcite and dolomite. Spinels occur within the macrocrysts and are fine-grained, 5 to 30 μm in size. Other macrocrysts include phlogopite that occurs as prisms with rounded terminations.

5.2.3 Magmaclasts:

Magmaclasts are 250 μm to 2.1 mm in size, averaging 0.6 mm. They are amoeboid-to-subrounded in shape and are well-defined against both types of interclast matrix. The matrix of the magmaclast encloses rounded macrocrysts and subhedral-euhedral phenocrysts. The phenocrysts are 5 to 500 μm in size with complex replacement by serpentine (see serpentine, section 6.2). The groundmass is very fine-grained and composed of pseudomorphed monticellite, and pseudomorphed olivine replaced by serpentine and carbonates (Figure 5.2.3). The mesostasis is cryptocrystalline, and composed of serpentine, calcite, and chlorite, with minor fine-grained (<3 μm) spinels, apatite, perovskite, anatase, and minor anhedral sulphides (Cu, Zn, Ni) and barite. The latter also occurs as thin (<2 μm) veins. Vesicles are a minor component of the magmaclast and are not always present. Vesicles are rounded and infilled by calcite with dolomite rims, similar in habit to the carbonate core replacement of macrocrysts (Figure 5.2.3). Vesicles infilled by a serpentine-carbonate mixture do occur in some magmaclasts but are very rare.

Variations between magmaclasts are minimal. Some magmaclasts have abundant vesicles while the majority contain a few or none. Barite only occurs in a few samples and is not present in all magmaclasts. Atoll structured spinels can occur in one magmaclast and not in an adjacent magmaclast. Perovskites may form and enclose type [3] spinels (see below) in one magmaclast but not in another.

The crystal tuff unit as well as having magmaclasts as noted above also has a different type of magmaclasts. These magmaclasts are 250 μm to 2 mm in size and are rounded-to-subhedral with a thin, 10-100μm selvage of matrix (Figure 5.2.2). Internal fracturing is present but is less prominent relative to the macrocrysts. Magmaclasts are dominated by pseudomorphed olivine that is replaced by one to three phases of serpentine. Samples containing increased amounts of pyrocryst reflect an increase in sorting, sample CL-06-003-186 (Figure 5.2.2).

5.2.4 Magmaclast Groundmass:

The matrix is dominantly a cryptocrystalline, relatively homogenous mixture of serpentine, carbonate and chlorite. However; there are well-defined irregular segregations of calcite which are interstitial to the clasts. These are infilled by fine grained (5 to 20 μm) angular calcite grains with a dolomite rim. The calcite segregations are surrounded by botryoidal serpentine. The second type of interclast matrix is a cryptocrystalline homogeneous calcite. The calcite in contact with macrocrysts and magmaclasts has an elevated magnesium content resulting from the interaction of the clasts with the interclast matrix during serpentinization of the clasts, or during the formation of the interclast matrix.

5.3 Resedimented Volcanic Kimberlite:

Fifteen samples are interpreted as resedimented volcanic kimberlite. This unit represents pyroclastic kimberlite that has been redeposited by diverse processes. These are light-to-dark green; fine-to-medium grained and poorly sorted (Figure 5.3.1) rocks. The clasts are poorly-defined within the interclast matrix. The ratio of macrocrysts and pyrocrysts to magmaclasts varies from 3:1 to 75:1, but on average is 15:1. There is commonly a preferred, sub-horizontal orientation of the magmaclasts and macrocrysts resulting from resedimentation. Samples with clast alignment contain clasts with a greater amount of selvage along the ventral part of the clast. This is more common with coarser clasts (>2 mm), and only occurs in extensively reworked samples. The interclast matrix is brown-to-green, cryptocrystalline, and is composed of serpentine and carbonates (Figure 5.3.1). The interclast matrix is heterogeneous with abundant irregular segregations of serpentine and carbonate.

Xenoliths and/or xenocrysts of quartz and carbonate are very abundant in some samples; the xenoliths and/or xenocrysts are equigranular within each sample but range in size between samples from 100 μm to 1.2 mm (Figure 5.3.2). The clasts are subrounded-to-fractured. Resedimented kimberlite is matrix-supported, but commonly the distinction between the interclast matrix and the clasts is difficult to discern. Late-forming secondary phases include thin calcite and barite veins.

Macrocrysts range in size from 0.6 μm to 2.2 mm and have abundant internal fracturing. The internal fractures are filled by carbonate and magnetite alteration (Figure 5.3.1). Serpentine replacement is similar to that in pyroclastic kimberlite macrocrysts, except that there is an increase in the amount of vermiform-textured serpentine. Vermiform-textured serpentines appear as thin, long, botryoidal-looping strands.

Magmaclasts range in size from 500 μm to 2.4 mm and are rounded-to-fragmented with irregular, diffuse contacts to the interclast matrix (Figure 5.3.1, 5.3.2). The diffuse contact originates from an increase in dolomite abundance from the core to the rim of the magmaclast selvage. Dolomite near the rim is similar in abundance, texture and composition to that of the interclast matrix. The interclast matrix encloses both macrocrysts and phenocrysts, resulting in the rounded shape, unlike pyroclastic kimberlite macrocrysts and phenocrysts, which protrude out of the magmaclast groundmass into the interclast matrix (Figure 5.3.4). Perovskite occurs as fine-grained anhedral grains that are completely or partially pseudomorphosed to anatase. Vesicles are not common, but when present, are rounded-to-sub-rounded and infilled with a single phase of serpentine or dolomite.

Magmaclasts are either less common in resedimented volcaniclastic kimberlite or the selvages around the clasts are indistinguishable from the interclast matrix due to the mixing of the selvages and interclast matrix during reworking.

The interclast matrix is heterogeneous and is a combination of cryptocrystalline serpentine, calcite and chlorite with minor spinels and anatase. There are two irregular segregation textures, one of serpentine and one of calcite. Both are a single phase cryptocrystalline material rimmed by botryoidal serpentine. Within the serpentine segregations there are fine-grained euhedral grains of calcite (Figure 5.3.3).

5.4 Crystal Tuff:

One sample is recognized as a crystal tuff. This sample is very well sorted, fine-grained, (50 μm to 2 mm), with an average size of 200 μm. The sample is dominated by pyrocrysts of pseudomorphed olivine with a ratio to magmaclasts of 15:1 (Figure 5.4.1, 5.4.2). The sample is clast-supported resulting in abundant grain-to-grain contact, however; there are no welding or bomb-sag textures

The matrix interstitial to the clasts is a carbonate-serpentine-chlorite mixture. There are thin late cross-cutting veins of calcite and few country xenoliths.

Pyrocrysts are 50 μm to 700 μm in size and are pseudomorphed olivines replaced by serpentine with calcite cores and trace iron nickel sulphides in the serpentine. The grains are rounded-to-subrounded with thin, selvages 5 to 50 μm, of cryptocrystalline serpentine-carbonate-chlorite (Figures 5.4.1, 5.4.3). The selvages are similar to the matrix of the magmaclasts from pyroclastic kimberlite.

Magmaclasts vary in size from 100 μm to 2.1 mm with an average grain size of 250 μm. They are rounded-to-sub-amoeboid in shape and enclose fine-to-medium grained phenocrysts of pseudomorphed olivine (Figure 5.4.2). The matrix is very fine-grained, dark green-to-brown, composed of pseudomorphed monticellite grains, 5 to 15μm in size, replaced by serpentine and carbonates. Other minerals within the matrix include perovskite, and spinels (<5 μm). Vesicles are present, but are rare, and infilled by anhedral calcite grains 20 to 30 μm in size.

The interclast matrix is dominantly a single phase of cryptocrystalline serpentine with rims of botryoidal serpentine around the clasts. Irregular segregations interstitial to the clasts are infilled by angular calcite with dolomite rims. The calcite infilling has a vug texture suggesting late infilling of void spaces (Figure 5.4.4).

5.5 Conclusion:

The three kimberlite phases defined by Great Western Diamond Corp. (see chapter 4), do not correspond to those recognized above. The two classifications are compared in Table 5.5.1. In conclusion, megascopic identification is inadequate to describe the main types of infill in this Fort à la Corne type kimberlite. Petrographic analysis is essential in understanding and classifying the different units in the Candle Lake Kimberlite.

Figure 5.5.1 shows a cross-sectional view of the same four drill holes as figure 4.1.2 (CL-06-003, CL-07-006, CL-07-010 and CL-07-014), however; they have been redrawn using the petrographic interpretations from this work. There are significant differences between Figure 4.1.2 and Figure 5.5.1.

Table 5.5.1: Terminology of this work compared to Great Western Diamond Corp.

This work	Great Western Diamon Corp. (2007)
Pyroclastic Kimberlite – poor-to-moderately sorted, fine-to-medium grained, matrix supported, with amoeboid magmaclasts, well defined magmaclasts to interclast matrix, very well preserved.	Kimberlite 1 – dark green, massive, uniform, fine-to-medium grained, increase in xenoliths. 50% olivine with a lower abundance of juvenile lapilli. Matrix supported
Resedimented Volcaniclastic Kimberlite – poorly sorted, fine-to-medium grained, matrix supported, rounded and fractured magmaclasts, abundant secondary veining, and very poorly defined magmaclasts to interclast matrix.	Kimberlite 2 – dark green-to-grey, bedded with inter-layers of carbonate and serpentine interclast matrix units. 60% olivine, with dominantly phenocrysts. Close packed, clast supported. Kimberlite 3 – pale green, bedded, very-fine to medium grained, 40% olivine, magnetite blebs and phlogopite laths are common. Interclast matrix is composed of serpentine and minor carbonate, close packed, clast supported.
Lapilli Tuff – very fine-grained, very well sorted, clast supported, interclast matrix is serpentine and carbonate. Dominantly pyrocrysts (<250 μm) with thin matrix selvages.	Described as kimberlite 2.

Pyroclastic kimberlite is equivalent to Great Western Diamond Corp. Kimberlite 1 and resedimented volcaniclastic kimberlite is equivalent to kimberlite 2 and 3. There is no equivalent kimberlite unit defined for the lapilli tuff kimberlite.

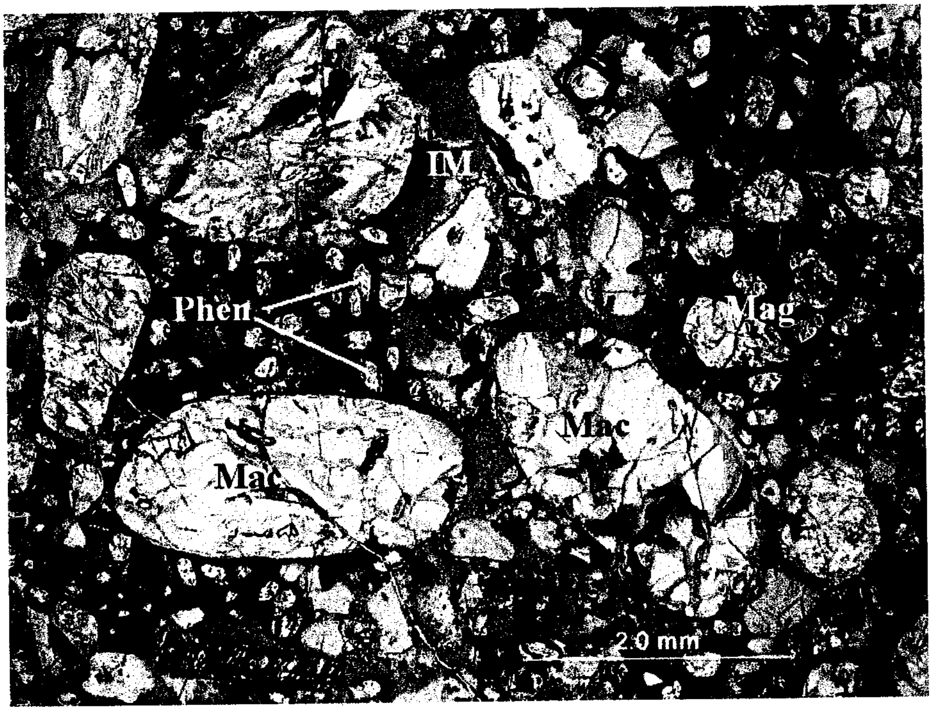

Figure 5.2.1 CL-06-003-236 (PPL) Pyroclastic volcanic kimberlite with amoeboid magmaclast (Mag) enclosing rounded macrocrysts (Mac) and euhedral phenocrysts (Phen) set in a carbonate interclast matrix (IM).

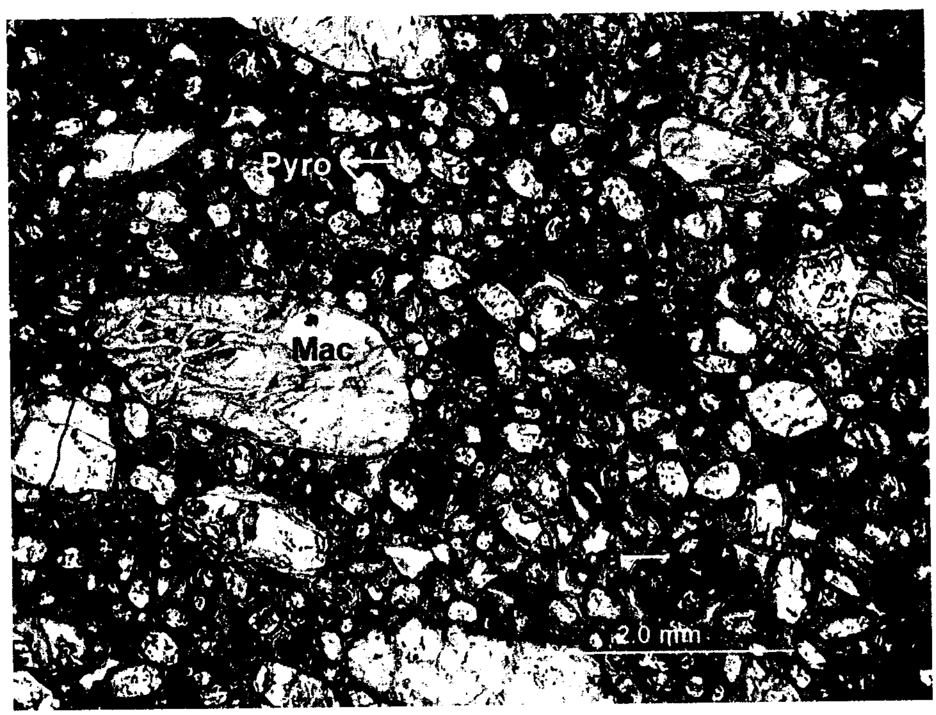

Figure 5.2.2 CL-06-003-186 (PPL) Pyroclastic volcanic kimberlite moderately sorted with abundant fine grained pyrocrysts (Pyro) and coarser rounded macrocrysts (Mac).

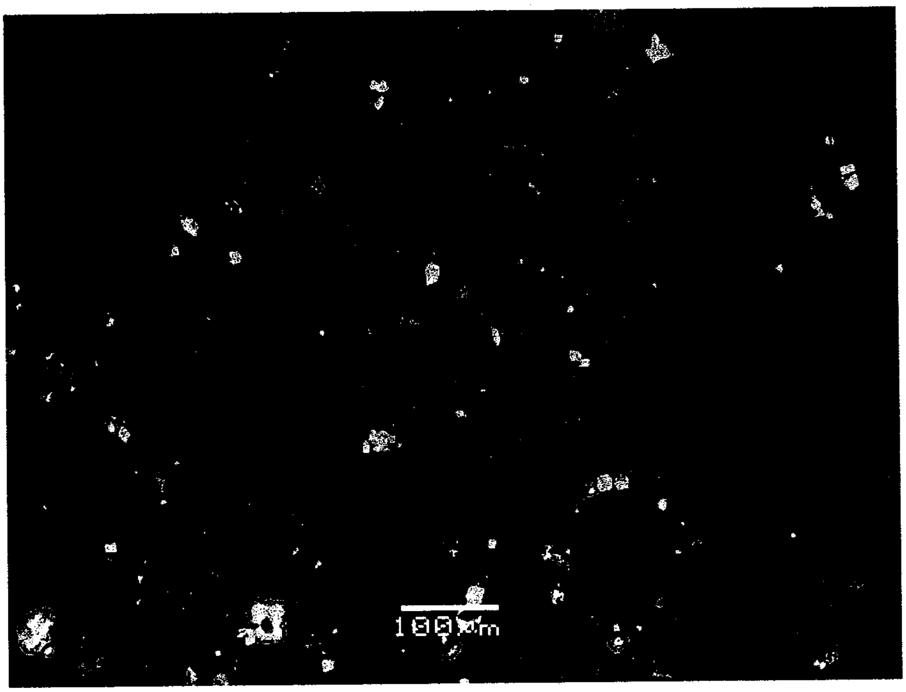

Figure 5.2.3 CL-06-003-182 (BSE) pyroclastic kimberlite, a magmaclast with subhedral zoned phenocrysts (Phen). Rounded vesicles (Ves) infilled by calcite (Cal) which is similar in composition to the calcite interclast matrix on the right. Minor phases are present spinels (Sp) and perovskite (Prv)

Figure 5.2.4 CL-06-003-247 (PPL) pyroclastic volcanic kimberlite that is poorly-sorted, has abundant amoeboid magmaclasts (Mag) and a serpentine-calcite-chlorite interclast matrix (IM).

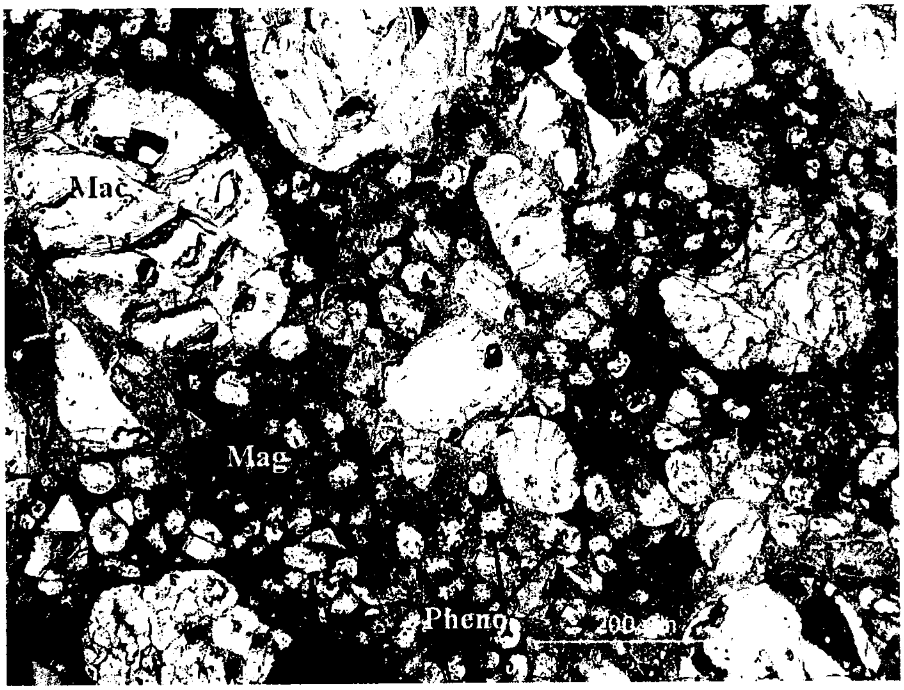

Figure 5.3.1 CL-06-003-222 (PPL), resedimented volcanic kimberlite, poorly sorted with a multiphase interclast matrix (IM) and poorly-defined magmaclasts (Mag). Macrocrysts (Mac) are rounded with internal fracturing.

Figure 5.3.2 CL-07-010-224 (PPL), resedimented volcanic kimberlite poorly sorted with xenocrysts of quartz (Qtz) and fractured macrocrysts (Mac) and phlogopite (Phl) set in a serpentine-carbonate-chlorite interclast matrix (IM).

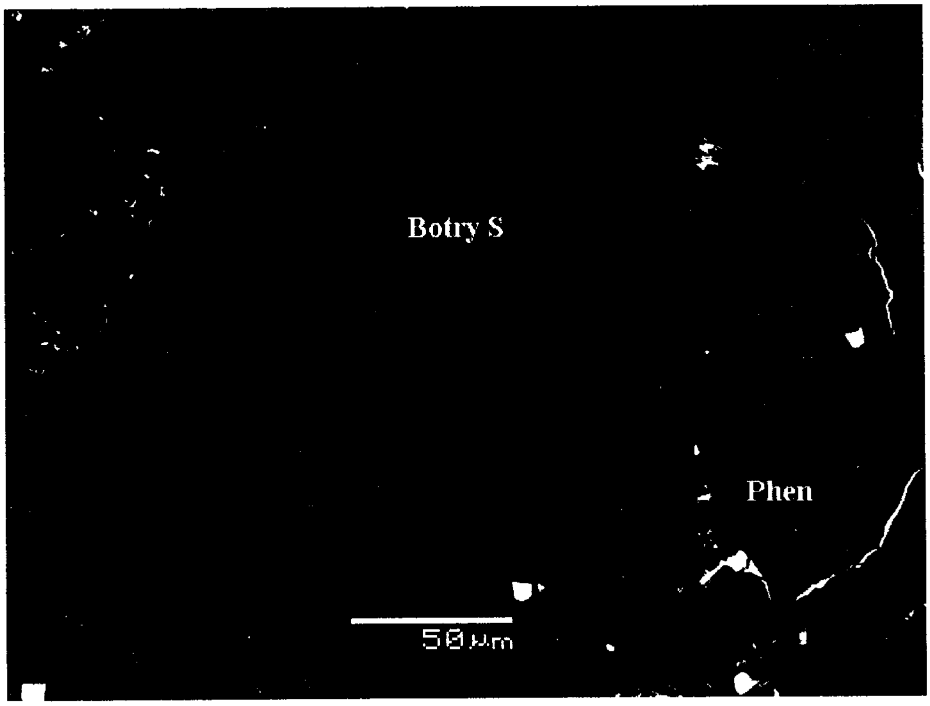

Figure 5.3.3 CL-06-003-219 (BSE), resedimented volcanic kimberlite, groundmass with a calcite (Cal) segregations and botryoidal serpentine (Botry S), surrounding serpentine replaced macrocrysts (Mac).

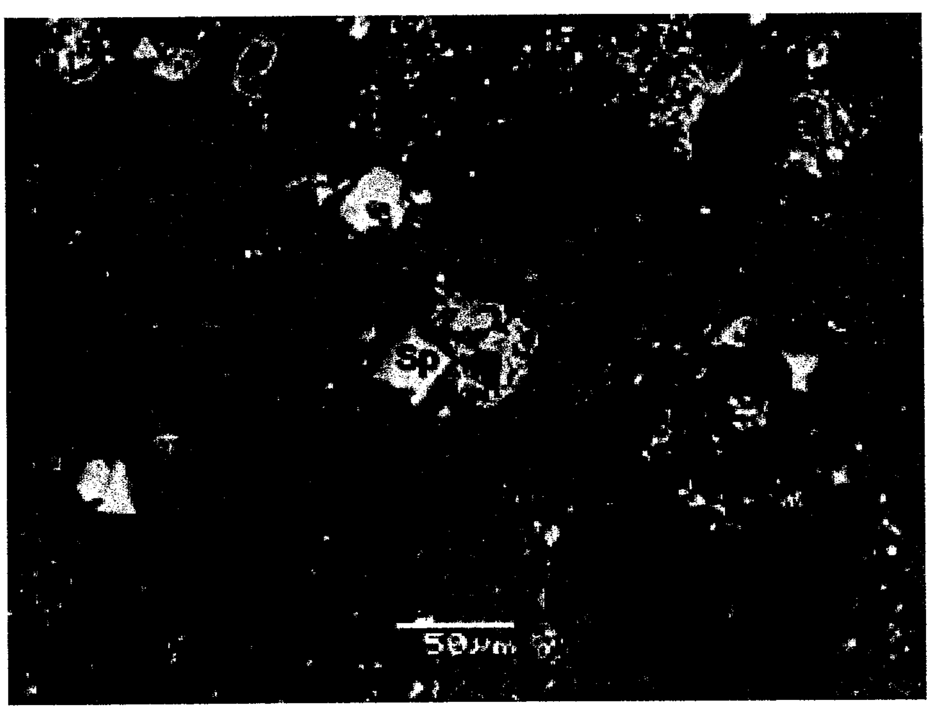

Figure 5.3.4 CL-07-010-169 (BSE), resedimented volcanic kimberlite, rounded phenocrysts replaced by serpentine (S) and calcite (Cal) set in a fine-grained pseudomorphed monticellite matrix (Mon) with interstitial serpentine and carbonate mesostasis (Mes).

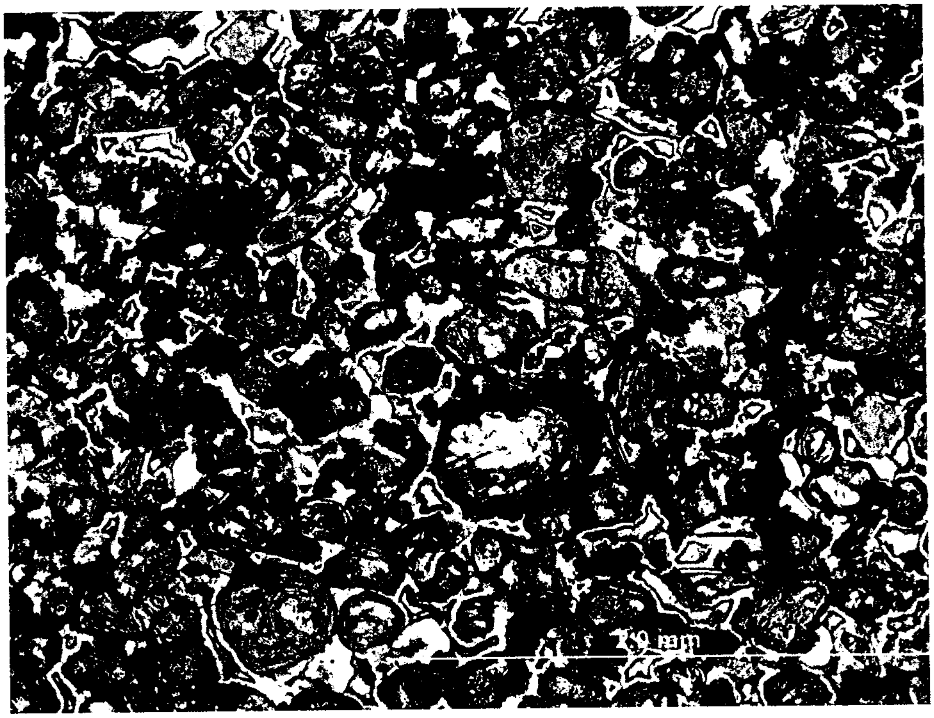

Figure 5.4.1 CL-06-003-173 (PPL) lapilli tuff, pyrocrysts of pseudomorphed olivine replaced by serpentine and calcite. The sample is clast-supported with serpentine-carbonated interstitial matrix and segregations of calcite.

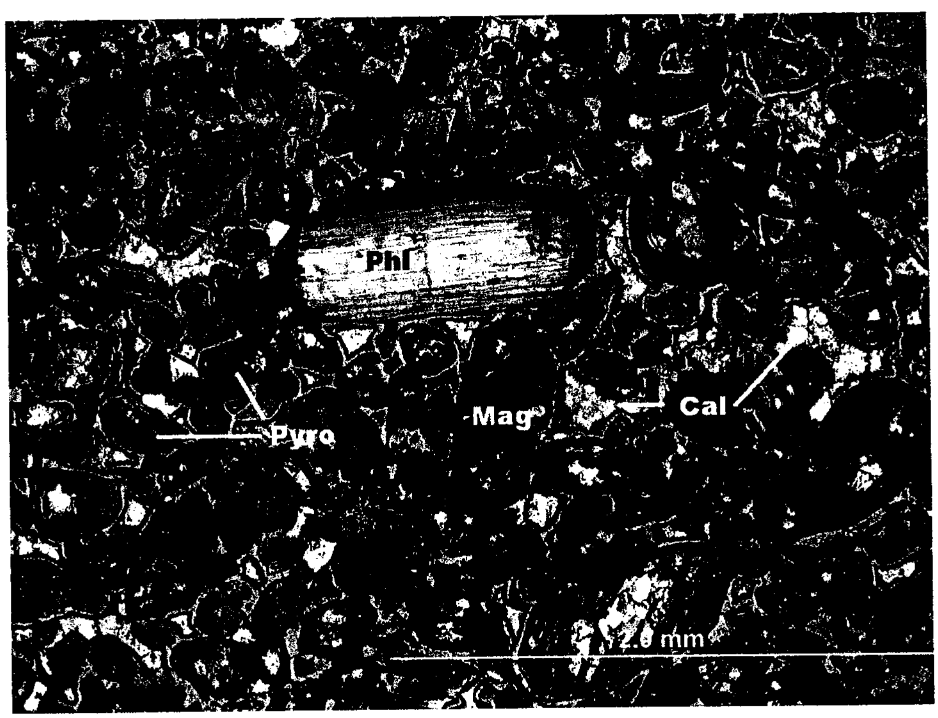

Figure 5.4.2 CL-06-003-173 (PPL), lapilli tuff. Pyrocrysts (Pyro) of pseudomorphed olivine, rounded magmaclasts (Mag) and a macrocryst of phlogopite (Phl) with a serpentine interstitial matrix and interstitial calcite (Cal).

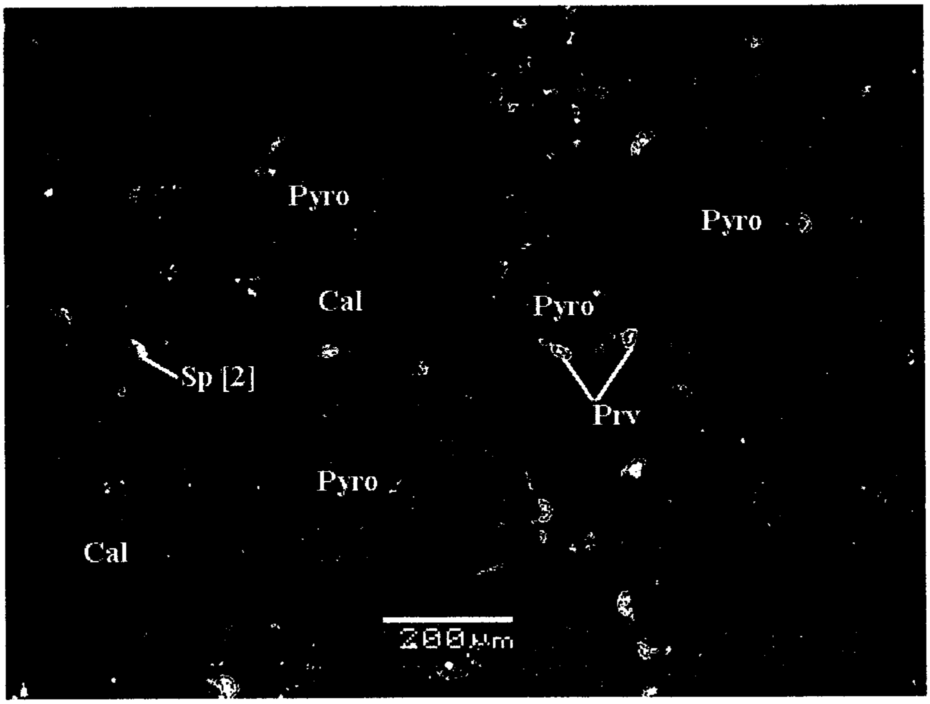

Figure 5.4.3 CL-06-003-173 (BSE), lapilli tuff. Clast-supported pyrocrysts (Pyro) with a thin selvages of matrix with interstitial calcite (Cal) vugs and serpentine-calcite interstitial matrix (GM).

Figure 5.4.4 CL-06-003-173 (PPL) lapilli tuff. Pseudomorphed olivine phenocrysts (Phen) surrounded by a serpentine and calcite groundmass (S – Cal) and interstitial

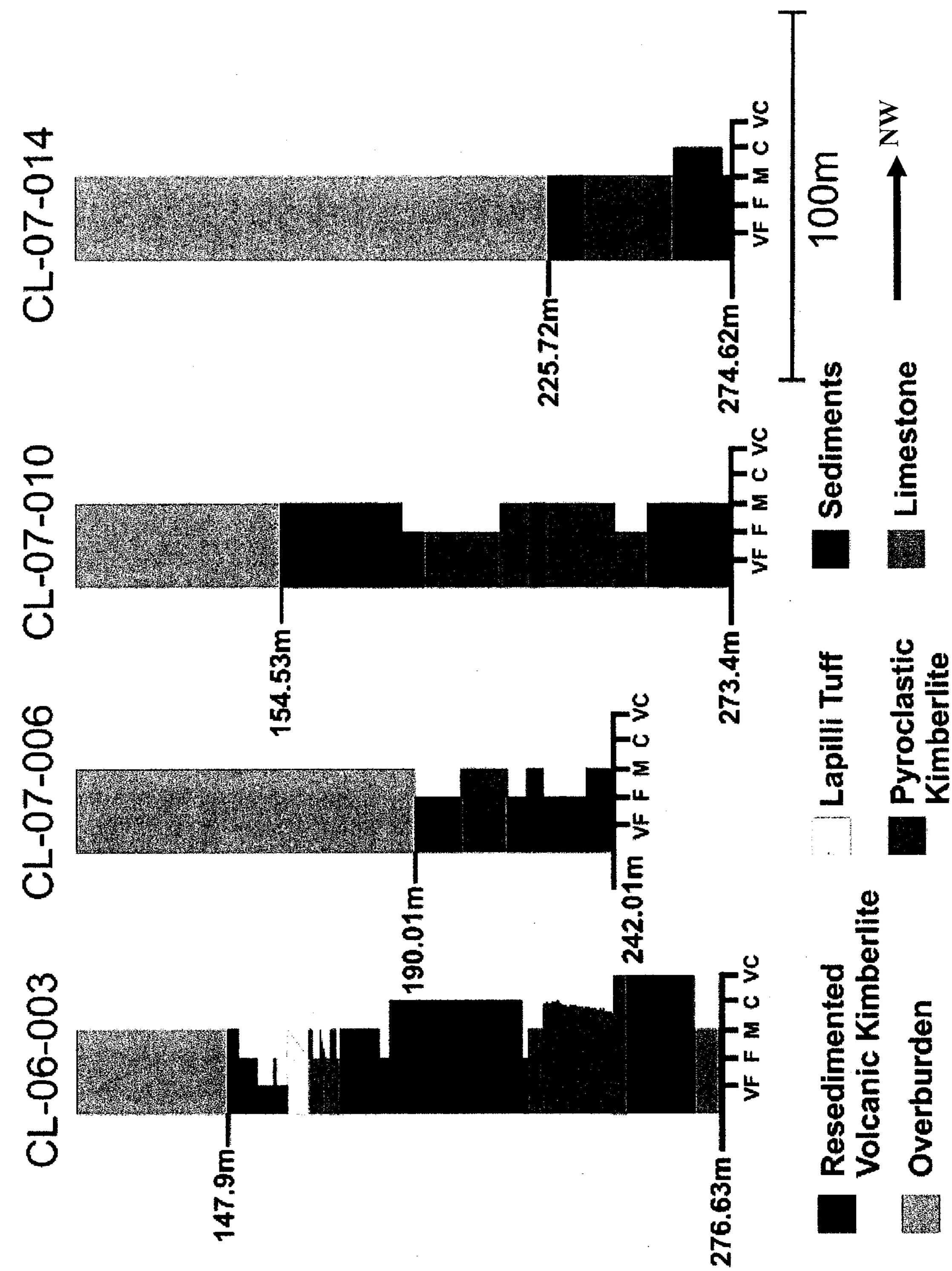

Figure 5.5.1: Petrographic interpretations using resedimented volcaniclasic kimberlite, pyroclastic kimberlite and lapilli tuff kimberlite units for drill holes CL-06-003, CL-07-006, CL-07-010 and CL-07-014.

Chapter 6: Mineralogy

6.1.1 Spinels:

Three parageneses of spinel are evident within the Candle Lake kimberlite on the basis of textural relationships with other phases (Figure 6.1.1). Type [1] spinels crystallized contemporaneously with macrocrysts and phenocrysts and are enclosed within these grains; type [2] spinels crystallized at the margins of the macrocrysts and phenocrysts (Figure 6.1.1); type [3] spinels occur as discrete grains within the matrix of the magmaclast. A fourth spinel (type [4]) is associated with phlogopite cumulates, (see section 6.3). The first three parageneses of spinels are present in all three varieties of kimberlite.

6.1.2 Parageneses of Spinels:

Type 1 primary spinels enclosed in serpentine are common in pyroclastic kimberlite and resedimented kimberlite units of the Candle Lake kimberlite, but rare in the lapilli tuff unit. The spinels are fine-grained, 5 to 30 μm in size, euhedral-to-anhedral in habit, and are opaque (Figure 6.1.1). Spinels were not observed to be enclosed within relict olivine, even though type [1] spinels and olivine formed contemporaneously. Type 1 spinels are similar in pyroclastic and resedimented kimberlite units; however, spinels in resedimented units have slightly lower chromium content and the spinel grains can be fractured (see below). These fractured spinels are broken due to internal fracturing of the pseudomorphed olivine grain.

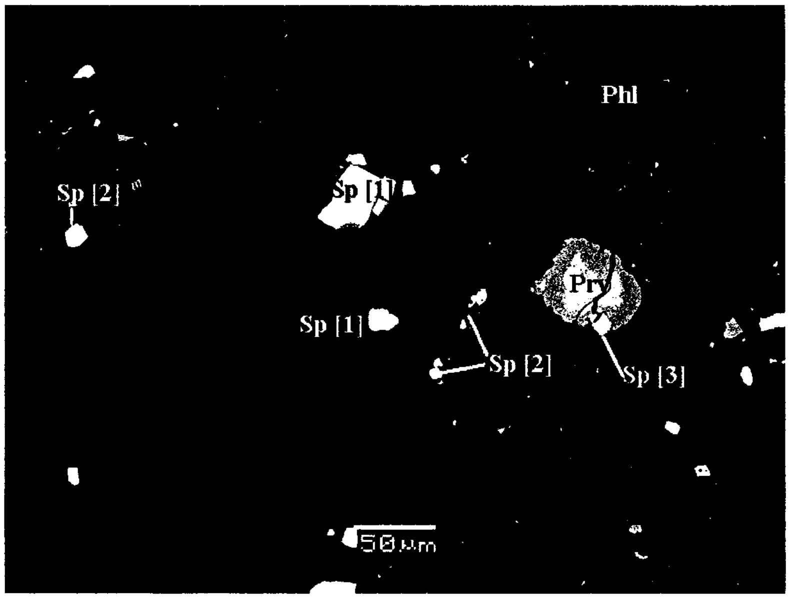

Figure 6.1.1: CL-06-003-247 (BSE) pyroclastic kimberlite. Subhedral type 1 spinels (Sp) enclosed within a serpentine (S) replaced pseudomorphic olivine macrocrysts. Subrounded type 2 spinels occur along the margin of the phenocrysts. A perovskite (Prv) grain in the matrix has marginal titanium rim.

Type 2 spinels nucleated along the edge of the macrocrysts and phenocrysts forming a necklace texture. Spinels were also observed to nucleate together with perovskite, although this is uncommon (Figure 6.1.1).

The contact between the spinel and the macrocrysts or phenocrysts can vary. The spinel can be enclosed within the grain (Figure 6.1.2a) but still exposed to the matrix along the outer edge, partially protruding and resorbed along the crystal face within the phenocrysts or macrocrysts (Figure 6.1.2b), or more commonly the spinel crystallizes at the outer margin of the macrocryst or phenocryst (Figure 6.1.2c). All three varieties of type 2 spinels can occur together. They are all considered type 2 spinels because at least some portion of the spinel grain is exposed to the matrix.

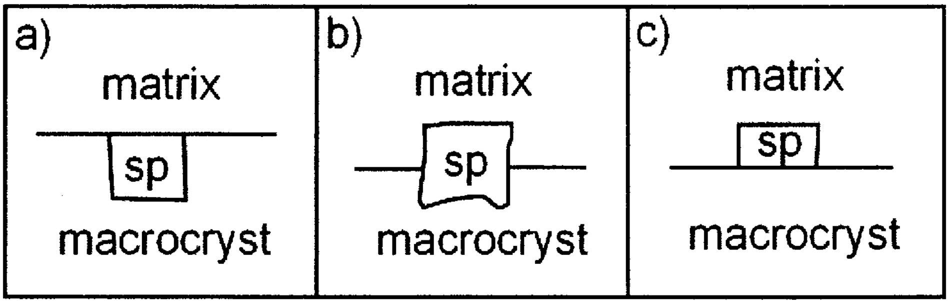

Figure 6.1.2: Type [2] spinel varieties a) spinel crystallized within the macrocryst or phenocryst, b) spinel occurring half in the macrocryst or phenocryst and half in the magmaclast matrix, c) spinel occuring within the magmaclast matrix with only one crystal face in contact with the macrocryst or phenocryst.

Type [2] spinels are common to all three types of Candle Lake kimberlite and are the dominant spinel observed in the lapilli tuff unit. The spinels are 10 to 50 μm in size, euhedral-to-subhedral in habit, and are opaque (Figure 6.1.3).

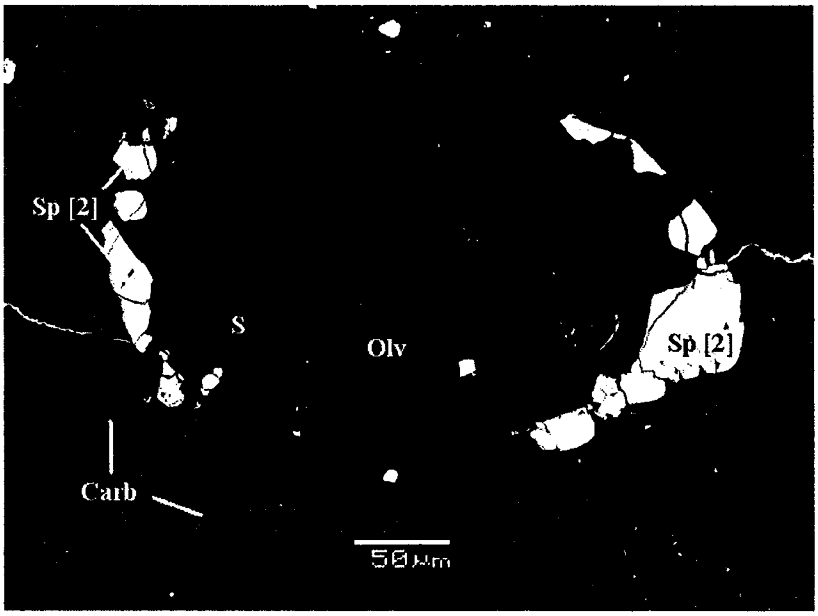

Figure 6.1.3: CL-06-003-195 (BSE) resedimented kimberlite. Macrocrysts of pseudomorphed olivine (Olv) showing a type [2] spinel (Sp) necklace texture.

Atoll structures are present but uncommon. The atoll structure consists of euhedral spinels with a thin selvage of matrix between the spinel core and a magnetite rim (Figure 6.1.4).

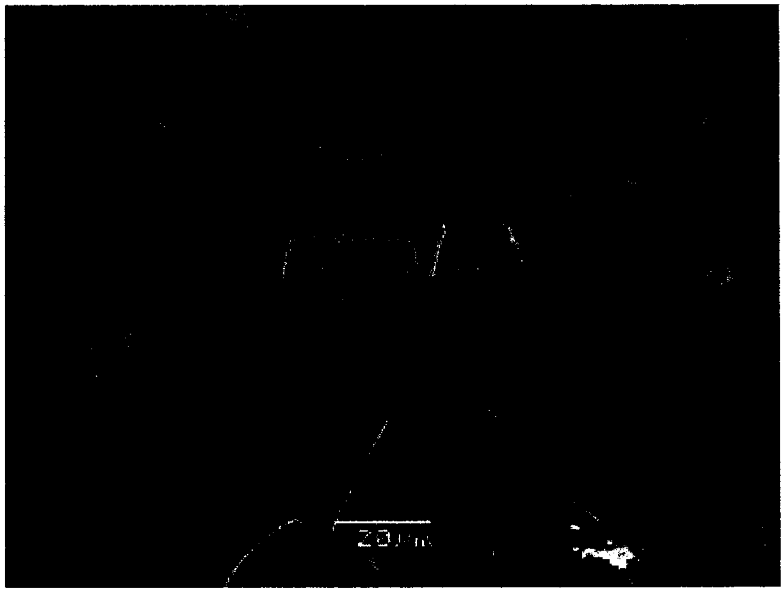

Figure 6.1.4: CL-06-003-222 (BSE) resedimented kimberlite. Macrocrysts of pseudomorphic olivine replaced by serpentine (S) with atoll structured type 2 spinels (Sp) along the edge of the grain. An atoll structured perovskite (Pvk) surrounded by an anatase margin is enclosed within the matrix.

Discrete type [3] spinels occur in small groups (Figure 6.1.5), or more commonly as individual grains (Figure 6.1.6), within the matrix of the magmaclast. These spinels are common to pyroclastic and resedimented units but are rare in the lapilli tuff unit. They are 10 to 100 μm in size, euhedral-to-anhedral in habit and are opaque. Well-preserved euhedral spinels are more commonly associated with pyroclastic kimberlite units, whereas a higher proportion of anhedral and fractured spinels are associated with resedimented kimberlite. Atoll-structured type [3] spinels were observed and consist of euhedral-to-subhedral spinel cores with a thin selvage of matrix between the spinel core and the magnetite rim. Atoll spinels are found adjacent to euhedral and subhedral spinels. The habits of type [3] spinels are consistent within each magmaclast. Adjacent magmaclasts can have spinels that are more anhedral or euhedral, fractured or lacking atoll structured spinels, compositionally the spinels are similar.

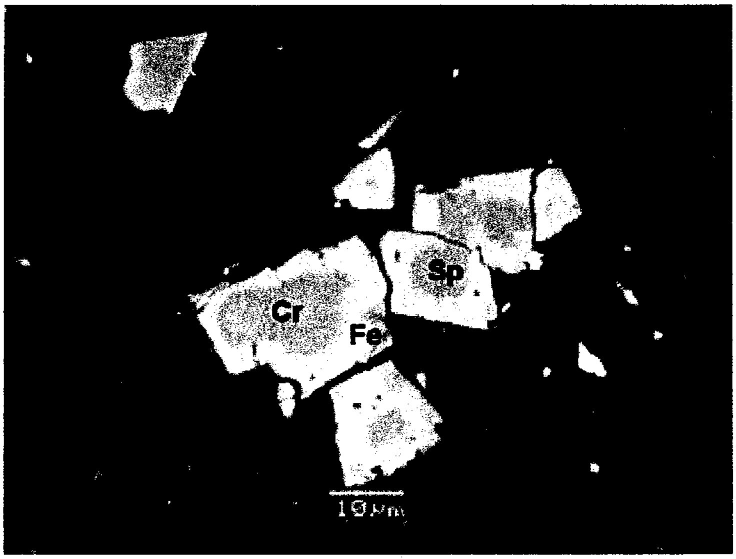

Figure 6.1.5: CL-06-003-236 (BSE) pyroclastic kimberlite. Zoned spinels type 3 (Sp) with chromium (Cr) rich core and an iron (Fe) rich rim set in a serpentine (S) matrix.

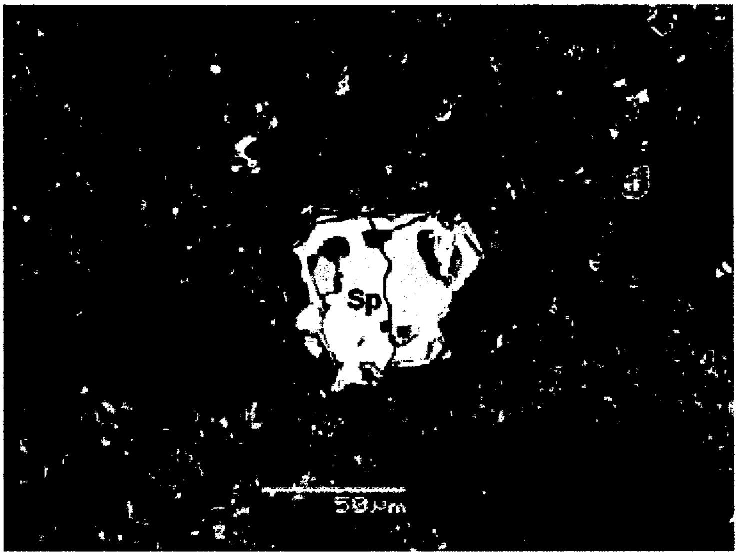

Figure 6.1.6: CL-07-014-233 (BSE) Resedimented kimberlite. Isolated spinel (Sp) grain within a magmaclast matrix with abundant fine grain phlogopite grains. The spinel is anhedral and fractured.

6.1.3 Spinel Composition:

There are two spinel major compositions, titaniferrous-magnesium aluminum chromites (TIMAC) and qandilite – ulvöspinel-magnetite (QUM), both of which are common to all three spinel habits.

Type [1] spinels are principally TIMAC in composition with high Cr_2O_3 contents (> 40.27 wt. %), TiO_2 (4.19-18.31 wt. %) and variable FeO_T content. (Table 6.1.1; 1 and 2). The chromium content decreases towards the margins of the spinel grains. Most type [1] spinels trend to a lower chromium TIMAC types (Cr_2O_3 18.27-40.77 wt. %), while some spinels trend to a QUM composition (Figure 6.1.7) with low Cr_2O_3 (<2.75 wt. %), high TiO_2 (>15 wt. %) and high FeO_T (>48.82 wt. %).

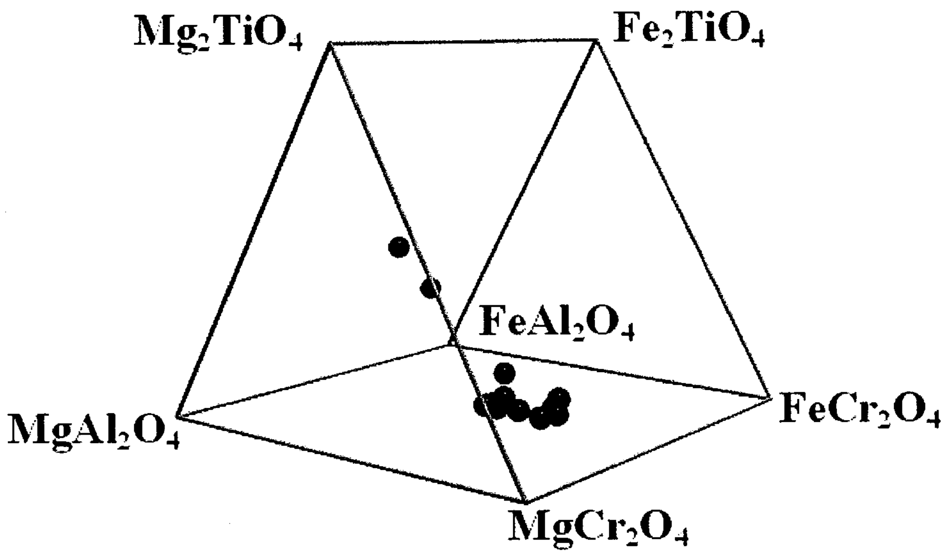

Figure 6.1.7: Representative data for type [1] spinel. The composition of type [1] spinels is dominantly high Cr_2O_3 TIMAC spinels with a trend towards QUM spinels.

Type [2] spinels occur in three compositional varieties, TIMAC to low chromium TIMAC (similar to type [1] spinels); highly zoned from TIMAC to QUM composition; and QUM composition (Table 6.1.1; 3 and 4). Type [2] spinels are dominantly zoned from TIMAC to QUM with similar chromium depletion towards the margin of the spinel grains (Figure 6.1.8).

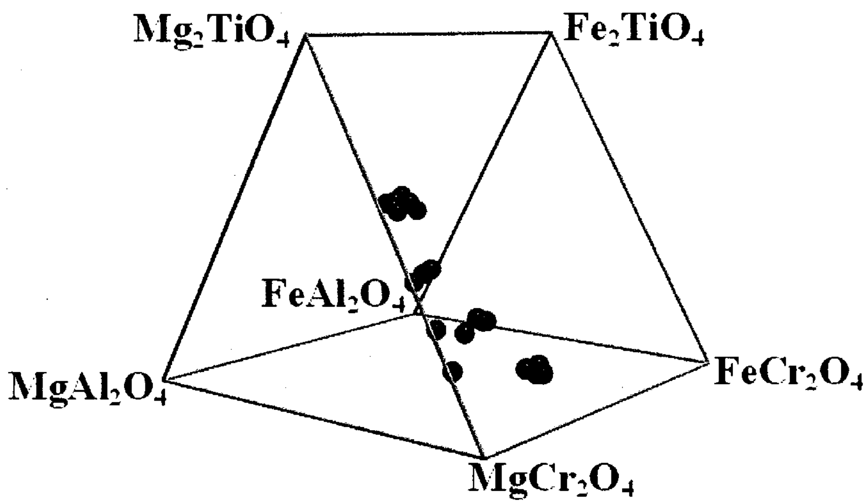

Figure 6.1.8: Representative data for type [2] spinel. The spinel prism shows a trend from TIMAC to QUM spinels.

Atoll structures are present but are rare. The different habits of spinels as shown in Figure 6.1.2 do not show significant composition variation other than the zoning. Atoll compositions are zoned from a TIMAC core to a QUM rim with matrix separating the spinel from the magnetite rim.

Type [3] spinels occur in three compositional varieties; rare TIMAC spinels commonly with low-chromium; zoned TIMAC to QUM; and QUM compositions (Figure 6.1.9).

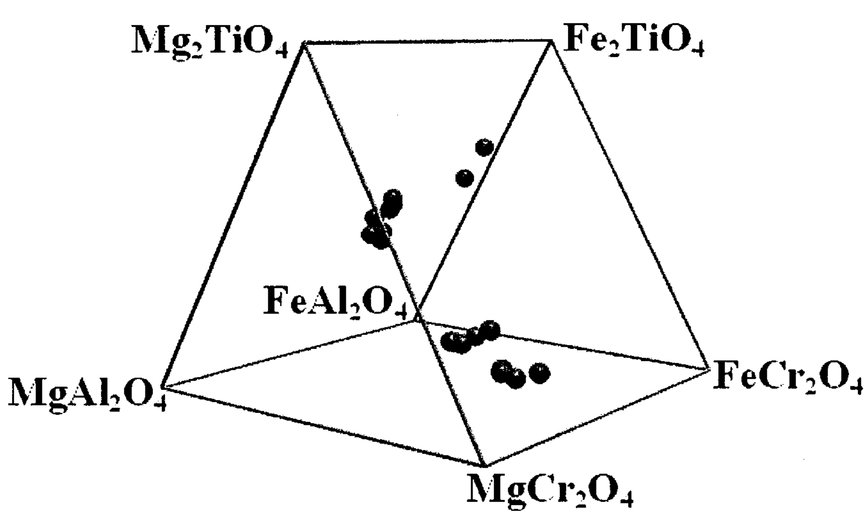

Figure 6.1.9: Representative data for type [3] spinels, high Cr_2O_3 TIMAC spinels, low Cr_2O_3, high FeO_T QUM spinel and very high FeO_T and TiO_2 magnetite spinels.

Type [3] spinels are commonly TIMAC-to-QUM or QUM compositions with thick outer margins around the spinel grains (Table 6.1.1; column 5). Atoll structures are present and are similar to type [2] atoll spinels (Table 6.1.1; column 6).

Aluminous magnesium chromites were observed in sample CL-07-014-233 (pyroclastic kimberlite) in a type [1] spinel within the core of the grain. Magnetite is commonly found as the rim around atoll-structured spinels. The magnetite has high TiO_2 content (<10.63 wt. %), (Table 6.1.1; column 6).

Table 6.1.1: Compositional data for the three types of Candle Lake spinels.

	1	2	3	4	5	6
TiO_2	4.47	5.33	7.58	14.49	15.88	9.59
Al_2O_3	8.11	7.24	10.37	11.37	8.4	4.67
FeO_T	25.11	27.99	36.57	44.99	53.13	76.18
MnO	n.d.	n.d.	.42	0.66	1.19	1.02
MgO	13.6	13.61	14.85	15.92	14.28	7.51
Cr_2O_3	48.65	46.2	30.23	10.7	4.65	1.67
Total	99.45	99.93	98.13	98.36	97.56	96.02
Fe Recalculated						
FeO	16.42	17.15	17.05	21.72	24.39	28.41
Fe_2O_3	8.69	10.84	19.52	25.86	31.94	47.77
Total	99.94	100.37	100.09	100.72	100.73	100.64
Mol %						
Ti	0.06	0.07	0.10	0.18	0.20	0.12
Al	0.08	0.07	0.1	0.11	0.08	0.05
Fe^{2+}	0.23	0.24	0.24	0.30	0.34	0.40
Fe^{3+}	0.05	0.07	0.12	0.16	0.20	0.30
Mn	0	0	0.01	0.01	0.02	0.01
Mg	0.34	0.34	0.37	0.40	0.35	0.19
Cr	0.32	0.3	0.2	0.07	0.03	0.01

1) Sample CL-07-006-214 (RVK) type [1] spinel with a TIMAC composition. 2) Sample CL-07-010-197 (PK) type [1] spinel with a TIMAC composition. 3) Sample CL-06-003-173 (LT) type [2] spinel, moderate chromium TIMAC. 4) Sample CL-06-003-236 (PK) type [2] spinel, low chromium TIMAC. 5) Sample CL-07-010-160 (RVK) type [3] spinel, moderate chromium QUM. 6) Sample CL-07-014-257 (PK) type [3] spinel, magnetite rim around atoll.

6.1.4 Spinel Compositional Variations:

Although type [1] spinels are commonly TIMAC and type [2] and type [3] spinels are commonly zoned TIMAC to QUM in composition, there are intraclast and interclast compositional variations between spinels.

Intra-unit Variation:

There are minor intra-unit compositional variation between spinels due to the difference in zoning and spinel type. However; there are adjacent magmaclasts varying beyond these minor compositional differences.

For example, sample CL-07-010-245 contains type [1] TIMAC spinels but one magmaclast has type [1] spinels with a QUM composition. The Al_2O_3 content (15.89 wt. %) is higher, which is proportional to the lower Cr_2O_3 content (40.06 wt. %) in the same spinel grain. Type [2] and [3] spinels are similar between magmaclasts. Type [1] spinels with QUM composition are also observed in sample CL-07-010-160.

Type [2] and type [3] spinels in adjacent magmaclasts can have different extents of zoning. Where one spinel maybe zoned to chromium poor TIMAC, another magmaclast can contain spinels zoned to a QUM composition. This variation between magmaclasts results in a large range in TiO_2 (3.16-15.84 wt. %) and Cr_2O_3 (13.96-44.24 wt. %) content.

Inter-unit Variation:

Compositional variation of spinels between samples is more evident. Resedimented kimberlite samples have a larger range in TiO_2 and FeO_T content (Appendix C (Ti vs. Fe)). This is due to the greater prevalence of QUM compositional spinels and magnetite atoll rims. Whereas pyroclastic kimberlites tend to have a lesser TiO_2 and FeO_T range due to the absence of magnetite rims. The abundance of type [1] spinels is variable in resedimented kimberlite from sample CL-07-010 because pseudomorphed olivines have been pitted, resulting in the removal of the enclosed serpentine and spinels (Figure 6.1.10).

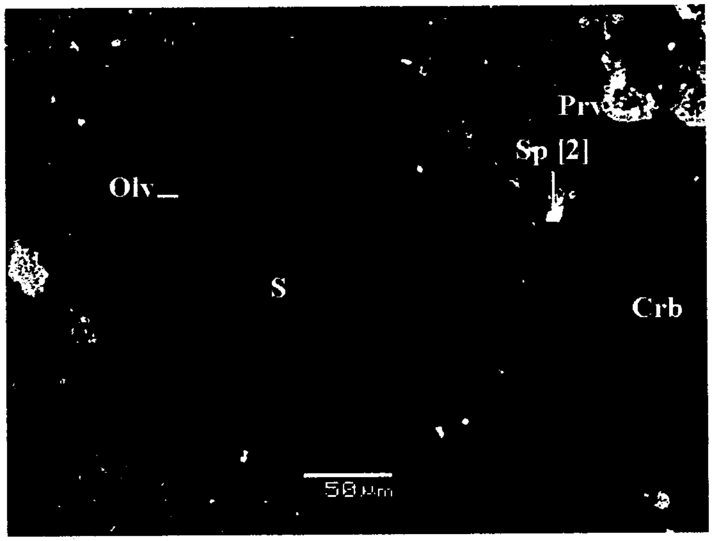

Figure 6.1.10: CL-07-010-169 (BSE), serpentine replacement has been removed by carbonate replacement and botryoidal serpentine.

Sample CL-07-014-260 has spinel types [1], [2] and [3] all having a similar TIMAC composition. This is unlike other samples where type [2] and [3] spinels trend towards a QUM composition. Zoning in this sample is less compared to other samples.

Sample CL-06-003-173 is a lapilli tuff unit containing mainly type [2] spinels because the sample is composed dominantly of magmaclasts which do not have a selvage thick enough to contain type [3] spinels. The reason the lapilli tuff unit lacks type [1] spinels is unknown.

6.1.5 Wesselton Kimberlite:

Candle Lake spinels are compared in Figure. 6.1.14 to spinels from the Wesselton kimberlite (Shee, 1985) a well established "type HK" kimberlite from South Africa. Wesselton spinels are divided into three groups; spinels occurring as inclusions in diamonds, spinels in peridotite and spinels in the groundmass of the kimberlite. Spinels from diamond inclusions and spinels from peridotite plot close to the $MgCr_2O_4$ corner of the spinel prism (Figure 6.1.11). Groundmass spinels have three distinct trends; anhedral chromites with decreasing chromium content and increasing titanium, chromium poor magnetites as rims around pre-existing grains, and magnetites with low chromium and decreasing titanium, due to the formation of perovskite. The overall trend of groundmass spinels is identical to Candle Lake spinels from $MgCr_2O_4$-$FeCr_2O_4$ with increasing iron and titanium (Figures 6.1.11 and 6.1.12). This overlap of data points in Figure 6.1.12 and similar trends in Figure 6.1.14 confirm that Candle Lake kimberlite is comparable to Wesselton trend 1 kimberlite spinel.

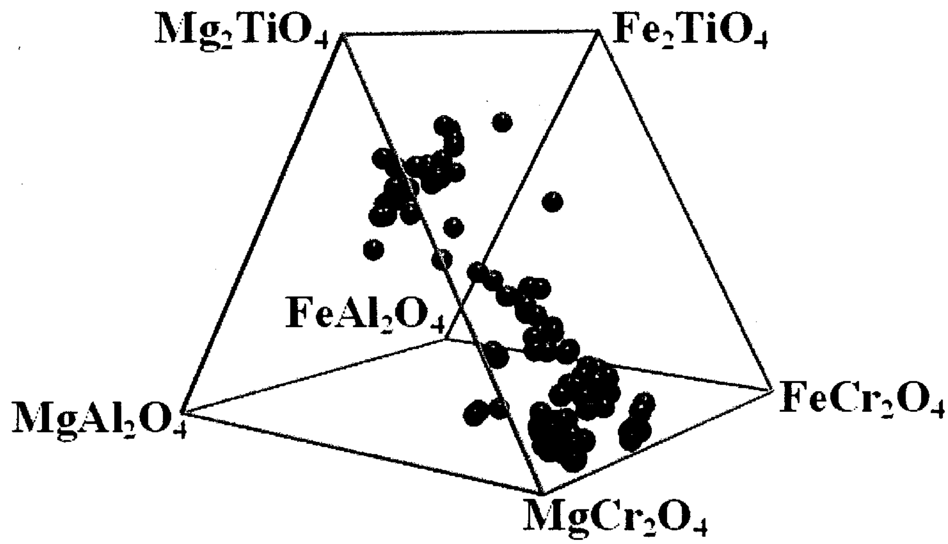

Figure 6.1.11: Spinel prism for Wesselton kimberlite a South African hypabyssal kimberlite. Red data are from diamond inclusions, blue from peridotites and green data are from the kimberlite groundmass.

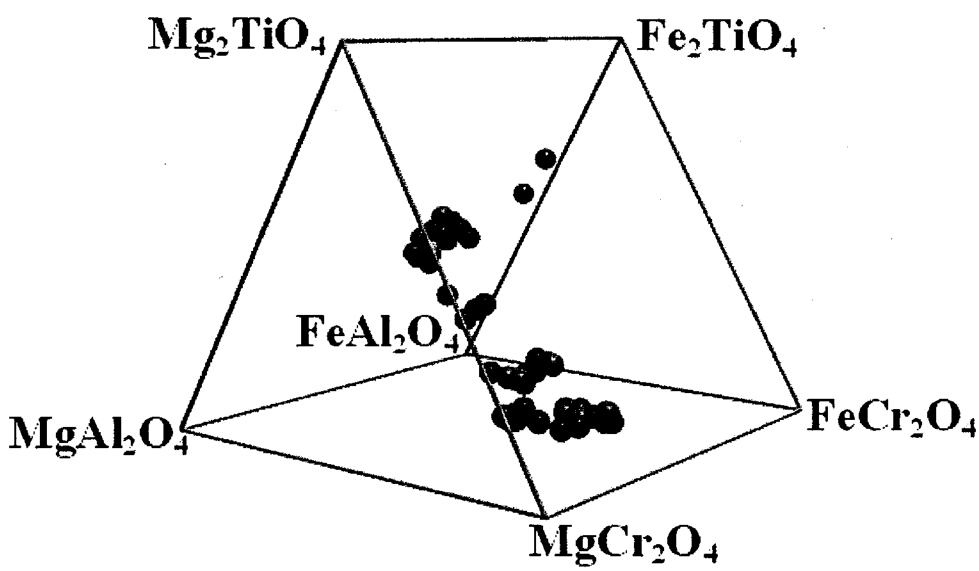

Figure 6.1.12: Spinel prism for Candle Lake kimberlite. Blue points are type [1] spinels, red points are type [2] spinels and green points are type [3] spinels.

6.1.6 Comparison with Other FALC-type Spinels:

Spinels from the Candle Lake kimberlite show an overall trend that type [1] spinels are high chromium TIMAC with a limited trend towards chromium poor TIMAC. Type [2] spinels are cored by a moderate chromium TIMAC and trend towards higher titanium and lower chromium TIMAC or QUM. Type [3] spinels are cored by a low-to-moderate chromium TIMAC and trend to a thick margin of QUM or magnetite in the case of atolls. Combined, all three Candle Lake spinel types plot directly over the HK kimberlite trend T1 field (Mitchell 1995) which indicates that Candle Lake kimberlite can be classified as an archetypal or group 1 kimberlite (as discussed below).

Candle Lake kimberlite spinels also have a lower $Fe^{2+}/(Mg + Fe^{2+})$ ratio relative to the type 2 spinel trend of lamproites and basalts (Mitchell 1995). Candle Lake spinels do not plot within the T2 field and therefore can be confidently ruled out as being a group 2 kimberlites or lamprophyres (Mitchell 1995) (Figure 6.1.14).

6.1.7 Fort à la Corne Kimberlite:

Spinels from ten different kimberlite intrusions investigated by Masun (1999) from the Fort à la Corne consist of three parageneses: rare Cr-rich macrocrysts spinels; TIAMC groundmass spinels; and relatively pure reaction-product magnetite spinels (Masun 1999).

Cr-rich macrocrysts are larger than 0.5 mm in size and are rounded with a reddish-brown-to-orange colour. They are low in TiO_2 (<2 wt. %) but have high chromium contents (Masun 1999).

TIAMC groundmass spinels have a composition trend from TIAMC-to-QUM. The spinels contain less than 5 wt. % TiO2 and increase to > 10 wt. % when compositionally zoned from TIAMC-to-QUM, respectively. FeO_T and Al_2O_3 increases with decreasing Cr_2O_3 (Masun 1999).

Reaction product spinels are small (<5 μm, in size), euhedral crystals that mantle serpentinized olivines. These spinels have almost a pure magnetite composition (Masun 1999).

A spinel plot of the FALC spinels (Figure 6.1.13) shows an identical trend to spinels from Candle Lake. Except that pure magnetite reactionary spinels are not present at Candle Lake. Magnetite that is present in Candle Lake has a significant titanium content as magnetite occurs as rimming around atoll structures.

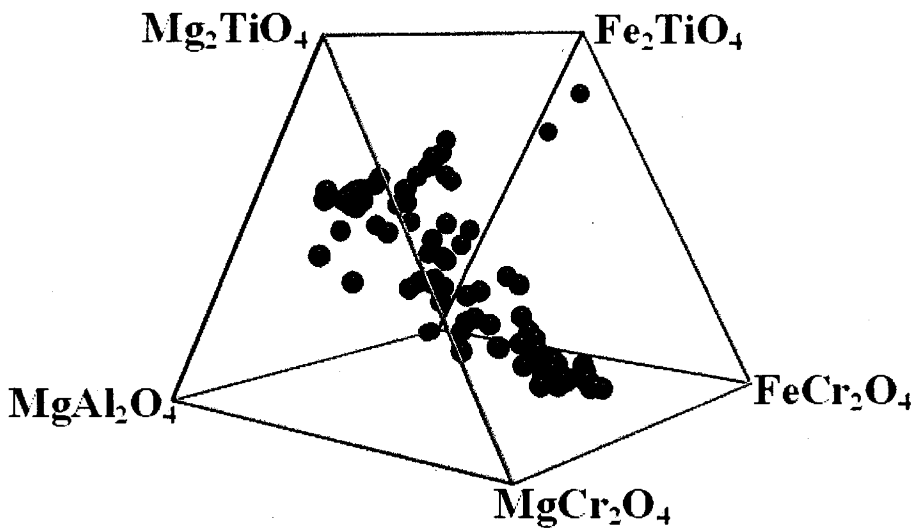

Figure 6.1.13: Spinel prism Fort à la Corne spinel analyses (after Masun 1999).

6.1.8 Smeaton:

The Smeaton 169 kimberlite is from the Fort à la Corne region and is petrographically similar to Candle Lake (Leckie et al. 1997), containing amoeboid magmaclasts with protruding rounded macrocrysts and subhedral-to-euhedral phenocrysts enclosed in a carbonate or serpentine interclast matrix (Leckie et al. 1997 and Mitchell et al. 2009) (Figure 6.1.15). Smeaton spinels have a lower $Fe^{2+}/(Mg + Fe^{2+})$ ratios compared to Candle Lake kimberlite spinels (Figure 6.1.14). These data show similar style kimberlites can have different spinel trends. The reason why the Smeaton 169 spinel have a lower $Fe^{2+}/(Mg + Fe^{2+})$ is unknown.

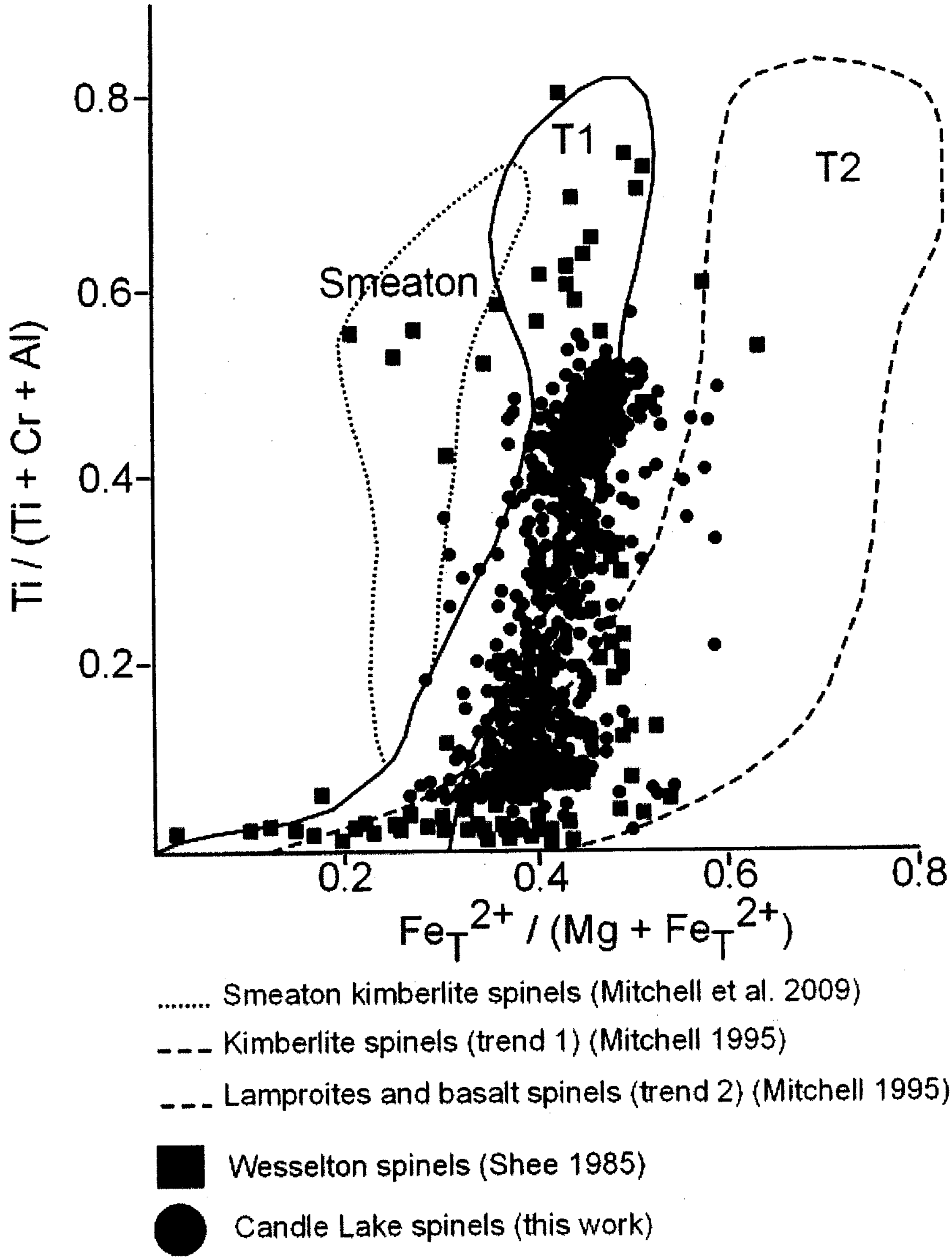

Figure 6.1.14: Compositional trend of Smeaton 169 kimberlite spinels (Mitchell et al, Smith 2009b), Trend T1 and Trend T2 kimberlites (Mitchell 1995). Candle Lake spinel (this work) data and Wesselton kimberlite spinel data (Shee 1985). have a strong correlation and overlay the Trend T1 field.

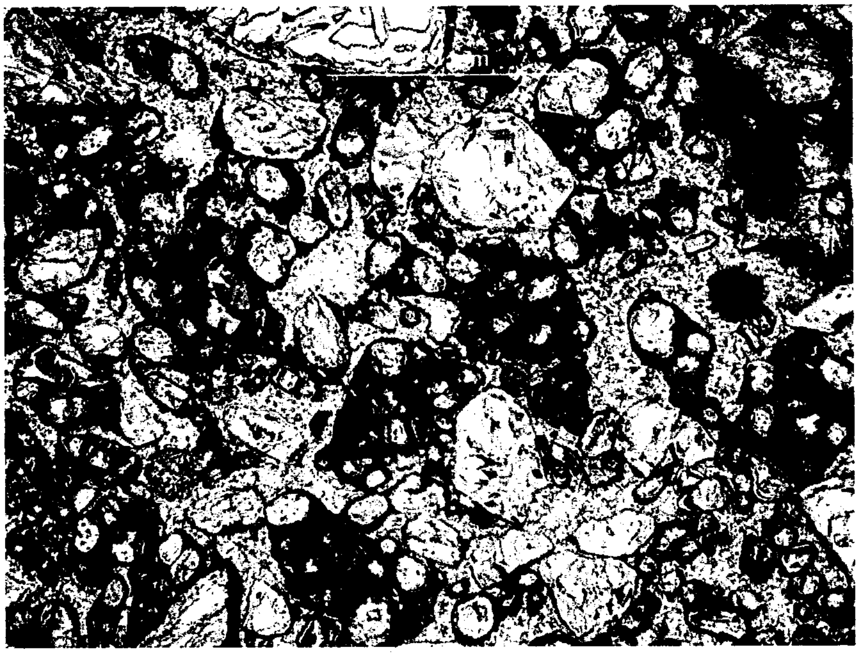

Figure 6.1.15 Smeaton 169 (PPL) amoeboid magmaclasts with rounded-to-subhedral pseudomorphed olivine phenocrysts and macrocrysts set in a carbonate interclast matrix. Pyroclast are identical to those in Candle Lake (see Figure 5.2.1)

6.1.9 Peuyuk Kimberlites:

The Peuyuk C kimberlite, Somerset Island, Nunavut (Mitchell and Clarke 1976) has recently been reclassified as a pyroclastic kimberlite (Mitchell et al. 2009b) Figure 6.1.15 shows a typical vesicular magmaclast in Peuyuk C; magmaclast with pseudomorphed olivine phenocrysts and macrocrysts set in a carbonate interclast matrix which is almost identical to Candle Lake pyroclastic kimberlite units (Figure 6.1.16).

Figure 6.1.16: A vesicular magmaclast from Peuyuk C kimberlite (PPL).

Peuyuk spinels (Mitchell and Clarke 1976) are; a) euhedral, opaque, 10 to 20 μm in size TIMAC in composition with no reaction rims or mantles, and form the cores of the other two parageneses of spinels, b) the spinels are 20 to 50 μm in size, complexly zoned from TIMAC-to-QUM with an atoll structure that is composed of magnetite, c) discrete grains with a TIMAC-to-QUM or QUM composition with increasing titanium from core-to-rim. When plotted on a spinel prism they show a trend from $MgCr_2O_4$-$FeCr_2O_4$ with increasing iron and titanium to Mg_2TiO_4-Fe_2TiO_4 following kimberlite trend 1 (Figure 6.1.17).

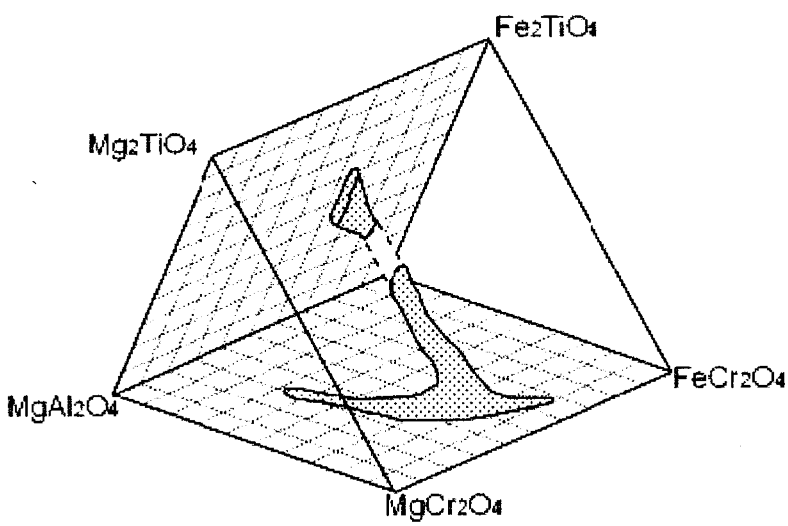

Figure 6.1.17: Spinel prism for Peuyuk kimberlite showing a trend from high chromium to increasing iron and titanium (Mitchell and Clarke 1976).

6.1.10 Diavik Kimberlite:

Candle Lake kimberlite has several similarities with the Diavik kimberlite from the Lac de Gras kimberlite field (Masun 1999). Diavik kimberlites are hypabyssal and resedimented kimberlites with three parageneses of spinels, including spinels that nucleate along pre-existing crystals, similar to type [2] spinels from Candle Lake. The three parageneses of spinels include: macrocrysts that are rounded, opaque with a magnesium-aluminous chromite composition: primary groundmass spinels that are subhedral-to-euhedral with a TIMAC-TMC-QUM composition; and atoll spinels rimmed by magnetite. Spinels with a TIMAC-to-TMC-to-QUM composition have a similar trend as Candle Lake spinels. However; there is a significant trend from the base of the prism at the $MgCr_2O_4$-$FeCr_2O_4$ towards the $MgAl_2O_4$-$FeAl_2O_4$ join (Figure 6.1.18). This trend is associated with aluminum rich groundmass spinels which are not present in Candle Lake kimberlite. The similar habit of type [2] spinels seen in both the Diavik kimberlite and Candle Lake along with a similar trend 1 composition from TIMAC-to-QUM suggest a group 1 kimberlite.

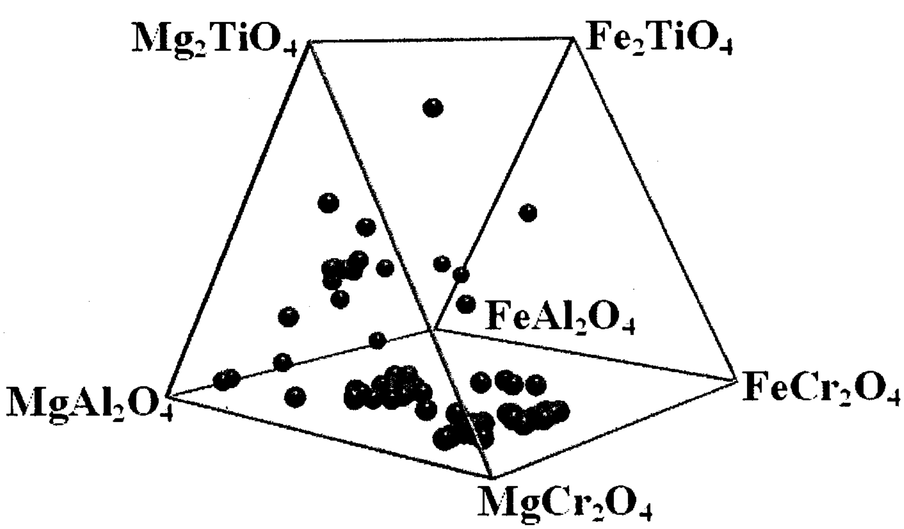

Figure 6.1.18: Spinel prism of Diavik spinels showing a pleonaste trend from $MgAl_2O_4$ to $MgCr_2O_4$-$FeCr_2O_4$ along the bottom of the prism and a Trend 1 kimberlite trend from TIMAC-to-QUM composition (from Masun, 1999).

6.2 Serpentine:

Serpentine has been analyzed in three different samples from three different drill cores. The samples were selected to represent each of the three kimberlite units; lapilli tuff, pyroclastic kimberlite and resedimented kimberlite. Serpentine occurs as a replacement mineral within; phenocrysts, macrocrysts, monticellite, groundmass and vesicle infilling.

6.2.1 Serpentine in Lapilli Tuff:

Sample CL-06-003-173 is a lapilli tuff unit with serpentine occurring in; macrocrysts, monticellite and the groundmass.

The macrocrysts have one to three phases of botryoidal-textured serpentine. The serpentine is zoned from a lower back scatter electron (BSE)-contrast to a higher BSE-contrast, reflecting an increase in iron content. The botryoidal serpentine occurs with an irregular vermiform texture. The macrocrysts are rimmed by botryoidal serpentine that is 3 to 10 μm in thickness, and can have cores of carbonates which overprint the serpentine alteration (Figure 6.2.1). Other minor phases present in the serpentine are magnetite and Fe-Ni sulphides; both are fine grained and <2 μm in size.

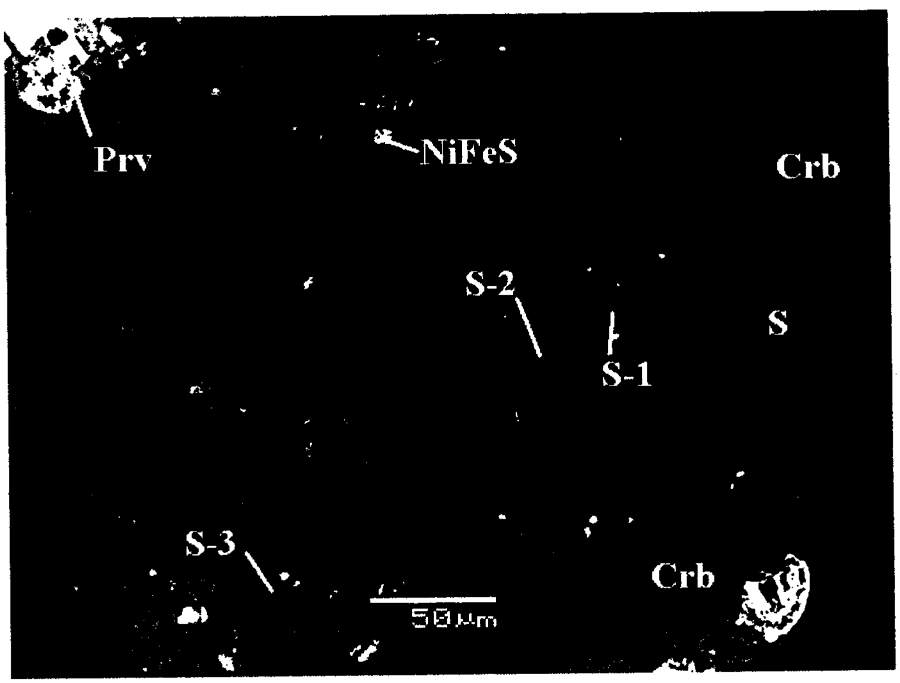

Figure 6.2.1: CL-06-003-173 (BSE), macrocryst with three phases of serpentine (S) replacement and carbonate (Crb) cores. Minor nickel-iron sulphide (NiFeS) phases occur in the low iron serpentine.

Pseudomorphed monticellite grains are 2 to 20 μm in size and are subrounded-to-irregular. They are replaced by a single phase of serpentine and rimmed by a 1 μm zone of carbonate (Figure 6.2.2). The serpentine in monticellite is similar to that of the serpentine in the macrocrysts. The matrix of the magmaclasts is a serpentine-carbonate mixture but due to the small grain size and intimate intergrowth, quantitative analysis was impossible.

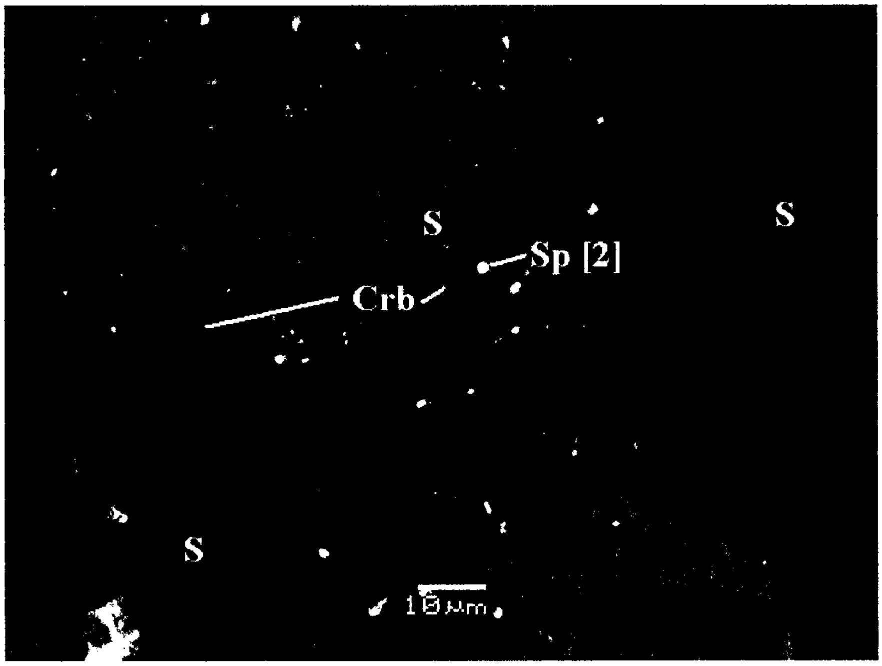

Figure 6.2.2: CL-06-003-173 (BSE), pyrocryst selvage with fine grained irregular monticellite replaced by serpentine (S) and carbonate (Crb) rims.

The mesostasis is a homogenous serpentine with interstitial carbonate (see carbonate section). The serpentine forms an intimate intergrowth of granular crystals with minor thin fractures, and has a composition similar to both macrocryst and pseudomorphed monticellite serpentine (Figure 6.2.3). In the bottom left of fig. 6.2.3 there is a macrocryst of pseudomorphed olivine enclosed by a thin selvage of pseudomorphed monticellite and serpentine-carbonate matrix. The selvage separates the macrocryst from the surrounding granular inter-grown serpentine (Figure 6.2.3).

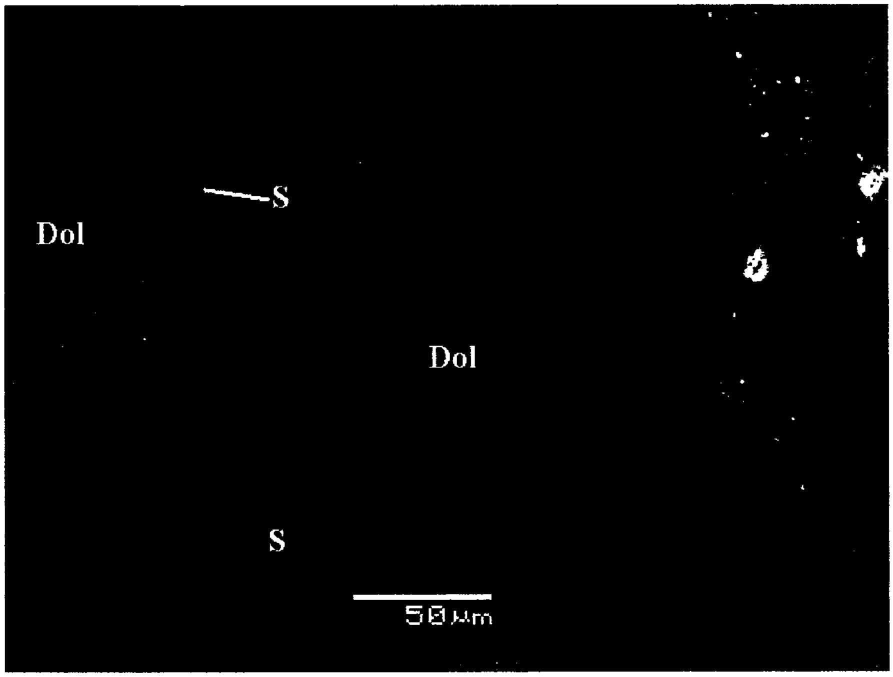

Figure 6.2.3: CL-06-003-173 (BSE), segregation texture of dolomite (Dol) from serpentine (S) in the interclast kimberlite groundmass. A thin selvage of pseudomorphed monticellite surrounds a macrocryst.

Serpentine in Pyroclastic Kimberlite:

Sample CL-06-003-182 represents a pyroclastic kimberlite with serpentine replacement of macrocrysts, phenocrysts and monticellite.

The macrocrysts are coarse-grained with two to three phases of serpentine alteration that are irregular and pervasive throughout the entire grain. The dominant phase is one or a combination of two zones of higher BSE contrast which represent serpentines of low-to-high iron content. A second serpentine phase occurs as thin bands, 2 to 20 µm, that cross-cut the macrocrysts and has a higher BSE contrast due to elevated iron content (Figure 6.2.4). The final phase of serpentine which rims the macrocrysts is botryoidal with elevated iron content and is similar to the cross-cutting serpentine phase. There are minor Fe-Ni sulphides associated with low iron serpentine.

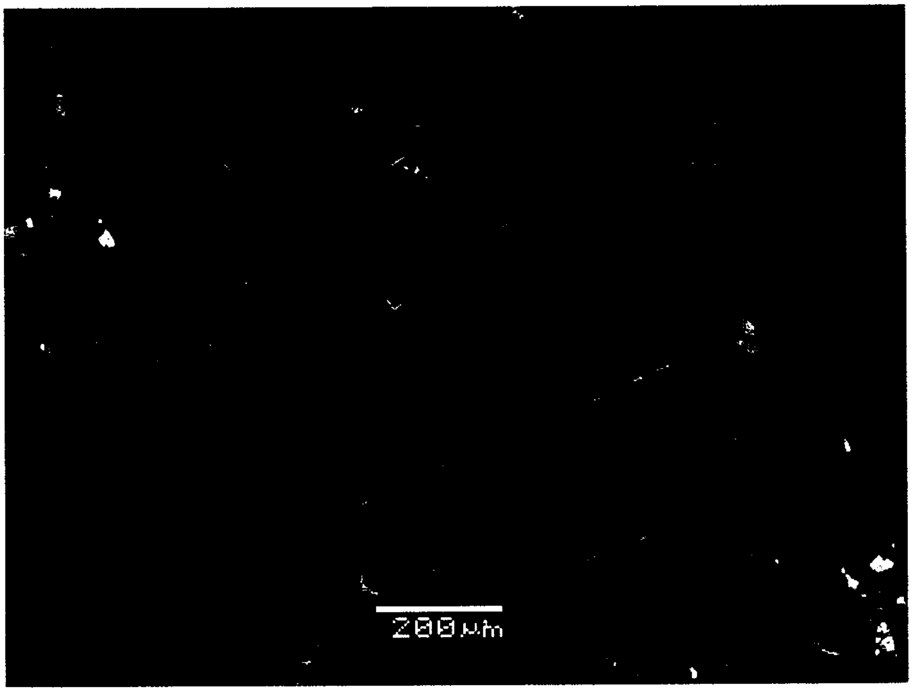

Figure 6.2.4: CL-06-003-182 (BSE), macrocryst with a pervasive serpentine phase (S-1) and a cross-cutting serpentine phase (S-2), with minor Fe-Ni sulphides. Macrocryst is surrounded by a calcite (Cal) interclast groundmass.

Phenocrysts are replaced by serpentine with a zoned alteration pattern. If the grain is orientated to show the euhedral habit, the zoning then parallels the crystal habit. The zones consist of two to three phases of serpentine reflected by a BSE contrast from low-to-high with increasing iron content. The lower BSE contrast cores are 5 to 20 µm wide and the higher BSE contrast phases are 2 to10 µm wide (Figure 6.2.5). Compositionally the phases become increasingly enriched in iron. Phenocrysts can exhibit up to four sequences of alteration (Figure 6.2.5). Commonly the second or third sequence is iron-enriched and is poorly-defined along the outer edge and is incorporated into the next sequence (sequence 3 in Figure 6.2.5). The entire phenocryst is enclosed by a rim of botryoidal serpentine. There are minor Fe-Ni sulphides associated with the low iron serpentines.

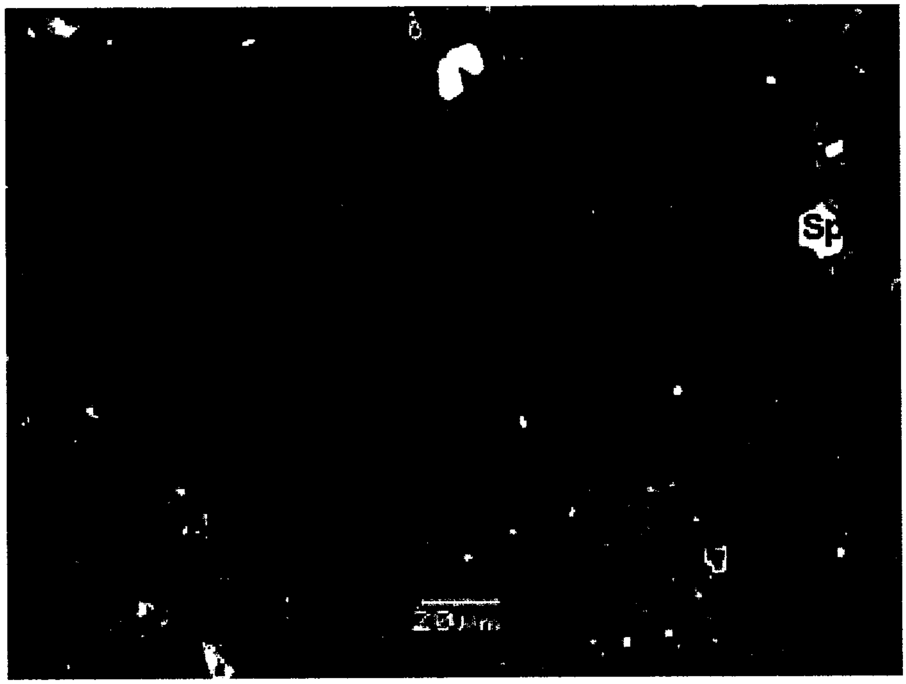

Figure 6.2.5: CL-06-003-182 (BSE), phenocryst with four sequences each consisting of two serpentines phases, going from a lower BSE contrast to higher BSE contrast (lower-to-higher iron content). The grain is enclosed by a thin botryoidal serpentine (S) with a euhedral type [2] spinel (Sp)

Pseudomorphed monticellite grains are 5 to 20 µm in size, and are subrounded-to-irregular with a two types of serpentine. The cores of the grains have a higher BSE contrast due to elevated iron and aluminum. There is a lower BSE contrast around the rim of the grain that has lower iron and aluminum. This dark rim is similar in composition to that of the low iron serpentines found in phenocrysts (Figure 6.2.6). The interstitial matrix of the magmaclast is a mixture of serpentine and carbonate but, due to the small grain size, quantitative analysis was impossible.

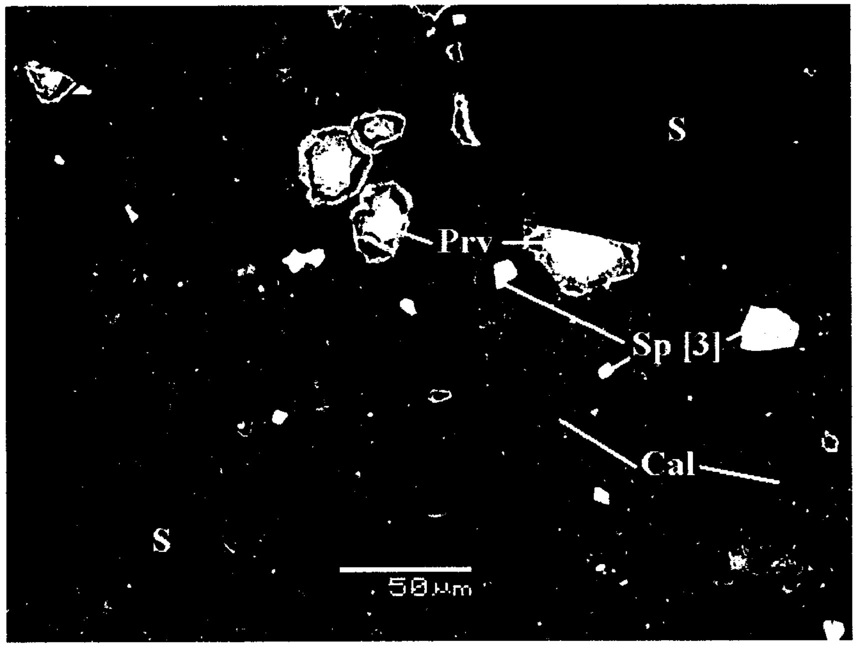

Figure 6.2.6: CL-06-003-182 (BSE), magmaclast matrix with monticellite infilled by calcite (Cal) and serpentine. Other minerals include rimmed perovskite (Prv) and type [3] spinels (Sp).

Resedimented Kimberlite Serpentine:

Sample CL-07-010-169 represents a resedimented kimberlite unit with serpentine occurring in macrocrysts, phenocrysts, monticellite and groundmass.

The macrocrysts and phenocrysts have similar textures and compositions. The serpentine occurs as two or three phases and is botryoidal, with an irregular thin vermiform texture (Figure 6.2.7). The inner phase of serpentine has a higher BSE contrast due to a slight increase in iron content relative to the outer rim. A portion of the macrocrysts or phenocrysts is commonly a single serpentine phase, with a low BSE contrast occurring as an intimate intergrowth of granular crystals (Figure 6.2.7). Compositionally, this single intimately intergrown serpentine is similar to the low BSE contrast of the thin irregular vermiform textured serpentine. There is a thin rim of botryoidal serpentine around the entire grain, which is slightly enriched in iron.

Figure 6.2.7: CL-07-010-169 (BSE), (RVK), resedimented macrocryst, showing an intimate intergrowth of granular serpentine (S), and a two phase botryoidal, vermiform-textured serpentine (S-1 and S-2).

Pseudomorphed monticellite is 2 to 20µm in size and is subrounded-to-irregular. The core is replaced by an iron-rich serpentine and rimmed by an iron-poor serpentine that is 1 to 2 µm thick (Figure 6.2.8). Carbonate is also commonly found within the core of the monticellite. The interstitial matrix of the magmaclast is a serpentine-carbonate mixture but due to the small grain size quantitative analysis is not possible.

Figure 6.2.8: CL-07-010-169 (BSE), (RVK), matrix of magmaclast with monticellite replaced by two serpentine phases, S-1 (iron rich) and S-2 (iron poor). The matrix of the groundmass is a cryptocrystalline serpentine and carbonate mixture (S + Crb).

Vesicles are infilled by a single phase of serpentine which is identical to serpentine found in the groundmass.

The interstitial kimberlite matrix is a mixture of serpentine and carbonate, too fine grained to analyze. However; there are serpentine segregations that are composed of a single phase of serpentine. There segregations are enclosed by botryoidal serpentine (Figure 6.2.9).

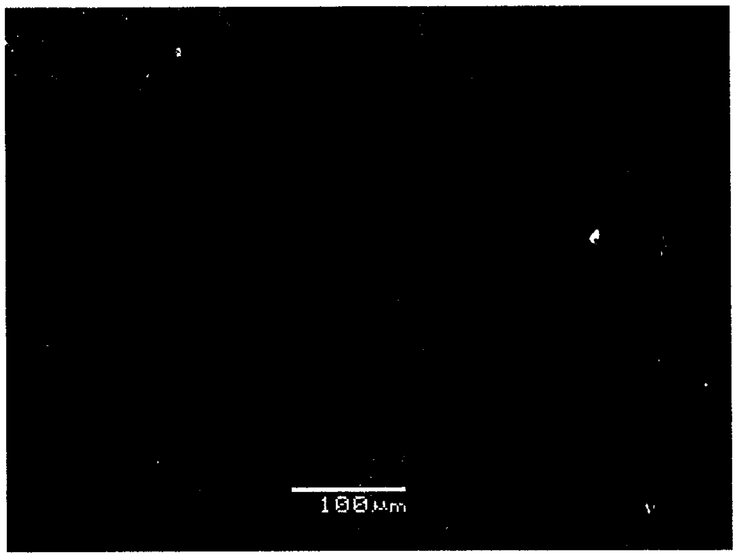

Figure 6.2.9: CL-07-010-169 (BSE), interclast kimberlite groundmass, a segregated serpentine (S) phase with botryoidal serpentine enclosing the segregation.

6.2.2 Composition:

Iron content varies within the serpentine of the magmaclasts, as expected due to the multiple sequences of zoning described above. What is not expected is the variation of iron content between the different types of kimberlite. In resedimented kimberlite units the iron content of serpentine is low FeO_T , (1.62-8.07 wt. %), where as in the lapilli tuff unit there is a more moderate iron content and range FeO_T, (6.51-8.66 wt. %). The serpentine in the pyroclastic kimberlite units has the highest iron content and range FeO_T, (5.27-19 wt. %). The large range in pyroclastic kimberlite reflects the botryoidal serpentine rimming macrocrysts and phenocrysts.

Aluminum content varies more significantly between clasts within a magmaclast than between samples. The aluminum content of serpentine within macrocrysts and phenocrysts, regardless of the type of kimberlite, is low Al_2O_3 (n.d.-0.62 wt. %). The

Al_2O_3 content of the groundmass and the pseudomorphic monticellite is higher (0.42-5.3 wt. %) and all three types of kimberlite exhibit this range in aluminum content. Botryoidal rims between clasts have similar aluminum content, Al_2O_3 (0.54-2.83 wt. %).

Magnesium contents show very little variation between individual clasts or between samples. Resedimented kimberlite units have a slightly larger magnesium range, MgO (28.59-41.56 wt. %) than pyroclastic kimberlite units MgO (25.64-37.76 wt. %). There is no significant variation between grains or samples with respect to sodium or manganese.

Composition:

Schiffman and Fridleiffson (1991) noted that when recalculating phyllosilicate data, chlorite end-members have a total of 20 non-interlayered (Si + Al + Fe + Mg + Mn) cations, whereas the smectite end-members would have 17.82 non-interlayered cations. Several paragenetic fields depicted on Figure 6.2.8 are smectite-to-chlorite, after olivine, after monticellite and vesicle fields. The smectite-to-chlorite trend is from the Wesselton tuffistic kimberlite (Mitchell et al. 2009b).

Candle Lake serpentine data for five parageneses are shown on a cation (Si + Al + Fe + Mg + Mn) versus Fe^{2+}_{Total} plot (Mitchell et al. 2009b) (Figure 6.2.10) together with serpentine data from Mitchell (1986) for comparison. The Candle Lake serpentine data plots between Fe^{2+}_{Total} (0.5-2) and (Si + Al + Fe + Mg +Mn) (19.1-20), and show, as these data plot well above the smectite-to-chlorite field, that most of the phyllosilicates analyzed are in fact serpentine.

However; Candle Lake data does plot below the Smeaton 169 field, which may be caused by minor chlorite interlayering in the serpentine which would reduce the (Si + Al + Fe + Mg + Mn) cation content.

The Candle Lake serpentine data has a large range across the three fields. Vesicle infilling and pseudomorphed olivine serpentine from Candle Lake does have a moderate overlap with the Smeaton 169 after olivine and vesicle fields. However; pseudomorphed monticellite data from Candle Lake does not correlate to the Smeaton 169 after monticellite field, which would suggest a difference in replacement history for the two monticellites.

Serpentine data from Mitchell (1986) are plotted on Figure 6.2.10, to compare other kimberlite serpentine with Candle Lake serpentine. The serpentine from Mitchell (1986) have a larger iron range, Fe_T (0.4-2.4) but the data groups more effectively in the after olivine and vesicle fields. There is a significant enough overlap between Mitchell's (1986) data and the Candle Lake kimberlite data to suggest that the phyllosilicates analyzed in the Candle Lake kimberlite are indeed replacement serpentines after olivine and monticellite.

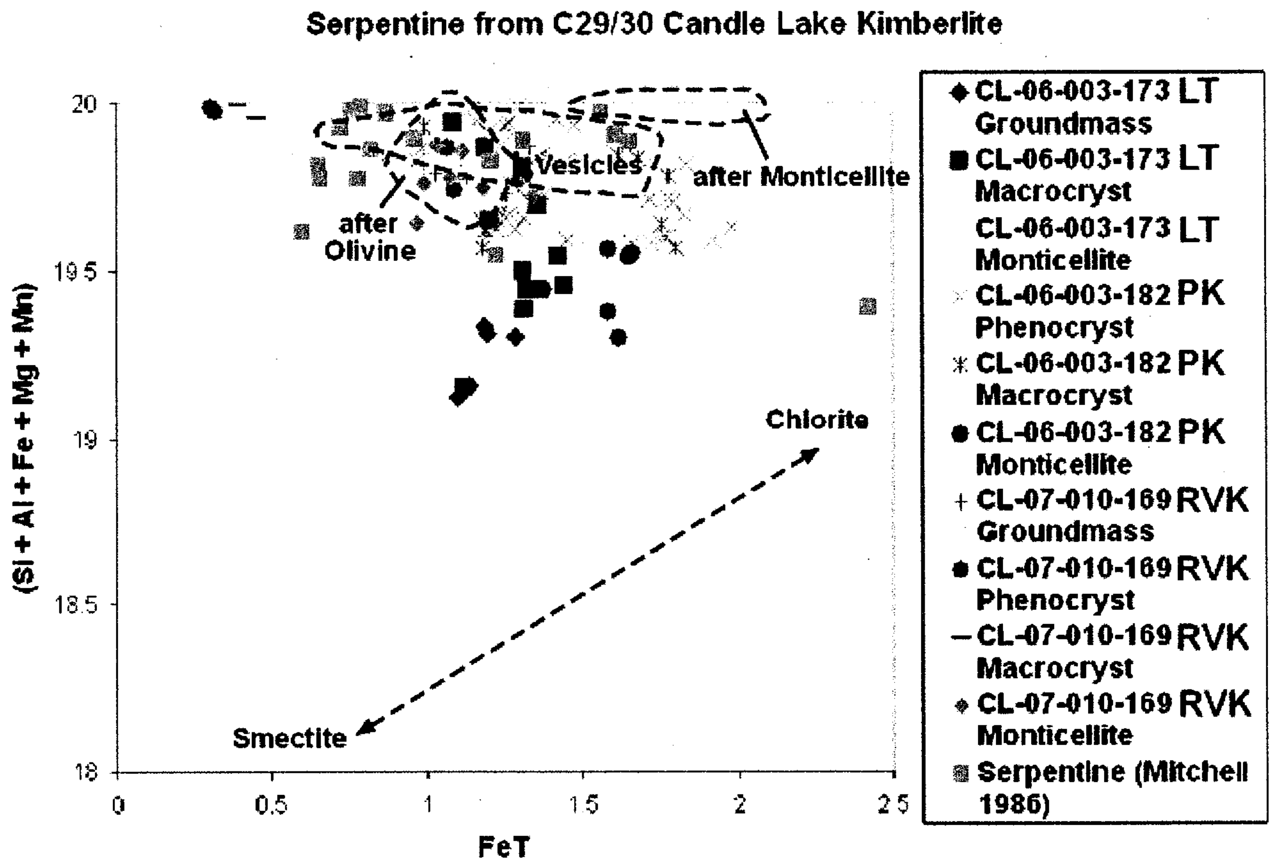

Figure 6.2.10: The diagram shows fields for serpentine after monticellite, olivine and infilling of vesicles (after Mitchell et al., 2009a). The serpentine from the Candle Lake kimberlite plots within the after olivine field, the vesicle field established for Smeaton PK and Wesselton TK.

6.3 Phlogopite:

Cumulates consisting of phlogopite and spinel were found in four samples from three different drill cores occurring in both resedimented kimberlite and pyroclastic kimberlite. The cumulates have been divided into two types on the basis of their texture and minor compositional differences.

Texture:

"Type 1" cumulates are 500 μm -10 mm in size and are rounded-to-sub-rounded. The sub-rounded grains exhibit fractured grain boundaries as a result of resorption. Internal fracturing is common in both rounded and sub-rounded cumulates.

Inequigranular phlogopite is the dominant component, varying from 20 to 150 μm in size. The grains are randomly-orientated and anhedral, commonly appearing fractured or resorbed (Figure 6.3.1). There are minor inclusions of iron nickel sulphide within the phlogopite grains. These inclusions are <2 μm and are irregular in habit.

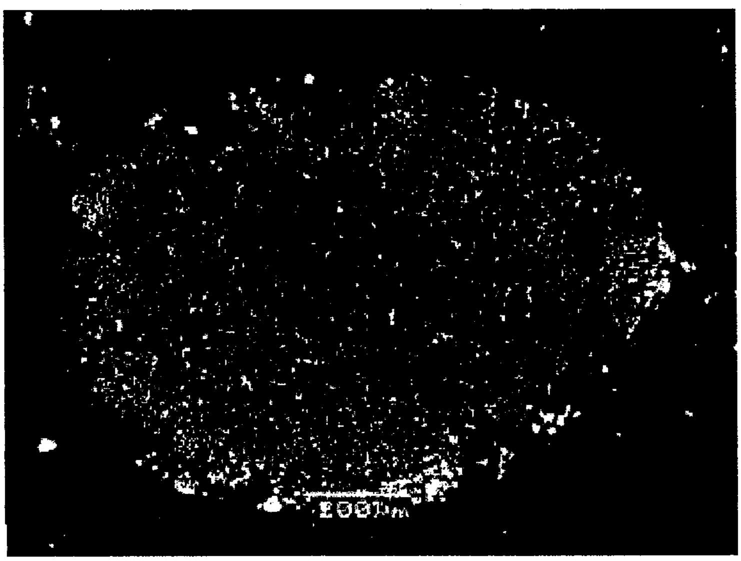

Figure 6.3.1: CL-07-014-257 (BSE), rounded "type 1" cumulate with fine-to-coarse grained size distribution of spinels (Sp) from the core to the rim of the phlogopite (Ph) cumulate. The cumulate is set in a serpentine (S) rich interclast matrix.

Spinels are interstitial to the phlogopite and are <1 μ to 3 μm in size, with a subhedral-to-anhedral habit. Spinel grains that occur at the core of the cumulate are commonly finer grained than those occurring at the rim of the cumulate. However; this grain size distribution is not evident in sample CL-06-003-222. Spinels in sample CL-06-003-222 are not interstitial to the phlogopite but are enclosed within, the phlogopite, similar to spinels in macrocrysts (Figure 6.3.2).

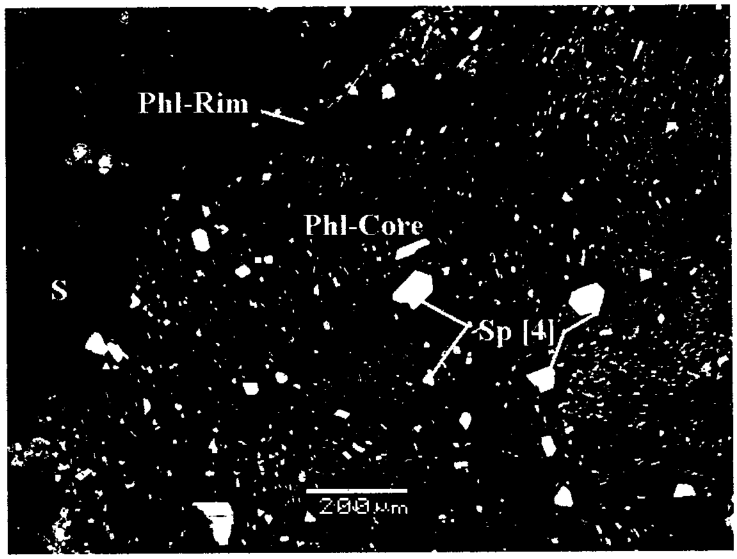

Figure 6.3.2: CL-06-003-222 (BSE), "type 1" cumulate with coarse spinels (Sp) that are not zoned. The phlogopite (Ph) is zoned with a greater Mg and Si content at the core and Al, Ti and Fe enrichment at the rim. The cumulate is set in a serpentine (S) rich interclast matrix.

"Type 2" cumulates are 1000-1500 µm in size and are rounded-to-irregular in shape with smooth edges and a well-defined contact with the interclast matrix (Figure 6.3.3).

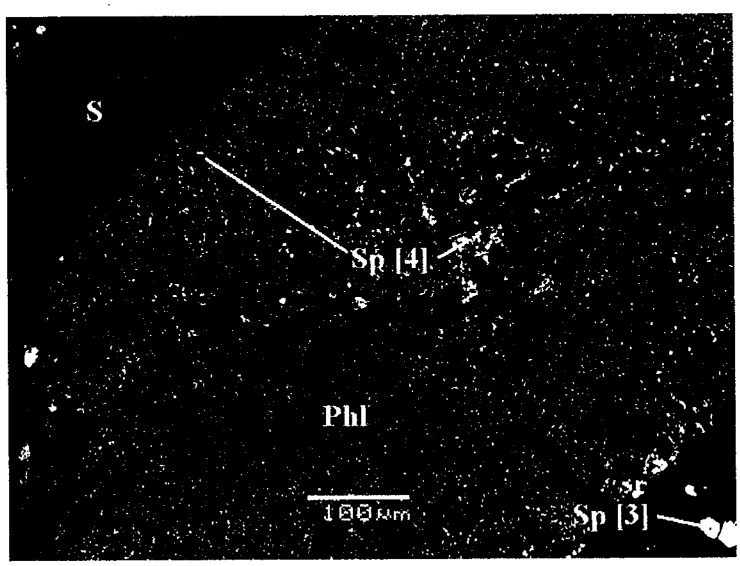

Figure 6.3.3: CL-07-014-245 (BSE), "type 2" cumulate with very fine grained phlogopite (Ph) and spinels (Sp) set in a serpentine (S) rich interclast matrix.

Phlogopite grains are the main component of the cumulate and are equigranular, 5 to 50 µm in size. The phlogopite forms randomly-orientated grains and is commonly broken or resorbed. There are trace amounts of iron nickel sulphide within the phlogopite grains.

The spinels occur interstitial to the phlogopite, <1 to 2 μm in size and are too small to analyze (Figure 6.3.4). The spinel grains are anhedral-to-subhedral and show a limited grain size distribution from very fine-grained at the core of the cumulate to fine grained at the rim.

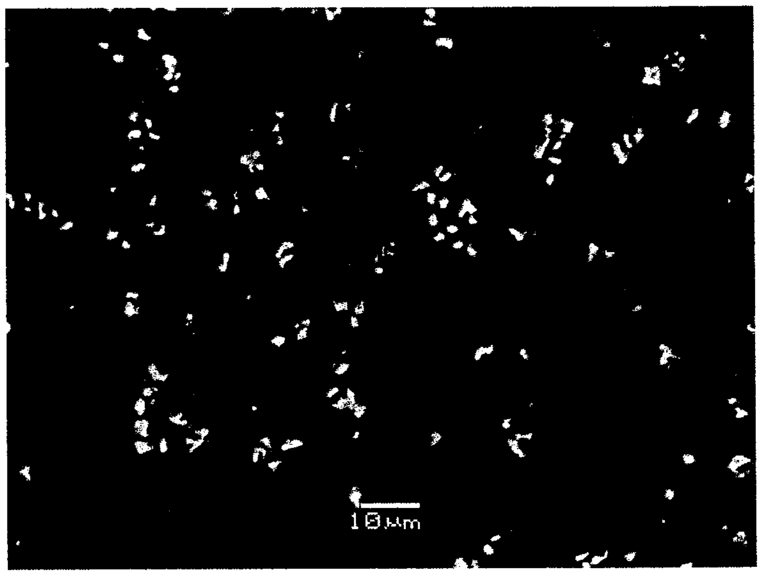

Figure 6.3.4: CL-07-006-208 (BSE), "type 2" cumulate. Phlogopite (Ph) cumulate with very fine grained interstitial spinels (Sp).

Composition:

Micas from type 1 and type 2 cumulates have a very similar composition except for chromium which is lower in type 1 cumulate micas (Cr_2O_3 = n.d.-2.74 wt. %) than in type 2 cumulate micas (Cr_2O_3 = 1.02-3.36 wt. %; Table 6.3.1)

Phlogopite in type 2 cumulates is not zoned, although phlogopite in type 1 cumulates is zoned. Phlogopite grains at the core of type 1 cumulate are poor in titanium whereas the grains along the margins of the cumulate are higher in titanium content. TiO_2 content of the phlogopite at the core of the cumulate has a range of TiO_2 (n.d.-0.65 wt. %) whereas the phlogopite at the margin of the cumulate has a TiO_2 range of (0.95-5.22 wt. %).

Macrocrysts of phlogopite have a relatively consistent composition throughout samples, although the barium content varies, Ba (n.d.-2.19 wt. of BaO). Exceptions include sample 07-014-245, which has a higher iron composition consistent with biotite (Table 6.3.1; 4)

Table 6.3.1 Representative compositional data for Candle Lake micas.

Oxide Wt. %	CL-07-014-245 Biotite (1)	CL-07-014-257 Macrocryst (2)	CL-07-014-257 Type 1 Core (3)	CL-07-014-257 Type 1 Rim (4)	CL-07-014-245 Type 2 (5)
SiO_2	35.21	35.72	35.36	38.68	35.63
Al_2O_3	16.39	17.15	17.73	13.9	16.51
TiO_2	3.51	4.16	n.d.	4.08	1.34
FeO_T	22.25	4.82	6.71	5.59	7.91
MnO	n.d.	n.d.	n.d.	n.d.	n.d.
MgO	9.19	22.93	25.77	22.87	26.57
Na_2O	0.37	n.d.	n.d.	n.d.	n.d.
K_2O	9.96	9.33	8.65	9	7.35
BaO	n.d.	1.87	n.d.	n.d.	n.d.
Cr_2O_3	n.d.	0.53	2.03	2.15	1.37
H_2O*	4.02	4.18	4.19	4.22	4.22
Total	100.9	100.63	100.44	100.49	100.9

Composition examples for (1) biotite, (2) unknown mica, (3) type 1 cumulate – core, (4) type 1 cumulate – rim, (5) Type 2 cumulate.

The differences in composition between macrocryst phlogopite and cumulate phlogopite are minor, barium is higher in macrocryst phlogopite. The composition of a macrocryst phlogopite is similar to marginal phlogopite from type 1 cumulate.

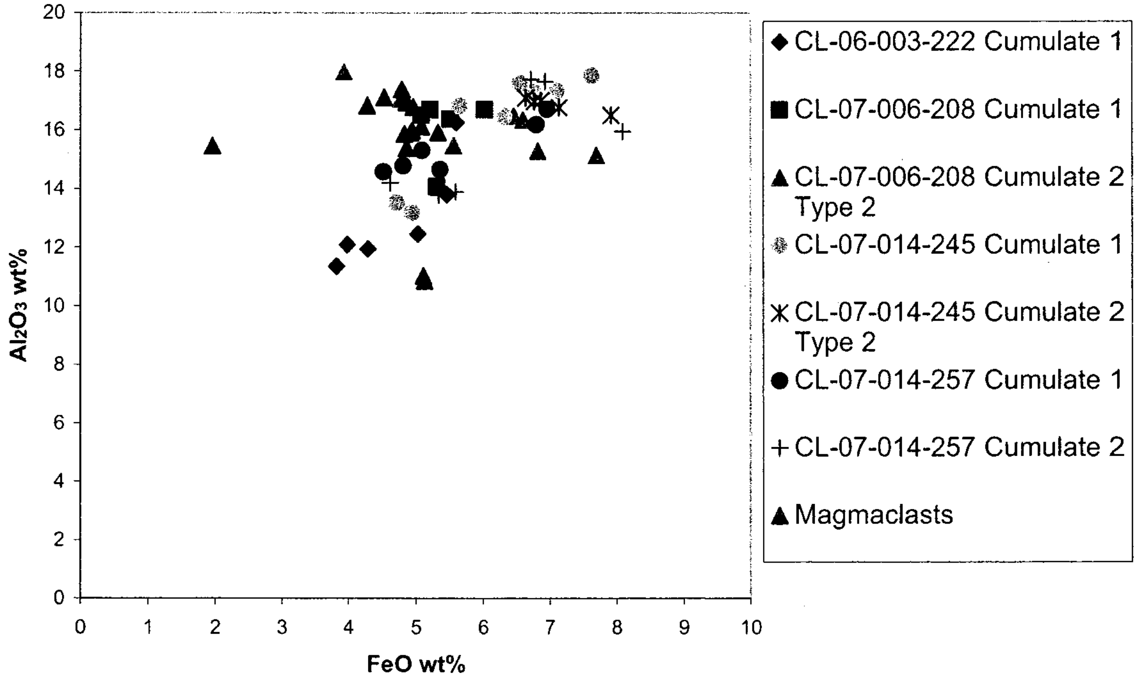

Figure 6.3.5: Al_2O_3 vs. FeO wt. % for phlogopite from type 1 and type 2 cumulates.

When Al_2O_3 is plotted against TiO_2 there is a trend of increasing titanium with increasing aluminum. This trend is a reflection of the zoning of type 1 cumulate phlogopite. Mitchell (1986) discusses phlogopite having three trends of crystallization dependent on their aluminum and titanium content (6.3.6). Trend 1) Al_2O_3 is constant, 2) Al_2O_3 decreases or 3) Al_2O_3 increases. The box in Figure 6.3.6 defines the least evolved composition of phlogopite (Mitchel 1986). The Candle Lake phlogopite follows trend 3, with increasing titanium, as aluminum increases.

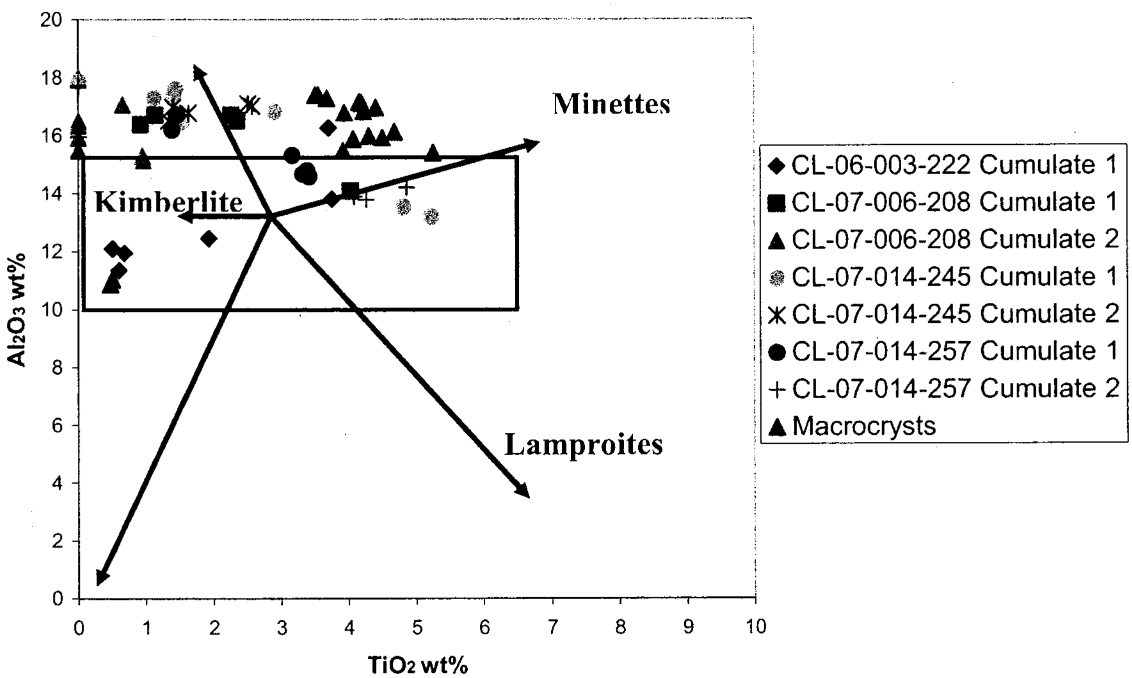

Figure 6.3.6: Al_2O_3 vs. TiO_2 wt. % plot for phlogopite from type 1 and type 2 cumulates. Comparative trends of pholognite crystallization shown by arrowed trend lines (after Mitchell 1995); Candle Lake cumulate phlogopite and macrocrysts show an increase in Al_2O_3 and TiO_2.

Spinel:

Three types of spinels occur with the phlogopite cumulates; TIMAC, QUM and TMC (titanium magnesium chromite). TIMAC spinels are the most common; they are not zoned, (Table 6.3.2; 1 and 2). There are minor QUM spinels, (Table 6.3.2; 3 and 4) that occur throughout the cumulates; however, a cumulate in sample CL-07-014-245 has spinels that are dominantly QUM composition.

Sample CL-06-003-222 is texturally unique as described above. Compositionally the spinels are also unique. The spinels have a TMC composition (Table 6.3.2; 4), with low aluminum content. The variation in spinel composition being unlike any other within the kimberlite and the differences in textures would suggest that this cumulate is not native to the kimberlite and is microxenolith.

Table 6.3.2: Representative compositions of spinel from phlogopite cumulates.

Oxide Wt. %	CL-07-006-208 TIMAC (1)	CL-07-006-208 TIMAC (2)	CL-07-014-257 QUM (3)	CL-06-003-222 TMC (4)
TiO_2	14.77	6.94	19.01	3.44
Al_2O_3	17.64	10.58	10.69	2.66
FeO_T	43.67	32.75	49.66	28.49
MnO	n.d.	n.d.	n.d.	n.d.
MgO	16.87	14.5	16.23	11.03
Cr_2O_3	8.11	33.15	2.99	53.26
Total	97.94	98.24	98.66	99.77
Fe Recalculated				
FeO	19.18	17.43	23.73	18.55
Fe_2O_3	25.9	17.03	29.83	11.05
Total	99.96	99.63	99.99	99.99
Mol %				
Ti	0.19	0.09	0.24	0.04
Al	0.17	0.10	0.11	0.03
Fe^{2+}	0.24	0.17	0.36	0.15
Fe^{3+}	0.06	0.03	0.16	0
Mn	0	0	0	0
Mg	0.12	0.36	0.40	0.27
Cr	0.05	0.22	0.02	0.35

Spinel 1 and spinel 2 are both TIMAC spinels from the same sample but have significantly different TiO_2, Al_2O_3, Fe_2O_3 and Cr_2O_3 content. Spinel 3 is a QUM spinel with low Cr_2O_3 content. Spinel 4 is a rare TMC spinel with low TiO_2 and Al_2O_3 content.

Type 2 cumulates have spinels that are to fine-grained for quantitative analyses. Qualitatively the spinels are high in chromium, moderate in magnesium, iron and aluminum, and low in titanium, and are most probably of TIMAC composition.

Type 1 cumulate spinels plot similarly to magmaclasts spinels on the spinel prism (Figure 6.3.7), which indicates that cumulate spinels belong to kimberlite trend 1.

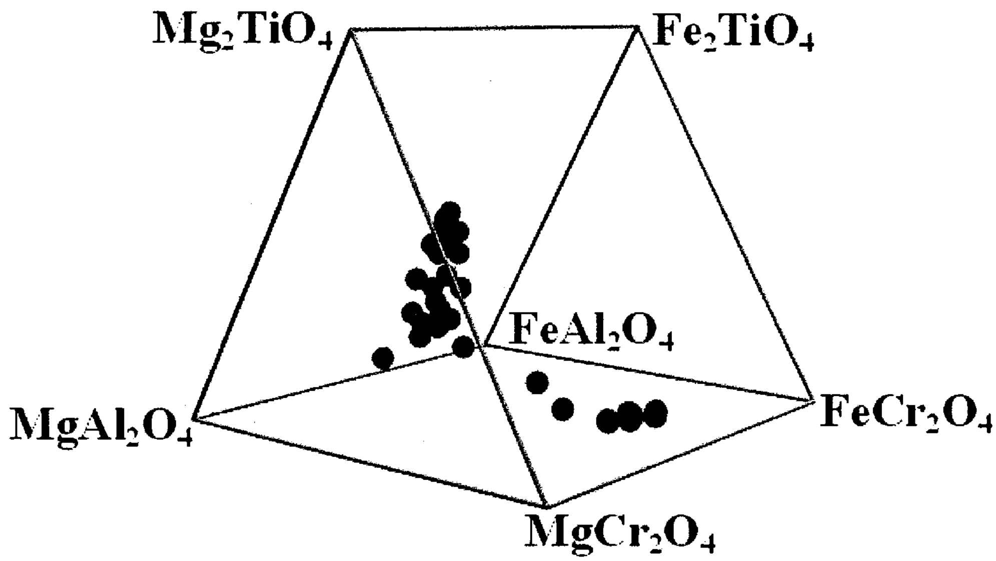

Figure 6.3.7: Spinels from phlogopite cumulates plotted in a prism. The spinels have a trend 1 curve similar to spinels from magmaclasts.

6.4 Olivine:

Olivine was found and analyzed in six different samples from two different drill cores, CL-06-003 and CL-07-014. Olivine occurs as relict cores within macrocrysts and phenocrysts. Five of the six samples analyzed are from drill hole CL-06-003, which is believed by Great Western Diamond Corp. to be situated over the feeder system of the kimberlite due to the thickness of the kimberlite in this location and the direction of resedimentation. The prevalence of samples with olivine originating from one drill core close to the proposed feeder system and olivine in the outer samples being minimal, this might suggest a spatial relationship for the preservation of olivine.

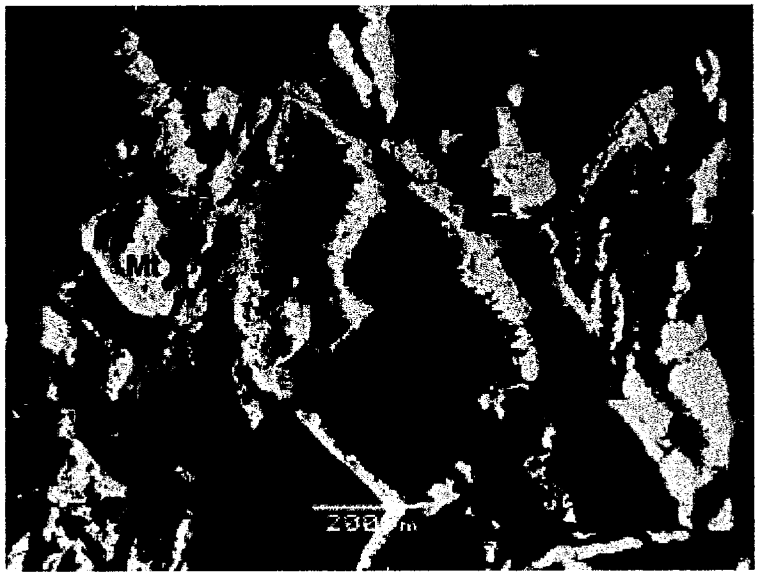

Figure 6.4.1: CL-06-003-205 (BSE), a resedimented volcanic kimberlite. Serpentinized (S) macrocryst with relict olivine (Olv), magnetite (Mt) alteration and minor dolomite (Dol).

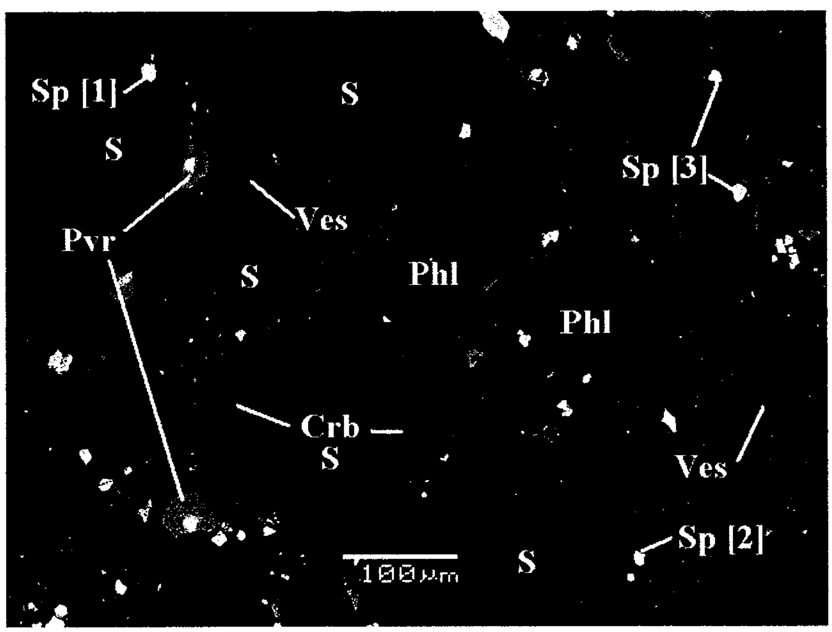

Figure 6.4.2: CL-07-014-257 (BSE), pyroclastic kimberlite. Magmaclast with phenocrysts of pseudomorphic olivine and macrocrysts of phlogopite (Phl). The olivine phenocrysts are replaced by serpentine (S). Other minor components include spinels (Sp), perovskite (Pvr) and vesicles (Ves).

Relict olivines are 20 to 500 µm in size and are anhedral-to-angular. Magnetite is uncommon but when present rims the olivine. The magnetite is 5 to 100 µm in width and is anhedral-to-irregular in habit. Magnetite rimming is not always present and occurs principally in resedimented samples. Olivine macrocrysts and phenocrysts are texturally similar; however, the olivine forming phenocrysts is on average smaller; (20 to 200 μm).

The olivine shows no zoning, and the composition of macrocrysts and phenocrysts are identical with the range in composition of $Fo_{86.92}$ to $Fo_{92.50}$, (Figure 6.4.3).

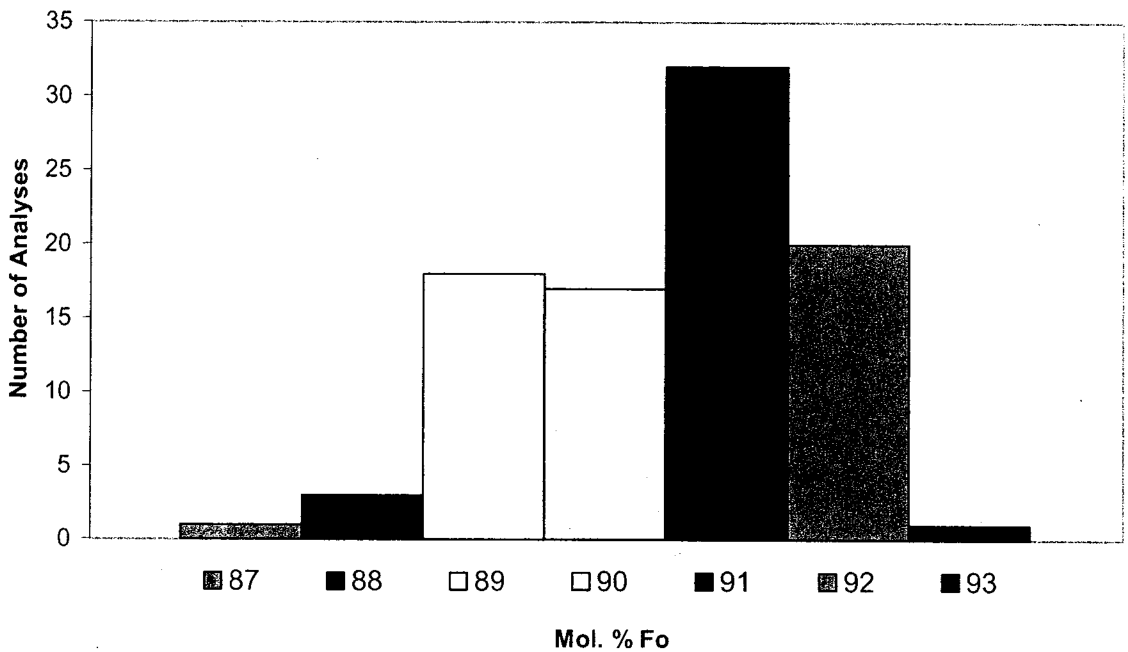

Figure 6.4.3: Histogram of olivine compositions (mol. % forsterite; Fo). Olivines are most abundant with a composition of Fo_{91}.

Sample CL-06-003-195 contains relict olivine associated with zoned serpentine-chlorite alteration (Figure 6.4.4). Calcium, magnesium and nickel are all below detection limits. Although serpentine replacement is derived from olivine, any spinels enclosed within the clasts are associated with the serpentine and not with relict olivine. This is observed in all samples.

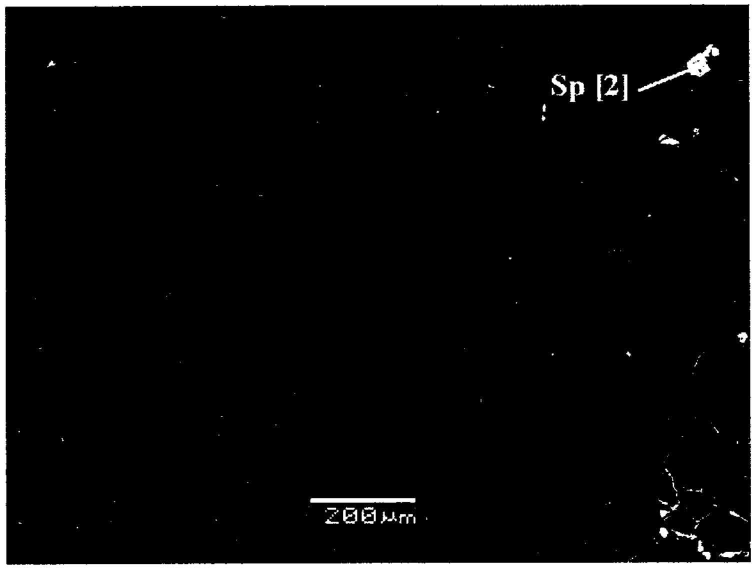

Figure 6.4.4: CL-06-003-195 (BSE), macrocryst with serpentine-chlorite zoning associated with relict olivine.

6.5 Carbonates:

Carbonates have been analyzed in three different samples from three different drill cores. The samples were selected to represent each of the three kimberlite units; lapilli tuff, pyroclastic kimberlite and resedimented kimberlite. Carbonate occurs as dolomite or calcite with minor iron, manganese, strontium and barium contents. The carbonates are found as replacement phases of macrocrysts, phenocrysts, as material infilling vesicles, within the matrix of the magmaclasts where it is cryptocrystalline and intergrown with serpentine. Carbonates are also found as irregular segregations within the interclast matrix as well as intergrown with interclast matrix serpentine.

Crystal Tuff:

Sample CL-06-003-173 is a lapilli tuff unit with carbonate occurring in macrocrysts, phenocrysts, and the interclast matrix, no vesicle filling was observed.

Although the macrocrysts and phenocrysts are dominantly replaced by serpentine, dolomite cores are common. These consist of an intergrowth of angular grains that are 20 to 150 µm in size (Figure 6.5.1).

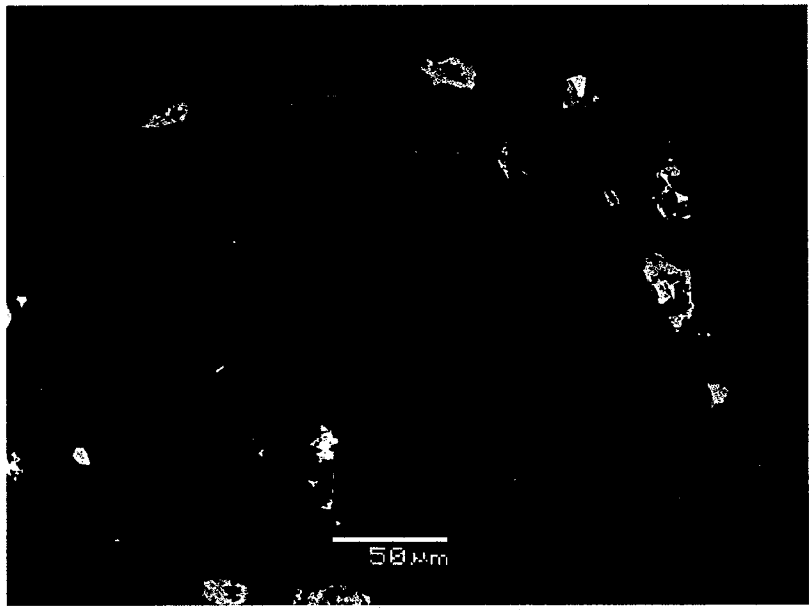

Figure 6.5.1: CL-06-003-173 (BSE), lapilli tuff unit with pyrocrysts of pseudomorphed olivine replaced by serpentine (S) and dolomite (Dol).

This intergrowth of dolomite grains has both a rounded and an angular face. Carbonates that occur in phenocrysts are similar to carbonates in macrocrysts but have a higher Fe content (Table 6.5.1).

Table 6.5.1: Representative analyses of carbonate compositions

Oxide Wt. %	CL-07-010-169 Macrocryst	CL-06-003-173 Macrocryst	CL-06-003-173 Phenocryst	CL-07-010-169 Matrix	CL-06-003-173 Matrix	CL-06-003-182 Vesicle	CL-07-010-169 Vesicle
$MgCO_3$	37.86	37.4	40.62	1.05	40.06	2.66	0.61
$CaCO_3$	58.86	59.06	55.88	95.07	55.88	90.84	95.39
$MnCO_3$	1.03	1.47	n.d.	n.d.	0.62	0.81	n.d.
$FeCO_3$	n.d.	1.71	3.31	n.d.	2.85	0.94	n.d.
$SrCO_3$	n.d.	n.d.	n.d.	n.d.	n.d.	0.71	0.48
$BaCO_3$	n.d.	n.d.	n.d.	n.d.	n.d.	1.95	1.25
Total	98.39	99.64	99.81	96.72	99.41	97.91	97.73

Composition of carbonates in samples CL-06-003-173, CL-06-003-182 and CL-07-006-169. Oxides have been converted to equivalent carbonate.

The interclast matrix of the lapilli tuff is dominated by a cryptocrystalline serpentine-carbonate intergrowth. In this interclast matrix there are also irregularly-shaped dolomite segregations (Figure 6.5.2). The dolomite segregations are fine-grained and zoned with increasing Fe content towards the margin of the segregation (Table 6.5.1; column 5).

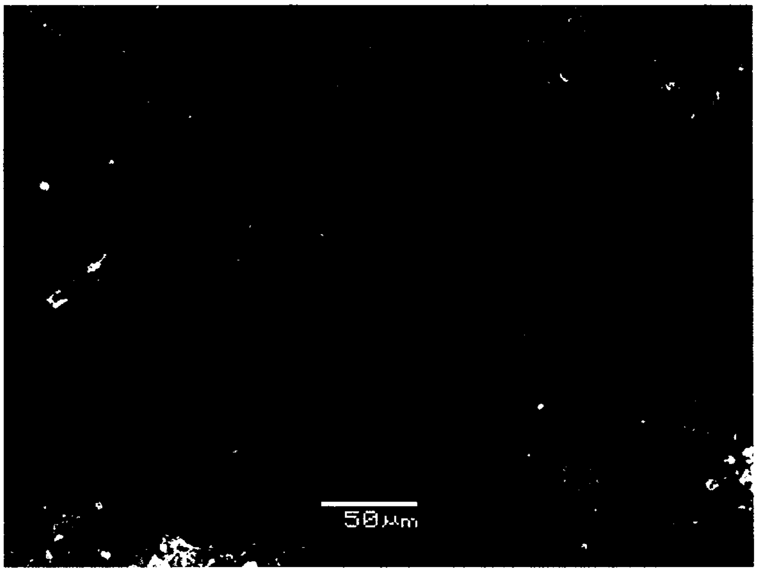

Figure 6.5.2: CL-06-003-173 (BSE), lapilli tuff unit. Dolomite (Dol) segregation within the interclast matrix, surrounded by botryoidal serpentine (S) and pyrocrysts (Pyro)

Pyroclastic Kimberlite:

Sample CL-06-003-182 is a representative pyroclastic kimberlite unit with carbonate occurring within macrocrysts, vesicle infill and as an almost pure interclast matrix. Other samples have an interclast matrix that has serpentine and carbonate intergrown with irregular segregations of carbonates.

The macrocrysts are dominated by serpentine replacement although these commonly have a carbonate core. The carbonate is fine-grained, 20 to 100 μm and has an anhedral habit. The carbonate is dominantly calcite at the core with increasing magnesium content towards the rim. Olivine phenocrysts are present in this sample but do not have carbonate replacement.

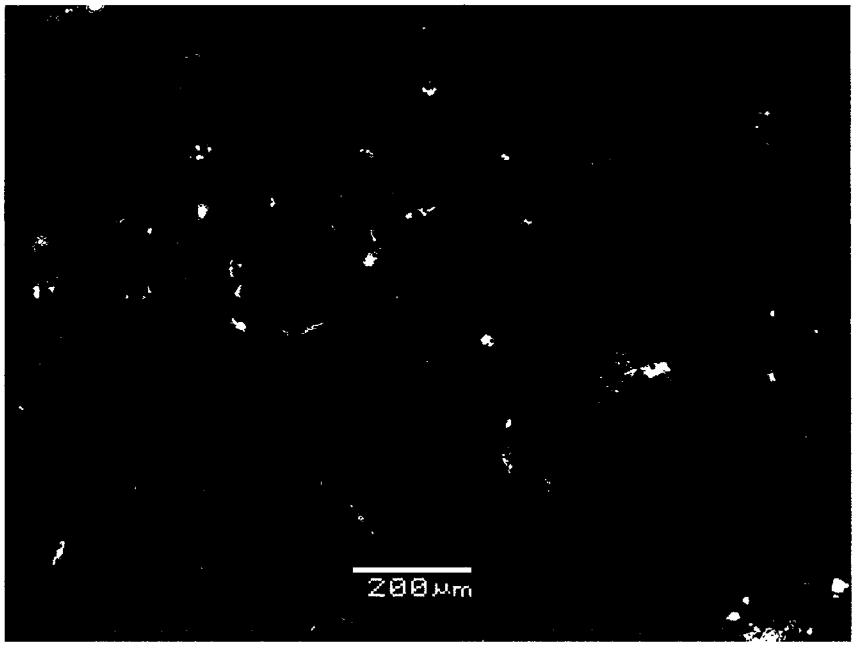

Figure 6.5.3: CL-06-003-182 (BSE), pyroclastic kimberlite. Macrocrysts enclosed in a magmaclast with a two phase of serpentine (S) replacement and minor calcite (Cal) replacement.

The groundmass is a homogenous calcite that is composed of fine-grained angular grains, resulting in a granular texture (Figure 6.5.4). The calcite is homogenous in composition except along the margins of clasts. The composition of the carbonate varies from a calcite with no detectable Ba and Sr content to a carbonate with a higher Ba and Sr content (BaO 1.58 wt. % and SrO 0.62 wt. %).

Vesicles are rounded-to-oval and are 20 to 50 µm in diameter. They are filled by fine-grained carbonate and rimmed by botryoidal serpentine. The calcite composition has two varieties. Vesicle fill can have relatively high Fe, Mn, Ba and Sr contents (Table 6.5.1, column 6) or no detectable Fe, Mn, Ba or Sr. The cores are dominantly calcite with minor Fe, and the rims have higher Ba, Sr and Mn.

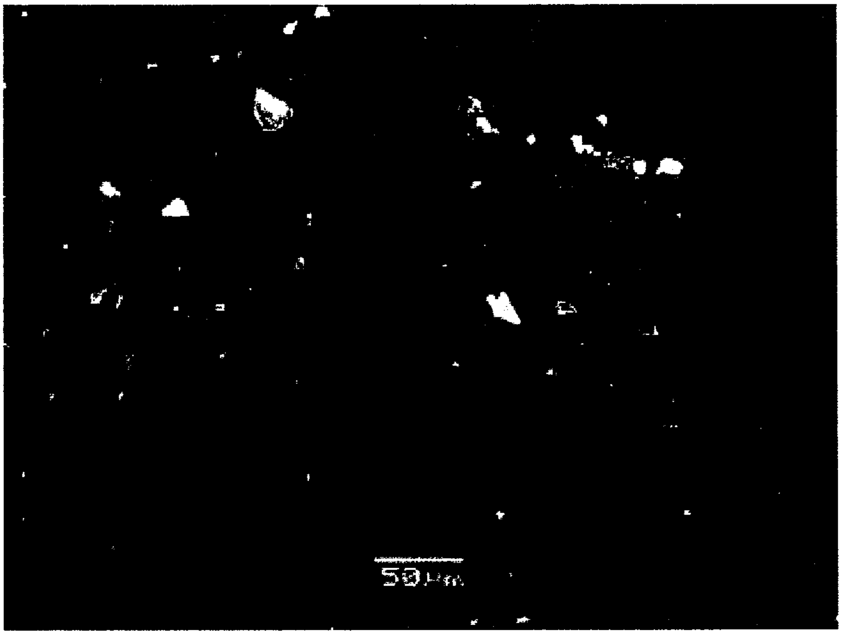

Figure 6.5.4: CL-06-003-182 (BSE), pyroclastic kimberlite. Magmaclast with phenocrysts of pseudomorphed olivines replaced by serpentine (S) and rounded vesicles infilled by calcite (Cal). The magmaclast is enclosed by a fine-grained calcite (Cal) interclast matrix (right side of figure).

Resedimented Kimberlite:

Sample CL-07-010-169 is a resedimented kimberlite with carbonates occurring in macrocrysts, interclast matrix and vesicles in clasts.

Macrocrysts are dominated by an intimate intergrowth of granular serpentine together with small, 20 to 50 µm sized carbonate grains. These are angular-to-irregular, single isolated grains. The carbonate is dolomitic in composition with a compositional trend to calcite towards the core of the macrocrysts.

The interclast matrix is a serpentine-carbonate mixture with both serpentine and dolomite segregations. The dolomite segregations are similar in size and shape to the serpentine segregations and are infilled by cryptocrystalline dolomite. Within these segregations there are single anhedral-to-subrounded calcite grains, varying in size from 5 to 75 µm (Figure 6.5.5). The carbonate grains are calcite with minor increases of Ba and Mn content at the rim.

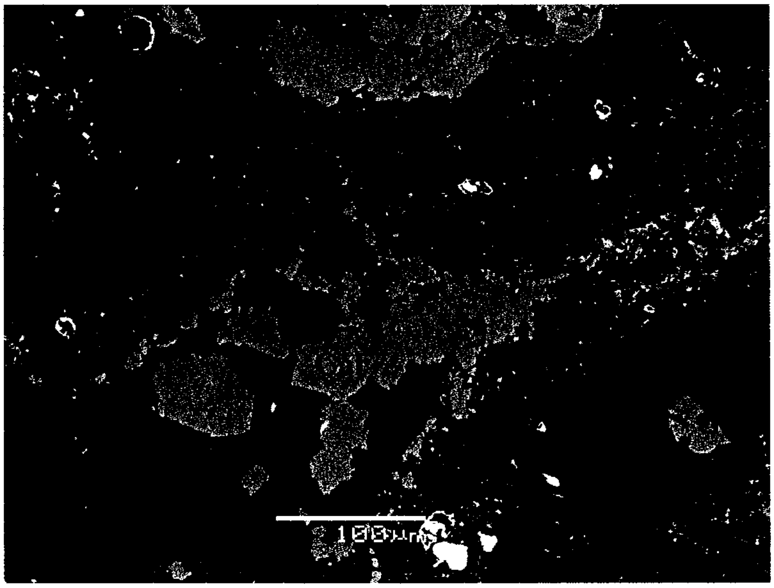

Figure 6.5.5: CL-07-010-169 (BSE), resedimented kimberlite. A reworked magmaclast with a former monticellite (Mo) matrix enclosing serpentine (S) replaced phenocrysts with minor calcite (Cal) and iron-nickel sulphides. The interclast matrix is a serpentine (S) segregation with minor calcite (Cal) grains.

Vesicles are rare but when present are 20 to 50 µm in size and are rounded-to-oval. They are infilled by fine-grained calcite with low Ba and Fe content (Table 6.5.1; column 7).

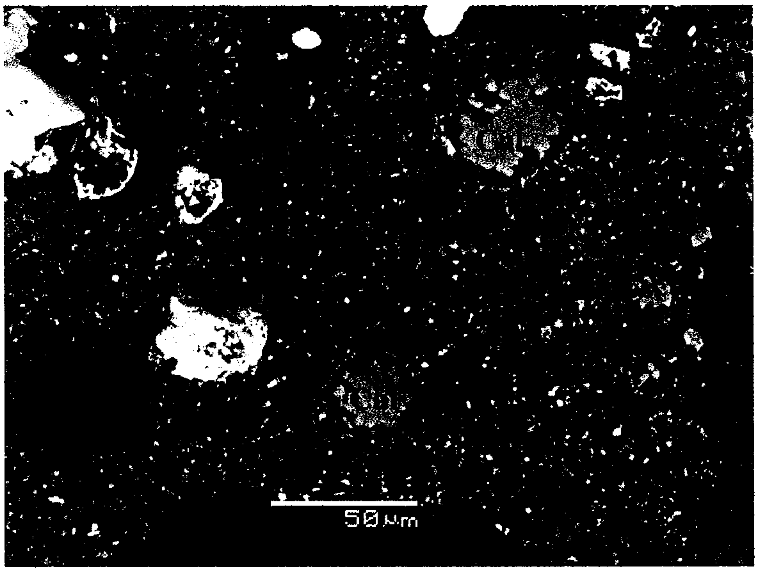

Figure 6.5.6: CL-07-010-169 (BSE), resedimented kimberlite. Magmaclast matrix composed of fine grained former monticellite (Mo) and vesicles infilled by calcite (Cal) and rimmed by serpentine (S).

Composition:

Two groups of carbonate are evident when data are plotted in the ternary system, $CaCO_3$-$MgCO_3$-$FeCO_3$ (Figure 6.5.7).

The dolomite field includes all carbonate data from sample CL-06-003-173; the lapilli tuff. The only other samples plotting within the dolomite field are carbonate replacements of macrocrysts from the resedimented unit, CL-07-010-169 (Figure 6.5.7). Macrocryst carbonate in the lapilli tuff unit has a higher Fe content than macrocrysts from the resedimented unit.

The calcite field represents replacement of phenocrysts and vesicle infilling from sample CL-07-010-169 (resedimented kimberlite) and all the data from sample CL-06-003-182 (pyroclastic kimberlite) (Figure 6.5.7). There are slight variations in composition due to zoning. Carbonate cores of macrocrysts and phenocrysts are lower in Mg (MgO 17.09-18.19 wt. %), relative to the margins of the carbonate that replace the macrocrysts and phenocrysts (MgO 18.02-20.25 wt. %). Vesicles from sample CL-07-010-169 (resedimented kimberlite) show only minor increases in iron and barium towards the rim, in contrast to zoned vesicles in sample CL-06-003-182 (pyroclastic kimberlite)

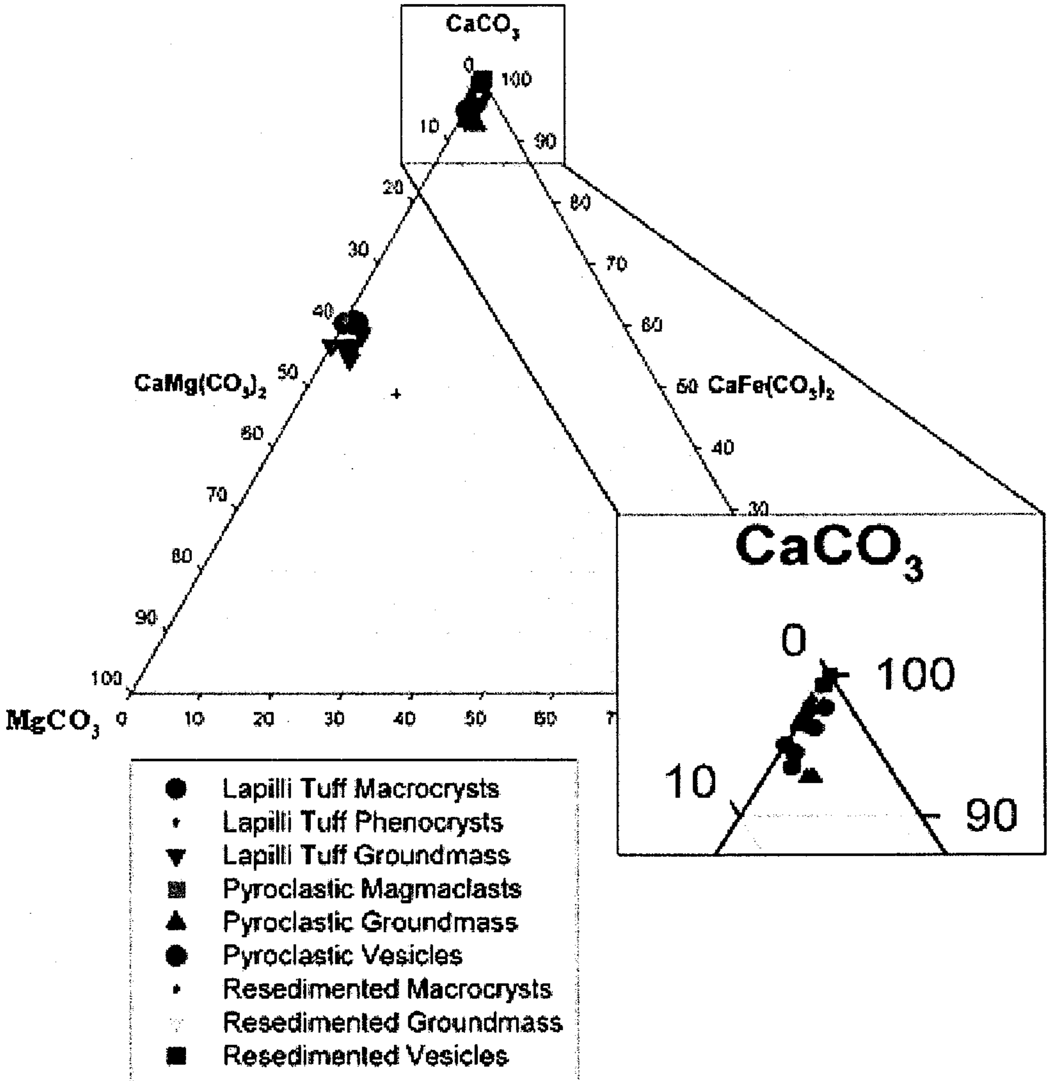

Figure 6.5.7: $CaCO_3$-$MgCO_3$-$FeCO_3$ ternary diagram for a lapilli tuff (CL-06-003-173), pyroclastic kimberlite (CL-06-003-182), and resedimented kimberlite (CL-07-010-169).

6.6 Perovskite:

There are two parageneses of perovskite in Candle Lake kimberlite. Type 1, nucleates along the edges of phenocrysts or macrocrysts and is analogous in this respect to type 2 spinels. Type 2, occurs as isolated grains in the matrix. Type 1 perovskites are far more common in Candle Lake kimberlite than type 2 perovskites.

Type 1 and type 2 perovskite grains are 5 to 100 μm in size, the finer-grained material is commonly fragments of coarser perovskite. Perovskites always have a rim of anatase (2 to 10 μm). There are two different types of anatase replacement, an atoll structure with a thin rim of anatase separated from the kernel by serpentine (Figure 6.6.1) or a marginal alteration in which the anatase alteration is along the outer rim of the grain and no separation from rim to core occurs (Figure 6.6.2).

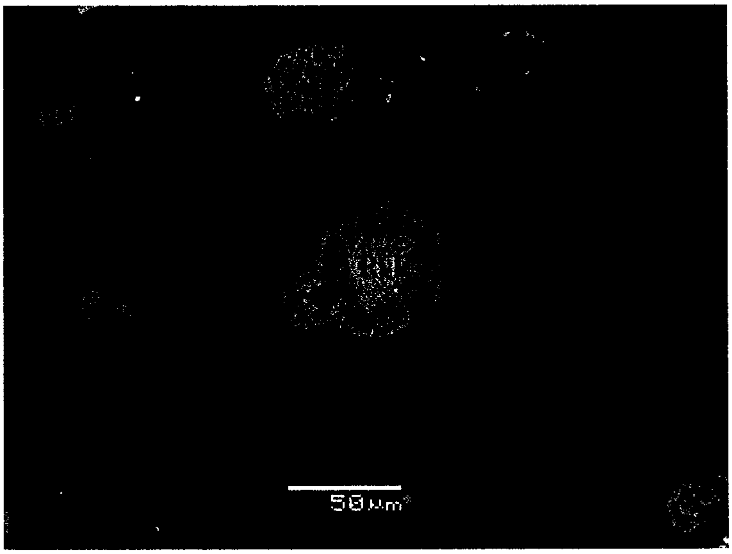

Figure 6.6.1: Sample CL-06-003-173 (BSE), atoll structured perovskite with anatase rim.

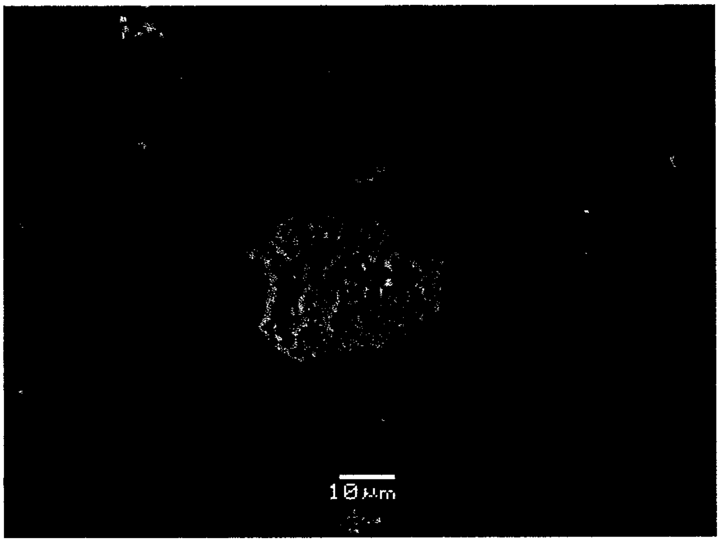

Figure 6.6.2: Sample CL-07-006-208 (BSE), perovskite replaced by anatase.

Perovskites when observed to nucleate against a spinel grain result in the spinel grain being enclosed in the perovskite or within the anatase rim. This textural relationship indicates that perovskite forms later than spinel.

Perovskite in Lapilli Tuff:

Perovskites in the lapilli tuff sample are dominantly type 1 forming around pyrocrysts. Type 2 perovskites where observed but due to the minimal amount of matrix they are rare. The perovskites average 25 μm in size. The kernels of the perovskite are almost completely replaced by anatase and have a granular texture with long needle-like grains. The kernel is commonly fragmented and infilled by matrix or left void. The anatase rims have variable thicknesses and the void spaces in the atoll structures are not uniform. There is minor anhedral $BaSO_4$ (<2 μm) at the core of some of the perovskite grains.

Perovskites in Pyroclastic Kimberlite:

All magmaclasts contain perovskites as a minor phase. These perovskite grains average 25 μm in size, but can vary between samples. Both type 1 and type 2 perovskites occur. Atoll structured perovskites are anhedral and the atoll structure is irregular. The kernel of the atoll is strongly altered to anatase although minor $CaTiO_3$ can remain at the core. Perovskites grains less than 20 μm in size are completely replaced by anatase or the kernel is removed.

In sample CL-06-003-247 the perovskites are dominantly replaced by marginal anatase. Grains less than 20 μm are completely replaced by anatase.

Spinels that are enclosed within the perovskite have high iron and titanium content with low chromium, and are QUM type spinels. They are commonly euhedral-to-subhedral but can be anhedral and are both type 2 and type 3 spinels (Figure 6.6.3). Perovskite that forms adjacent to a spinel have the anatase rim terminating when contacting the spinel grain or the rim follows the habit of the spinel (Figure 6.6.4).

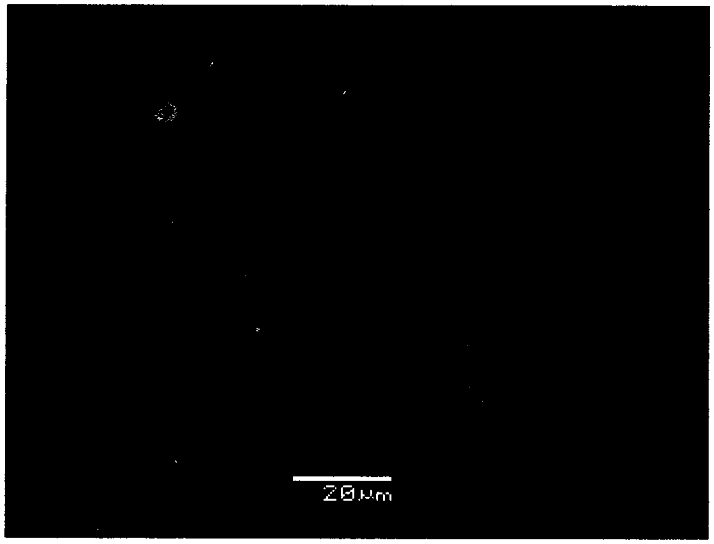

Figure 6.6.3: Sample CL-06-003-182 (BSE), perovskite nucleated against a spinel grain. The anatase rim terminates against the spinel.

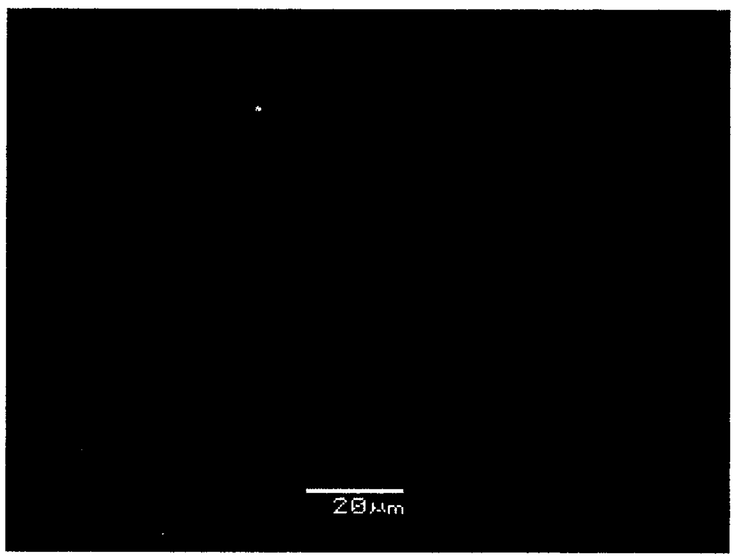

Figure 6.6.4: Sample CL-06-003-182 (BSE), perovskite adjacent to spinel with the anatase rim following the contact with the spinel grain.

Perovskite in Resedimented Volcanic Kimberlite:

Perovskites average 20 µm in size, are anhedral and less abundant in resedimented kimberlite than in pyroclastic kimberlite. Perovskites exhibit both an atoll structure alteration and a marginal replacement. The anatase replacement is extensive. In sample CL-07-010-169, all perovskite has been replaced by anatase. There are anatase rims around a pitted and replaced kernel. Sample CL-06-003-195 has minor perovskites remaining in the kernel, showing that there is variation in the degree of anatase alteration between samples.

The spinels that are enclosed in the perovskite are high in FeO_T and TiO_2, low in Cr_2O_3, and are QUM spinels.

Composition:

There is very little variation in composition in the Candle Lake perovskite. Perovskites are dominantly $CaTiO_3$ with consistently minor amounts of iron, niobium and cerium. There are slight variations in the light rare earth element (LREE) content. An increase in LREE is not reflected in a difference in perovskite type between kimberlite units.

When the composition of Candle Lake perovskites are plotted on a lueshite-loparite-perovskite ternary diagram, they plot near the $CaTiO_3$ endmember (Figure 6.6.5). There is very little range in composition of the perovskites. Kimberlite perovskites from Chakhmouradian and Mitchell (2000) are plotted for comparison.

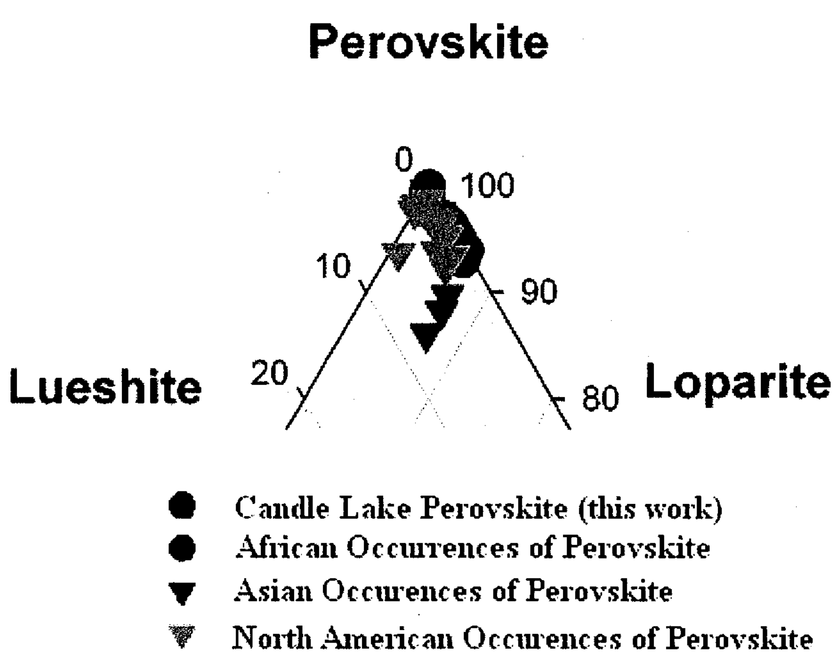

Figure 6.6.5: Lueshite-Laparite-Perovskite ternary diagram for Candle Lake perovskites. African, Asian and North American occurrences are representative data from Chakhmouradian and Mitchell (2000).

6.7 Apatite:

Apatite occurs as an accessory mineral in the matrix of magmaclasts, and is present in all samples. It is commonly very fine-grained (<1 μm in size) and is optically indistinguishable from the serpentine and carbonate in the matrix. However, some apatite grains are up to 6 μm in size and can be distinguished from the matrix as euhedral-to-subhedral grains. Other apatite grains are rounded or lath shaped (Figure 6.7.1). All magmaclasts within a sample do not have visible apatite, adjacent magmaclasts vary in the size and abundance of visible apatite. Coarse apatite, (> 100 μm in size) occurs in several samples as subrounded grains within the interclast-matrix (Figure 6.7.2).

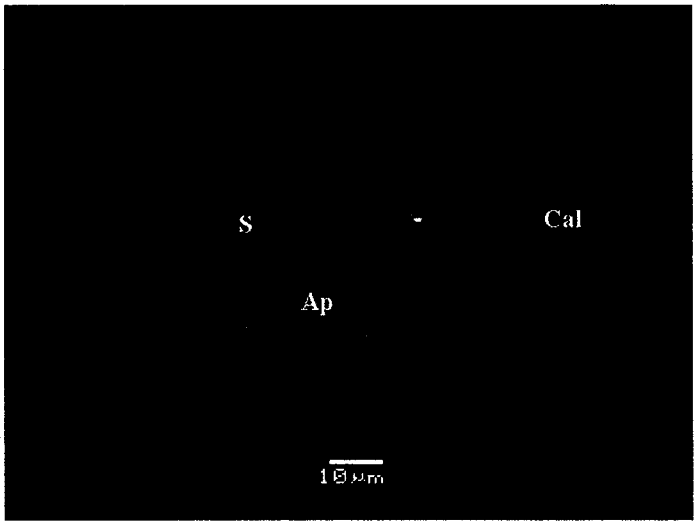

Figure 6.7.1: Sample CL-07-014-269 (BSE), fine-grained euhedral apatite in a magmaclast matrix.

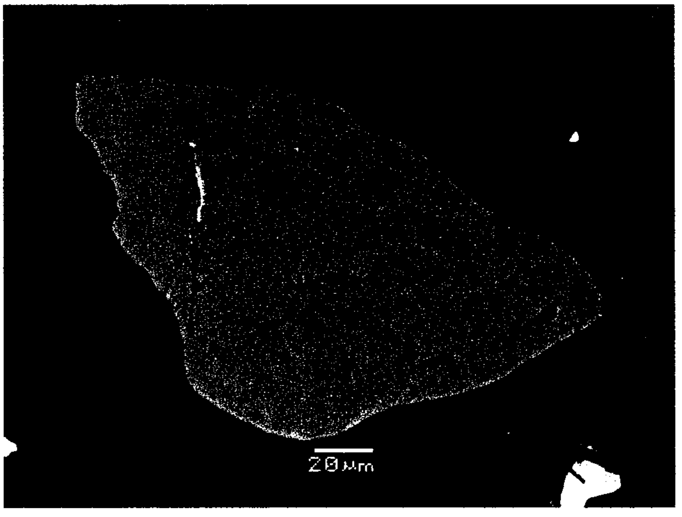

Figure 6.7.2: Sample CL-06-003-236 (BSE), coarse, anhedral apatite grain within the interclast matrix.

Apatite is essentially calcium phosphate [$Ca_5(PO_4)_3(OH,F)$] with minor fluorine contents (Table 6.7.1). There are no detectable light rare-earth elements present in the apatite except for samples which are too fine-grained to analyze and have high background interference. Chlorine is also absent except in apatite from sample CL-07-014-285. However, these apatites are enclosed in a calcium silicate xenolith and are possibly xenocrysts.

Table 6.7.1: Apatite compositions

Oxide Wt. %	CL-06-003-158 (1)	CL-06-003-158 (2)	CL-07-010-261 (3)	CL-07-010-261 (4)	CL-07-014-285 (5)
P_2O_5	43.58	45.17	43.63	43.56	45.15
La_2O_3	n.d.	n.d.	n.d.	n.d.	n.d.
Ce_2O_3	n.d.	n.d.	n.d.	n.d.	n.d.
Pr_2O_3	n.d.	n.d.	n.d.	n.d.	n.d.
Nd_2O_3	n.d.	n.d.	n.d.	n.d.	n.d.
Sm_2O_3	n.d.	n.d.	n.d.	n.d.	n.d.
CaO	56.08	55.2	56.19	56.88	57.86
SrO	n.d.	n.d.	n.d.	0.58	n.d.
F	2.5	4.77	3.9	5.02	2.91
Cl	n.d.	n.d.	n.d.	n.d.	1.78
Total	101.65	102.43	100.21	100.19	102.35
Fluorine and Chlorine Correction					
O ≡ F, Cl	1.05	2.01	1.64	2.11	1.63
Total	100.60	100.42	98.57	98.08	100.72

Composition data for course interclast matrix apatite in resedimented and pyroclastic kimberlites. Sample CL-07-014-285 is a xenocryst within a calcium-silicate xenolith.

6.8 Garnet:

Garnets are a minor accessory mineral that occurs as microcrysts and xenocrysts. They are visible in hand sample and are fine-grained (<2 mm in size) pink-orange to black in colour. Garnets are rarely observed in thin section but are consistently rimmed by kelyphite that can be up to 1 mm thick (Figure 6.8.1). Garnets grains are also commonly fractured. They occur as xenocrysts within the interclast matrix of the kimberlite but are also rarely observed within pseudomorphed olivine macrocrysts. This textural relationship shows that in some instances garnet and olivine formed contemporaneously and are microxenoliths of mantle-derived material (Figure 6.8.2).

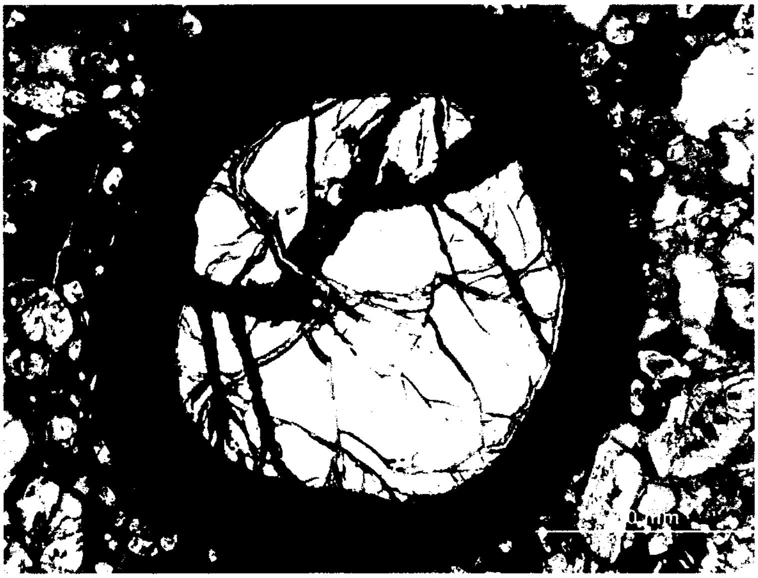

Figure 6.8.1: Sample CL-07-014-257 (PPL), fractured garnet with kelyphite rim.

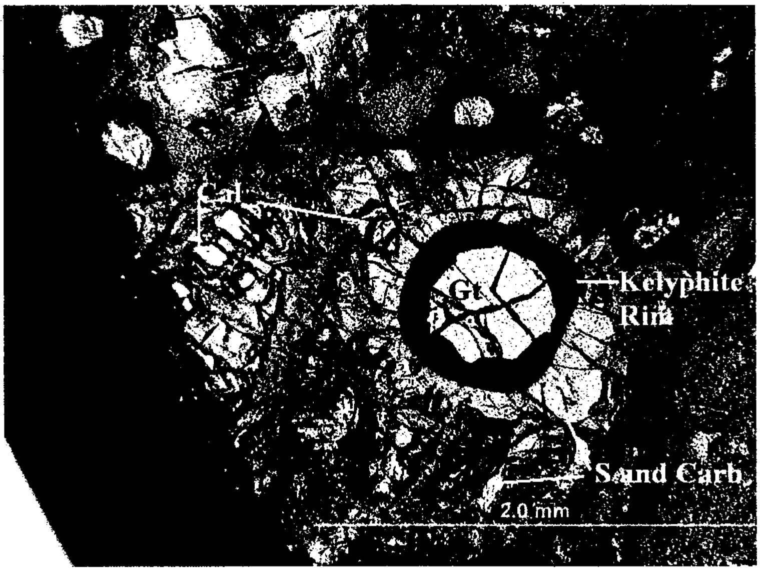

Figure 6.8.2: Sample CL-07-014-233 (PPL), rounded garnet (Gt) xenocryst enclosed in a pseudomorphed olivine macrocryst within a magmaclast.

Due to the limited abundance of garnets in thin section, heavy mineral separations (see analytical methods section) were performed to concentrate the garnets.

The Dawson and Stephens (1975) approach of classifying garnets by cluster analyses, using compositional data, and separating the clusters into twelve different groups was applied to Candle Lake garnets. On this basis Candle Lake garnets include groups: 1; 2; 3; 4; 5; 6; 9; and 11, and are dominantly type 5 and 9, i.e. crustal granulite garnets and lherzolitic garnets, respectively. No garnet group is confined to a particular kimberlite type (Figure 6.6.1).

Composition:

Garnet compositions plotted on a Mg-Fe-Ca ternary diagram show two clusters of data: a high Mg cluster and a high Fe cluster (Figure 6.8.3). The high magnesium cluster consists of Dawson and Stephens (1975) groups 1, 2, 9 and 11. The high iron cluster consists of Dawson and Stephens (1975) groups 3, 4, 5, and 6.

Group 1 and 2 garnets are high in MgO (17.55-22.5 wt. %) and have low Cr_2O_3 (n.d.-3.58 wt. %), (Table 6.6.1). They occur in all drill cores except for CL-07-006, however; there are a limited number of samples from this drill cores resulting in a smaller sample size.

Groups 9 and 11 garnets are high in MgO (19.31-23.03 wt. %) and high in Cr_2O_3 (n.d.-8.52 wt. %). Group 9 garnets are very abundant in Candle Lake kimberlite and are common to all samples. Groups 1, 2, 9 and 11 garnets are dominantly pyrope (Appendix 3), and form cluster 1 with a small compositional range (Figure 6.8.3).

Cluster 2 (Figure 6.8.3) consists of eclogite garnets and crustal garnet granulite, groups 3, 4, 5 and 6. There is a larger compositional range in cluster 2 relative to cluster 1. Cluster 2 garnets have high iron content and no detectable chromium. Group 3 garnets are found in samples CL-07-006-195 (RVK) and CL-07-010-245 (PK). The FeO_T content is high (14.58-14.88 wt. %) but the CaO content is not detectable (Table 6.8.1). Only one group 4 garnet was found in sample CL-07-010-245. The FeO_T content is (8.78 wt. %) which is lower than data from Dawson and Stevens (Table 1). Group 5 garnets are the most abundant type. They have a very high FeO_T content (27.1-36.01 wt. %) which is higher than the accepted FeO_T for eclogite garnets of (21-22 wt. %), and no detectable Cr_2O_3 or TiO_2. Group 6 garnets are only found in sample CL-07-006-195 (RVK) and CL-07-006-208 (PK) and have a low-to-moderate CaO content (0.76-4.78 wt. %), high FeO_T content (22.29-22.88 wt. %) and no Cr_2O_3 or TiO_2. However; group 6 garnets have high MnO content (13.68-18.42 wt. %), (table 1). Groups 3 and 5 are dominantly almandine garnets, whereas groups 4 and 6 are spessartine garnets.

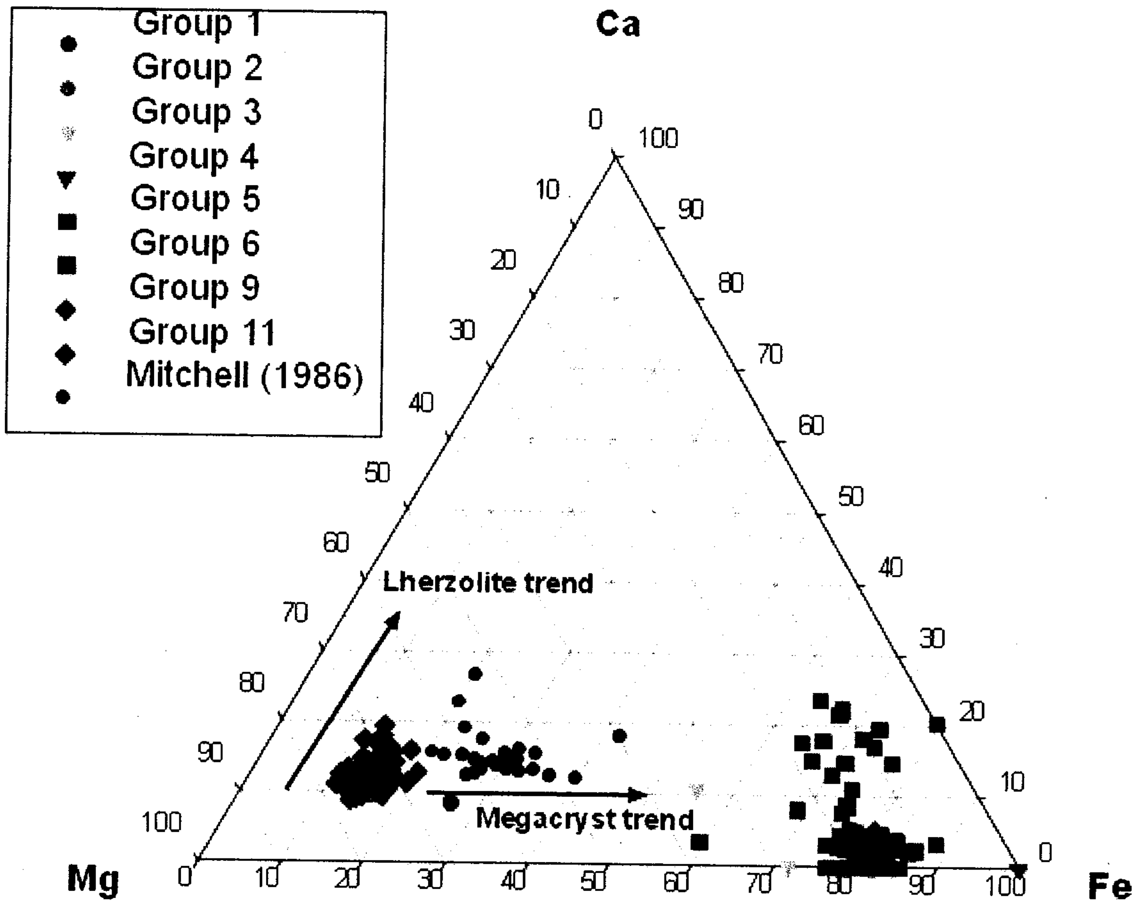

Figure 6.8.3: Fe-Ca-Mg ternary diagram for garnets. Groups 1, 2, 9 and 11 plot near the Mg endmember and groups 3, 4, 5, and 6 plot near the Fe endmember (this work). No distinct trend is seen along the lherzolite or megacrysts compositional trends (Mitchell, 1986).

Figure 6.8.4 shows the correlation between CaO and Cr_2O_3 (Grütter et al. 2004). There is a general trend of increasing CaO with increasing Cr_2O_3. Garnets in this diagram can belong to the G10 (diamond inclusions), G9 (lherzolite) and G12 (peridotite) garnet types. Garnets lacking CaO can have a variable Cr_2O_3 content and are dominantly G10 (diamond inclusions) and G0 (unclassified garnets).

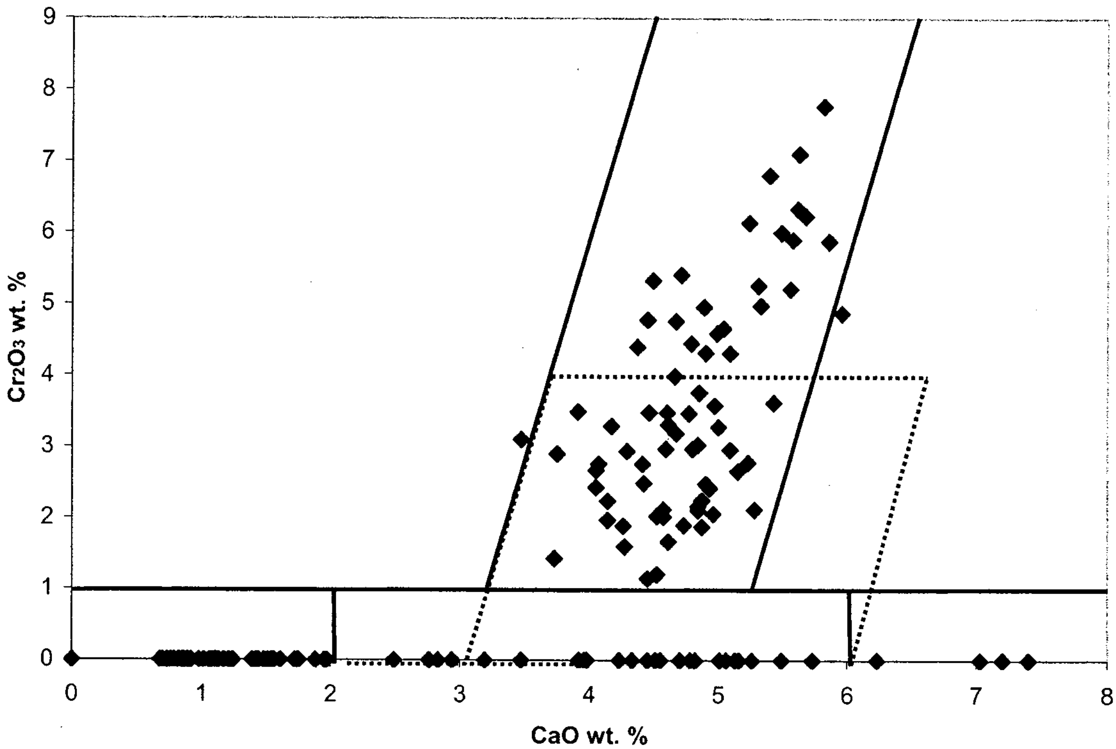

Figure 6.8.4: G-number nomenclature of the garnet classification scheme for this work in a conventional Cr_2O_3 vs. CaO diagram (Grütter et al. 2004).

Variation of garnet populations between kimberlite types is negligible and variation between drill holes is only minor, and all contain kimberlites with type 5 and type 9 garnets with lesser type 1 garnets except for drill hole CL-07-006 which has only group 6 spessartine garnets.

Table 6.8.1: Compositional data for the various garnet types in Candle Lake Kimberlite.

Garnet Type (Dawson and Stevens (1975)	1 – CL-06-003-173	2 – CL-07-010-264	3 – CL-07-006-195	4 – CL-07-010-245	5 – CL-06-003-182	6 – CL-07-006-208	9 – CL-07-014-245	11 – CL-07-014-257
Oxide %								
SiO_2	41.43	41.77	26.36	35.67	37.6	36.41	41.79	40.67
TiO_2	0.56	n.d.	0.85	n.d.	n.d.	n.d.	0.29	0.98
Cr_2O_3	1.21	1.6	n.d.	n.d.	n.d.	n.d.	3.47	6.23
Al_2O_3	21.53	21.27	53.96	19.54	20.23	21.04	20.77	17.48
FeO_T	8.57	7.85	14.72	8.78	28.6	22.29	6.82	8.49
MnO	n.d.	n.d.	n.d.	33.56	3.7	18.42	0.79	n.d.
MgO	21.94	21.83	3.24	n.d.	2.51	0.94	21.27	19.76
CaO	4.52	4.27	n.d.	n.d.	7.4	0.76	4.77	5.68
Total	99.76	99.75	99.35	99.51	99.99	99.75	99.97	99.96
# Ions in Formula								
Si	5.87	5.98	3.91	6.04	6.01	5.96	5.95	5.94
Al	0.13	0.02	2.09	-	-	0.04	0.05	0.06
Total	6	6	6	6.04	6.01	6	6	6
Al	3.47	3.57	7.36	3.9	3.81	4.03	3.43	2.95
Fe^{3+}	0.41	0.27	-	.02	0.18	0.01	0.17	0.18
Cr	0.14	0.18	-	-	-	-	0.39	0.72
Total	4.01	4.02	7.59	3.92	3.99	4.04	3.99	3.85
Mg	4.63	4.22	0.48	0	0.6	0.23	4.51	4.3
Fe^{2+}	0.61	0.67	1.84	1.23	3.64	3.05	0.64	0.86
Mn	-	-	-	4.81	0.5	2.56	0.1	0
Ca	0.69	0.65	-	-	1.27	0.13	0.73	0.89
Total	5.93	5.98	2.32	6.04	6.01	5.96	5.98	6.05
End Members								
Korringite	0	0	0	0	0	0	9.78	18.7
Uvarovite	3.38	4.5	0	0	0	0	0	0
Andradite	8.19	6.45	0	0	4.5	0.2	4.22	4.69
Grossular	0	0	0	0	16.59	2.03	7.95	10.01
Spessartine	0	0	0	79.69	8.34	42.85	1.59	0
Almandine	10.28	11.14	79.14	20.31	60.63	51.06	10.76	14.16
Pyrope	78.15	77.91	20.86	0	9.95	3.85	65.69	52.44

Using Dawson and Stephens (1975) classification of garnets sample 1 analyzed from CL-06-003-173 a lapilli tuff unit and is a type 1 garnet. Sample 2 is analyzed from CL-07-010-264 a pyroclastic kimberlite and is a type 2 garnet. Sample 3 is analyzed from CL-07-006-195 a resedimented kimberlite and is a type 2 garnet. Sample 4 is analyzed from CL-07-010-245 a pyroclastic kimberlite and is a type 4 garnet. Sample 5 is from CL-06-003-182 a pyroclastic kimberlite and is a type 5 garnet. Sample 6 is from CL-07-006-208 a pyroclastic kimberlite and is a type 6 garnet. Sample 7 is analyzed from CL-07-014-245 a pyroclastic kimberlite and is a type 9 garnet. Sample 8 is analyzed from CL-07-014-257 a pyroclastic kimberlite and is a type 11 garnet.

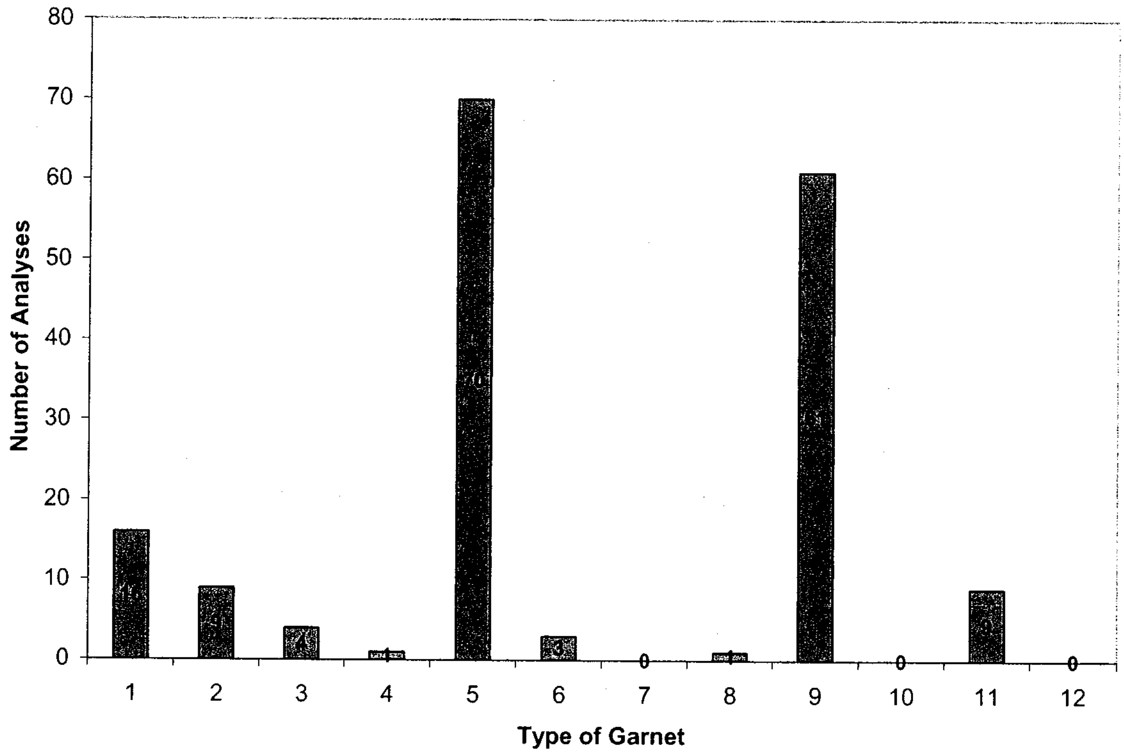

Figure 6.8.5. Histogram of garnet populations from the Candle Lake kimberlite based on the Dawson and Stevens (1975) garnet classification.

This study has shown that G10 garnet indicator minerals are absent from the C29/30 kimberlite (Figure 6.8.5) However, other indicator mineral studies show that the C29/30 kimberlite as well as an additional 31 kimberlite bodies in Fort à la Corne kimberlite field have a significant proportion of G10 garnets (Table 6.8.2). Table 6.8.2 shows data for thirty three different Fort à la Corne kimberlite bodies, the number of total garnets and the number of G10 garnets. This table is composed of data that has undergone different sampling procedures, mineral selection, and analytical methods all of which results in a highly variable grain count. It is therefore difficult to compare garnet data between kimberlite bodies but this table does show that within the Fort à la Corne kimberlite field there is significant variation of garnet populations from one kimberlite body to the next.

The percentage of G10 garnets relative to all garnets found within the Candle Lake kimberlites C28, C29 and C30, are 10%, 12.5% and 5.2% respectively (Harvey et al. 2001). This high G10 garnet count reflects a high diamond preservation potential which results in the Candle Lake kimberlites being a good potential source of diamonds (Dawson and Stephens 1975).

It is most likely that there were no G10 garnets detected in the C29/30 kimberlite from this work due to a smaller sample size.

Table 6.8.2: Garnet composition and counts from the Fort à la Corne kimberlite field.

Kimberlite	Total Number of Garnets	Cr-Garnet (>2 wt%)	"G10" Garnets
116	34	31	2
118	53	22	0
119	400	338	0
120	392	191	12
121	46	18	3
122	500	433	11
126	399	355	8
133	589	547	12
140	700	676	40
141	100	89	5
145	100	77	2
147	200	157	3
150	247	217	4
151	48	17	0
158	42	14	1
163	203	186	8
168	99	86	0
169	294	134	25
216	99	71	1
219	66	38	4
326	19	13	0
426	192	115	1
Candle LK C28	**652**	**588**	**65**
Candle LK C29	**176**	**156**	**22**
Candle LK C30	**518**	**438**	**27**
Foxford 179	101	67	2
Foxford 180	180	159	0
Smeaton RS-1	29	19	0
Snowden 603	47	44	0
Snowden 614	28	28	0
Snowden 611	63	32	2
Sturgeon SL-1	89	53	0
Weirdale 501	4	3	0

Garnet counts from thirty three different kimberlite bodies located in the Fort à la Corne kimberlite field (modified from Harvey et al. 2001)

6.9 Ilmenite:

Ilmenite occurs within the interclast-matrix of the kimberlite as anhedral-to-subrounded microcrysts, and ranges in size from 30 μm to 500 μm. Due to the low modal content concentration of ilmenite in thin section, heavy mineral separations were performed to concentrate the ilmenite. Ilmenite is observed most commonly as a rounded, moderately fractured homogenous grains, although anhedral fractured grains are also present (Figure 6.9.1). Ilmenite also exhibits an atoll structure with serpentine separating the ilmenite grain from the TiO_2 rim (Figure 6.9.2). This rimming of ilmenites is extremely rare and was not observed in the mineral separates.

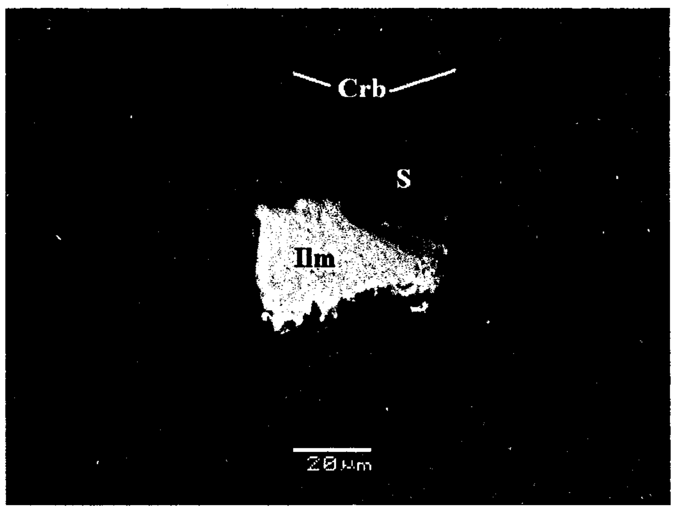

Figure 6.9.1: Sample CL-07-014-267 (BSE), fine-grained, anhedral ilmenite grain enclosed in serpentine and calcite interclast matrix.

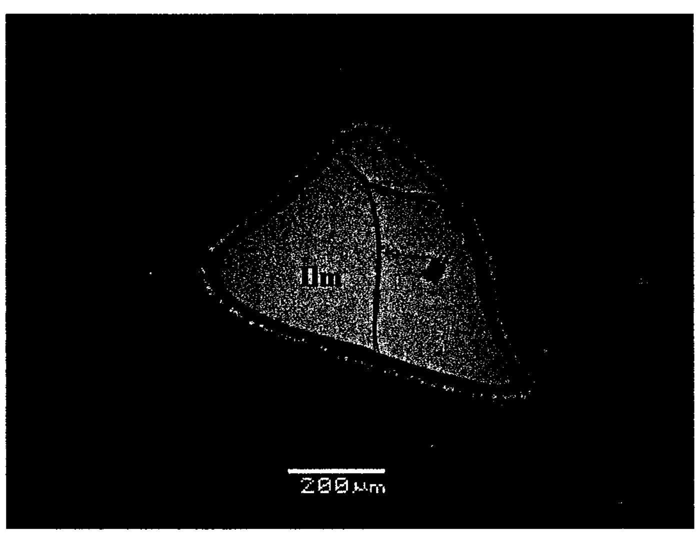

Figure 2: Sample CL-06-003-236 (BSE), coarse, subrounded ilmenite grain with a TiO_2 rim within a serpentine interclast matrix.

Composition:

Ilmenites are dominantly iron-titanium oxides [(Fe,Mg)TiO_3] but with some variation in minor components. Some ilmenites exhibit an increase in MgO (n.d.-18.54 wt. %) towards the geikielite end member. Cr_2O_3 content although commonly not detectable can be high in some grains of high MgO content. Although high Cr_2O_3 content are associated with MgO, not all Mg-rich ilmenites are Cr-rich (Table 6.9.1; CL-06-003-236). Zoning was not observed.

Table 6.9.1: Representative analyses of ilmenite compositions

Oxide Wt. %	CL-06-003-158	CL-06-003-236	CL-06-003-186
TiO_2	50.25	52.43	36.00
Al_2O_3	n.d.	n.d.	n.d.
Cr_2O_3	n.d.	n.d.	11.95
FeO_T	48.73	37.42	35.69
MnO	1.28	4.83	n.d.
MgO	n.d.	4.08	13.26
Total	99.34	98.7	98.82
Recalculated Oxide Wt. %			
TiO_2	50.25	52.43	36.00
Al_2O_3	n.d.	n.d.	n.d.
Cr_2O_3	n.d.	n.d.	11.95
FeO^{2+}	43.0	34.99	8.73
FeO^{3+}	5.37	2.7	29.96
MnO	1.28	4.83	n.d.
MgO	n.d.	4.08	13.26
Total	100.80	99.03	99.90
End Members			
$FeTiO_3$	94.79	80.47	19.03
$MgTiO_3$	0	16.73	51.56
Fe_2O_3	5.21	80.47	29.4

Composition data for Candle Lake ilmenite, 1) common ilmenite with no MgO or Cr_2O_3 content. 2) Ilmenite with MgO content <5 wt. %, but no detectable Cr_2O_3. 3) Ilmenite with high Cr_2O_3 and high MgO.

When ilmenite data are plotted on a $FeTiO_3$-$MgTiO_3$-Fe_2O_3 ternary diagram the majority of these data plot at the $FeTiO_3$ endmember although there is a trend of increasing magnesium towards $MgTiO_3$. When compared to other kimberlite megacryst and groundmass ilmenite data, there is a greater similarity between megacryst ilmenite than the groundmass ilmenites (Figure 6.9.3) (Mitchell 1986). Therefore, it is suggested that Candle Lake ilmenites are microcrysts that follow an evolutionary trend towards $FeTiO_3$ (Mitchell 1986).

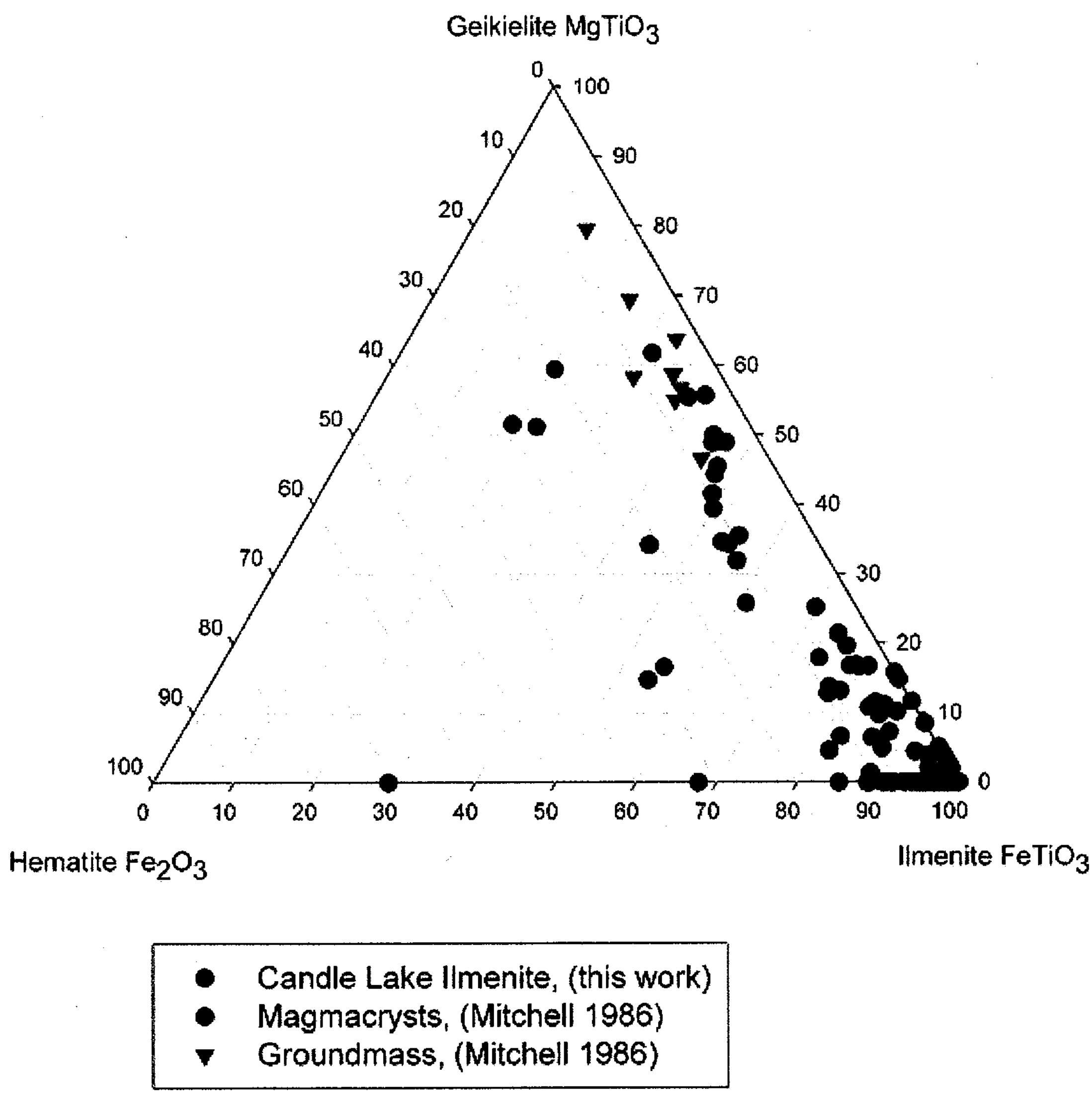

Figure 6.9.3: Fe_2O_3-$FeTiO_3$-$MgTiO_3$ ternary diagram to represent Candle Lake ilmenites. The ilmenites plot close to the $FeTiO_3$ endmember with some grains trending towards $MgTiO_3$ endmember similar to ilmenites from Mitchell (1986).

6.10 Magnetite:

Magnetite is rarely observed in Candle Lake kimberlite. Primary magnetite does occur in atoll spinels as thin rims; however, commonly these rims are too narrow to quantitatively analyze. Magnetite atoll rims have high TiO_2 (8.5-9.92 wt. %) due to contamination from perovskite or anatase.

Secondary magnetite is also observed as a late replacement phase in macrocrysts and phenocrysts that have relict olivine. The olivine is rimmed by a serpentine with a low iron content, which is then rimmed by the magnetite (Figure 6.10.1). The magnetite crystals are angular and the thickness around the serpentine is variable. This secondary magnetite is devoid of titanium and is similar in composition to magnetite obtained from heavy mineral separations.

Figure 6.10.1: Sample CL-06-003-205 (BSE), resedimented kimberlite, macrocrysts with relict olivine (Olv) rimmed by secondary serpentine (S) and secondary magnetite (Mt).

Composition:

Magnetites from heavy mineral separations were only observed in eight samples, of which five were pyroclastic kimberlite. Magnetite collected by heavy mineral separation is likely to be secondary magnetite because the grains are all greater than 100 μm in size, which is much larger than any atoll magnetite. Magnetite from all eight samples have a similar compositions, TiO_2 (n.d.), MnO (n.d.-1.71 wt. %), FeO (26.77-34.96 wt. %) and Fe_2O_3 (62.68-69.8 wt. %). Atoll magnetite compositions are plotted in spinel prisms in Section 6.1.

Chapter 7: Discusion and Conclusions

7.1 Discussion:

Macroscopic vs. Microscopic Petrography

Detailed petrographic work has resulted in the recognition of three different units of kimberlite in the C29/30 vent; pyroclastic kimberlite, resedimented volcaniclastic kimberlite, and lapilli tuff kimberlite. It is highly doubtful that the characteristics that distinguish these three units on a microscopic scale can be used on a macroscopic scale during core logging as seen when comparing Figures 4.1.2 and Figure 5.5.1. It is therefore necessary to undertake petrographic thin section work to identify confidently the pyroclastic, resedimented or lapilli tuff kimberlite units.

Magmaclasts:

Table 7.1 compares magmaclasts occurring in either pyroclastic or tuffistic kimberlite. Pyroclastic kimberlite magmaclasts have a distinct amoeboid shape a result of solidification and crystallization during subaerial pyroclastic eruption. Magmaclasts in tuffistic kimberlite have a sub-spherical-to-elliptical shape as a result of fluidization within the kimberlite pipe (Mitchell et al. 2009b).

Vesicles are a common component of pyroclastic magmaclasts but are absent in tuffistic kimberlite magmaclasts. This suggests that pyroclastic magmaclasts have a higher volatile component.

The groundmass of the pyroclastic magmaclasts is dominantly fine-grained pseudomorphed monticellite where as tuffistic kimberlite magmaclasts have diopside and phlogopite resulting from different volatile conditions and contamination (Mitchell et al. 2009b) during emplacement. This is supported by the presents of atoll structured spinels in the pyroclastic magmaclasts which are absent in tuffistic magmaclasts.

Table 7.1 Magmaclast Comparison between pyroclastic and tuffistic kimberlites:

	Pyroclastic Kimberlite[1]	Tuffistic Kimberlite[2]
Size and Shape	They are 0.25 to 3 mm in size and are amoeboid-to-subrounded in shape with well defined outlines. They commonly have pseudomorphed olivine macrocrysts and phenocrysts enclosed in a very fine grained matrix.	They are <10mm in size and are subspherical-to-elliptical and less commonly curviplaner. They have a kernel of olivine or xenolithic material set in a microcrystalline matrix.
Macrocrysts and Phenocrysts	Macrocrysts are dominantly rounded, moderately fractured pseudomorphed olivines, 0.7 to 10mm in size, but phlogopite is also observed. The olivine is replaced by serpentine and carbonate, relict olivine is not commonly observed. Phenocrysts are fine grained euhedral-to-subhedral pseudomorphed olivine with zoned serpentine replacement. They are on average 0.3mm in size.	Macrocrysts are dominantly anhedral pseudomorphed olivines. Olivines are completely replaced by chlorite and layered chlorite-smectite. Phenocrysts are subhedral-to-euhedral and are less abundant than macrocrysts. Other macrocrysts included garnet and ilmenite but in less abundance.
Mineral Assemblage	Pyroclastic kimberlite is dominantly pseudomorphed olivine and monticellite with minor phlogopite macrocrysts and phenocrysts, set in a spinel, perovskite, apatite, anatase and minor sulphide groundmass. The metastasis is a serpentine-carbonate mixture. Pseudomorphed olivine replaced by serpentine and carbonate is a significant feature of the magmaclast groundmass. Diopside is not present in the C29/30 kimberlite.	Tuffistic kimberlite is dominantly pseudomorphed olivine with and diopside with moderate phlogopite, set in a groundmass of spinels, perovskite, and apatite. The metastasis is a serpentine-carbonate mixture. There is no monticellite present. Diopside is a significant component of the kimberlite.
Vesicles	Vesicles are a minor component and are rounded and infilled by either calcite with dolomite rims or by serpentine and carbonate mixture.	Vesicles are absent from tuffistic kimberlite.

[1] Magmaclast descriptions from this work and Scott-Smith (2008a).
[2] Magmaclast descriptions from Mitchell et al. (2009) and Leckie et al. (2007)

Kimberlite Comparison:

Table 7.2 compares the three types of kimberlites: pyroclastic kimberlite (this work); tuffistic kimberlite from Wesselton (Mitchell, Skinner and Scott Smith 2009); and hypabyssal kimberlite (Mitchell 1995), on the basis of phenocryst mineralogy, interclast matrix and xenolithic material.

The mineralogy of the three types of kimberlite is relatively similar. Olivine is dominantly replaced by serpentine and chlorite-smectite. Phlogopite is present in all three kimberlite types but to a lesser extent in pyroclastic kimberlite.

Spinels are present in all three kimberlite types and all have a TIMAC-QUM zoned composition resulting in similar spinel evolution trend. The compositional similarities between spinels from the three kimberlite types indicate that all kimberlite magmas have a similar source composition and evolution. Atoll structured spinels are absent from most tuffistic kimberlite suggesting an early termination of the spinel evolution (Mitchell et al. 2009b). Monticellite is present in pyroclastic and hypabyssal kimberlite but is always pseudomorphed by serpentine in pyroclastic kimberlite. Diopside is absent from pyroclastic kimberlite, but common in tuffistic kimberlite.

Phenocrysts are similar in the kimberlite types although pyroclastic kimberlite phenocrysts have a distinct serpentine zoned replacement texture, and are better sorted than olivines in tuffistic and hypabyssal kimberlites.

The interclast matrix is significantly different in hypabyssal kimberlite in which there is commonly a two phase segregation texture of a calcite serpentine mixture. Tuffistic magmaclast groundmass is dominantly a diopside-phlogopite mixture. Pyroclastic kimberlite can either be a mixture of serpentine-carbonate, common to resedimented units or a homogenous calcite, observed only in some pyroclastic units.

The abundance of xenolithic material between kimberlite types is very different. Xenoliths are extremely common in both tuffistic and hypabyssal kimberlites and can be megaxenoliths (>100 m; Mitchell 1995). Xenoliths in pyroclastic kimberlite are only 2-5 modal %, angular-to-rounded depending on the amount of resedimentation and <5 cm in size. The lack of xenolithic material in pyroclastic kimberlite maybe a result of the eruption into unconsolidated country rock or, a higher volatility of the magma, or a shallower eruptive center (Lorenz and Kurszlaukis 2006).

Table 7.2 Comparison of pyroclastic, tuffistic and hypabyssal kimberlite components and mineralogy:

	Pyroclastic Kimberlite	Tuffistic Kimberlite	Hypabyssal Kimberlite
Occurrences	Occurs in the crater of class 2 kimberlites and is fine grained moderately sorted clast-to-matrix supported.	Occurs between the crater and root zones of a class 1 kimberlite pipe and is massive, unsorted and matrix-to-clast supported.	Occurs in the root zone of a class 1 kimberlite pipe, and as dikes and sills. Typical igneous textures.
Mineralogy			
Olivine	Olivine is commonly replaced by serpentine and calcite but can be present in some macrocrysts.	Olivine is commonly completely replaced by chlorite and chlorite-smectite.	Olivine is abundant and occurs as subhedral-to-euhedral macrocrysts and phenocrysts
Phlogopite	Phlogopite occurs as macrocrysts and phenocrysts with an elongated lath habit with rounded ends. Phlogopite is also observed as fine and coarse grained cumulates enclosing TIMAC spinels.	Phlogopite occurs as fresh and chloritized macrocrysts and fine grains in the groundmass.	Phlogopite-Kinoshitalite occurs dominantly in the groundmass as a primary late stage phase. Macrocrysts of phlogopite are also present.
Spinels	Spinels are 0.03 to 0.1mm in size and are commonly zoned from TIMAC-to-QUM composition which follows the kimberlite spinel evolutionary Trend 1. Atoll structured spinels are common.	Spinels are common in the magmaclasts and typically have a TIMAC composition and belong to the kimberlite spinel evolutionary Trend 1. There are no atoll structured spinels suggesting early termination of the spinel evolution.	Spinels are 0.01-0.1mm in size and are typically Mg-chromites zoned to Mg-ulvöspinel which follows the kimberlite spinel evolutionary Trend 1. Atoll spinels are very common.
Monticellite	Monticellite is common to the matrix of the magmaclasts and is fine grained <0.08mm and is pseudomorphed by serpentine-carbonate.	Not present.	Monticellite is present and not commonly pseudomorphed by serpentine-carbonate.
Diopside	Not present.	Diopside occurs as fine grained subhedral blocky prisms within the groundmass and magmaclasts.	Primary diopside is absent but secondary diopside can occur rarely in the groundmass of contaminated kimberlites together with pectolite.

Perovskite	Perovskite occurs as subhedral-to-anhedral crystals <0.01mm in size commonly altered or partially altered to anatase.	Perovskite is a minor mineral within the magmaclasts.	Perovskite is commonly rounded-to-euhedral.
Apatite	Apatite is fine grained, euhedral and occurs within the matrix of the magmaclasts.	Apatite occurs as fine grained rounded crystal in the magmaclasts.	Apatite is common and occurs as euhedral prisms or acicular radiating aggregates.
Carbonate	Carbonates occur as calcite and dolomite with minor iron content (<5% FeO_T). Carbonate occurs as replacement of olivine within macrocrysts and phenocrysts, as well as in the magmaclast groundmass and the interclast matrix.	Carbonates occur rarely within the groundmass of the magmaclast and some interclast matrix.	Carbonates are abundant and dominantly calcite with minor dolomites.
Serpentine	Serpentine is very abundant within the groundmass and the interclast matrix. It also occurs as zoned replacement of olivine and monticellite.	Serpentine is abundant as a primary and secondary mineral. It commonly replaces olivine.	Serpentine is abundant as a primary and secondary mineral. Secondary serpentine commonly replaces olivine and monticellite. Primary serpentine occurs in segregations.
Phenocrysts	Phenocrysts are dominantly pseudomorphed olivines replaced by multiple phases of serpentine and rimmed by a botryoidal serpentine. They are 0.1-0.5mm in size and are euhedral-to-subhedral. Phlogopite is also minor phenocrysts.	Phenocrysts are dominantly olivine but diopside and phlogopite are also observed. Olivines are completely pseudomorphed by chlorite and layered chlorite-smectite. Broken crystals are rare. The phenocrysts are surrounded by a thin mantle of diopside and phlogopite.	Phenocrysts are dominantly olivine and are larger than tuffistic kimberlite olivines. They can be fresh or pseudomorphed by serpentine and chlorite.
Interclast Matrix	Two interclast matrices occur, a homogenous calcite, and a serpentine-calcite mixture. The serpentine-calcite matrix is cryptocrystalline homogenous mixture, however; well defined irregular	The interclast matrix is dominantly serpentine or chlorite. Diopside occurs as fine grained prismatic crystals but is uncommon.	Two groundmasses occur, uniform and non-uniform depending on the extent of crystallization. Uniform groundmass is homogeneous and fine-grained consisting of dominantly serpentine and carbonate.

	Pyroclastic Kimberlite	Tuffistic Kimberlite	Hypabyssal Kimberlite
Interclast Matrix (continued)	segregations of calcite occur interstitially to the clasts, they are 0.05-0.2mm angular calcite grains with dolomite rim, the calcite segregations are surrounded by botryoidal serpentine. The second interclast matrix is a cryptocrystalline homogenous calcite with dolomite riming the macrocrysts and magmaclasts.		Non-uniform has a segregation texture with a non uniform distribution of groundmass minerals and mesostasis. Segregations are amoeboid to spherical discrete regions of calcite and primary serpentine.
Xenoliths	Xenoliths are present but in a low abundance 2-5 modal%. They are commonly angular but can be subrounded depending on the amount of resedimentation. Resedimented kimberlite is similar to the PK kimberlite but there is an increase in xenolithic and xenocrystal (quartz) material.	Xenoliths occur in a high abundance >15-90 modal% and range greatly in size from microscopic clasts to extremely large megaxenoliths (>100m) and are angular-to-less commonly subrounded	Abundant within some hypabyssal kimberlites. If the xenoltihic material is >15 modal % and the grains are >4mm in size then it is considered a breccia.

Comparison of pyroclastic kimberlite (this work), tuffistic kimberlite from Wesselton (Mitchell et al. 2009), and hypabyssal kimberlite (Mitchell 1995) showing distinct similarities based on mineralogy, phenocrysts, interclast matrix and xenoliths.

Although there are significant textural differences between the three types of kimberlite, the overall mineralogy of pyroclastic, tuffistic and hypabyssal kimberlite is similar, with all having the same spinel evolutionary kimberlite Trend 1. The mineralogy and spinel composition suggest that Candle Lake pyroclastic kimberlite are archetypal kimberlites having a similar magmatic origin and evolution to tuffistic and hypabyssal kimberlite with the textural differences resulting from emplacement processes.

7.2 Vent Formation at Candle Lake:

As it has been shown above that pyroclastic kimberlite is an archetypal kimberlite by comparison to a hypabyssal and tuffistic kimberlite, and that the emplacement environment of the kimberlite results in variations between kimberlites, then it is important to interpret the Candle Lake C29/30 kimberlite emplacement history.

All drill holes from the 2006 and 2007 exploration season were used to interpret the overall eruptive sequence (Great Western Diamond Corp 2007). The kimberlite magma intruded through the Paleozoic limestone, the sand and siltstones of the Mannville group, and poorly-consolidated mud and siltstones of the lower Colorado Group (Verigeanu et al. 2009). Shale intermixing is seen throughout the upper levels of core including CL-06-003 and mid levels of CL-07-002. The lack of shale along the lower contacts suggests that it may not have been preserved or it was not present at the time of initial eruption. Six main stages of emplacement are postulated; other minor resedimentation events may have occurred.

Stage 1 – an explosive event originating around the location of the CL-06-003 drill hole, excavating Mannville sandstones, Paleozoic limestone and any Colorado mudstone present. At the base of drill holes surrounding the explosive centre there is an increase in the abundance of country rock fragments, up to 5%, where normally country rock fragments account for only 1-2%. The eruption style was probably dry-phreatomagmatic. The absence of accretionary lapilli and soft sediment deformation (bomb-sag textures) support a dry eruption where all water was converted to steam during the eruption process (Brand et al. 2009). Maar volcanism commonly results from phreatomagmatic eruptions, when compared to the C29/30 kimberlite they have a similar shallow bowl shape with a depth to width ratio of 1:5 as well as the absence of dikes and a diatreme. There is however; a minimal amount of crustal xenolithic material incorporated into the kimberlite relative to other studied phreatomagmatic eruptions, which can be 10 to 25% lithic material and may form a breccia (Brand et al., 2009). The minimal amount of xenolithic material present in the Candle Lake kimberlite maybe due to; the higher volatility of the kimberlite magma; the very unconsolidated Mannville group sediments; or an extremely shallow eruptive centre.

Stage 2 – After the initial explosive event there is a period when the pyroclastic kimberlite is reworked and redeposited as resedimented kimberlite. This resedimented kimberlite overlies pyroclastic volcanic kimberlite that has not been reworked around the eruptive center, as observed in drill hole CL-06-003. The pyroclastic unit is not preserved laterally due to processes of resedimentation observed in samples CL-07-006, CL-07-010 and CL-07-014 each progressively further from the explosive center (Figure 5.5.1).

Stage 3 – The resedimented volcaniclastic kimberlites are overlain by a second pyroclastic kimberlite eruption. The thickness of the second eruption sequence is significantly less closer to drill hole CL-06-003 but is substantially thicker in sample CL-07-010 possibly a result of a topographic depression. A lull time in eruption and resedimentation followed, which is followed by the deposition of the lapilli tuff unit (Figure 5.5.1).

Stage 4 – Overlying stage 3 is a resedimented volcaniclastic kimberlite that is intermixed with sediments and shows iron staining? from the overlying sediments (Appendix A). Probably a resurgent (storm event) reworked the upper layers of the pyroclastic kimberlite.

Stage 5 – Deposition of remaining Colorado group sediments and burial.

Stage 6 – Erosion of overlying sediments and deposition of glacial till.

Fort à la Corne Kimberlite

The C29/30 Candle Lake kimberlite has the typical mineralogy and texture of other kimberlites from the Fort à la Corne kimberlite field (Table 7.3). The common characteristics of Fort à la Corne kimberlites are: the shallow bowl shape; pseudomorphed olivine macrocrysts, phenocrysts and amoeboid shaped magmaclasts set in a serpentine-carbonate interclasts matrix; magmaclasts with a monticellite groundmass; and a low abundance of xenolithic material (<5 modal %).

Table 7.3: Comparison of Fort à la Corne Kimberlites.

Fort à la Corne Kimberlites	Candle Lake C29/30	Orion (Pattari et al., 2008)	147 Kimberlite (Lefebvre and Kurszlaukis, 2008)	140/141 Kimberlite (Berryman et al., 2004, Kjarsgaard et al., 2009)
Kimberlite Body Shape	Shallow bowl shape with a north-west to south-east trend. Composed of matrix-to-clast supported pyroclastic kimberlite.	Laterally complex successions of interbedded kimberlite and sediment in a shallow bowl shape.	Poorly sorted, matrix-to-clast supported. Shallow bowl shaped kimberlite body.	Shallow bowl structure, champagne glass shaped with mega graded beds.
Mineralogy	Fine-grained, rounded pseudomorphed olivine macrocrysts and euhedral olivine phenocrysts being more abundant than magmaclasts. Set in a serpentine-carbonate or carbonate interclast matrix.	Fine-grained (<1mm) euhedral crystals of serpentine-carbonated altered olivine (20-50 modal %), minor garnet, ilmenite and phlogopite (<2%).	Altered angular discrete olivine grains which are more abundant than magmaclasts. The interclast matrix is serpentine-carbonated mixture. Pseudomorphed olivine macrocrysts and phenocrysts compose 55-65 modal % of the kimberlite.	Completely pseudomorphed discrete olivines and minor magmaclasts set in a uniform serpentine interclast matrix. Olivines are pseudomorphed by serepentine and carbonate.
Magmaclasts	Amoeboid-to-rounded depending on the extent of resedimentation. With pseudomorphed olivine macrocrysts and phenocrysts protruding	Ameoboid magmaclasts with serpentine-carbonate interstitial matrix. And rounded macrocrysts.	Subelongated-to-irregular-to-curvilinear shape, with abundant olivine phenocrysts, phlogopite laths (rare) and amygdales infilled by carbonate. The groundmass is composed of monticellite,	Subrounded-to-oval-to-curvilinear-to-irregular shaped. Pseudomorphed olivine or xenoliths can form the kernel. The groundmass is composed of spinels,

Fort à la Corne Kimberlites	Candle Lake C29/30	Orion (Pattari et al., 2008)	147 Kimberlite (Lefebvre and Kurszlaukis, 2008)	140/141 Kimberlite (Berryman et al., 2004)
Magmaclasts (continued)	from the margin of the magmaclasts. With abundant spinels, perovskite (altered to anatase), minor phlogopite, and apatite. The groundmass is a fine-grained psuedomorphed monticellite (altred by serpentine and carbonate).		rare perovskite altered to rutile, black euhedral-to-anhedral opaque oxides (spinels) set in a cryptocrystalline carbonate.	perovskite,phenocrysts of olivine protruding from the magmaclast margin, garnet and ilmenite set in a serpentine-carbonate mesostasis.
Xenolithic Material	Dominantly sedimentary angular fragments but granitic clasts are observed (<5%)	Sedimentary angular lithic clasts (<5%)	Minor sedimentary angular clasts with minor rounded granitic xenoliths (<10%).	Xenolith material is rare (<5%), except around the eruptive center.

Comparison of the C29/30 Candle Lake kimberlite to other Fort à la Corne kimberlites; Orion (Pattari et al., 2008), 147 Kimberlite (Lefebvre and Kurszlaukis, 2008) and 140/141 Kimberlite (Berryman et al., 2004 and Kjarsgaard et al., 2009).

Magma Chamber

The presence of pre-eruptive crystallized grains such as phlogopite-spinel cumulates, spinels and perovskites suggests that there is a magma chamber in which the kimberlite magma had a resident time long enough to begin crystallizing. The presence of carbonate infilled vesicles indicates that there was no loss of CO_2 prior to eruption. Although there is mineralogical evidence that a magma chamber should exist there is no geophysical evidence to support a magma chamber (Scott-Smith, 2008a).

7.3 General Conclusions:

Candle Lake kimberlite have similar textures and mineralogy compared to other Fort à la Corne kimberlite and is considered a typical kimberlite found within the Fort à la Corne kimberlite field. Petrographic interpretations are needed in order to identify the different pyroclastic units of Fort à la Corne kimberlite, macroscopic interpretations are insufficient.

References

Ansdell K (2005) Tectonic Evolution of the Manitoba-Saskatchewan Segment of the Paleoproterozoic Trans-Hudson Orogen, Canada. Canadian Journal of Earth Sciences 42: 741-759

Berryman AD, Scott Smith BH, and Jellicoe BC (2004) Geology and Diamond Distribution of the 140/141 Kimberlite, Fort à la Corne, Central Saskatchewan, Canada. Lithos 76: 99-114

Brand BD, Clarke AB and Smeken S (2009) Eruptive Conditions and Depositional Processes of Narbona Pass Maar Volcano, Navajo Volcanic Field, Navajo Nation, New Mexico (USA). Bulletin of Volcanology 71: 49-77

Chakhmouradian AR and Mitchell RH (2000) Occurrence, Alteration Patterns and Compositional Variation of Perovskites in Kimberlites. Canadian Mineralogist 38: 975-994.

Clement CR and Skinner EMW (1985) A Textural-Genetic Classification of Kimberlites, South Africa. Journal of Geology 88: 403-409

Dawson JB and Stephens WE (1975) Statistical Classification Of Garnets From Kimberlite and Associated Xenoliths. Journal of Geology 83: 589-607

Droop GTR (1987) A General Equation for Estimating Fe3+ Concentrations In Ferromagnesian Silicates And Oxides From Microprobe Analyses, Using Stoichiometric Criteria. Mineralogical Magazine 51: 431-435

Field M and Scott Smith BH (1999) Near Survace Emplacemant of Kimberlites: Contrasting Models and Why. Proceeding Volumes of the 7th Kimberlite Conference.

Geological Survey of Canada (2002) Geological Map of Saskatchewan. www.nrcan.gc.ca

Great Western Diamand Corp. (2007) Candle Lake Diamond Project Results of the 2006/2007 Drilling Program Core and LDD Drilling C29/30 Kimberlite. Internal Report.

Grütter HS, Gurney JJ, Menzies AH and Winter F (2004) An Updated Classification Scheme For Mantle-Derived Garnet, For Use By Diamond Explorers. Lithos 77: 841-857

Harvey SE, Kjarsgaard BA and Kelley LI (2001) Kimberlites of Central Saskatchewan: Compilation and Significants of Indicator Mineral Geochemistry with Respect to Diamond Potential; in Summary of Investigations. 2: Saskatchewan Geological Survey, Sask. Energy Mines, Misc. Rep. 2001-4.2

Leckie Da, Kjarsgaard BA, Peirce JW, Grist AM, Collins M, Sweet A, Stasiuk L, Tomica MA, Eccles DR, Duffesne MB, Fenton HM, Pawlowrez JG, Balzer SA, McIntyre DJ, McNeil DH (1997) Geology of a Late Cretaceous Possible Kimberlite at Mountain Lake, Alberta – Chemistry, Petrology, Indicator Minerals, Aeromagnetic Signature, Age, Stratigraphic Position and Setting. GSA Bulletin 3441: 202

Irvine TN (1965) Chromian Spinel As A Petrogenetic Indicator. Canadian Journal of Earth Sciences 2: 648-672

Kjarsgaard B, Harvey S, McCintock M, Shimell, Fourie L, Du Plessis D and Read G (2009) Geology and Evaluation Strategy of the Star and Orion South Kimberlite, Fort à la Corne, Canada. Lithos 112: Supplement 1 47-60

Lefebver N and Kurszlaukis (2008) Contrasting Eruption Styles of the 147 Kimberlite, Fort à la Corne, Saskatchewan, Canada. Journal of Volcanology and Geothermal Research 174: 171-185

Lorenz V. and Kurszlaukis (2006) Root Zone Processes in the Phreatomagmatic Pipe Emplacement Model and Consequences for the Evolution of Maar-Diatreme Volcanoes. Journal of Volcanology and Geothermal Research 159: 4-32

Masun KM (1999) The Petrography and Mineralogy of the Lac de Gras Kimberlite Field, Slave Province, Northwest Territories: A Comparative Study. M.Sc. Thesis. Lakehead University

Mitchell RH (1978) Mineralogy of the Elwin Bay Kimberlite, Somerset Island, N.W.T., Canada. American Mineralogist 63: 47-57

Mitchell RH (1986) Kimberlites: Mineralogy, Geochemistry and Petrology. Pleunum Press, New York.

Mitchell RH (1995) Kimberlites, Orangeites, and Related Rocks. Plenum Press, New York.

Mitchell RH (1997) Kimberlites, Orangeites, Lamproites, Melilitites, and Minettes: A Petrographic Atlas. Almaz Press Inc. 243 pp.

Mitchell RH and Clarke DB (1976) Oxide and Sulphide Mineralogy of the Peuyuk Kimberlite, Somerset Island, N.W.T., Canada. Contributions to Mineralogy and Petrology 56: 157-172

Mitchell RH, Kjarsgaard BA and McBride JA (2009) Mineralogy of Juvenile Lapilli Fort à la Corne Pyroclastic Kimberlites. [Abstract] V 24A-03 Presented at the Joint Assembly AGU, Toronto Canada.

Mitchell RH, Skinner EM and Scott Smith BH (2009) Tuffistic Kimberlites from the Wesselton Mine, South Africa: Mineralogical Characteristics Relevant to Their Formation. Lithos. 112S: 452-464

Pattari A, Cas RF, Lefebvre N, Robey J, Kurszlaukis S and Webb K (2008) Eruption Processes and Facies Architecture of the Orion Central Kimberlite Volcanic Complex, Fort à la Corne, Saskatchewan; Kimberlite Mass Flow Deposits in a Sedimentary Basin. Journal of Volcanology and Geothermal Research 174: 152-170

Scott Smith BH (2008a) The Fort a la Corne Kimberlites, Saskatchewan, Canada: Geology, Emplacement and Economics. Journal of the Geological Society of India 71: 11-55

Scott Smith BH (2008b) Canadian Kimberlites: Geological Characteristics Relevant to Emplacement. Journal of Volcanology and Geothermal Research 174: 9-19

Scott Smith BH, Nowicki TE, Russell JK, Webb KJ, Hetman CM, Harder M and Mitchell RH (In Press) Kimberlites: Descriptive Geological Nomenclature and Classification. Abstract 9th International Kimberlite Conference.

Shee SR (1985) The Petrogenesis of the Wesselton Mine Kimberlites, Kimberly, Cape Province, R.S.A. Ph.D. Thesis. University of Cape Town.

Schiffman P and Fridleiffson GO (1991) The Smectite-Chlorite Transition in Drillhole NJ-15 Nesjavellir Geothermal Field, Iceland: XRD, BSE and Electron Microprobe Investigation. Journal of Metamorphic Geology 9: 679-696

Verigeanu D, Getman CM, Jellicoe B and Baumgartner MC (2009) Preliminary Geology, Mineral Chemistry and Diamond Results from the C29/30 Candle Lake Volcanic Complex, Saskatchewan, Canada. Lithos 112: 529-540

Zonneveld JP, Kjarsgaard BA, Harvey SE, Heaman LM, McNeil DH and Marcia KY (2004) Sedimentologic and Stratigraphic Constraints On Emplacement of the Star Kimberlite, East-Central Saskatchewan. Lithos 76: 115-138

APPENDIX A

THIN SECTION AND HANDSAMPLE DESCRIPTIONS

C29/30 Kimberlite: CL-06-003 Thin Section & Hand sample Descriptions:

Drill Hole Description:

Diamond drill hole CL-06-003 was drilled to test the north-eastern portion of the southern C29/30 kimberlite. The drilling project is located in the Candle Lake area. CL-06-003 has a vertical dip, with an intersection of kimberlite from 147.90m to 251.3m. The drill hole was stopped at 276.83m after intersecting the Manville Group sands and the Paleozoic limestone. The following ten samples where taken within the kimberlite interval.

All thin sections are oriented so the north-south axis of the photograph is parallel to the vertical axis of the drill core.

Sample 158A:

The sample was taken from a depth of 158.49 to 158.61m from surface. It is very fine grained, predominantly pseudomorphic olivine with a ratio of 75:1 to magmaclasts. The sample is set in a cryptocrystalline brown-green interclast matrix (serpentine and calcite). The grains show no preferred orientation and are commonly fractured along the edges. The magmaclasts have a poorly defined amoeboid shape.

There is minor occurrence of rounded-to-subrounded open vesicles that are surrounded by a ring of fine calcite grains. The vesicles are on average 0.4mm in diameter. There are coarse fragments, 0.3-1.2mm in size, of angular-subangular carbonate country rock fragments. This sample, based on the textures of the phenocrysts, magmaclasts and heavily altered matrix, is a resedimented volcanic kimberlite.

Phenocrysts:

Pseudomorphic olivines are the most abundant phenocryst. The olivine is replaced with a light brown-green serpentine, and commonly has a calcite core. The replacement serpentine shows a intimately intergrown texture which is also seen in the surrounding interclast matrix. The pseudomorphic olivine is rounded and shows interclast fracturing, suggestive of reworking. The maximum grain size reaches 2.5mm but on average is 0.4mm.

Phlogopite grains are less common and make up only about 4% of the total sample. The grains are on average 0.8mm but reach a maximum size of 2mm (measured with respect to the long axis).

Magmaclasts:

Magmaclasts are a minor component of the sample compared to the phenocrysts. The magmaclasts matrix is composed of serpentine, calcite and chlorite which are a darker brown-green than the interclast matrix. Within the magmaclasts matrix there are perovskite, spinels, calcite rimming grains and serpentinized relict olivine grains. The magmaclasts range in size from 0.8mm to 1.5mm. The perovskites within the matrix have an average size of 0.2mm.

80% - Serpentine
15% - Calcite

3% - Perovskite
2% - Chlorite
Trace Opaques

Interclast Matrix:

The interclast matrix is a cryptocrystalline brown-green colour composed of serpentine, calcite and chlorite with minor opaques. Magnetite is a minor component of the opaques, whereas the rest of the opaques are extremely fine grained serpentine. Magnetite is found dominantly as rim textures which are associated with serpentine, but occur also as very fine-to-fine grained euhedral crystals in the interclast matrix. Calcite occurs as very fine grained component of the matrix, but also as fine grained cumulates of deformed interstitial infilling. The interclast matrix encloses both phenocrysts and magmaclasts masking majority of grain or magmaclasts edges and distorts the boundaries of the grains.

70% - Serpentine
20% - Calcite
10% - Chlorite

Sample 173B:

The sample was taken at a depth of 173.53m to 173.65m. It is very fine grained with a minor mineral orientation parallel to the core axis (horizontal). The main components of the sample include pseudomorphic olivine and magmaclasts set in a serpentine-calcite matrix. The pseudomorphic olivines are the dominant feature of the sample with a ratio to Magmaclasts of 15:1. Calcite is a significant component of the matrix, 40%; it is also found as late thin calcite veins that crosscut the sample parallel to the core axis (vertical). Overall the grains tend to be rounded and mainly matrix-supported with minor grain to grain contact. It appears to be a crystal tuff unit.

Phenocrysts:

Phenocrysts are predominantly pseudomorphic olivine with an average grain size of 0.2mm within a range of 0.05 to 0.7mm. The phenocrysts have undergone extensive serpentinization with minor calcite replacement at the core. The pseudomorphic olivines are dominantly rounded but some do show a subhedral habit, and thin rims of the magmaclasts matrix. The rims are thin less than 0.02mm which contain trace opaques and perovskites.

Phlogopite grains are a minor component of the rock; they are subhedral, with a definite cleavage, pleochroic and have a 2nd order birefringence. The average size is 0.25mm, parallel to the cleavage, but has a maximum size of 1.1mm and is found in a similar manner as the pseudomorphic olivine, within the interclast matrix.

Magmaclasts:

Range in size from 0.1mm to 2.1mm; the average being about 0.25mm. The coarser magmaclasts (>0.7mm) have a rounded pseudomorphic olivine (>0.4mm) within the core of the magmaclasts. The matrix of the magmaclasts is very fine grained, dark green-to-brown, and if the magmaclasts are large enough, then they may show a zoning.

The zoning is defined by a colour change from the core to the rim; from dark brown to dark green respectively. The matrix encloses fine to medium grained pseudomorphic olivines that are rounded-to-subhedral. There is also minor phlogopite. Both olivine and phlogopite have an average size of 0.2mm. The matrix is also composed of fine grained (>0.2mm) perovskite-magnetite-opaques-chlorite-serpentine-calcite-spinel and vesicles.

80% Serpentine as pseudomorphic olivine and within the matrix
10% Calcite
5% Opaques
4% Chlorite
1% Perovskite
Trace Phlogopite

Interclast Matrix:

Very fine grained, composed of serpentine-calcite and chlorite. The interclast matrix is visible around the rim of most components as a light yellow coloured serpentine. Voids within the matrix are in filled by calcite, formed as fine grained aggregates. The voids are angular and as large as 250μm.

45% Yellow Serpentine
15% Grey Serpentine
40% Calcite

Sample 182A:

This sample was taken from a depth of 182.08 to 182.27m. In handsample there is a distinct banding of moderately sorted fine and coarse grained zones. The fine to medium gained bands are 1cm thick and are dark grey-to-black with a white calcite matrix, whereas the coarse grained bands are light grey-to-green colour with grains up to 1cm but on average 3mm. In thin section the sample is poorly sorted and shows a close relative abundance of phenocrysts to magmaclasts, 2:1 respectively. The phenocrysts and magmaclasts are set in a matrix that is dominated by angular interstitial calcite with dark brown rims of serpentine and chlorite. Calcite is also found as thin veins cutting parallel to the core axis. This sample is considered a pyroclastic kimberlite.

Phenocrysts:

Phenocrysts are only slightly more abundant then the magmaclasts component. Pseudomorphic olivines are the most abundant phenocrysts; they are rounded but may show some subhedral form and are replaced with a light green serpentine. 1 in 10 pseudomorphic olivines have a calcite core. The size range is from 0.2mm to 10mm but on average is 0.3mm. The grains show a calcite-chlorite rimming which is less than 0.5mm. The phenocrysts show now alignment.

Phlogopite is almost absent as a phenocryst, but does occur up to 1mm in size. Phlogopite does have a greater presence in the magmaclasts matrix and reach up to 1cm measured along the long axis.

Magmaclasts:

Magmaclasts range in size from 0.3mm to 13mm but on average is 0.6mm. They have an undefined shape but are subrounded, not amoeboid. They have a defined rim against the calcite matrix. The matrix is composed of a dark brown serpentine and contains serpentine altered pseudomorphic olivine, phlogopite as discussed above, opaques which are mostly very fine grained serpentine, chlorite and minor calcite. There is also an unknown isotropic mineral that is white in plane light, with rimmed alteration of serpentine causing a rounding of the grain. Along the edge of the magmaclasts matrix there are serpentinized pseudomorphic olivine grains that are euhedral-to-subhedral that are partially enclosed within the matrix but extruded into the interclast matrix. If abrasion where to occur, these fragments would have been separated from the magmaclasts.

85% - Serpentine
5% - Phlogopite
5% - Opaques
3% - Chlorite
1% - Spinel
1% - Calcite

Interclast Matrix:

The interclast matrix is composed almost entirely of fine grained calcite, >1 to 30μm. There are minor opaques and serpentine along grain contacts. There is also calcite veining crosscutting the matrix and grains.

97% - Calcite
2% - Opaques
1% - Serpentine

Sample186B:

Sample was taken from a depth of 185.97 to 186.12m. The dominate components are fine-to-coarse pseudomorphic olivines, with additional phlogopite macrocrysts, and magmaclasts in a interclast matrix of dominantly calcite and serpentine. The ratio of phenocrysts to magmaclasts is 20:1, respectively. It is moderately sorted with a fabric at 80° to the core axis, indicative of a shallow dip. In handsample there is a visible 4mm thick, dark black, serpentine vein that runs 40-50° to the core axis. The interclast matrix is a very light brown to grey, composed of calcite serpentine and chlorite. Calcite also occurs as very thin veins which cut at 40° to the core axis. Sample 186B represents a pyroclastic kimberlite unit.

Phenocrysts:

Pseudomorphic olivines are the primary constituent and are rounded-subrounded with serpentine replacement and calcite cores. There is a slight orientation to the phenocrysts perpendicular to the core axis. The grains are rimmed by two phases of interclast matrix, first a very fine grained calcite rim followed by a thin dark brown serpentine rich rim. Coarse pseudomorphic olivines, >1.5mm, are rounded to subrounded, whereas the fine grained <1.5mm are rounded-to-subhedral. The maximum grain size is 10.2mm but grains less than 0.5mm dominates the sample.

Phlogopite is a minor component, occurring as small laths, with parallel cleavage, 2nd to 3rd order birefringence and is randomly orientated in both the magmaclasts and free phenocrysts. The maximum lengths of the grains are 4mm and on average 1.4mm along the cleavage.

Magmaclasts:

The magmaclasts are variable in size and range from 0.3mm to 12mm. Within the coarser magmaclasts there is commonly a coarse pseudomorphic olivine or phlogopite. The coarse internal pseudomorphic grains reach a maximum of 10.5mm. There are minor vesicles within the magmaclasts matrix, <1mm. The magmaclasts form shows no visible sagging or welding textures. The magmaclasts matrix is fine grained with two phase, dark-grey to a dark green-brown colour, and is composed of serpentine-chlorite-perovskite-opaques and trace spinel.

85% - Serpentine
5% - Calcite
5% - Opaques
2% - Phlogopite
2% - Chlorite
1% - Perovskite

Interclast Matrix:

The interclast matrix is composed of two phases of serpentine distinguished by a colour change from a dark cryptocrystalline serpentine to a light brown serpentine-calcite interclast matrix. There is interstitial calcite between distinguished grains. The interclast matrix does not overprint the grain boundaries but supports the grains and minimizes contact between grains. Moderate amount of rounded opaques and brown perovskites up to 1mm, occur freely in the interclast matrix.

50% - Serpentine
40% - Calcite
5% - Opaques
5% - Perovskite

Sample 195A:

This sample was taken from a depth of 195.78 to 195.98m. Appears coarse grained, dark black, with abundant pseudomorphic olivine macrocrysts, and magmaclasts up to 15mm. Pseudomorphic olivines proportional to magmaclasts are 15:1 respectively. Macrocrysts of shiny white phlogopite are visible in handsample. The sample is poorly sorted with a minor grain orientation perpendicular to the core axis. There is calcite veining from 1 to 4mm thick at 30° and 80° from the core axis. Calcite is also found as medium to coarse grained interstitial infilling between macrocrysts and magmaclasts. The serpentine alteration shows three phases of mantling, all fine grained brown to brown-green, becoming lighter away from the core. Both the phenocrysts and the magmaclasts are poorly defined against the matrix and are fractured or have concoidal fractures along edges suggesting reworking as a resedimented volcanic kimberlite.

Phenocrysts:

The main phenocrysts are pseudomorphic olivine, and they have a variable grain size reaching a maximum of 2.2cm but on average they are 0.4mm. Pseudomorphic olivine has been replaced by yellow-green serpentine as well as calcite along internal fractures. Unlike previous samples up cross-section there is a significant amount of unaltered relict olivine at the cores of the pseudomorphic olivine phenocrysts. The grains are rounded-to-subrounded but do show moderate fracturing.

60% - Serpentine
30% - Calcite
10% - Olivine

Phlogopite is only a minor component of this sample and is located in the matrix. The grains on average are 1mm but reach a maximum of 15mm, measured along the long axis and are rounded along the lath ends.

Brown unknown mineral – characteristics include, pleochroic brown, brown under polarized light with edges showing high birefringence as well as a cleavage parallel to the long axis, possibly a mica.

Magmaclasts:

The magmaclasts reach a maximum size of 14mm, but averages 4mm. They contain coarse-to-fine pseudomorphic olivines that reach a maximum size of 13mm, as well as perovskite, spinel, chlorite, calcite, minor phlogopite, serpentine and opaques. The pseudomorphic olivines vary from rounded-subhedral as the grains range from coarse-fine respectively.

There are fine rounded cumulates of calcite most likely due to secondary vesicle infilling, during resedimentation. The matrix is a light grey, cryptocrystalline most likely composed of serpentine and calcite. The magmaclasts edges have concoidal fracturing with proximal fine fragmentation in the interclast matrix. Perovskite is in higher concentration in the brown magmaclasts matrix then in previous samples.

80% - Serpentine
7% - Calcite
5% - Opaques
3% - Chlorite
2% - Phlogopite
2 % - Perovskite

Interclast Matrix:

There is a segregation texture between a light-brown interclast matrix and a charcoal-grey interclast matrix. This variation in colour is due to the increase of calcite in the latter. The light- brown interclast matrix rims the grains and blurs the contact between the interclast matrix and the phenocrysts and magmaclasts components. The charcoal-grey is a calcite rich and occurs between the grains which resembles interstitial calcite that has been reworked.

65% - Serpentine
35% - Calcite

Sample 205A:

The sample location is from 205.12 to 205.30m. The sample is poorly sorted with abundant pseudomorphic olivine and moderate magmaclasts, 20:1 respectively. Other macrocrysts included phlogopite, and garnet, visible in handsample. In handsample there are also visible coarse xenoliths of carbonate host rock, 4mm in size. There is no preferred orientation to any of the components. Magmaclasts are only a minor component of the rock, but they do vary in size. The interclast matrix is light green, composed of serpentine and mica, with minor perovskite and differentiates of calcite in irregular fine to medium grained pockets. Calcite is also found as thin veins. The sample shows resedimented textures, including undefined magmaclasts and macrocrysts variably angled though the core, fractured magmaclasts and internal fracturing of phenocrysts, as well as a multiphase interclast matrix.

Phenocrysts:

The dominate phenocrysts are pseudomorphic olivines that have been serpentinized with only minor calcite replacement along internal fractures. There is, however, as in sample 295A relict olivine at the core of the grains. The grains reach a maximum of 17mm but on average are 2.2mm. The grains are commonly rounded but there are examples of euhedral-to-subhedral grains, as the grains reduce in size.

75% - Serpentine
15% - Olivine
10% - Calcite

Phlogopite – is only a minor component, with rounded edges and is on average only 0.1mm but can be up to 0.4mm.

Magmaclasts:

The magmaclasts are poorly formed and have an amoeboid shape with abundant fragments surrounding the magmaclasts and associated to conchoidal fractures along the edges. Calcite has in filled the void spaces in the magmaclasts matrix producing round fine grained calcite aggregates. The matrix is a slightly green colour (darker than interclast matrix) with abundant opaques, perovskite, phlogopite, and chlorite. The matrix also contains fine-coarse grained subhedral to euhedral pseudomorphic olivine with olivine cores. The magmaclasts do not have well defined edges, slightly intermixed with interclast matrix and small olivine grains. The magmaclasts reach a maximum size of 24mm but on average are 3mm.

70% - Serpentine
10% - Calcite
10% - Opaques
5% - Chlorite
3% - Phlogopite
2% - Perovskite
Trace – Garnet

Interclast Matrix:

The matrix is homogenous very fine grained light grey-green with abundant serpentine and calcite, however; there are cumulates of calcite grains possibly interstitial calcite infilling before resedimentation.

70% - Serpentine
25% - Calcite
5% - Chlorite

Sample 219A:

Similar to sample 205A and 205B but is located further down hole at 219.77 to 219.92m. The sample is coarse grained, dark grey-to-black, with coarse pseudomorphic olivine macrocrysts, which is the slightly more dominate feature of this rock, with respect to magmaclasts, 3:1. The sample is poorly sorted with no preferred orientation of grains. Interclast matrix is very fine grained with a green colouring and relatively abundant calcite. There is less phlogopite macrocrysts than viewed in sample 205A. However; in handsample there are a moderate amount of phlogopite phenocrysts. In handsample carbonate xenoliths from the country rock are visible as angular fragments. The sample is a resedimented volcanic kimberlite.

Phenocrysts:

Pseudomorphic olivine is the most abundant phenocrysts and on average has a grain size of 0.8mm but reaches a maximum size of 2.6mm. The grains are rounded but the finer grains do show subhedral form. The grains have been replaced by serpentine and minor calcite along internal fracturing. The pseudomorphic olivines do have an unaltered relict olivine core.

94% - Serpentine
5% - Olivine
1% - Calcite

Magmaclasts:

The magmaclasts have a poorly defined amoeboid shape with a maximum size of 2.5mm but on average they are 0.75mm. The magmaclasts are composed of pseudomorphic olivine (with olivine cores) phlogopite, perovskite, spinel, serpentine, calcite and opaques. Calcite has in filled rounded voids. The magmaclasts have concoidal fracturing along the grain boundary and fragmentation into the interclast matrix suggesting abrasion reworking.

80% - Serpentine
5% - Calcite
5% - Opaques
3% - Olivine
3% - Chlorite
2% - Phlogopite
2% - Perovskite

Interclast Matrix:

Is homogenous, light brown and cryptocrystalline, composed of what is believed to be serpentine and calcite with minor calcite cumulates as relict interstitial infilling. The interclast matrix obscures the grain boundary and edges of phenocrysts and magmaclasts. There are also minor fine grained opaques set in the interclast matrix.

85% - Serpentine
10% - Calcite
3% - Chlorite
2% - Opaques

Sample 222A:

This sample was taken from a depth of 222.80 to 222.92m. The sample is medium-to-coarse grained, poorly sorted composed dominantly of phenocrysts of pseudomorphic olivine, phlogopite and juvenile magmaclasts. The ratio of pseudomorphic olivine to magmaclasts is 5:1. Fragments of carbonates are found in the matrix, and are angular and tan coloured. There is minor calcite veining parallel to the core axis. There are thin opaque linear features at 30° to the core axis, in reflected light the linear features are still black, indicating possible thin fractures. The grains show no distinct fabric but the interclast fracturing and overprinting of the matrix suggest a resedimented volcanic kimberlite unit.

Phenocrysts:

Pseudomorphic olivine are the dominate component of the sample and are rounded to oval shaped with extreme serpentinization; however, some cores still have primary olivine. The grains show an internal fracturing which is recognized by calcite and serpentine interclast matrix infilling. The grains have a maximum size of 6mm but on average is 1.2mm. The grains that are fractured can show an angular edge.

90% - Serpentine
5% - Olivine
5% - Calcite

Magmaclasts:

The magmaclasts are poorly defined with an amoeboid shape, with no preferred orientation. The maximum magmaclasts size is 1.4cm but on average they are 3mm. The matrix of the magmaclasts is a dark green serpentine with minor calcite. The enclosed pseudomorphic olivine are subhedral to euhedral whereas the free pseudomorphic phenocrysts are typically rounded (Figure 222A). The magmaclasts often have a coarse relict olivine at the core. The matrix edge does show concave fracturing. Other components of the matrix are phlogopite, perovskite, chlorite, opaques, and spinels, all fine grained.

80% - Serpentine
10% - Opaques
3% - Calcite
3% - Phlogopite
2% - Perovskite

2% - Olivine

Interclast Matrix:

The interclast matrix is light brown composed of serpentine, calcite and chlorite. The calcite is very fine grained as is the serpentine but calcite also occurs as irregular pockets possibly interstitial infilling before resedimentation. The interclast matrix does grade into the phenocrysts and magmaclasts masking the grain outlines.

Sample 236A:

The sample was taken from a depth of 236.64 to 236.82m. The handsample shows an abundant amount of coarse angular xenoliths of country rock (carbonate). Also visible in handsample are thin, non oriented, green-white calcite veins. The interclast matrix is dark black; fine grained, composed of serpentine-chlorite-perovskite and minor calcite surrounding pseudomorphic olivine, phlogopite and magmaclasts. The pseudomorphic olivine relative to magmaclasts is 3:2 respectively. The thin section orientation maybe incorrect, the up direction is assumed by country rock xenoliths. The sample is poorly sorted with no preferred orientation but the grains are well defined within the matrix. The sample represents a pyroclastic kimberlite deposit.

Phenocrysts:

Pseudomorphic olivines are the dominate feature of the sample and have a grain size ranging from 0.1 to 2.5mm and are completely replaced by serpentine and calcite. Grains that are 2.5mm or larger are replaced by platy serpentine and fine grained calcite but do have a relict olivine at the core. The coarse grains are rounded where as the finer grains are subhedral.

80% - Serpentine
10% - Calcite
10% - Olivine

Phlogopite is rounded with no preferred orientation and has an average size of 3mm.

Magmaclasts:

The magmaclasts have a maximum size of 2.3mm but on average is 0.6mm and have an amoeboid shape with minor fragmentation. There is a minor fabric associated to the magmaclasts, sub-horizontal to the core axis. The matrix of the magmaclasts is very fine grained composed of serpentine, calcite and chlorite with minor phlogopite, pseudomorphic olivine that range up to 1.4cm, opaques, perovskite and spinel. There are no visible vesicles but minor subrounded calcite nodules that may have in filled the vesicles.

80% - Serpentine
8% - Calcite
5% - Opaques
3% - Chlorite
2% - Phlogopite

2% - Perovskite

Interclast Matrix:

The interclast matrix is cryptocrystalline composed of serpentine and calcite. There is a multiphase interclast matrix which is recognized by the variable colour change from a dark grey to a light brown. The difference arises because of the increase of calcite in the dark grey interclast matrix. The light brown is associated to surrounding the magmaclasts possibly interchange from the magmaclasts matrix to the interclast matrix. The dark grey interclast matrix contains more calcite.

Sample 247B:

Sampled from a depth of 247.53m to 247.64m, this sample contains coarse xenoliths of country rock up to 1cm in size that are angular carbonated fragments. Overall the sample is poorly sorted with no fabric or mineral alignment. There is minor calcite veining (at variable angles) and late in filling of interstitial spaces and vesicles. The sample shows moderate compact textures with only moderate matrix supported grains. This sample shows defined amoeboid magmaclasts structures and in tacked pseudomorphic olivines suggesting a pyroclastic deposit.

Magmaclasts:

Coarse grained, ranging in size form 0.3mm to 2.4mm with an average size of 2mm and are randomly distributed. The matrix is a dark heterogeneous grey-green colour with very fine components less then 0.2mm and forms amoeboid magmaclasts. The main components of the matrix are opaques-perovskite-chlorite-serpentine and vesicles, which do enclose some rounded-subhedral pseudomorphic olivine and phlogopite. The pseudomorphic olivines are also observed to be only partially enclosed in the magmaclasts matrix, and project out of the magmaclasts into the interclast matrix of the rock. These pseudomorphic olivines range in size form 0.1mm to 1.8mm but on average is 0.2mm. The phlogopite has an average size of 0.2mm. There is a minor zoning within the matrix, visible only in larger magmaclasts but is not a universal texture of all magmaclasts. The zone grades to a darker grey colour.

80% Serpentine as pseudomorphic olivine and within the matrix
5% Opaques
1% Phlogopite
5% Perovskite
5% Calcite
4% Chlorite

Phenocrysts:

Pseudomorphic olivines are rounded-subhedral with an average size of 0.4mm but range from 0.1mm to 0.8mm and are completely serpentinized. There is minor calcite replacement at the core. The pseudomorphic olivine are much smaller on average to the magmaclasts but are more common with a ratio of 10:1.

Phlogopite is medium grained with an average size of 0.25 (along the cleavage) rounded and found within the interclast matrix. Phlogopite is pleochroic brown, 2nd order birefringence and distinct parallel cleavage.

Interclast Matrix:

Very fine grained, light brown, homogenous, cryptocrystalline and composed mostly of serpentine and calcite. There is late calcite in filling of voids, and crosscutting veins. The main components of the sample are only in minor contact with each other.

80% Serpentine
20% Calcite

C29/30 Kimberlite: CL-07-006 Thin Section & Hand sample Descriptions:

Drill Hole Description:

DDH CL-07-006 was drilled to test the north-west trending low magnetic anomaly. The hole intersected kimberlite from 190.01-240.39 a total of 50.38m. Above the kimberlite there was glacial till. The hole was terminated at 242.01m as it intersected sands from the Manville Group.

Sample 195A (897-171):

Sample 195 was taken from a depth below surface at 195.44 to 195.67m. It is a fine-to-medium grained sample that is light green with minor thin, less than 1mm, dark black serpentine-magnetite bands. There is no mineral alignment and the sample is poorly sorted. There are a moderate amount of angular fragmented quartz and carbonate grains. Pseudomorphic olivines are the dominate clast in this sample with a ratio to magmaclasts of 20:1. There is only minor internal fracturing, with most PMO being subhedral. The magmaclasts are small due to fragmentation and are poorly defined against the interclast matrix. This sample shows no textures of being reworked and is therefore considered a resedimented volcanic kimberlite.

Phenocrysts:

Pseudomorphic olivines are the predominate clast and are fine grained up to 1mm. They have a subhedral shape and are replaced by serpentine with small calcite cores and very thin cryptocrystalline calcite rims. Some grains are completely replaced by fine to medium grained calcite. There is no major internal fracturing. The lack of internal fracturing is most likely due to the small grain size where internal fracturing is naturally minimal.

Angular fragmented quartz grains are moderately abundant. They have a maximum grain size of 1mm. They are white in plain light and have undgulose extinction.

Phlogopite grains vary in size from 2mm to 0.3mm, with an average grain size of 1mm. They are mostly rounded but some do have angular fractured ends. Others are bent perpendicular to the cleavage and have undgulose extinction.

Magmaclasts:

The magmaclasts are only a minor component of this sample. They have a rounded-to-amoeboid shape with a grain size up to 1.5mm but on average are 1mm. There are only trace vesicles the dominant phenocryst enclosed in the matrix is subhedral pseudomorphic olivine that is replace by serpentine and calcite. Phlogopite, opaques and perovskite are also common within the magmaclasts matrix but on a much small scale. The matrix is slightly darker brown than the interclast matrix. There appears to be a slight absorption of the magmaclasts into the interclast matrix.

75% - Serpentine
10% - Chlorite
5% - Calcite
5% - Opaques

3% - Phlogopite
2% - Perovskite

Interclast Matrix:

The interclast matrix is cryptocrystalline and is a light brown colouring. There are minor single opaques as well as perovskite within the interclast matrix. There are poorly defined calcite rich zones which appear to be interstitial.

60% - Serpentine
25% - Calcite
8% - Chlorite
5% - Opaques
2% - Perovskite

Sample 208 (897-172):

This sample was taken from a depth of 208.31 to 208.56m from surface. It is medium-to-coarse grained dominated by PMO and magmaclasts clasts in a ration of 1:1. There are moderate coarse mudstone angular fragments up to 5mm and minor carbonate fragments up to 2mm randomly dispersed throughout the sample. The sample is moderately sorted and shows no mineral alignment. There is minor irregular carbonate veining, horizontal to the core axis. The PMO are rounded to subhedral and the magmaclasts have an amoeboid shape with moderate rounded vesicles. This sample is interpreted as a pyroclastic volcanic kimberlite based on the lack of reworked interclast matrix and minimal fracturing of PMO and magmaclasts.

Phenocrysts:

Pseudomorphic olivines have an average size of 0.5mm but have a maximum size of 2mm. They are completely replaced by very fine grained serpentine and calcite with calcite infilling along internal fracturing. Most grains are rounded but some are subhedral.

Phlogopite is up to 0.5mm but on average it 0.4mm has fractured and grounded edges. Commonly elongated oval shaped, not fractured to the extent of being reworked.

Unknown mineral is rounded, dark brown colouring in plain light with calcite infilling and a dark brown intimate intergrowth texture.

Magmaclasts:

Magmaclasts have an average grain size of 0.4mm similar to the PMO but have a larger maximum size of 3mm. The magmaclasts have an amoeboid shape some are slightly rounded with grains within the matrix extruding out into the interclast matrix which would not occur if they magmaclasts would have been reworked. There are moderate vesicles rounded with calcite infilling. The matrix is dark brown composed of subhedral calcite replaced PMO and minor opaques and perovskite, with minor phlogopite.

60% - Serpentine
30% - Calcite
5% - Opaques
3% - Chlorite

1% - Phlogopite
1% - Perovskite

Interclast Matrix:

The interclast matrix is dominated by a dark brown serpentine with moderate opaques and perovskite. There is a second lighter brown phase attributed to an increase in calcite. The lighter zones are irregular shaped most likely an interstitial phase. Both interclast matrix phases are cryptocrystalline and are well defined against both the magmaclasts and PMO.

55% - Serpentine
35% - Calcite
13% - Chlorite
5% - Opaques
1% - Phlogopite
1% - Perovskite
Minor carbonate and mudstone components

Sample 214 (897-173):

This sample was taken from a depth of 214.79 to 215.05m from surface. The top direction of the thin section is unknown. There is minor bedding present with one side of the thin section having and increase in magmaclasts. It is light green very fine grained with minor medium grained clasts. There is no late carbonated or serpentinized veining. The sample is well sorted relative to pyroclastic volcanic kimberlite samples, with an average grain size of 0.2mm. The dominate clasts are angular fragments of quartz and carbonate which are matrix supported. Magmaclasts are absent from this sample while the pseudomorphic olivines are minimal with a grain size less than 1mm. This sample is interpreted as a resedimented volcanic kimberlite based on fine grained reworked magmaclasts.

Phenocrysts:

Quartz grains are the dominate clasts in this sample. They have an average grain size of 0.2mm and are angular fractured grains. They are clear in plain light with undgulose extinction with cross polarized light and are uniaxial positive. All grains are well supported by the interclast matrix with a minor orientation where the flat edge of some grains is in the same direction, however, orientation is unknown.

Pseudomorphic olivines are a very minor component of this sample. They have an average grain size of 0.2mm although there are some grains up to 2mm. They are rounded with fine grained calcite and serpentine replacement. They are poorly defined against the interclast matrix which is a similar fine grained serpentine.

Phlogopite is also only a minor component with an average grain size of 0.25mm. They are angular with minor rounded edges and show no preferred orientation.

Interclast Matrix:

The interclast matrix is cryptocrystalline, varying between a dark yellow to a dark brown colour. The difference in colour possibly reflects a variation in the amount of serpentine and chlorite. There are small irregular calcite-serpentine rich zones, poorly defined to be interstitial infilling. There are minor very fine grained subhedral opaques and rounded perovskite.

45% - Serpentine
30% - Quartz
20% - Calcite
7% - Chlorite
5% - Opaques
2% - Phlogopite
1% - Perovskite

Magmaclasts:

Magmaclasts are very fine grained averaging about 0.25mm; they are rounded and well absorbed into the interclast matrix. They are more abundant on one side of the slide interpreted as a bedding plane. Very few magmaclasts have a pseudomorphic olivine core and are simply rounded matrix with minor perovskite and opaques.

90% - Serpentine
5% - Opaques
5% - Perovskite

Sample 235B (897-175):

Sample 235 was taken from a depth below surface between 235.31 to 235.62m. It is medium to coarse grained poorly sorted with a medium green colouring. There is no visible mineral alignment in hand sample or in thin section. There are angular carbonate and quartz fragments up to 2mm. There are minor, very thin 0.1mm, orientated late stage carbonate veins cross cutting coarse quartz fragments. The veins are orientated at 50° to the core axis, but in thin section they appear to be subhorizontal. Pseudomorphic olivines are more abundant than the magmaclasts in a ratio 2:1, but the magmaclasts on average are coarser. There are a moderate amount of rounded vesicles in the interclast matrix and in the magmaclasts. The magmaclasts are subrounded with a simple rounded-to-amoeboid shape, and both the magmaclasts and PMO are poorly defined against the interclast matrix and are partially reworked. Based on these factors this sample is a resedimented volcanic kimberlite.

Phenocrysts:

Angular fragmented quartz grains are the dominate component in this sample. They have a wide range in grain size from 0.2mm up to 20mm. The average grain size is 0.4mm. They are well supported by the interclast matrix. They show undgulose extinction and are uniaxial positive.

Pseudomorphic olivines have a maximum grain size of 2mm but have an average size of 0.25mm. They have a subhedral to rounded shape and are replaced by very fine grained serpentine and have medium grained calcite cores. They are well defined against the interclast matrix.

Phlogopite is only a minor component and has a rounded elongated shape with a maximum size of 0.25mm. Some minor grains show calcite infilling along cleavage plains.

Unknown mineral that is light tan to dark blue in cross polarized light and uniaxial negative. It has a white colour in plain light with moderate relief.

Magmaclasts:

The magmaclasts are medium grained with an average grain size of 1.5mm and reach up to 2.5mm. They have a sub-amoeboid shape to slightly round with only minor phenocrysts within the matrix extruding into the interclast matrix. But there are only trace occurrences of fractured matrix edges. There are an abundant amount of rounded small vesicles that have been infilled with calcite. The matrix is homogenously a dark brown with no fracturing and minor carbonated veining cross cutting the magmaclasts. Very fine grained subhedral opaques and rounded perovskite are common. The magmaclasts are well defined against the interclast matrix suggest a very different composition and minimal reworking and mixing.

73% - Serpentine
10% - Calcite
5% - Opaques
5% - Phlogopite
5% -Chlorite
2% - Perovskite

Interclast Matrix:

The interclast matrix is cryptocrystalline, medium brown colour with abundant thin calcite veins, with no preferred orientation. There is minimal composition or colour variation throughout the sample suggesting a very homogenous interclast matrix. There are minor opaques and perovskite, both being very fine grained subhedral-to-rounded. The phenocrysts and magmaclasts are well defined against the interclast matrix and very little reworking and mixing is evident.

55% - Serpentine
20% - Calcite
15% - Quartz
5% - Chlorite
3% - Phlogopite
2% - Opaques

C29/30 Kimberlite: CL-07-010 Thin Section & Hand sample Descriptions:

Drill Hole Description:

Drill hole CL-07-010 is located in the northern portion of the C29/30 kimberlite occurrence. The drill hole intersected kimberlite beginning at 158.52m and continues for a 114.27m interval. Above the kimberlite is glacial till, no sediments where intersected. The drill hole was terminated at 273.40m as it intersected the Mannville group sediments.

Sample 160E (897-255):

The sample was taken from a depth of 160.65 to 160.93m. The sample is poorly sorted, mainly fine grained, light green with moderate fine grained opaque showing a minor preferred orientation perpendicular to the core axis. The opaque grains are on average 2mm. There are minor xenoliths of angular, fine grained carbonate rocks. Pseudomorphic olivines are the dominate feature of the rock and tend to be rounded-to-subrounded with a ratio to magmaclasts of 15:1, respectively. The interclast matrix is significantly more serpentine rich than the colour suggests being 80% serpentine. Only one minor calcite veins is observed and runs parallel to the core axis. Based on the fracturing of the grains, and the reworked interclast matrix this sample is consistent with a resedimented volcanic kimberlite.

Phenocrysts:

Pseudomorphic olivines are the main component of the rock and are rounded to subrounded ranging in size from 2.5-to-0.5mm. The grains show only minor internal fracturing with calcite replacement along these fractures. There are no relict olivine cores indicating complete replacement. The replacement consists of platy and very fine grained serpentine and minor calcite coring. Magnetite is only a minor component of the replacement minerals.

75% - Serpentine
20% - Calcite
5% - Magnetite

Phlogopite is only a minor component; they are elongated with rounded ends. The average grain size is about 0.4mm (measured along the long axis). There is no visible fracturing also suggestive of a pyroclastic deposition.

Magmaclasts:

The magmaclasts are subrounded, and range in size from 0.5-2.5mm. They contain minor rounded vesicles <1mm that have been infilled by calcite. There is also a minor rimming, <1mm, of calcite partially around the edge of the magmaclasts. The matrix is a darker brown-green colour, predominantly serpentine and chlorite with abundant subhedral clasts. The clasts included pseudomorphic olivine which is fine grained subhedral-to-euhedral, spinel, phlogopite, perovskite, magnetite and calcite.

70% - Serpentine
15% - Calcite

5% - Opaques
5% - Chlorite
2% - Phlogopite
2% - Perovskite
1% - Spinel

Interclast Matrix:

The interclast matrix is a light brown colour with minor pockets of darker brown, possibly where there is a decrease in calcite. It is composed of mainly serpentine, calcite and chlorite mostly being cryptocrystalline. There are also very fine grained opaque mostly magnetite and perovskite, with an average size of 1mm. The interclast matrix does show a intimate intergrowth texture, as well as anhedral pockets of calcite infilling interstitial space. There are also minor calcite veins; however, they do not have a preferred orientation. The grains do show a minor lineation in a sub-perpendicular direction to the core axis.

75% - Serpentine
25% - Calcite
5% - Chlorite
5% - Opaques
Trace – Phlogopite

Sample 169B (897-257):

This sample is from a depth of 169.87 to 170.08m. The sample is poorly sorted with abundant fine-to-medium grained phenocrysts and magmaclasts. It is light green with a defined preferred orientation in a sub-perpendicular direction to the core axis. Large calcite veining is absent and only minor xenoliths are present. Pseudomorphic olivines are the dominate component of this sample. The ratio between phenocrysts and magmaclasts is 3:1 respectively. The interclast matrix overprints much of the magmaclasts and there is extensive alteration of the phenocrysts. Based on the shape of the grains and the lack of definition between the clasts and the interclast matrix this sample is interpreted to be a resedimented volcanic kimberlite.

Phenocrysts:

Pseudomorphic olivines are the main phenocrysts in this sample. They are rounded to oval shaped, with abundant fracturing and have calcite and magnetite alteration along the fracture edges. The grains have been completely replaced by fine grained yellow serpentine, as well as fine grained single euhedral grains of calcite. Around some grains there is a dark green rim against the interclast matrix, this appears to be a chlorite rim. The grain size ranges from 2.5mm to 0.2mm.

Phlogopite is a minor component, all grains being less than 0.6mm. They are commonly rounded, but not fractured. Fracturing of phlogopite is a typical characteristic of a resedimented sample, the lack of fracturing of the phlogopite maybe due to the smaller grain size.

Unknown isotropic mineral shows a pentagonal shape, with only a minor yellow alteration rim radiating form the unknown mineral. There is an example of a fractured grain where the isotropic mineral and the dark rim are fractured together.

Magmaclasts:

The magmaclasts range in size form 2.2mm to 0.15mm and are heavily reworked. The magmaclasts are rounded with uneven edges. The inconsistent shape of the edge is caused by the breaking up of the magmaclasts causing partial to complete fracturing of the magmaclasts. The matrix of the magmaclasts is homogenous, dark green and cryptocrystalline, with minor voids infilled with calcite. There are abundant opaques and calcite and the pseudomorphic olivine are rounded to subhedral. The magmaclasts appear to be absorbed into the interclast matrix where the contact between the two is very difficult to distinguish.

65% - Serpentine
15% - Calcite
8% - Chlorite
5% - Perovskite
5% - Opaques
2% - Phlogopite

Interclast Matrix:

The interclast matrix consists of two phases. The first and most abundant is cryptocrystalline dark green, intimate intergrowth textured and calcite rich. Within this first interclast matrix there are abundant fine grained anhedral-to-euhedral grains. The second phase is a cryptocrystalline light yellow colour and is consistent with infilling of interstitial spaces after resedimentation. The xenoliths are fine grained fractured and are limited to carbonates and granites.

60% - Calcite
35% - Serpentine
5% - Opaques

Sample 188A (897-260):

This sample was taken from a depth of 188.54 to 188.77m from surface. It is a poorly sorted med grained dark green rock with abundant vesicles. The vesicles occur in the matrix as well as the cores of pseudomorphic olivines that have been replaced with calcite. The voids have in internal rimming of calcite and they are commonly oval not rounded. A minor alignment is seen in sample 188B horizontal to the core axis. There is a distinct yellow alteration banding throughout the sample. The alteration is gradation from non-altered to heavily altered, where the interclast matrix, phenocrysts and magmaclasts take on a much more altered appearance. Pseudomorphic olivines are the dominate clast with a ratio to magmaclasts of 3:1 but on average the magmaclasts are much coarser. The PMO are subrounded with abundant oval vesicles and appear to be absorbed into the interclast matrix. The magmaclasts are slightly broken with minor fragmenting along the edges. The interclast matrix is multiphased with a dark serpentine rich zone and reworked calcite interstitial phase. Based on the appearance of the PMO, magmaclasts and interclast matrix which all appear to have been moderately reworked suggest that this sample is a resedimented volcanic kimberlite.

Phenocrysts:

Pseudomorphic olivines are the dominate component of this sample. The maximum grain size is 2.5mm but on average is only 0.3mm. The grains have no relict olivine remaining and have been completely replaced by fine grained serpentine and calcite. The calcite occurs in the cores and along fracturing. Internal fracturing is visible only in the larger grains which are limited. There are abundant voids in the PMO were calcite replacement was incomplete or was not recovered during sample prep. In the altered zone it is very difficult to distinguish boundaries between the interclast matrix and the PMO.

Phlogopite is only a minor component with an average gain size of 0.25mm but occurs in cumulate zones with interstitial serpentine matrix. These cumulate are as large as 6mm. The grains are well fractured.

Magmaclasts:

The magmaclasts are subrounded and partially reworked with minor magmaclasts fragmentation. In sample 188B the magmaclasts appear to be much more reworked and are broken up along the edges. The grain size on average is 0.5m but can be up to 2mm. There are an abundant amount of voids within the magmaclasts matrix which are infilled by calcite. The magmaclasts has a cryptocrystalline multiphased matrix composed of a dark brown core with a lighter brown rim, this is only visible in coarse magmaclasts.

70% - Serpentine
17% - Calcite
5% - Chlorite
5% - Opaques
2% - Phlogopite
1% - Perovskite

Interclast Matrix:

The interclast matrix is cryptocrystalline with a medium brown colour and with poorly defined calcite rich reworked interstitial zones. The interclast matrix becomes a strong yellow colour as the alteration increases. There is a sharp contact between the alteration phases were the grains are half altered. There are minor calcite stringers working around the grains less than 0.5mm, orientated sub-horizontal, visible in sample 188B.

75% - Serpentine
15% - Calcite
5% - Chlorite
5% - Opaques

Sample 197 (897-261)

This sample was taken from a depth of 197.35 to 197.58m from surface. It is fine grained with a variable light to dark green interclast matrix. There are altered gossans red bands at 35° to the core axis. Some alteration bands boudinage where others are consistent bands up to 5mm thick. There are also calcite veins up to 1mm thick along the same angle as the alteration bands. There are minor xenoliths up to 4mm of mudstone and carbonates all angular fragments. There is no visible layering or mineral alignment and the grains are poorly sorted and well supported by the matrix. The PMO are rounded and have minimal internal fracturing where as the magmaclasts are amoeboid in shape with abundant rounded vesicles infilled by calcite. PMO are the dominate component of this sample with a ration to magmaclasts of 4:1. The interclast matrix is a single homogenous, cryptocrystalline light brown phase. The shape and definition of the phenocrysts and magmaclasts along with the minimal single phased interclast matrix suggest this sample is a pyroclastic volcanic kimberlite.

Phenocrysts:

Pseudomorphic olivines are the dominate component of this sample and have an average grain size of 0.5mm but have a maximum size of 2.5mm. They are completely replaced by fine grained calcite, and some have a coarse grained calcite core surrounded by the finer grained calcite. The PMO grains are subrounded-to-oval shaped but some do have a subhedral from. Internal fracturing is minimal but in coarser grains there is minor fracturing that has coarse yellow serpentine infilling with subhedral fine grained magnetite.

Phlogopite grains have an elongated oval shape with rounded ends and very few bent cleavages. They are medium grained up to 1.5mm but are only a limited component of the sample.

Magmaclasts:

The magmaclasts are amoeboid shaped but they do show minor characteristics of slight reworking. The edges have minor fracturing and fragments of the magmaclasts matrix separated from the main magmaclasts. The number of phenocrysts extruding from the magmaclasts matrix in the interclast matrix are minimal but still present. However, the moderate amounts of vesicles present in the matrix are rounded and infilled with calcite. The matrix is a dark brown colour dominated by serpentine and chlorite. Other components include perovskite minor phlogopite and opaques.

50% - Serpentine
35% - Calcite
5% -Opaques
5% - Chlorite
3% - Phlogopite
2% - Perovskite

Interclast Matrix:

The interclast matrix is light brown, cryptocrystalline with minor fine grained subhedral opaques and rounded perovskite and phlogopite. The gossan zone has caused a red staining of the interclast matrix, phenocrysts and magmaclasts. The alteration occurs from strings of calcite infilled with red elongated intimate intergrowth textured grained as well as opaque needled grains up to 0.1mm.

50% - Serpentine
30% - Calcite
10% - Chlorite
6% - Opaques
3% - Phlogopite
1% - Perovskite
Trace Unknown intimate intergrowth textured grains within alteration stringers.

Sample 221A (897-263):

This sample was taken from a depth of 211.00 to 211.24m from surface. The sample is poorly sorted with a minor horizontal alignment with abundant vesicles. There are minor thin 1mm black horizontal anatomizing serpentine and calcite bands associated with minor yellow alteration. The rock is a dark to medium green colour and in thin section there are very thin late stage calcite veins cross cutting all grains. PMO are the dominate component of the sample with a ratio to magmaclasts of 15:1. The phenocrysts and magmaclasts are matrix supported. There is poor distinction between the interclast matrix and the PMO they are also rounded with internal fracturing. The magmaclasts are rounded with irregular fragmentation and have minimal extruding phenocrysts within the magmaclasts matrix. The interclast matrix has a minor two phase component a serpentine rich zone and a calcite-serpentine zone. Based on the fracturing of the magmaclasts and the PMO as well as the multiphased interclast matrix this sample appears to be a resedimented volcanic kimberlite.

Phenocrysts:

Pseudomorphic olivines are the dominate component of the sample. They are poorly sorted and have a variation of alteration. Some are completely replaced by fine grained calcite. Other pseudomorphic olivines are replaced by coarser grained calcite while still others are replaced by fine serpentine-calcite. The serpentine altered PMO are poorly defined against the interclast matrix. The average size of the grains is 0.25mm but have a maximum of 2mm. Internal fracturing is minimal due to the lack of coarse grains. The smaller grains are rounded and anhedral.

Phlogopite reach a maximum size of 1.5mm with an average size of 1mm measured along the long axis. They are rounded with abundant small fractured fragments.

Unknown mineral is isotropic, grey in plain light, rounded-to-subrounded and up to 0.1mm in size. It is found within the serpentine vein with the yellow alteration. There is an opaque halo.

Magmaclasts:

The magmaclasts are up to 1.5mm with an average size of 0.25mm. The magmaclasts have an irregular from due to fracturing of minor fragments from the edge of the grains. There are very few magmaclasts with phenocrysts that are extruding out from the matrix. The matrix is dark brown homogenous with subhedral-to-rounded PMO that have been replaced by fine grained calcite. There are moderate subrounded vesicles infilled by calcite and perovskite that shows a brown alteration rim.

70% - Serpentine
15% - Calcite
10% - Chlorite
3% - Opaques
2% - Perovskite
Trace Unknown

Interclast Matrix:

The interclast matrix supports most grains and has two phase cryptocrystalline component. The dominant is a light yellow that is calcite rich and the other is a dark serpentine rich matrix. There are abundant opaques within the serpentine matrix. The serpentine that replaced PMO are poorly defined and appear to be absorbed into the matrix were as the magmaclasts matrix are moderately defined against the interclast matrix.

60% - Serpentine
20% - Calcite
10% - Chlorite
5% - Opaque
3% - Phlogopite
2% - Perovskite
1% - Unknown

Sample 224B (897-266):

This sample was taken from a depth of 224.35 to 224.68m from the surface. It is dark green with abundant undefined black clasts throughout the sample. Poorly sorted but does have a minor preferred orientation which is seen in both hand sample and thin section, and trends 60° from the core axis. There is no coarse calcite veining; however, there is very thin minor calcite veining, with no preferred orientation. There are minor xenoliths, fractured and angular fragments mostly carbonates. Pseudomorphic olivines are the most abundant clast in the sample with a ratio to magmaclasts of 2:1. The interclast matrix is composed of a single phase and the phenocrysts are rounded and show only minor fracturing. The magmaclasts are amoeboid and have definition against the interclast matrix; due to these factors this sample is consistent with a pyroclastic volcanic kimberlite.

Phenocrysts:

Pseudomorphic olivines are poorly sorted and have a grain size range from 2.5mm to 0.5mm. The grains are only moderately fractured with minimal magnetite and calcite alteration along the factures. There is no relict olivine but there is minor calcite coring of the grains. The pseudomorphic olivines are mainly replaced by platy yellow serpentine. The coarse grains are rounded to oval shaped but the smaller grains can be subhedral-to-euhedral.

Phlogopite occurs in a moderate amount. The maximum grain sized observed was 2mm along the long axis (which is parallel to the cleavage plane). The grains are elongated but with rounded ends and are found more commonly in the magmaclasts matrix rather than the interclast matrix.

Unknown isotropic mineral is light green to blue, non pleochroic, fine grained and slightly fractured. It is 1mm along the long axis and has high relief.

Apatite is uniaxial (-), has high birefringence, and is rounded at 1mm in diameter.

Magmaclasts:

The magmaclasts are amoeboid shaped and range in size from 3mm to 0.5mm. There are minor small, rounded voids that have been infilled by calcite. The clasts within the matrix along the edge of the magmaclasts are not completely surrounded by the matrix and extend into the interclast matrix. This texture of the magmaclasts indicates that reworking has not occurred; otherwise those grains along the edge would be removed from the magmaclasts. The pseudomorphic olivines in the magmaclasts are fine grained subhedral-to-euhedral and have a maximum grain size of 2mm. Other minerals observed in the magmaclasts include phlogopite, perovskite, spinel and magnetite. The matrix is a cryptocrystalline dark brown-grey and is homogenous.

80% - Serpentine
8% - Calcite
5% - Opaques
3% - Phlogopite
3% - Chlorite
1% - Perovskite
Trace Spinel

Interclast Matrix:

The interclast matrix is a light brown with a intimate intergrowth texture. The interclast matrix is consistent throughout the sample. There are minor anhedral interstitial zones where calcite has proceeded to infill. There are also minor fine grained opaques that are anhedral and euhedral. There is very minor calcite veining, as well there is minor magnetite veining, neither has a preferred orientation.

40% - Serpentine
40% - Calcite
15% - Chlorite
5% - Opaques

Sample 233B (897-267):

This sample was obtained from a depth of 233.2 to 233.5m. The sample is poorly sorted, fine grained with dark green colouring. There are abundant clasts of phenocrysts and magmaclasts. Pseudomorphic olivines dominate the sample, in a ratio to magmaclasts of 2:1 respectively. There is no preferred orientation of the grains and there is abundant grain to grain contact. There are minimal xenoliths within the sample; the only observed xenoliths are angular fragments of carbonate. There is very thin, minor calcite veining, with no preferred orientation throughout the sample; this is observed in hand sample and thin-section. The interclast matrix has two phases, a light brown cryptocrystalline phase that is the majority as well as a light calcite rich interclast matrix, most likely an interstitial phase. The interclast matrix overprints on the magmaclasts slightly. There appears to be very minor reworking of this sample but will be classified as a pyroclastic volcanic kimberlite, because the resedimented textures are only minor.

Phenocrysts:

Pseudomorphic olivines are subhedral with moderate fracturing, and show minor angular fragmentation. The finer the grain size the more euhedral the grains become. The most euhedral grains are found in the magmaclasts matrix. There are no relict olivine cores but there is minor calcite core replacement. The majority of the pseudomorphic olivine has been replaced by fine grained yellow-green serpentine as well as platy serpentine. There is minor magnetite and calcite alteration along the fracture edges. The grain size ranges from 6mm to 0.1mm averaging about 0.4mm.

Phlogopite is occurs only as a minor component. It shows a distinct cleavage, which is distinctly deformed possibly by minor reworking. The grain size ranges from 2.2mm to 0.2 mm.

There are two cumulates that occur within this sample the first is a fine grained phlogopite and pseudomorphic olivines all less than 0.4mm in a brown-grey matrix with magnetite spotted rimming around the sample.

The second cumulate is highly fractured with concave edges, consisting of pseudomorphic olivine and altered phlogopite and a light brown interclast matrix. There are abundant very fine grained brown-red grains spotted throughout (spinels).

Magmaclasts:

The magmaclasts are rounded and amoeboid, with a grain size of 3.25mm to 0.3mm. There is an abundant amount of small magmaclasts, possibly due to fragmentation from reworking but possibly just a very poorly sorted sample. There is abundant subhedral to euhedral pseudomorphic olivine within the matrix, as well as phlogopite, and magnetite. The matrix is a dark grey-green colour which is separate from the interclast matrix but some magmaclasts do show a moderate blending into the interclast matrix.

80% - Serpentine
8% - Calcite
5% - Chlorite
5% - Opaques
1% - Phlogopite
1% - Perovskite

Interclast Matrix:

The interclast matrix is cryptocrystalline, a light brown-green colour with very fine grained brown-grey grains, perovskite. The interclast matrix does have minor zones of a lighter grey, due to increased calcite, possibly interstitial zones. There are fine grained cubic to anhedral opaque grains (magnetite). The contact of the magmaclasts to the interclast matrix is vague on finer grained magmaclasts but defined on course grained.

65% - Serpentine
20% - Calcite
10% - Chlorite
5% - Opaques.

Sample 245A (897-270):

This sample was taken from a depth of 245.8 to 245.93m. The sample is moderately sorted with no preferred orientation of grains. Pseudomorphic olivines are the dominate feature of the rock with a ratio to magmaclasts of 4:1, respectively. The magmaclasts are amoeboid-to-round and are set in a cryptocrystalline interclast matrix. The clast component of this sample is abundant resulting in a moderate amount of grain-to-grain contact. The hand sample does not show calcite veining but in thin section calcite veining does occur. The direction of the calcite veining is perpendicular to the core axis. There are minor xenoliths, including fractured carbonates and rounded granites. The sample is classified as a pyroclastic volcanic kimberlite.

Phenocrysts:

Pseudomorphic olivines are the main component of the rock and are fine grained, rounded to angular due to minor fracturing. The grain size ranges from 2.2mm to 0.2mm. They are replaced by very fine grained serpentine and calcite, having a light yellow colouring. There are no relict olivine cores or calcite coring.

Phlogopite is a minor component and is commonly rounded. Some grains show a bending observed from the deformation of the cleavage and the interference pattern. Some grains show angular fracturing. The average grain size is 0.7mm.

Garnet is fragmented, with a black rim directly along the mineral and transitions to a dark brown against the interclast matrix. The isotropic mineral is 2mm thick and the rim is 1mm thick.

Magmaclasts:

The magmaclasts are rounded to slightly amoeboid. There is a minor fragmentation of some of the magmaclasts causing a tail around the magmaclasts. Where as other magmaclasts are amoeboid and have clasts along the edge extending into the interclast matrix that have not been reworked. Another grain is fractured into two parts with interclast matrix infilling the space, this is suggestive of a resedimented unit. The pseudomorphic olivines in the magmaclasts are subhedral but the larger grains, greater than 1mm are rounded. The matrix is a dark grey and has abundant fine grained opaques and perovskite. There is a distinct colour change from the matrix to the interclast matrix but some magmaclasts show a grading from the matrix to the interclast matrix, this is seen commonly in finer grained magmaclasts. The magmaclasts range in size from 2.5mm to 0.3mm.

Interclast Matrix:

The interclast matrix is cryptocrystalline and is a dark brown colour, with abundant opaques, all less than 0.5mm. The interclast matrix is consistent throughout the sample. There is only minor calcite veining, and no magnetite veining. There are no interstitial voids and no calcite infilling. There are xenoliths of carbonates and granites but also of quartz grains and microcline, less than 0.7mm.

Sample 255A (897-271):

This sample was taken from a depth of 255.93 to 256.15m below surface. Poorly sorted very fine grained dark green colour no preferred orientation, with abundant angular carbonate fragments. There are very small vesicles within the interclast matrix as well as in the magmaclasts. Pseudomorphic olivines are the dominate feature of the rock with to magmaclasts of 1:4. The pseudomorphic olivines are fine grained with rounded shape. The interclast matrix is heterogeneous with a varying amount of serpentine and calcite. There is no secondary late stage calcite veining. The magmaclasts are subrounded, with poor definition to the interclast matrix. This sample based on the textures and relationships of the resedimented country rock is consistent with a resedimented volcanic kimberlite.

Phenocrysts:

Pseudomorphic olivines have an average grain size of 0.5mm but are up to 5mm. They are replaced by fine grained brown serpentine and chlorite, with thin calcite rims around the outer edge. There is also calcite infilling along internal fractures. They are rounded so subhedral.

Phlogopite is only a minor component and is rounded to oval and is up to 1mm measured along the long axis.

Magmaclasts:

The Magmaclasts have an average size of 1mm but are as large as 2mm. They have an amoeboid shape with abundant internal phenocrysts protruding from the magmaclasts matrix into the interclast matrix which are not broken off by reworking. The phenocrysts that are within the matrix include subhedral serpentine-calcite replaced PMO, phlogopite and moderate perovskite with brown rims and opaques. These grains have a maximum size of 0.5mm. The matrix is a dark brown serpentine rich and is well defined against the much lighter brown interclast matrix.

85% - Serpentine
5% - Phlogopite
5% - Opaques
4% - Calcite

Interclast Matrix:

The interclast matrix is slightly heterogeneous with a variation in colour from a light brown to a medium brown. The light brown is a very fine grained serpentine, chlorite calcite mixture with very fine grained spots of the medium brown. The colour change is possibly due to the reduction of calcite. There are moderate fragments of quartz and carbonates, as well as abundant fine grained opaques and perovskite.

60% - Serpentine
15% - Calcite
10% - Chlorite
7% - Opaques
5% - Quartz
2% - Phlogopite
1% - Perovskite

Sample 264B (897-273):

This sample was taken from a depth of 264.65 to 264.86m. It is very fine grained, poorly sorted with a light green colouring. There are an abundant amount of xenoliths including, granitic fragments as well as angular limestone. These xenoliths are also incorporated into the magmaclasts which suggest emplacement with eruption as oppose to resedimentation. The sum of all xenoliths composes about 5% of the total rock. The xenoliths range in size from 4cm to 0.4mm and are extremely fractured and occur as fine fragments in the matrix of the magmaclasts. There is minor calcite veining perpendicular to the core axis, some veins seem to be offset possibly due to slumping or settling of the pyroclastics. The matrix is a dark brown cryptocrystalline with moderate fine grained opaques. There is a second interstitial infilling by calcite and miner serpentine into anhedral spaces. There is no mineral alignment. Pseudomorphic olivine are the dominate feature of this sample with a ratio of magmaclasts of 2:1. This sample is a pyroclastic volcanic kimberlite.

Phenocrysts:

Pseudomorphic olivines are rounded, medium to fine grained ranging in size from 3.5mm to 0.3mm. They are extensively replaced by platy serpentine as well as fine grained serpentine. Calcite replacement is dominated along the internal fracturing of the grains.

65% - Serpentine
25% - Calcite
5% - Chlorite
5% - Opaques

Phlogopite is a very minor component, fine grained always less than 0.5mm, and is rounded. Some grains appear to be fractured but maybe poorly orientated. Phlogopite has a higher abundance of phlogopite in the matrix of the magmaclasts.

Unknown isotropic mineral is rounded to elongate. During cross-polars the mineral goes grey. There is a dark black rim that transitions into a dark brown when in contact with the interclast matrix. The grain is about 1cm in length along the extended axis.

Magmaclasts:

The magmaclasts are slightly rounded with irregular edges. There are abundant vesicles within the matrix that are rounded and infilled with calcite. The cores of the magmaclasts can be a variety of grains including pseudomorphic olivines, quartz, and other xenoliths. There is an abundant amount of fine grained phlogopite within the matrix. The matrix is heterogeneous transitioning between a dark brown and a lighter grey, possibly due to the variation in calcite. The grain size ranges from 3mm to 0.4mm.

75% - Serpentine
5% - Calcite
5% - Opaques
5% - Xenoliths (quartz, microcline, carbonates)
4% - Chlorite
3% - Perovskite
3% - Phlogopite

Interclast Matrix:

The interclast matrix is very fine grained and a cryptocrystalline dark brown colour. There are an abundant amount of fine fragmented xenoliths, as well as phlogopite, perovskite and opaques. There is also a very fine grained interstitial phase that is a light yellow-grey colour. It infills anhedral areas between grains, these areas are absent of fragmented grains.

65% - Serpentine
15% - Calcite
5% - Opaques
5% - Xenoliths

C29/30 Kimberlite: CL-07-014 Thin Section & Hand sample Descriptions:

Drill Hole Description:

Diamond drill hole CL-07-014 was drilled to test the Northern portion of the C29/30 occurrence. The drill hole recovered no overburden sediments only glacial till, but drilled a total of 48.90m of kimberlite from 225.72 to 274.62m. The final depth of the hole is 274.8m and was terminated in the consolidated sands of the Mannville Group. The drill hole had a dip of 90°. The following seven samples were taken within the kimberlite interval.

Sample 233C (897-278):

The sample was taken at a depth of 233.30 to 233.53m. It is a medium green colour with abundant dark grains. There is a minor mineral alignment, visible with coarse grains in a sub-perpendicular direction to the core axes. The sample is poorly sorted and clast supported, grain to grain contact is common. There are moderate amount of xenoliths, 2-3%, shales and carbonates with a maximum size of 3cm. The xenoliths are angular and fractured. There is no coarse calcite veining but there are very thin calcite veins throughout the sample, in a network pattern. Pseudomorphic olivines are the dominate grains within the sample at a ratio to magmaclasts of 5:1. This sample is classified as a resedimented volcanic kimberlite; however, sample 233A is less reworked and could be classified as a slightly reworked pyroclastic volcanic kimberlite.

Phenocrysts:

Pseudomorphic olivines are the dominate phenocrysts and are rounded to moderately fractured. They range in size from 4mm to 0.1mm. The pseudomorphic olivines are replaced by dark green sheeted serpentine and chlorite, as well as calcite and magnetite along the internal fractured edges. There is also minor calcite coring.

Phlogopite again is only minor phenocrysts (2%), with a maximum grain size of 3mm measured along the long axis. The phlogopite does appear to be angular along the ends not rounded which suggest fracturing by reworking.

Unknown isotropic mineral (assumed garnet with k is coarse; minimum 2mm in diameter with a dark serpentine rimming that is also 2mm thick. One of these grains is fractured in half as well as the serpentine rim, suggesting reaction rim is prior to reworking and external environment.

Magmaclasts:

The magmaclasts range in size from 2.5mm to 0.12mm. They are commonly rounded to oval, with smooth edges; no internal grains extend into the interclast matrix. If the magmaclasts are not rounded then they are fractured with small (< 0.2mm) fragments of the matrix absorbed into the interclast matrix. The interclast matrix is dark brown to green and is homogenous with minor components of phlogopite, opaques and perovskites. There are no distinct rounded voids. However, in sample A the magmaclasts are more defined against the interclast matrix, slightly less rounded and show minor voids infilled with calcite-dolomite.

80% - Serpentine
8% - Calcite
5% - Opaques
3% - Chlorite
2% - Phlogopite
2% - Perovskite

Interclast matrix:

The interclast matrix is a light brown, with areas of very fine grained calcite infilling. The interclast matrix is poorly defined against the magmaclasts and phenocrysts, but relatively to other resedimented samples it is only moderately reworked. There is no alignment of grains or any preferred vein orientation. The xenoliths are mostly carbonates and shales, but there are some xenoliths that are elongated and heavily altered, with a distinct hatch pattern and blue-to-black interference colours, and has a high birefringence, the mineral is unknown (microcline?).

60% - Serpentine
30% - Calcite
5% - Chlorite
5% - Opaques

Sample 245B (897-279):

This sample was taken from a depth of 245.37 to 245.67m. It is poorly sorted and the main components are pseudomorphic olivine and magmaclasts in a ratio of 4:1, respectively. The sample has a very dark grey colouring, fine grained interclast matrix with numerous fragmented and angular xenoliths of granite, carbonates and shales. There is calcite veining orientated parallel to the core axis, and are thin veins from 1mm to less than 1mm. There are also moderate amounts of magnetite veining between the pseudomorphic olivine. The sample represents a pyroclastic volcanic kimberlite, based on the shape of the magmaclasts and the form of the interclast matrix.

Phenocrysts:

The pseudomorphic olivines which are the dominate phenocrysts are 5 to 0.1mm in size. They are rounded but the smaller grains are subhedral to euhedral. The replacement is dominantly serpentine but there is minor calcite coring. Calcite along with magnetite is also found infilling internal fracture space. The grains are well in tacked and mostly matrix supported. There is no preferred orientation of the minerals.

Phlogopite has a maximum size of 1.5mm but on average is 0.2mm. Some of the grains show a bent texture but commonly are elongated with rounded ends not fractured.

Magmaclasts:

The Magmaclasts are rounded to amoeboid, at a maximum size of 9mm but on average are 1.5mm. Within the amoeboid magmaclasts there are pseudomorphic clasts that extent from the magmaclasts matrix into the interclast matrix and have not been broken off by abrasion. The matrix is dark brown homogenous composed mostly of serpentine but minor phlogopite, perovskite, spinels, opaques and calcite.

70% - Serpentine
5% - Opaques
5% - Chlorite
15% - Calcite
3% - Phlogopite
2% - Perovskite
Trace Spinel

Interclast matrix:

The interclast matrix is a light brown-yellow colour with abundant calcite, homogenous with spotted very fine grained opaque grains throughout. There is minor calcite veining visible in thin section that cross-cuts the calcite rich interclast matrix. There is also moderate amount of magnetite veining between the altered pseudomorphic olivine. There are quartz rich xenoliths between 3 to 0.5mm in size. Other xenoliths include shales and carbonates.

50% - Calcite
35% - Serpentine
10% - Chlorite
5% - Opaques

Sample 257B (897-281):

This sample was taken from a depth of 257.46 to 257.72m. This sample is poorly sorted and is mostly matrix supported. The interclast matrix is very fine grained a very dark grey-to-green with abundant carbonate and granitic xenoliths with an average size of 2.5mm. There is minor thin calcite veining with no preferred orientation. There is no preferred mineral orientation visible. Pseudomorphic olivine are the dominate clast with a ration to magmaclasts of 3:1. This sample is interpreted to be a pyroclastic volcanic kimberlite.

Phenocrysts:

Pseudomorphic olivines are the primary phenocrysts and range in size from 3mm to 0.2mm. Some grains do show relict olivine cores, others show calcite coring but are mainly replaced with serpentine. They are rounded to oval, with minor internal fracturing. Along the fractured boundaries there is calcite and magnetite infilling.

85% - Serpentine
5% - Calcite
5% - Olivine
5% - Opaques

Phlogopite is a very minor component of this sample and average in size at 0.5mm. The grains are typically elongated with rounded ends.

Garnets are about 2mm in diameter, fracture and rounded. There is a thick, 2mm, alteration rim around the grain that is dark black to brown and is cryptocrystalline.

Magmaclasts:

The magmaclasts have a maximum size of 3mm but average about 0.75mm. They are amoeboid in shape, with internal grains extending from the magmaclasts matrix into the interclast matrix, suggesting a lack of reworking. The matrix is a dark brown, distinct against the interclast matrix, and has minor calcite concentration. The pseudomorphic olivines within the magmaclasts are subhedral-to-euhedral and show a relict olivine core.

80% - Serpentine
5% - Opaques
5% - Chlorite
3% - Calcite
3% - Perovskite
2% - Olivine
2% - Phlogopite

Interclast matrix:

The interclast matrix in thin section appears to be a light grey-to-yellow colour with a second phase of calcite infilling interstitial phases. The infilling is anhedral but structured to fit around grains. The calcite infilling does not appear to be reworked. There is minor calcite veining present in thin section as well as a thin vein that is biaxial and has a 90° extinction angle. There is no preferred orientation of the veins or minerals. There are abundant xenoliths present mostly fractured carbonates with minor quartz rich rounded xenoliths.

Sample 260B (897-283):

This sample was taken from a depth of 260. 49 to 260.77m. It is poorly sorted and is a medium to dark green colour. There is no preferred grain orientation, but there are abundant opaques. The xenoliths are up 1cm in diameter and consist of carbonates and shales as well as minor granite clasts up to 3.5mm. There is calcite veining sub-vertical to the core axis and 60° to the core axis. The calcite veining cuts the entire sample except for the granitic xenoliths, possibly due to strength of the clast. The magmaclasts are poorly defined against the interclast matrix. Pseudomorphic olivine are the dominate clast within this sample at a ratio to magmaclasts of 5:1. This sample is believed to be a pyroclastic volcanic kimberlite but is poor example relative to other pyroclastic units.

Phenocrysts:

Pseudomorphic olivines are the most abundant phenocrysts and are rounded-to-moderately fractured. Along the internal fracturing there is replacement by calcite and minor magnetite. The grains range in size from 5 to 0.2mm, and the finer grained pseudomorphic olivines are subhedral to euhedral. The grains are replaced mainly with light brown fine grained serpentine, but there are a few grains that still have relict olivine cores.

Phlogopite is up to 1mm in diameter measured along the long axis. It is rounded partially fractured, but not a major component of the sample.

Magmaclasts:

The magmaclasts are a minor component of the sample. They are rounded but some magmaclasts and have internal clasts (mostly pseudomorphic olivine) extent from the magmaclasts matrix into the interclast matrix. These clasts in a resedimented unit would be broken off by abrasion. The matrix has a calcite rich area that is a lighter grey where the serpentine rich areas are a darker brown. The distinction between the matrix and the interclast matrix is difficult to determine, depending from magmaclasts-to-magmaclasts.

75% - Serpentine
10% - Calcite
5% - Chlorite
5% - Opaques
3% - Perovskite
2% - Phlogopite

Interclast matrix:

The interclast matrix is mainly a medium yellow to brown colour, cryptocrystalline but transitions into two other phases. There is also a light grey most likely due to an increase in calcite, and a dark brown phase possibly due to an increase in serpentine. The interclast matrix is obscured to the grain boundaries of the phenocrysts and the magmaclasts. Calcite veining is common and cross cuts everything except for the granitic xenoliths. The xenoliths are fractured and matrix supported.

Sample 269B (897-285):

This sample was taken from a depth of 269.08 to 269.33m. It is poorly sorted with minor alignment of grains in a direction sub-horizontal to the core axis. There is moderate amount of calcite veining at about 45° to the core axis. The main components are pseudomorphic olivine with a ratio to magmaclasts of 3:1. There is a variety of xenoliths including shale, carbonate and granite all fractured and angular, with a maximum size of 5cm. The other xenoliths include microcline, quartz, and fine grained olivine. The xenoliths on average are 2.5mm. This sample is interpreted to be a resedimented pyroclastic volcanic kimberlite.

Phenocrysts:

Pseudomorphic olivines are the predominate phenocryst and are rounded, with a grain size range of 4mm to 0.3mm. The finer the grain size the more subhedral shape they have. They have been replaced by fine grained light yellow-brown serpentine, as well as calcite. Some grains show minor fracturing but fracture infilling by magnetite is minimal. Calcite is a significant component of the pseudomorphic olivines up to 60%.

Phlogopite has a maximum grain size of 2.5mm; it is rounded and partially replaced by calcite.

Magmaclasts:

The Magmaclasts are rounded and dominantly matrix supported. Some magmaclasts show an amoeboid but the majority are rounded or selvages around coarse macrocrysts. There are moderate amount of voids in the magmaclasts matrix that are infilled by calcite. The matrix is a very dark grey with sections being a more brown colouring, the difference is mostly likely due to the variation of serpentine and calcite.

80% - Serpentine
8% - Calcite
5% - Opaques
3% - Chlorite
2% - Phlogopite
2% - Perovskite

Interclast matrix:

The interclast matrix consists of three phases the dominate one being a light brown. The other phases are a grey around magmaclasts, possibly due to assimilation of magmaclasts into interclast matrix and a yellow-brown as an interstitial phase. There is no calcite infilling but increased calcite maybe the cause of variation in the interclast matrix. There is abundant calcite veining and xenoliths. There are minor opaques throughout the magmaclasts.

Sample 273A (897-287)

This sample was taken from a depth of 273.1 to 273.42m below surface. It has a light brown to tan colouring in handsample and has a carbonate based matrix and is very brittle. There is a distinct mineral alignment with tail structures on the back side of coarser grains and is orientated horizontally to the core axis. There are and abundant xenoliths of carbonate, shale and granitic rounded to subrounded fragments up to 7cm wide. There is an abundant amount of vesicles within the interclast matrix. There is later stage horizontal cross cutting thing carbonate veins, less than 1mm thick. The pseudomorphic olivines are in a ratio to magmaclasts of 4:1 and have a subhedral to rounded shape. There is abundant internal fracturing within the PMO. The magmaclasts have an elongated form and rounded and the matrix has a distinct phase change from the core to the rim. The interclast matrix is intermixed with most of the magmaclasts. The rounded and fractured appearance of the phenocrysts and magmaclasts along with the heavily reworked interclast matrix suggest this sample is a resedimented volcanic kimberlite.

Phenocrysts:

Pseudomorphic olivines are the main component of this sample and they are subhedral-to-angular. They have been replaced by very fine grained calcite and serpentine as well as having medium grained calcite cores. They have a maximum size of 6mm but on average are 0.75mm. There is abundant internal fracturing with calcite infilling.

Phlogopite is a minor component and is angular and fractured with minor calcite infilling along cleavage plains. They are only small fragments remaining; they are up to 1mm.

Magmaclasts:

The magmaclasts are medium grained up to 5mm but on average are 1mm. They have rounded edges with no internal phenocrysts extruding from the matrix into the interclast matrix. Reworking has removed any of these grains. The magmaclasts are often stretched into elongated shapes. The magmaclasts are well absorbed into the interclast matrix. The matrix of the magmaclasts has a dark interior core with a lighter brown rim. Other grains within the matrix of the magmaclasts are subhedral, fine grained pseudomorphic olivines, phlogopite and subhedral opaques and calcite infilled voids that are oval shaped. Perovskite is only a very minor component.

72% - Serpentine
10% - Chlorite
10% - Calcite
5% - Phlogopite
3% - Opaques
Minor Perovskite

Interclast matrix:

The interclast matrix is cryptocrystalline, calcite rich with moderate chlorite and serpentine. There is a secondary phase within the calcite interclast matrix of a dark brown chlorite and serpentine rich. The interclast matrix is well reworked and abundant absorption of the magmaclasts and phenocrysts.

50% - Calcite
30% - Serpentine
16% - Chlorite
2% - Phlogopite
1% - Opaques
Minor perovskite and garnet.

APPENDIX B

SPINEL PRISM PLOTS

Spinel Prism Legend

Groundmass Spinels

Magmaclast 1

Magmaclast 2

Magmaclast 3

Magmaclast 4

Magmaclast 5

Magmaclast 6

Magmaclast 7

Magmaclast 8

Magmaclast 9

Magmaclast 10

Magmaclast 11

Magmaclast 12

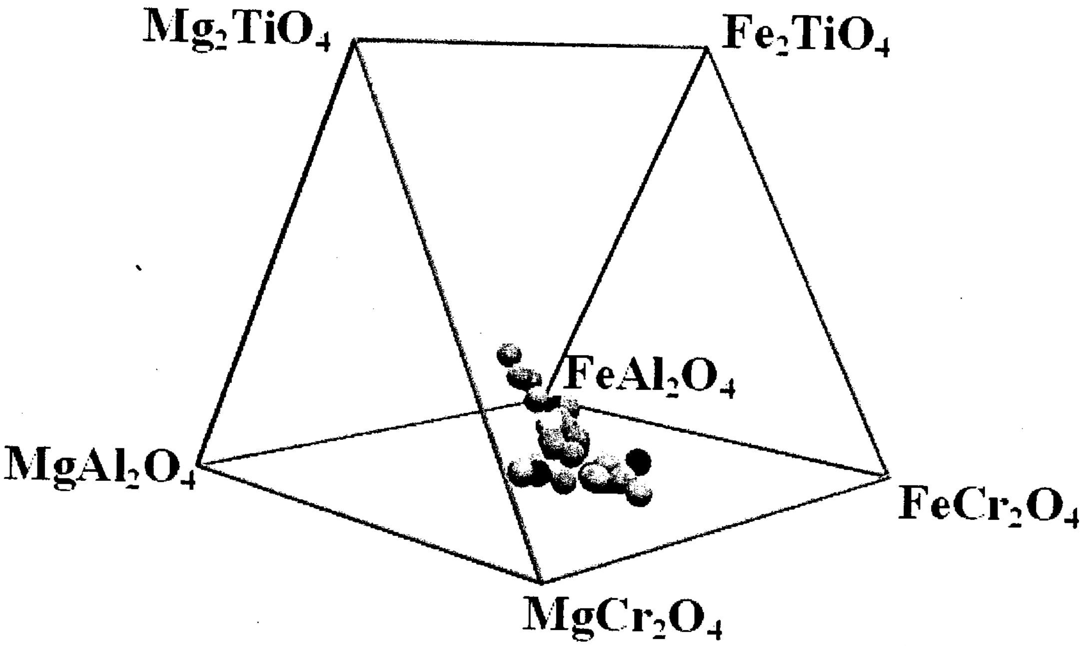

Spinel Prism for CL-06-003-158

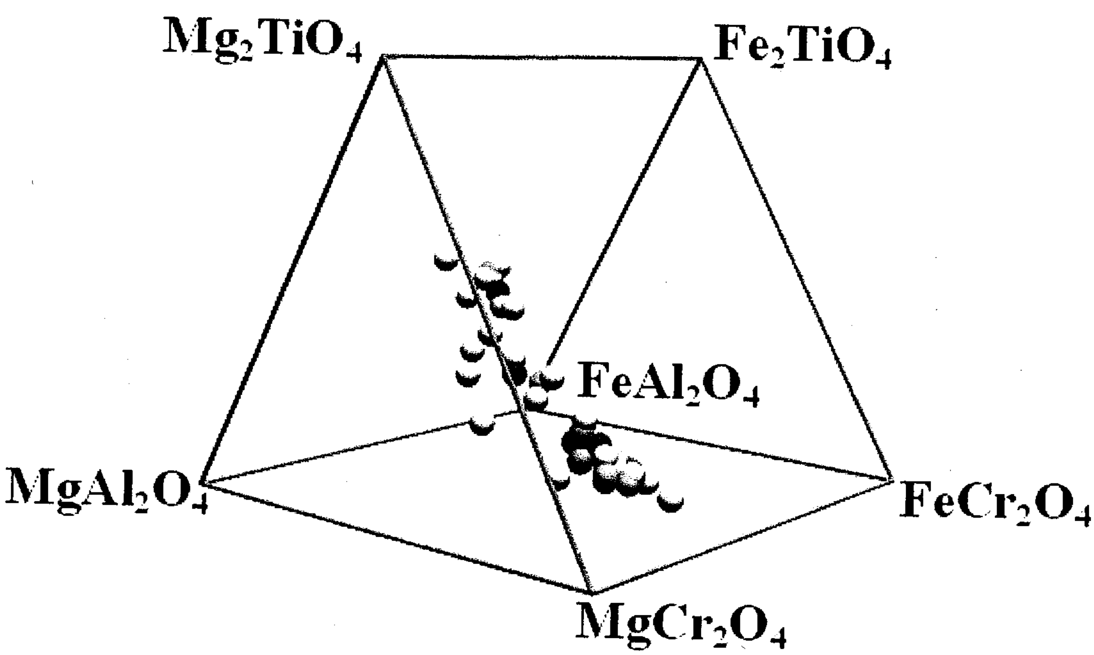

Spinel Prism for CL-06-003-173

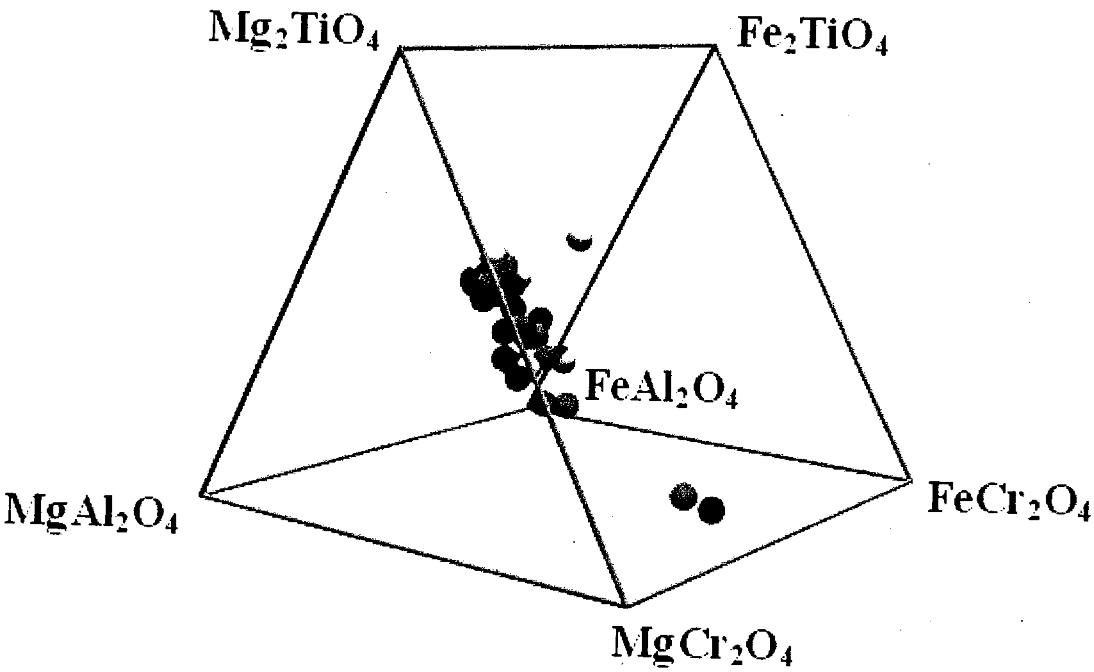

Spinel Prism for CL-06-003-182

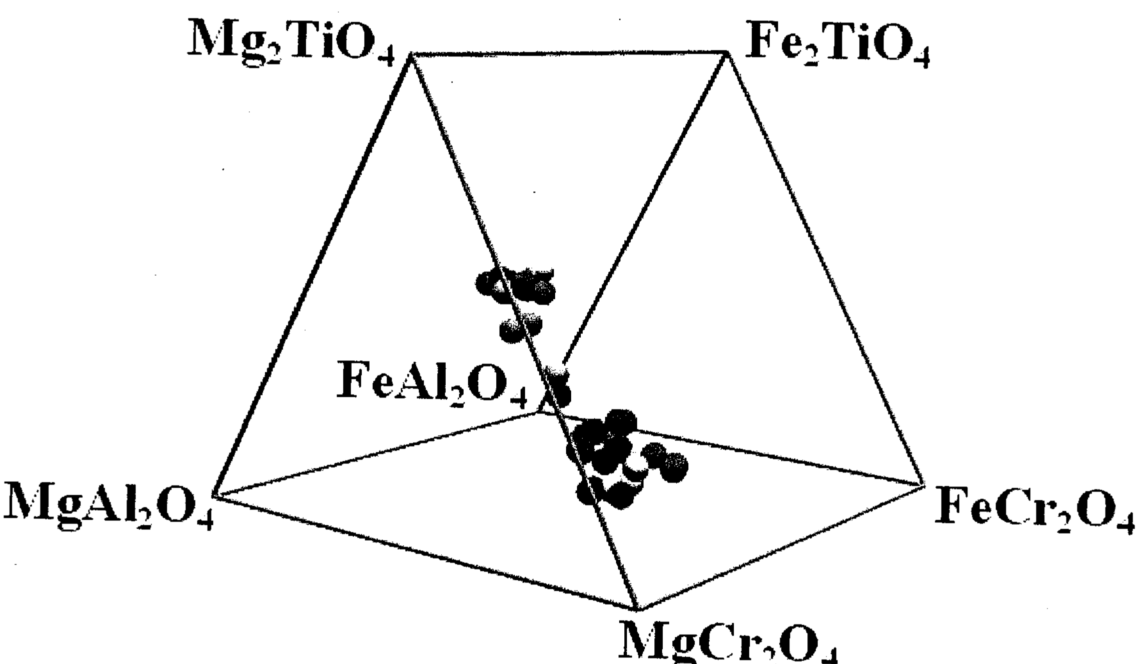

Spinel Prism for CL-06-003-186

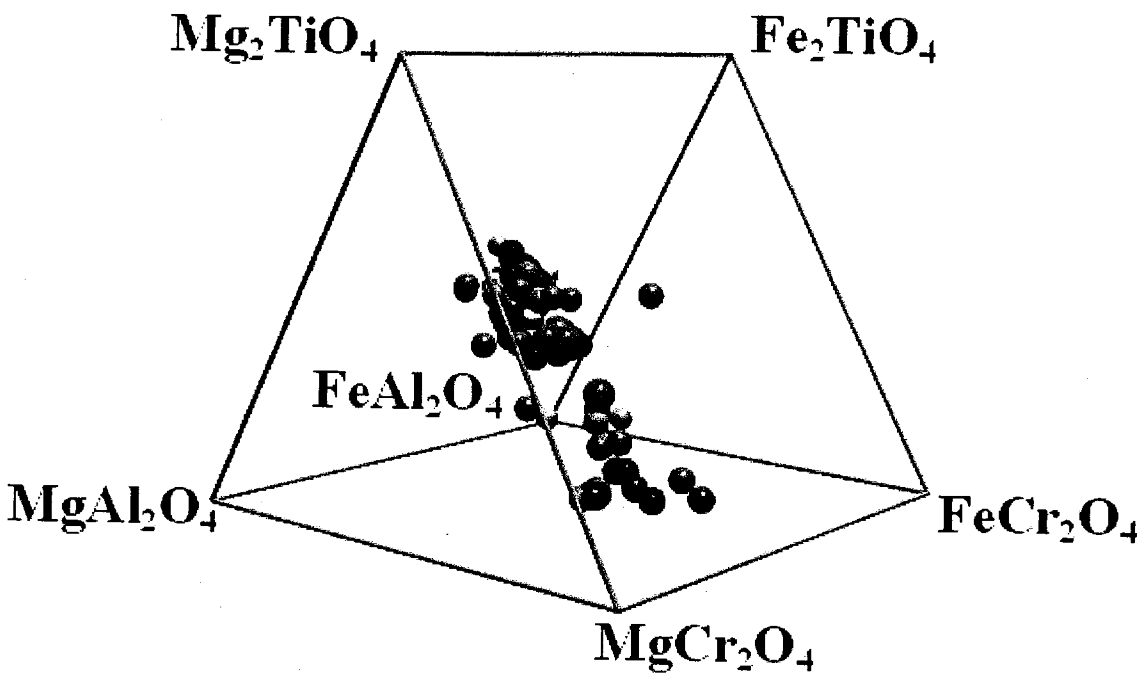

Spinel Prism for CL-06-003-195

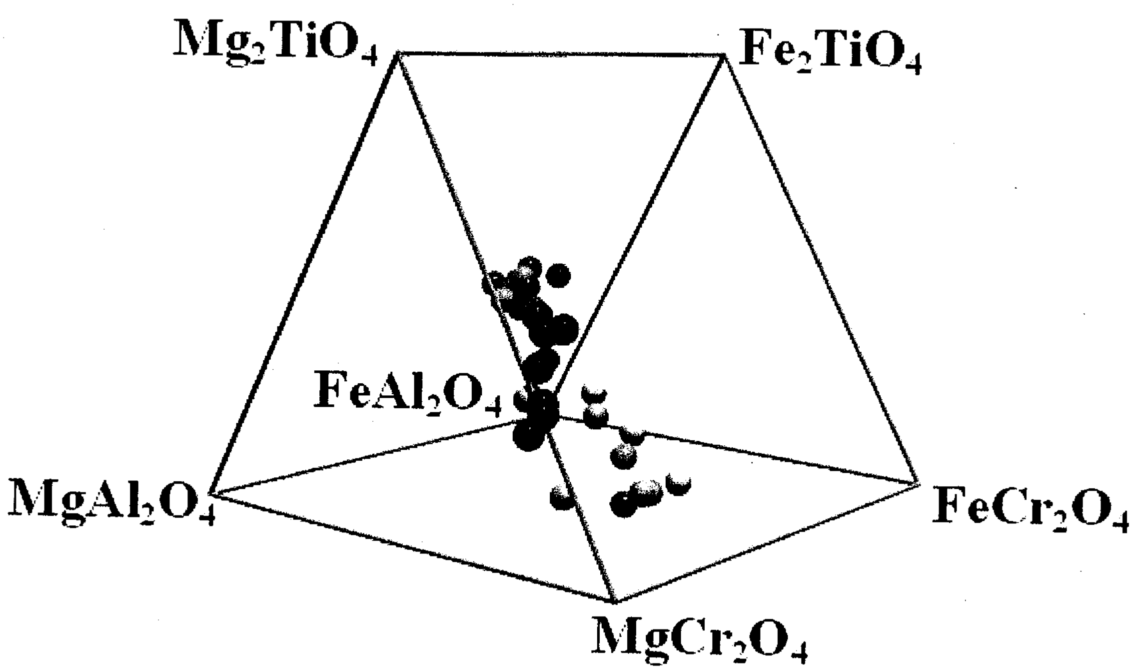

Spinel Prism for CL-06-003-205

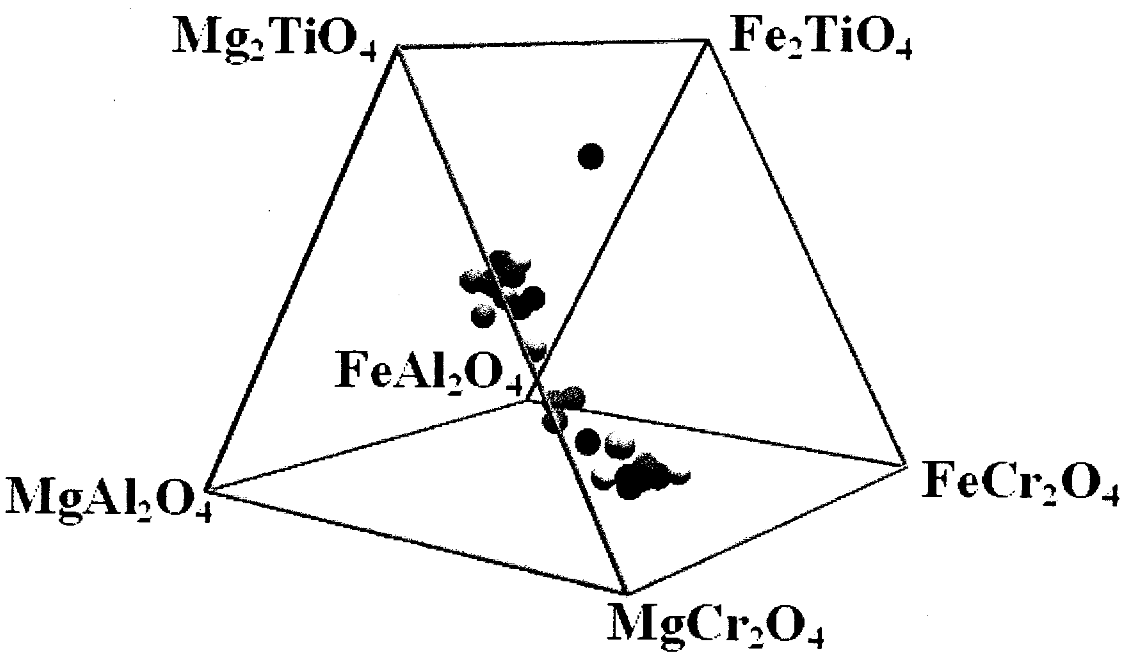

Spinel Prism for CL-06-003-219

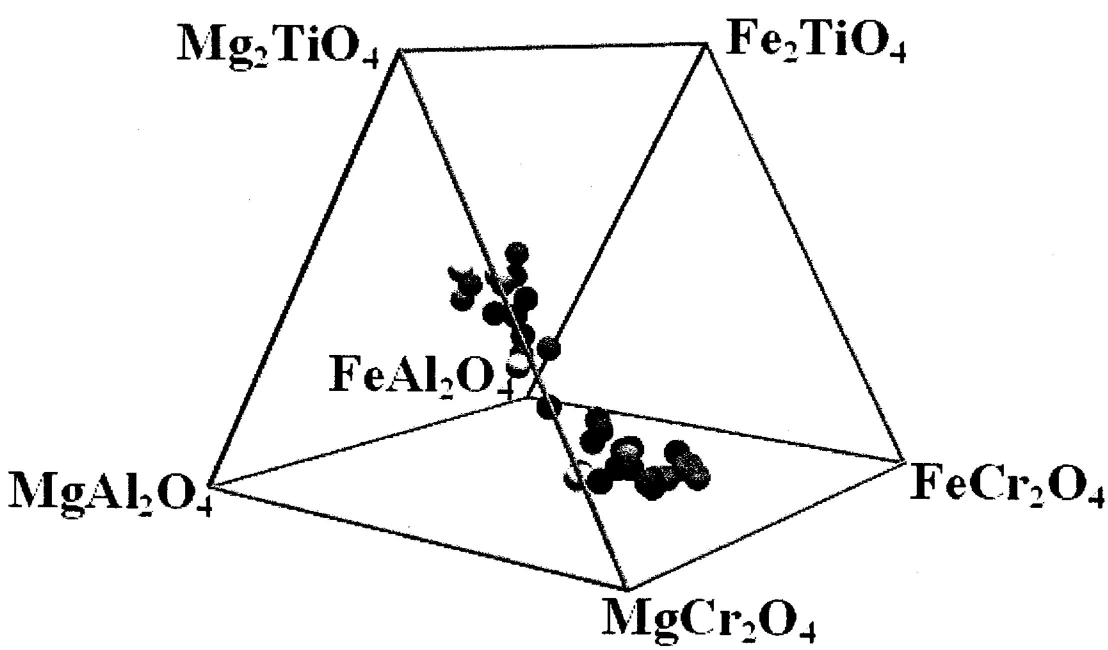

Spinel Prism for CL-06-003-222

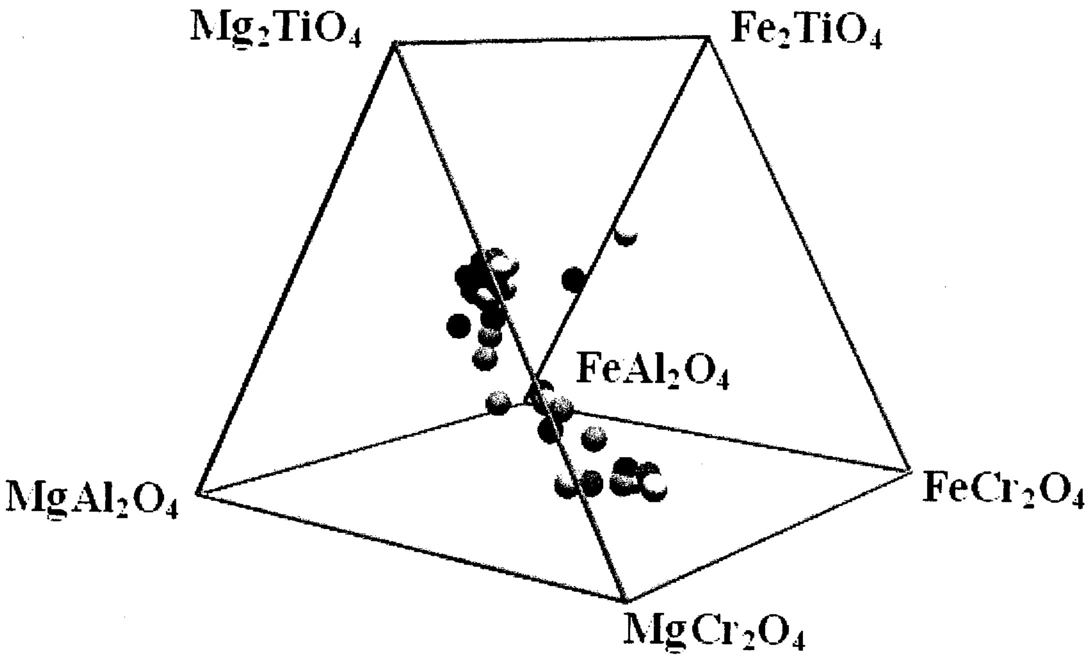

Spinel Prism for CL-06-003-236

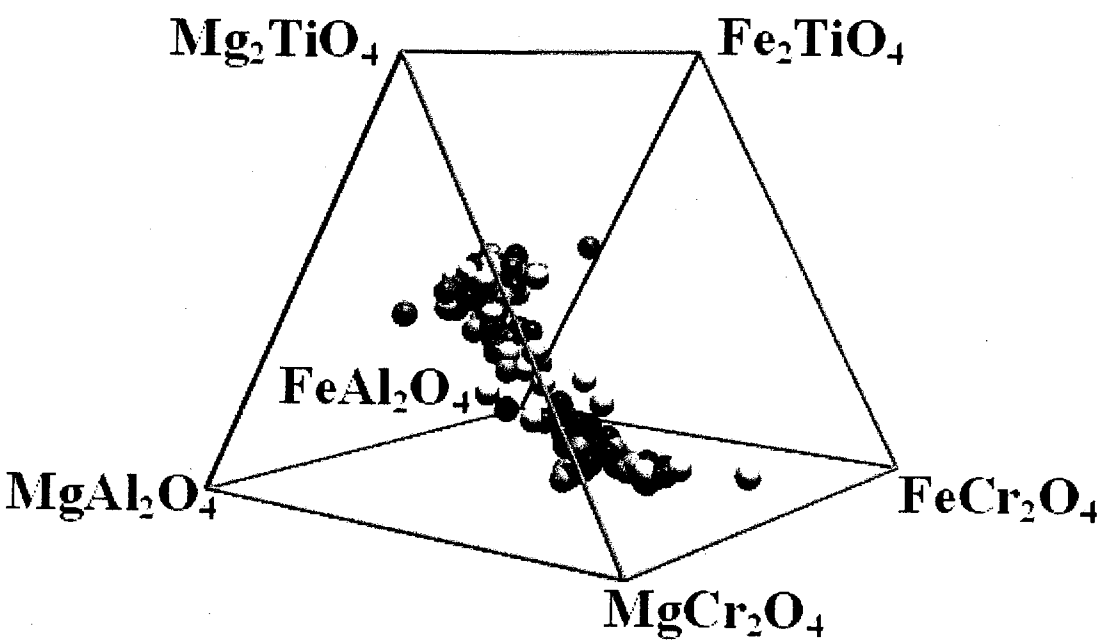

Spinel Prism for CL-06-003-236

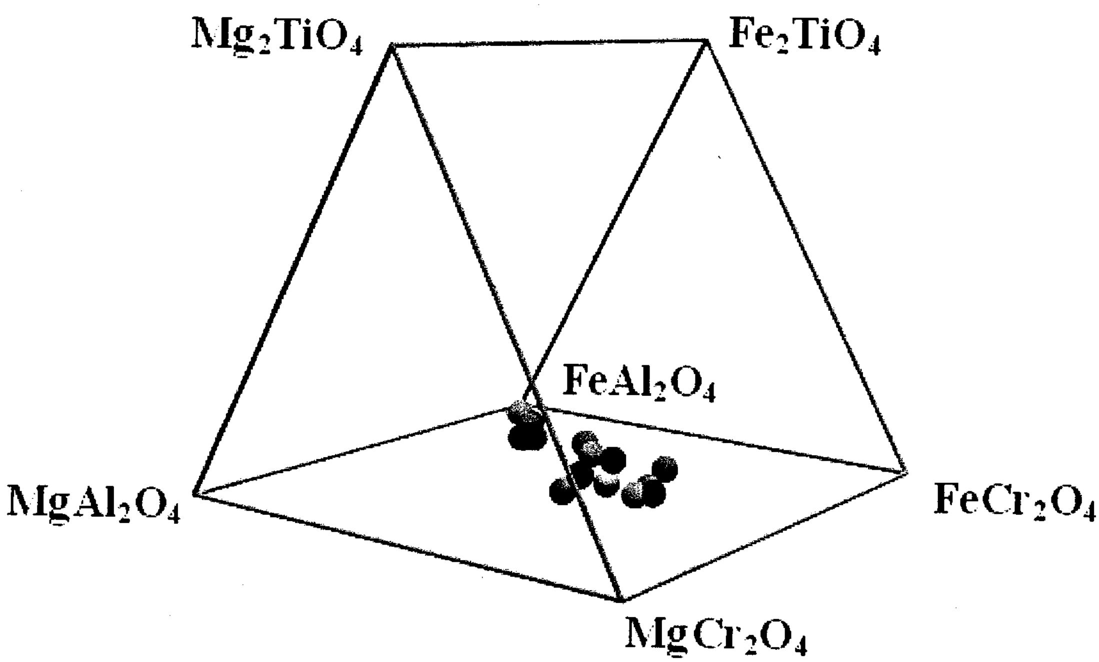

Spinel Prism for CL-07-006-195

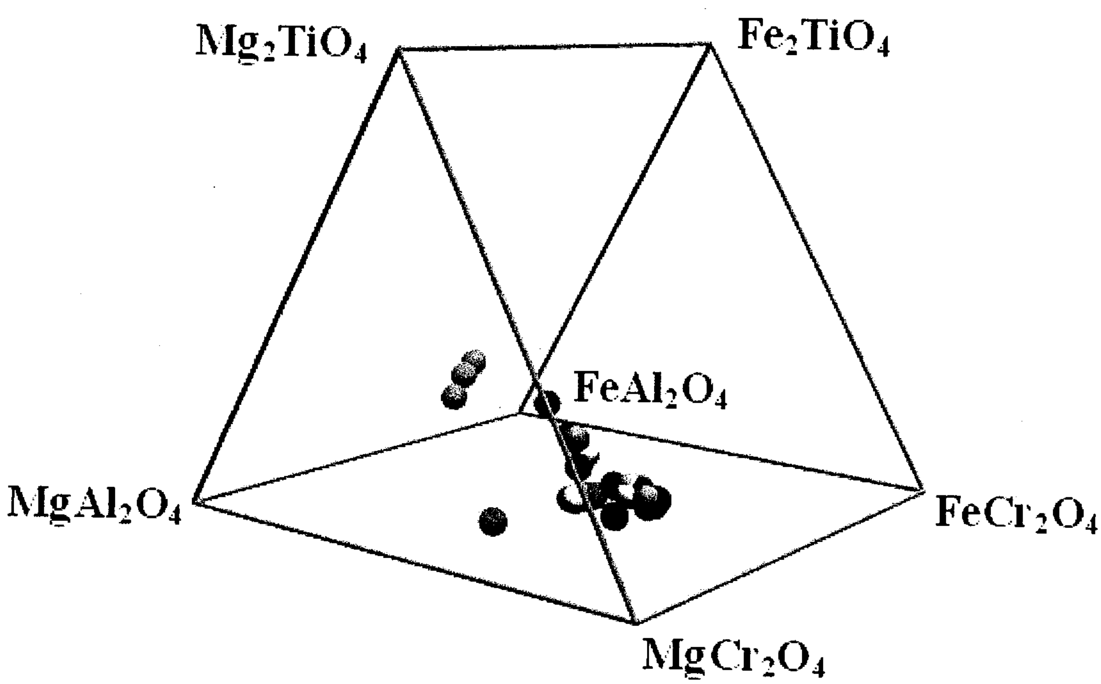

Spinel Prism for CL-07-006-208

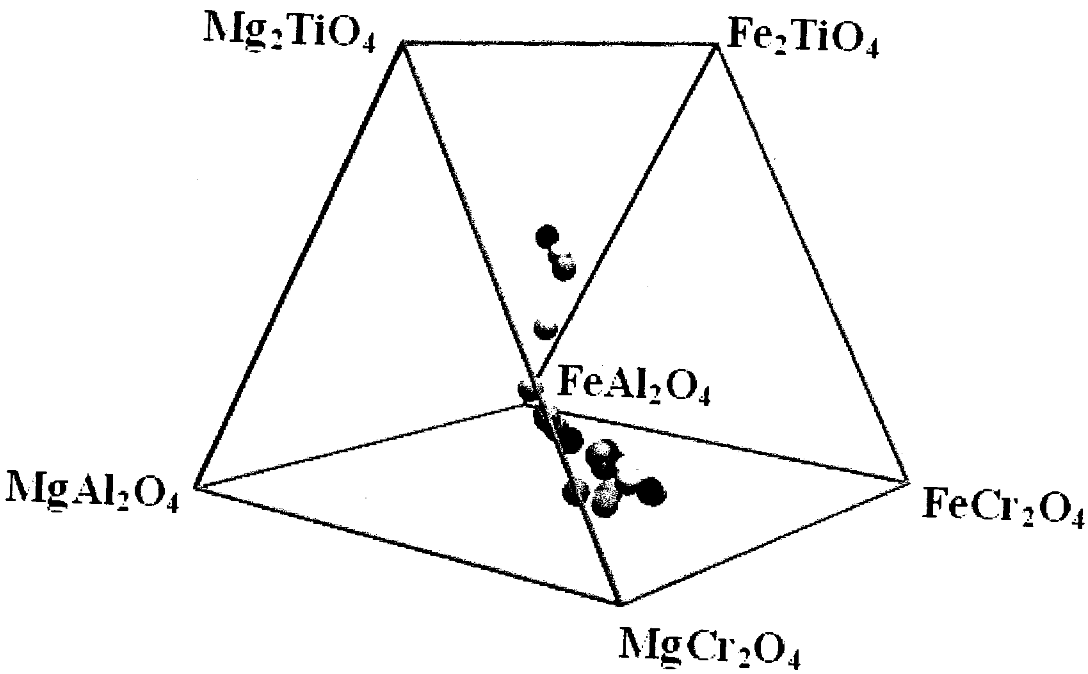

Spinel Prism for CL-07-006-214

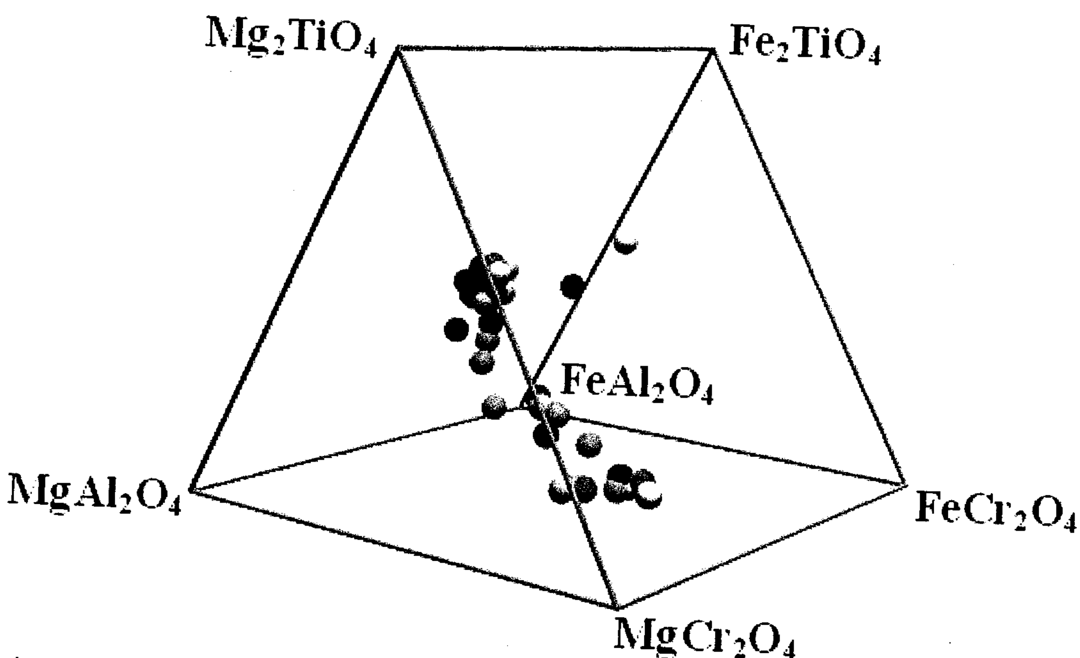

Spinel Prism for CL-07-006-235

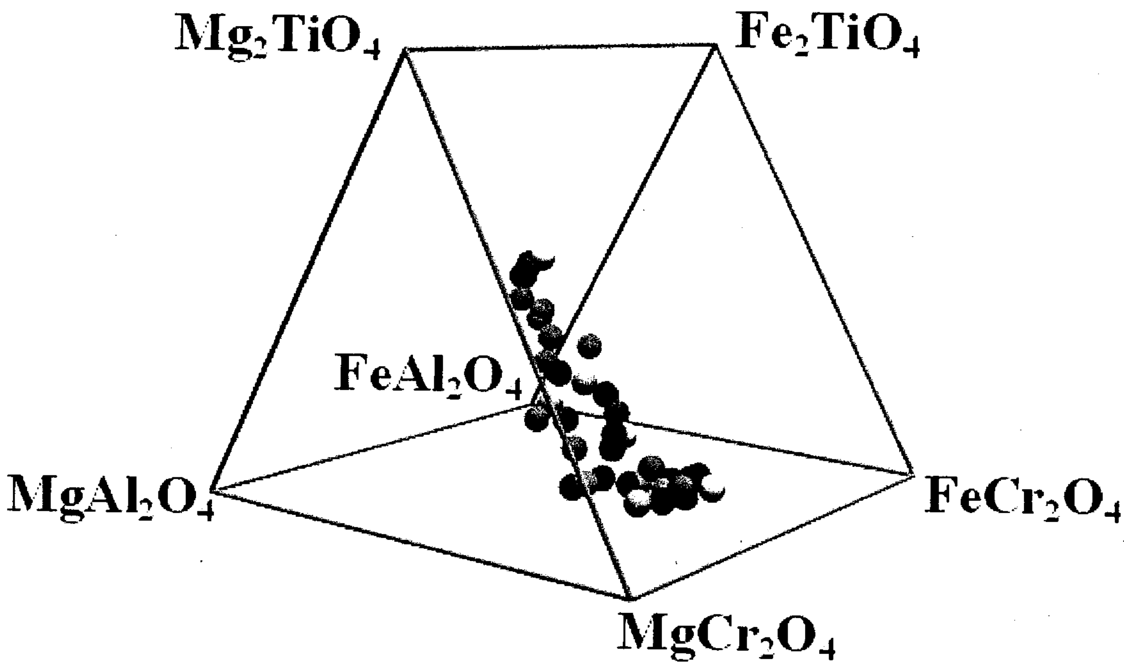

Spinel Prism for CL-07-010-160

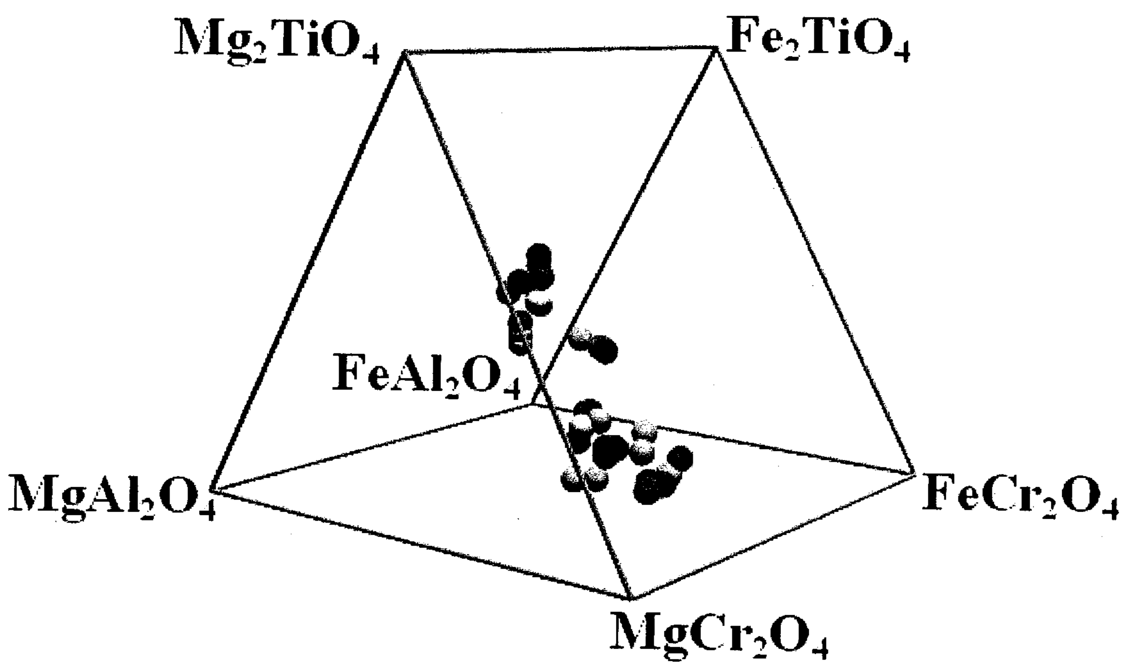

Spinel Prism for CL-07-010-169

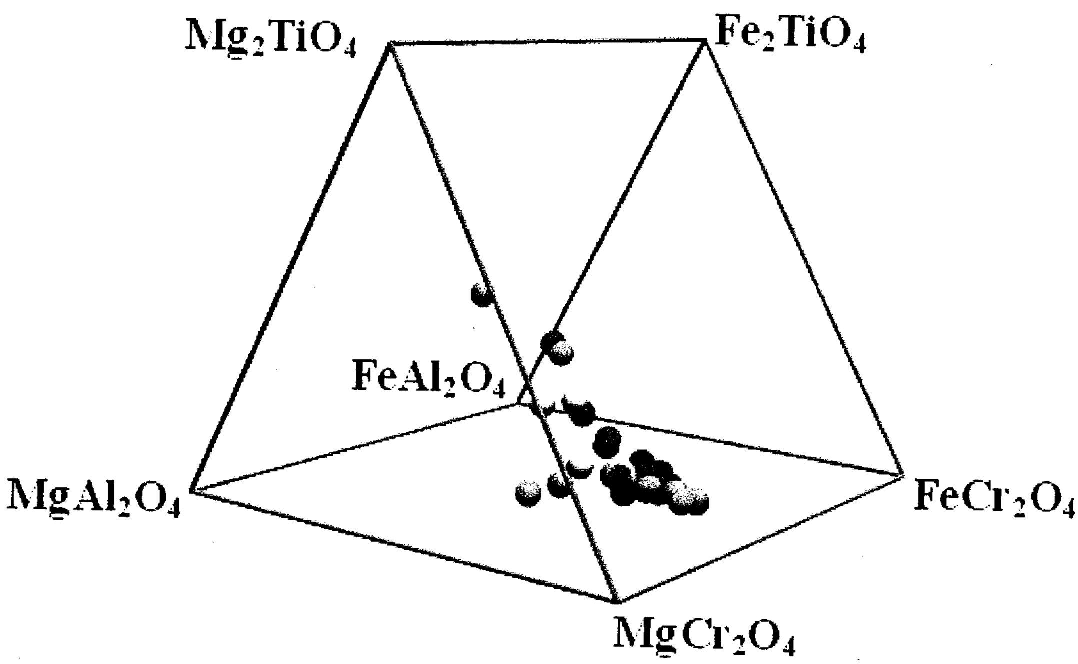

Spinel Prism for CL-07-010-188

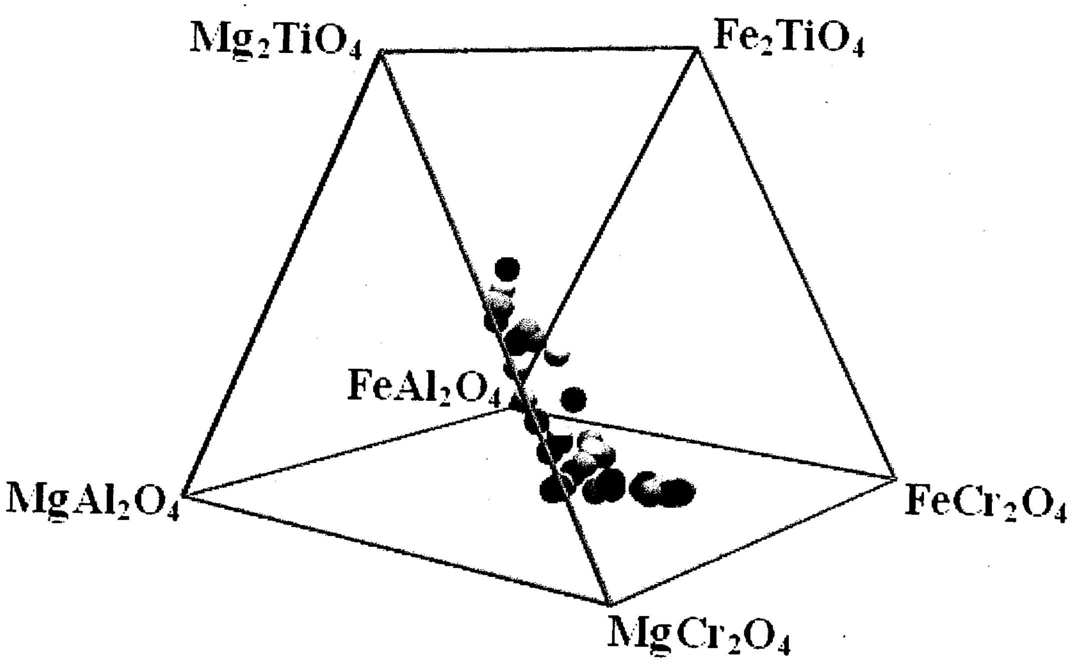

Spinel Prism for CL-07-010-188

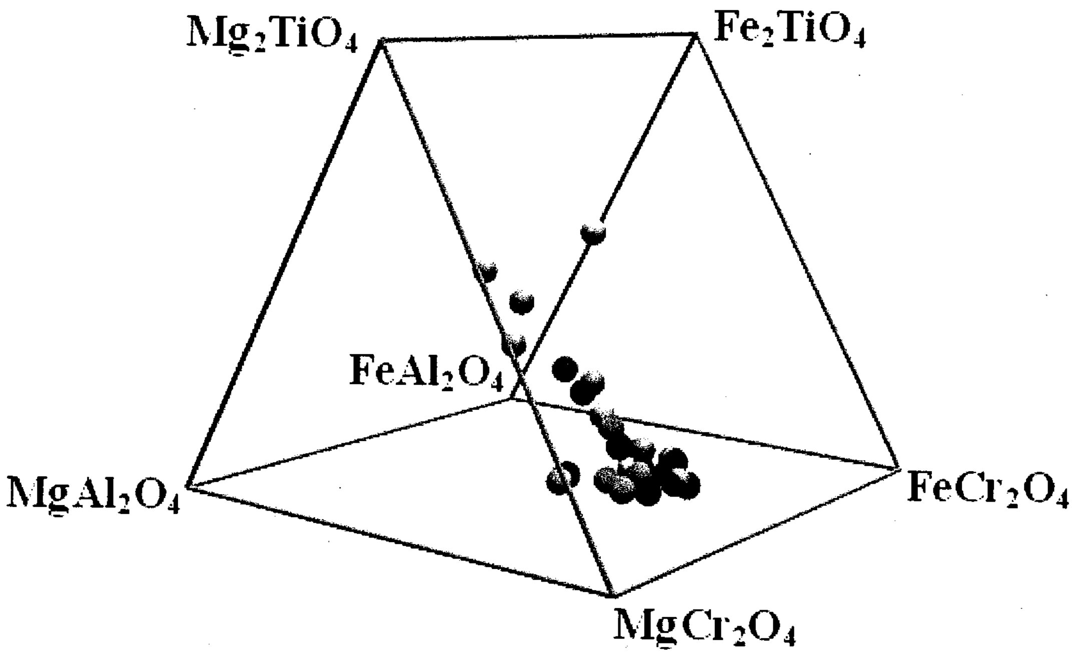

Spinel Prism for CL-07-010-221

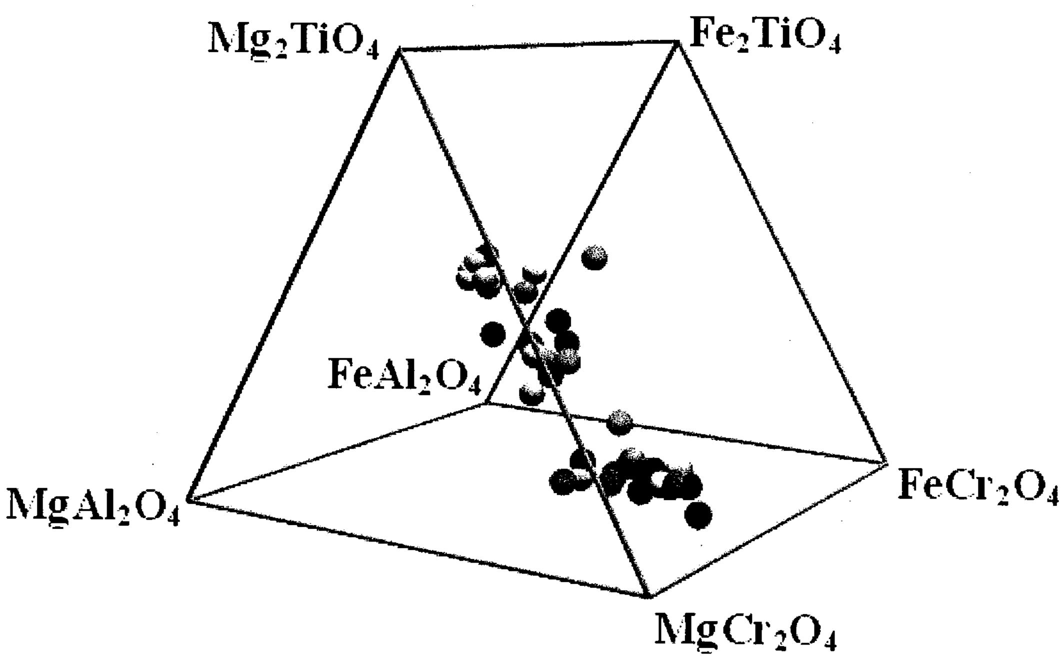

Spinel Prism for CL-07-010-224

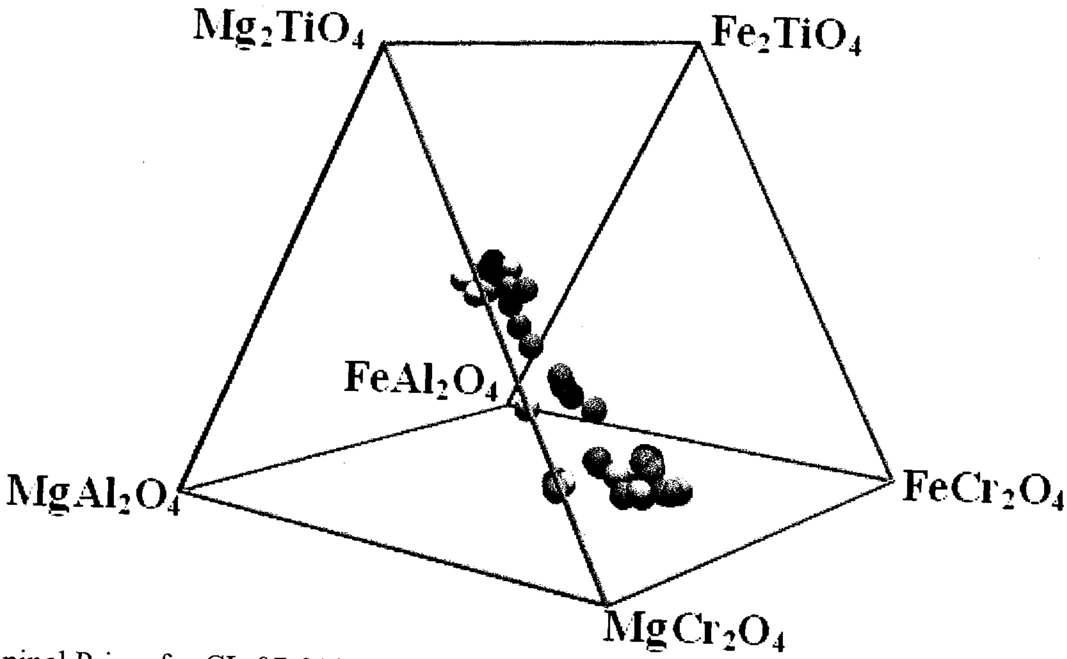

Spinel Prism for CL-07-010-233

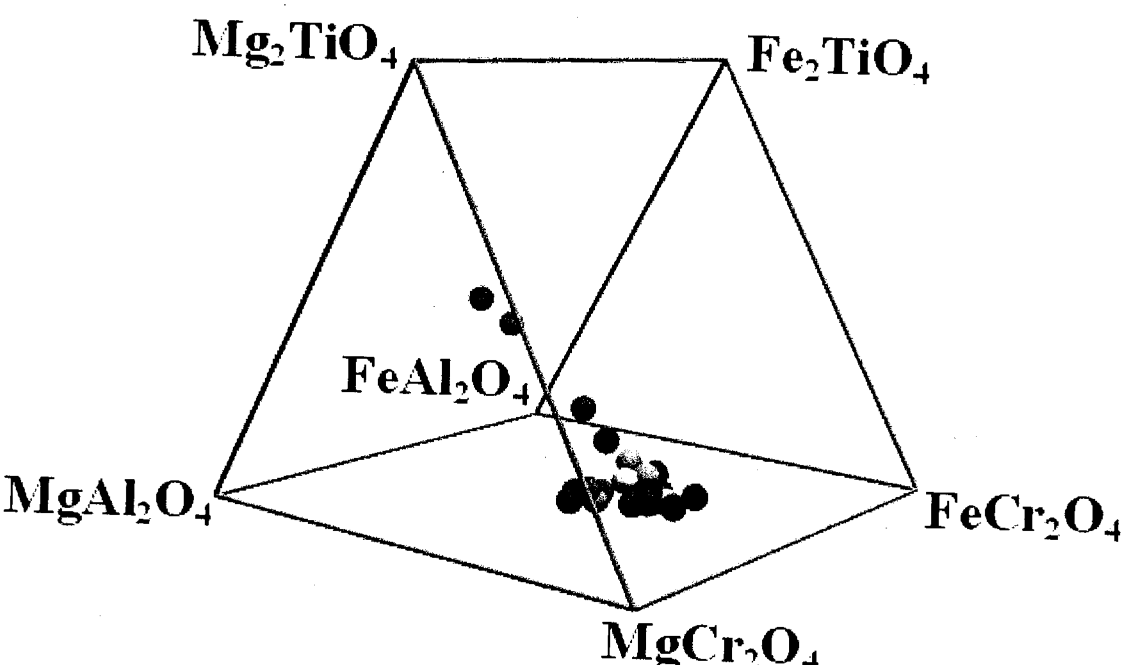

Spinel Prism for CL-07-010-245

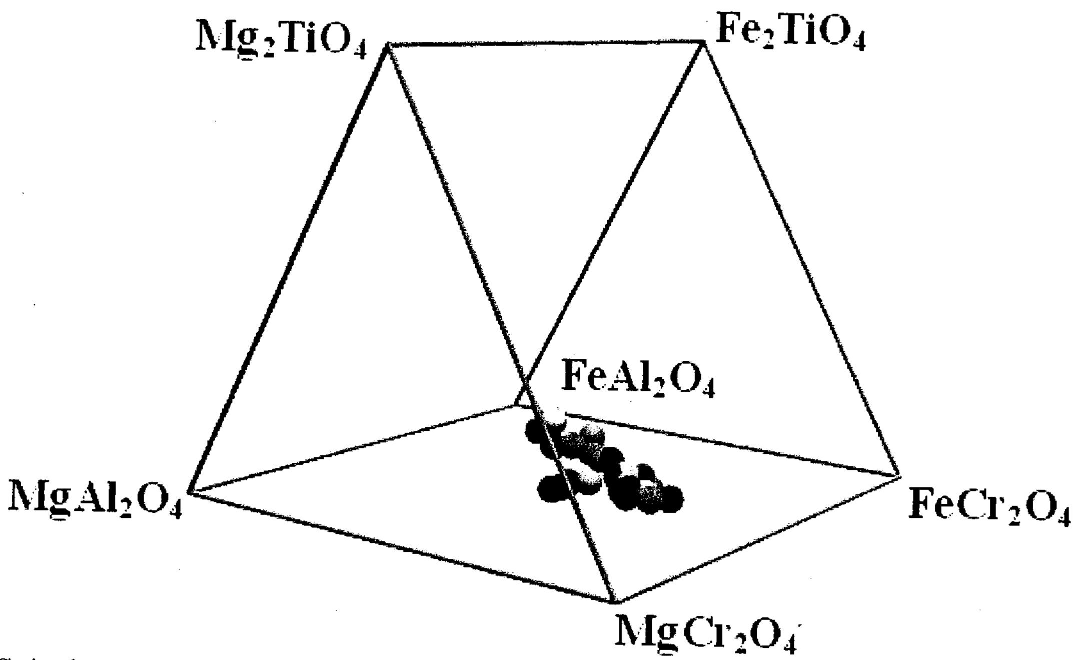

Spinel Prism for CL-07-010-255

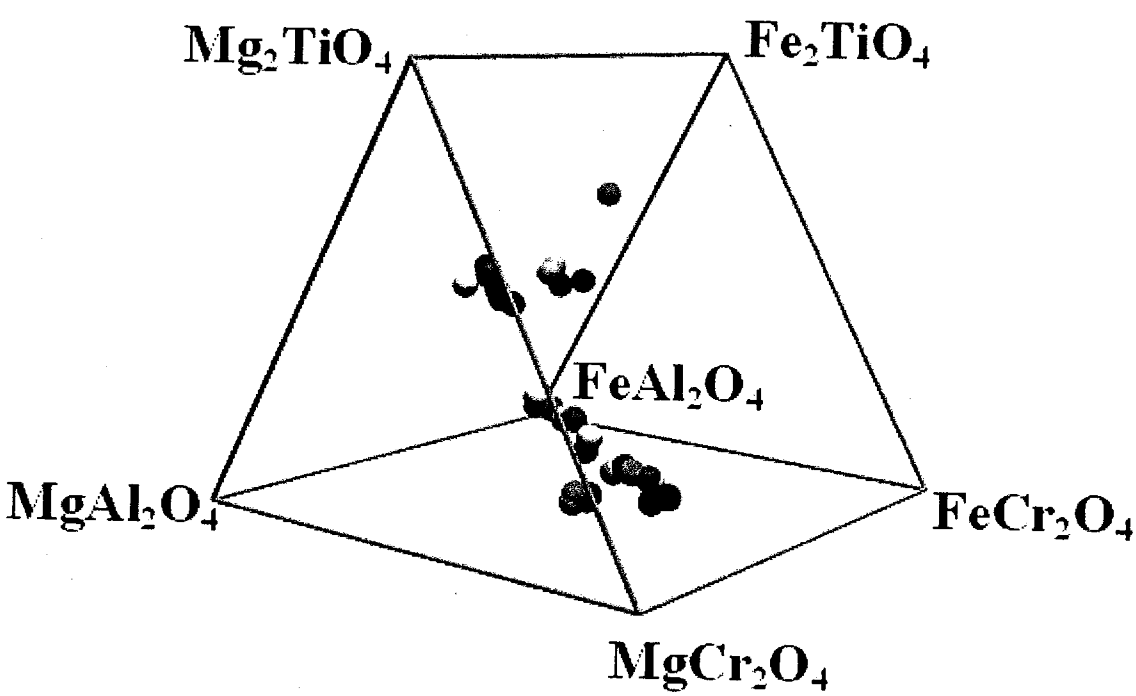

Spinel Prism for CL-07-010-264

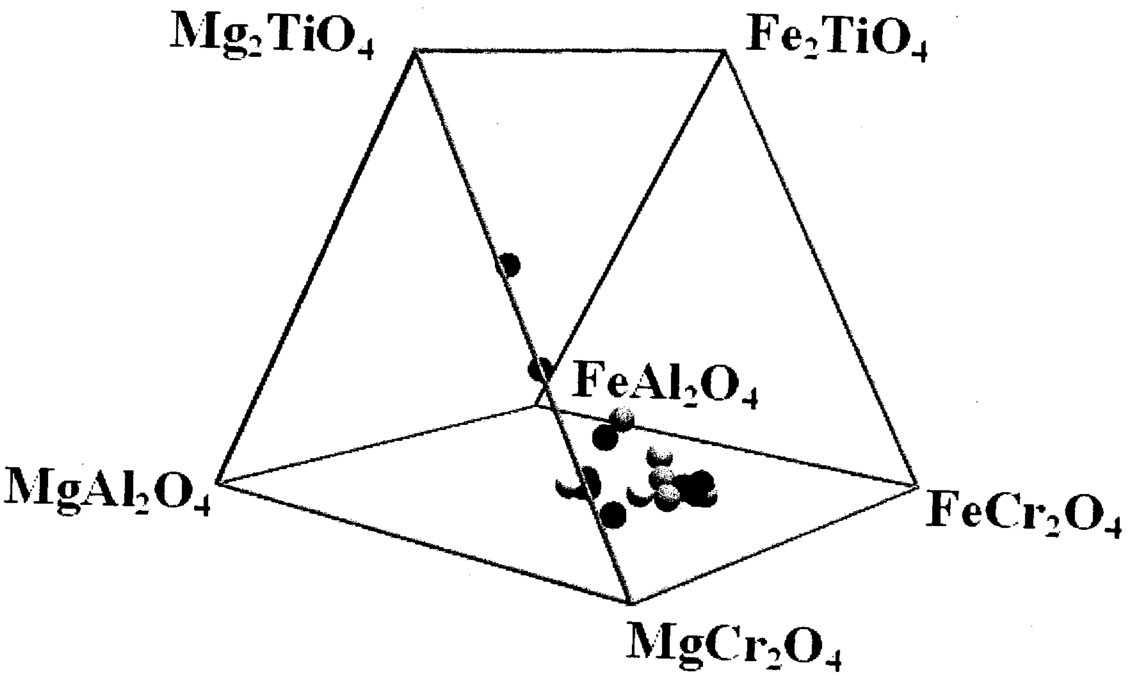

Spinel Prism for CL-07-014-233

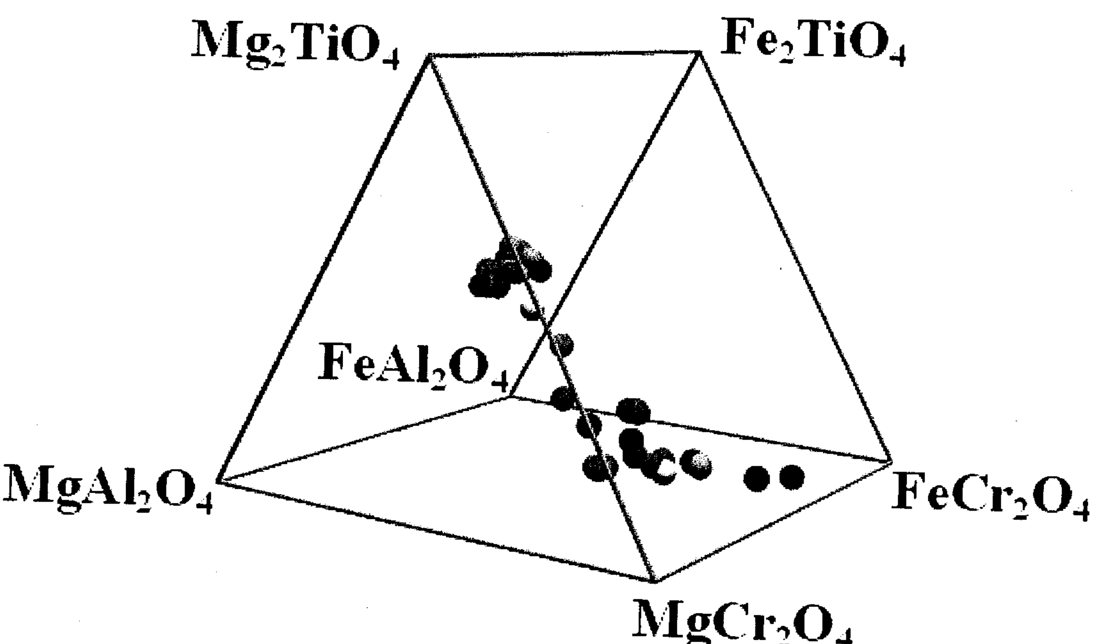

Spinel Prism for CL-07-014-245

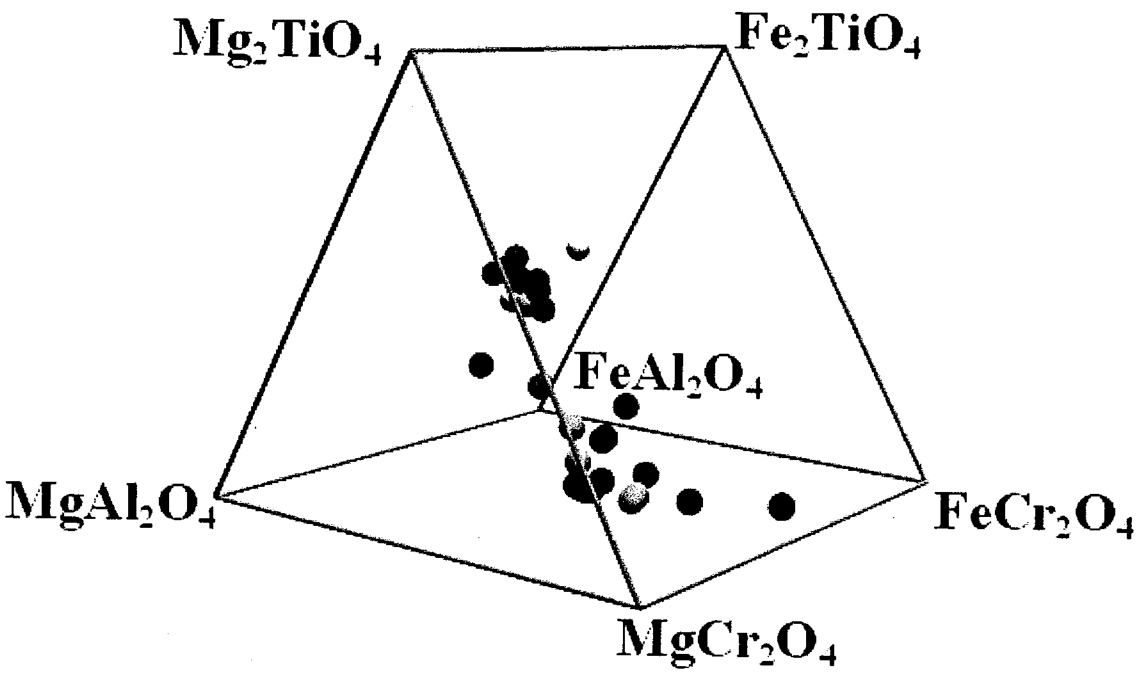

Spinel Prism for CL-07-014-257

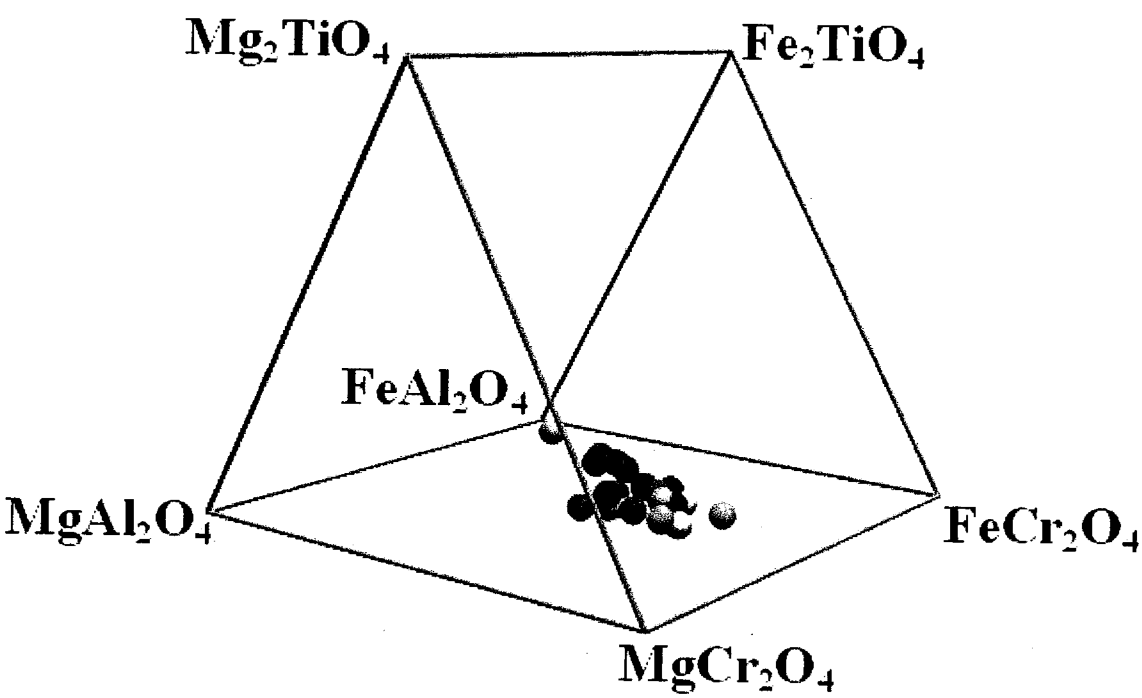

Spinel Prism for CL-07-014-260

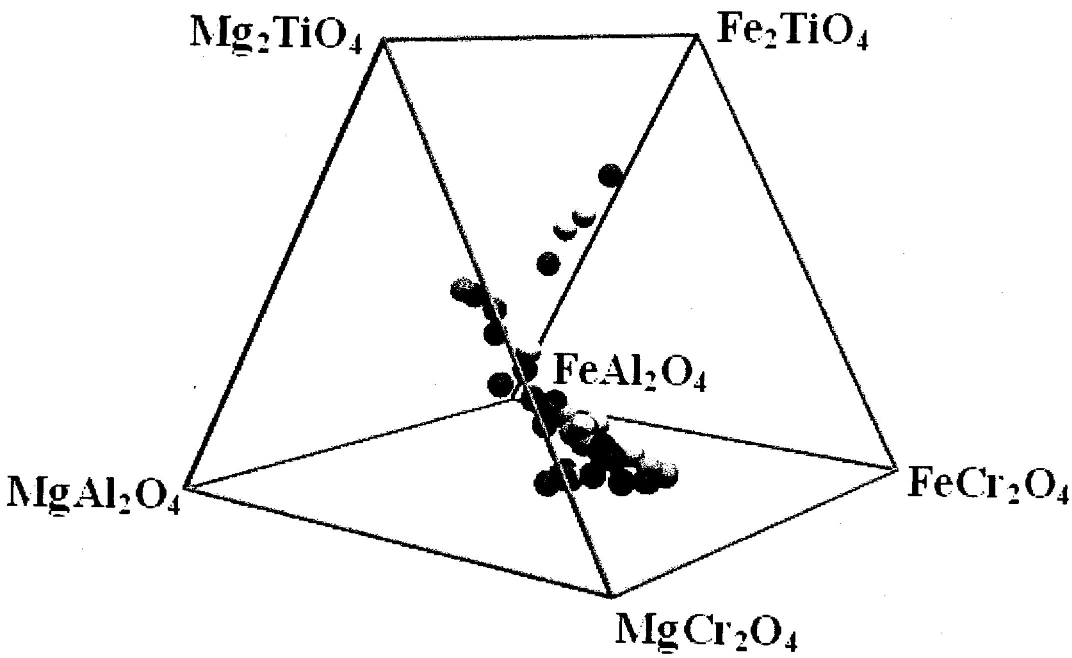

Spinel Prism for CL-07-014-269

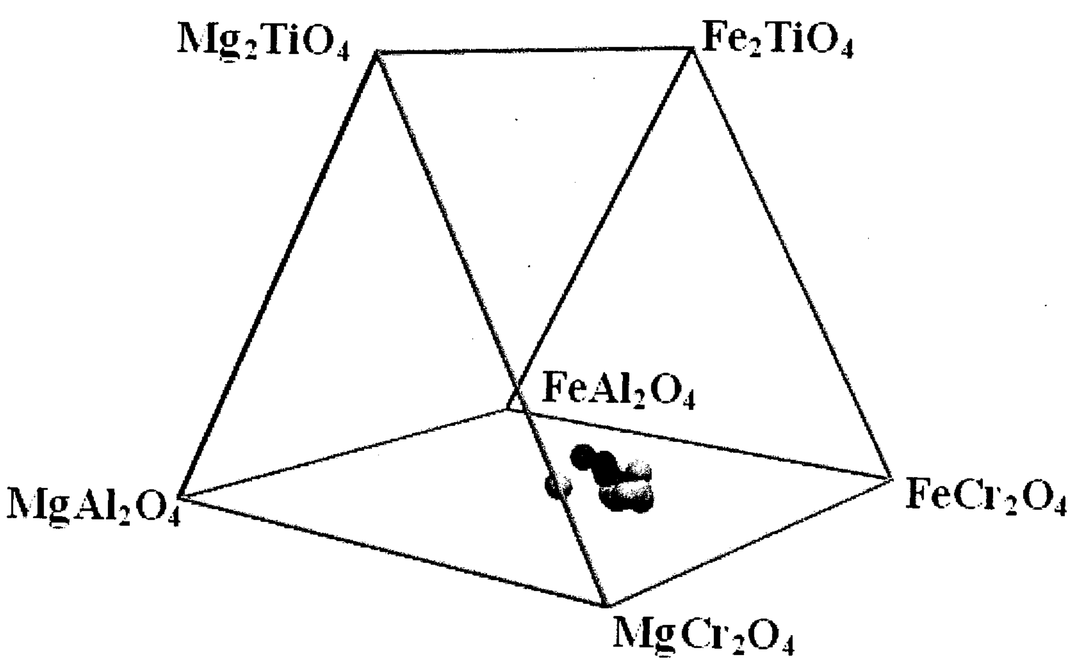

Spinel Prism for CL-07-014-273

APPENDIX C

Ti / (Ti + Cr + Al) vs. Fe^{2+} / (Mg + Fe^{2+}) PLOTS FOR SPINELS

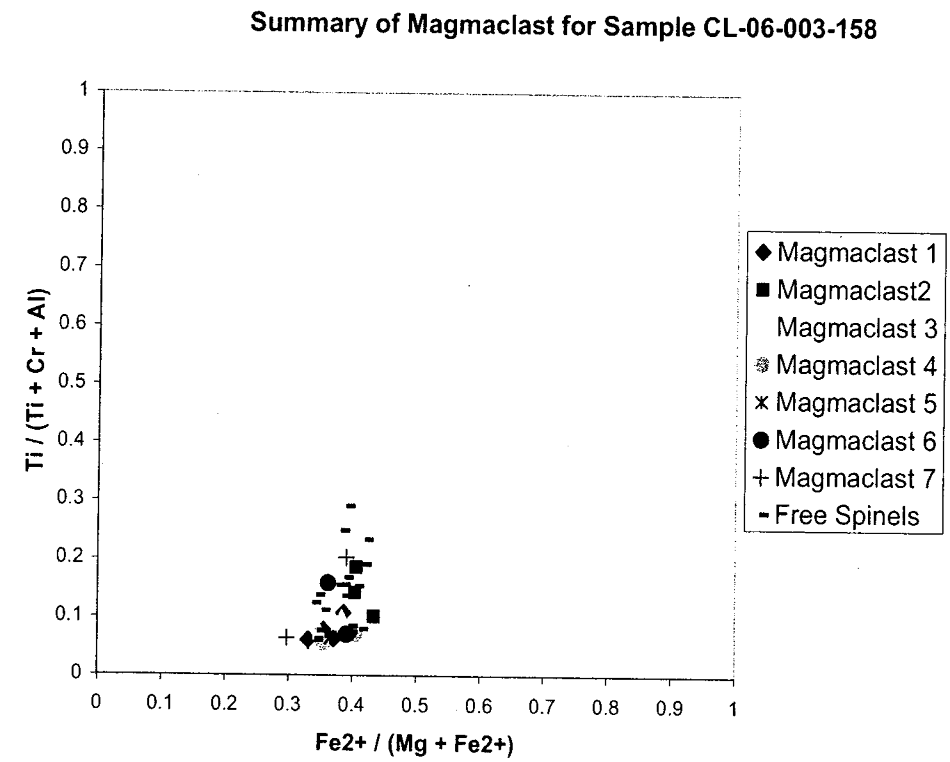

Plot for Sample CL-06-003-158

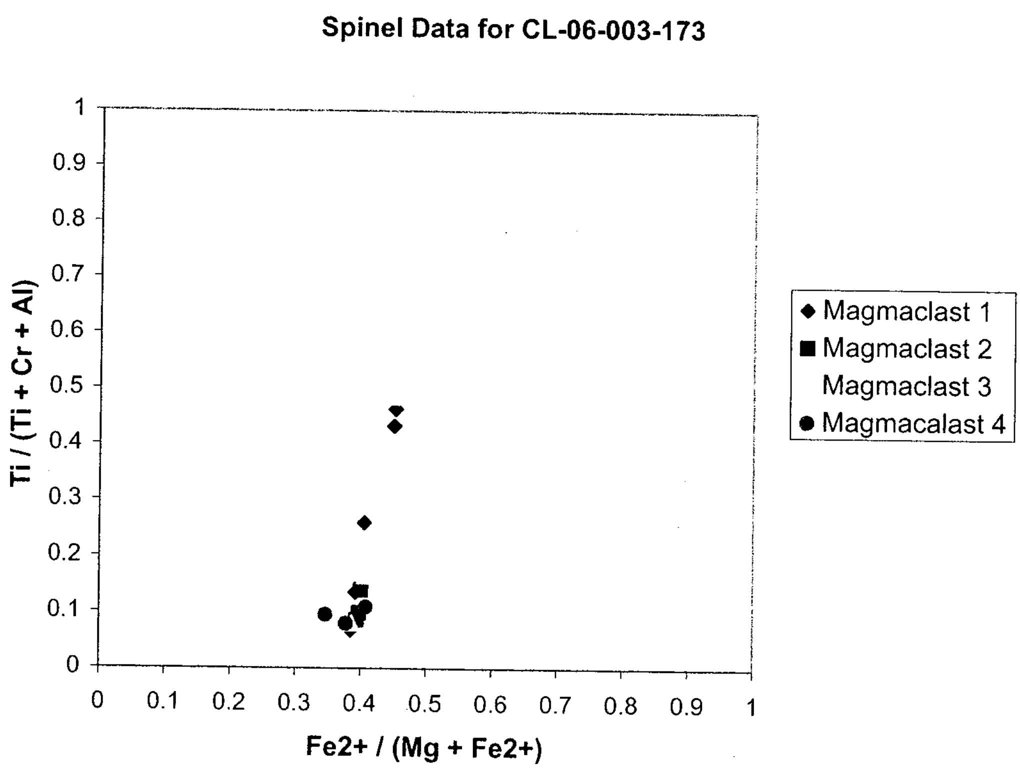

Plot for Sample CL-06-003-173

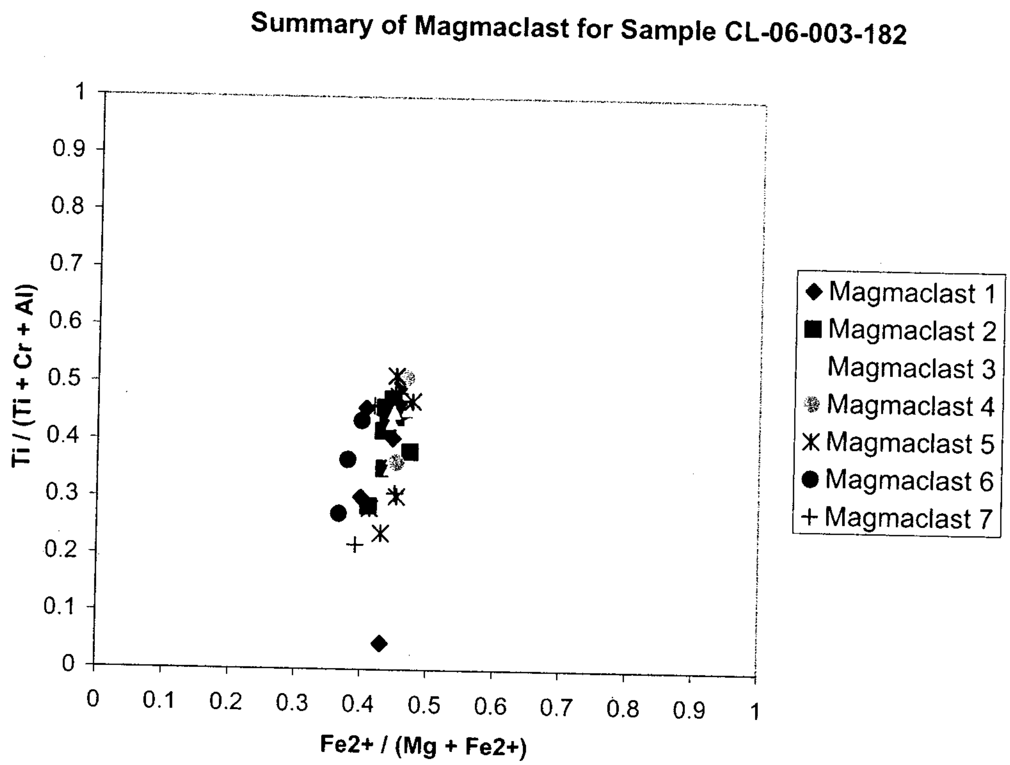

Plot for Sample CL-06-003-182

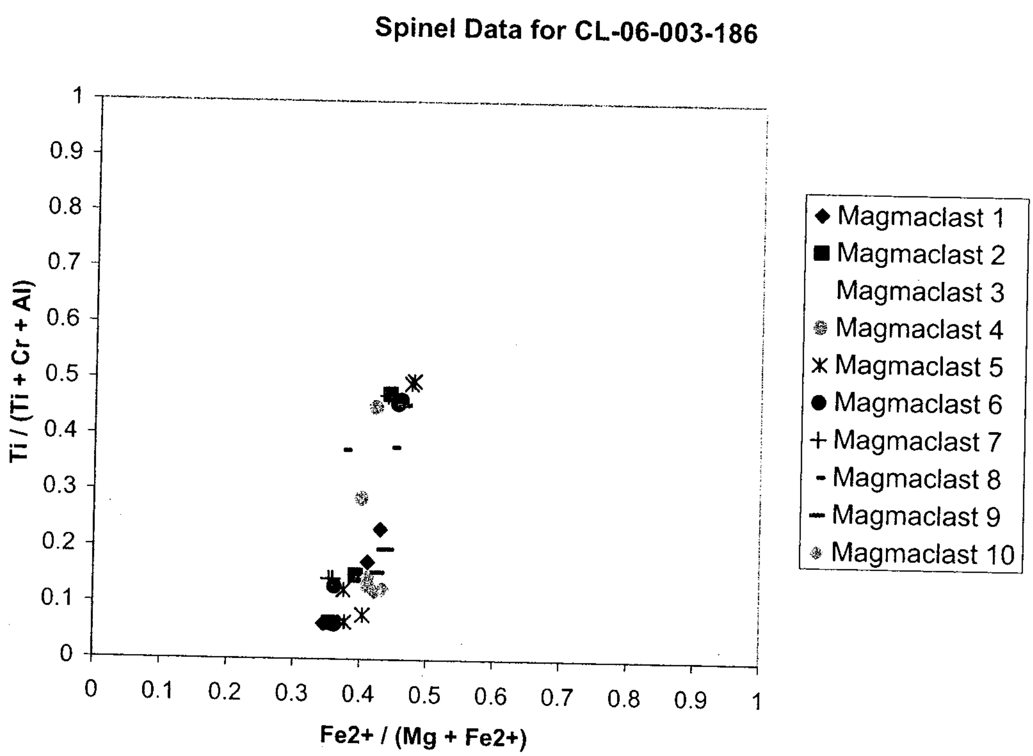

Plot for Sample CL-06-003-186

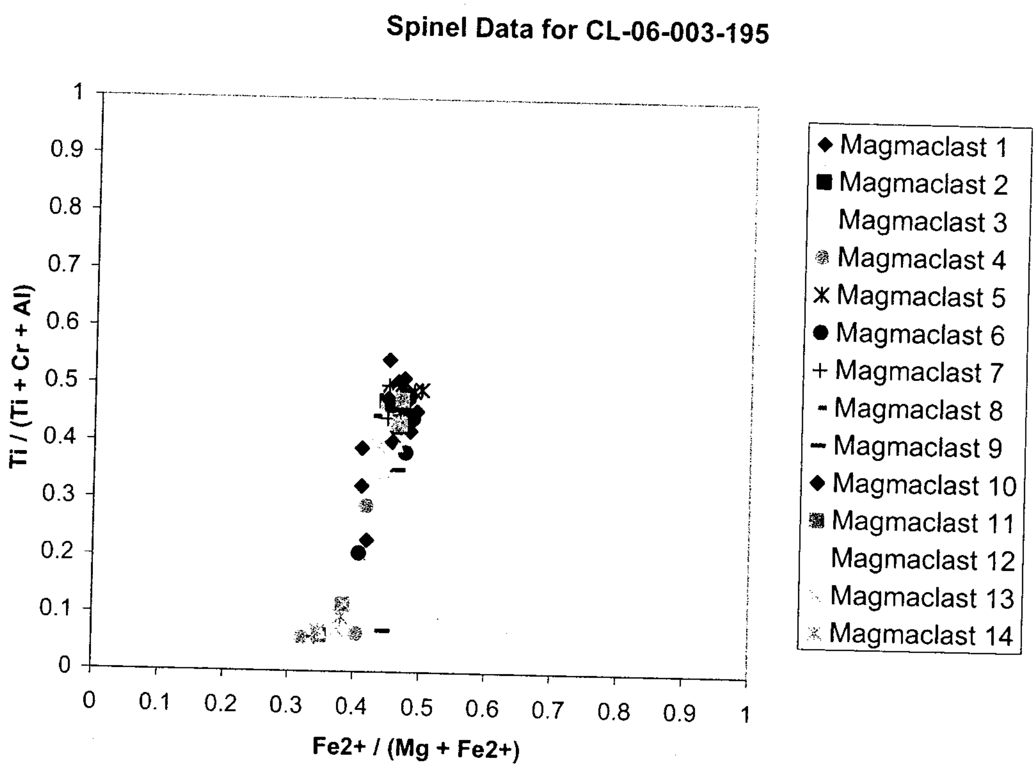

Plot for Sample CL-06-003-195

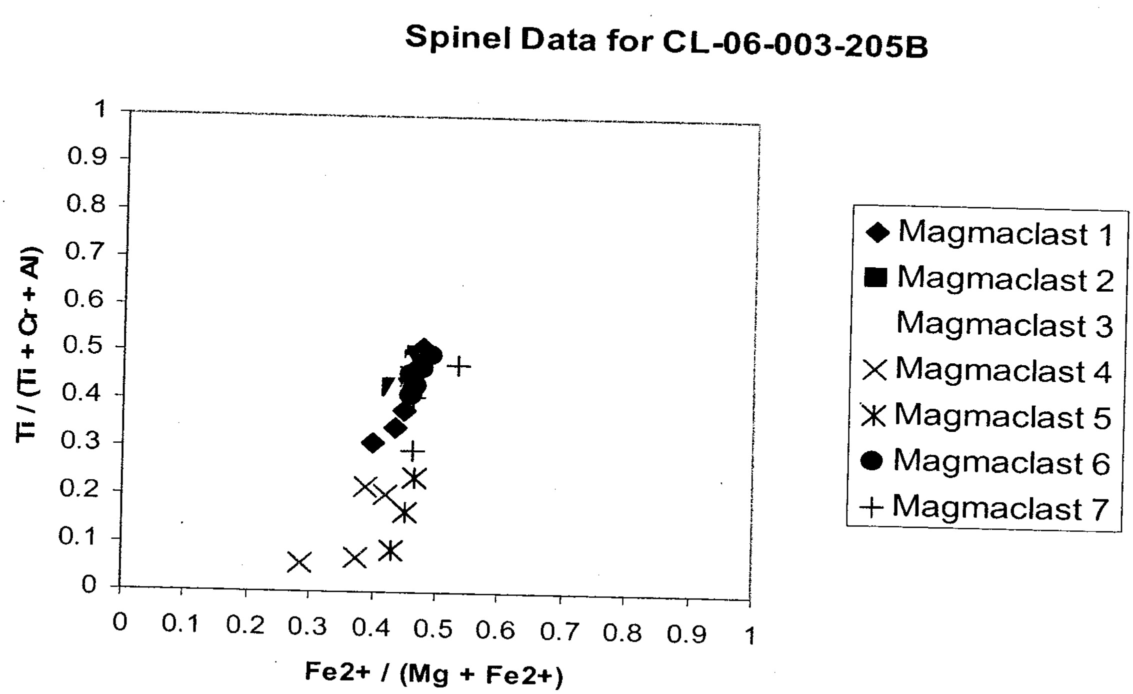

Plot for Sample CL-06-003-205

Spinel Data for CL-06-003-219

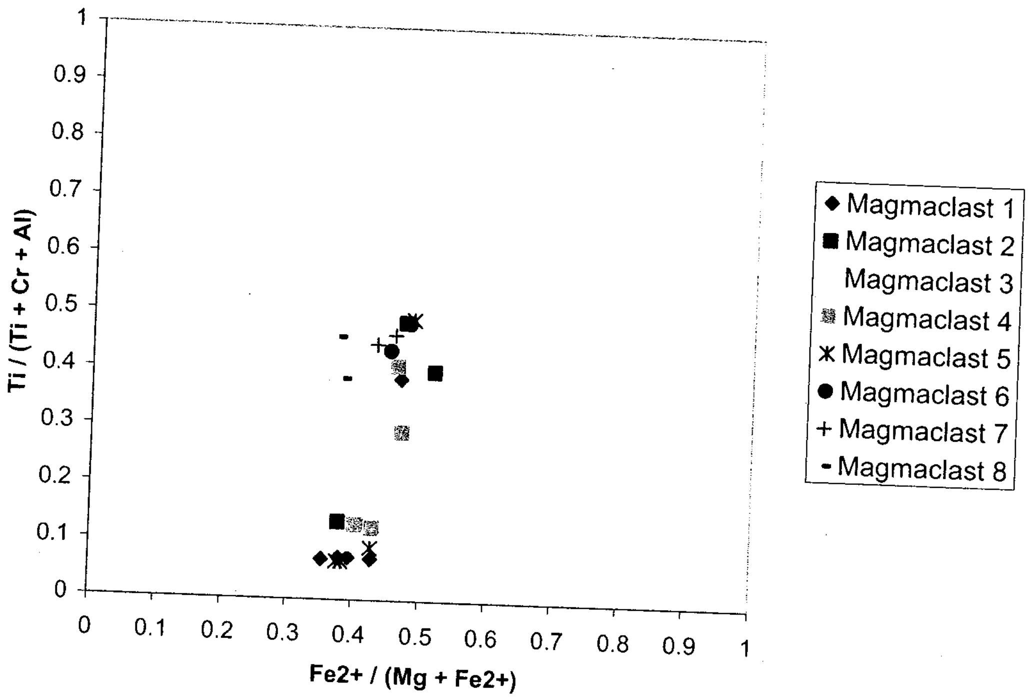

Plot for Sample CL-06-003-219

Spinel Data for CL-06-003-222

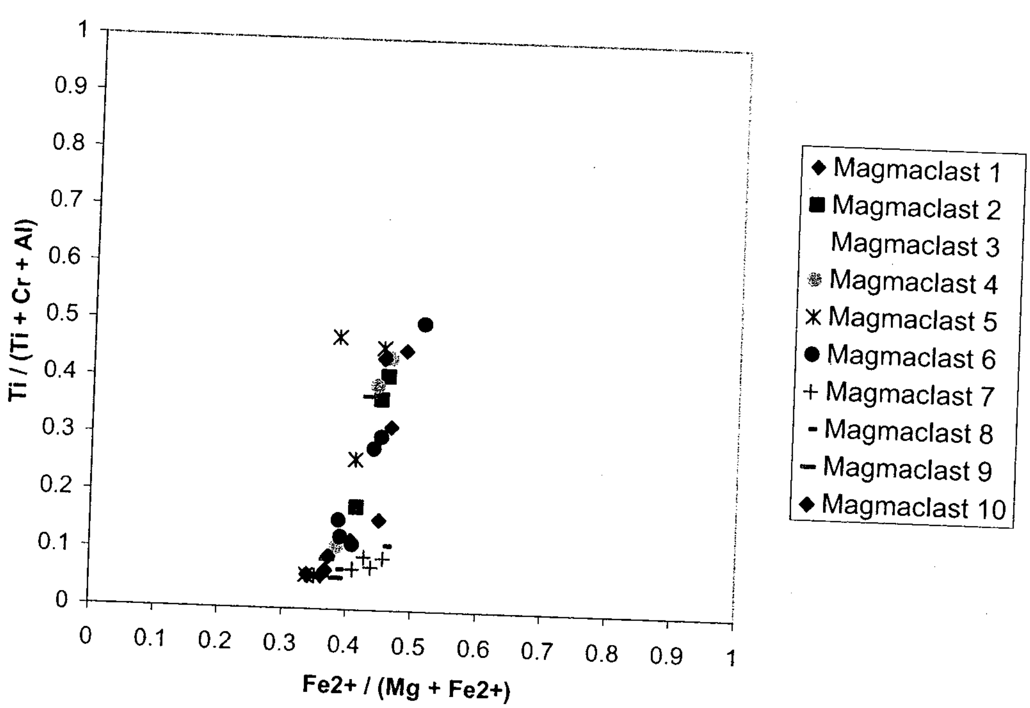

Plot for Sample CL-06-003-222

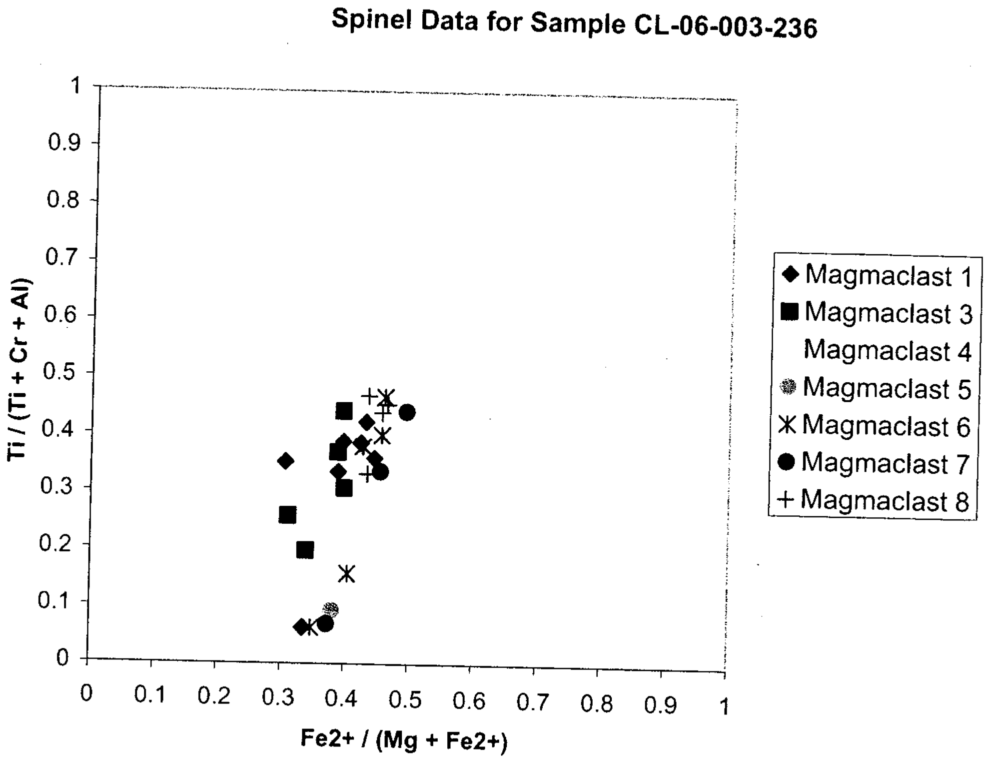

Plot for Sample CL-06-003-236

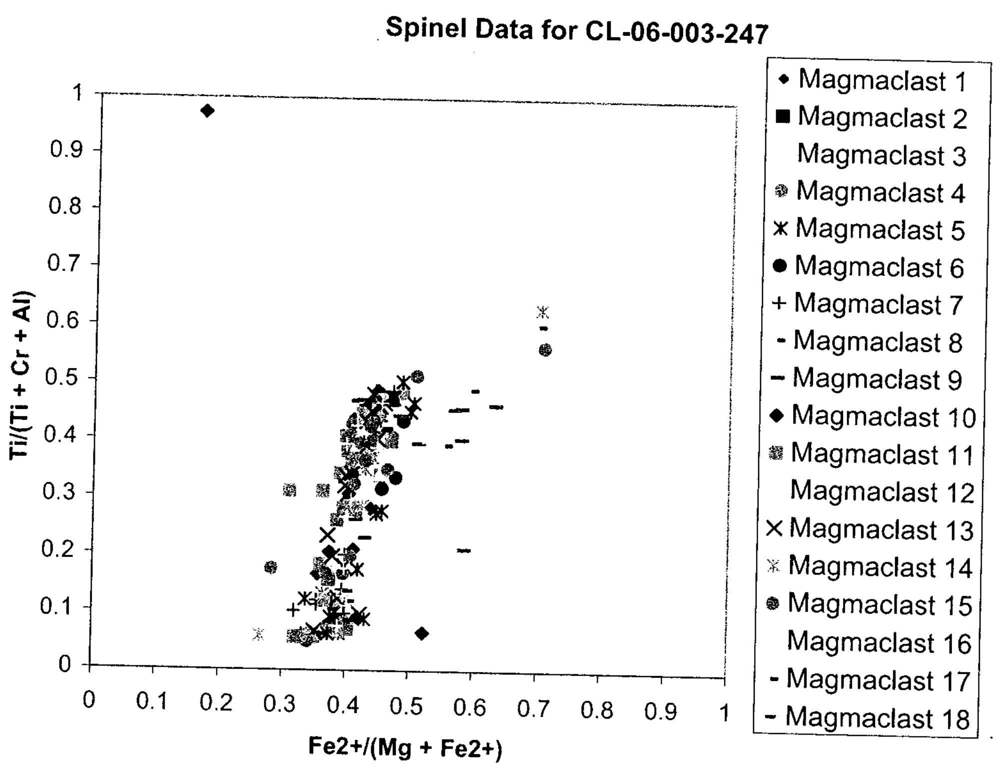

Plot for Sample CL-06-003-247

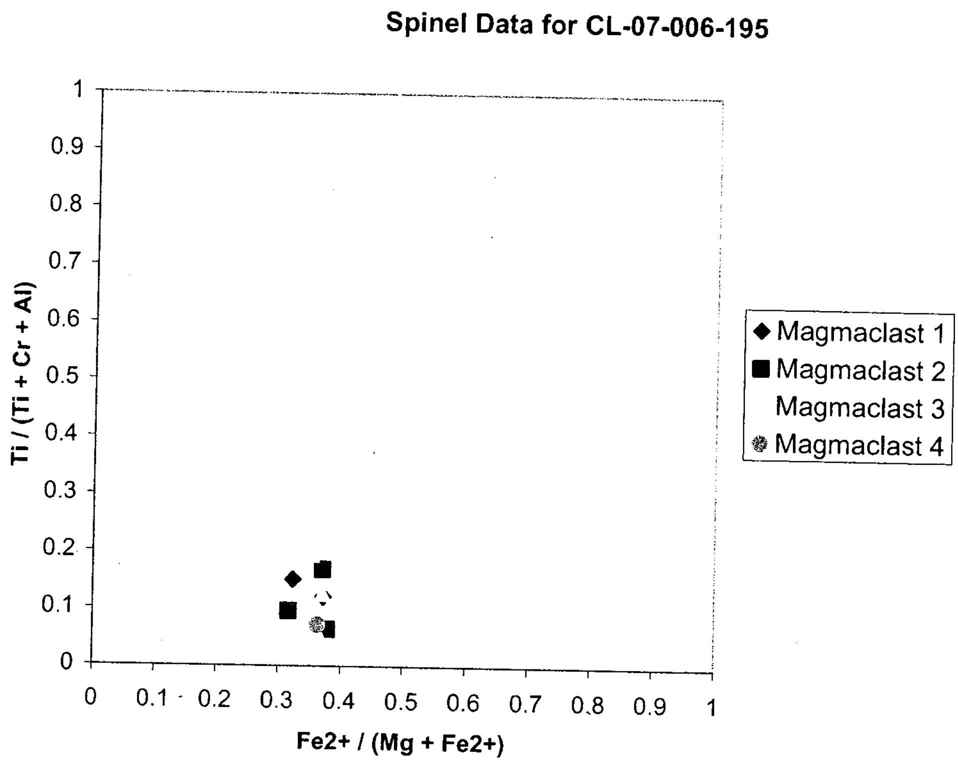

Plot for Sample CL-07-006-195

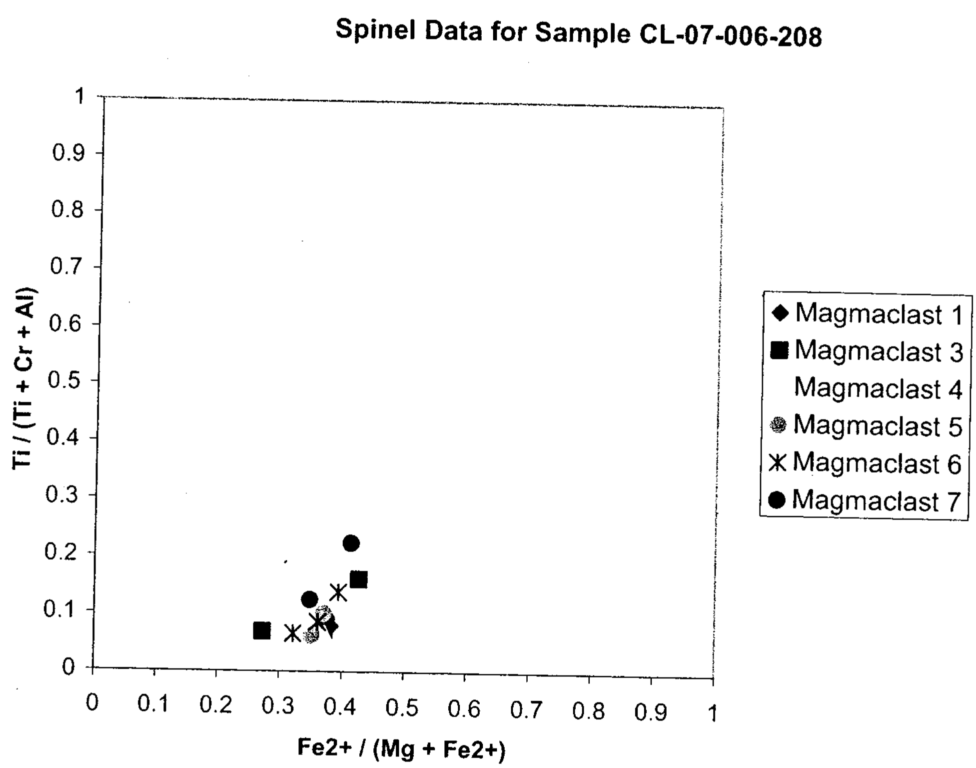

Plot for Sample CL-07-006-208

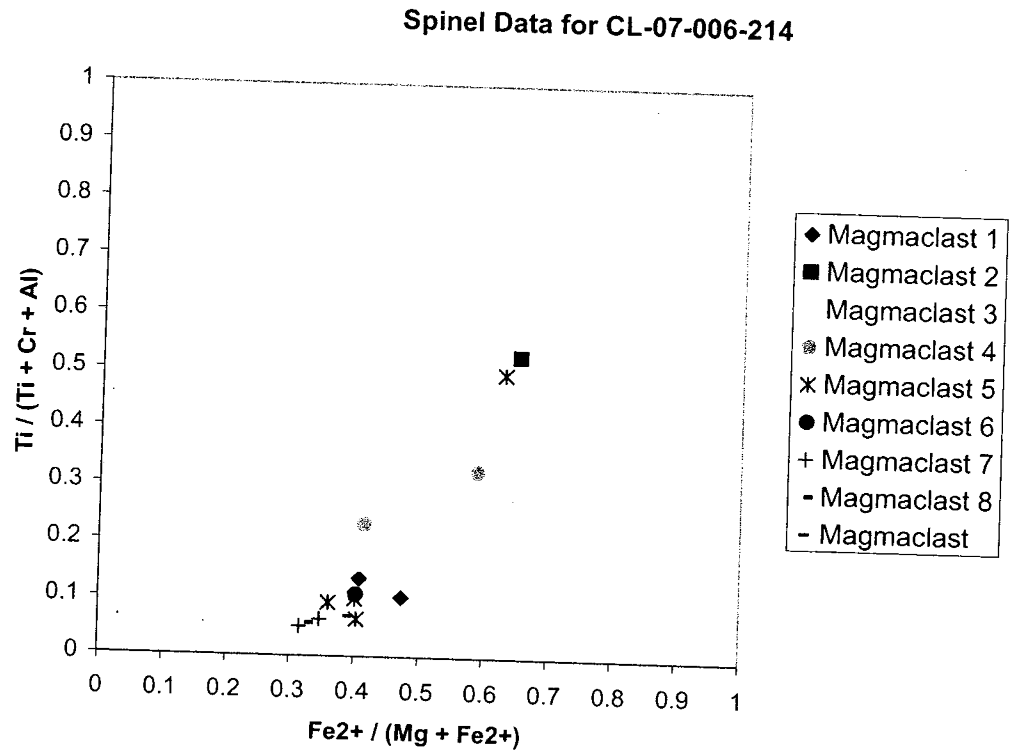

Plot for Sample CL-07-006-214

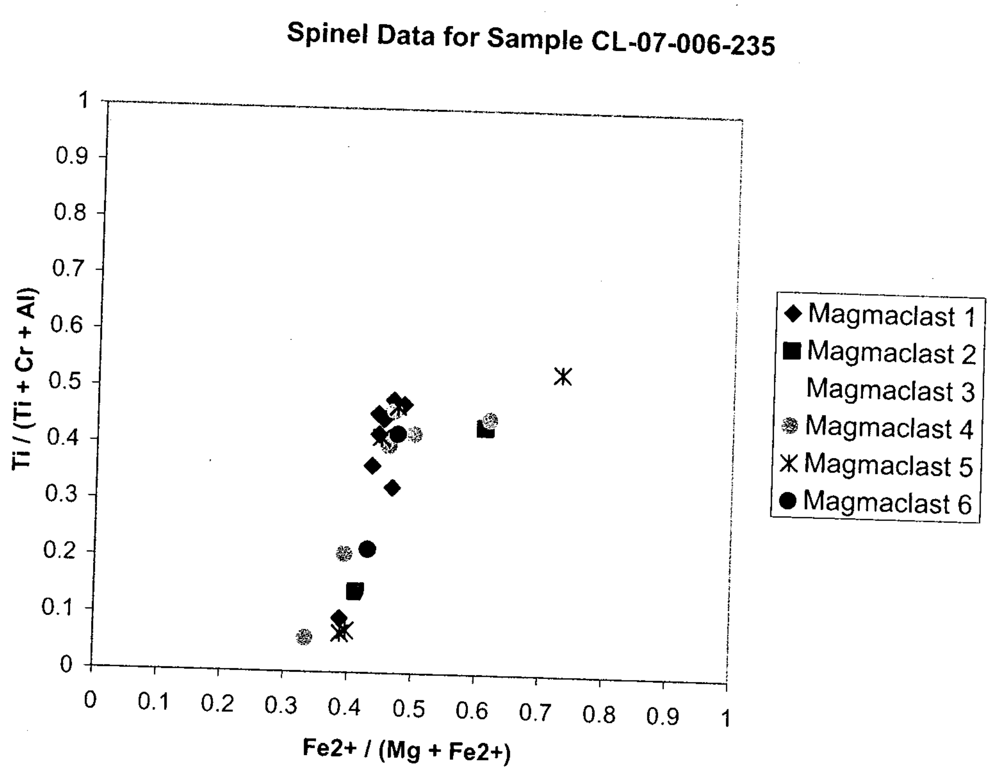

Plot for Sample CL-07-006-235

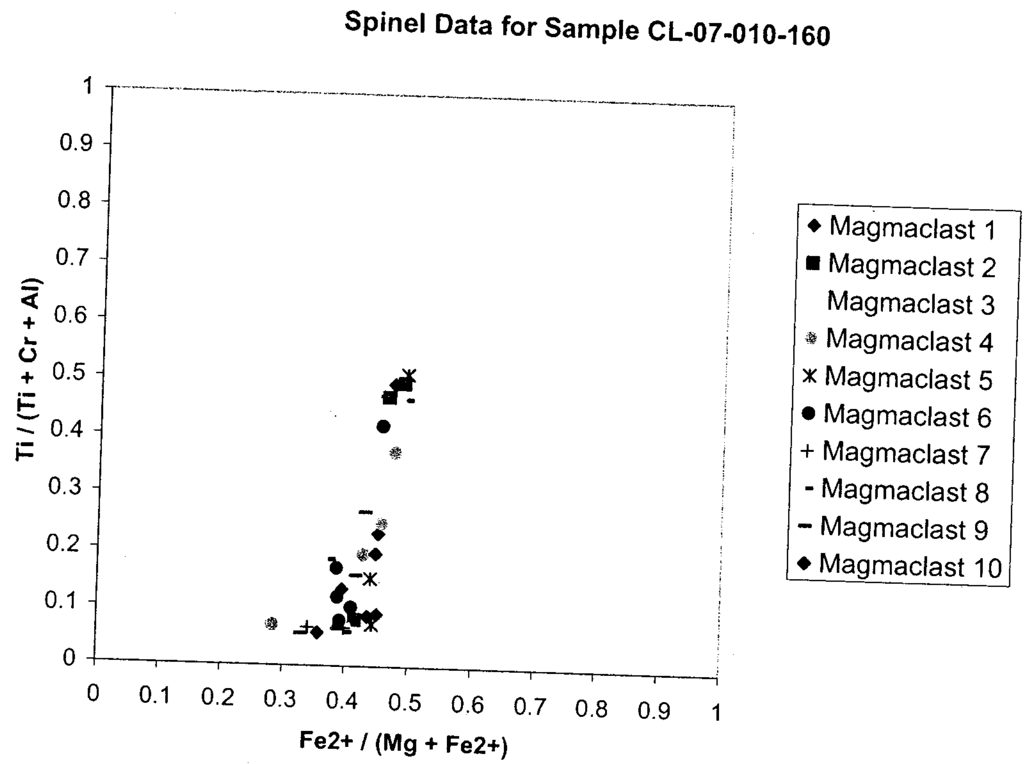

Plot for Sample CL-07-010-160

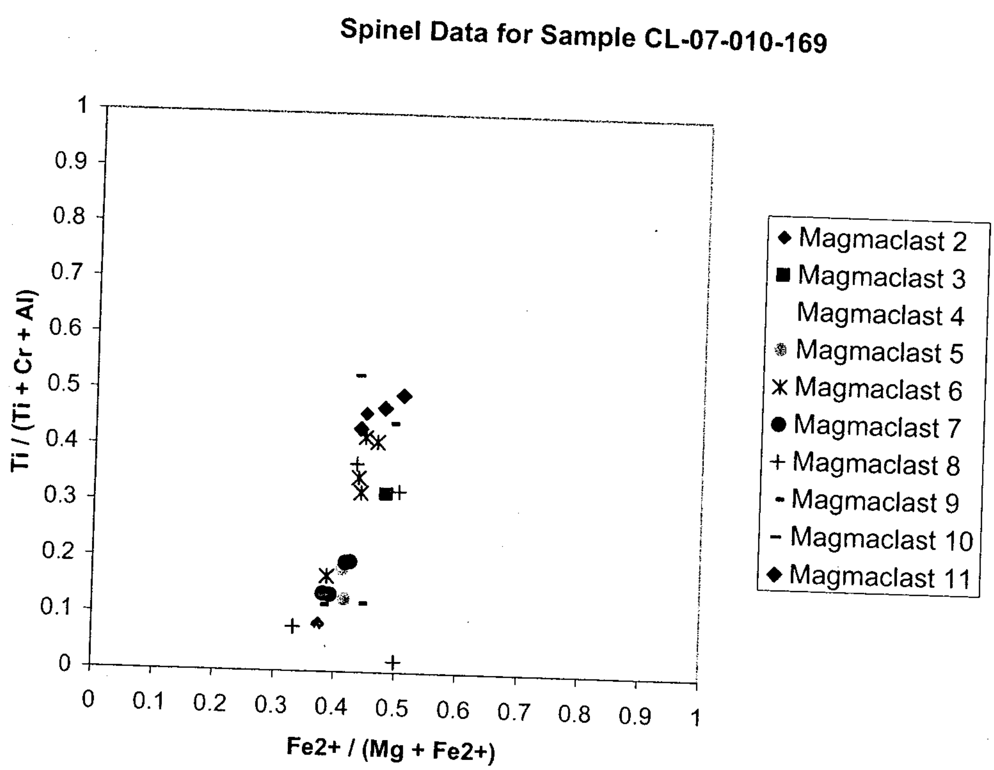

Plot for Sample CL-07-010-169

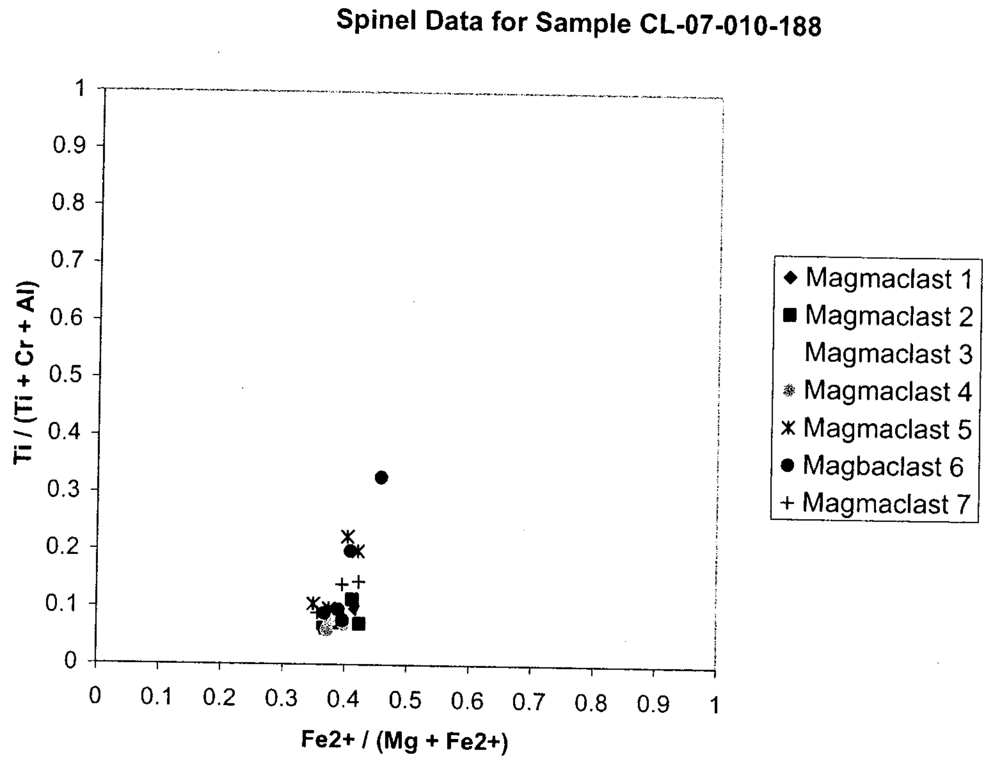

Plot for Sample CL-07-010-188

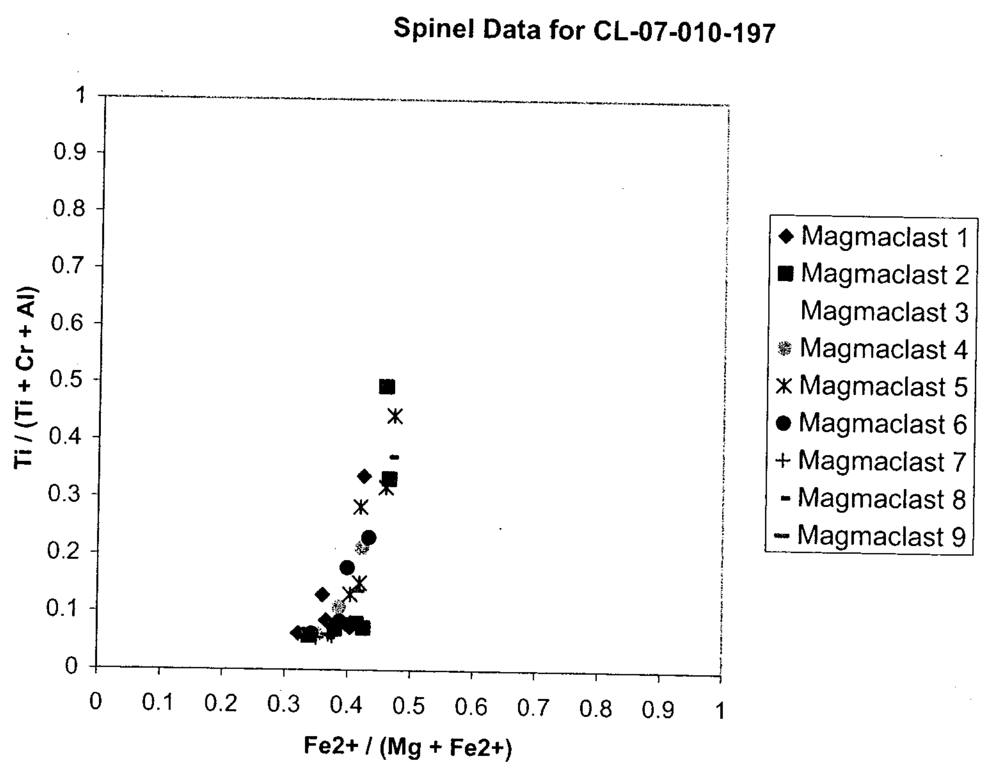

Plot for Sample CL-07-010-197

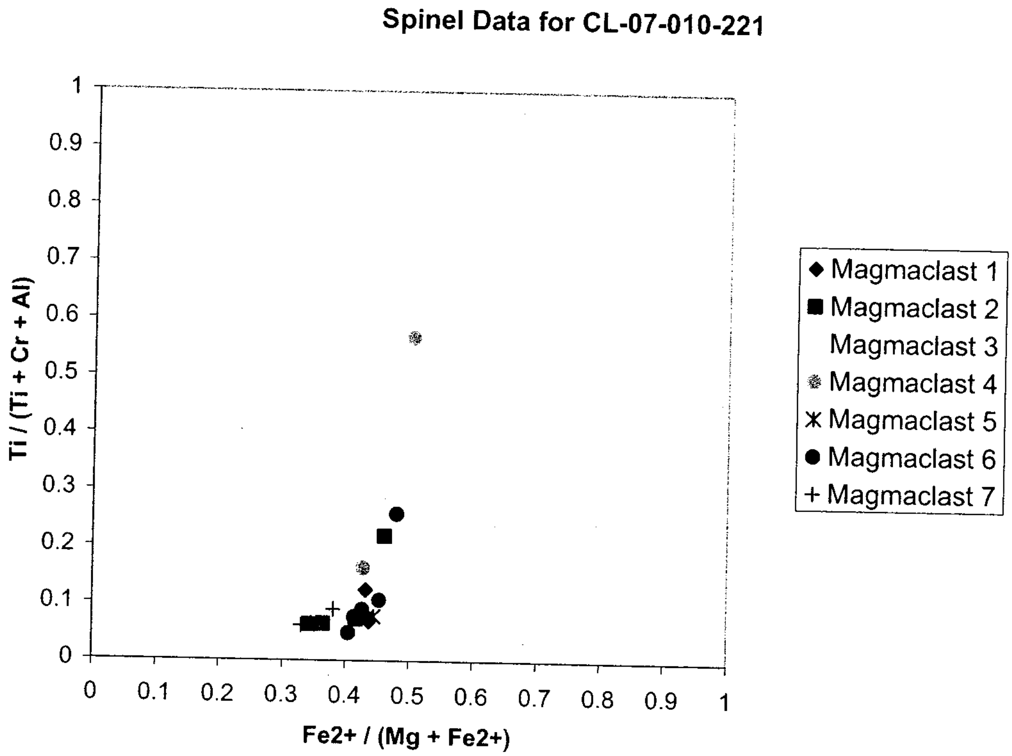

Plot for Sample CL-07-010-221

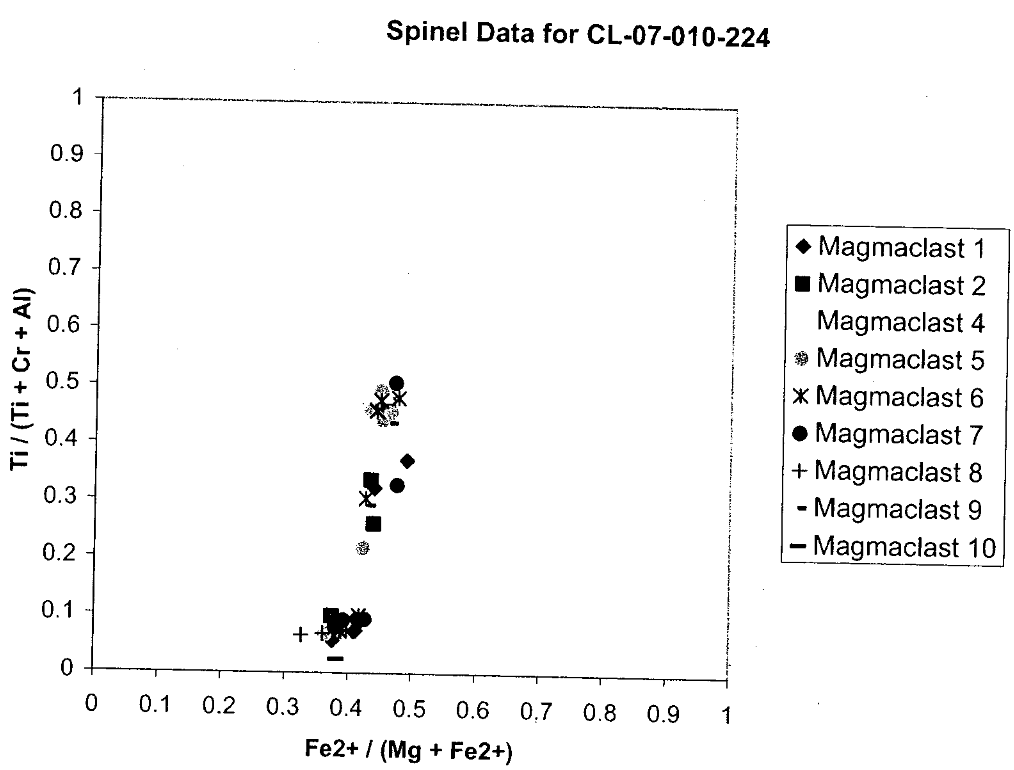

Plot for Sample CL-07-010-224

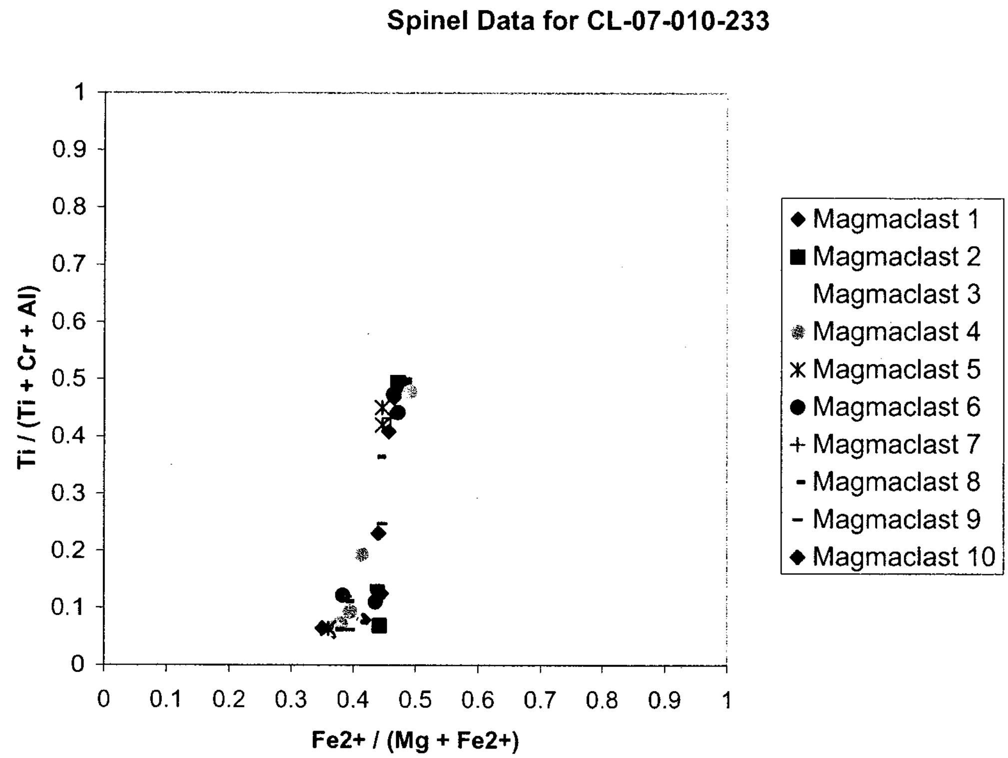

Plot for Sample CL-07-010-233

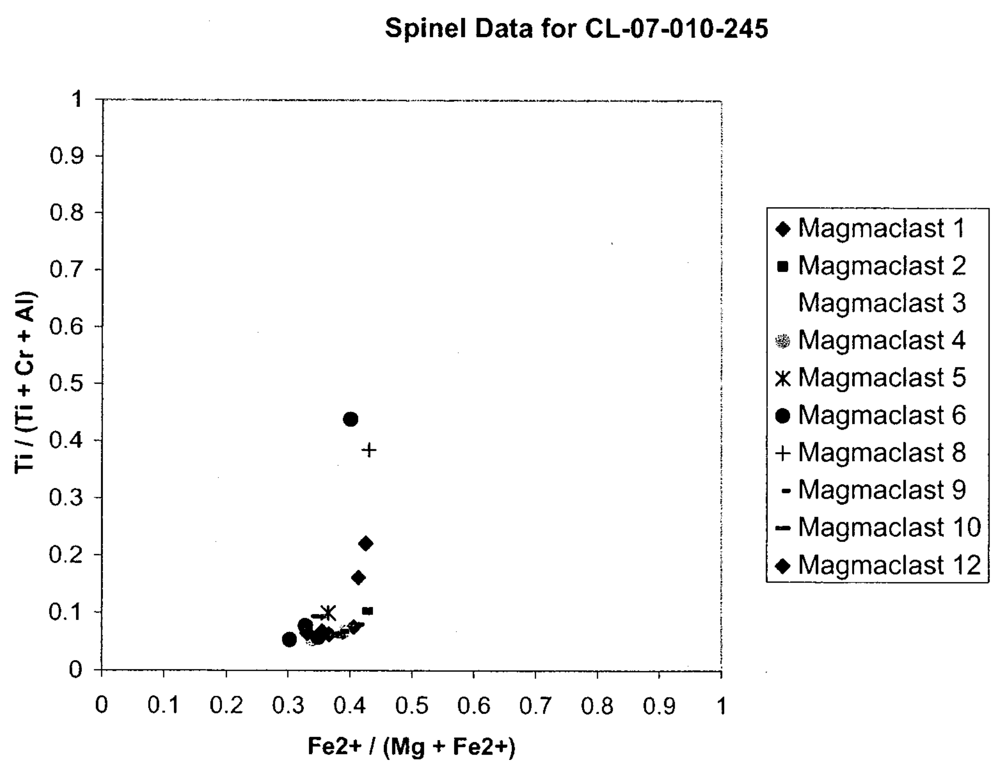

Plot for Sample CL-07-010-245

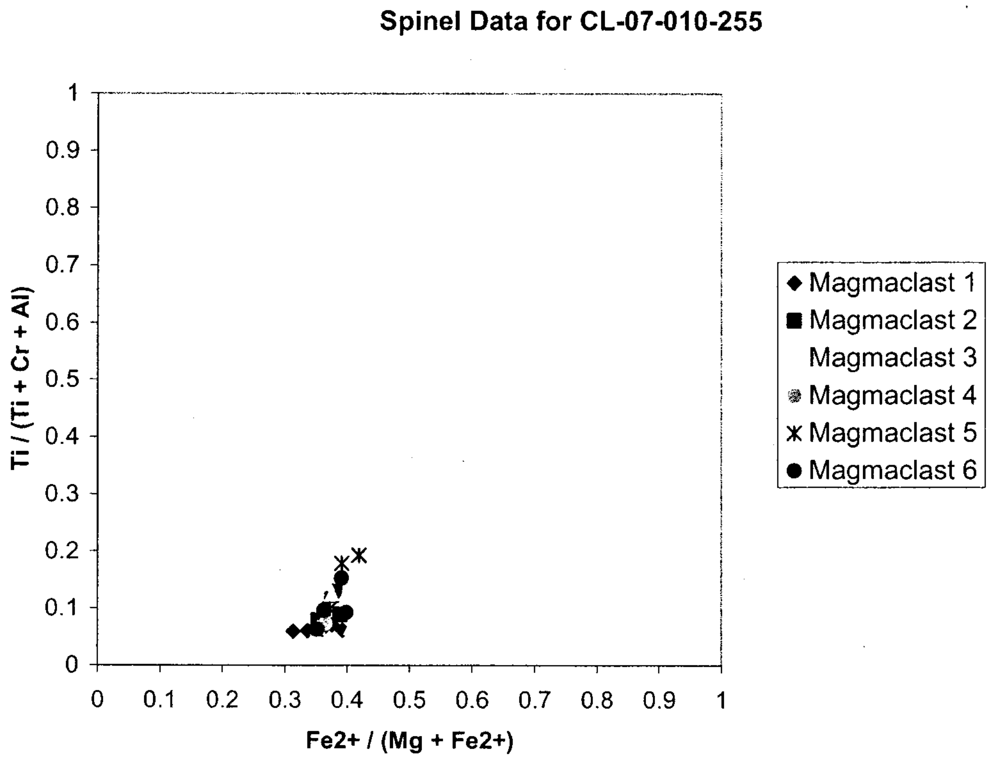

Plot for Sample CL-07-010-255

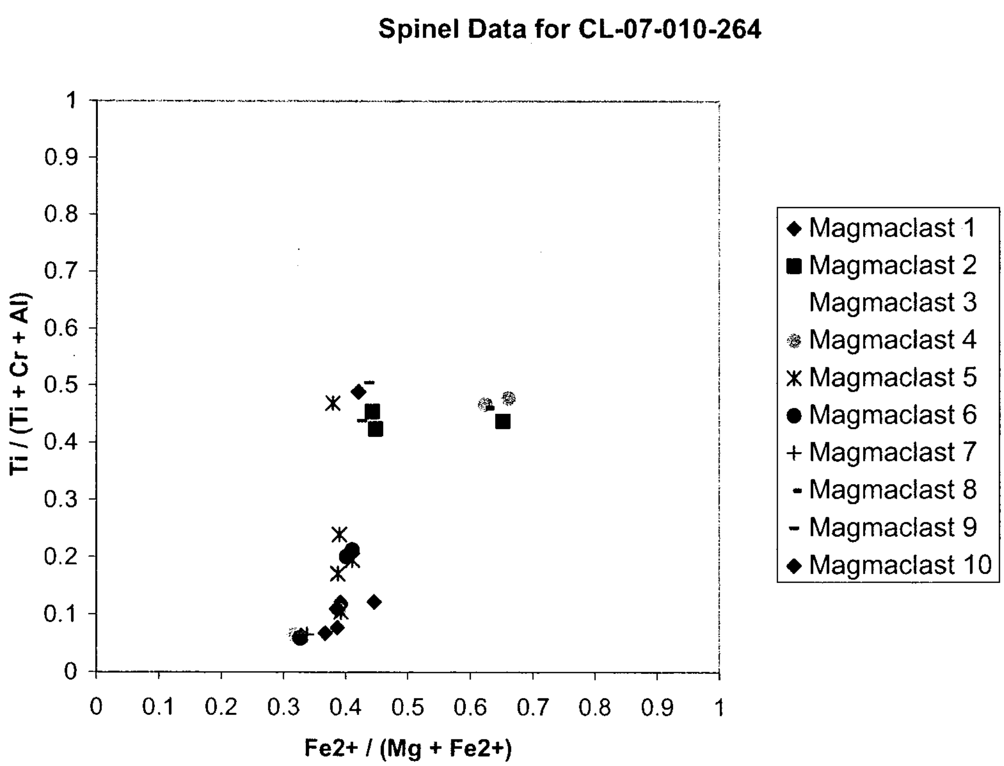

Plot for Sample CL-07-010-264

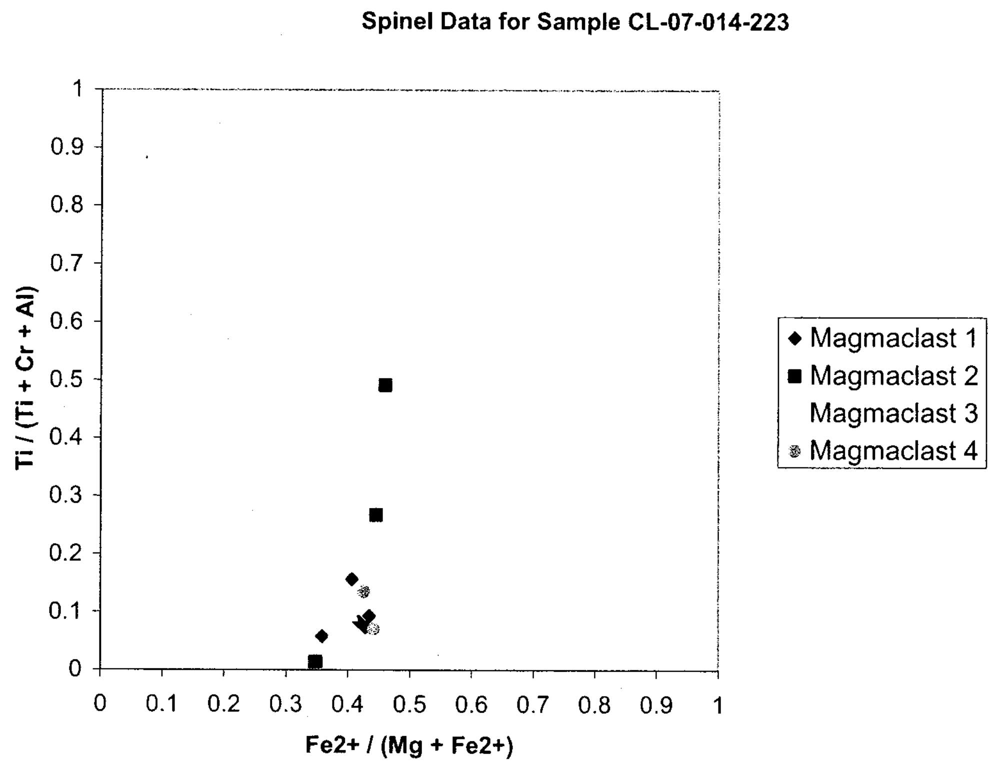

Plot for Sample CL-07-014-223

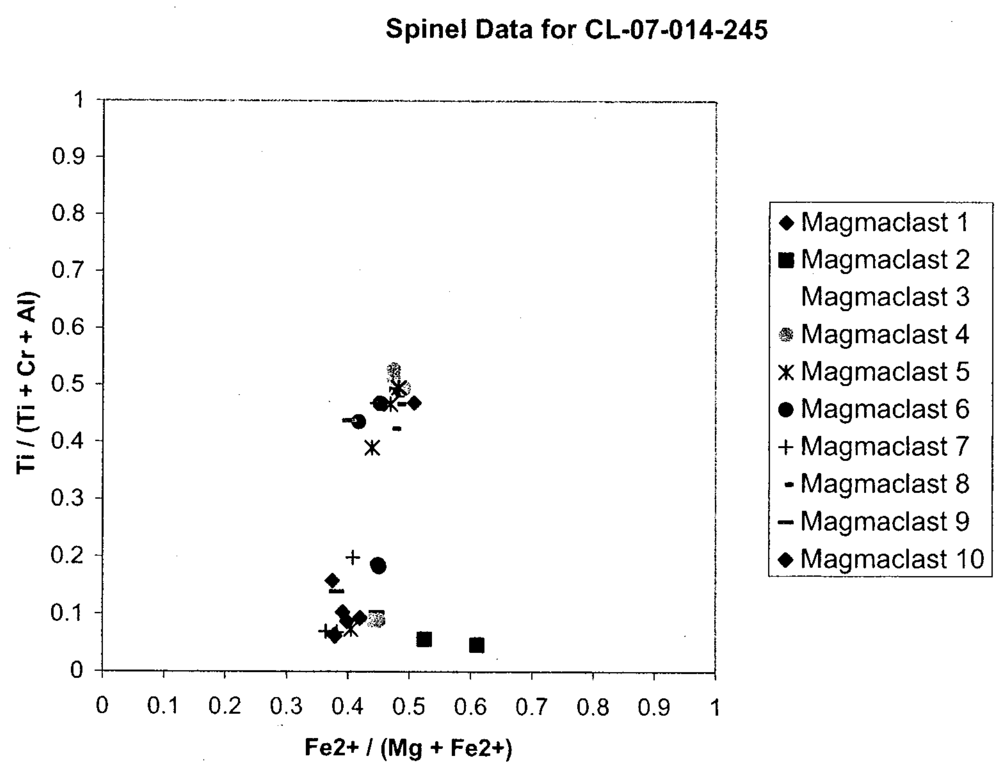

Plot for CL-07-014-245

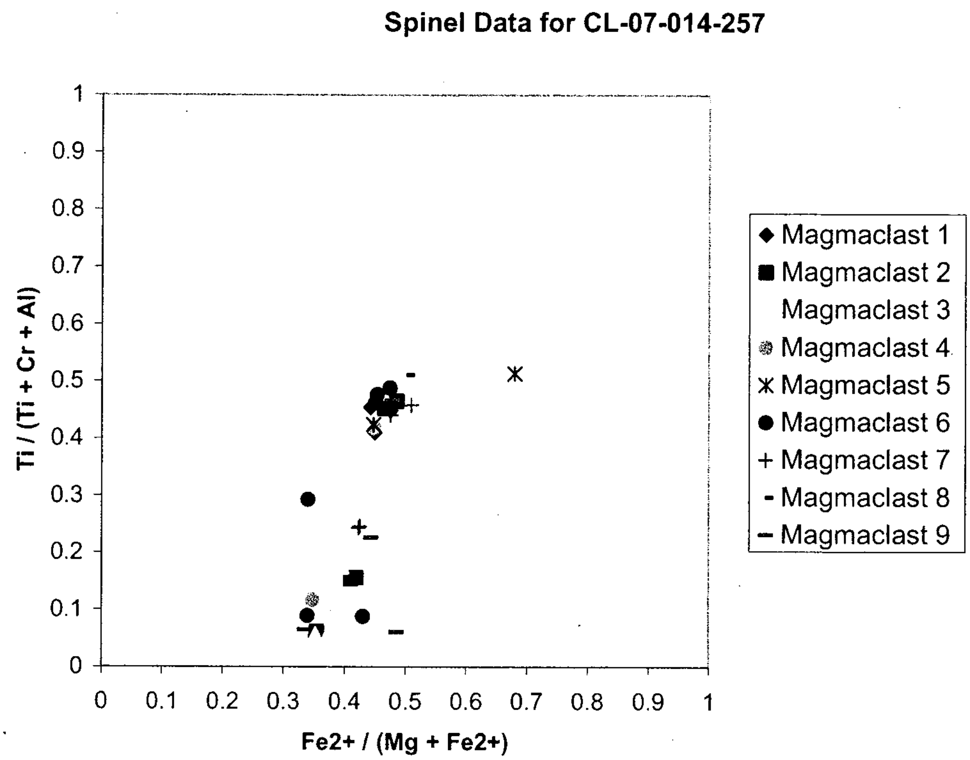

Plot for Sample CL-07-014-257

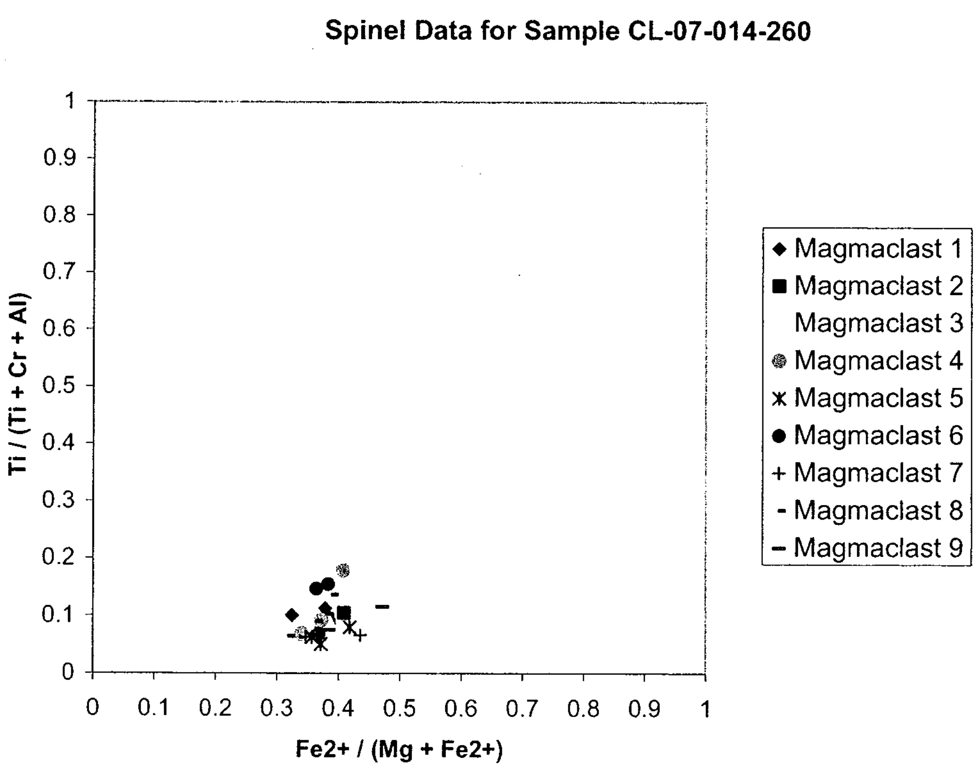

Plot for Sample CL-07-014-260

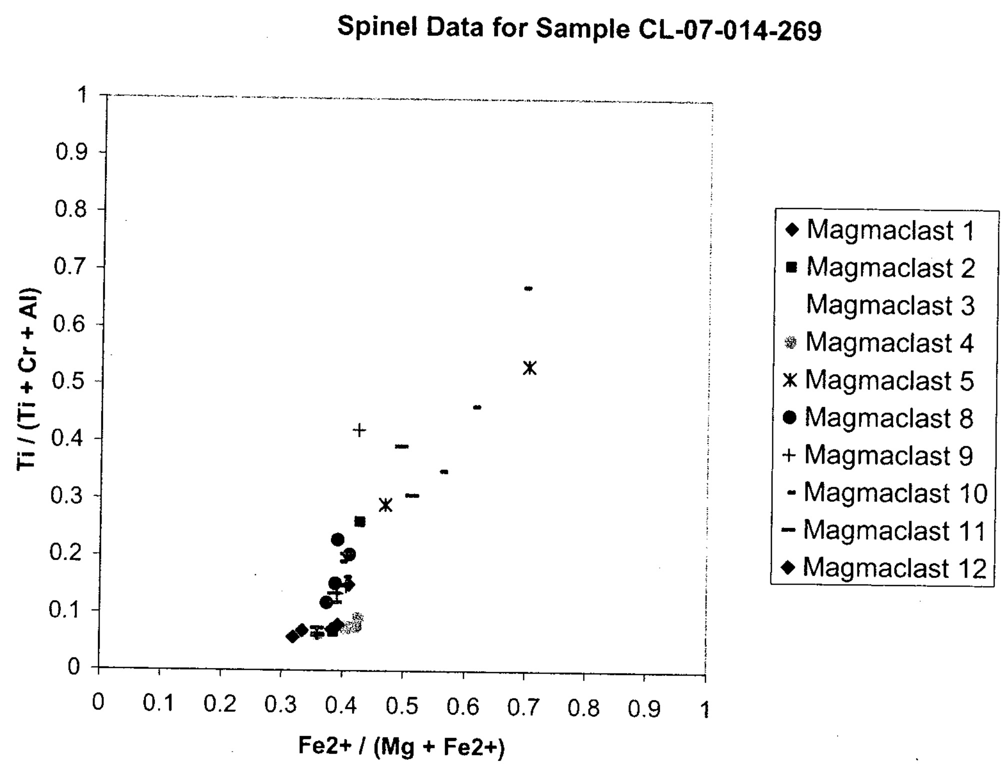

Plot for Sample CL-07-014-269

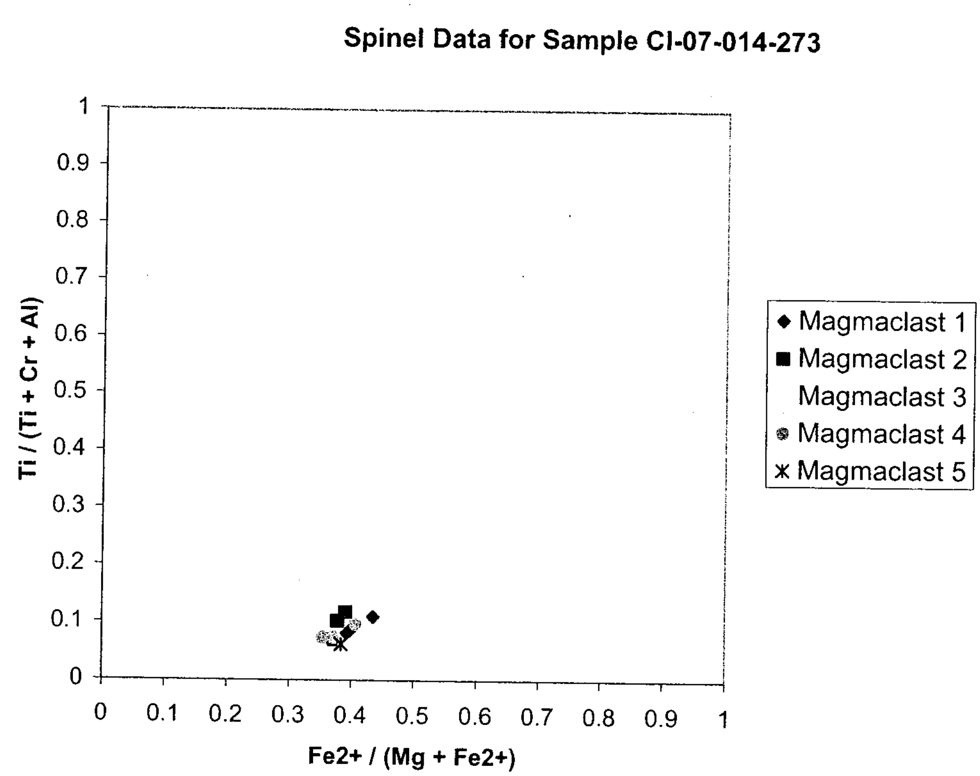

Plot for Sample CL-07-014-273

APPENDIX D

COMPOSITION OF ROCK FORMING AND MINOR MINERALS

Microprobe analyses and various recalculations for each of the rock forming and minor minerals, are presented in the following section. Minerals are listed in order presented in text. Abbreviations are listed below, identifying sample location, or grain type. Spinel data associated with the phlogopite cumulates are considered all type [4] spinels. Garnets are numbered based on Dawson and Stevens (1975) classification.

1 – Spinel type [1], enclosed within macrocrysts or phenocrysts. This also indicates type 1 perovskites.

2 – Spinel type [2], along the edge of the macrocrysts or phenocrysts, partially exposed to the interclast matrix. This also indicates type 2 perovskites

3 – Spinel type [3], completely separate from macrocrysts and phenocrysts set in the interclast matrix.

IM – interclast matrix

Macro – macrocrysts

Meso - mesostasis

Mont – monticellite

Pheno – phenocrysts

PC-1 – Phlogopite cumulate type 1

PC-2 – Phlogopite cumulate type 2

Appendix D-1 Spinels

Sample	CL-06-003-158															
Oxide%																
TiO_2	6.67	4.48	4.33	4.95	4.49	11.34	6.13	7.93	9.55	5.39	4.47	4.99	4.72	5.59	12.42	7.53
Al_2O_3	9.68	14.82	14.09	7.55	8.17	10.67	5.02	11.09	9.03	7.08	14.4	7.22	6.73	7.78	10.5	9.51
Cr_2O_3	38.18	40.98	41.61	44.06	49.5	19.45	43.78	28.75	26.17	48.53	41.33	45.54	50.23	45.61	19.98	35.8
FeO_T	28.99	24.42	23.4	27.2	24.25	42.16	30.63	36.22	39.21	23.95	24.25	26.63	24.12	26.39	39.22	30.67
MnO	0	0	0	0.88	0	0.71	0	0	0	0	0.58	0	0	0	0.5	0.8
MgO	14.64	14.75	15.62	14.46	14.16	15.38	13.03	14.73	15.31	13.55	15.52	15.13	13.95	14.22	16.96	16.22
Total	98.6	99.87	99.65	99.63	100.75	99.95	99.59	99.66	99.82	98.94	100.59	100.07	100.39	99.93	99.73	100.98
Recalculated Fe																
FeO	16.40	15.51	13.78	14.20	16.08	19.84	17.75	17.76	18.63	16.97	14.40	14.28	16.11	16.63	18.71	14.80
Fe_2O_3	13.99	9.90	10.69	14.45	9.08	24.81	14.32	20.51	22.87	7.76	10.95	13.73	8.90	10.85	22.80	17.63
Total	100.08	100.85	100.57	101.09	101.48	102.44	100.59	101.47	101.78	99.28	101.65	101.30	100.64	100.68	101.86	102.75
$Fe^{2+}/(Mg + Fe^{2+}$	0.386	0.371	0.331	0.355	0.389	0.420	0.433	0.404	0.406	0.413	0.342	0.346	0.393	0.396	0.382	0.339
Cr/(Cr + Al)	0.726	0.650	0.665	0.797	0.803	0.550	0.854	0.635	0.660	0.821	0.658	0.809	0.834	0.797	0.561	0.716
Ti/Ti + Cr + Al)	0.108	0.063	0.062	0.078	0.065	0.234	0.102	0.143	0.187	0.080	0.063	0.078	0.069	0.085	0.249	0.125

Sample																
Oxide%																
TiO_2	8.83	6.87	3.29	4.94	5.11	6.46	5.11	4.73	4.05	4.49	4.8	8.55	4.36	4.43	10.887	8.99
Al_2O_3	10.43	8.67	5.48	7.7	7.31	6.92	7.12	6.61	15.28	13.18	9.38	9.2	17.06	14.16	10.65	10.37
Cr_2O_3	30.11	38.55	53.31	47.73	48.77	45.38	49.35	48.55	41.34	41.87	46.14	29.33	40.3	40.1	24.91	31.68
FeO_T	34.69	28.49	24.11	25.47	23.58	26.66	23.78	25.05	23.46	24.26	24.23	35.99	22.29	23.17	36.51	31.92
MnO	0.64	0.65	0	0	0	0	0	0.69	0	0	0	0	0	0.53	0	0.58
MgO	15.94	15.49	13.11	13.91	15.06	14.89	13.99	13.33	15.17	14.57	14.06	16.18	15.86	16.14	16.29	14.93
Total	100.69	98.91	99.81	100.31	100.73	100.98	99.64	98.96	99.21	99.16	99.09	100	100.71	99.26	99.8	98.52
Recalculated Fe																
FeO	17.17	15.11	15.78	16.34	14.37	16.49	16.33	16.12	14.86	15.02	16.07	16.33	14.03	12.16	18.56	18.14
Fe_2O_3	19.47	14.87	9.26	10.15	10.24	11.30	8.28	9.92	9.56	10.26	9.07	21.85	9.18	12.23	19.95	15.31
Total	102.59	100.21	100.23	101.01	101.48	101.44	100.18	99.95	100.26	100.01	99.52	101.74	101.37	100.49	101.44	100.00
$Fe^{2+}/(Mg + Fe^{2+}$	0.377	0.354	0.403	0.397	0.349	0.383	0.396	0.404	0.355	0.366	0.391	0.362	0.332	0.297	0.390	0.405
Cr/(Cr + Al)	0.659	0.749	0.867	0.806	0.817	0.815	0.823	0.831	0.645	0.681	0.767	0.681	0.613	0.655	0.611	0.672
Ti/Ti + Cr + Al)	0.155	0.113	0.048	0.074	0.075	0.099	0.075	0.072	0.057	0.065	0.071	0.159	0.059	0.064	0.203	0.154

Sample																
Oxide%										CL-06-003-173						
TiO_2	14.13	9.29	9.23	4.9	10.56	8.22	4.21	4.44	8.09	4.82	18.38	7.58	17.42	12.9	5.4	5.6
Al_2O_3	10.71	9.26	9.18	15.75	9.07	8.68	10.09	15.6	9.59	10.8	10.34	10.37	10.17	12.51	6.35	6.68
Cr_2O_3	16.75	33.92	29.6	40.76	29.05	36.32	44.08	41.41	33.67	46.02	4.76	30.23	6.46	16.19	46.9	45.7
FeO_T	40.41	31.78	35.67	22.49	35.56	30.28	24.73	22.24	31.48	23.7	49.55	34.61	48.1	40.61	25.35	26.18
MnO	0.74	0	0	0	0	0	0.59	0	0.69	0.45	0.52	0.49	0.48	0.48	0	0.58
MgO	17.28	15.98	15.77	15.38	15.25	15.31	15.31	15.47	16.17	14.29	16.79	14.85	16.42	16.51	13.58	13.88
Total	100.13	100.84	99.69	99.5	100.2	99.3	99.24	99.52	100.22	100.08	100.34	98.13	99.06	99.2	98.09	98.61
Recalculated Fe																
FeO	19.69	17.79	17.86	15.34	19.46	17.12	13.15	14.36	15.17	15.97	24.61	17.05	23.90	20.04	16.55	16.10
Fe_2O_3	23.02	15.55	19.79	7.94	17.89	14.63	12.87	8.76	18.13	8.59	27.71	19.52	26.89	22.86	9.78	11.21
Total	102.33	101.79	101.43	100.08	101.69	100.47	100.51	100.48	102.05	100.94	103.12	100.09	101.74	101.49	98.56	99.74
$Fe^{2+}/(Mg + Fe^{2+}$	0.390	0.384	0.389	0.359	0.417	0.386	0.325	0.342	0.345	0.385	0.451	0.392	0.450	0.405	0.406	0.394
Cr/(Cr + Al)	0.512	0.711	0.684	0.634	0.682	0.737	0.746	0.640	0.702	0.741	0.236	0.662	0.299	0.465	0.832	0.821
Ti/Ti + Cr + Al)	0.291	0.156	0.169	0.068	0.191	0.137	0.063	0.061	0.138	0.069	0.464	0.136	0.434	0.261	0.084	0.087

Sample																
Oxide%																
TiO_2	6.22	8.47	16.32	5.43	18.28	9.4	11.94	5.8	16.78	4.14	14.84	11.22	11.95	8.89	13.82	4.83
Al_2O_3	7.03	9.01	11.31	7.77	9.5	9.7	10.93	10.6	9.58	4.02	11.08	11.98	14.31	15.27	13.82	15.56
Cr_2O_3	43.17	35.72	4.26	46.79	4.21	30.47	17.8	42.74	9.03	52.35	9.64	20.81	11.5	19.46	9.18	40.85
FeO_T	27.55	30.81	49.67	24.31	49.77	34.68	42.49	26.31	47.15	24.95	46.1	39.84	43.18	36.88	44.51	23.5
MnO	0	0	0	0	0.64	0	0.47	0	0.59	0	0.45	0	0.42	0	0.53	0
MgO	14.19	15.09	17.15	14.29	16.4	15.36	15.17	14.28	16.38	13.58	17.44	16.19	17.69	17.94	17.12	15.53
Total	98.64	99.55	99.15	99.09	98.84	99.73	98.8	99.95	99.51	99.56	99.55	100.4	99.05	98.58	98.7	100.52
Recalculated Fe																
FeO	16.69	17.99	22.41	16.03	24.38	18.74	20.88	17.21	23.32	15.53	20.38	19.68	17.77	14.94	20.10	15.35
Fe_2O_3	12.07	14.25	30.30	9.20	28.21	17.71	24.01	10.12	26.48	10.47	28.58	22.40	28.24	24.38	27.13	9.05
Total	99.37	100.53	101.75	99.51	101.63	101.38	101.21	100.74	102.16	100.09	102.41	102.28	101.88	100.88	101.70	101.18
$Fe^{2+}/(Mg + Fe^{2+}$	0.398	0.401	0.423	0.386	0.455	0.406	0.436	0.403	0.444	0.391	0.396	0.406	0.360	0.318	0.397	0.357
Cr/(Cr + Al)	0.805	0.727	0.202	0.802	0.229	0.678	0.522	0.730	0.387	0.897	0.369	0.538	0.350	0.461	0.308	0.638
Ti/Ti + Cr + Al)	0.099	0.141	0.424	0.081	0.486	0.166	0.250	0.086	0.406	0.063	0.351	0.216	0.257	0.167	0.306	0.067

Sample																**CL-06-003-182**
Oxide%																
TiO_2	18.9	16.53	10.63	17.88	18.15	13.21	19	5.99	7.95	6.38	13.22	6.73	6.82	5.93	5.15	3.21
Al_2O_3	9.34	10.13	8.99	9.79	9.93	10.19	9.01	6.47	7.58	7.55	10.74	9.35	8.18	7.68	7.16	57.08
Cr_2O_3	4.45	7.71	29.85	4.68	4.83	19.73	2.94	43.6	39.15	41.4	13.52	34.88	40.34	41.52	45.44	4.23
FeO_T	50.69	48.3	34.03	49.98	49.68	38.94	50.58	27.95	23.66	28.86	45.82	32.63	28.46	28	27.13	21.49
MnO	0.5	0.73	0.55	0.75	0.53	0.81	0.66	0.81	0.64	0	0.69	0.87	0	0.77	0	0.51
MgO	16.24	16.77	15.5	16.98	16.56	15.39	17.34	14.18	14.95	14.81	16.58	15.71	14.16	15.28	14.48	12.09
Total	100.13	100.17	99.55	100.05	99.67	98.27	99.53	99	98.93	99.51	100.58 sorr		99.39	99.17	99.75	98.67
Recalculated Fe																
FeO	25.72	22.69	18.93	23.49	24.48	20.99	23.76	15.88	15.12	16.27	20.27	15.08	17.39	14.46	15.70	16.28
Fe_2O_3	27.75	28.46	16.78	29.44	28.01	19.95	29.81	13.41	9.49	14.00	28.40	19.51	12.30	15.05	12.71	5.79
Total	102.90	103.02	101.23	103.01	102.49	100.27	102.52	100.34	94.88	100.40	103.42	102.12	99.19	100.69	100.63	99.19
$Fe^{2+}/(Mg + Fe^{2+}$	0.470	0.432	0.407	0.437	0.453	0.434	0.435	0.386	0.362	0.381	0.407	0.350	0.408	0.347	0.378	0.430
Cr/(Cr + Al)	0.242	0.338	0.690	0.243	0.246	0.565	0.180	0.819	0.776	0.786	0.458	0.714	0.768	0.784	0.810	0.901
Ti/Ti + Cr + Al)	0.495	0.408	0.190	0.469	0.468	0.265	0.525	0.097	0.130	0.103	0.299	0.116	0.110	0.096	0.080	0.046

Sample																
Oxide%																
TiO_2	18.34	12.74	16.76	15.62	16.24	16.86	16.99	17.84	16.4	12.47	16.4	16.41	15.14	15.68	16.92	11.28
Al_2O_3	3.36	10.7	3.62	7.24	10.32	2.92	4.97	3.38	2.52	11.96	4.55	3.68	11.37	4.46	5.71	22.23
Cr_2O_3	9.36	11.65	10.27	9.8	9.85	11.02	9.56	10.37	10.65	11.79	10.66	10.75	10.13	10.91	9.09	10.29
FeO_T	50.29	45.57	49.44	47.92	46.33	50.88	49.71	49.16	50.6	45.36	48.45	50.19	44.45	49.55	49.54	38.82
MnO	0.51	0.8	0.65	0	0.57	0.47	0.66	0.61	0.74	0	0.77	0.58	0.57	0.58	0.6	0.53
MgO	16.29	16.29	17.4	15.81	15.27	16.1	15.65	16.55	16.34	16.18	16.11	16	15.98	16.33	15.85	16.07
Total	98.34	98.03	98.54	97	98.67	98.37	97.62	97.96	97.46	98.28	97.26	97.74	97.85	97.63	97.82	99.35
Recalculated Fe																
FeO	24.51	19.17	21.08	22.60	24.27	23.83	23.96	23.64	22.24	19.99	22.33	23.22	21.77	22.06	23.64	18.85
Fe_2O_3	28.65	29.34	31.52	28.14	24.52	30.06	28.62	28.36	31.52	28.20	29.03	29.98	25.20	30.56	28.79	22.19
Total	101.02	100.98	101.71	99.45	101.04	101.26	100.41	100.75	100.62	100.79	100.16	100.61	100.37	100.57	100.59	101.44
$Fe^{2+}/(Mg + Fe^{2+}$	0.458	0.398	0.405	0.445	0.471	0.454	0.462	0.445	0.433	0.409	0.437	0.449	0.433	0.431	0.456	0.397
Cr/(Cr + Al)	0.194	0.381	0.191	0.331	0.413	0.151	0.259	0.179	0.137	0.405	0.223	0.187	0.430	0.215	0.296	0.592
Ti/Ti + Cr + Al)	0.502	0.302	0.457	0.405	0.382	0.453	0.457	0.474	0.459	0.287	0.433	0.442	0.352	0.419	0.455	0.222

Sample																
Oxide%																
TiO_2	14.88	18.48	16.41	4.51	16.09	14.68	18.01	14.8	13.93	17.16	14.93	18.28	17.43	12.84	17.75	13.65
Al_2O_3	10.61	3.53	2.65	48.93	5.24	8.48	3.79	11.42	14.34	5.45	8.86	2.94	2.25	14.04	5.46	15.8
Cr_2O_3	11.08	9.63	10.98	5.43	9.96	10.16	9.33	9.76	10.61	9.44	10.76	9.2	10.6	11.41	9.13	9.4
FeO_T	44.8	49.97	50.77	25.94	49.78	48.37	49.65	45.46	42.7	49.3	47.04	50.9	50.36	43.1	49.41	42.92
MnO	0	0.57	0.77	0	0.5	0	0.68	0.45	0.5	0.58	0.56	0.61	0.36	0.48	0.56	0.59
MgO	15.7	15.93	16.02	13.15	16.04	15.74	15.38	15.7	15.37	15.45	15.49	15.9	16.04	16.03	15.5	14.93
Total	97.38	98.1	97.74	98.38	97.61	97.64	97.04	97.7	97.43	97.63	97.76	98.11	97.83	98.12	97.94	97.44
Recalculated Fe																
FeO	22.67	25.14	23.04	16.40	22.82	22.47	24.82	22.13	21.84	24.18	22.65	24.60	23.70	19.98	24.97	21.93
Fe_2O_3	24.59	27.59	30.82	10.60	29.96	28.78	27.59	25.93	23.18	27.92	27.11	29.23	29.63	25.69	27.16	23.32
Total	99.53	100.87	100.69	99.02	100.61	100.31	99.80	100.19	99.77	100.46	100.36	101.03	100.45	100.70	100.53	99.63
$Fe^{2+}/(Mg + Fe^{2+}$	0.448	0.470	0.447	0.412	0.444	0.445	0.475	0.442	0.444	0.467	0.451	0.465	0.453	0.412	0.475	0.452
Cr/(Cr + Al)	0.391	0.197	0.139	0.858	0.261	0.359	0.214	0.440	0.476	0.279	0.356	0.177	0.125	0.452	0.286	0.530
Ti/Ti + Cr + Al)	0.343	0.496	0.451	0.070	0.432	0.372	0.492	0.352	0.305	0.455	0.363	0.511	0.479	0.282	0.470	0.303

Sample											**CL-06-003-186**					
Oxide%																
TiO_2	11.52	18.38	15.71	12.62	16.61	18.39	17.44	10.93	13.96	17.34	11.15	4.41	9.27	17.51	4.69	8.46
Al_2O_3	20.73	2.89	10.11	15.01	5.15	4.72	3.59	19.72	15.45	4.7	11.76	14.34	10.64	9.95	14.76	9.04
Cr_2O_3	9.54	9.15	10.5	11.42	10.29	9.37	9.35	11.75	9.54	9.75	17.5	39.92	26.08	3.59	41.44	32.02
FeO_T	40.31	50.88	42.41	41.3	46.18	48.96	49.9	38.45	42.6	48.16	41.51	23.72	36.78	49.98	23.54	32.69
MnO	1.08	0.81	0.65	0.48	0.77	0.64	0	0.52	0	0.72	0	0.24	0	0	0	0.93
MgO	14.86	16.52	17.82	17.47	17.43	16.29	16.19	15.93	15.25	17.13	15.11	14.99	14.92	16.71	15.46	14.83
Total	98.08	98.74	97.44	98.47	97.18	98.68	97.3	97.52	97.3	98.08	97.75	98.12	98.35	97.69	99.86	97.89
Recalculated Fe																
FeO	19.88	24.03	19.29	17.91	20.54	24.22	23.47	18.21	22.17	21.84	20.29	14.10	18.56	23.61	15.09	17.13
Fe_2O_3	22.70	29.83	25.70	25.99	28.50	27.50	29.38	22.50	22.70	29.25	23.58	10.69	20.25	29.31	9.39	17.29
Total	100.31	101.62	100.00	100.90	99.28	101.42	99.84	99.75	99.07	101.00	99.39	99.20	100.08	100.68	100.83	99.70
$Fe^{2+}/(Mg + Fe^{2+}$	0.429	0.449	0.378	0.365	0.398	0.455	0.448	0.391	0.449	0.417	0.430	0.345	0.411	0.442	0.354	0.393
Cr/(Cr + Al)	0.593	0.175	0.392	0.469	0.251	0.253	0.205	0.530	0.521	0.244	0.500	0.651	0.622	0.195	0.653	0.704
Ti/Ti + Cr + Al)	0.239	0.514	0.367	0.273	0.435	0.484	0.486	0.218	0.309	0.462	0.232	0.064	0.174	0.475	0.066	0.150

Sample																
Oxide%																
TiO_2	7.98	15.61	14.95	7.92	15.96	13.16	17.4	17.35	5.51	4.65	6.88	7.42	4.39	16.65	17.12	17.83
Al_2O_3	12.06	8.97	7.4	8.82	9.24	9.98	7.54	7.84	11.83	13.24	7.56	9.78	11.88	9.48	10.32	8.82
Cr_2O_3	30.06	4.59	6.34	35.85	4.72	16.09	5.44	5.27	42.98	41.88	34.85	32.26	44.24	4.16	3.98	5.86
FeO_T	34.74	52.71	53.57	31	50.37	42.02	51.26	51.31	24.67	23.61	33.2	33.27	24.03	50.75	49.56	47.88
MnO	0	1.11	0	0.49	0.85	0	0	0.45	0	0.63	0	0	0	0.44	0	0
MgO	13.08	14.47	15.01	14.37	16.57	16.62	15.32	15.37	14.15	14.31	14.99	15.82	14.92	15.68	16.16	16.77
Total	98.09	97.66	97.38	98.57	97.88	98.45	97.56	97.84	99.36	98.34	98.21	99.33	100	97.29	97.44	98.16
Recalculated Fe																
FeO	20.75	24.01	23.42	17.87	21.50	19.80	25.01	24.69	17.12	15.43	16.04	15.95	15.07	23.72	23.95	23.41
Fe_2O_3	15.55	31.90	33.50	14.60	32.09	24.70	29.18	29.59	8.39	9.09	19.07	19.25	9.96	30.04	28.46	27.20
Total	99.48	100.66	100.63	99.91	100.93	100.34	99.88	100.55	99.98	99.23	99.39	100.48	100.46	100.17	99.99	99.88
$Fe^{2+}/(Mg + Fe^{2+}$	0.471	0.482	0.467	0.411	0.421	0.401	0.478	0.474	0.404	0.377	0.375	0.361	0.362	0.459	0.454	0.439
Cr/(Cr + Al)	0.626	0.256	0.365	0.732	0.255	0.520	0.326	0.311	0.709	0.680	0.756	0.689	0.714	0.227	0.206	0.308
Ti/Ti + Cr + Al)	0.136	0.453	0.450	0.133	0.451	0.288	0.498	0.493	0.080	0.067	0.124	0.131	0.063	0.464	0.457	0.472

Sample														CL-06-003-195		
Oxide%																
TiO_2	7.82	7.81	17.8	14.2	13.61	17.06	8.49	8.04	9.53	9.91	7.99	7.35	6.99	18.05	8.95	16.82
Al_2O_3	11.23	10.85	9.55	9.56	9.01	11.6	12.26	12.41	8.12	8.08	6.44	6.15	6	8.12	10.35	10.33
Cr_2O_3	27.44	28	6.06	7.88	8.28	2.15	25.47	26.12	24.77	26.331	34.44	39.15	39.14	2.83	30.32	5.25
FeO_T	36.04	34.78	48	50.3	48.85	50.71	37.21	36.74	40.85	39.39	35.27	32.3	31.99	51.98	34.26	49.23
MnO	0	0.62	0	0	0	0	0	0	0.44	0.53	0	0	0.66	0.64	0.68	0.61
MgO	16.16	15.95	16.11	15.5	17.52	15.94	14.5	15.14	14.17	14.22	14.49	13.63	13.55	16.06	15.29	16.27
Total	98.94	98.12	97.85	97.88	97.23	98.02	98.37	99.03	98.08	98.64	99.27	99.42	98.63	98.22	99.99	98.53
Recalculated Fe																
FeO	16.11	15.51	24.60	22.35	18.63	24.55	19.14	17.96	19.53	19.85	18.00	18.61	17.65	23.70	17.94	23.34
Fe_2O_3	22.15	21.42	26.01	31.06	33.59	29.07	20.08	20.87	23.69	21.71	19.19	15.21	15.93	31.43	18.13	28.77
Total	100.91	100.16	100.13	100.55	100.63	100.37	99.94	100.54	100.25	100.64	100.55	100.10	99.93	101.37	101.67	101.39
$Fe^{2+}/(Mg + Fe^{2+}$	0.359	0.353	0.461	0.447	0.374	0.464	0.425	0.400	0.436	0.439	0.411	0.434	0.422	0.453	0.397	0.446
Cr/(Cr + Al)	0.621	0.634	0.299	0.356	0.381	0.111	0.582	0.585	0.672	0.686	0.782	0.810	0.814	0.535	0.157	0.437
Ti/Ti + Cr + Al)	0.144	0.144	0.455	0.379	0.374	0.455	0.156	0.146	0.197	0.197	0.147	0.126	0.122	0.189	0.663	0.254
Sample																
Oxide%																
TiO_2	17.11	17.4	13.89	15.01	16.85	15.31	16.63	17.47	17.17	10.82	18.5	18.12	17.95	15.32	13.47	17.73
Al_2O_3	7.35	11.73	11.94	11.13	11.35	9.32	11.6	7.52	7.85	8.05	7.75	8.15	8.97	10.33	9.79	8.36
Cr_2O_3	9.28	1.63	7.4	9.95	6.8	6.09	5.76	4.94	5.99	22.44	3.14	4.21	4.3	7.33	12.04	5.96
FeO_T	50.08	49.25	45.7	45.18	46.51	50.22	46.69	52.39	50.61	41.18	52.1	50.62	49.7	48.08	46.5	50.41
MnO	0.28	0.64	0.69	0.48	0.6	0.61	0.42	0.53	0.62	0	0.58	0.47	0.39	0.44	0.51	0.45
MgO	14.78	17.66	17.68	16.92	17.05	16.2	16.71	15.81	15.09	15.16	16.52	15.57	16.33	16.99	16.4	15.74
Total	99.11	98.34	97.47	98.74	99.17	98.04	97.87	98.87	97.4	98.15	98.95	97.39	97.9	98.71	98.88	98.81
Recalculated Fe																
FeO	25.84	21.89	18.36	21.00	22.52	21.50	22.63	24.18	24.69	19.40	23.89	24.73	23.78	20.88	20.22	24.87
Fe_2O_3	26.94	30.40	30.39	26.88	26.66	31.92	26.74	31.35	28.81	24.21	31.35	28.78	28.80	30.23	29.21	28.39
Total	101.58	101.36	100.34	101.36	101.83	101.23	100.49	102.01	100.22	100.25	102.05	100.27	100.78	101.75	101.64	101.49
$Fe^{2+}/(Mg + Fe^{2+}$	0.495	0.410	0.368	0.410	0.426	0.427	0.432	0.462	0.479	0.418	0.448	0.471	0.450	0.408	0.409	0.470
Cr/(Cr + Al)	0.446	0.464	0.344	0.350	0.403	0.422	0.407	0.507	0.480	0.230	0.545	0.513	0.491	0.391	0.325	0.478
Ti/Ti + Cr + Al)	0.459	0.085	0.294	0.375	0.287	0.305	0.250	0.306	0.339	0.652	0.214	0.257	0.243	0.322	0.452	0.324
Sample																
Oxide%																
TiO_2	18	16.87	17.73	17.96	17.38	17.38	5	14.9	15.51	16.53	17.58	17.49	4.54	12.49	16.72	4
Al_2O_3	8.23	7.38	8.03	8.23	8.83	8.23	14.77	11.12	7.91	7.9	8.49	7.78	7.7	11.29	8.97	14.03
Cr_2O_3	5.38	8.44	6.21	6	5.69	6.1	41.89	0.88	11.75	11.3	4.89	5.87	48.82	12.29	4.89	39.9
FeO_T	49.11	48.34	50.23	50.21	50.16	49.46	22.81	53.64	47.43	47.16	50.86	49.45	23.32	46.05	51.41	24.14
MnO	0.47	0.53	0.79	0.44	0.53	0.57	0	0.69	0	0.58	0.71	0.76	0	0.62	0.43	0
MgO	16.29	15.73	15.56	15.57	15.74	16.34	14.75	15.89	15.85	16.08	16.36	15.67	13.45	15.9	16.29	15.78
Total	97.59	97.49	98.69	98.45	98.42	98.1	99.85	97.28	98.93	99.76	98.97	97.27	98.36	98.75	98.84	98.3
Recalculated Fe																
FeO	23.84	23.42	24.71	25.23	24.44	23.32	16.21	21.90	22.78	23.13	23.65	23.62	16.24	20.19	23.30	13.26
Fe_2O_3	28.08	27.69	28.36	27.76	28.58	29.05	7.33	35.27	27.39	26.71	30.24	28.71	7.87	28.74	31.24	12.09
Total	100.29	100.06	101.39	101.19	101.19	100.99	99.95	100.65	101.44	102.45	101.92	100.15	98.62	101.52	101.84	99.06
$Fe^{2+}/(Mg + Fe^{2+}$	0.451	0.455	0.471	0.476	0.466	0.445	0.381	0.436	0.446	0.447	0.448	0.458	0.404	0.416	0.445	0.320
Cr/(Cr + Al)	0.492	0.452	0.481	0.483	0.467	0.474	0.069	0.448	0.385	0.405	0.488	0.488	0.067	0.290	0.466	0.059

Ti/Ti + Cr + Al)	0.305	0.434	0.342	0.328	0.302	0.332	0.655	0.050	0.499	0.490	0.279	0.336	0.810	0.422	0.268	0.656
Sample																
Oxide%																
TiO_2	15.92	17.12	17.57	15.28	17.86	18.13	17.61	13.11	10.18	17.02	15	17.7	4.36	15.49	16.45	17.44
Al_2O_3	7.84	8.55	9.63	10.07	8.37	8.01	7.79	6.77	8.64	9.16	8.63	7.77	15.04	8.4	8.03	10.91
Cr_2O_3	12.14	6.42	4.98	2.12	5.19	5.08	5.57	5.59	24.09	4.91	10.03	5.23	41.86	7.04	7.69	4.26
FeO_T	46.61	51.3	49.13	55.27	50.29	49.89	51.23	57.41	40.08	50.39	49.24	51.34	22.71	51.2	50.15	49.03
MnO	0.61	0.53	0.43	0.6	0.48	0.73	0.36	0.57	0.47	0.47	0.66	0.61	0	0.47	0.68	0.51
MgO	16.61	15.62	15.36	14.92	15.12	15.68	14.68	13.7	15.26	15.94	14.72	16.25	15.7	15.23	16.05	17.19
Total	99.78	99.71	97.16	98.47	97.35	97.71	97.4	97.36	98.92	98.16	98.43	99.38	99.87	97.9	99.19	99.6
Recalculated Fe																
FeO	21.99	24.75	25.00	23.83	25.46	24.61	25.92	22.97	18.59	23.56	23.68	23.50	14.40	23.39	23.11	22.72
Fe_2O_3	27.36	29.50	26.82	34.95	27.60	28.09	28.12	38.28	23.88	29.82	28.41	30.94	9.24	30.90	30.05	29.24
Total	102.47	102.50	99.79	101.98	100.07	100.33	100.06	101.19	101.32	101.16	101.13	102.49	100.60	100.93	102.06	102.55
Fe^{2+}/(Mg + Fe^{2+}	0.426	0.471	0.477	0.473	0.486	0.468	0.498	0.485	0.406	0.453	0.474	0.448	0.340	0.463	0.447	0.426
Cr/(Cr + Al)	0.389	0.459	0.464	0.459	0.490	0.503	0.494	0.443	0.208	0.466	0.384	0.500	0.061	0.430	0.443	0.447
Ti/Ti + Cr + Al)	0.509	0.335	0.258	0.124	0.294	0.298	0.324	0.356	0.652	0.264	0.438	0.311	0.651	0.360	0.391	0.208
Sample																
Oxide%																
TiO_2	15.78	16.86	17	17.43	17.04	16.35	9.99	7	18.32	4.88	14.08	14.63	15.45	15.11	16.9	16
Al_2O_3	9.66	10.01	9.77	8.66	9.19	10.65	9.84	5.56	9.47	5.36	7.44	8.68	8.59	9.26	7.91	8.05
Cr_2O_3	4.14	3.98	4.54	6.03	4.4	1.44	33.11	44.98	3.57	51.46	13.4	6.39	5.72	7.56	5.8	6.2
FeO_T	51.6	49.85	50.03	48.29	53.68	55.1	31.8	28.19	53.62	24.68	48.34	52	53.24	51.34	51.82	52.09
MnO	0.59	0.52	0.41	0.37	0.57	0.41	0	0.63	0.39	0	0	0	0.4	0.48	0.51	0.5
MgO	15.42	16.28	15.94	16.79	13.94	14	15.06	13.55	14.8	12.55	14.94	15.05	14.7	15.58	16.26	14.44
Total	97.54	97.6	97.94	97.81	98.41	97.85	99.53	99.27	99.61	99.51	98.69	97.46	98.24	99.43	99.28	97.26
Recalculated Fe																
FeO	22.94	23.10	23.65	22.58	27.08	26.52	19.74	18.05	27.57	17.90	22.96	22.74	24.38	23.13	23.42	24.79
Fe_2O_3	31.85	29.73	29.31	28.57	29.56	31.76	13.40	11.27	28.95	7.53	28.20	32.52	32.08	31.35	31.56	30.34
Total	100.74	100.48	100.88	100.65	101.78	101.13	101.14	101.04	103.07	99.68	101.03	100.42	101.31	102.47	102.36	100.32
Fe^{2+}/(Mg + Fe^{2+}	0.455	0.443	0.454	0.430	0.522	0.515	0.424	0.428	0.511	0.445	0.463	0.459	0.482	0.454	0.447	0.491
Cr/(Cr + Al)	0.447	0.459	0.458	0.467	0.472	0.473	0.166	0.111	0.496	0.072	0.354	0.419	0.442	0.402	0.478	0.455
Ti/Ti + Cr + Al)	0.223	0.211	0.238	0.318	0.243	0.083	0.693	0.844	0.202	0.866	0.547	0.331	0.309	0.354	0.330	0.341
Sample																
Oxide%																
TiO_2	14.91	10.54	14.32	11.5	13.77	14.38	16.42	17.97	7.09	4.39	4.65	16.66	15.8	14.87	15.8	6.9
Al_2O_3	9.38	13.55	11.65	14.75	11.98	13.34	10.6	10	9.77	14.15	13.28	10.96	11.26	11.88	10.72	8.64
Cr_2O_3	5.51	16.65	7.54	4.7	8.22	2.18	4.62	3.95	36.19	40.7	42.4	5.26	6.33	8.93	7.04	35.99
FeO_T	52.37	41.72	48.84	46.76	48.88	52.16	50.61	49.61	30.9	24.03	23.43	49.17	48.62	46.96	48.59	31.17
MnO	0.59	0.43	0.77	0.84	0.42	0.75	0.68	0.83	0	0.58	0.79	0.39	0.54	0.77	0.45	0
MgO	14.46	16.12	15.76	18.19	14.78	15.78	15.53	15.78	15.18	15.14	15.09	16.44	15.42	15.82	16.53	14.77
Total	97.37	99.4	99.27	97.18	98.24	98.6	98.57	98.23	99.48	99.09	99.66	98.84	98.05	99.3	99.29	98.09
Recalculated Fe																
FeO	23.90	18.37	21.73	15.24	23.18	22.33	24.08	24.72	16.76	14.37	14.52	23.38	23.75	22.56	22.45	16.51
Fe_2O_3	31.64	25.95	30.13	35.03	28.56	33.15	29.48	27.66	15.72	10.74	9.90	28.66	27.64	27.11	29.05	16.29
Total	100.39	102.01	102.28	100.68	100.91	101.91	101.41	100.91	100.70	100.07	100.63	101.75	100.74	101.95	102.04	99.10
Fe^{2+}/(Mg + Fe^{2+}	0.481	0.390	0.436	0.320	0.468	0.443	0.465	0.468	0.382	0.347	0.351	0.444	0.464	0.444	0.432	0.385

Cr/(Cr + Al)	0.421	0.214	0.354	0.291	0.334	0.383	0.433	0.476	0.117	0.063	0.066	0.423	0.394	0.347	0.395	0.118
Ti/Ti + Cr + Al)	0.283	0.452	0.303	0.176	0.315	0.099	0.226	0.209	0.713	0.659	0.682	0.244	0.274	0.335	0.306	0.736
Sample								**CL-06-003-205**								
Oxide%																
TiO_2	4.79	4.89	17.1	6.02	14.96	16.32	15.17	13.6	14.4	15.46	18.2	16.01	17.53	17.89	11.89	4.57
Al_2O_3	7.73	13.33	11.58	8.77	11.22	9.56	10.75	12.11	11.41	10.81	8.85	9.45	7.79	9.04	13.64	8.81
Cr_2O_3	46.35	41.98	3.78	41.37	9.8	5.04	2.9	10.08	9.1	7.58	3.12	6.11	5.24	4.38	18.02	47.12
FeO_T	25.44	23.57	50.67	26.96	46.63	52.09	54.48	45.51	47.25	47.71	50.79	50.43	51.48	50.67	39	24.4
MnO	0	0	0.39	0.67	0.48	0.38	0.78	0.61	0.47	0	0.66	0.61	0.84	0.73	0	0
MgO	14.41	15.62	16.07	14.45	16.14	15.09	15.55	16.83	15.93	15.9	15.52	16.51	15.57	15.94	16.72	13.83
Total	99.19	99.98	99.74	98.3	99.37	98.7	99.7	98.95	98.82	98.01	97.25	99.29	98.57	98.76	99.82	98.84
Recalculated Fe																
FeO	15.34	14.65	24.67	15.74	22.34	24.63	23.31	19.76	21.79	22.86	25.01	22.19	24.43	24.54	19.48	16.17
Fe_2O_3	11.23	9.91	28.89	12.47	26.99	30.52	34.64	28.62	28.30	27.62	28.65	31.38	30.07	29.04	21.70	9.15
Total	99.84	100.38	102.48	99.49	101.93	101.77	103.10	101.82	101.65	100.42	100.01	102.44	101.46	101.56	101.44	99.65
$Fe^{2+}/(Mg + Fe^{2+}$	0.374	0.345	0.463	0.379	0.437	0.478	0.457	0.397	0.434	0.446	0.475	0.430	0.468	0.463	0.395	0.396
Cr/(Cr + Al)	0.073	0.070	0.436	0.095	0.349	0.446	0.433	0.358	0.349	0.320	0.191	0.303	0.311	0.245	0.470	0.782
Ti/Ti + Cr + Al)	0.801	0.679	0.180	0.760	0.369	0.261	0.153	0.315	0.344	0.383	0.515	0.430	0.497	0.488	0.228	0.067
Sample																
Oxide%																
TiO_2	7.02	17.6	14.89	17.54	4.91	10.79	17.49	10.05	4.12	17.48	2.95	5.49	11.38	9.23	17.28	16.69
Al_2O_3	8.11	8.51	9.38	10.36	8.62	13.02	10.25	8.84	13.79	8.63	12.17	5.89	9.35	8.07	9.65	9.64
Cr_2O_3	32.19	5.47	4.93	3.88	47.58	16.62	4.7	24.35	40.27	6.55	49.94	44.15	20.32	30.74	4.57	4.53
FeO_T	35.33	49.93	52.17	48.43	23.59	41.69	49.89	39.54	24.18	49.73	19.6	28.36	42.43	36.89	50.25	51.41
MnO	0.55	0.61	0.63	0.64	0	0.49	0.38	0	0	0.44	0	0.69	0	0	0.48	0.51
MgO	14.15	16.24	16.04	16.71	14.59	16.37	16.06	15	16.94	16.25	14	12.62	13.93	13.87	15.6	15.78
Total	97.47	98.54	98.11	97.66	99.62	99.13	99.05	98.35	99.45	99.14	99.09	97.54	98.28	99.41	97.9	98.78
Recalculated Fe																
FeO	16.96	23.76	21.72	22.98	15.46	18.41	24.33	19.24	12.04	24.05	14.89	16.97	21.67	20.18	24.59	23.83
Fe_2O_3	20.41	29.08	33.84	28.28	9.04	25.87	28.40	22.57	13.49	28.54	5.23	12.65	23.07	18.57	28.52	30.65
Total	99.39	101.27	101.43	100.39	100.20	101.57	101.89	100.04	100.65	101.94	99.18	98.80	100.15	100.87	100.69	101.84
$Fe^{2+}/(Mg + Fe^{2+}$	0.402	0.451	0.432	0.436	0.373	0.387	0.459	0.418	0.285	0.454	0.374	0.430	0.466	0.449	0.469	0.459
Cr/(Cr + Al)	0.727	0.301	0.261	0.201	0.787	0.461	0.235	0.649	0.662	0.337	0.734	0.834	0.593	0.719	0.241	0.240
Ti/Ti + Cr + Al)	0.131	0.480	0.428	0.463	0.072	0.222	0.454	0.203	0.061	0.461	0.040	0.090	0.240	0.170	0.464	0.457
Sample								**CL-06-003-219**								
Oxide%																
TiO_2	17.39	17.2	15.63	14.92	13.22	17.51	16.13	4.83	15.5	4.9	4.9	5.06	7.72	16.62	17.8	9.55
Al_2O_3	8.22	9.23	8.93	8.65	11.15	7.86	10.39	13.26	10.3	8.56	9.76	9.03	10.55	10.62	9.65	12.18
Cr_2O_3	4.45	4.59	6.08	7.24	12.95	6.34	6.74	40.62	7.96	47.29	44.26	46.6	30.77	7.72	3.52	20.18
FeO_T	52.13	51.46	52.3	51.09	45.51	51.53	49.19	24.39	47.3	25.37	25.31	24.33	33.26	47.95	49.96	42.47
MnO	0.57	0.72	0.83	0.6	0.44	0.69	0	0	0	0	0	0.82	0.78	0	0.64	0
MgO	14.82	15.31	15.3	15.09	14.78	13.49	15.71	15.16	15.17	13.18	14.42	13.86	15.2	14	15.54	13.05
Total	97.85	98.47	99.1	97.78	98.18	97.64	98.61	98.66	96.68	99.19	99.16	99.7	98.49	97.72	97.19	98.04
Recalculated Fe																
FeO	25.27	24.89	23.55	22.77	22.48	27.18	24.08	14.77	23.68	17.60	15.71	16.08	16.41	26.70	24.75	22.18
Fe_2O_3	29.85	29.53	31.95	31.47	25.59	27.06	27.91	10.69	26.25	8.64	10.67	9.17	18.73	23.61	28.02	22.54
Total	100.84	101.47	102.27	100.93	100.61	100.35	100.96	99.53	98.86	100.17	99.72	100.62	100.16	99.28	99.92	99.69

$Fe^{2+}/(Mg + Fe^{2+}$	0.489	0.477	0.463	0.458	0.460	0.531	0.462	0.353	0.467	0.428	0.379	0.394	0.377	0.517	0.472	0.488
Cr/(Cr + Al)	0.266	0.250	0.314	0.360	0.438	0.351	0.303	0.673	0.341	0.787	0.753	0.776	0.662	0.328	0.197	0.526
Ti/Ti + Cr + Al)	0.498	0.471	0.434	0.413	0.298	0.480	0.408	0.071	0.387	0.072	0.073	0.074	0.136	0.402	0.486	0.192
Sample																
Oxide%																
TiO_2	9.45	2.65	6.21	9.13	7.4	15.71	7.92	7.92	13.69	4.8	4.77	5.65	18.31	18.18	16.86	16.76
Al_2O_3	13.01	12.58	7.87	12.71	9.88	10.4	9.31	8.9	12.28	13.35	12.98	5.62	8.74	9.6	10.67	8.59
Cr_2O_3	19.61	46.57	42.3	24.43	33.82	5.98	35.67	36.25	12.79	43.62	43.53	44.99	4.99	4.07	4.74	5.6
FeO_T	41.82	24.95	27.31	36.05	33.33	49.38	29.8	30.48	43.71	23.09	23.1	28.24	49.54	49.67	49.13	49.59
MnO	0.56	0	0	0	0	0	1.38	0.74	0.52	0	0	0.73	0	0.4	0.33	0.81
MgO	13.96	12.81	13.95	15.76	13.96	15.49	14.28	14.49	14.62	14.57	14.69	12.81	15.45	15.56	16.21	15.6
Total	98.67	99.83	98.04	98.35	98.88	97.3	98.5	98.93	97.66	99.58	99.26	98.33	97.6	98.33	97.56	97.34
Recalculated Fe																
FeO	20.60	16.86	16.84	17.91	18.70	23.66	17.15	17.55	23.06	16.16	15.78	17.04	25.80	25.39	23.62	23.35
Fe_2O_3	23.58	8.99	11.64	20.16	16.26	28.58	14.06	14.38	22.94	7.70	8.13	12.45	26.39	26.98	28.35	29.17
Total	100.77	100.46	99.00	100.10	100.02	99.82	99.77	100.22	99.91	100.20	99.89	99.59	99.68	100.18	100.78	99.87
$Fe^{2+}/(Mg + Fe^{2+}$	0.453	0.425	0.404	0.389	0.429	0.462	0.402	0.405	0.470	0.384	0.376	0.427	0.484	0.478	0.450	0.456
Cr/(Cr + Al)	0.503	0.713	0.783	0.563	0.697	0.278	0.720	0.732	0.411	0.687	0.692	0.843	0.277	0.221	0.230	0.304
Ti/Ti + Cr + Al)	0.187	0.037	0.099	0.167	0.127	0.410	0.132	0.132	0.295	0.067	0.067	0.092	0.492	0.485	0.437	0.464
Sample				**CL-06-003-222**												
Oxide%																
TiO_2	17.88	16.45	14.59	8.78	13.7	4.43	6.86	16.7	4.26	11.33	6.94	17.65	12.26	12.95	10.98	9.3
Al_2O_3	10.81	9.42	10.27	11.12	11.7	15.51	7.89	9.38	12.19	14.14	10.58	10.78	14.68	14.66	15.21	12.92
Cr_2O_3	4.9	4.36	6.69	28.23	10.3	41.67	35.63	5.13	44.55	12.63	33.15	3.4	10.64	9.61	11.7	21.18
FeO_T	47.07	49.21	47.93	35.95	46.87	23.06	34.61	50.85	23.76	43.29	32.75	49.75	43.14	43.53	43.25	39.55
MnO	0	0	0	0.67	0	0	0	0.74	0.71	0.53	0	0.51	0	0.55	0	0.67
MgO	17.29	18.69	17.71	13.71	14.95	15.21	14.45	14.86	15.4	16	14.5	15.73	16.42	16.42	16.59	15.02
Total	97.98	97.82	97.93	98.64	97.76	100.34	99.86	97.83	100.61	98.03	98.24	98.82	97.5	98.98	98.24	98.73
Recalculated Fe																
FeO	23.21	19.72	19.36	19.89	23.03	15.34	17.53	24.84	14.02	19.27	17.43	24.85	19.82	19.84	18.70	18.78
Fe_2O_3	26.52	32.77	31.75	17.85	26.49	8.58	18.98	28.90	10.83	26.69	17.03	27.67	25.92	26.32	27.28	23.08
Total	100.61	101.41	100.37	100.25	100.17	100.74	101.34	100.56	101.95	100.59	99.63	100.59	99.74	100.63	100.46	100.95
$Fe^{2+}/(Mg + Fe^{2+}$	0.430	0.372	0.380	0.449	0.464	0.361	0.405	0.484	0.338	0.403	0.403	0.470	0.404	0.404	0.387	0.412
Cr/(Cr + Al)	0.233	0.237	0.304	0.630	0.371	0.643	0.752	0.268	0.710	0.375	0.678	0.175	0.327	0.305	0.340	0.524
Ti/Ti + Cr + Al)	0.447	0.460	0.387	0.157	0.320	0.061	0.121	0.454	0.061	0.242	0.119	0.463	0.264	0.281	0.233	0.180
Sample																
Oxide%																
TiO_2	14.66	14.56	16.2	14.49	16.17	6.93	4.07	4.17	12.56	17.41	16.89	18.22	7.08	7.59	13.46	13.77
Al_2O_3	8.49	10.36	10.59	12.59	9.76	8.69	14.58	14.58	12.98	10.39	9.81	9.03	9.56	11.11	10.19	13.4
Cr_2O_3	7.47	8.28	3.87	2.59	5.01	40.25	41.07	41.13	14.2	2.79	4.38	3.68	37.98	32.79	14.28	13.36
FeO_T	51.21	49.1	49.85	51.72	50.11	28.22	24.78	24.07	42.34	47.91	50.39	50.87	29.54	32	43.68	41.32
MnO	0.53	0.52	0.56	0	0.59	0.68	0	0	0	0	0.23	0.82	0	0	0.4	0.39
MgO	15.04	15.57	17.8	15.93	15.43	14.82	15.33	15.68	16.4	18.71	16.23	14.36	14.41	15.21	15.05	15.74
Total	97.67	98.45	98.98	97.96	97.31	99.98	99.67	99.99	99.03	97.31	97.73	97.24	99.31	98.8	97.8	98.28
Recalculated Fe																
FeO	22.54	22.45	20.71	22.42	23.53	16.41	14.72	14.20	20.26	20.38	23.60	26.59	17.67	17.25	21.84	21.83
Fe_2O_3	31.86	29.62	32.38	32.56	29.54	13.12	11.18	10.97	24.54	30.60	29.77	26.98	13.19	16.39	24.28	21.66
Total	100.85	101.36	102.11	100.58	100.03	100.90	100.95	100.73	100.94	100.28	100.91	99.68	99.89	100.34	99.49	100.15

$Fe^{2+}/(Mg + Fe^{2+}$	0.457	0.447	0.395	0.441	0.461	0.383	0.350	0.337	0.409	0.379	0.449	0.510	0.408	0.389	0.449	0.438
Cr/(Cr + Al)	0.371	0.349	0.197	0.121	0.256	0.757	0.654	0.654	0.423	0.153	0.230	0.215	0.727	0.664	0.485	0.401
Ti/Ti + Cr + Al)	0.409	0.369	0.439	0.392	0.440	0.110	0.058	0.059	0.263	0.475	0.458	0.503	0.114	0.128	0.303	0.282
Sample														**CL-06-003-236**		
Oxide%																
TiO_2	9.19	5.77	4.94	5.83	4.84	4.8	6.81	3.84	5.85	15.15	5.45	4.64	16.83	13.25	12.58	15.44
Al_2O_3	9.67	5.45	4.73	4.95	7.22	7.72	5.85	8.24	10.19	11.6	8.93	7.83	9.99	14.77	15.39	10.42
Cr_2O_3	32.72	47.05	50.85	47.21	49.71	48.73	41.98	50	42.74	6.9	37.29	48.76	5.49	1.11	0.73	7.56
FeO_T	30.97	28.84	25.87	27.15	24.22	24.39	31.79	23.87	25.79	48.01	32.8	23.79	49.72	47.58	51.66	47.31
MnO	0.93	0	0.66	0.84	0	0.56	0	0	0	0	0	0	0	0.4	0	0.43
MgO	15.43	12.64	12.56	13	13.61	14.11	12.9	14.01	15.19	16.53	14.93	14.67	16.3	19.7	17.07	17.55
Total	99.1	99.85	99.6	99.1	100.83	100.51	99.16	99.91	99.64	98.55	99.26	99.69	98.88	96.89	97.94	98.8
Recalculated Fe																
FeO	17.24	18.90	17.42	17.23	16.76	15.72	19.41	15.54	15.82	22.15	15.67	15.11	23.81	15.36	19.25	20.42
Fe_2O_3	15.26	11.05	9.39	11.02	8.29	9.63	13.76	9.26	11.08	28.73	19.03	9.65	28.79	35.81	36.02	29.88
Total	100.44	100.86	100.55	100.08	100.43	101.27	100.71	100.89	100.87	101.07	101.31	100.66	101.21	100.40	101.31	101.70
$Fe^{2+}/(Mg + Fe^{2+}$	0.385	0.456	0.438	0.426	0.409	0.385	0.458	0.384	0.369	0.429	0.371	0.366	0.450	0.304	0.388	0.395
Cr/(Cr + Al)	0.694	0.853	0.878	0.865	0.822	0.809	0.828	0.803	0.738	0.285	0.737	0.807	0.269	0.048	0.031	0.327
Ti/Ti + Cr + Al)	0.156	0.090	0.075	0.092	0.071	0.070	0.113	0.055	0.088	0.373	0.093	0.068	0.440	0.353	0.336	0.389
Sample																
Oxide%																
TiO_2	12.68	4.16	16.71	15.03	12.19	10.1	10.01	16.8	15.1	11.76	5.42	15.53	13.17	7.55	15.88	5.78
Al_2O_3	14.36	14.02	11.19	12.55	16.69	18.5	14.353	11.16	12.27	14.74	7.04	12.52	12.59	9.69	10.13	11.73
Cr_2O_3	0	38.31	5	3.94	1.24	0	17.21	3.52	6.09	0	47.2	2.08	7.32	35.71	4.53	35.97
FeO_T	54.28	26.61	48.17	48.64	49.64	50.23	38.62	47.47	45.88	56.03	25.46	52.28	48.47	30.94	51.95	29.99
MnO	0.61	0.61	0.55	0.53	0.49	0	0	0.62	0	0.4	0	0.68	0.47	0	0.71	1.02
MgO	15.17	15.32	16.78	16.46	16.54	18.72	17.53	17.82	17.66	14.88	13.59	15.13	15.88	14.77	14.5	14.42
Total	97.42	98.64	98.56	97.28	96.96	98.33	98.27	97.54	97.64	98.13	99.31	98.38	98.07	99	97.77	99.12
Recalculated Fe																
FeO	21.61	13.71	22.62	21.46	19.41	14.94	15.97	20.73	19.85	21.75	17.02	24.15	20.99	17.62	24.84	15.76
Fe_2O_3	36.31	14.33	28.40	30.21	33.59	39.22	25.18	29.72	28.92	38.09	9.38	31.26	30.54	14.80	30.13	15.81
Total	100.74	100.69	101.24	100.18	100.16	101.90	100.54	100.37	100.19	101.63	99.65	101.35	100.96	100.14	100.72	100.71
$Fe^{2+}/(Mg + Fe^{2+}$	0.444	0.334	0.431	0.422	0.397	0.309	0.338	0.395	0.387	0.451	0.413	0.472	0.426	0.401	0.490	0.380
Cr/(Cr + Al)	0.000	0.647	0.231	0.174	0.047	0.000	0.446	0.175	0.250	0.000	0.818	0.100	0.281	0.712	0.231	0.673
Ti/Ti + Cr + Al)	0.360	0.063	0.423	0.387	0.307	0.258	0.198	0.442	0.371	0.337	0.082	0.416	0.324	0.125	0.435	0.093
Sample														**CL-06-003-247**		
Oxide%																
TiO_2	15.4	4.43	16.78	9.02	13.86	4.97	14.85	15.57	4.53	14.49	16.62	17.05	17.26	17.58	6.19	19.14
Al_2O_3	11.68	14.6	10.01	10.24	13.85	14.33	12.15	11.46	7.46	11.37	9.47	10.09	10.84	8.73	8.21	9.98
Cr_2O_3	4.51	40.74	3.32	30.51	0.82	41.74	9.65	1.62	49.4	10.7	4.9	5.64	2.43	6.19	45.04	5
FeO_T	49.21	23.28	51.38	33.3	52.1	23.23	44.94	53.36	24.26	44.99	49.64	48.72	49.44	50.66	27.44	49.63
MnO	0.94	0	0.52	0.67	0.43	0	0.44	0.68	0	0.66	0.47	0.49	0.78	0.67	0	0
MgO	15.37	15.33	15.77	14.98	15.99	14.96	15.38	14.33	13.21	15.92	15.37	16	16.65	13.72	14.47	15.74
Total	97.21	99.06	97.95	98.78	97.41	99.57	97.62	97.14	99.75	98.36	96.68	98.22	97.72	97.69	101.93	99.89
Recalculated Fe																
FeO	22.88	14.55	23.91	18.09	21.16	15.81	22.79	24.87	16.60	21.72	23.70	23.86	22.73	27.27	17.26	27.06
Fe_2O_3	29.26	9.70	30.53	16.90	34.39	8.24	24.62	31.67	8.52	25.86	28.83	27.63	29.69	26.00	11.31	25.08

Total	100.04	99.35	100.84	100.41	100.86	100.06	100.09	100.19	100.06	100.72	99.58	100.76	100.37	100.15	102.67	102.00
$Fe^{2+}/(Mg + Fe^{2+})$	0.455	0.348	0.460	0.404	0.426	0.372	0.454	0.493	0.413	0.434	0.464	0.456	0.434	0.527	0.401	0.491
Cr/(Cr + Al)	0.206	0.652	0.182	0.667	0.038	0.661	0.348	0.087	0.816	0.387	0.258	0.273	0.131	0.466	0.093	0.478
Ti/Ti + Cr + Al)	0.401	0.063	0.467	0.158	0.381	0.070	0.337	0.442	0.066	0.333	0.454	0.440	0.469	0.322	0.786	0.252
Sample																
Oxide%																
TiO_2	16.8	15.52	9.8	14.64	13.53	7.97	14.5	11.68	19.51	17.76	5.42	19.12	8.76	5.5	18.73	17.42
Al_2O_3	12.8	13.41	15.48	12.6	12.98	12.96	13.13	15.26	11.05	11.15	15.82	11.1	11.42	6.38	9.11	10.15
Cr_2O_3	5.07	8	18.98	10.88	11.02	28.07	9.46	17.25	3.55	4.79	41.7	3.7	29.65	49.2	3.81	4.81
FeO_T	47.21	47.77	38.66	46.8	45.43	35.13	46.53	40.29	49.35	47.37	23.53	49.74	35.75	26.32	50.58	51.46
MnO	0.69	0.41	0.56	0.77	0.66	0.38	0.53	0.52	0	0.48	0	0.37	0.33	0	0.55	0.49
MgO	16.19	16.59	16.26	16.4	17.13	15.34	16.88	16.38	17.26	17.91	15.01	16.53	14.62	12.84	14.46	16.55
Total	98.95	101.74	99.88	101.22	100.89	99.88	101.17	101.67	101.06	99.67	101.6	100.48	100.66	100.66	97.4	101.27
Recalculated Fe																
FeO	23.79	23.37	18.19	22.50	20.14	17.69	21.63	19.98	25.65	22.06	17.04	26.00	19.54	18.61	27.25	24.01
Fe_2O_3	26.03	27.12	22.75	27.01	28.11	19.38	27.67	22.57	26.34	28.13	7.22	26.38	18.02	8.56	25.93	30.51
Total	101.37	104.42	102.02	104.80	103.57	101.82	103.80	103.93	103.36	102.48	102.25	103.20	102.34	101.10	99.84	104.32
$Fe^{2+}/(Mg + Fe^{2+}$	0.452	0.441	0.386	0.435	0.397	0.393	0.418	0.406	0.455	0.409	0.389	0.469	0.428	0.449	0.514	0.449
Cr/(Cr + Al)	0.210	0.286	0.451	0.367	0.363	0.592	0.326	0.431	0.177	0.224	0.639	0.183	0.635	0.838	0.219	0.241
Ti/Ti + Cr + Al)	0.398	0.345	0.181	0.320	0.298	0.138	0.322	0.217	0.481	0.441	0.073	0.473	0.152	0.082	0.506	0.454
Sample																
Oxide%																
TiO_2	16.55	5.46	9.51	10.06	4.92	4.81	5.34	16.58	18.29	17.25	13.83	17.83	4.86	18.22	12.99	5.92
Al_2O_3	10.31	5.8	16.14	3.84	11.87	16.08	9.21	11.19	10.48	11.13	13.55	10.22	16.04	9.78	11.67	7.32
Cr_2O_3	5.14	44.27	18.7	3.21	40.6	41.01	45.5	6.23	2.9	7.28	13.87	5.37	42.36	5.2	15.47	46.1
FeO_T	51.28	28.39	38.11	74.95	27.83	22.63	24.18	49.04	50.57	48.53	43.46	49.31	23.01	49.48	42.07	27.03
MnO	0.43	0.64	0	0.66	0.86	0	0.96	0.51	0.48	0.47	0.47	0.66	0	0.55	0.66	0
MgO	15.46	13.1	16.31	8	12.99	15.86	14.35	15.54	15.41	16.79	15.49	14.74	14.77	14.77	15.03	13.46
Total	99.58	98.03	99.59	101.14	99.34	100.89	99.81	99.21	98.13	101.74	100.84	98.4	101.69	98.08	98.05	100.33
Recalculated Fe																
FeO	24.40	16.37	17.75	29.55	17.28	14.90	15.21	24.52	25.99	23.86	23.09	26.12	16.83	26.66	21.65	18.08
Fe_2O_3	29.87	13.36	22.63	50.45	11.72	8.59	9.97	27.25	27.31	27.41	22.64	25.77	6.87	25.37	22.69	9.94
Total	102.56	99.37	101.57	106.19	100.53	101.30	100.80	101.96	100.87	104.50	102.94	100.98	101.73	100.54	100.16	100.83
$Fe^{2+}/(Mg + Fe^{2+}$	0.470	0.412	0.379	0.675	0.427	0.345	0.373	0.470	0.486	0.444	0.455	0.499	0.390	0.503	0.447	0.430
Cr/(Cr + Al)	0.251	0.837	0.437	0.359	0.696	0.631	0.768	0.272	0.157	0.305	0.407	0.261	0.639	0.263	0.471	0.809
Ti/Ti + Cr + Al)	0.434	0.089	0.175	0.517	0.074	0.066	0.079	0.408	0.484	0.407	0.279	0.452	0.065	0.467	0.273	0.090
Sample																
Oxide%																
TiO_2	9.53	4.63	19.54	15.46	17.51	7.07	9.24	8.22	15.87	13.72	6.65	17.63	4.62	17.46	19.13	19.06
Al_2O_3	12.16	15.67	11.58	11.68	10.39	9.73	12.17	9.64	10.31	12.19	9.86	9.97	13.29	11.26	10.7	10.12
Cr_2O_3	24.36	41.4	4.2	11.52	6.12	37.52	26.14	5.03	10.88	13.38	37.19	5.08	42.3	6.2	3.49	3.61
FeO_T	36.98	22.97	50.19	45.46	47.92	30.34	36.46	51.13	48.35	43.8	30.56	49.3	24.36	49.36	49.75	52.21
MnO	0.78	0	0.67	0.69	0.45	0.87	0.32	0.53	0	0.4	0	0.69	0	0.71	0.77	0.79
MgO	14.84	14.98	17.78	15.08	15	15.01	15.37	15.99	14.5	16.31	15.04	15.56	10.06	16.39	16.59	16.41
Total	98.77	100.08	104.28	100.05	97.68	100.37	99.87	100.68	100.26	99.92	99.7	98.51	100.01	101.39	100.5	102.41
Recalculated Fe																
FeO	18.98	15.82	25.08	24.43	25.41	16.56	18.56	13.66	26.19	21.35	16.64	24.74	21.28	24.68	25.36	25.96

Fe_2O_3	20.00	7.95	27.90	23.38	25.02	15.31	19.89	41.65	24.63	24.95	15.47	27.29	3.42	27.43	27.10	29.17
Total	100.65	100.45	107.07	102.23	100.19	102.07	101.86	94.71	102.38	102.30	100.85	101.15	94.97	104.13	103.21	105.31
$Fe^{2+}/(Mg + Fe^{2+}$	0.418	0.372	0.442	0.476	0.487	0.382	0.404	0.324	0.503	0.423	0.383	0.472	0.543	0.458	0.462	0.470
Cr/(Cr + Al)	0.573	0.639	0.196	0.398	0.283	0.721	0.590	0.259	0.414	0.424	0.717	0.255	0.681	0.270	0.180	0.193
Ti/Ti + Cr + Al)	0.176	0.064	0.464	0.337	0.435	0.114	0.166	0.287	0.365	0.293	0.109	0.457	0.066	0.420	0.484	0.492
Sample																
Oxide%																
TiO_2	16.25	4.2	11.53	18.4	17.85	6.43	16.33	4.63	5.1	17.96	18.5	6.49	16.89	16.86	14.93	4.51
Al_2O_3	11.46	7.95	12.15	10.53	10.78	9.93	11.53	15.32	6.68	10.37	10.68	7.45	11.1	11.42	12.31	8.02
Cr_2O_3	4.93	48.16	25.42	3.05	5.26	38.12	6.24	41.94	47.78	3.79	2.54	45.19	6.01	4.19	8.43	48.2
FeO_T	49.66	25.06	35.46	49.12	48.66	29.61	47.66	21.74	25.14	49.02	49.55	25.44	46.31	48.11	44.86	23.15
MnO	0.51	0	0	0.72	0.69	0.51	0.61	0.63	0.55	0.34	0.73	0.65	0.45	0.51	0.77	0
MgO	17.2	13.99	16.66	16.44	17.28	16.77	16.96	15.83	13.72	16.96	16.82	14.09	16.4	17.61	16.86	13.87
Total	100.06	99.88	101.63	98.33	100.63	101.51	99.35	100.17	99.18	98.66	99.06	99.53	97.25	98.73	98.31	98.14
Recalculated Fe																
FeO	22.20	15.46	19.57	24.33	23.35	13.99	22.29	13.98	15.84	23.37	23.85	16.63	23.01	21.67	20.56	15.34
Fe_2O_3	30.52	10.67	17.66	27.55	28.13	17.36	28.20	8.63	10.34	28.50	28.57	9.80	25.89	29.38	27.01	8.67
Total	103.07	100.69	102.99	101.02	103.34	103.11	102.15	100.95	100.22	101.52	101.91	100.52	99.75	101.64	101.09	98.92
$Fe^{2+}/(Mg + Fe^{2+}$	0.420	0.383	0.397	0.454	0.431	0.319	0.424	0.331	0.393	0.436	0.443	0.398	0.440	0.408	0.406	0.383
Cr/(Cr + Al)	0.224	0.803	0.584	0.163	0.247	0.720	0.266	0.647	0.828	0.197	0.138	0.803	0.266	0.198	0.315	0.801
Ti/Ti + Cr + Al)	0.413	0.062	0.201	0.483	0.443	0.104	0.399	0.064	0.078	0.470	0.488	0.099	0.416	0.431	0.347	0.067
Sample																
Oxide%																
TiO_2	17.31	15.73	16.68	8.39	17.99	18.62	7.32	7.54	18.03	6.91	16.39	10.57	14.56	4.81	17.16	4.89
Al_2O_3	11.83	11.9	12.12	9.32	9.47	10.18	9.91	12.71	10.31	10.71	11.08	13.2	10.9	7.64	10.72	10.64
Cr_2O_3	3.67	6.88	2.86	34.86	3.88	4.27	38.98	32.53	4.33	34.85	7.86	21.79	10.04	47.03	6.02	41.37
FeO_T	49.08	47.29	47.8	32.1	48.64	47.74	28.9	29	48.71	30.07	46.59	37.61	45.81	24.45	47.41	26.3
MnO	0.5	0.58	0	0.55	0.48	0.39	0.67	0	0.53	0.52	0	0	0.39	0.56	0.67	0
MgO	16.4	16.99	18.86	15.24	15.55	16.11	15.5	16.07	16.76	15.69	17.29	16.77	15.66	14.83	16.72	15.43
Total	98.89	99.49	99.88	100.64	96.07	97.47	101.41	98.28	98.79	98.89	99.68	100.46	97.58	99.44	98.81	99.05
Recalculated Fe																
FeO	24.01	21.81	19.93	17.65	24.66	24.97	16.48	15.65	23.79	15.33	22.14	18.17	21.95	14.33	23.00	14.33
Fe_2O_3	27.86	28.32	30.98	16.06	26.65	25.31	13.80	14.84	27.69	16.38	27.18	21.60	26.52	11.25	27.13	13.30
Total	101.58	102.21	101.65	102.07	98.68	99.85	102.66	99.56	101.44	100.39	102.15	102.31	100.25	100.45	101.42	99.96
$Fe^{2+}/(Mg + Fe^{2+}$	0.451	0.419	0.372	0.394	0.471	0.465	0.374	0.353	0.443	0.354	0.418	0.378	0.440	0.352	0.436	0.343
Cr/(Cr + Al)	0.172	0.279	0.137	0.715	0.216	0.220	0.725	0.632	0.220	0.686	0.322	0.525	0.382	0.805	0.274	0.723
Ti/Ti + Cr + Al)	0.436	0.378	0.431	0.141	0.487	0.477	0.115	0.122	0.465	0.115	0.390	0.195	0.345	0.073	0.426	0.075
Sample																
Oxide%																
TiO_2	6.39	17.49	18.44	8.53	4.58	4.23	16.09	15.29	10.51	17.35	17.93	18.78	17	16.47	17.79	18.67
Al_2O_3	8.54	11.3	9.88	11.26	9.29	11.37	10.7	12.71	12.67	11.08	9.95	9.92	12.28	11.01	10.69	11.35
Cr_2O_3	40.18	4.44	3.66	28.04	42.11	44.55	7.4	9.55	21.09	5.64	2.83	4.51	4.39	5.51	4.08	3.06
FeO_T	27.81	48.38	48.26	33.74	27.67	22.44	46.7	45.38	38.67	48.42	49.67	49.2	47.74	47.59	48.4	47.79
MnO	0	0.44	0.45	0.07	0	0	0.94	0.39	0.45	0.51	0.55	0.41	0.42	0.6	0	0.68
MgO	15.36	16.71	16.42	15.92	14.86	16.44	16.57	17.09	17.14	16.78	16.67	16.95	18.36	17.08	16.72	18.36
Total	98.62	99.02	97.29	97.81	98.89	99.47	98.59	100.45	100.66	99.98	97.81	99.97	100.26	98.4	98.1	100.11
Recalculated Fe																

FeO	15.36	23.42	24.18	16.42	14.69	12.40	21.74	21.87	17.42	23.65	23.27	24.42	21.35	21.70	23.91	22.34
Fe_2O_3	13.84	27.74	26.76	19.24	14.42	11.16	27.74	26.12	23.61	27.53	29.34	27.54	29.32	28.77	27.22	28.28
Total	99.67	101.82	99.79	99.74	99.95	100.15	101.37	103.03	102.90	102.54	100.75	102.73	103.13	101.28	100.41	102.74
$Fe^{2+}/(Mg + Fe^{2+}$	0.359	0.440	0.452	0.367	0.357	0.297	0.424	0.418	0.363	0.442	0.439	0.447	0.395	0.416	0.445	0.406
Cr/(Cr + Al)	0.759	0.209	0.199	0.626	0.753	0.724	0.317	0.335	0.528	0.255	0.160	0.234	0.193	0.251	0.204	0.153
Ti/Ti + Cr + Al)	0.103	0.439	0.488	0.153	0.072	0.061	0.396	0.338	0.200	0.427	0.491	0.481	0.416	0.417	0.458	0.471
Sample																
Oxide%																
TiO_2	16.29	17.97	17.47	11.7	18.31	14.92	10.87	7.66	10.38	11.23	11.07	12.08	12.8	5.68	9.13	17.55
Al_2O_3	11.89	11.02	11.17	7.15	11.22	14.24	7.43	7.88	7.91	11.9	8.82	9.19	12.42	7.38	11.1	10.77
Cr_2O_3	4.46	3.52	5.23	2.2	2.75	2.16	1.18	41.33	0	17.72	0	3.28	15.45	46.42	15.63	2.97
FeO_T	47.76	47.37	47.37	66.34	47.79	50.07	66.22	27.09	65.48	39.92	61.83	60.1	40.94	25.73	50.03	50.59
MnO	0.53	0.4	0.48	0.88	0.52	0.51	0.61	0.65	0.6	0	0.7	0.79	0	0.58	0.52	0.54
MgO	17.74	17.11	16.86	9.34	17.45	16.2	10.54	14.3	10.58	14.89	12.95	10.75	16.22	14.53	10.1	16.28
Total	99.05	97.87	98.75	97.75	98.25	98.19	97.1	99.24	95.49	96.41	96.47	96.47	98.13	100.36	96.61	99.09
Recalculated Fe																
FeO	20.67	22.62	23.28	28.50	22.75	22.36	25.82	17.23	24.73	19.94	21.43	26.32	20.43	15.83	25.41	23.86
Fe_2O_3	30.11	27.51	26.77	42.05	27.83	30.80	44.90	10.96	45.28	22.20	44.90	37.54	22.80	11.01	27.36	29.70
Total	102.09	100.63	101.26	101.82	101.05	101.19	101.60	100.34	99.82	98.25	100.74	100.24	100.11	101.42	99.25	102.07
$Fe^{2+}/(Mg + Fe^{2+}$	0.395	0.426	0.436	0.631	0.422	0.436	0.579	0.403	0.567	0.429	0.481	0.579	0.414	0.379	0.585	0.451
Cr/(Cr + Al)	0.201	0.176	0.239	0.171	0.141	0.092	0.096	0.779	0.000	0.500	0.000	0.193	0.455	0.808	0.486	0.156
Ti/Ti + Cr + Al)	0.411	0.462	0.432	0.464	0.472	0.378	0.458	0.121	0.456	0.232	0.445	0.404	0.264	0.086	0.213	0.467
Sample																
Oxide%																
TiO_2	16.02	16.26	16.17	13.57	4.06	13.49	5.98	17.59	13.62	9.27	18.87	8.7	10.76	12.92	17.07	17.52
Al_2O_3	11.56	11.45	10.43	11.47	1.66	12.94	4.94	9.68	9.76	13.53	7.67	9.44	7.67	11.63	10.26	11.27
Cr_2O_3	7.51	4.78	2.65	2.54	50.55	13.3	48.26	4.26	14.56	23.6	8.68	26.75	26.87	11.89	5.28	5.23
FeO_T	47.12	49.46	51.22	55.32	32.75	41.98	26.57	49.91	43.25	35.49	46.91	36.09	37.2	44.13	49.3	47.61
MnO	0.72	0.69	0.65	0.87	0	0	0	0.56	0.45	0.65	0.68	0.47	0	0.48	0.61	0
MgO	17.17	16.91	15.79	13.06	10.36	15.71	13.57	16.73	16.52	16.56	16.61	15.77	15.39	16.46	17.07	17.08
Total	100.16	99.75	97.32	97.31	99.4	97.74	99.66	98.91	98.67	99.58	99.49	97.26	98.23	97.7	99.71	99.15
Recalculated Fe																
FeO	21.83	22.15	22.66	24.38	20.18	21.77	17.43	23.36	19.83	16.21	24.41	16.27	19.09	19.53	22.69	23.16
Fe_2O_3	28.11	30.35	31.74	34.39	13.96	22.46	10.16	29.50	26.03	21.42	25.01	22.02	20.13	27.34	29.57	27.17
Total	102.92	102.78	100.49	100.77	100.78	99.67	100.34	101.69	100.96	101.73	101.93	99.43	99.91	100.25	102.55	101.86
$Fe^{2+}/(Mg + Fe^{2+}$	0.416	0.424	0.446	0.512	0.522	0.437	0.419	0.439	0.402	0.355	0.452	0.367	0.410	0.400	0.427	0.432
Cr/(Cr + Al)	0.304	0.219	0.146	0.129	0.953	0.408	0.868	0.228	0.500	0.539	0.432	0.655	0.701	0.407	0.257	0.237
Ti/Ti + Cr + Al)	0.381	0.415	0.458	0.397	0.068	0.283	0.093	0.472	0.308	0.168	0.472	0.169	0.211	0.296	0.441	0.431
Sample																
Oxide%																
TiO_2	18.74	18.89	15.86	16.01	16.49	17.88	10.14	16.45	17.19	14.58	18.05	14.56	4.26	7.62	14.9	4.1
Al_2O_3	10.38	10.1	11.62	11.48	11.28	11.35	15.45	12.07	11.66	12.7	10.96	13.08	16.29	9.64	12.3	15.38
Cr_2O_3	4.01	3.75	4.07	3.71	3.22	3.18	14.09	4.97	5.56	7.85	3.37	2.51	40.9	38.39	6.52	40.91
FeO_T	48.74	48.79	49.37	49.88	48.79	47.95	40.83	46.7	47.04	44.8	47.7	51.14	22.97	28.8	47.7	23
MnO	0.49	0.46	0.53	0.54	0.65	0.55	0.6	0.52	0	0.54	0.44	0.5	0	0	0.48	0
MgO	16.87	16.94	16.52	16.69	16.52	17.21	16.31	17.45	17.22	16.78	17.57	16.72	15.43	15.18	16.73	16.13
Total	99.3	99.08	98.02	98.33	96.93	98.17	97.9	98.53	98.78	97.31	98.17	99.17	100.25	99.91	98.75	99.56

Recalculated Fe																
FeO	24.48	24.40	22.23	22.19	22.28	22.94	17.27	21.12	23.06	20.56	22.58	20.68	14.97	17.33	21.40	13.53
Fe_2O_3	26.96	27.10	30.16	30.77	29.46	27.80	26.18	28.43	26.65	26.94	27.91	33.85	8.89	12.75	29.23	10.52
Total	101.93	101.65	100.99	101.39	99.90	100.90	100.52	101.39	101.34	99.95	100.89	102.55	100.74	100.91	101.56	100.57
$Fe^{2+}/(Mg + Fe^{2+}$	0.449	0.447	0.430	0.427	0.431	0.428	0.373	0.404	0.429	0.407	0.419	0.410	0.352	0.390	0.418	0.320
Cr/(Cr + Al)	0.206	0.199	0.190	0.178	0.161	0.158	0.380	0.216	0.242	0.293	0.171	0.114	0.627	0.728	0.262	0.641
Ti/Ti + Cr + Al)	0.478	0.489	0.414	0.422	0.439	0.458	0.206	0.405	0.416	0.341	0.466	0.386	0.059	0.121	0.363	0.058
Sample																
Oxide%																
TiO_2	15.62	12.04	15.85	16.95	4.42	15.57	14.48	15.85	16.68	8.22	12.49	13.72	15.42	13.09	4.51	18.12
Al_2O_3	11.25	12.46	12.04	11.55	15.82	11.09	12.76	11.3	11.85	8.76	15.78	16.06	12.57	13.49	6.58	10.62
Cr_2O_3	7.27	13.68	6.55	2.55	41.21	5.69	7.28	3.55	4.08	38.49	2.67	4.82	4.91	11.52	49.23	3.33
FeO_T	46.52	42.02	46.31	49.48	22.6	46.77	45.99	48.83	48.91	28.89	47.4	45.85	47.5	42.45	23.54	49.52
MnO	0.1	0.46	0.57	0.48	0	0.53	0.5	0.6	0.41	0.5	0	0	0.56	0.55	0	0.38
MgO	16.59	16.52	16.46	17.15	15.7	14.82	17.41	16.5	17.43	15.19	19.4	18.46	17.33	16.7	13.69	16.55
Total	97.63	97.49	98.13	98.34	100.29	94.63	98.69	96.86	99.86	100.12	98.64	99.54	98.49	98.04	97.91	98.63
Recalculated Fe																
FeO	22.03	18.41	21.94	22.35	14.60	23.30	19.74	21.49	21.82	17.35	15.47	18.59	20.64	19.40	15.59	24.35
Fe_2O_3	27.21	26.23	27.08	30.15	8.89	26.09	29.18	30.39	30.10	12.83	35.49	30.29	29.85	25.62	8.83	27.97
Total	100.08	100.11	100.82	101.18	100.64	97.08	101.60	99.92	102.79	101.34	101.90	102.26	101.48	100.61	98.43	101.32
$Fe^{2+}/(Mg + Fe^{2+}$	0.427	0.385	0.428	0.422	0.343	0.469	0.389	0.422	0.413	0.390	0.309	0.361	0.401	0.395	0.390	0.452
Cr/(Cr + Al)	0.302	0.424	0.267	0.129	0.636	0.256	0.277	0.174	0.188	0.747	0.102	0.168	0.208	0.364	0.834	0.174
Ti/Ti + Cr + Al)	0.382	0.262	0.381	0.449	0.061	0.400	0.344	0.425	0.422	0.132	0.312	0.312	0.383	0.283	0.068	0.474
Sample																
Oxide%																
TiO_2	15.92	5.08	10	17.68	17.77	13.35	13.4	14.93	7.42	16.38	4.32	4.28	17.64	4.93	14.27	16.11
Al_2O_3	13.31	15.13	13.66	11.51	11.12	12.96	13.1	12.56	10.85	11.15	12.15	15.63	11.3	6.62	10.9	11.62
Cr_2O_3	3.51	40.29	21.62	3.8	3.54	13.82	12.06	5.93	34.92	4.45	43.86	41.75	3.01	50.1	10.05	4.83
FeO_T	47.8	23.47	34.44	48.71	48.85	41.25	42.17	47.34	31.04	48.8	22.03	22.27	49.38	23.55	44	48.12
MnO	0.35	0	0	0	0.37	0.54	0	0	0	0.46	0.58	0	0	0.18	0.61	0.45
MgO	16.98	15.3	16.8	16.81	16.64	16.3	16.55	16.99	15.93	16.64	14.8	15.37	17.05	13.59	14.91	17.6
Total	98.14	99.53	97.05	98.93	98.43	97.4	97.99	98.62	100.61	98.12	97.91	99.76	98.94	99.02	94.87	99.25
Recalculated Fe																
FeO	21.75	15.37	16.74	24.07	23.91	20.47	20.07	20.79	16.42	22.25	14.08	14.79	23.37	16.39	21.94	20.67
Fe_2O_3	28.95	9.00	19.67	27.38	27.72	23.09	24.57	29.51	16.25	29.50	8.84	8.31	28.90	7.96	24.52	30.50
Total	101.03	100.37	98.49	101.25	101.07	100.53	100.15	101.27	101.79	101.09	98.63	100.13	101.56	99.77	97.20	102.32
$Fe^{2+}/(Mg + Fe^{2+}$	0.418	0.360	0.359	0.445	0.446	0.413	0.405	0.407	0.366	0.429	0.348	0.351	0.435	0.404	0.452	0.397
Cr/(Cr + Al)	0.150	0.641	0.515	0.181	0.176	0.417	0.382	0.241	0.683	0.211	0.708	0.642	0.152	0.835	0.382	0.218
Ti/Ti + Cr + Al)	0.393	0.071	0.185	0.445	0.457	0.277	0.288	0.366	0.121	0.425	0.062	0.059	0.458	0.073	0.340	0.409
Sample																
Oxide%																
TiO_2	16.81	16.81	8.86	17.99	17.68	15.77	10.98	13.42	15.46	8.85	9.02	10.71	14.93	16.19	16.87	11.81
Al_2O_3	11.37	12.36	13.31	10.97	10.95	11.76	10.1	11.93	11.93	9.73	4.57	13.23	13.35	11.56	11.65	13.87
Cr_2O_3	3.13	3.23	25.01	4.49	4.28	2.98	0	6.65	4.91	0	2.07	21.35	7.79	6.6	3.51	15.89
FeO_T	49.4	49.42	34.33	48.34	48.66	50.9	63.11	48.97	47.76	63.02	71.63	37.47	44.36	46.74	48.51	39.35
MnO	0	0.5	0	0.43	0.47	0	0.5	0.66	0.8	0.83	0.53	0	0.6	0.5	0.4	0.61
MgO	16.86	17.18	15.99	16.54	16.4	16.85	12.06	14.78	16.71	14	7.01	16.74	17.34	16.66	16.9	17.17
Total	98	99.72	98.4	99.08	98.84	98.77	97.19	96.91	97.74	97.07	95.3	99.86	98.49	98.4	97.1	98.86

Recalculated Fe																
FeO	22.92	22.52	16.93	24.03	23.78	22.14	23.94	21.68	21.05	18.50	28.40	18.14	20.41	22.37	22.63	17.99
Fe_2O_3	29.43	29.90	19.34	27.02	27.65	31.96	43.53	30.33	29.68	49.48	48.04	21.48	26.62	27.08	28.76	23.74
Total	100.52	102.72	99.76	101.80	101.60	101.67	101.51	99.95	100.73	101.97	100.11	101.94	101.04	100.96	100.72	101.08
Fe^{2+}/(Mg + Fe^{2+}	0.433	0.424	0.373	0.449	0.449	0.424	0.527	0.451	0.414	0.426	0.694	0.378	0.398	0.430	0.429	0.370
Cr/(Cr + Al)	0.156	0.149	0.558	0.215	0.208	0.145	0.000	0.272	0.216	0.000	0.233	0.199	0.281	0.277	0.168	0.435
Ti/Ti + Cr + Al)	0.443	0.425	0.158	0.451	0.449	0.422	0.410	0.343	0.393	0.367	0.491	0.520	0.339	0.393	0.435	0.235
Sample																
Oxide%																
TiO_2	7.55	13.78	5	18.29	18.43	17.35	6.08	18.14	13.57	17.08	45	9.37	15.79	12.71	12.69	4.09
Al_2O_3	9.92	12.2	16.31	9.78	11.07	10.52	8.66	10.3	11.86	11.23	14.7	12.36	11.59	13.42	13.87	13.99
Cr_2O_3	34.95	9.43	40.07	5.27	2.39	4.32	40.26	3.65	7	2.28	41.13	21.73	7.29	10.1	1.67	42.19
FeO_T	30.48	45.21	21.79	48.33	49.44	48.77	28.09	48.61	46.82	50.48	21.77	38.03	46.7	44.69	54.68	22.95
MnO	0	0	0	0.39	0	0.46	0	0.64	0.89	0.58	0	0.5	0.68	0	0.54	0
MgO	15.08	17.01	15.59	16.36	17.19	16.55	13.41	15.62	16.09	16.2	15.12	15.27	16.32	15.85	15.9	15.45
Total	98.25	98.19	9.79	98.48	99	98.5	97.15	97.28	96.58	97.89	97.43	97.48	98.31	97.37	99.44	98.65
Recalculated Fe																
FeO	16.97	19.92	15.02	24.60	24.11	22.94	17.48	24.69	19.65	23.66	21.77	17.90	22.39	20.79	21.23	14.06
Fe_2O_3	15.01	28.11	7.52	26.38	28.15	28.71	11.80	26.58	30.20	29.80	0.00	22.37	27.01	26.56	37.17	9.88
Total	99.48	100.65	99.51	101.06	101.34	101.38	97.68	99.93	99.60	100.84	137.72	99.72	101.08	99.43	103.07	99.66
Fe^{2+}/(Mg + Fe^{2+}	0.387	0.396	0.351	0.458	0.440	0.437	0.422	0.470	0.407	0.450	0.447	0.397	0.435	0.424	0.428	0.338
Cr/(Cr + Al)	0.703	0.341	0.622	0.265	0.127	0.216	0.757	0.192	0.284	0.120	0.652	0.541	0.297	0.335	0.075	0.669
Ti/Ti + Cr + Al)	0.126	0.322	0.069	0.467	0.481	0.452	0.098	0.476	0.343	0.461	0.404	0.182	0.379	0.287	0.351	0.058
Sample																
Oxide%																
TiO_2	4.01	10.42	12.98	14.34	7.3	9.17	3.67	16.14	17.34	16.97	13.73	15.42	15.17	8.62	9.19	4.01
Al_2O_3	14.56	1.93	12.54	13.08	12.22	10.43	16.08	10.23	11.07	12.1	12.26	10.4	11.47	2.9	15.92	12.59
Cr_2O_3	38.23	2.88	12.13	3.64	26.83	27.54	40.93	5.88	3.18	3.37	8.86	9.93	4.03	1.97	16.96	41.47
FeO_T	23.79	73.07	43.04	50.23	34.78	35.25	21.71	49.36	49.78	48.4	46.21	45.9	49.11	75.45	37.69	23.29
MnO	0	0.69	0.43	0.54	0	0	0	0.39	0.61	0.56	0.52	0	0.47	0.77	0.57	0
MgO	17.27	7.05	16.46	15.67	15.42	15.36	15.24	15.94	17.45	17.5	16.36	16.54	16.94	6.74	19.08	15.35
Total	98.15	96.48	97.53	97.88	97.64	98.41	97.59	98.18	99.69	99.71	98.28	98.72	97.92	96.55	99.35	97.39
Recalculated Fe																
FeO	11.11	29.45	19.78	21.91	15.67	17.90	13.98	23.07	22.23	21.37	20.33	21.99	20.17	28.94	13.35	13.15
Fe_2O_3	14.10	48.48	25.85	31.47	21.23	19.28	8.59	29.22	30.62	30.04	28.76	26.57	32.16	51.69	27.05	11.27
Total	99.27	101.34	100.17	101.04	99.32	99.88	98.49	101.10	102.75	102.72	101.17	101.04	101.12	101.63	102.12	98.03
Fe^{2+}/(Mg + Fe^{2+}	0.265	0.701	0.403	0.440	0.363	0.395	0.340	0.448	0.417	0.407	0.411	0.427	0.400	0.707	0.282	0.325
Cr/(Cr + Al)	0.638	0.500	0.394	0.157	0.596	0.639	0.631	0.278	0.162	0.157	0.326	0.390	0.191	0.313	0.417	0.688
Ti/Ti + Cr + Al)	0.060	0.633	0.286	0.371	0.134	0.168	0.051	0.421	0.456	0.430	0.325	0.366	0.406	0.566	0.177	0.060
Sample															**CL-07-006-195**	
Oxide%																
TiO_2	15.67	16.71	8.88	18.97	15.77	17	6.86	15.22	17.72	15.56	4.34	5.72	16.53	18.52	7.68	8.01
Al_2O_3	12.08	10.55	13.63	9.05	12.82	10.56	10.26	12.04	10.88	11.95	12.29	7.63	11.41	10.77	9.1	13.08
Cr_2O_3	2.16	3.81	21.19	3.55	3.71	5.37	40.17	4.25	3.74	2.7	41.62	44.56	6.27	1.63	39.37	23.29
FeO_T	50.24	50.94	38.95	50.27	49.37	48.88	26.79	49.26	49.36	49.95	24.79	25.42	46.26	50.65	27.25	35.72
MnO	0.71	0.7	0	0.38	0.57	0.55	0	0.62	0.59	0.58	0	0.56	0.45	0.48	0.59	0.67
MgO	16.14	15.79	16.42	14.77	16.95	16.61	15.14	17.23	16.99	15.29	14.92	13.28	16.8	16.95	15.43	16.96
Total	97.11	98.7	99.63	97.12	99.39	98.82	99.89	99.16	99.41	96.12	98.57	97.14	97.88	99.08	99.56	97.83

Recalculated Fe																
FeO	22.24	23.77	16.98	26.97	21.28	23.10	16.72	20.10	22.31	23.01	14.90	16.84	21.96	23.73	16.24	14.39
Fe_2O_3	31.12	30.19	24.42	25.69	29.80	28.36	11.72	31.87	27.49	29.45	11.51	9.60	26.20	28.82	12.23	23.70
Total	100.12	101.73	101.78	99.22	99.82	101.29	102.42	101.41	97.38	98.13	100.95	98.34	98.82	99.95	100.65	100.10
$Fe^{2+}/(Mg + Fe^{2+}$	0.436	0.458	0.367	0.463	0.406	0.507	0.420	0.440	0.378	0.398	0.440	0.406	0.395	0.402	0.371	0.323
Cr/(Cr + Al)	0.107	0.195	0.510	0.146	0.603	0.208	0.163	0.254	0.724	0.743	0.256	0.372	0.724	0.596	0.744	0.544
Ti/Ti + Cr + Al)	0.425	0.449	0.169	0.350	0.200	0.514	0.397	0.434	0.105	0.085	0.402	0.298	0.130	0.114	0.121	0.151
Sample														**CL-07-006-208**		
Oxide%																
TiO_2	8.95	6.51	8.68	4.95	8.22	4.26	9.47	5.88	4.42	10.31	4.12	7.42	5.09	6.19	5.78	5.26
Al_2O_3	12.54	6.57	10.81	7.9	14.68	14.06	14.05	10.54	7.39	13.22	8.52	10.16	11.65	8.21	10.39	7.39
Cr_2O_3	22.27	44.89	32.73	48.91	25.62	41.35	23.24	36.6	49.92	20.69	47.38	33.44	45.12	43.59	38.83	46.97
FeO_T	37.03	27.56	30.35	23.47	34.1	22.63	35.27	29.33	22.75	35.97	24.01	31.06	22.22	26.41	29.23	24.24
MnO	0.71	0	0	0	0	0	0	0	0	0.69	0	0.63	0.71	0.64	0	0.62
MgO	16.67	13.41	15.85	14.21	16.36	16.6	16.57	16.569	14.13	16.85	14.41	15.26	14.86	14.79	14.96	14.01
Total	98.25	99.25	98.69	99.48	99.54	99.47	99.1	99.22	98.92	98.08	99.01	98.15	99.93	99.91	99.84	98.7
Recalculated Fe																
FeO	15.70	18.29	17.08	16.00	16.75	12.56	17.35	13.63	15.30	16.30	14.57	16.00	15.07	15.81	16.02	15.42
Fe_2O_3	23.71	10.30	14.74	8.30	19.28	11.19	19.92	17.45	8.28	21.86	10.49	16.73	7.95	11.78	14.69	9.81
Total	100.55	99.97	99.90	100.27	100.91	100.02	100.60	100.67	99.44	100.27	99.71	99.65	100.45	101.01	100.66	99.68
$Fe^{2+}/(Mg + Fe^{2+}$	0.346	0.434	0.377	0.387	0.365	0.298	0.370	0.316	0.378	0.352	0.362	0.370	0.363	0.375	0.375	0.382
Cr/(Cr + Al)	0.544	0.821	0.670	0.806	0.539	0.664	0.526	0.700	0.819	0.512	0.789	0.688	0.722	0.781	0.715	0.810
Ti/Ti + Cr + Al)	0.172	0.102	0.145	0.072	0.141	0.061	0.169	0.097	0.065	0.195	0.061	0.127	0.072	0.095	0.092	0.079
Sample																
Oxide%																
TiO_2	9.09	4.87	4.45	13.22	12.32	11.19	4.78	3.83	4.51	4.51	6.41	4.37	4.39	9.14	5.55	7.76
Al_2O_3	12.94	7.63	7.97	15.07	15.49	18	13.74	15.04	8.52	15.36	8.59	14.4	14.7	10.4	8.95	11.11
Cr_2O_3	25.55	47.69	44.4	8.5	9.27	10.88	41.99	36.02	47.64	41.25	41.31	40.4	39.54	26.54	42.53	29.21
FeO_T	36.26	24.45	25.44	43.93	42.42	40.13	23.2	21.93	23.83	22.62	27.63	24.2	23.5	35.75	27.13	34.69
MnO	0.54	0	0	0	0.49	0.49	0	0	0	0	0	0	0	0.66	0	0
MgO	14.61	14.53	16.84	16.564	17.12	17.57	15.05	20.63	14.28	15	15.17	15.23	15.54	15.53	15.17	15.04
Total	98.92	99.46	99.17	97.47	97.11	98.4	99.26	99.29	99.4	99.22	99.62	98.76	99.17	98.38	99.89	97.86
Recalculated Fe																
FeO	19.39	15.34	11.25	20.57	18.44	17.47	15.27	5.81	15.10	15.34	15.92	14.71	13.56	16.91	15.28	17.42
Fe_2O_3	18.74	10.13	15.77	25.96	26.65	25.18	8.81	17.92	9.70	8.09	13.01	10.55	11.04	20.94	13.17	19.19
Total	100.87	100.18	101.02	99.88	99.78	100.78	99.64	99.25	100.10	99.55	100.41	99.66	99.29	100.49	100.65	99.73
$Fe^{2+}/(Mg + Fe^{2+}$	0.427	0.372	0.273	0.411	0.377	0.358	0.363	0.136	0.372	0.365	0.371	0.351	0.329	0.379	0.361	0.394
Cr/(Cr + Al)	0.570	0.807	0.789	0.274	0.286	0.288	0.672	0.616	0.790	0.643	0.763	0.653	0.643	0.631	0.761	0.638
Ti/Ti + Cr + Al)	0.162	0.073	0.070	0.289	0.266	0.220	0.068	0.059	0.066	0.063	0.101	0.063	0.064	0.171	0.086	0.139
Sample					**CL-07-006-214**											
Oxide%																
TiO_2	4.71	5.54	11.14	7.26	8.04	5.56	9.16	9.09	6.7	10.54	8.5	11.59	7.48	4.47	5.97	9.35
Al_2O_3	14.43	7.6	11.76	11.14	13.02	11.11	4.57	13	11.23	12.93	7.66	12.93	10.47	8.11	8.07	4.54
Cr_2O_3	41.64	45.59	19.06	31.69	28.88	28.76	0.98	25.35	32.5	23.37	5.26	17.31	34.63	48.65	42.89	2.26
FeO_T	22.29	25.85	40.04	32.38	33.61	39.46	70.82	35.75	33.13	35.37	65.02	39.74	31.47	24.24	27.15	70.15
MnO	0	0	0	0.86	0	0.78	0.66	0	0	0	0.69	0.68	0	0	0	0.62
MgO	16.1	15	15.66	15.95	14.96	12.05	8.12	15.62	13.82	16.31	9.82	15.64	15.22	13.6	15.32	8.81

Total	99.76	100.26	98.11	99.41	99.13	97.83	94.45	99.25	98.08	99.12	96.99	98.07	99.68	99.45	100.1	95.9
Recalculated Fe																
FeO	13.63	15.17	19.63	15.19	18.29	19.26	26.95	18.35	17.96	18.49	24.99	19.63	17.21	16.42	15.31	26.55
Fe_2O_3	9.63	11.87	22.68	19.11	17.03	22.45	48.75	19.33	16.86	18.76	44.49	22.35	15.85	8.69	13.16	48.45
Total	100.39	101.01	99.93	101.19	100.22	99.97	99.19	100.75	99.32	100.40	101.41	100.13	100.86	99.94	100.72	100.58
$Fe^{2+}/(Mg + Fe^{2+}$	0.322	0.362	0.413	0.348	0.407	0.473	0.651	0.397	0.422	0.389	0.588	0.413	0.388	0.404	0.359	0.628
Cr/(Cr + Al)	0.659	0.801	0.521	0.656	0.598	0.635	0.126	0.567	0.660	0.548	0.315	0.473	0.689	0.801	0.781	0.250
Ti/Ti + Cr + Al)	0.066	0.085	0.225	0.125	0.137	0.105	0.528	0.162	0.115	0.190	0.327	0.232	0.124	0.065	0.094	0.496
Sample										**CL-07-006-235**						
Oxide%																
TiO_2	6.31	9.45	6.67	4.42	3.46	6.34	4.09	4.79	10.15	17.95	17.71	6.22	18.15	16.23	17.29	15
Al_2O_3	9.26	4.65	9.9	10.82	10.16	10.93	13.76	7.88	11.79	10.24	12.31	9.44	10.67	11.8	10.34	11.73
Cr_2O_3	39.74	3.287	36.8	45.04	45.05	37.19	42.16	48.03	23.71	4.23	2.31	41.74	2.56	3.53	3.64	7.17
FeO_T	29.17	68.74	29.64	23.77	25.22	28.78	22.54	24.38	35.47	49.18	48.78	27.61	49.36	49.41	50.22	47.34
MnO	0.92	0.59	0.76	0	0	0	0	0.83	0.64	0.67	0.69	0	0.76	0.84	0.5	0.56
MgO	14.09	9.45	14.09	15.24	15.69	14.42	15.52	13.77	16.56	15.61	16.46	14.79	15.92	16.15	15.79	16.14
Total	99.57	96.23	97.99	99.93	100.16	98.34	99.01	99.76	98.44	98.09	98.11	99.85	97.48	98.23	97.93	98.03
Recalculated Fe																
FeO	16.80	25.84	16.87	14.39	12.88	16.67	13.38	15.79	16.90	24.88	23.99	16.68	24.61	22.83	24.38	21.98
Fe_2O_3	13.75	47.68	14.19	10.42	13.71	13.46	10.18	9.55	20.64	27.00	27.56	12.15	27.51	29.54	28.72	28.18
Total	100.87	100.94	99.28	100.33	100.95	99.30	99.50	100.64	100.39	100.80	101.02	101.02	100.18	100.92	100.66	100.76
$Fe^{2+}/(Mg + Fe^{2+}$	0.401	0.605	0.402	0.346	0.315	0.393	0.326	0.391	0.364	0.472	0.450	0.387	0.464	0.442	0.464	0.433
Cr/(Cr + Al)	0.742	0.322	0.714	0.736	0.748	0.695	0.673	0.803	0.574	0.217	0.112	0.748	0.139	0.167	0.191	0.291
Ti/Ti + Cr + Al)	0.101	0.468	0.110	0.064	0.052	0.101	0.058	0.071	0.190	0.467	0.449	0.096	0.483	0.422	0.463	0.367
Sample																
Oxide%																
TiO_2	10.9	18.4	17.16	8.39	8.73	18.32	5.71	4.42	7.86	10.32	16.87	4.56	4.96	9.5	14.12	12.56
Al_2O_3	12.36	10.4	10.43	14.79	4.43	10.43	8.07	13.91	11.51	11.79	10.73	15.16	10.54	16.69	13.06	14.41
Cr_2O_3	2.79	3.78	3.7	25.48	4.08	2.82	44.29	42.41	30.2	23.25	3.61	42.02	45.1	15.29	8.17	9.59
FeO_T	56.42	49.39	49.37	34.6	68.47	50.16	27.07	23.14	34.13	36.54	51.56	22.47	24.15	40.24	46.23	45.2
MnO	0.71	0.43	0.65	0	0.76	0.59	0	0	0.58	0.52	0.5	0	0	0	0.53	0
MgO	13.92	15.6	16.45	15.02	9.06	15.12	14.01	14.81	13.83	15.26	14.88	15.17	14.61	15.47	16.07	16.23
Total	97.19	98.13	97.98	98.7	95.73	98	99.86	99.24	98.4	97.79	98.06	99.9	99.77	97.74	98.17	98.48
Recalculated Fe																
FeO	21.54	25.78	23.12	18.73	25.21	26.11	16.97	15.06	18.66	18.94	25.58	15.30	15.80	19.08	21.60	20.64
Fe_2O_3	38.76	26.24	29.18	17.64	48.08	26.72	11.22	8.98	17.19	19.56	28.87	7.97	9.28	23.51	27.37	27.30
Total	100.98	100.63	100.68	100.05	100.55	100.12	100.27	99.89	100.11	99.64	101.04	100.18	100.29	99.55	100.92	100.73
$Fe^{2+}/(Mg + Fe^{2+}$	0.465	0.481	0.441	0.412	0.610	0.492	0.405	0.363	0.431	0.410	0.491	0.361	0.378	0.409	0.430	0.416
Cr/(Cr + Al)	0.132	0.196	0.192	0.536	0.382	0.154	0.786	0.672	0.638	0.569	0.184	0.650	0.742	0.381	0.296	0.309
Ti/Ti + Cr + Al)	0.328	0.476	0.459	0.144	0.437	0.487	0.088	0.062	0.136	0.194	0.450	0.063	0.072	0.184	0.327	0.278
Sample														**CL-07-010-160**		
Oxide%																
TiO_2	16.24	10.93	15.49	9.92	4.21	17.15	14.89	4.68	9.46	17.24	5.06	16.11	10.65	7.51	6.94	12.03
Al_2O_3	10.89	12.04	11.47	7.29	15.02	10.31	10.96	7.6	2.89	9.58	9.87	10.77	12.35	6.68	6.99	8.61
Cr_2O_3	4.8	21.14	4.78	0.61	39.75	3.45	3.5	47.94	3.52	4.04	44.9	4.8	17.8	39.12	37.69	19.98
FeO_T	50.2	38.21	49.78	69.03	23.6	49.67	51.14	24.07	73.66	50.44	25.39	50.46	41.14	31.5	32.06	41.64
MnO	0.69	0	0.46	0.38	0.72	0.82	0.51	0	0.74	0.43	0	0	0.48	0	0.89	0.79

MgO	14.29	16.32	15.49	9.45	15.19	15.49	15.42	13.93	6.34	15.48	14.12	15.36	14.87	13.47	14.04	14.72
Total	97.31	99.23	97.65	96.9	98.99	97.08	95.92	98.62	96.71	97.38	100.14	98.04	97.37	98.8	98.83	97.86
Recalculated Fe																
FeO	25.21	18.77	23.35	27.04	13.54	24.10	22.15	15.76	30.33	24.58	16.54	24.46	19.90	18.97	16.89	20.62
Fe_2O_3	27.77	21.60	29.37	46.67	11.19	28.42	32.22	9.23	48.15	28.74	9.84	28.89	23.60	13.93	16.86	23.36
Total	100.10	100.80	100.41	101.36	100.11	99.74	100.05	99.15	101.43	100.09	100.33	100.39	99.65	99.68	100.30	100.11
$Fe^{2+}/(Mg + Fe^{2+}$	0.497	0.392	0.458	0.616	0.333	0.466	0.446	0.388	0.729	0.471	0.397	0.472	0.429	0.441	0.403	0.440
Cr/(Cr + Al)	0.228	0.541	0.218	0.053	0.640	0.183	0.176	0.809	0.450	0.221	0.753	0.230	0.492	0.797	0.783	0.609
Ti/Ti + Cr + Al)	0.423	0.210	0.402	0.451	0.061	0.464	0.417	0.070	0.535	0.472	0.075	0.424	0.219	0.127	0.121	0.259
Sample																
Oxide%																
TiO_2	19.2	4.81	6.74	4.47	5.9	7.39	11.08	3.82	5.8	18.27	18.18	5.16	5.18	14.14	14.34	15.89
Al_2O_3	8.49	10.87	8.22	10.71	5.08	9.03	8.09	6.49	5.53	8.36	8.83	6.53	8.04	7.47	9.27	9.21
Cr_2O_3	6.15	44.55	39.99	45.55	48.2	31.76	22.6	49.55	49.14	5.15	6.17	45.51	39.45	16.14	12.27	9.27
FeO_T	48.47	24.36	27.92	23.38	27.18	34.57	41.66	24.46	25.47	49.17	47.61	27.13	29.98	45.55	45.59	47.87
MnO	0	0	0	0	0	0	0	0	0.73	0.57	0	0.68	0.65	0	0.54	0
MgO	15.12	14.45	14.76	14.62	12.74	14.47	14.41	14.46	12.91	15.15	16.12	13.11	13.98	14.69	15.2	15.11
Total	97.84	99.32	98.22	99.19	99.54	98.74	98.59	99.13	99.54	96.74	97.45	98.61	97.78	98.38	97.28	97.65
Recalculated Fe																
FeO	27.14	15.86	16.21	15.17	18.57	16.76	20.97	14.22	17.70	25.46	24.61	16.60	14.93	23.28	22.19	24.31
Fe_2O_3	23.70	9.44	13.01	9.13	9.57	19.79	22.99	11.38	8.64	26.35	25.56	11.70	16.73	24.75	26.01	26.19
Total	99.80	99.99	99.05	99.64	100.06	100.00	100.14	99.92	100.45	99.31	99.47	99.29	99.47	100.47	99.82	99.97
$Fe^{2+}/(Mg + Fe^{2+}$	0.502	0.381	0.381	0.368	0.450	0.394	0.450	0.355	0.435	0.485	0.461	0.415	0.375	0.471	0.450	0.474
Cr/(Cr + Al)	0.327	0.733	0.765	0.740	0.864	0.702	0.652	0.837	0.856	0.292	0.319	0.824	0.767	0.592	0.470	0.403
Ti/Ti + Cr + Al)	0.493	0.070	0.109	0.065	0.091	0.135	0.233	0.058	0.088	0.497	0.472	0.082	0.087	0.330	0.343	0.397
Sample																
Oxide%																
TiO_2	4.57	13	13.52	5.87	14.25	11.6	4.52	9.91	17.15	16.56	16.96	4.76	8.36	18.05	7.96	16.94
Al_2O_3	10.49	10.86	10.91	9.69	9.15	9.18	6.19	12.979	8.97	9.11	8.35	3.97	8.75	7.14	14.57	9.85
Cr_2O_3	45.48	14.25	12.01	35.68	8.87	19.25	47.39	19.32	6.665	7.25	5.41	51.3	30.63	5.73	33.18	7.41
FeO_T	24.85	44.18	45.78	31.3	50.14	42.94	24.12	41.02	49.03	48.61	50.3	26.15	36.94	50.92	27.02	47.33
MnO	0	0	0.72	0.97	0.54	0	0	0	0	0.62	0.55	0	0	0.51	0.85	0
MgO	13.71	15.32	15.18	14.2	14.55	14.37	16.46	15.01	15.45	15.8	15.55	12.47	13.99	14.97	15.28	16.19
Total	99.46	98.14	98.58	98.01	97.62	98.03	99.48	98.45	97.84	97.98	97.4	98.73	99.45	97.47	98.84	97.77
Recalculated Fe																
FeO	16.73	21.71	21.86	15.48	23.24	21.34	11.55	19.91	24.57	23.43	23.89	17.64	19.48	25.65	17.12	23.82
Fe_2O_3	9.02	24.98	26.58	17.58	29.89	24.00	13.97	23.46	27.19	27.98	29.36	9.46	19.41	28.09	11.00	26.13
Total	100.00	100.11	100.78	99.77	100.49	99.96	100.31	100.59	100.34	100.75	100.06	99.60	100.61	100.13	99.96	100.34
$Fe^{2+}/(Mg + Fe^{2+}$	0.406	0.443	0.447	0.380	0.473	0.454	0.282	0.427	0.471	0.454	0.463	0.442	0.439	0.490	0.386	0.452
Cr/(Cr + Al)	0.744	0.468	0.425	0.712	0.394	0.584	0.837	0.500	0.333	0.348	0.303	0.897	0.701	0.350	0.604	0.335
Ti/Ti + Cr + Al)	0.066	0.289	0.313	0.100	0.376	0.251	0.071	0.196	0.449	0.431	0.475	0.073	0.154	0.512	0.121	0.422
Sample																
Oxide%																
TiO_2	6.51	5.03	9.12	4.53	4.77	4.02	9.77	4.98	15.88	4.58	8.55	12.2	17.15	3.98	9.79	17.54
Al_2O_3	7.77	5.07	13.97	7.45	14.19	5.8	10.85	13.58	8.4	11.01	8.77	9.9	8.42	15.26	8.06	7.8
Cr_2O_3	42.14	47.58	20.97	49.03	42.1	51.37	24.25	41.94	4.65	45.74	29.78	16.52	5.58	40.3	25.84	5.44
FeO_T	28.72	26.3	37.1	24.82	22.85	25.08	36.24	24.31	53.13	24.13	36.28	43.06	49.68	23.46	39.53	50.11

MnO	0	0.87	0	0	0	0	0.64	0	1.19	0	0	0.69	0	0	0.56	0.7
MgO	14.17	13.46	15.87	13.79	15.81	13.49	15.9	14.73	14.28	14.29	14.51	15.2	15.9	15.75	13.9	15.39
Total	100	98.56	97.66	99.82	100.25	100.21	98.19	99.72	97.56	100.09	98.58	97.67	97.43	99.09	97.74	97.3
Recalculated Fe																
FeO	17.47	15.38	17.62	16.27	14.48	16.06	16.75	16.17	24.39	16.14	18.40	20.31	23.95	13.75	19.95	24.36
Fe_2O_3	12.50	12.14	21.65	9.50	9.30	10.02	21.66	9.05	31.94	8.88	19.87	25.28	28.60	10.80	21.76	28.62
Total	100.56	99.78	99.20	100.57	100.65	100.76	100.36	100.45	100.73	100.64	100.13	100.10	99.60	99.83	99.86	99.85
Fe^{2+}/(Mg + Fe^{2+}	0.409	0.391	0.384	0.398	0.339	0.401	0.371	0.381	0.489	0.388	0.416	0.428	0.458	0.329	0.446	0.470
Cr/(Cr + Al)	0.784	0.863	0.502	0.815	0.666	0.856	0.600	0.674	0.271	0.736	0.695	0.528	0.308	0.639	0.683	0.319
Ti/Ti + Cr + Al)	0.103	0.080	0.172	0.067	0.067	0.060	0.187	0.071	0.468	0.066	0.160	0.271	0.474	0.057	0.197	0.494
Sample	**CL-07-010-169**															
Oxide%																
TiO_2	8.82	5.61	17.16	4.33	13.55	8.8	14.36	5.92	4.69	4.77	7.47	9.5	8.86	16.09	16.28	14.29
Al_2O_3	10.57	6.48	8.64	15.4	6.67	7.29	7.86	7.35	16.3	13.778	7.6	9.22	10.22	8.8	8.42	10.8
Cr_2O_3	27.02	47.69	6.13	40.43	17.37	32.17	14.4	45.71	40.3	40.64	35.99	26.4	25.78	8.77	8.88	9.51
FeO_T	35.64	24.22	48.51	22.11	45.22	35.98	46.19	25.9	23.07	23.67	33.48	36.98	36.62	48	47.63	46.8
MnO	0.49	0	0.57	0	0	0	0.52	0	0	0.86	0	0	0	0	0.66	0
MgO	14.89	14.43	16.18	16.02	14.08	13.61	14.41	13.3	15.61	14.41	14.28	14.96	15.49	15.42	15.94	15.95
Total	97.6	99.07	97.61	98.81	97.37	98.49	98.1	98.5	100.24	98.27	99.32	97.46	97.23	97.6	97.91	97.74
Recalculated Fe																
FeO	17.91	15.31	23.13	13.50	23.20	19.94	23.37	17.79	15.12	15.19	18.06	18.59	17.35	23.87	22.77	21.86
Fe_2O_3	19.70	9.90	28.21	9.57	24.47	17.83	25.36	9.02	8.83	9.43	17.13	20.43	21.41	26.82	27.63	27.72
Total	99.40	99.91	100.02	99.25	99.34	99.64	100.28	99.08	100.85	99.07	100.54	99.11	99.12	99.77	100.58	100.13
Fe^{2+}/(Mg + Fe^{2+}	0.403	0.373	0.445	0.321	0.480	0.451	0.476	0.429	0.352	0.372	0.415	0.411	0.386	0.465	0.445	0.435
Cr/(Cr + Al)	0.632	0.832	0.322	0.638	0.636	0.747	0.551	0.807	0.624	0.664	0.761	0.658	0.629	0.401	0.414	0.371
Ti/Ti + Cr + Al)	0.164	0.085	0.462	0.061	0.321	0.163	0.343	0.090	0.065	0.069	0.131	0.184	0.170	0.412	0.420	0.347
Sample																
Oxide%																
TiO_2	13.5	10.01	10.01	7.64	8.19	1.23	14.37	14.81	5.16	7.53	6.95	16.87	18.79	8.02	5.51	18.05
Al_2O_3	11.48	9.84	10.03	11.86	8.94	0.54	7.85	10.09	6.77	5.58	9.97	8.96	6.2	9.95	7.69	8.06
Cr_2O_3	10.12	24.21	24.25	27.73	34.68	58.04	16.93	8.81	46.66	42.59	33.64	6.61	6.6	33.53	45.72	5.45
FeO_T	46.67	38.34	38.47	34.96	30.98	28.32	43.94	47.11	24.91	29.85	32.61	49.48	48.63	31.13	23.97	49.87
MnO	0	0.67	0.53	0	0	0	0.83	0.8	0	0	0	0	0	0	1.41	1
MgO	15.61	14.65	14.98	15.05	15.48	9.93	13.52	15.93	15.62	13.48	15.17	14.94	17.13	15.42	14.14	14.33
Total	97.86	97.87	98.43	97.9	98.77	98.43	97.41	97.58	99.59	98.75	98.37	97.68	97.69	98.71	98.64	96.94
Recalculated Fe																
FeO	21.78	19.18	19.02	17.24	16.88	17.66	24.28	21.51	13.82	19.01	16.46	25.26	23.38	16.91	14.86	26.07
Fe_2O_3	27.66	21.30	21.61	19.69	15.67	11.85	21.85	28.45	12.33	12.05	17.94	26.91	28.06	15.80	10.12	26.45
Total	100.15	99.85	100.44	99.21	99.84	99.25	99.63	100.40	100.36	100.24	100.14	99.56	100.16	99.63	99.45	99.41
Fe^{2+}/(Mg + Fe^{2+}	0.439	0.423	0.416	0.391	0.380	0.499	0.502	0.431	0.332	0.442	0.378	0.487	0.434	0.381	0.371	0.505
Cr/(Cr + Al)	0.372	0.623	0.619	0.611	0.722	0.986	0.591	0.369	0.822	0.837	0.694	0.331	0.417	0.693	0.800	0.312
Ti/Ti + Cr + Al)	0.320	0.197	0.195	0.138	0.140	0.019	0.323	0.371	0.080	0.123	0.120	0.446	0.530	0.136	0.084	0.496
Sample			**CL-07-010-188**													
Oxide%																
TiO_2	16.53	17.4	4.43	5.87	6.3	4.75	7.17	4.84	4.29	6.24	3.8	13.63	4.53	4.97	4.55	5.11
Al_2O_3	9.7	7.67	15.37	8.51	6.38	6.35	7.38	7.37	9.34	7.24	4.78	8.7	15.91	9.25	5.01	6.87
Cr_2O_3	5.97	7.07	40.57	39.52	45.78	49.18	41.82	47.45	46	42.6	51.72	15.91	40.56	46.37	49.76	47.75

FeO_T	48.25	49.61	23.36	29.58	26.29	24.96	28.25	25.32	24.9	28.92	25.13	44.5	23.05	24.82	26.31	24.33
MnO	0	0.88	0	0	0	0	0	0	0	0	0.73	0.95	0	0	0	0.64
MgO	16.49	15.21	15.88	15.22	13.6	13	14.12	14.31	14.58	13.4	13.14	14.76	15.58	14.82	13.63	14.13
Total	97.06	98.1	99.63	98.66	99.02	98.7	98.95	99.71	100.06	98.89	99.45	98.71	100.1	100.38	100.02	99.08
Recalculated Fe																
FeO	22.75	24.57	14.24	15.27	17.39	17.05	17.64	15.66	15.00	18.03	15.37	22.10	14.86	15.58	16.07	15.29
Fe_2O_3	28.34	27.83	10.14	15.91	9.90	8.79	11.80	10.74	11.00	12.11	10.85	24.89	9.10	10.27	11.39	10.05
Total	99.78	100.63	100.63	100.29	99.57	99.12	100.21	100.37	100.21	99.61	100.39	100.94	100.54	101.26	100.40	99.84
$Fe^{2+}/(Mg + Fe^{2+}$	0.436	0.475	0.335	0.360	0.418	0.424	0.412	0.380	0.366	0.430	0.396	0.457	0.349	0.371	0.398	0.378
Cr/(Cr + Al)	0.292	0.382	0.639	0.757	0.828	0.839	0.792	0.812	0.768	0.798	0.879	0.551	0.631	0.771	0.869	0.823
Ti/Ti + Cr + Al)	0.435	0.472	0.062	0.097	0.098	0.072	0.114	0.073	0.064	0.100	0.058	0.310	0.063	0.073	0.070	0.077
Sample																
Oxide%																
TiO_2	4.06	4.52	5.63	3.56	10.15	6.15	10.88	6.15	6.36	5.12	14.18	9.52	5.64	5.84	15.27	8.26
Al_2O_3	9.57	7.04	8.09	4.67	12.45	8.38	8.64	10.45	7.03	6.77	8.8	8.43	8.31	7.51	8.93	9.01
Cr_2O_3	46.13	49.62	44.28	54.96	20.39	41.13	23.06	33.77	46.05	47.74	14.47	23.9	41.86	46.27	5.86	34.77
FeO_T	24.07	23.79	26.79	23.43	39.61	28.39	39.97	32.5	25.22	25.85	45.84	40.07	27.77	25.31	48.67	30.38
MnO	0	0	0	0	0	0.66	0	0	0.69	0	0.49	0	0	0	0.57	0.6
MgO	14.14	13.59	14.74	12.52	15.16	14.77	15.74	15.74	14.36	13.97	15.14	14.99	14.91	14.43	17.13	14.79
Total	98.66	98.89	100.08	99.22	97.94	99.71	98.94	99.07	99.96	100.03	98.88	97.16	99.21	100.2	97.04	98
Recalculated Fe																
FeO	14.89	16.15	15.92	16.72	19.64	15.74	18.99	15.06	16.32	16.38	22.66	18.45	15.40	16.40	19.84	17.24
Fe_2O_3	10.20	8.49	12.08	7.46	22.20	14.06	23.31	19.39	9.89	10.52	25.76	24.02	13.75	9.90	32.04	14.60
Total	99.26	99.41	100.74	99.89	99.98	100.89	100.63	100.55	100.70	100.50	101.50	99.32	99.87	100.35	99.64	99.27
$Fe^{2+}/(Mg + Fe^{2+}$	0.371	0.400	0.377	0.428	0.421	0.374	0.404	0.349	0.389	0.397	0.456	0.409	0.367	0.389	0.394	0.395
Cr/(Cr + Al)	0.764	0.825	0.786	0.888	0.523	0.767	0.642	0.684	0.815	0.825	0.524	0.655	0.772	0.805	0.306	0.721
Ti/Ti + Cr + Al)	0.060	0.067	0.087	0.052	0.199	0.098	0.224	0.106	0.097	0.078	0.328	0.199	0.090	0.088	0.431	0.140
Sample			**CL-07-010-197**													
Oxide%																
TiO_2	5.7	8.54	5.02	5.13	4.59	5.51	13.99	5.05	5.93	7.45	7.23	4.8	4.33	5.33	14.69	17.73
Al_2O_3	8.38	9.53	4.87	6.43	14.98	8.92	9.54	5.16	15.74	12	9.89	9.93	15.26	7.24	11.01	7.61
Cr_2O_3	42.11	33.63	50.79	48.43	41.7	41.78	11.8	51.59	41.66	28.98	34.6	44.3	41.04	46.2	11.37	5.77
FeO_T	28.13	32.41	25.62	25.05	22.32	27.16	46.38	24.4	21.17	34	33.1	24.68	22.34	26.9	45.74	50
MnO	0	0	0	0	0	0.61	0.44	0	0	0.55	0	0.79	0	0	0	0.63
MgO	15.36	14.49	12.75	13.17	16.32	14.73	16.05	13.72	14.64	15.84	14.04	14.08	15.48	13.61	15.23	15.85
Total	100.06	99.2	99.6	98.77	100.24	98.93	98.57	100.67	99.24	98.92	99.48	98.7	99.02	99.93	98.26	97.81
Recalculated Fe																
FeO	15.17	18.90	17.70	16.91	13.73	15.10	21.07	16.57	17.29	15.84	18.57	15.34	14.07	17.15	23.52	23.88
Fe_2O_3	14.41	15.01	8.80	9.04	9.55	13.40	28.13	8.70	4.31	20.18	16.15	10.38	9.20	10.84	24.69	29.02
Total	101.12	100.10	99.93	99.38	100.87	100.05	101.02	100.79	99.57	100.84	100.48	99.62	99.70	100.37	100.51	100.71
$Fe^{2+}/(Mg + Fe^{2+}$	0.356	0.423	0.438	0.419	0.321	0.365	0.424	0.404	0.399	0.359	0.426	0.379	0.338	0.414	0.464	0.458
Cr/(Cr + Al)	0.771	0.703	0.875	0.835	0.651	0.759	0.453	0.870	0.640	0.618	0.701	0.750	0.643	0.811	0.409	0.337
Ti/Ti + Cr + Al)	0.090	0.145	0.076	0.078	0.064	0.087	0.338	0.075	0.080	0.131	0.122	0.072	0.061	0.082	0.335	0.496
Sample																
Oxide%																
TiO_2	4.85	15.03	15.88	15.82	8.29	4.36	4.51	6.45	10.72	8.21	17.04	13.77	7.54	12.45	4.7	5.14
Al_2O_3	4.73	9	9.45	9.48	10.57	5.98	15.45	10.48	12.88	11.82	9.36	8.23	9.76	10.65	8.5	8.99

Cr_2O_3	50.55	11.35	7.61	6.87	31.41	50.58	41.47	33.9	18.44	25.99	6.26	15.64	32.68	13.81	47.93	39.5
FeO_T	25.09	46.46	48.75	49.36	33.56	24.71	22.72	32.32	40.55	36.41	48.88	45.04	33.59	44.74	24.18	29.33
MnO	0	0.63	0.7	0.67	0	0	0	0	0.5	0.62	0	0	0	0.58	0	0.67
MgO	12.9	15.38	15.82	15.94	14.13	13.65	15.45	14.77	15.22	14.29	15.5	14.92	14.67	15.68	13.2	13.9
Total	98.74	98.08	98.46	98.33	98.27	100.06	99.86	98.47	98.49	97.36	97.47	98.07	98.96	97.98	98.93	97.61
Recalculated Fe																
FeO	17.00	22.62	22.86	22.65	19.20	15.99	14.95	16.56	19.81	18.33	24.68	22.59	17.69	20.18	17.11	15.64
Fe_2O_3	8.99	26.50	28.77	29.68	15.96	9.69	8.64	17.51	23.05	20.10	26.89	24.95	17.67	27.30	7.86	15.21
Total	99.02	100.50	101.09	101.11	99.56	100.25	100.47	99.67	100.62	99.35	99.73	100.10	100.01	100.65	99.30	99.05
$Fe^{2+}/(Mg + Fe^{2+}$	0.425	0.452	0.448	0.444	0.433	0.397	0.352	0.386	0.422	0.418	0.472	0.459	0.404	0.419	0.421	0.387
Cr/(Cr + Al)	0.878	0.458	0.351	0.327	0.666	0.850	0.643	0.685	0.490	0.596	0.310	0.560	0.692	0.465	0.791	0.747
Ti/Ti + Cr + Al)	0.074	0.366	0.410	0.417	0.143	0.065	0.062	0.110	0.213	0.152	0.445	0.319	0.132	0.285	0.069	0.085
Sample												**CL-07-010-221**				
Oxide%																
TiO_2	9.69	4.54	11.77	4.97	4.12	4.37	4.33	4.2	14.84	14.19	7.64	7.41	4.99	4.49	4.62	4.86
Al_2O_3	12.8	15.14	9.14	5.88	15.77	15.61	11.7	16.48	10.88	9.09	12.19	8.74	7.53	4.59	15	7.54
Cr_2O_3	23.37	41.29	23.53	47.25	41.14	42.12	44.05	41.12	7.51	12.35	27.14	36.34	41.03	50.83	40.76	47.06
FeO_T	36.18	22.51	38.71	26.14	22.54	23.28	23.52	22.45	48.25	45.87	36.32	32.13	31.21	26.11	23.35	25.97
MnO	0	0	0	0	0	0	0	0	0.6	0.72	0	0	0	0	0	0
MgO	15.63	15.63	15.2	14.25	15.1	14.88	14.45	14.91	14.93	14.75	14.51	13.84	13.04	12.55	14.95	13.37
Total	98.04	99.18	98.88	98.87	99.64	99.99	98.56	99.61	97.05	97.1	98.17	99.16	98.43	99.73	99.34	99.73
Recalculated Fe																
FeO	18.49	14.50	20.67	15.39	14.48	15.93	15.05	15.50	23.21	22.46	18.31	18.71	17.36	17.35	15.27	16.97
Fe_2O_3	19.66	8.90	20.05	11.94	8.95	8.17	9.41	7.72	27.83	26.02	20.02	14.92	15.39	9.74	8.98	10.00
Total	99.64	100.00	100.36	99.69	100.04	101.08	99.21	99.93	99.80	99.58	99.81	99.95	99.34	99.55	99.79	99.80
$Fe^{2+}/(Mg + Fe^{2+}$	0.399	0.342	0.433	0.377	0.350	0.375	0.369	0.368	0.466	0.461	0.414	0.431	0.428	0.437	0.364	0.416
Cr/(Cr + Al)	0.551	0.647	0.633	0.844	0.636	0.644	0.716	0.626	0.316	0.477	0.599	0.736	0.785	0.881	0.646	0.807
Ti/Ti + Cr + Al)	0.178	0.063	0.232	0.078	0.057	0.060	0.063	0.057	0.373	0.343	0.138	0.125	0.083	0.069	0.065	0.073
Sample																
Oxide%																
TiO_2	4.54	10.92	17.12	7.05	4.06	9.03	11.76	20.55	8.66	4.94	5.18	6.81	6.62	4.95	5.72	12.21
Al_2O_3	14.87	9.21	10.82	7.47	11.64	8.71	8.36	2.92	10.21	5.23	9.96	5.52	5.18	4.87	5.54	9.85
Cr_2O_3	41.33	23.21	3.61	38.19	43.55	32.14	22.85	10.51	26.96	49.59	43.05	44.54	44.91	48.94	46.51	18.55
FeO_T	22.84	39.89	51.9	33.19	25.65	35.36	42.56	49.49	37.71	26.25	26.94	29.14	29.2	26.06	27.58	43.34
MnO	0.69	0.59	0	0	0	0.53	0	0.63	0	0	0	0	0.71	0	0.59	0.61
MgO	15.41	13.9	14.83	13.08	13.75	13.97	14.09	15.19	14.26	12.68	12.72	12.84	12.68	13.22	13.1	13.85
Total	99.77	98.31	98.68	99.74	99.41	99.88	100.06	99.43	98.39	99.73	98.48	99.35	99.47	98.55	99.38	98.62
Recalculated Fe																
FeO	14.29	21.12	26.43	19.52	16.27	19.88	22.68	27.35	18.94	17.26	18.12	19.25	18.71	16.62	17.35	22.69
Fe_2O_3	9.50	20.86	28.31	15.19	10.42	17.21	22.10	24.60	20.86	9.99	9.80	10.99	11.66	10.49	11.37	22.95
Total	100.63	99.81	101.12	100.50	99.69	101.46	101.83	101.76	100.32	100.19	99.07	99.95	100.47	99.09	100.18	100.71
$Fe^{2+}/(Mg + Fe^{2+}$	0.342	0.460	0.500	0.456	0.399	0.444	0.474	0.503	0.427	0.433	0.444	0.457	0.453	0.414	0.426	0.479
Cr/(Cr + Al)	0.651	0.628	0.183	0.774	0.715	0.712	0.647	0.707	0.639	0.864	0.744	0.844	0.853	0.871	0.849	0.558
Ti/Ti + Cr + Al)	0.064	0.220	0.452	0.120	0.060	0.160	0.241	0.568	0.163	0.076	0.078	0.109	0.107	0.077	0.090	0.259
Sample								**CL-07-010-224**								
Oxide%																
TiO_2	3.47	4.399	4.39	5.78	13.68	15.91	5.27	5.95	15.35	3.92	5.73	4.85	13.86	4.82	12.07	5.88

Al_2O_3	8.38	8.26	14.54	6.92	11.05	8.58	4.78	7.76	7.86	8.88	8.82	6.11	9.69	4.71	9.95	11.49
Cr_2O_3	51.58	47.32	41.01	45.12	12.58	9.57	49.95	45.76	12.96	48.65	38.81	48.33	13.24	51.26	17.7	33.49
FeO_T	23.13	24.16	23.23	25.75	45.17	50.02	26.03	26.26	46.52	22.65	31.57	26.18	45.23	24.12	42.65	31.77
MnO	0	0	0.62	0.78	0.53	0.77	0	0	0.64	0.86	0.56	0.58	0	0	0.55	0
MgO	13.36	15.08	15.66	14.23	15.76	15.89	13.33	13.73	14.2	13.8	13.71	13.22	15.61	13.2	14.94	14.93
Total	100.53	99.82	99.57	98.7	99.04	100.99	100.01	99.92	97.69	98.91	99.28	99.52	98.37	98.93	97.94	98.04
Recalculated Fe																
FeO	16.19	14.20	13.74	15.55	21.53	23.40	17.14	17.64	24.39	14.78	17.10	16.54	21.87	16.26	20.82	15.85
Fe_2O_3	7.72	11.07	10.55	11.34	26.27	29.59	9.88	9.58	24.60	8.75	16.08	10.71	25.96	8.73	24.26	17.69
Total	100.69	100.33	100.51	99.72	101.40	103.70	100.35	100.42	99.99	99.64	100.81	100.34	100.23	99.26	100.29	99.33
Fe^{2+}/(Mg + Fe^{2+}	0.405	0.346	0.330	0.380	0.434	0.452	0.419	0.419	0.491	0.375	0.412	0.412	0.440	0.409	0.439	0.373
Cr/(Cr + Al)	0.805	0.794	0.654	0.814	0.433	0.428	0.875	0.798	0.525	0.786	0.747	0.841	0.478	0.880	0.544	0.662
Ti/Ti + Cr + Al)	0.049	0.066	0.062	0.090	0.309	0.404	0.081	0.090	0.372	0.057	0.095	0.074	0.323	0.073	0.261	0.100
Sample																
Oxide%																
TiO_2	14.32	16.99	17.91	10	10.06	12.83	4.83	16.42	18.43	16.85	17.73	11.05	13.71	4.96	17.65	6.2
Al_2O_3	11.64	9.88	9.59	8.45	7.24	8.08	14.49	9.47	9.66	9.08	9.81	12.61	9.87	6.72	10.65	4.92
Cr_2O_3	9.41	3.5	3.71	26.79	31.56	17.36	41.46	5.51	3.63	5.23	5.5	18.85	15.03	49.03	3.94	45.47
FeO_T	46.6	50.15	50.25	38	34.61	43.59	22.49	49.38	49.24	49.4	48.46	40.32	43.37	23.53	48.66	27.82
MnO	0.54	0.63	0	0	0	0	0	0	0.65	0.63	0	0	0	0	0.52	0
MgO	15.97	15.7	16.33	15.25	15.02	14.74	15.02	15.95	16.59	16.46	16.02	15.47	16.03	14.01	16.64	13.54
Total	98.58	96.98	98.12	98.5	98.85	97.13	99.04	97.12	98.19	97.86	97.91	98.82	98.51	98.82	98.28	98.1
Recalculated Fe																
FeO	21.80	23.76	24.50	18.95	19.10	21.67	15.31	23.38	24.05	22.43	24.72	20.17	21.22	15.75	23.51	17.26
Fe_2O_3	27.56	29.33	28.62	21.17	17.24	24.36	7.98	28.89	28.00	29.97	26.38	22.39	24.61	8.64	27.95	11.74
Total	101.24	99.79	100.66	100.61	100.22	99.04	99.09	99.62	101.01	100.85	100.16	100.54	100.48	99.12	100.86	99.13
Fe^{2+}/(Mg + Fe^{2+}	0.434	0.459	0.457	0.411	0.416	0.452	0.364	0.451	0.448	0.433	0.464	0.423	0.426	0.387	0.442	0.417
Cr/(Cr + Al)	0.352	0.192	0.206	0.680	0.745	0.590	0.657	0.281	0.201	0.279	0.273	0.501	0.505	0.830	0.199	0.861
Ti/Ti + Cr + Al)	0.337	0.470	0.486	0.195	0.184	0.293	0.068	0.443	0.493	0.461	0.456	0.218	0.305	0.074	0.459	0.100
Sample																
Oxide%																
TiO_2	17.17	16.81	6.09	17.59	13.79	5.96	5.18	5.93	4.66	4.73	4.67	4.73	6.84	12.45	15.94	1.72
Al_2O_3	6.59	9.56	7.94	8.55	7.75	5.19	10.15	4.95	15.07	5.88	10.92	5.46	7.52	8.86	7.56	4.45
Cr_2O_3	7.78	3.33	44.9	3.49	15.22	46.88	40.82	47.2	40.31	49.13	43.79	47.7	38.77	15.39	8.27	57.6
FeO_T	50	51.14	25.57	51.95	45.96	27.74	27.98	27.89	22.46	24.78	23.83	26.31	30.39	44.95	49.82	23.18
MnO	0.55	0.58	0.57	0.68	0.53	0	0.66	0	0	0	0.57	0	0	0.46	0.56	0
MgO	15.1	16.07	14.25	15.5	14.24	13.37	14.35	13.73	16.02	13.75	14.64	13.55	14.67	15.24	15.19	13.13
Total	97.43	97.8	99.57	97.86	97.7	99.75	99.26	100.13	98.65	98.72	98.37	98.14	98.61	97.56	97.53	100.43
Recalculated Fe																
FeO	24.49	23.26	16.39	24.65	23.02	17.72	15.67	17.29	13.82	15.61	14.69	15.94	16.65	20.51	23.45	14.43
Fe_2O_3	28.35	30.98	10.20	30.34	25.50	11.14	13.68	11.78	9.60	10.19	10.16	11.53	15.27	27.16	29.30	9.72
Total	100.03	100.59	100.34	100.80	100.04	100.26	100.51	100.88	99.48	99.56	99.44	98.90	99.72	100.07	100.28	101.05
Fe^{2+}/(Mg + Fe^{2+}	0.476	0.448	0.392	0.472	0.476	0.426	0.380	0.414	0.326	0.389	0.360	0.398	0.389	0.430	0.464	0.381
Cr/(Cr + Al)	0.442	0.189	0.791	0.215	0.568	0.858	0.730	0.865	0.642	0.849	0.729	0.854	0.776	0.538	0.423	0.897
Ti/Ti + Cr + Al)	0.481	0.476	0.093	0.508	0.329	0.094	0.081	0.094	0.066	0.072	0.069	0.075	0.115	0.293	0.437	0.025
Sample	**CL-07-010-233**															
Oxide%																

TiO_2	4.24	16.64	15.23	5.33	17.31	4.89	7.75	17.79	17.44	4.72	4.71	10.15	6.92	12.25	6.72	13.84
Al_2O_3	15.48	8.66	8.7	9	9.06	5.05	6.46	9.12	8.59	5.55	16.46	7.18	5.79	8.53	6.4	9.4
Cr_2O_3	40.65	5.07	7.99	45.37	4.32	52.03	40.37	3.98	4.17	52.15	40.61	24.89	38.03	18.65	44.9	13.37
FeO_T	23.88	51.41	49.12	25.45	50.97	25.22	30.69	50.69	51.36	23.79	21.89	40.03	33.21	42.83	26.59	44.73
MnO	0	0.5	0.54	0	0.5	0	0	0.68	0.42	0	0	0.58	0.61	0.51	0	0.62
MgO	14.86	15.49	15.2	13.56	15.66	12.81	13.66	15.21	15.5	12.54	14.91	14.33	13.5	14.89	13.59	15.04
Total	99.55	98.13	96.87	99.35	97.99	100.23	99.65	97.51	97.51	99.35	98.76	97.36	98.42	97.86	98.54	97.31
Recalculated Fe																
FeO	15.47	24.01	22.82	17.29	24.42	17.82	19.05	25.24	24.68	17.73	15.76	19.31	17.62	20.81	17.93	21.58
Fe_2O_3	9.35	30.45	29.23	9.07	29.50	8.23	12.94	28.29	29.65	6.73	6.81	23.02	17.33	24.47	9.62	25.72
Total	100.05	100.82	99.71	99.62	100.78	100.82	100.23	100.30	100.45	99.42	99.26	99.47	99.80	100.11	99.16	99.89
Fe^{2+}/(Mg + Fe^{2+}	0.369	0.465	0.457	0.417	0.467	0.438	0.439	0.482	0.472	0.442	0.372	0.431	0.423	0.440	0.425	0.446
Cr/(Cr + Al)	0.638	0.282	0.381	0.772	0.242	0.874	0.807	0.226	0.246	0.863	0.623	0.699	0.815	0.595	0.825	0.488
Ti/Ti + Cr + Al)	0.060	0.468	0.409	0.079	0.480	0.072	0.129	0.491	0.494	0.069	0.064	0.213	0.124	0.271	0.105	0.325
Sample																
Oxide%																
TiO_2	4.03	4.95	17.05	5.06	6.04	10.09	4.76	4.57	16.42	16.84	6.68	17.4	7.33	17.27	15.31	4.8
Al_2O_3	14.26	5.57	8.21	15.6	8.94	13	7.1	14.92	10.98	10.95	6.11	9.45	9.17	8.11	9.35	4.88
Cr_2O_3	40.22	50.28	5.45	40.78	42.35	20.51	47.74	41.14	5.16	3.2	41.96	4.29	36.4	8.66	5.19	48.93
FeO_T	25.33	24.11	50.94	22.41	27.06	38.27	24.68	22.67	48.67	49.54	30.28	50.13	29.99	48.11	51.11	26.75
MnO	0	0	0.53	0.73	0	0	0.68	0	0.46	0.59	0	0.53	0.64	0.72	0.53	0
MgO	15.66	13.23	14.67	14.79	14.37	15.21	13.96	15.08	16.13	16.17	13.33	15.73	14.87	15.4	15.19	13.25
Total	99.79	98.59	96.99	99.59	99.25	97.73	99.08	98.71	98.06	97.44	98.88	97.65	98.46	98.41	96.95	99.26
Recalculated Fe																
FeO	14.04	16.53	25.21	15.65	16.73	19.11	15.27	15.09	23.22	23.25	18.36	24.32	16.46	24.50	23.02	16.64
Fe_2O_3	12.55	8.42	28.59	7.51	11.48	21.30	10.46	8.42	28.28	29.22	13.25	28.68	15.03	26.24	31.22	11.24
Total	100.76	99.19	99.71	100.12	99.91	99.50	99.97	99.22	100.65	100.22	99.69	100.40	99.91	100.90	99.81	99.74
Fe^{2+}/(Mg + Fe^{2+}	0.335	0.412	0.491	0.373	0.395	0.413	0.380	0.360	0.447	0.446	0.436	0.464	0.383	0.472	0.460	0.413
Cr/(Cr + Al)	0.654	0.858	0.308	0.637	0.761	0.514	0.819	0.649	0.240	0.164	0.822	0.233	0.727	0.417	0.271	0.871
Ti/Ti + Cr + Al)	0.059	0.074	0.478	0.070	0.094	0.194	0.072	0.064	0.421	0.451	0.111	0.474	0.122	0.442	0.432	0.075
Sample											**CL-07-010-245**					
Oxide%																
TiO_2	14.29	16.46	4.24	6.8	4.06	6.83	4.65	11.78	7.34	11.12	4.53	5.22	9.13	4.62	4.65	6.89
Al_2O_3	8.79	8.78	8.61	9.44	7.29	8.74	14.99	9.23	6.05	8.89	14.98	8.63	10.21	15.64	15.89	8.67
Cr_2O_3	10.57	6.94	47.27	37.34	47.4	34.43	40.34	20.25	39.58	21.97	39.71	47.61	29.54	40.06	41.53	42.06
FeO_T	48.24	49.88	24.64	29.93	25.66	33.65	23.64	42.36	32.34	41	24.05	23.7	33.73	22.18	22.65	27.07
MnO	0.69	0	0	0.64	0	0.74	0	0	0	0	0	0	0.6	0.55	0	0.57
MgO	15.52	15.46	14.33	14.58	13.53	14.57	15.17	14.84	13.32	14.7	15.34	13.7	14.59	15.7	15.17	13.47
Total	98.17	98.11	99.96	98.9	98.59	99.01	99.11	98.86	99.01	98.06	98.73	99.4	98	98.83	100.44	98.93
Recalculated Fe																
FeO	21.77	24.31	15.21	16.58	15.71	16.55	15.18	21.33	19.07	20.63	14.77	16.72	18.38	13.88	15.65	18.05
Fe_2O_3	29.42	28.42	10.48	14.84	11.06	19.00	9.40	23.37	14.75	22.63	10.31	7.76	17.06	9.23	7.78	10.02
Total	101.05	100.37	100.14	100.22	99.05	100.86	99.73	100.80	100.11	99.95	99.64	99.90	99.72	99.67	100.67	99.93
Fe^{2+}/(Mg + Fe^{2+}	0.440	0.469	0.373	0.389	0.394	0.389	0.360	0.446	0.445	0.441	0.351	0.406	0.414	0.332	0.367	0.429
Cr/(Cr + Al)	0.446	0.346	0.786	0.726	0.813	0.725	0.644	0.595	0.814	0.624	0.640	0.787	0.660	0.632	0.637	0.765
Ti/Ti + Cr + Al)	0.365	0.439	0.063	0.112	0.062	0.120	0.066	0.248	0.126	0.231	0.065	0.076	0.163	0.065	0.064	0.107

Sample

Oxide%																
TiO_2	6.91	7.7	4.36	4.82	3.95	4.72	6.14	5.17	3.99	3.77	16.47	4.76	15.01	4.4	4.67	5.34
Al_2O_3	8.69	10.2	8.63	14.31	13.72	7.93	9.13	7.04	9.97	15.03	10.89	13.81	10.6	8.49	9.29	5.11
Cr_2O_3	41.65	36.56	47.21	40.99	42.96	50.38	38.56	47.24	46.3	40.12	3.76	41.81	6.97	47.67	46.72	50.46
FeO_T	26.86	30.3	25.43	22.61	23.88	22.65	29.44	24.14	23.78	22.61	48.45	23.24	48.25	23.92	23.32	24.53
MnO	0	0	0	0	0	0	0	0	0	0.3	0	0	0.72	0	0.4	0
MgO	14.42	14.23	14.13	15.04	15.55	14.13	15.19	15.75	14.91	15.99	17.71	15.18	16.06	14.31	13.93	13.52
Total	99.26	99.45	100.34	98.19	99.82	99.76	99.05	99.82	99.25	98.01	97.85	99.14	97.83	99.03	98.5	99
Recalculated Fe																
FeO	17.31	18.74	15.85	15.09	14.20	16.02	15.57	13.73	14.27	12.38	21.16	15.08	21.69	15.26	15.64	16.82
Fe_2O_3	10.61	12.85	10.65	8.36	10.75	7.37	15.42	11.57	10.57	11.37	30.33	9.07	29.52	9.63	8.54	8.57
Total	99.59	100.28	100.83	98.61	101.14	100.55	100.00	100.50	100.01	99.17	100.32	99.71	100.57	99.75	99.19	99.82
$Fe^{2+}/(Mg + Fe^{2+}$	0.402	0.425	0.386	0.360	0.339	0.389	0.365	0.328	0.349	0.303	0.401	0.358	0.431	0.374	0.386	0.411
Cr/(Cr + Al)	0.763	0.706	0.786	0.658	0.677	0.810	0.739	0.818	0.757	0.642	0.188	0.670	0.306	0.790	0.771	0.869
Ti/Ti + Cr + Al)	0.107	0.124	0.065	0.069	0.056	0.067	0.101	0.079	0.058	0.054	0.439	0.068	0.385	0.065	0.068	0.080
Sample						**CL-07-010-255**										
Oxide%																
TiO_2	6.01	3.95	4.53	4.77	11.38	4.32	4.54	4.25	4.1	4.87	8.96	5.15	7.63	5.78	7.44	4.8
Al_2O_3	7.13	6.51	13.37	13.19	10.48	15.03	15.19	15.32	6.97	7.43	9.93	7.72	13.16	7.32	8.44	8.94
Cr_2O_3	44.13	48.6	40.87	41.69	22.31	40.95	41	40.46	48.72	49.33	31.26	45.18	29.01	45.22	37.69	46.29
FeO_T	26.05	26.52	24.6	24.44	37.65	22.93	23.22	23.87	24.53	23.31	32.4	25.61	33.49	25.3	29.07	23.78
MnO	0	0	0	0	0.5	0	0	0	0	0	1.03	0	0	0	0	0
MgO	15.43	14.01	15.82	15.31	15.07	15.56	14.93	16.49	13.31	14.45	14.58	14.88	15.65	14	14.92	14.73
Total	99.33	99.71	99.53	99.8	98.07	99.36	99.77	100.74	98.44	100.15	98.66	99.17	99.51	98.83	98.69	99.29
Recalculated Fe																
FeO	14.81	15.30	13.99	15.01	19.91	14.06	14.94	13.41	15.29	15.48	18.04	14.53	17.04	15.84	16.00	14.61
Fe_2O_3	12.49	12.47	11.79	10.48	19.72	9.86	9.21	11.63	10.27	8.71	15.96	12.32	18.28	10.52	14.53	10.19
Total	100.00	100.84	100.37	100.45	99.37	100.06	100.46	101.56	99.38	100.26	99.76	100.20	100.77	99.35	99.87	99.98
$Fe^{2+}/(Mg + Fe^{2+}$	0.350	0.380	0.332	0.355	0.426	0.336	0.359	0.313	0.392	0.375	0.410	0.354	0.379	0.388	0.376	0.357
Cr/(Cr + Al)	0.806	0.834	0.672	0.680	0.588	0.061	0.064	0.060	0.062	0.071	0.156	0.080	0.130	0.089	0.123	0.071
Ti/Ti + Cr + Al)	0.095	0.061	0.066	0.069	0.222	0.646	0.644	0.639	0.824	0.817	0.679	0.797	0.597	0.806	0.750	0.776
Sample																
Oxide%																
TiO_2	6.18	8.47	4.48	4.51	7.5	7.65	5.12	6.33	9.91	9.57	4.84	5.48	6.05	6	4.29	8.26
Al_2O_3	7.79	10.98	6.26	7.75	10.71	9.44	12.78	8.21	12.07	11.48	9.56	8.07	7.5	8.24	8.49	13.27
Cr_2O_3	44	31.71	50.54	49.2	33.81	36.84	42.73	42.68	21.43	24.68	46.7	44.73	45.14	40.69	47.69	23.73
FeO_T	25.64	31.86	23.36	23.48	32.22	29.81	23.41	27.1	38.71	36.65	22.35	25.09	25.54	27.62	24.07	37.46
MnO	0.66	0.56	0	0	0	0	0	0	0.65	0.64	0.96	0	0	1.03	0	0
MgO	14.53	15.98	14.68	13.46	14.97	15.57	14.96	14.98	14.74	15.62	13.69	14.75	14.02	14.52	14.95	15.49
Total	99.08	99.86	100.24	98.73	99.71	99.6	99.44	100.23	97.86	98.76	98.68	99.21	99.1	98.57	100.15	98.97
Recalculated Fe																
FeO	15.54	16.56	14.28	16.39	17.63	16.65	15.33	15.79	18.96	17.87	15.04	14.82	16.56	14.75	14.42	17.70
Fe_2O_3	11.22	17.00	10.10	7.88	16.21	14.62	8.98	12.57	21.95	20.87	8.12	11.42	9.98	14.31	10.72	21.96
Total	100.19	101.26	100.69	99.19	100.83	100.77	100.26	100.96	100.06	100.73	99.50	99.82	99.60	100.00	100.56	100.41
$Fe^{2+}/(Mg + Fe^{2+}$	0.375	0.368	0.353	0.406	0.398	0.375	0.365	0.372	0.419	0.391	0.381	0.360	0.399	0.363	0.351	0.391
Cr/(Cr + Al)	0.096	0.144	0.066	0.066	0.125	0.125	0.073	0.099	0.193	0.179	0.070	0.084	0.093	0.097	0.063	0.153
Ti/Ti + Cr + Al)	0.791	0.660	0.844	0.810	0.679	0.724	0.692	0.777	0.544	0.591	0.766	0.788	0.801	0.768	0.790	0.545

Sample	CL-07-010-264															
Oxide%																
TiO_2	4.63	5.3	4.63	7.45	6.34	17.27	17.18	9.82	4.64	7.42	8.98	4.05	5.03	10.89	4.68	6.31
Al_2O_3	15.36	7.52	8.68	9.88	12.65	10.69	10.84	6.48	14.95	8.86	2.12	15.43	14.27	13.38	15.29	10.51
Cr_2O_3	41.2	48.4	46.97	36.49	24.22	3.73	5.98	2.31	41.67	38.4	1.14	40.81	38.88	17.11	40.3	33.68
FeO_T	22.9	23.95	23.69	29.89	40.12	49.35	48.12	68.65	22.6	29.29	76.05	22.05	23.3	40.4	22.6	33.64
MnO	0	0.73	0	0	0.63	0.49	0	0	0.62	0	0.49	0	0.78	0.75	0	0
MgO	16.21	14.13	14.4	15.01	13.01	16.52	16.55	8.49	15.51	15.49	7.28	16.4	16.12	15.9	16.38	14.8
Total	100.38	100.25	99.02	99.7	97.85	98.82	99.24	97.03	100.02	100.11	96.48	99.16	98.75	98.65	99.88	99.61
Recalculated Fe																
FeO	14.12	15.84	14.87	17.20	18.67	23.40	23.95	28.34	14.40	16.52	28.49	12.83	12.76	18.80	13.56	16.75
Fe_2O_3	9.75	9.01	9.80	14.10	23.84	28.84	26.86	44.79	9.11	14.19	52.85	10.25	11.72	24.00	10.04	18.78
Total	101.28	100.93	99.76	100.13	99.36	100.94	101.36	100.24	100.90	100.88	101.36	99.77	99.92	100.83	100.26	100.82
$Fe^{2+}/(Mg + Fe^{2+})$	0.328	0.386	0.367	0.391	0.446	0.443	0.448	0.652	0.343	0.374	0.687	0.305	0.307	0.399	0.317	0.388
Cr/(Cr + Al)	0.643	0.812	0.784	0.712	0.562	0.190	0.270	0.193	0.652	0.744	0.265	0.640	0.646	0.462	0.639	0.682
Ti/Ti + Cr + Al)	0.064	0.078	0.068	0.122	0.123	0.455	0.425	0.438	0.065	0.120	0.665	0.057	0.074	0.219	0.066	0.108

Sample																
Oxide%																
TiO_2	9.46	12.18	10.46	9.67	16.02	6.7	11.59	10.46	10.87	4.22	4.79	9.69	4.92	17.24	18.05	6.95
Al_2O_3	5.86	7.41	12.77	10.99	10.06	8.12	12.38	12.35	11.69	14.49	15.01	4.87	14.2	10.65	10.01	7.96
Cr_2O_3	1.51	1.57	21.88	27.87	2.19	41.97	16.43	18.26	23.51	41.35	41.63	3.5	41.57	5.07	1.85	40.99
FeO_T	70.3	66.41	37.88	33.74	49.12	27.32	40.65	40.72	36.15	23.32	22.71	67.64	22.21	47.16	49.66	27.17
MnO	0.2	0	0	0.52	0.88	0	0.82	0	0.72	0	0	0.79	0	0.51	0	0
MgO	9.14	8.74	15.66	15.75	17.76	14.49	16.3	15.51	15.75	15.91	15.96	8.88	16.06	16.97	16.87	14.66
Total	97.59	96.78	99.5	99.22	97.03	99.1	98.65	97.79	99.02	100.03	100.72	95.7	99.68	98	96.94	98.24
Recalculated Fe																
FeO	27.01	30.33	19.46	17.72	19.30	16.67	18.52	19.24	18.79	13.77	14.52	26.47	13.99	22.49	23.44	16.38
Fe_2O_3	48.11	40.09	20.47	17.80	33.14	11.84	24.59	23.87	19.30	10.62	9.10	45.75	9.13	27.42	29.14	11.99
Total	101.29	100.33	100.70	100.32	99.35	100.14	100.63	99.69	100.62	100.35	101.01	99.95	99.88	100.35	99.36	99.22
$Fe^{2+}/(Mg + Fe^{2+})$	0.624	0.661	0.411	0.387	0.379	0.392	0.389	0.410	0.401	0.327	0.338	0.626	0.328	0.426	0.438	0.385
Cr/(Cr + Al)	0.147	0.124	0.535	0.630	0.127	0.776	0.471	0.498	0.574	0.657	0.650	0.325	0.663	0.242	0.110	0.775
Ti/Ti + Cr + Al)	0.468	0.479	0.196	0.172	0.470	0.105	0.240	0.213	0.202	0.060	0.066	0.461	0.069	0.439	0.506	0.111

Sample		CL-07-014-233														
Oxide%																
TiO_2	18.28	8.31	4.19	5.07	4.78	5.88	1.09	12.61	17.19	10.71	4.44	5.82	4.72	7.81	5.17	4.64
Al_2O_3	10.25	9.47	15.1	5.46	5.14	4.41	14.19	12.52	9.12	8.04	6.67	7.64	4.92	6.54	14.56	8.4
Cr_2O_3	2.84	28.43	42	44.7	49.37	47.57	52.4	14.12	3.31	28.92	48.32	41.03	51.39	37.78	39.71	44.77
FeO_T	48.53	36.72	23.37	29.42	26.31	28.36	17.34	42.93	51.61	35.18	25.11	29.28	25.19	32.02	22.63	26.46
MnO	0.51	0.62	0	0.67	0	0	0	0.65	0.71	0.77	0.81	0.72	0	0	0	0
MgO	17.51	14.62	15.19	13.01	12.79	13.11	14.16	15.01	15.77	14.71	13.88	13.52	12.53	13.95	16.85	14.92
Total	98.26	99.06	100.27	98.64	99.18	100.13	99.53	97.88	98.03	98.48	99.36	98.29	99.24	98.59	99.46	99.99
Recalculated Fe																
FeO	22.66	17.82	15.09	16.63	17.06	17.99	13.44	21.49	23.93	19.46	15.02	16.47	17.67	18.44	13.08	14.71
Fe_2O_3	28.75	21.00	9.20	14.22	10.28	11.53	4.33	23.83	30.76	17.47	11.22	14.24	8.35	15.09	10.62	13.06
Total	100.80	100.27	100.77	99.75	99.67	100.48	99.61	100.23	100.79	100.08	100.35	99.72	99.59	99.61	99.98	100.50
$Fe^{2+}/(Mg + Fe^{2+})$	0.421	0.406	0.358	0.418	0.428	0.435	0.347	0.445	0.460	0.426	0.378	0.406	0.442	0.426	0.303	0.356
Cr/(Cr + Al)	0.157	0.668	0.651	0.846	0.866	0.879	0.712	0.431	0.196	0.707	0.829	0.783	0.875	0.795	0.647	0.781
Ti/Ti + Cr + Al)	0.490	0.157	0.058	0.084	0.074	0.094	0.014	0.268	0.492	0.199	0.068	0.096	0.071	0.135	0.074	0.072

Sample			CL-07-014-245													
Oxide%																
TiO_2	5.01	4.31	4.55	4.41	17.12	8.34	2.39	3.06	5.96	18.06	16.72	16.66	13.72	17.56	17.16	18.62
Al_2O_3	14.82	15.25	14.7	14.59	8.25	9.93	0.74	1.82	5.42	9.58	8.16	8.82	8.55	8.01	8.26	8.46
Cr_2O_3	40.01	40.88	40.39	41.47	6.07	27.27	44.63	45.07	46.11	3.41	3.15	4.04	14.81	3	3.33	5.42
FeO_T	23.47	22.75	24.71	24.14	50.82	37.13	41.32	37.62	27.58	50.57	54.62	52.07	43.98	52.26	52.48	49.57
MnO	0.46	0	0	0	0.69	0.51	0	0.59	0	0.39	0	0.43	0	0.92	0.76	0
MgO	15.03	15.01	14.68	14.63	14.16	15.65	7.8	9.78	12.71	15.5	14.1	15.31	16.03	15.23	15.2	15.33
Total	99.1	98.57	99.14	99.41	97.18	99.29	97.21	98.05	98.42	97.57	97.55	97.54	97.6	97.04	97.36	97.52
Recalculated Fe																
FeO	15.23	14.46	15.88	15.87	25.97	16.70	21.78	19.25	18.31	25.41	26.33	24.27	20.75	24.47	24.43	26.32
Fe_2O_3	9.16	9.21	9.81	9.19	27.62	22.71	21.71	20.42	10.30	27.96	31.44	30.89	25.82	30.89	31.18	25.84
Total	99.72	99.71	100.01	100.16	99.88	101.11	99.06	99.99	98.81	100.31	99.90	100.43	99.68	100.07	100.31	99.99
$Fe^{2+}/(Mg + Fe^{2+}$	0.362	0.351	0.378	0.378	0.507	0.374	0.610	0.525	0.447	0.479	0.512	0.471	0.421	0.474	0.474	0.491
Cr/(Cr + Al)	0.644	0.643	0.648	0.656	0.330	0.648	0.976	0.943	0.851	0.193	0.206	0.235	0.537	0.201	0.213	0.301
Ti/Ti + Cr + Al)	0.071	0.061	0.065	0.062	0.470	0.159	0.047	0.057	0.095	0.493	0.509	0.480	0.321	0.528	0.511	0.496

Sample																
Oxide%																
TiO_2	5.79	5.79	17.2	17.98	4.92	14.02	9.63	9.52	15.82	16.64	10.76	16.95	4.74	4.9	17	18.18
Al_2O_3	5.13	4.77	9.14	9.1	7.74	8.37	7.2	7.25	10.14	8.81	12.41	10.31	13.41	13.75	11.74	9.67
Cr_2O_3	48.04	48.41	5.01	3.77	46.59	8.29	29.19	29.46	4.29	4.79	22.63	2.9	41.06	40.85	4.41	5.27
FeO_T	27.06	26.8	50.44	50.9	26.58	50.87	38.1	37.93	49.53	50.56	35.79	50.56	24.98	24.92	48.24	48.71
MnO	0.43	0	0.46	0.61	0	0	0	0	1.32	0	0	0.66	0	0	0.44	0
MgO	12.55	12.89	15.57	15.3	13.79	15.61	13.94	13.87	16.53	15.96	15.65	16.14	14.53	15.18	15.43	15.56
Total	99.12	99.03	97.75	97.67	99.44	97.66	98.92	98.64	97.79	97.44	98.3	97.81	99.37	100.15	97.53	98.1
Recalculated Fe																
FeO	18.31	18.06	24.50	25.40	16.69	21.77	20.27	20.27	21.06	23.49	19.20	23.31	15.98	15.48	24.74	25.75
Fe_2O_3	9.72	9.72	28.83	28.34	10.99	32.34	19.82	19.63	31.63	30.08	18.44	30.28	10.00	10.49	26.12	25.51
Total	99.97	99.63	100.71	100.50	100.72	100.40	100.05	100.00	100.80	99.77	99.09	100.55	99.72	100.65	99.88	99.95
$Fe^{2+}/(Mg + Fe^{2+}$	0.450	0.440	0.469	0.482	0.404	0.439	0.449	0.451	0.417	0.452	0.408	0.448	0.382	0.364	0.474	0.481
Cr/(Cr + Al)	0.863	0.872	0.269	0.217	0.801	0.399	0.731	0.732	0.221	0.267	0.550	0.159	0.673	0.666	0.201	0.268
Ti/Ti + Cr + Al)	0.090	0.090	0.468	0.497	0.075	0.391	0.187	0.184	0.437	0.469	0.199	0.469	0.069	0.071	0.425	0.468

Sample								CL-07-014-257								
Oxide%																
TiO_2	10.2	10.15	7.8	15.34	6.58	5.67	6.22	16.62	17.15	16.12	16	4.47	8.33	4.3	8.26	16.46
Al_2O_3	7.87	7.84	7.52	9.93	9.15	8.07	7.84	7.92	9.18	8.87	8.46	15.33	10.33	15.36	10.43	8.33
Cr_2O_3	30.05	29.61	34.27	3.87	40.36	43.79	45.09	7.15	5.01	8.8	6.07	41.31	27.42	41.57	27.59	5.56
FeO_T	35.34	36.18	32.92	50.53	29.2	26.95	26.93	49.21	48.78	47.73	51.77	22.42	37.34	22.84	36.84	51.73
MnO	0	0	0	0	0	0	0	0.59	0.66	0.7	0.44	0.7	0	0.6	0.51	0
MgO	14.09	14.46	15.16	17.22	14.85	14.1	13.86	16.09	15.97	15.77	15	15.02	14.5	15.1	14.58	14.86
Total	98.24	98.68	98.24	97.6	99.56	99.53	100.37	97.82	96.91	98.1	98.03	99.43	98.35	99.9	98.33	97.79
Recalculated Fe																
FeO	20.44	20.06	16.65	20.66	17.00	16.62	17.86	22.79	23.30	22.97	24.21	14.73	18.70	14.74	18.11	24.99
Fe_2O_3	16.56	17.91	18.09	33.19	13.56	11.48	10.08	29.36	28.32	27.52	30.63	8.54	20.71	9.00	20.81	29.72
Total	99.21	100.03	99.48	100.22	101.50	99.73	100.95	100.52	99.59	100.75	100.81	100.11	100.00	100.67	100.30	99.92
$Fe^{2+}/(Mg + Fe^{2+}$	0.449	0.438	0.381	0.402	0.391	0.398	0.420	0.443	0.450	0.450	0.475	0.355	0.420	0.354	0.411	0.485
Cr/(Cr + Al)	0.719	0.717	0.754	0.207	0.747	0.784	0.794	0.377	0.268	0.400	0.325	0.644	0.640	0.645	0.640	0.309

Ti/Ti + Cr + Al)	0.188	0.190	0.140	0.439	0.104	0.088	0.094	0.455	0.466	0.411	0.449	0.062	0.156	0.060	0.154	0.466
Sample																
Oxide%																
TiO_2	16	10.58	15.63	13.63	15.55	9.79	9.62	3.97	16.18	4.23	15.52	6.78	16.44	9.59	17.42	5.94
Al_2O_3	8.51	12.16	9.27	10.53	9.83	12.66	12.43	10.66	9.85	10.96	9.15	12.17	10.46	4.67	10.47	6.44
Cr_2O_3	5.72	16.38	5.11	9.13	6.57	24.83	24.81	45.92	4.17	46.01	6.89	30.2	5.62	1.67	2.58	48.51
FeO_T	51.43	41.22	50.57	47.2	49.86	35.24	35.94	23.45	52.83	23.44	48.74	32.15	47.34	71.39	50.43	24.81
MnO	0.61	0.441	0.67	0.83	0	0	0	1.17	1.23	0	0.56	1.18	0.59	1.02	0.57	0
MgO	15.21	14.58	15.52	16.05	16.06	15.8	15.85	14.48	13.08	14.43	15.53	15.59	15.88	7.51	16.14	13.29
Total	97.76	95.47	96.94	97.59	98.14	98.53	98.9	99.8	97.42	99.55	96.37	98.08	96.32	96.02	97.71	99.07
Recalculated Fe																
FeO	23.65	19.68	22.67	20.27	22.87	18.49	18.34	14.06	26.58	15.39	22.50	14.76	22.91	28.41	23.87	17.91
Fe_2O_3	30.88	23.94	31.00	29.93	29.99	18.62	19.56	10.44	29.17	8.95	29.16	19.33	27.15	47.77	29.52	7.66
Total	100.57	97.76	99.88	100.37	100.87	100.19	100.61	100.70	100.26	99.97	99.31	100.01	99.05	100.64	100.57	99.76
$Fe^{2+}/(Mg + Fe^{2+}$	0.466	0.431	0.450	0.415	0.444	0.396	0.394	0.353	0.533	0.374	0.448	0.347	0.447	0.680	0.453	0.431
Cr/(Cr + Al)	0.311	0.475	0.270	0.368	0.310	0.568	0.572	0.743	0.221	0.738	0.336	0.625	0.265	0.193	0.142	0.835
Ti/Ti + Cr + Al)	0.453	0.226	0.440	0.343	0.411	0.176	0.174	0.058	0.449	0.061	0.418	0.118	0.424	0.514	0.477	0.089
Sample														**CL-07-014-260**		
Oxide%																
TiO_2	5.31	12.55	17.76	16.07	16.04	12.14	11.9	17.08	6.14	3.6	16.8	11.5	4.53	6.1	7.2	5.61
Al_2O_3	10.78	13	9.97	8.86	9.41	13.13	13.08	8.84	7.55	0	9.33	7.69	14.72	10.09	8.73	7.13
Cr_2O_3	35.32	9.37	2.85	4.86	5.31	15.79	15.59	2.36	45.05	52.3	4.33	25.87	39.58	36.47	40.65	46.89
FeO_T	31.41	43.93	50.4	52.99	50.8	40.68	40.54	54.26	26.12	29.61	50.99	37.21	24.59	29.26	27.17	24.22
MnO	0	0	0.45	0	0.69	0.68	0.6	0	0	0	0	1.56	0	0	0	0.58
MgO	15.71	18.4	15.5	14.03	14.91	15.49	15.4	14.55	13.58	10.68	15.2	14.14	15.82	16.29	15.22	14.01
Total	98.41	97.6	97.14	97.51	97.15	97.94	97.18	97.66	99.32	97.02	97.35	98.3	99	99.03	99.59	98.79
Recalculated Fe																
FeO	14.37	16.89	24.96	25.96	24.08	20.40	20.14	26.18	17.68	17.98	24.83	20.10	14.22	13.94	16.52	15.60
Fe_2O_3	18.94	30.05	28.27	30.04	29.69	22.54	22.67	31.21	9.38	12.93	29.07	19.01	11.53	17.02	11.84	9.58
Total	100.43	100.26	99.76	99.82	100.13	100.17	99.38	100.22	99.38	97.49	99.56	99.87	100.39	99.92	100.16	99.74
$Fe^{2+}/(Mg + Fe^{2+}$	0.339	0.340	0.475	0.509	0.475	0.425	0.423	0.502	0.422	0.486	0.478	0.444	0.335	0.324	0.378	0.384
Cr/(Cr + Al)	0.687	0.326	0.161	0.269	0.275	0.446	0.444	0.152	0.800	1.000	0.237	0.693	0.643	0.708	0.757	0.815
Ti/Ti + Cr + Al)	0.090	0.293	0.488	0.458	0.441	0.246	0.244	0.511	0.094	0.061	0.467	0.227	0.065	0.101	0.113	0.085
Sample																
Oxide%																
TiO_2	5.83	6.77	5.98	6.15	4.62	9.58	4.41	5.31	3.58	4.78	8.54	9.02	4.94	4.51	4.19	4.64
Al_2O_3	7.57	7.57	7.86	7.72	12.23	14.12	13.64	7.33	7.39	14.15	10.92	10.97	12.68	4.75	7.68	15.28
Cr_2O_3	44.8	43.5	44.67	45.56	40.69	20.59	41.79	46.73	51.62	40.53	30.6	30.27	43.31	52.96	47.53	40.5
FeO_T	26.69	27.3	26.51	25.18	25.65	38.47	23.54	26.68	22.83	24.21	32.39	32.18	23.1	24.88	24.91	22.33
MnO	0	0	0	0	0.6	0	0	0	0	0	0	0	0	0	0.71	0
MgO	14.66	14.23	14.65	15.04	15.29	15.49	15.02	13.53	14.12	14.92	16.21	15.78	15.08	12.72	14.72	16.3
Total	99.74	100.01	100.24	100.01	99.26	98.73	98.78	99.85	99.99	98.76	98.85	98.76	99.36	100.1	99.66	99.39
Recalculated Fe																
FeO	16.14	17.57	16.37	15.88	14.08	19.03	14.86	17.35	14.86	15.49	16.55	17.49	15.31	17.51	13.94	13.58
Fe_2O_3	11.72	10.81	11.27	10.33	12.85	21.61	9.64	10.36	8.85	9.69	17.60	16.33	8.66	8.19	12.19	9.72
Total	100.72	100.45	100.80	100.69	100.37	100.41	99.37	100.62	100.43	99.56	100.42	99.86	99.98	100.64	100.96	100.02
$Fe^{2+}/(Mg + Fe^{2+}$	0.382	0.409	0.385	0.372	0.341	0.408	0.357	0.418	0.371	0.368	0.364	0.383	0.363	0.436	0.347	0.319

Cr/(Cr + Al)	0.799	0.794	0.792	0.798	0.691	0.494	0.673	0.810	0.824	0.658	0.653	0.649	0.696	0.882	0.806	0.640
Ti/Ti + Cr + Al)	0.090	0.105	0.092	0.093	0.069	0.180	0.063	0.081	0.052	0.069	0.148	0.155	0.070	0.067	0.063	0.065
Sample												**CL-07-014-269**				
Oxide%																
TiO_2	4.5	7.91	5.81	6.56	5.12	4.48	6.74	5.81	5.64	8.1	10.72	5.19	8.58	4.53	12.36	9.62
Al_2O_3	10.5	9.22	11.36	7.74	8.31	11.74	8.15	10.97	7.57	8.94	12.28	12.74	13.63	9.24	11.6	10.88
Cr_2O_3	43.86	33.44	38.29	42.35	46.66	42.35	41.49	25.5	47.14	36.23	19.7	44.24	25.68	45.19	15.95	26.86
FeO_T	25.41	32.5	28.63	26.84	24.24	23.74	28	42.02	25.14	30.51	39.01	22.54	36.14	25.88	42.47	35.78
MnO	0	0	0	0	0.61	0	0	0.89	0	0	0	0	0	1.1	0.51	0.58
MgO	15.03	15.06	15.37	14.65	14.62	15.54	14.99	12.07	13.63	13.49	15.08	14.72	15.19	13.86	15.54	15.04
Total	99.39	98.52	99.68	98.73	99.58	98.36	99.54	97.38	99.26	97.93	97.35	100.17	99.85	100.18	98.87	99.19
Recalculated Fe																
FeO	14.76	17.11	15.65	16.11	15.04	13.68	16.51	19.22	17.36	19.47	19.92	16.17	18.78	15.43	20.65	18.78
Fe_2O_3	11.83	17.11	14.42	11.92	10.22	11.18	12.77	25.34	8.65	12.27	21.22	7.08	19.29	11.61	24.25	18.90
Total	100.49	100.06	100.91	99.65	100.58	98.97	100.65	99.80	99.99	98.50	98.92	100.14	101.15	100.96	100.86	100.65
$Fe^{2+}/(Mg + Fe^{2+}$	0.355	0.389	0.364	0.382	0.366	0.331	0.382	0.472	0.417	0.447	0.426	0.381	0.410	0.384	0.427	0.412
Cr/(Cr + Al)	0.737	0.709	0.693	0.786	0.790	0.708	0.773	0.609	0.807	0.731	0.518	0.700	0.558	0.766	0.480	0.623
Ti/Ti + Cr + Al)	0.067	0.138	0.091	0.104	0.076	0.066	0.107	0.117	0.084	0.135	0.212	0.072	0.151	0.068	0.261	0.175
Sample																
Oxide%																
TiO_2	9.45	9.56	6.67	8.17	5.17	6.01	4.99	4.93	4.6	13.54	10.63	7.21	8.96	11.06	10.53	8.14
Al_2O_3	9.73	3.16	9.16	11.1	7.66	7.36	6.97	7.5	14.69	11.67	4.6	7.89	10.29	13.32	12.55	10.66
Cr_2O_3	30.54	2.15	39.77	28.56	47.35	46.1	47.05	47.71	42.32	13.96	1.97	39	31.95	15.57	20.49	33.68
FeO_T	32.41	73.37	30.26	37.7	24.92	26.29	25.55	24.72	22.32	43.34	69.53	28.2	31.59	41	38.34	31.29
MnO	0.59	0.77	0	0	0	0	0	0	0	0.48	0.85	0.55	0	0	0	0
MgO	15.24	6.94	12.93	12.62	13.25	13.55	13.55	13.6	15.18	14.58	6.91	14.76	15.63	16.33	15.54	15.38
Total	98.41	96.78	99.36	99.54	99.09	99.89	99.39	98.96	99.51	98.17	95.3	98.14	99.19	98.21	98.11	100.1
Recalculated Fe																
FeO	17.82	29.32	19.56	21.58	17.28	17.86	16.50	16.55	15.16	22.92	29.24	15.69	17.61	18.69	19.30	17.54
Fe_2O_3	16.21	48.96	11.89	17.91	8.49	9.37	10.06	9.08	7.96	22.70	44.78	13.90	15.54	24.79	21.16	15.28
Total	99.58	100.85	99.98	99.94	99.20	100.25	99.12	99.37	99.91	99.84	99.78	99.52	99.98	99.76	99.57	100.68
$Fe^{2+}/(Mg + Fe^{2+}$	0.396	0.703	0.459	0.490	0.423	0.425	0.406	0.406	0.359	0.469	0.704	0.374	0.387	0.391	0.411	0.390
Cr/(Cr + Al)	0.678	0.313	0.744	0.633	0.806	0.808	0.819	0.810	0.659	0.445	0.223	0.768	0.676	0.439	0.523	0.679
Ti/Ti + Cr + Al)	0.166	0.570	0.106	0.147	0.077	0.091	0.076	0.074	0.064	0.291	0.534	0.119	0.153	0.229	0.204	0.135
Sample																
Oxide%																
TiO_2	8.25	16.54	4.71	7.25	9.35	8.9	11.14	10.03	9.23	5.38	8.3	7.28	12.12	11.34	4.44	13.22
Al_2O_3	10.94	11.57	15.5	9.36	4.77	1.46	10.62	11.13	9.69	14.86	8.89	8.56	12.7	11.45	15.62	10.76
Cr_2O_3	28.84	4.34	40.76	34.73	3.18	1.95	3.81	23.82	30.27	40.84	36.9	37.97	7.02	24.83	40.17	3.34
FeO_T	34.6	46.96	23.28	31.43	68.87	74.72	59.44	37.14	33.01	22.23	29.56	29.33	51.94	34.54	23.51	55.17
MnO	0	0	0	0	0.6	0.82	0.664	0.62	0	0	0	0.69	0.81	0	0	0
MgO	14.85	16.71	15.25	14.48	9.24	6.93	11.27	15.46	14.98	15.44	15.44	14.55	12.9	15.91	15.16	13.77
Total	98.37	97.1	100.11	97.73	96.5	95.72	97.53	98.48	97.84	99.26	99.41	98.74	97.84	98.58	99.08	97.07
Recalculated Fe																
FeO	18.01	21.95	15.20	17.09	26.03	28.09	25.52	18.12	18.08	15.37	17.27	16.44	24.15	19.41	15.14	23.99
Fe_2O_3	18.44	27.80	8.98	15.93	47.61	51.82	37.69	21.14	16.59	7.63	13.66	14.33	30.88	16.81	9.30	34.65
Total	99.33	99.47	100.65	99.10	100.78	99.97	100.72	100.60	99.17	99.51	100.46	100.17	100.58	99.75	99.83	99.73

$Fe^{2+}/(Mg + Fe^{2+}$	0.405	0.424	0.359	0.398	0.612	0.695	0.560	0.397	0.404	0.358	0.386	0.388	0.512	0.406	0.359	0.494
Cr/(Cr + Al)	0.639	0.201	0.638	0.713	0.309	0.473	0.194	0.589	0.677	0.648	0.736	0.748	0.270	0.593	0.633	0.172
Ti/Ti + Cr + Al)	0.148	0.422	0.066	0.124	0.464	0.672	0.350	0.191	0.164	0.075	0.136	0.120	0.308	0.205	0.062	0.394
Sample				**CL-07-014-273**												
Oxide%																
TiO_2	4.88	5.36	4.19	5.31	5.24	6.34	7.05	4.77	6.25	4.84	4.24	4.42	6.59	4.83	4.83	5.95
Al_2O_3	13.89	6.78	15.78	7.21	8.4	11.32	8.57	7.93	8.36	15.07	8.94	15.09	7	6.91	7.21	8.81
Cr_2O_3	40.6	48.26	40.71	42.66	42.92	31.41	36.7	47	38.85	40.23	46.9	41.03	43.66	46.04	46.06	39.06
FeO_T	23.26	25.17	21.9	28.61	27.93	35.16	30.25	23.97	29.53	23.31	24.34	23.43	27.61	26.46	25.64	30.12
MnO	0	0	0	0	0.69	0	0.63	0	0	0	0	0	0.82	0	0	0
MgO	15.83	14.21	15.95	13.4	13.93	13.01	14.18	14.02	14.4	15.02	14.55	15.26	13.7	13.97	14.29	13.96
Total	99.07	100.39	99.2	98.95	99.9	99.01	98.16	99.42	98.51	99.43	100.04	100.57	99.42	100.02	100.07	99.1
Recalculated Fe																
FeO	14.12	16.33	13.28	15.74	16.05	17.88	16.18	14.56	15.60	14.89	14.89	15.00	17.32	14.72	13.98	17.04
Fe_2O_3	10.16	9.83	9.58	14.31	13.21	19.21	15.64	10.45	15.48	9.35	10.50	9.37	11.44	13.05	12.96	14.54
Total	99.48	100.76	99.88	99.88	100.43	100.57	99.74	99.94	99.87	100.10	100.02	100.17	100.53	100.75	100.83	99.36
$Fe^{2+}/(Mg + Fe^{2+}$	0.333	0.392	0.318	0.397	0.393	0.435	0.390	0.368	0.378	0.357	0.365	0.355	0.415	0.371	0.354	0.406
Cr/(Cr + Al)	0.662	0.827	0.634	0.799	0.774	0.651	0.742	0.799	0.757	0.642	0.779	0.646	0.807	0.817	0.811	0.748
Ti/Ti + Cr + Al)	0.070	0.080	0.058	0.086	0.083	0.111	0.119	0.072	0.104	0.068	0.063	0.062	0.104	0.075	0.075	0.098

Sample			
Oxide%			
TiO_2	4.21	4.92	4.34
Al_2O_3	7.32	7.42	10.06
Cr_2O_3	49.24	48.32	45.86
FeO_T	24.93	24.12	23.97
MnO	0	0	0
MgO	13.95	13.92	13.75
Total	100.03	99.94	99.17
Recalculated Fe			
FeO	15.74	16.11	15.27
Fe_2O_3	10.22	8.90	9.67
Total	100.67	99.59	99.85
$Fe^{2+}/(Mg + Fe^{2+}$	0.388	0.394	0.384
Cr/(Cr + Al)	0.819	0.814	0.754
Ti/Ti + Cr + Al)	0.062	0.073	0.064

Appendix D-2 Serpentine

CL-06-003-173

	Sample: Notes:	Groundmas 1	Groundmass Rim of Pheno	In Pheno 1	In Pheno 2	In Pheno 3 2 With NiS	In Pheno 4	Rim	Matrix of Magmaclast	Monticellite	In Pheno 3	In pheno core
Oxide%	**Na2O**	0	0.32	0.32	0.37	0	0.48	0	0	0	0	0
	MgO	31.91	30.5	30.85	36.13	34.04	33.84	30.5	29.51	29.76	36.22	31.68
	Al2O3	3.12	2.84	0.46	0.59	0.5	0.62	3.22	2.3	2.71	0	0.47
	SiO2	43.37	43.1	40.72	40.83	38.91	40.76	43.03	41.82	42.18	40.31	41.38
	CaO	0.32	0.35	0	0	1	0	0.65	0.78	0	0	0
	FeOT	7.48	6.73	7.85	7.27	7.71	7.17	6.9	8.16	8.55	6.51	7.68
	Total	85.41	83.89	80.3	85.21	82.39	83.05	84.13	82.53	83.56	83.83	81.75

Oxide%	**Na2O**	0.00	0.32	0.32	0.37	0.00	0.48	0.00	0.00	0.00	0.00	0.00
	MgO	31.91	30.50	30.85	36.13	34.04	33.84	30.50	29.51	29.76	36.22	31.68
	Al2O3	3.12	2.84	0.46	0.59	0.50	0.62	3.22	2.30	2.71	0.00	0.47
	SiO2	43.37	43.10	40.72	40.83	38.91	40.76	43.03	41.82	42.18	40.31	41.38
	CaO	0.32	0.35	0.00	0.00	1.00	0.00	0.65	0.78	0.00	0.00	0.00
	FeOT	7.48	6.73	7.85	7.27	7.71	7.17	6.90	8.16	8.55	6.51	7.68
	H2O	3.13	3.06	2.89	3.06	2.93	2.99	3.07	2.98	3.01	3.00	2.94
	Total	89.33	86.90	83.09	88.25	85.09	85.86	87.37	85.55	86.21	86.04	84.15

	Sample: Notes:	In pheno Edge	Groundmass	Groundmas edge by calcite	Magmaclast Monticellite	Monticellite	Pheno	Pheno	Groundmass	Phenocrysts 4	Pheno 5	CL-06-003-18: rain 1 orientate Core zoning core dark
Oxide%	**Na2O**	0	0.4	0	0	0	0	0	0	0	0	0
	MgO	30.5	30.81	31.78	29.76	29.43	29.99	31.15	31.19	30.66	32.94	36.73
	Al2O3	3.53	2.92	2.57	2.6	2.41	0.46	0.53	2.84	0.46	0.51	0
	SiO2	40.81	43.22	42.52	4.98	41.86	39.08	41.34	43.28	41.44	40.56	41.32
	CaO	0	0.21	0.63	0.19	0.18	0	0.19	0	0.19	0	0
	FeOT	8.66	7.02	7.32	7.68	7.87	7.92	7.74	7.93	7.64	7.97	5.27
	Total	84.13	84.66	83.76	82.08	81.78	77.85	81.14	85.3	80.61	82.14	83.91

Oxide%	**Na2O**	0.00	0.40	0.00	0.00	0.00	0.00	0.00	0.00	0.00	0.00	0.00
	MgO	30.50	30.81	31.78	29.76	29.43	29.99	31.15	31.19	30.66	32.94	36.73
	Al2O3	3.53	2.92	2.57	2.60	2.41	0.46	0.53	2.84	0.46	0.51	0.00
	SiO2	40.81	43.22	42.52	4.98	41.86	39.08	41.34	43.28	41.44	40.56	41.32
	CaO	0.00	0.21	0.63	0.19	0.18	0.00	0.19	0.00	0.19	0.00	0.00
	FeOT	8.66	7.02	7.32	7.68	7.87	7.92	7.74	7.93	7.64	7.97	5.27
	H2O	3.01	3.08	3.08	1.40	2.97	2.79	2.93	3.10	2.91	2.95	3.03
	Total	86.51	87.66	87.90	46.61	84.72	80.24	83.88	88.34	83.30	84.93	86.35

CL-06-003-182

	Sample:							Grain 2 unorientated				
	Notes:	outer lighter gre	Second Zone Dark	Third Zone Dark	'ery bright zon	Fourth Zone Dark	Botyriodal Rim	Core Zone dark	ghter outer zor	Second Zone Dark	Bright iron zone	Third Zone Botryiodal rim
Oxide%	**Na2O**	0	0.31	0	0	0	0	0	0	0	0	0
	MgO	36.73	33.05	33.2	31.91	33.65	32.15	34.77	34.47	33.63	33.36	31.38
	Al2O3	0	0	0	0	0	0.99	0	0	0	0	1.36
	SiO2	40.53	39.11	40.61	36.99	41.58	42.63	39.41	41.26	40.13	38.84	40.94
	CaO	0	0	0	0	0	0	0	0	0	0	0
	FeOT	6.94	7.26	8.08	19	7.33	10.91	7	9.03	8.46	13.6	10.96
	Total	84.91	80.12	82.27	87.51	83.37	86.9	81.72	85.47	82.71	86.17	84.66
Oxide%	**Na2O**	0.00	0.31	0.00	0.00	0.00	0.00	0.00	0.00	0.00	0.00	0.00
	MgO	36.73	33.05	33.20	31.91	33.65	32.15	34.77	34.47	33.63	33.36	31.38
	Al2O3	0.00	0.00	0.00	0.00	0.00	0.99	0.00	0.00	0.00	0.00	1.36
	SiO2	40.53	39.11	40.61	36.99	41.58	42.63	39.41	41.26	40.13	38.84	40.94
	CaO	0.00	0.00	0.00	0.00	0.00	0.00	0.00	0.00	0.00	0.00	0.00
	FeOT	6.94	7.26	8.08	19.00	7.33	10.91	7.00	9.03	8.46	13.60	10.96
	H2O	3.03	2.86	2.94	2.94	2.98	3.08	2.92	3.03	2.94	2.97	3.00
	Total	87.23	82.59	84.83	90.84	85.54	89.76	84.10	87.79	85.16	88.77	87.64

	Sample:	ellite in Magmaclast 1		Macrocryst 1		Grain 3 Orientated						Monticellite
	Notes:	Monti 1	Monti 2	Core Dark with NiS	im/Crosscuttir no sulphides	Core Dark with NiS	Rim	Second Zone Core	Rim	Third Zone Dark	im - Botryiodi	Magma 2 Grain1
Oxide%	**Na2O**	0	0	0	0	0	0	0.32	0	0	0.37	0
	MgO	30.57	31.4	33.75	32.1	36.15	35.48	33.76	31.03	32.84	32.21	28.64
	Al2O3	1.77	2.03	0	2.2	0	0	0.41	0.63	0	1.53	2.33
	SiO2	39.79	41.7	41.93	38.48	41.18	40	40.16	39.91	40.92	42.01	41.35
	CaO	0.31	0.31	0	0	0	0	0	0	0.18	0	0
	FeOT	9.24	8.3	7.14	9.43	5.83	8.78	7.65	8.31	7.56	10.58	9.51
	Total	81.88	83.97	83.2	82.41	83.53	84.79	83.65	83.01	82.09	86.7	82.22
Oxide%	**Na2O**	0.00	0.00	0.00	0.00	0.00	0.00	0.32	0.00	0.00	0.37	0.00
	MgO	30.57	31.40	33.75	32.10	36.15	35.48	33.76	31.03	32.84	32.21	28.64
	Al2O3	1.77	2.03	0.00	2.20	0.00	0.00	0.41	0.63	0.00	1.53	2.33
	SiO2	39.79	41.70	41.93	38.48	41.18	40.00	40.16	39.91	40.92	42.01	41.35
	CaO	0.31	0.31	0.00	0.00	0.00	0.00	0.00	0.00	0.18	0.00	0.00
	FeOT	9.24	8.30	7.14	9.43	5.83	8.78	7.65	8.31	7.56	10.58	9.51
	H2O	2.92	3.02	3.00	2.92	3.02	3.00	2.95	2.87	2.94	3.08	2.94
	Total	84.60	86.76	85.82	85.13	86.18	87.26	85.25	82.75	84.44	89.78	84.77

	Sample:	Unorientated Grain 2				Magmaclast 2			Magmaclast			
	Notes:		Zone 1 Core	Zone 1 Rim		Core Zone 1	Rim Zone 1	Iron Phase	Zoned Pheno			
		Grain 2	Dark	Lighter	ɔn Phase and Cross Cutting		Main Phase	m/Cross Cutti	Core	Dark Core	ɛr rim to dark	Fe rich rim
Oxide%	**Na2O**	0	0	0.39	0	0.33	0	0	0	0	0	0
	MgO	29.58	33.49	33.95	31.46	36.45	36.22	31.42	36.62	35.63	35.18	34.16
	Al2O3	2.41	0	0	1.21	0	0	2.94	0	0.67	0.57	0
	SiO2	41.08	41.69	39.92	41.46	40.24	40.86	38.35	40.44	40.18	40.16	38.45
	CaO	0.28	0	0	0	0	0	0	0	0	0	0
	MnO	0	0	0	0	0.36	0	0	0	0	0	0
	FeOT	9.39	7.29	8.43	9.95	7.01	5.94	10.15	9.97	7.62	8.55	14.8
	Total	82.88	83.07	83.12	84.4	84.56	83.28	82.98	87.52	84.4	84.89	87.59
Oxide%	**Na2O**	0.00	0.00	0.39	0.00	0.33	0.00	0.00	0.00	0.00	0.00	0.00
	MgO	29.58	33.49	33.95	31.46	36.45	36.22	31.42	36.62	35.63	35.18	34.16
	Al2O3	2.41	0.00	0.00	1.21	0.00	0.00	2.94	0.00	0.67	0.57	0.00
	SiO2	41.08	41.69	39.92	41.46	40.24	40.86	38.35	40.44	40.18	40.16	38.45
	CaO	0.28	0.00	0.00	0.00	0.00	0.00	0.00	0.00	0.00	0.00	0.00
	MnO	0.00	0.00	0.00	0.00	0.36	0.00	0.00	0.00	0.00	0.00	0.00
	FeOT	9.39	7.29	8.43	9.95	7.01	5.94	10.15	9.97	7.62	8.55	14.80
	H2O	2.97	2.98	2.95	3.00	3.02	3.01	2.94	3.08	3.02	3.02	3.00
	Total	85.71	85.45	85.64	87.08	87.41	86.03	85.80	90.11	87.12	87.48	90.41

	Sample:										NiS	
	Notes:	Second Zone		Monticellite	Monticellite	orientated Pheno			Cross Cuts		Macrocryst	
		Inner Dark	RIM	light	dark	Dark core	light Fe rich	Dark outer rim	Botry Rim	Cross Cut	dark	light
Oxide%	**Na2O**	0	0	0	0.35	0	0	0	0	0	0	0
	MgO	32.93	32.66	27.68	29.22	35.94	32.04	35.29	31.48	32.26	37.76	35.9
	Al2O3	0	1.08	5.3	4.42	0	0	0	1.5	2.71	0	0
	SiO2	40.58	41.45	37.53	37.64	40.17	37.55	39.98	41.67	39.34	41.83	40.62
	CaO	0	0	0	0	0	0	0	0	0.48	0	0
	FeOT	7.85	10.42	17.07	16.27	7.77	16.66	7.42	10.66	11.12	6.15	9.27
	Total	82.04	85.9	87.59	87.82	84.58	86.85	83.2	85.48	86.1	86.23	86.22
Oxide%	**Na2O**	0.00	0.00	0.00	0.35	0.00	0.00	0.00	0.00	0.00	0.00	0.00
	MgO	32.93	32.66	27.68	29.22	35.94	32.04	35.29	31.48	32.26	37.76	35.90
	Al2O3	0.00	1.08	5.30	4.42	0.00	0.00	0.00	1.50	2.71	0.00	0.00
	SiO2	40.58	41.45	37.53	37.64	40.17	37.55	39.98	41.67	39.34	41.83	40.62
	CaO	0.00	0.00	0.00	0.00	0.00	0.00	0.00	0.00	0.48	0.00	0.00
	FeOT	7.85	10.42	17.07	16.27	7.77	16.66	7.42	10.66	11.12	6.15	9.27
	H2O	2.93	3.04	2.99	3.01	3.00	2.93	2.97	3.03	3.02	3.10	3.05
	Total	84.29	88.65	90.57	90.91	86.88	89.18	85.66	88.34	88.93	88.84	88.84

	Sample:		Megmaclast 2									
	Notes:	Rim	heno Orientated			Second Zone		Monticellite	Monticellite	Monticellite	eno Unorientated	
		lightest	Core	ark Middel Zor	Fe rich light	Dark	Botyr Rim	Light Core	Dark Rim	light core	Core	Dark Core
Oxide%	**Na2O**	0.34	0.33	0	0.43	0	0	0	0	0	0	0
	MgO	32.94	35.37	34.27	33.65	33.89	31.92	25.64	30.53	27.42	35.62	34.79
	Al2O3	2.04	0.54	0.5	0	0	1.04	5.75	2.5	5.38	0.49	0
	SiO2	40.42	40.26	40.44	38.4	41.6	40.69	37.02	40.36	37.38	40.6	40.98
	CaO	0	0	0	0	0	0	0	0.26	0	0	0
	FeOT	10.85	8.94	8.24	14.69	7.41	10.62	18.38	9.83	17.04	9.76	8.19
	Total	65.52	85.42	83.8	87.12	83.44	84.46	87.36	83.73	87.41	86.62	84.52

Oxide%	**Na2O**	0.34	0.33	0.00	0.43	0.00	0.00	0.00	0.00	0.00	0.00	0.00
	MgO	32.94	35.37	34.27	33.65	33.89	31.92	25.64	30.53	27.42	35.62	34.79
	Al2O3	2.04	0.54	0.50	0.00	0.00	1.04	5.75	2.50	5.38	0.49	0.00
	SiO2	40.42	40.26	40.44	38.40	41.60	40.69	37.02	40.36	37.38	40.60	40.98
	CaO	0.00	0.00	0.00	0.00	0.00	0.00	0.00	0.26	0.00	0.00	0.00
	FeOT	10.85	8.94	8.24	14.69	7.41	10.62	18.38	9.83	17.04	9.76	8.19
	H2O	3.06	3.04	2.99	2.99	2.99	2.99	2.95	2.98	2.98	3.07	3.01
	Total	89.65	88.48	86.44	90.16	85.89	87.26	89.74	86.46	90.20	89.54	86.97

	Sample:			Macrocryst		Magmaclast 3						
	Notes:			FeNiS		Pheno Orientated			Second Zone		Monticellite	Monticellite
		Fe Cross Cut	Bot Rim	Dark	Light	Core	Dark Inner Rim	Fe Zone	Dark Inner zone	Botry Rim	light	light
Oxide%	**Na2O**	0.41	0.45	0	0	0	0	0	0	0	0	0
	MgO	32.74	32.91	34.43	34.08	37.02	34.35	32.44	33.77	30.07	28.07	27.85
	Al2O3	0	1.13	0	0.87	0	0	0	0.47	1.33	4.46	5.41
	SiO2	37.44	41.43	42.32	41.36	39.85	40.4	37.51	41.93	40.61	37.87	38.67
	CaO	0	0	0	0	0	0	0	0	0	0	0
	FeOT	16.27	11	7.13	10.29	8.12	8.16	16.23	7.95	11.3	15.83	16.79
	Total	86.91	87.02	84.58	86.98	85.48	83.32	86.61	84.59	83.66	86.23	89.11

Oxide%	**Na2O**	0.41	0.45	0.00	0.00	0.00	0.00	0.00	0.00	0.00	0.00	0.00
	MgO	32.74	32.91	34.43	34.08	37.02	34.35	32.44	33.77	30.07	28.07	27.85
	Al2O3	0.00	1.13	0.00	0.87	0.00	0.00	0.00	0.47	1.33	4.46	5.41
	SiO2	37.44	41.43	42.32	41.36	39.85	40.40	37.51	41.93	40.61	37.87	38.67
	CaO	0.00	0.00	0.00	0.00	0.00	0.00	0.00	0.00	0.00	0.00	0.00
	FeOT	16.27	11.00	7.13	10.29	8.12	8.16	16.23	7.95	11.30	15.83	16.79
	H2O	2.95	3.07	3.04	3.07	3.03	2.97	2.93	3.03	2.95	2.97	3.05
	Total	89.81	89.99	86.92	89.67	88.02	85.88	89.11	87.15	86.26	89.20	91.77

	Sample:	NiS								CL-07-010-169	
	Notes:	Monticellite dark	Macrocryst Dark Core	Botry Rim	Pheno Unorientated m Cross Cutti	Dark Core	Lighter Core	Fe Zone	ark Second Zo	Botry Rim	Macrocrysts Core	Rim
Oxide%	**Na2O**	0	0.35	0	0	0.32	0	0	0	0	0	0
	MgO	30.9	33.66	31.7	31.91	35.34	35.44	32.52	33.62	31.56	37.37	39.2
	Al2O3	2.42	0	1.51	1.46	0	0.61	0	0.6	1.56	0.66	0.56
	SiO2	41.04	41.86	42.57	41.68	40.16	40.03	37.39	41.35	42.12	38.99	39.49
	CaO	0	0	0	0	0	0	0	0	0.2	0	0
	FeOT	9.97	7.06	11.11	10.69	7.41	9.08	17.3	7.58	12.24	2.63	2.64
	Total	84.71	83.27	87.07	86.01	83.7	85.15	87.26	83.44	87.85	79.94	82.17

Oxide%	**Na2O**	0.00	0.35	0.00	0.00	0.32	0.00	0.00	0.00	0.00	0.00	0.00
	MgO	30.90	33.66	31.70	31.91	35.34	35.44	32.52	33.62	31.56	37.37	39.20
	Al2O3	2.42	0.00	1.51	1.46	0.00	0.61	0.00	0.60	1.56	0.66	0.56
	SiO2	41.04	41.86	42.57	41.68	40.16	40.03	37.39	41.35	42.12	38.99	39.49
	CaO	0.00	0.00	0.00	0.00	0.00	0.00	0.00	0.00	0.20	0.00	0.00
	FeOT	9.97	7.06	11.11	10.69	7.41	9.08	17.30	7.58	12.24	2.63	2.64
	H2O	3.01	3.00	3.09	3.05	2.98	3.03	2.95	3.00	3.09	2.93	3.01
	Total	87.34	85.93	89.98	88.79	86.21	88.19	90.16	86.15	90.77	82.58	84.90

	Sample:	Groundmass	Pheno	Groundmass	Groundmass	Groundmass	Groundmass	Groundmass	Groundmass	Pheno		
	Notes:	Interstital 1	1	Rim around interstital	Between and Rim of Int	Rim around pheno	Interstital 2	Interstitial rim	granular	2 Core	dark rim inner rim	light rim outer rim
Oxide%	**Na2O**	0	0	0.38	0	0	0	0	0	0.38	0	0
	MgO	40.37	38.95	33.77	32.96	34.65	40.79	33.29	30.3	40.45	29.98	32.13
	Al2O3	0	0.47	3.34	1.69	2.96	0.42	2.85	2.73	0.5	0.77	2.88
	SiO2	41.46	40.04	39.75	38.19	40.05	41.47	38.35	35.08	40.67	33.95	38.02
	CaO	0	0	0	0	0	0	0	0.21	0	0	0
	FeOT	4.79	6.82	7.66	6.42	6.75	3.84	7.85	6.05	2.31	5.4	7.63
	Total	86.77	86.67	84.83	79.71	84.81	86.77	82.86	74.66	84.22	70.4	81.05

Oxide%	**Na2O**	0.00	0.00	0.38	0.00	0.00	0.00	0.00	0.00	0.38	0.00	0.00
	MgO	40.37	38.95	33.77	32.96	34.65	40.79	33.29	30.30	40.45	29.98	32.13
	Al2O3	0.00	0.47	3.34	1.69	2.96	0.42	2.85	2.73	0.50	0.77	2.88
	SiO2	41.46	40.04	39.75	38.19	40.05	41.47	38.35	35.08	40.67	33.95	38.02
	CaO	0.00	0.00	0.00	0.00	0.00	0.00	0.00	0.21	0.00	0.00	0.00
	FeOT	4.79	6.82	7.66	6.42	6.75	3.84	7.85	6.05	2.31	5.40	7.63
	H2O	3.15	3.10	3.05	2.86	3.05	3.16	2.95	2.68	3.10	2.53	2.90
	Total	89.77	89.38	87.95	82.12	87.46	89.68	85.29	77.05	87.41	72.63	83.56

	Sample:	Pheno	rim	Groundmass	Magmaclast			Monticellite	Monticellite	Monticellite	Interstital	
	Notes:	3		Granular	1			1	2	3		Dark
				Dark	Pheno	Pheno 2	Pheno 3	dark	light	light		inner rim
Oxide%	**Na2O**	0	0	0	0	0	0	0	0	0	0	0
	MgO	41.35	30.48	30.99	40.39	41.56	41.36	32.96	34.1	34.05	40.62	31.56
	Al2O3	0	2.08	1.87	0.47	0	0.57	2.79	4.6	4.43	0	0.54
	SiO2	41.99	35.88	35.31	41.46	42.1	41.24	38.18	39.98	39.94	41.36	36.02
	CaO	0	0	0.32	0	0	0	0	0.17	0.35	0	0
	FeOT	2	5.85	5.52	1.98	1.81	1.62	6.25	8.02	8.07	2.91	5.94
	Total	85.75	74.62	74.11	84.67	86.06	84.97	80.51	86.67	86.94	85.37	74.33
Oxide%	**Na2O**	0.00	0.00	0.00	0.00	0.00	0.00	0.00	0.00	0.00	0.00	0.00
	MgO	41.35	30.48	30.99	40.39	41.56	41.36	32.96	34.10	34.05	40.62	31.56
	Al2O3	0.00	2.08	1.87	0.47	0.00	0.57	2.79	4.60	4.43	0.00	0.54
	SiO2	41.99	35.88	35.31	41.46	42.10	41.24	38.18	39.98	39.94	41.36	36.02
	CaO	0.00	0.00	0.32	0.00	0.00	0.00	0.00	0.17	0.35	0.00	0.00
	FeOT	2.00	5.85	5.52	1.98	1.81	1.62	6.25	8.02	8.07	2.91	5.94
	H2O	3.15	2.69	2.68	3.12	3.16	3.13	2.90	3.12	3.12	3.12	2.67
	Total	88.49	76.98	76.69	87.42	88.63	87.92	83.08	89.99	89.96	88.01	76.73

	Sample:		Magmaclast 2					Pheno	
	Notes:	Light	Pheno	Vesicle	Monticellite		Monticellite	Core	Rim
		Botryiodal rim		Dominatly Cal	Core	Rim			
Oxide%	**Na2O**	0	0	0	0	0	0	0	0
	MgO	33.28	39.18	28.59	32.76	30.94	30.59	37.59	38.3
	Al2O3	2.83	0	1.84	2.14	1.47	4.16	0.5	0
	SiO2	39.33	40.13	33.81	37.92	34.53	36.69	38.56	39.95
	CaO	0	0	0.45	0	0.18	0.23	0	0
	FeOT	7.03	1.83	4.91	5.63	5.42	7.64	2.25	4.47
	Total	82.8	81.66	69.73	78.69	72.81	79.51	79.21	83.2
Oxide%	**Na2O**	0.00	0.00	0.00	0.00	0.00	0.00	0.00	0.00
	MgO	33.28	39.18	28.59	32.76	30.94	30.59	37.59	38.30
	Al2O3	2.83	0.00	1.84	2.14	1.47	4.16	0.50	0.00
	SiO2	39.33	40.13	33.81	37.92	34.53	36.69	38.56	39.95
	CaO	0.00	0.00	0.45	0.00	0.18	0.23	0.00	0.00
	FeOT	7.03	1.83	4.91	5.63	5.42	7.64	2.25	4.47
	H2O	2.98	3.00	2.53	2.85	2.62	2.85	2.91	3.01
	Total	85.45	84.14	72.13	81.30	75.16	82.46	81.81	85.73

Appendix D-3 Phlogopite and Spinels

Phlogopite

CL-06-003-222

	Sample	Macrocryst	Phlogopite 1	Macrocryst	Phlogopite	Phlogopite	Cumulate				
	Notes:			Rounded		Core	Core	Core	Rim	Rim	Rim
Oxide%											
	SiO2	36.32	35.97	36.12	36.24	42.48	42.27	41.42	37.8	36.26	40.69
	TiO2	4.07	4.68	4.3	4.19	0.68	0.5	0.6	3.75	3.7	1.93
	Al2O3	15.88	16.13	15.99	17.12	11.95	12.1	11.36	13.81	16.27	12.46
	Cr2O3	0.65	0.36	0.54	0	0.56	0.46	0.42	0.83	0	0.9
	FeO	4.83	5.08	4.94	4.53	4.29	3.98	3.82	5.46	5.6	5.03
	MgO	22.41	22.41	22.35	22.79	26.94	27.3	26.21	23.49	23.22	24.51
	Na2O	0.47	0	0.34	0.37	0	0	0	0	0	0
	K2O	9.92	9.73	9.88	9.84	10.84	11.15	10.56	9.52	10.04	10.27
	BaO	1.61	1.33	1.11	2.19	0	0	0	0.8	1.41	0
	Total	96.16	95.89	95.33	97.51	97.46	97.61	94.24	97.28	97.28	96.46
Oxide% Recalculated											
	SiO2	36.32	35.97	36.12	36.24	42.48	42.27	41.42	37.80	36.26	40.69
	TiO2	4.07	4.68	4.30	4.19	0.68	0.50	0.60	3.75	3.70	1.93
	Al2O3	15.88	16.13	15.99	17.12	11.95	12.10	11.36	13.81	16.27	12.46
	Cr2O3	0.65	0.36	0.54	0.00	0.56	0.46	0.42	0.83	0.00	0.90
	FeO	4.83	5.08	4.94	4.53	4.29	3.98	3.82	5.46	5.60	5.03
	MgO	22.41	22.41	22.35	22.79	26.94	27.30	26.21	23.49	23.22	24.51
	Na2O	0.47	0.00	0.34	0.37	0.00	0.00	0.00	0.00	0.00	0.00
	K2O	9.92	9.73	9.88	9.84	10.84	11.15	10.56	9.52	10.04	10.27
	BaO	1.61	1.33	1.11	2.19	0.00	0.00	0.00	0.80	1.41	0.00
	H2O	4.15	4.15	4.14	4.20	4.31	4.31	4.18	4.16	4.17	4.21
	Total	100.31	99.84	99.71	101.47	102.05	102.07	98.57	99.62	100.67	100.00

CL-07-006-208

Sample	Macrocryst Phlogopite 1		Macrocryst Phlogopite		Phlogopite Cumluate 1					Phlogpite cumulate 2	
Notes:	Rounded		Core	Rim	Resorbed					Core	Mid
Oxide%											
Na2O	0	0	0.86	0.7	0	0	0.39	0	0	0	0
MgO	21.69	22.19	22.82	22.7	24.83	24.5	22.01	23.11	22.72	23.22	23.15
Al2O3	17.4	16.79	15.47	16.84	16.71	16.39	14.09	16.71	16.52	17.06	15.48
SiO2	35.18	36	36.61	35.54	37.3	36.63	37.47	38.14	37.98	36.95	35.11
K2O	10.19	9.47	9.42	9.32	9.21	9.08	9.72	9.84	9.86	9.61	10.27
TiO2	3.55	3.94	3.92	4.22	1.14	0.92	4.03	2.26	2.35	0.65	0
Cr2O3	0	0.3	0	0	0.59	0.57	1.69	1.11	1.05	2.1	3.36
FeO	4.79	4.96	1.96	4.28	6.02	5.51	5.31	5.21	5.08	4.77	5.56
BaO	0	1.72	1.08	1.02	0	0	0	0.85	0.81	0	2.6
Total	92.8	95.1	96.15	95.81	95.97	94.15	95.94	97.58	96.44	94.84	95.59

Oxide% Recalculated											
Na2O	0	0	0.86	0.7	0	0	0.39	0	0	0	0
MgO	21.69	22.19	22.82	22.7	24.83	24.5	22.01	23.11	22.72	23.22	23.15
Al2O3	17.4	16.79	15.47	16.84	16.71	16.39	14.09	16.71	16.52	17.06	15.48
SiO2	35.18	36	36.61	35.54	37.3	36.63	37.47	38.14	37.98	36.95	35.11
K2O	10.19	9.47	9.42	9.32	9.21	9.08	9.72	9.84	9.86	9.61	10.27
Cr2O3	0	0.3	0	0	0.59	0.57	1.69	1.11	1.05	2.1	3.36
TiO2	3.55	3.94	3.92	4.22	1.14	0.92	4.03	2.26	2.35	0.65	0
FeO	4.79	4.96	1.96	4.28	6.02	5.51	5.31	5.21	5.08	4.77	5.56
BaO	0.00	1.72	1.08	1.02	0.00	0.00	0.00	0.85	0.81	0	2.6
H2O	4.07	4.14	4.07	4.13	4.22	4.12	4.13	4.25	4.21	4.15	4.05
Total	96.87	99.51	96.21	98.75	100.46	97.72	98.84	101.48	100.58	98.51	99.58

CL-07-006-208

	Sample	coarse grained			
	Notes:	Mid	Mid	Rim	Rim
Oxide%					
	Na2O	0.51	0.4	0	0
	MgO	24.44	24.37	24.66	23.03
	Al2O3	16.5	16.35	15.15	15.3
	SiO2	36.49	36.55	34.82	34.53
	K2O	8.91	9	7.09	8.11
	TiO2	0	0	0.96	0.95
	Cr2O3	1.77	1.71	1.32	1.64
	FeO	6.45	6.59	7.69	6.81
	Total	96.19	95.7	92.01	90.99

Oxide% Recalculated					
	Na2O	0.51	0.4	0	0
	MgO	24.44	24.37	24.66	23.03
	Al2O3	16.5	16.35	15.15	15.3
	SiO2	36.49	36.55	34.82	34.53
	K2O	8.91	9	7.09	8.11
	Cr2O3	1.77	1.71	1.32	1.64
	TiO2	0	0	0.96	0.95
	FeO	6.45	6.59	7.69	6.81
	H2O	4.15	4.14	4.01	3.94
	Total	99.22	99.11	95.70	94.31

CL-07-014-245

Sample Notes: Macrocryst Phlogopite 1 Macrocryst Phlogopite Phlogopite cumulate very fine grained

Oxide%

Na2O	0.37	0	0	0	0	0	0	0	0	0	0
MgO	9.19	9.3	35.98	34.75	26.57	24.86	24.78	24.07	24.11	23.82	23.4
Al2O3	17.39	17.28	4.83	5.31	16.51	16.98	16.78	17.01	17.1	16.83	17.6
SiO2	36.21	35.66	43.78	42.81	35.63	36.19	35.52	35.65	37.07	38.62	37.13
K2O	9.96	9.66	4.82	4.58	7.35	9.13	9.07	8.8	9.86	9.8	9.07
TiO2	3.51	3.68	0	0	1.34	1.4	1.63	2.57	2.51	2.9	1.44
Cr2O3	0	0	0	0	1.37	2.52	2.42	2.84	1.02	1.08	1.65
MnO	0	0.29	0	0.43	0	0	0	0	0	0	0
FeO	22.25	23.34	7	7.65	7.91	6.76	7.13	6.86	6.63	5.65	6.54
Total	98.83	99.08	95.99	95.68	97.47	97.92	97.76	98.51	98.66	99.22	96.36

Oxide% Recalculated

Na2O	0.37	0	0	0	0	0	0	0	0	0	0
MgO	9.19	9.3	35.98	34.75	26.57	24.86	24.78	24.07	24.11	23.82	23.4
Al2O3	17.39	17.28	4.83	5.31	16.51	16.98	16.78	17.01	17.1	16.83	17.6
SiO2	36.21	35.66	43.78	42.81	35.63	36.19	35.52	35.65	37.07	38.62	37.13
K2O	9.96	9.66	4.82	4.58	7.35	9.13	9.07	8.8	9.86	9.8	9.07
Cr2O3	0	0	0	0	1.37	2.52	2.42	2.84	1.02	1.08	1.65
MnO	0	0.29	0	0.43	0	0	0	0	0	0	0
TiO2	3.51	3.68	0	0	1.34	1.4	1.63	2.57	2.51	2.9	1.44
FeO	22.25	23.34	7	7.65	7.91	6.76	7.13	6.86	6.63	5.65	6.54
H2O	4.02	4.01	4.32	4.26	4.22	4.25	4.21	4.24	4.28	4.33	4.24
Total	102.90	103.22	100.73	99.79	100.90	102.09	101.54	102.04	102.58	103.03	101.07

CL-07-014-245

	Sample	Phlogopite cumulate 2 coarse grained					
	Notes:						
Oxide%							
	Na2O	0	0	0	0	0	0
	MgO	23.23	24.12	24.3	24.75	23.22	23.19
	Al2O3	16.48	17.3	17.87	17.33	13.19	13.53
	SiO2	37	37.81	37.32	37.22	38.87	39.58
	K2O	9.47	9.66	8.57	9.01	9.86	10.19
	TiO2	1.53	1.12	0	1.4	5.22	4.81
	Cr2O3	1.63	1.22	1.02	1.07	1.76	1.88
	MnO	0	0	0	0	0	0
	FeO	6.31	6.75	7.62	7.09	4.94	4.71
	BaO	0	0.98	0	0	0	0
	Total	95.78	98.94	98.49	98.14	97.81	98.62

Oxide% Recalculated							
	Na2O	0	0	0	0	0	0
	MgO	23.23	24.12	24.3	24.75	23.22	23.19
	Al2O3	16.48	17.3	17.87	17.33	13.19	13.53
	SiO2	37	37.81	37.32	37.22	38.87	39.58
	K2O	9.47	9.66	8.57	9.01	9.86	10.19
	Cr2O3	1.63	1.22	1.02	1.07	1.76	1.88
	MnO	0	0	0	0	0	0
	TiO2	1.53	1.12	0	1.4	5.22	4.81
	FeO	6.31	6.75	7.62	7.09	4.94	4.71
	BaO	0	0.98	0	0	0	0
	H2O	4.18	4.29	4.23	4.28	4.25	4.29
	Total	99.83	103.25	100.93	102.15	101.31	102.18

CL-07-014-257

	Sample	Macrocryst Phlogopite In Magmaclast				Macrocryst Phlogopite Phlogopite Cumluate 1						
	Notes:											
Oxide%												
	Na2O	0	0.36	0	0	0	0	0	0	0	0	0
	MgO	21.3	22.96	22.93	22.97	26.48	26.68	21.88	24.79	24.6	22.42	22.09
	Al2O3	15.4	15.93	17.15	16.96	10.87	11.04	14.59	16.72	16.2	14.79	15.32
	SiO2	36.26	36.59	35.72	35.92	41.73	42.02	39.08	36.07	36.1	37.41	37.96
	K2O	9.87	9.65	9.33	9.35	10.81	10.79	10.24	8.76	8.66	10.43	10.19
	TiO2	5.25	4.5	4.16	4.4	0.47	0.5	3.42	1.46	1.39	3.39	3.17
	Cr2O3	1.01	0.33	0.53	0.41	0	0.3	2.74	1.91	1.63	2.4	2.35
	FeO	4.86	5.33	4.82	4.86	5.13	5.11	4.52	6.95	6.79	4.81	5.09
	BaO	0	1.49	1.87	1.89	0	0	0	0	0	0	0
	Total	95.54	97.3	96.61	96.66	95.84	96.31	97.91	97.28	95.87	96.69	96.46

Oxide% Recalculated												
	Na2O	0	0.36	0	0	0	0	0	0	0	0	0
	MgO	21.3	22.96	22.93	22.97	26.48	26.68	21.88	24.79	24.6	22.42	22.09
	Al2O3	15.4	15.93	17.15	16.96	10.87	11.04	14.59	16.72	16.2	14.79	15.32
	SiO2	36.26	36.59	35.72	35.92	41.73	42.02	39.08	36.07	36.1	37.41	37.96
	K2O	9.87	9.65	9.33	9.35	10.81	10.79	10.24	8.76	8.66	10.43	10.19
	Cr2O3	1.01	0.33	0.53	0.41	0	0.3	2.74	1.91	1.63	2.4	2.35
	TiO2	5.25	4.5	4.16	4.4	0.47	0.5	3.42	1.46	1.39	3.39	3.17
	FeO	4.86	5.33	4.82	4.86	5.13	5.11	4.52	6.95	6.79	4.81	5.09
	BaO	0	1.49	1.87	1.89	0	0	0	0	0	0	0
	H2O	4.11	4.20	4.18	4.19	4.19	4.24	4.23	4.21	4.16	4.17	4.20
	Total	98.06	101.34	100.69	100.95	99.68	100.68	100.70	100.87	99.53	99.82	100.37

CL-07-014-257

	Sample	Phlogopite Ccumluate 2						
	Notes:							
Oxide%								
	Na2O	0	0	0	0	0	0	0
	MgO	23.38	25.77	25.75	26.72	23.53	23.24	22.87
	Al2O3	14.67	17.73	17.66	15.96	13.79	14.21	13.9
	SiO2	38.48	35.36	35.79	35.31	38.6	39.15	38.68
	K2O	9.58	8.65	8.68	6.96	9.06	9.36	9
	TiO2	3.33	0	0	0	4.26	4.86	4.08
	Cr2O3	2.13	2.03	2.09	1.22	2.12	1.91	2.15
	FeO	5.36	6.71	6.92	8.08	5.34	4.62	5.59
	Total	97.82	97.91	98.09	94.41	97.18	96.29	96.58

Oxide% Recalculated								
	Na2O	0	0	0	0	0	0	0
	MgO	23.38	25.77	25.75	26.72	23.53	23.24	22.87
	Al2O3	14.67	17.73	17.66	15.96	13.79	14.21	13.9
	SiO2	38.48	35.36	35.79	35.31	38.6	39.15	38.68
	K2O	9.58	8.65	8.68	6.96	9.06	9.36	9
	Cr2O3	2.13	2.03	2.09	1.22	2.12	1.91	2.15
	TiO2	3.33	0	0	0	4.26	4.86	4.08
	FeO	5.36	6.71	6.92	8.08	5.34	4.62	5.59
	H2O	4.24	4.19	4.22	4.12	4.24	4.29	4.22
	Total	101.17	100.44	101.11	98.37	100.94	101.64	100.49

Spinels

CL-06-003-222 Locations are based on spinel grains within the cumulate.

	Sample	Phlogopite Cumulate 1 - Macrocryst?						Phlogopite Cumulate 2				
	Notes:	Core	Mid	Core	Mid	Edge	Edge					
Oxide%	**MgO**	11.03	10.39	12.87	14.11	12.29	12.54	16	14.5	15.73	16.42	16.42
	Al2O3	2.66	3.13	3.14	3.67	3.58	3.5	14.14	10.58	10.78	14.68	14.66
	TiO2	3.44	3.4	4.28	3.8	3.7	3.49	11.33	6.94	17.65	12.26	12.95
	Cr2O3	53.26	49.57	49.16	47.93	50.3	51.32	12.63	33.15	3.4	10.64	9.61
	MnO	0	0	0	0	0	0	0.53	0	0.51	0	0.55
	FeOT	28.49	31.51	29.73	29.52	29.41	28.02	43.29	32.75	49.75	43.14	43.53
	Total	99.77	98.38	98.92	99.3	98.91	98.94	98.03	98.24	98.82	97.5	98.98
Oxide wt%	Recalculated											
	TiO2	3.44	3.40	4.28	3.80	3.70	3.49	11.33	6.94	17.65	12.26	12.95
	Al2O3	2.66	3.13	3.14	3.67	3.58	3.50	14.14	10.58	10.78	14.68	14.66
	FeO	18.55	19.33	16.72	14.46	17.17	16.44	19.27	17.43	24.85	19.82	19.84
	Fe2O3	11.05	13.54	14.46	16.74	13.60	12.87	26.69	17.03	27.67	25.92	26.32
	MnO	0.00	0.00	0.00	0.00	0.00	0.00	0.53	0.00	0.51	0.00	0.55
	MgO	11.03	10.39	12.87	14.11	12.29	12.54	16.00	14.50	15.73	16.42	16.42
	Cr2O3	53.26	49.57	49.16	47.93	50.30	51.32	12.63	33.15	3.40	10.64	9.61
	Total	99.99	99.36	100.63	100.71	100.64	100.16	100.59	99.63	100.59	99.74	100.63

CL-06-003-222

	Sample Notes:	
Oxide%	**MgO**	16.59
	Al2O3	15.21
	TiO2	10.98
	Cr2O3	11.7
	MnO	0
	FeOT	43.25
	Total	98.24
Oxide wt%	Recalculated	
	TiO2	10.98
	Al2O3	15.21
	FeO	18.70
	Fe2O3	27.28
	MnO	0.00
	MgO	16.59
	Cr2O3	11.70
	Total	100.46

CL-07-006-208

	Sample	Phlogopite Cumulate 1			
	Notes:	Core	Mid	Edge	Mid
Oxide%	**MgO**	16.87	18.79	16.08	16.17
	Al2O3	17.64	12.87	15.07	17.18
	TiO2	11.86	14.77	14.11	11.06
	Cr2O3	8.11	7.02	7.35	12.56
	MnO	0	0	0	0
	FeOT	42.49	43.67	44.18	40.39
	Total	97.52	97.94	97.14	98.13
Oxide wt%	Recalculated				
	TiO2	11.86	14.77	14.11	11.06
	Al2O3	17.64	12.87	15.07	17.18
	FeO	19.18	18.20	21.94	19.54
	Fe2O3	25.90	28.31	24.72	23.17
	MnO	0.00	0.00	0.00	0.00
	MgO	16.87	18.79	16.08	16.17
	Cr2O3	8.11	7.02	7.35	12.56
	Total	99.57	99.96	99.27	99.68

CL-07-014-245

	Sample	Phlogopite Cumulate 1		
	Notes:	Core	Core	Edge
Oxide%	**MgO**	16.6	16.81	17.67
	Al2O3	8.15	8.45	10.78
	TiO2	15.82	15.38	17.75
	Cr2O3	5.45	5.12	4.84
	MnO	0.64	0.68	0
	FeOT	50.08	50.89	47.1
	Total	97.77	97.51	98.78
Oxide wt%	Recalculated			
	TiO2	15.82	15.38	17.75
	Al2O3	8.15	8.45	10.78
	FeO	21.05	20.56	22.58
	Fe2O3	32.26	33.71	27.25
	MnO	0.64	0.68	0.00
	MgO	16.60	16.81	17.67
	Cr2O3	5.45	5.12	4.84
	Total	99.97	100.71	100.87

CL-07-014-257

	Sample	Phlogopite Cumulate 1			
	Notes:	core	Edge	Edge	Mid
Oxide%	**MgO**	17.61	16.23	15.59	16.75
	Al2O3	15.87	10.69	10.6	9.78
	TiO2	11.16	19.01	16.34	16.87
	Cr2O3	10.98	2.99	7.01	5.31
	MnO	0	0	0.9	0.97
	FeOT	42.2	49.66	46.62	51.9
	Total	97.77	98.66	97.06	101.7
Oxide wt%	Recalculated				
	TiO2	17.78	16.82	10.28	8.22
	Al2O3	8.38	9.96	17.55	25.08
	FeO	23.81	23.73	16.77	15.22
	Fe2O3	29.88	29.83	24.94	21.31
	MnO	0.00	0.85	0.00	0.00
	MgO	16.39	15.52	17.57	18.20
	Cr2O3	3.57	3.28	12.70	11.87
	Total	99.81	99.99	99.81	99.91

CL-07-014-257

	Sample	Phlogopite Cumulate grain 2				
	Notes:	Edge	Edge	Mid	Core	Edge
Oxide%	**MgO**	16.39	15.52	17.57	18.2	13.72
	Al2O3	8.38	9.96	17.55	25.08	10.05
	TiO2	17.78	16.82	10.28	8.22	4.23
	Cr2O3	3.57	3.28	12.7	11.87	43.02
	MnO	0	0.85	0	0	0
	FeOT	50.7	50.57	39.21	34.4	28.42
	Total	97.25	97.3	98.06	97.91	99.32
Oxide wt%	Recalculated					
	TiO2	4.23	11.16	19.01	16.34	16.87
	Al2O3	10.05	15.87	10.69	10.60	9.78
	FeO	16.52	17.44	26.03	23.19	23.24
	Fe2O3	13.22	27.52	26.26	26.04	31.85
	MnO	0.00	0.00	0.00	0.90	0.97
	MgO	13.72	17.61	16.23	15.59	16.75
	Cr2O3	43.02	10.98	2.99	7.01	5.31
	Total	100.76	100.58	101.21	99.67	104.77

Appendix D-4 Olivine

Sample No.:		CL-06-003-195										
		Magmaclast 1			Magmaclast 2							M 3
	Note:	Phenocryst	Phenocryst	Phenocryst	Phenocryst	Phenocryst	Macrocryst	Macrocryst	Macrocryst	Macrocryst	Macrocryst	Phenocryst
Oxide%	**MgO**	48.64	49.79	49.34	50.26	49.04	49.95	49.92	51.35	50.90	50.99	49.63
	SiO2	41.48	41.29	42.33	39.15	41.28	41.38	41.76	41.27	41.42	41.39	40.84
	FeO	9.86	8.26	7.65	9.46	10.10	8.37	7.98	8.04	7.64	7.73	8.80
	Total	99.78	99.94	99.54	99.49	100.64	99.72	100.28	100.66	99.99	100.14	99.81
No. Ions in Formula												
	Mg	1.77	1.81	1.80	1.83	1.79	1.82	1.82	1.87	1.85	1.86	1.81
	Si	1.01	1.01	1.03	0.96	1.01	1.01	1.02	1.01	1.01	1.01	1.00
	Fe	0.20	0.17	0.16	0.19	0.21	0.17	0.16	0.16	0.16	0.16	0.18
End Members												
	Fo	90	91	92	90	90	91	92	92	92	92	91
	Fa	10.21	8.51	8.00	9.55	10.36	8.59	8.23	8.07	7.77	7.84	9.05

Sample No.:												
	Note:	Phenocryst	Phenocryst	Macrocryst	Macrocryst				Macrocryst			
					Same Grain, No Zoning				Same Grain, No Zoning			
Oxide%	**MgO**	49.40	50.75	47.95	49.86	49.51	48.37	48.68	48.15	48.91	48.46	48.55
	SiO2	40.32	40.62	41.63	40.91	40.90	40.97	40.90	40.76	40.60	40.92	40.62
	FeO	8.87	8.39	9.96	9.55	9.18	9.85	10.10	10.86	10.38	10.37	10.84
	Total	98.95	99.63	99.62	99.95	99.79	99.70	99.96	99.88	99.82	99.64	100.21
No. Ions in Formula												
	Mg	1.80	1.85	1.75	1.82	1.80	1.76	1.77	1.75	1.78	1.77	1.77
	Si	0.99	0.99	1.02	1.00	1.00	1.00	1.00	1.00	0.99	1.00	0.99
	Fe	0.18	0.17	0.20	0.20	0.19	0.20	0.21	0.22	0.21	0.21	0.22
End Members												
	Fo	91	92	90	90	91	90	90	89	89	89	89
	Fa	9.15	8.49	10.44	9.70	9.42	10.25	10.43	11.23	10.64	10.72	11.13

Sample No.:						CL-06-003-205						
		Magmaclast 4										
	Note:	Phenocryst		Phenocryst	Phenocryst	Macrocryst		Macrocryst		Macrocryst	Macrocryst	Macrocryst
			Same Grain			Same Grain, No Zonin		Same Grain, No Zoning				
Oxide%	**MgO**	47.96	48.96	49.24	49.02	51.16	50.26	50.27	49.98	51.12	50.46	50.66
	SiO2	42.75	40.98	40.01	40.41	41.92	40.73	40.49	40.15	39.15	40.68	40.98
	FeO	8.86	9.79	10.27	9.72	7.75	8.01	8.83	9.48	9.11	8.65	8.43
	Total	99.70	99.95	99.91	99.71	100.93	99.22	99.65	99.60	99.99	100.11	99.87
No. Ions in Formula												
	Mg	1.75	1.78	1.79	1.79	1.83	1.80	1.80	1.79	1.83	1.81	1.81
	Si	1.04	1.00	0.98	0.99	1.01	0.98	0.97	0.96	0.94	0.98	0.98
	Fe	0.18	0.20	0.21	0.20	0.16	0.16	0.18	0.19	0.18	0.17	0.17
End Members												
	Fo	91	90	90	90	92	92	91	90	91	91	91
	Fa	9.39	10.09	10.48	10.01	7.83	8.21	8.97	9.62	9.09	8.77	8.54

Sample No.:										CL-06-003-219		
	Note:	Macrocryst			Macrocryst					Macrocryst	Macrocryst	Macrocryst
		Same Grain, No Zoning			Same Grain, No Zoning							
Oxide%	**MgO**	50.27	50.53	50.70	50.57	50.86	50.44	50.34	51.05	48.97	49.95	48.87
	SiO2	40.66	40.36	40.96	41.20	41.23	41.30	41.47	40.58	40.24	40.20	40.63
	FeO	8.83	8.27	8.66	7.87	8.43	8.69	7.87	8.92	9.97	9.30	10.41
	Total	99.77	99.51	100.31	99.68	100.52	99.88	99.79	100.55	99.20	99.82	99.64
No. Ions in Formula												
	Mg	1.80	1.81	1.81	1.81	1.82	1.81	1.80	1.83	1.80	1.84	1.80
	Si	0.98	0.97	0.98	0.99	0.99	0.99	1.00	0.97	0.99	0.99	1.00
	Fe	0.18	0.17	0.17	0.16	0.17	0.17	0.16	0.18	0.21	0.19	0.22
End Members												
	Fo	91	92	91	92	91	91	92	91	90	91	89
	Fa	8.97	8.41	8.74	8.03	8.51	8.81	8.06	8.93	10.25	9.46	10.67

Sample No.: CL-06-003-222

	Note:	Macrocryst	Macrocryst	Macrocryst	Macrocryst	Macrocryst	Macrocryst		Phenocryst	Macrocryst	Macrocryst	Macrocryst
							Same Grain, No Zoning					
Oxide%	**MgO**	50.48	50.62	49.79	52.40	48.11	49.50	49.04	48.70	51.03	49.91	50.71
	SiO2	41.20	41.19	40.58	40.78	38.99	40.33	40.31	39.91	40.64	40.66	41.32
	FeO	8.61	8.02	8.98	6.92	12.90	9.39	10.72	10.27	8.00	8.90	7.36
	Total	100.40	99.84	99.48	100.00	99.83	99.76	100.28	99.15	99.88	99.74	99.64
No. Ions in Formula												
	Mg	1.86	1.87	1.83	1.93	1.77	1.82	1.81	1.80	1.89	1.85	1.88
	Si	1.02	1.02	1.00	1.01	0.96	1.00	1.00	0.99	1.01	1.01	1.03
	Fe	0.18	0.17	0.19	0.14	0.27	0.19	0.22	0.21	0.17	0.18	0.15
End Members												
	Fo	91	92	91	93	87	90	89	89	92	91	92
	Fa	8.73	8.16	9.19	6.90	13.08	9.62	10.92	10.58	8.08	9.09	7.53

Sample No.: Magmaclast 1

	Note:	Macrocrysts	Macrocrysts	Macrocrysts	Macrocrysts		Macrocryst	Phenocryst	Phenocryst	Phenocryst	Macorcryst	Macorcryst
					same grain							
Oxide%	**MgO**	49.13	50.14	49.27	48.29	49.99	49.73	49.52	48.95	49.66	48.14	48.45
	SiO2	40.91	40.77	40.43	41.01	38.10	40.24	41.66	41.32	40.86	40.52	40.23
	FeO	9.08	9.01	9.82	10.53	12.20	9.77	8.61	9.08	9.80	11.20	10.71
	Total	99.38	100.03	99.86	100.01	100.00	100.00	99.79	99.66	100.40	99.90	99.65
No. Ions in Formula												
	Mg	1.82	1.86	1.82	1.79	1.85	1.84	1.80	1.78	1.80	1.75	1.76
	Si	1.02	1.01	1.00	1.02	0.95	1.00	1.01	1.01	0.99	0.99	0.98
	Fe	0.19	0.19	0.20	0.22	0.25	0.20	0.18	0.18	0.20	0.23	0.22
End Members												
	Fo	91	91	90	89	88	90	91	91	90	88	89
	Fa	9.39	9.16	10.06	10.90	12.04	9.93	8.89	9.43	9.97	11.55	11.03

Sample No.:						CL-06-003-236						
						Magmaclast 1						
	Note:	Macorcryst	Macorcryst	Macorcryst	Macorcryst	Macorcryst	Phenocryst	Phenocryst	Phenocryst	Macorcryst	Macorcryst	Macorcryst
Oxide%	**MgO**	51.20	51.47	50.33	48.00	48.33	49.52	48.95	49.66	48.14	48.45	51.2
	SiO2	41.87	41.13	41.22	40.58	40.56	41.66	41.32	40.86	40.52	40.23	41.87
	FeO	7.41	7.44	9.03	10.87	10.40	8.61	9.08	9.8	11.2	10.71	7.41
	Total	100.24	100.13	100.56	99.65	99.32	99.79	99.66	100.4	99.9	99.65	100.24
No. Ions in Formula												
	Mg	1.86	1.87	1.83	1.74	1.75	1.80	1.78	1.80	1.75	1.76	1.86
	Si	1.02	1.00	1.00	0.99	0.99	1.01	1.01	0.99	0.99	0.98	1.02
	Fe	0.15	0.15	0.18	0.22	0.21	0.18	0.18	0.20	0.23	0.22	0.15
End Members												
	Fo	92	92	91	89	89	91	91	90	88	89	92
	Fa	7.51	7.50	9.15	11.27	10.77	8.89	9.43	9.97	11.55	11.03	7.51

Sample No.:						CL-07-014-257						
	Note:	Macorcryst	Macorcryst	Macorcryst	Macorcryst	Phenocryst	Macrocryst	Macrocryst	Phenocryst	Phenocryst	Macrocryst	
											Same Grain, No Zone	
Oxide%	**MgO**	51.47	50.33	48	48.33	50.65	51.13	49.50	49.37	49.62	50.51	50.54
	SiO2	41.13	41.22	40.58	40.56	40.27	41.14	39.35	40.54	39.15	40.43	40.61
	FeO	7.44	9.03	10.87	10.4	8.36	7.57	10.70	10.45	10.58	8.70	8.86
	Total	100.13	100.559	99.65	99.32	99.91	99.95	99.74	100.37	99.80	99.65	100.02
No. Ions in Formula												
	Mg	1.87	1.83	1.74	1.75	1.85	1.87	1.81	1.81	1.81	1.85	1.85
	Si	1.00	1.00	0.99	0.99	0.99	1.01	0.97	0.99	0.96	0.99	1.00
	Fe	0.15	0.18	0.22	0.21	0.17	0.16	0.22	0.21	0.22	0.18	0.18
End Members												
	Fo	92	91	89	89	92	92	89	89	89	91	91
	Fa	7.50	9.15	11.27	10.77	8.48	7.67	10.82	10.61	10.68	8.81	8.95

Sample No.:

	Note:	Macrocryst	Macrocryst	Pyrocryst	Pyrocryst
Oxide%	**MgO**	50.28	50.59	49.42	49.36
	SiO2	40.89	41.08	41.03	39.70
	FeO	8.51	8.76	9.09	11.01
	Total	99.99	100.43	99.70	100.06
No. Ions in Formula					
	Mg	1.84	1.85	1.81	1.81
	Si	1.00	1.01	1.01	0.97
	Fe	0.17	0.18	0.19	0.23
End Members					
	Fo	91	91	91	89
	Fa	8.67	8.85	9.35	11.12

Appendix D-5 Carbonates

	Sample	CL-06-003-173										
	Notes:	Cored PMO	Interstitial	Core PMO	Interstitial	Cored PMO	Interstitial	Cored PMO	Interstitial	Cored Pheno	Edge of Pheno	Interstitial
Oxide%												
	MgO	17.09	19.67	17.72	19.15	17.88	20.25	17.23	18.02	19.42	18.19	18.76
	CaO	32.08	30.14	31.66	31.31	33.09	32.25	32.53	32.74	31.31	27.39	31.39
	MnO	1.08	0.52	1.91	0.38	0.91	0	1.83	1.12	0	0	0.59
	FeOT	0.77	2.32	0	1.77	1.06	1.39	1.1	2.14	2.05	8.2	1.93
	SrO	0	0	0	0	0	0	0	0	0	0	0
	BaO	0	0	0	0	0	0	0	0	0	0	0
	Total	51.23	52.92	51.85	50.67	53.77	54.45	52.85	54.93	53.46	54.28	52.48
Oxide%												
	MgCO3	35.75	41.15	37.07	40.06	37.40	42.36	36.04	37.70	40.62	38.05	39.24
	CaCO3	57.25	53.79	56.50	55.88	59.06	57.56	58.06	58.43	55.88	48.88	56.02
	MnCO3	1.75	0.84	3.10	0.62	1.47	0.00	2.97	1.81	0.00	0.00	0.96
	FeCO3	1.24	3.74	0.00	2.85	1.71	2.24	1.77	3.45	3.31	13.22	3.11
	SrCO3	0.00	0.00	0.00	0.00	0.00	0.00	0.00	0.00	0.00	0.00	0.00
	BaCO3	0.00	0.00	0.00	0.00	0.00	0.00	0.00	0.00	0.00	0.00	0.00
	Total	96.00	99.52	96.67	99.41	99.64	102.16	98.84	101.39	99.81	100.16	99.33

	Sample			CL-06-007-182								
	Notes:	Interstitial		Core of Macro		Groundmass		Groundmass		Groundmass		Vesicle
		Core	Rim	core	edge	core	Rim	Core	Rim	Core	Rim	Core
Oxide%												
	MgO	19.57	18.36	0.64	1.02	2.08	1.14	1.04	1.55	0.68	2.23	2.49
	CaO	30.13	30.25	50.76	51.55	49.28	50.11	51.57	49.98	51.71	49.25	50.58
	MnO	0	0.52	0.65	0.57	0	0.5	0.43	0.42	0	0.52	0
	FeOT	0	1.88	0	0	1.55	0	0	0	0	1.38	0.67
	SrO	0	0	0	0	0	0.51	0	0.45	0	0	0
	BaO	0	0	0	0	0	1.22	0	0.81	0	0	0
	Total	50.1	50.93	52.31	53.29	53.26	53.78	53.18	53.46	53.23	53.35	53.12
Oxide%												
	MgCO3	40.94	38.41	1.34	2.13	4.35	2.38	2.18	3.24	1.42	4.66	5.21
	CaCO3	53.77	53.99	90.59	92.00	87.95	89.43	92.04	89.20	92.29	87.90	90.27
	MnCO3	0.00	0.84	1.05	0.92	0.00	0.81	0.70	0.68	0.00	0.84	0.00
	FeCO3	0.00	3.03	0.00	0.00	2.50	0.00	0.00	0.00	0.00	2.23	1.08
	SrCO3	0.00	0.00	0.00	0.00	0.00	0.73	0.00	0.64	0.00	0.00	0.00
	BaCO3	0.00	0.00	0.00	0.00	0.00	1.50	0.00	1.00	0.00	0.00	0.00
	Total	94.71	96.27	92.99	95.06	94.80	94.86	94.91	94.76	93.71	95.63	96.56

Sample							CL-07-010-169				
Notes:		Vesicle		Vesicle		Macro	In Macro	In Macro		In Macro	
	Rim	ı cross sectional		Core	Rim		Single Grains	Single Grains		One Grain	
Oxide%											
MgO	1.34	0.64	1.27	2.32	2.19	0.67	18.1	21.46	17.8	17.82	18.26
CaO	51.03	50.46	50.9	52.07	51.27	52.61	32.98	32.85	32.91	32.53	33.64
MnO	0	0	0.5	0	0	0.44	1.03	0.35	0.6	0.51	0
FeOT	0.35	0.5	0.58	0	0.47	0	0	0.4	0	0	0
SrO	0.62	0.38	0.5	0	0	0	0	0	0	0	0
BaO	1.02	0.93	1.58	0	0	0	0	0	0	0	0
Total	54.41	53.04	55.34	54.65	54.28	53.94	52.29	55.08	51.48	50.86	52.18
Oxide%											
MgCO3	2.80	1.34	2.66	4.85	4.58	1.40	37.86	44.89	37.23	37.28	38.20
CaCO3	91.07	90.06	90.84	92.93	91.50	93.89	58.86	58.63	58.74	58.06	60.04
MnCO3	0.00	0.00	0.81	0.00	0.00	0.71	1.67	0.57	0.97	0.83	0.00
FeCO3	0.56	0.81	0.94	0.00	0.76	0.00	0.00	0.65	0.00	0.00	0.00
SrCO3	0.88	0.54	0.71	0.00	0.00	0.00	0.00	0.00	0.00	0.00	0.00
BaCO3	1.26	1.15	1.95	0.00	0.00	0.00	0.00	0.00	0.00	0.00	0.00
Total	96.58	93.89	97.91	97.78	96.84	96.01	98.39	104.73	96.94	96.16	98.24

Sample									
Notes:		Interstitial Groundmass			Interstitial GM		Vesicle	Vesicle	
		anhedral			In GM	Out of GM			
Oxide%									
MgO	0.5	0	0	0.36	0.54	0	0.29	0	0.33
CaO	53.27	52.66	52.09	51.98	52.21	53.68	53.45	52.93	52.7
MnO	0.37	0.85	0.46	0	0.83	0	0	0	0
FeOT	0	0	0	0	0	0	0	0	0
SrO	0	0	0	0	0	0	0.34	0	0.37
BaO	0	0	0	0.62	0	0.66	1.01	0.46	0
Total	54.21	54.08	52.48	53.75	53.3	54.59	55.34	53.89	53.41
Oxide%									
MgCO3	1.05	0.00	0.00	0.75	1.13	0.00	0.61	0.00	0.69
CaCO3	95.07	93.98	92.97	92.77	93.18	95.80	95.39	94.47	94.06
MnCO3	0.60	1.38	0.75	0.00	1.34	0.00	0.00	0.00	0.00
FeCO3	0.00	0.00	0.00	0.00	0.00	0.00	0.00	0.00	0.00
SrCO3	0.00	0.00	0.00	0.00	0.00	0.00	0.48	0.00	0.53
BaCO3	0.00	0.00	0.00	0.76	0.00	0.81	1.25	0.57	0.00
Total	96.72	95.36	93.71	94.29	95.66	96.62	97.73	95.03	95.27

Appendix D-6 Perovskite

	CL-06-003-173						CL-06-003-182					
Sample	Lapilli 1		Pyrocryst 2	Pyrocryst 3	Pyrocryst 4	Pyrocryst 5	Lapilli 1				Lapilli 2	
Note:	Pyrocryst 1	Interclast									Adjacent to lapilli 1	
	2	3	2	3	2	2	3	3	3	3	2	3
Na2O	0.56	0.41	0.8	0	0.46	0.62	0.51	0.55	0	0.44	0.54	0.51
CaO	35	36.75	35.45	35.88	36.03	34.99	36.52	36.74	36.64	36.69	37.14	39.2
TiO2	52.64	52.09	52.29	52.79	52.34	52.13	54.75	54.35	53.81	53.34	54.61	56.16
FeO	0	1.21	1.63	1.36	1.61	1.51	1.76	1.64	1.34	1.14	1.38	1.47
SrO	1.14	0	0	0	0	0.62	0.51	0	0	0.34	0	0
Nb2O5	0	1.08	1.61	0.93	0.91	0.6	0.96	0.76	1.03	0.71	1	1.07
BaO	0	0	0	0	0	1.9	0	0	0	0	0	0
La2O3	0	0	2.2	0	2.04	2.52	0	0	0	2.52	0	0
Ce2O3	2.51	2.91	2.85	2.65	2.27	2.57	3.11	2.8	2.08	2.53	2.71	1.76
Pr2O3	0	1.19	0	1.74	0	0	0	0	0	0	0	0
Nd2O3	1.76	1.1	1.27	0	1.3	1.22	0	0	1.08	0.99	0	0
Total	99.84	99.21	100.13	99.78	99.64	99.48	100.02	99.88	99.14	99.98	100.54	100.82
Na	0.11	0.08	0.15	0.00	0.09	0.12	0.09	0.10	0.00	0.08	0.10	0.09
Ca	3.74	3.84	3.67	3.77	3.76	3.66	3.71	3.77	3.79	3.77	3.78	3.87
Ti	3.95	3.82	3.80	3.89	3.83	3.82	3.91	3.91	3.91	3.84	3.90	3.89
Fe	0.00	0.10	0.13	0.11	0.13	0.12	0.14	0.13	0.11	0.09	0.11	0.11
Sr	0.07	0.00	0.00	0.00	0.00	0.04	0.03	0.00	0.00	0.02	0.00	0.00
Nb	0.00	0.05	0.07	0.04	0.04	0.03	0.04	0.03	0.04	0.03	0.04	0.04
Ba	0.00	0.00	0.00	0.00	0.00	0.07	0.00	0.00	0.00	0.00	0.00	0.00
La	0.00	0.00	0.08	0.00	0.07	0.09	0.00	0.00	0.00	0.09	0.00	0.00
Ce	0.09	0.10	0.10	0.10	0.08	0.09	0.11	0.10	0.07	0.09	0.09	0.06
Pr	0.00	0.04	0.00	0.06	0.00	0.00	0.00	0.00	0.00	0.00	0.00	0.00
Nd	0.06	0.04	0.04	0.00	0.05	0.04	0.00	0.00	0.04	0.03	0.00	0.00
Total	8.02	8.06	8.05	7.97	8.05	8.08	8.03	8.04	7.97	8.04	8.03	8.06
Loparite	4.98	3.96	7.63	0.00	4.42	6.11	4.81	0.00	0.00	4.18	4.74	2.95
Lueshite	0.00	0.00	0.00	0.00	0.00	0.00	0.00	0.00	0.00	0.00	0.13	0.79
Perovskite	95.02	96.04	92.38	100.00	95.58	93.89	95.19	100.00	100.00	95.83	95.13	96.26

Sample		Lapilli 3		Lapilli 4						Lapilli 5	
Note:		with spinel									
	2	3	3	3	2	3	2	3	3	2	2	3
Na2O	0	0.36	0.49	0	0	0.44	0.4	0	0.43	0.37	0.55	0.59
CaO	39.53	38.73	36.66	39.57	36.76	37.22	37.41	37.81	37.38	37.27	37	37.3
TiO2	55.35	54.83	54.32	56.27	53.89	54.47	53.62	55.15	54.51	54.39	53.71	54.4
FeO	2.27	1.58	1.78	1.4	1.3	1.18	1.41	1.59	1.4	1.38	1.31	1.63
SrO	0	0.38	0	0.35	0	0	0	0	0	0	0	0
Nb2O5	1.28	0.64	0.69	0.7	0.87	0.98	0.93	0	0.94	1.18	0.98	0.82
BaO	0	0	0	0	0	1.99	0	0	0	0	0	0
La2O3	0	0	0	0	1.96	0	0	0	0	0	1.97	0
Ce2O3	0	1.53	1.94	0	1.8	1.57	2.94	2.38	2.04	2.78	2.11	0.275
Pr2O3	0	0	0	0	0	0	0	0	0	0	0	0
Nd2O3	0	0	0	0	1.37	0	0	0	0	0	0	1.09
Total	100.3	99.96	100.4	99.6	100.01	99.62	99.8	99.58	99.37	99.27	99.22	100.5
Na	0.00	0.07	0.09	0.00	0.00	0.08	0.07	0.00	0.08	0.07	0.10	0.11
Ca	3.94	3.91	3.78	3.94	3.77	3.80	3.85	3.85	3.82	3.80	3.79	3.82
Ti	3.87	3.88	3.93	3.93	3.88	3.90	3.87	3.95	3.91	3.89	3.87	3.92
Fe	0.18	0.12	0.14	0.11	0.10	0.09	0.11	0.13	0.11	0.11	0.10	0.13
Sr	0.00	0.02	0.00	0.02	0.00	0.00	0.00	0.00	0.00	0.00	0.00	0.00
Nb	0.05	0.03	0.03	0.03	0.04	0.04	0.04	0.00	0.04	0.05	0.04	0.04
Ba	0.00	0.00	0.00	0.00	0.00	0.07	0.00	0.00	0.00	0.00	0.00	0.00
La	0.00	0.00	0.00	0.00	0.07	0.00	0.00	0.00	0.00	0.00	0.07	0.00
Ce	0.00	0.05	0.07	0.00	0.06	0.05	0.10	0.08	0.07	0.10	0.07	0.01
Pr	0.00	0.00	0.00	0.00	0.00	0.00	0.00	0.00	0.00	0.00	0.00	0.00
Nd	0.00	0.00	0.00	0.00	0.05	0.00	0.00	0.00	0.00	0.00	0.00	0.04
Total	8.05	8.08	8.04	8.03	7.97	8.05	8.05	8.01	8.03	8.02	8.05	8.06
Loparite	0.00	2.64	3.47	0.00	0.00	2.78	3.74	0.00	3.59	3.47	5.14	5.42
Lueshite	0.00	0.33	0.59	0.00	0.00	0.67	0.00	0.00	0.21	0.00	0.00	0.00
Perovskite	100.00	97.04	95.95	100.00	100.00	96.54	96.26	100.00	96.20	96.53	94.86	94.59

							CL-06-003-247					CL-06-003-
Sample	Lapilli 6		Lapilli 7				same phen	lapillus 2			Pheno	
Note:			with spinel			with spinel	but no spin	2	2	2	2	3
	3	3	3	2	2	2	2					
Na2O	0.38	0	0	0	0	0.42	0.37	0	0	0	0.5	0
CaO	38.21	37.65	37.31	38.24	35.33	37.83	37.9	37.16	34.24	34.53	37.4	36.8
TiO2	53.87	54.69	55.41	54.78	56.21	55.51	55.21	53.25	53.36	53.89	53.31	53.87
FeO	1.26	1.73	1.3	1.14	1.59	1.5	1.43	1.88	1.22	1.52	1.21	1.65
SrO	0.41	0	0	0	0	0.43	0	0	0	0	0	0
Nb2O5	0.75	0.7	0.69	0.96	0.93	0	0.73	1.2	0	1.01	1.07	0.81
BaO	0	0	0	0	0	0	0	0	0	0	0	0
La2O3	0	0	0	0	1.86	0	0	0	3.09	2.44	0	2.24
Ce2O3	2.93	2.3	2.63	2.57	2.17	1.72	1.85	2.22	5.35	3.53	2.42	3.02
Pr2O3	0	0	0	0	0	0	0	1.76	0	0	0	0
Nd2O3	0	0	0.86	0	0	1.23	0	1.48	0	0	1.53	1.23
Total	100.54	99.56	100.73	99.94	100.48	100.28	99.55	99.9	99.83	99.31	99.62	100.65
Na	0.07	0.00	0.00	0.00	0.00	0.08	0.07	0.00	0.00	0.00	0.09	0.00
Ca	3.90	3.84	3.77	3.88	3.58	3.81	3.84	3.80	3.59	3.59	3.84	3.75
Ti	3.86	3.91	3.93	3.90	3.99	3.93	3.92	3.82	3.93	3.93	3.85	3.85
Fe	0.10	0.14	0.10	0.09	0.13	0.12	0.11	0.15	0.10	0.12	0.10	0.13
Sr	0.02	0.00	0.00	0.00	0.00	0.02	0.00	0.00	0.00	0.00	0.00	0.00
Nb	0.03	0.03	0.03	0.04	0.04	0.00	0.03	0.05	0.00	0.04	0.05	0.03
Ba	0.00	0.00	0.00	0.00	0.00	0.00	0.00	0.00	0.00	0.00	0.00	0.00
La	0.00	0.00	0.00	0.00	0.06	0.00	0.00	0.00	0.11	0.09	0.00	0.08
Ce	0.10	0.08	0.09	0.09	0.08	0.06	0.06	0.08	0.19	0.13	0.08	0.11
Pr	0.00	0.00	0.00	0.00	0.00	0.00	0.00	0.06	0.00	0.00	0.00	0.00
Nd	0.00	0.00	0.03	0.00	0.00	0.04	0.00	0.05	0.00	0.00	0.05	0.04
Total	8.08	8.00	7.96	8.00	7.88	8.06	8.03	8.01	7.92	7.90	8.06	7.99
Loparite	3.57	0.00	0.00	0.00	0.00	3.86	3.23	0.00	0.00	0.00	4.72	0.00
Lueshite	0.00	0.00	0.00	0.00	0.00	0.00	0.10	0.00	0.00	0.00	0.00	0.00
Perovskite	96.43	100.00	100.00	100.00	100.00	96.14	96.68	100.00	100.00	100.00	95.28	100.00

Sample	Lapillus 1			Lapillus 2			Lapillu 3		Lapillus 4			
Note:		3	2	2	2	2	3	3	3	2	3	2
Na2O	0	0	0	0.54	0.46	0.47	0	0	0.39	0.61	0.55	0.45
CaO	37.94	37.75	38.06	38.02	37.61	37.48	38.77	36.97	36.94	36.42	37.15	37.09
TiO2	54.63	55.33	52.54	54.37	53.05	52.32	54.37	54.24	54.16	52.51	53.41	54.45
FeO	1.13	1.79	2.1	1.59	1.34	1.74	1.31	1.53	1.63	1.23	1.75	1.78
SrO	0.38	0.39	0	0	0	0	0.5	0	0	0	0	0
Nb2O5	1	0.74	0	0.78	0.59	0.68	0.67	0.87	0.92	0.98	0.96	0.62
BaO	0	0	0	0	0	0	0	0	0	0	0	0
La2O3	0	0	0	2.13	0	0	0	0	0	2.41	0	0
Ce2O3	2.22	2.92	0	1.96	2.77	1.96	1.46	2.67	2.38	2.88	2.36	3.59
Pr2O3	0	0	0	0	0	0	1.29	1.84	1.55	1.17	0	0
Nd2O3	0	0	2.27	0	0.94	1.31	1.12	1.07	1.16	1.39	0	0
Total	99.48	100.97	99.86	100.63	99.81	99.14	99.61	99.91	99.65	100.95	99.24	100.12
Na	0.00	0.00	0.00	0.10	0.09	0.09	0.00	0.00	0.07	0.11	0.10	0.08
Ca	3.86	3.80	3.99	3.83	3.89	3.91	3.91	3.76	3.75	3.74	3.84	3.78
Ti	3.90	3.91	3.86	3.85	3.85	3.83	3.85	3.87	3.86	3.79	3.87	3.89
Fe	0.09	0.14	0.17	0.13	0.11	0.14	0.10	0.12	0.13	0.10	0.14	0.14
Sr	0.02	0.02	0.00	0.00	0.00	0.00	0.03	0.00	0.00	0.00	0.00	0.00
Nb	0.04	0.03	0.00	0.03	0.03	0.03	0.03	0.04	0.04	0.04	0.04	0.03
Ba	0.00	0.00	0.00	0.00	0.00	0.00	0.00	0.00	0.00	0.00	0.00	0.00
La	0.00	0.00	0.00	0.07	0.00	0.00	0.00	0.00	0.00	0.09	0.00	0.00
Ce	0.08	0.10	0.00	0.07	0.10	0.07	0.05	0.09	0.08	0.10	0.08	0.12
Pr	0.00	0.00	0.00	0.00	0.00	0.00	0.04	0.06	0.05	0.04	0.00	0.00
Nd	0.00	0.00	0.08	0.00	0.03	0.05	0.04	0.04	0.04	0.05	0.00	0.00
Total	7.99	8.00	8.10	8.08	8.09	8.11	8.04	7.98	8.03	8.06	8.08	8.05
Loparite	0.00	0.00	0.00	4.96	4.35	4.47	0.00	0.00	3.68	5.84	4.14	4.21
Lueshite	0.00	0.00	0.00	0.00	0.00	0.00	0.00	0.00	0.00	0.00	0.49	0.00
Perovskite	100.00	100.00	100.00	95.04	95.65	95.53	100.00	100.00	96.32	94.16	95.38	95.79

Sample			CL-010-169
Note:	2	2	No Perserved Perovskites
Na2O	0	0	
CaO	38.16	37.89	
TiO2	54.14	54.38	
FeO	1.44	1.35	
SrO	0	0	
Nb2O5	0.93	0.76	
BaO	0	0	
La2O3	0	0	
Ce2O3	0	3.19	
Pr2O3	0	0	
Nd2O3	0	0	
Total	99.51	100.25	
Na	0.00	0.00	
Ca	3.94	3.86	
Ti	3.92	3.89	
Fe	0.12	0.11	
Sr	0.00	0.00	
Nb	0.04	0.03	
Ba	0.00	0.00	
La	0.00	0.00	
Ce	0.00	0.11	
Pr	0.00	0.00	
Nd	0.00	0.00	
Total	8.02	8.00	
Loparite	0.00	0.00	
Lueshite	0.00	0.00	
Perovskite	100.00	100.00	

Appendix D-7 Apatite

	CL-06-003-158						CL-06-003-236		CL-07-010-261		CL-07-014-285				
	1	2	3	4	5	6	1	2	1	2	1	2	3	4	5
		Mg BG		Mg BG	Mg+S BG	CL=0.64	Mg BG	Mg BG			Cl = 1.38	Cl = 1.78	Cl=1.68	Cl = 1.6	to small
F	2.5	2.94	4.77	1.32	2.68	3.41	2.53	4.24	3.9	5.02	2.93	2.91	3.99	2.97	1.39
P2O5	43.58	38.69	45.17	35.1	33.4	43.11	35.31	35.54	43.63	43.56	43.2	45.18	44.15	43.2	36.16
CaO	56.08	55.47	55.2	54.03	49.41	55.52	50.66	48.93	56.19	56.88	56.23	60.56	57.86	57.46	56.06
SrO	0	1.1	0	1.05	0	0.56	0.66	1.2	0	0.58	0.57	0	0	0	1.59
La2O3	0	0	0	0	0	0	0	0.68	0	0	0	0	0	0	0
Ce2O3	0	0	0	0	0.84	0	0	1.5	0	0	0	0	0	0	0
Pr2O3	0	0	0	0	0	0	0	0	0	0	0	0	0	0	0
Nd2O3	0	0	0	0	0	0	0	0	0	0	0	0	0	0	0
Sm2O3	0	0	0	0	0	0	0	0	0	0	0	0	0	0	0
Total	101.65	95.51	102.43	90.16	86.19	99.95	85.86	88.78	100.21	100.19	100.29	102.35	102.19	100.39	94.61

No. Ions in Formula

F	1.315	1.649	2.417	0.805	1.717	1.792	1.559	2.559	2.020	2.557	1.538	1.449	2.028	1.549	0.818
P2O5	6.138	5.809	6.127	5.728	5.729	6.066	5.827	5.742	6.051	5.940	6.071	6.023	6.008	6.030	5.697
CaO	9.996	10.540	9.475	11.159	10.725	9.886	10.579	10.004	9.862	9.816	10.000	10.217	9.965	10.150	11.177
SrO	0.000	0.113	0.000	0.117	0.000	0.054	0.075	0.133	0.000	0.054	0.055	0.000	0.000	0.000	0.172
La2O3	0.000	0.000	0.000	0.000	0.000	0.000	0.000	0.048	0.000	0.000	0.000	0.000	0.000	0.000	0.000
Ce2O3	0.000	0.000	0.000	0.000	0.062	0.000	0.000	0.105	0.000	0.000	0.000	0.000	0.000	0.000	0.000
Pr2O3	0.000	0.000	0.000	0.000	0.000	0.000	0.000	0.000	0.000	0.000	0.000	0.000	0.000	0.000	0.000
Nd2O3	0.000	0.000	0.000	0.000	0.000	0.000	0.000	0.000	0.000	0.000	0.000	0.000	0.000	0.000	0.000
Sm2O3	0.000	0.000	0.000	0.000	0.000	0.000	0.000	0.000	0.000	0.000	0.000	0.000	0.000	0.000	0.000
Total	17.450	18.111	18.018	17.810	18.234	17.798	18.040	18.590	17.934	18.368	17.663	17.690	18.002	17.729	17.864

Appendix D-8 Garnet

		CL-06-003-158							CL-06-003-173		
	Garnet Type	9	5	5	5	5	9	5	5	9	1
Oxide%	**SiO2**	40.99	39.2	37.7	36.73	37.27	42.05	37.35	36.75	40.55	41.43
	TiO2	0	0	0	0	0	0	0	0.00	0	0.56
	Al2O3	18.71	19.78	20.68	20.43	20.09	22.18	20.58	21.96	19.92	21.53
	FeOT	7.45	29.95	34.27	34.93	35.06	6.5	34.29	31.10	7.64	8.57
	MnO	0	3.08	1.91	1.78	0	0	0	1.26	0	0
	MgO	20.44	3.39	5.34	4.65	3.95	21.24	5.68	5.83	20.26	21.94
	CaO	5.49	3.47	0	0.74	1.54	3.91	1.11	2.83	5.33	4.52
	Cr2O3	6	0	0	0	0	3.49	0	0.00	4.98	1.21
	Total	99.26	99.36	99.87	99.19	99.13	99.68	99.74	99.64	99.17	99.76
No. Ions in Formula											
	Si	5.94	6.34	6.01	5.92	6.10	5.99	5.98	5.80	5.88	5.87
	Al	0.06	0.00	0.00	0.08	0.00	0.01	0.02	0.20	0.12	0.13
	Total	6.00	6.34	6.01	6.00	6.10	6.00	6.00	6.00	6.00	6.00
	Al	3.14	3.77	3.89	3.80	3.87	3.72	3.86	3.88	3.29	3.47
	Fe3+	0.23	0.00	0.09	0.28	0.00	0.00	0.16	0.32	0.25	0.41
	Cr	0.69	0.00	0.00	0.00	0.00	0.39	0.00	0.00	0.57	0.14
	Total	4.06	3.77	3.97	4.08	3.87	4.11	4.02	4.20	4.12	4.01
	Mg	4.42	0.82	1.27	1.12	0.96	4.51	1.36	1.37	4.38	4.63
	Fe2+	0.67	4.05	4.49	4.43	4.80	0.77	4.43	3.78	0.67	0.61
	Mn	0.00	0.42	0.26	0.24	0.00	0.00	0.00	0.17	0.00	0.00
	Ca	0.85	0.60	0.00	0.13	0.27	0.60	0.19	0.48	0.83	0.69
	Total	5.94	5.89	6.01	5.92	6.03	5.89	5.98	5.80	5.88	5.93
End Members											
	$Mg_3Cr_2Si_3O_{12}$	16.95	0.00	0.00	0.00	0.00	9.56	0.00	0.00	13.88	0.00
	Uvarovite	0.00	0.00	0.00	0.00	0.00	0.00	0.00	0.00	0.00	3.38
	Andradite	5.69	0.00	0.00	2.16	0.00	0.00	3.18	7.69	6.18	8.19
	Grossular	8.66	10.21	0.00	0.00	4.48	10.15	0.00	0.56	7.91	0.00
	Spessartine	0.00	7.16	4.29	4.10	0.00	0.00	0.00	2.90	0.00	0.00
	Almandine	11.31	68.76	74.59	74.86	79.55	13.17	74.15	65.20	11.44	10.28
	Pyrope	57.39	13.87	21.11	18.87	15.97	67.13	22.67	23.65	60.60	78.15

CL-06-003-182

	Garnet Type	1	1	9	9	9	5	5	5	5	5
Oxide%	**SiO2**	41.59	41.38	42.71	42.61	40.98	37.60	38.08	37.76	38.02	37.09
	TiO2	0.63	0.86	0	0	0	0.00	0	0	0	0
	Al2O3	21.57	20.78	15.99	20.01	21.4	20.23	20.48	19.22	21.14	20.38
	FeOT	8.17	8.26	6.38	8.64	9.39	28.60	36.31	30.38	29.3	36.83
	MnO	0	0	0	0	0	3.70	0	4.2	2.71	1.79
	MgO	21.87	20.76	21.05	21.5	21.6	2.51	2.73	2.13	3.8	3
	CaO	4.45	4.29	5.96	4.14	4.33	7.40	0.77	5.49	4.23	0.73
	Cr2O3	1.15	2.94	7.39	1.97	0	0.00	0	0	0	0
	Total	99.59	99.66	100.02	99.53	99.79	99.99	99.64	99.94	99.79	99.82
No. Ions in Formula											
	Si	5.91	5.95	6.18	6.12	5.91	6.01	6.25	6.14	6.09	6.01
	Al	0.09	0.05	0.00	0.00	0.09	0.00	0.00	0.00	0.00	0.00
	Total	6.00	6.00	6.18	6.12	6.00	6.01	6.25	6.14	6.09	6.01
	Al	3.52	3.47	2.73	3.39	3.55	3.81	3.96	3.68	3.99	3.89
	Fe3+	0.30	0.06	0.06	0.16	0.54	0.18	0.00	0.04	0.00	0.08
	Cr	0.13	0.33	0.85	0.22	0.00	0.00	0.00	0.00	0.00	0.00
	Total	3.96	3.87	3.63	3.77	4.09	3.99	3.96	3.73	3.99	3.97
	Mg	4.63	4.45	4.54	4.60	4.65	0.60	0.67	0.52	0.91	0.73
	Fe2+	0.67	0.93	0.72	0.88	0.60	3.64	4.98	4.09	3.92	4.92
	Mn	0.00	0.00	0.00	0.00	0.00	0.50	0.00	0.58	0.37	0.25
	Ca	0.68	0.66	0.92	0.64	0.67	1.27	0.14	0.96	0.73	0.13
	Total	5.98	6.04	6.18	6.12	5.91	6.01	5.79	6.14	5.92	6.01
End Members											
	$Mg_3Cr_2Si_3O_{12}$	0.00	0.00	23.30	5.93	0.00	0.00	0.00	0.00	0.00	0.00
	Uvarovite	3.27	8.65	0.00	0.00	0.00	0.00	0.00	0.00	0.00	0.00
	Andradite	7.68	1.58	1.56	4.20	11.32	4.50	0.00	1.15	0.00	1.97
	Grossular	0.39	0.71	13.39	6.21	0.00	16.59	2.34	14.43	12.25	0.14
	Spessartine	0.00	0.00	0.00	0.00	0.00	8.34	0.00	9.42	6.20	4.09
	Almandine	11.16	15.43	11.58	14.37	10.11	60.63	86.12	66.59	66.23	81.75
	Pyrope	77.50	73.64	50.17	69.28	78.57	9.95	11.54	8.41	15.31	12.06

		CL-06-003-186					CL-06-003-195				
	Garnet Type	9	1	2	1	9	9	9	2	9	9
Oxide%	**SiO2**	42.54	42.3	41.54	42.3	40.05	41.24	40.85	42.92	41.13	41.11
	TiO2	0.00	0.4	1.06	0.86	0	0.41	0	1.84	0	0
	Al2O3	20.32	20.35	20.92	19.8	19.84	19.95	21.45	21.4	19.11	18.81
	FeOT	8.47	8.22	6.52	8.73	7.85	6.68	9.11	8.09	7.61	7.95
	MnO	0.00	0.36	0	0	0	0.00	0	0	0	0
	MgO	21.42	21.61	22.92	21.29	21.37	21.27	20.7	20.36	19.41	19.31
	CaO	4.87	4.84	4.96	4.84	5.31	4.79	4.37	5.01	6.47	6.15
	Cr2O3	2.25	2.17	2.06	2.11	5.26	4.45	4.4	0	6.12	6.45
	Total	99.86	100.25	99.69	99.97	99.48	99.00	99.85	99.85	99.84	99.91
No. Ions in Formula											
	Si	6.05	6.00	5.85	6.03	5.74	5.94	5.80	6.13	5.94	5.96
	Al	0.00	0.00	0.15	0.00	0.26	0.06	0.20	0.00	0.06	0.04
	Total	6.05	6.00	6.00	6.03	6.00	6.00	6.00	6.13	6.00	6.00
	Al	3.41	3.40	3.33	3.33	3.09	3.33	3.38	3.60	3.20	3.17
	Fe3+	0.24	0.28	0.37	0.18	0.58	0.13	0.33	0.00	0.16	0.13
	Cr	0.25	0.24	0.23	0.24	0.60	0.51	0.49	0.00	0.70	0.74
	Total	3.90	3.92	3.92	3.75	4.26	3.97	4.20	3.60	4.06	4.04
	Mg	4.54	4.57	4.81	4.53	4.56	4.57	4.38	4.34	4.18	4.17
	Fe2+	0.77	0.69	0.40	0.86	0.36	0.68	0.75	0.97	0.76	0.83
	Mn	0.00	0.04	0.00	0.00	0.00	0.00	0.00	0.00	0.00	0.00
	Ca	0.74	0.74	0.75	0.74	0.81	0.74	0.66	0.77	1.00	0.95
	Total	6.05	6.04	5.97	6.13	5.74	5.99	5.80	6.07	5.94	5.96
End Members											
	$Mg_3Cr_2Si_3O_{12}$	6.49	0.00	0.00	0.00	13.97	12.78	11.74	0.00	17.24	18.28
	Uvarovite	0.00	6.21	5.85	6.35	0.00	0.00	0.00	0.00	0.00	0.00
	Andradite	6.17	5.97	6.70	4.86	13.64	3.19	7.79	0.00	3.92	3.28
	Grossular	6.09	0.00	0.00	0.87	0.56	9.16	3.67	12.64	12.93	12.75
	Spessartine	0.00	0.72	0.00	0.00	0.00	0.00	0.00	0.00	0.00	0.00
	Almandine	12.67	11.49	6.75	14.03	6.25	11.33	13.00	15.93	12.80	13.95
	Pyrope	68.57	75.62	80.70	73.90	65.57	63.53	63.80	71.44	53.11	51.74

				CL-06-003-205				CL-06-003-219			
	Garnet Type	9	9	5	9	9	9	1	11	11	9
Oxide%	**SiO2**	41.86	41.68	35.82	43.02	41.97	45.11	40.29	40.11	40.29	42.72
	TiO2	0.51	0.58	0.00	0	0	0	1.34	1.77	1.34	0
	Al2O3	23.07	23.17	20.73	20.6	20.49	19.85	21.94	15.58	15.08	17.79
	FeOT	8.71	8.73	35.30	6.55	6.89	5.89	8.19	5.57	6.99	6.92
	MnO	0	0	2.33	0	0	0	0.00	0	0.51	0
	MgO	20.29	20.4	4.46	21.76	22.1	20.47	20.90	19.7	19.88	19.31
	CaO	5.26	5.06	0.79	4.46	4.6	4.66	4.07	6.72	6.61	5.42
	Cr2O3	0	0	0.00	3.48	3.48	3.99	2.76	9.84	9.28	7.15
	Total	99.71	99.61	99.82	99.95	99.87	100.05	99.59	99.82	99.97	99.53
No. Ions in Formula											
	Si	5.95	5.92	5.77	6.10	5.97	6.44	5.77	5.90	5.89	6.23
	Al	0.05	0.08	0.23	0.00	0.03	0.00	0.23	0.10	0.11	0.00
	Total	6.00	6.00	6.00	6.10	6.00	6.44	6.00	6.00	6.00	6.23
	Al	3.81	3.81	3.71	3.45	3.40	3.34	3.47	2.60	2.49	3.06
	Fe3+	0.13	0.14	0.51	0.00	0.24	0.00	0.15	0.00	0.25	0.00
	Cr	0.00	0.00	0.00	0.39	0.39	0.45	0.31	1.14	1.07	0.82
	Total	3.94	3.95	4.23	3.84	4.03	3.79	3.94	3.74	3.81	3.88
	Mg	4.30	4.32	1.07	4.60	4.69	4.36	4.46	4.32	4.33	4.20
	Fe2+	0.90	0.89	4.25	0.78	0.58	0.70	0.83	0.68	0.61	0.84
	Mn	0.00	0.00	0.32	0.00	0.00	0.00	0.00	0.00	0.06	0.00
	Ca	0.80	0.77	0.14	0.68	0.70	0.71	0.62	1.06	1.04	0.85
	Total	6.00	5.99	5.77	6.06	5.97	5.77	5.92	6.06	6.04	5.89
End Members											
	$Mg_3Cr_2Si_3O_{12}$	0.00	0.00	0.00	10.18	9.71	11.88	0.00	30.57	28.14	21.23
	Uvarovite	0.00	0.00	0.00	0.00	0.00	0.00	7.93	0.00	0.00	0.00
	Andradite	3.33	3.66	2.36	0.00	5.88	0.00	2.63	0.00	6.51	0.00
	Grossular	10.02	9.22	0.00	11.19	5.87	12.35	0.00	17.47	10.64	14.38
	Spessartine	0.00	0.00	5.51	0.00	0.00	0.00	0.00	0.00	1.05	0.00
	Almandine	15.06	14.92	73.57	12.83	9.76	12.18	14.00	11.30	10.04	14.33
	Pyrope	71.60	72.21	18.56	65.80	68.79	63.59	75.44	40.66	43.62	50.05

		CL-06-003-222					CL-06-003-236				
	Garnet Type	11	11	9	9	1	9	9	9	9	9
Oxide%	**SiO2**	40.96	40.14	40.73	41.18	40.61	41.25	43.27	41.62	40.85	40.62
	TiO2	1.16	1.16	0.00	0	0.81	0.63	0	0.00	0	0
	Al2O3	14	13.97	20.11	18.41	21.2	19.34	23.45	21.20	19.22	18.85
	FeOT	6.7	6.77	9.32	7.17	8.88	8.06	7.63	5.73	8.47	7.87
	MnO	0	0	0.00	0	0	0	0	1.08	1.15	0
	MgO	19.66	19.67	20.41	20.2	20.77	24.87	21.74	22.54	22.15	20.64
	CaO	7.87	7.23	4.85	5.62	4.17	3.98	3.92	5.16	5.43	5.24
	Cr2O3	9.58	10.47	3.76	6.33	3.29	0	0	0.00	3.62	6.14
	Total	99.98	99.78	99.85	99.79	99.74	99.72	99.82	99.21	99.85	99.67
No. Ions in Formula											
	Si	6.00	5.92	5.88	5.99	5.82	5.86	6.08	5.98	5.77	5.87
	Al	0.00	0.08	0.12	0.01	0.18	0.14	0.00	0.02	0.23	0.13
	Total	6.00	6.00	6.00	6.00	6.00	6.00	6.08	6.00	6.00	6.00
	Al	2.42	2.35	3.30	3.14	3.40	3.10	3.88	3.56	2.97	3.09
	Fe3+	0.22	0.25	0.39	0.14	0.23	0.90	0.00	0.46	0.85	0.34
	Cr	1.11	1.22	0.43	0.73	0.37	0.00	0.00	0.00	0.40	0.70
	Total	3.75	3.82	4.12	4.01	4.01	4.00	3.88	4.02	4.23	4.13
	Mg	4.29	4.32	4.39	4.38	4.44	5.27	4.55	4.82	4.66	4.45
	Fe2+	0.60	0.58	0.74	0.73	0.83	0.05	0.90	0.23	0.15	0.61
	Mn	0.00	0.00	0.00	0.00	0.00	0.00	0.00	0.13	0.14	0.00
	Ca	1.23	1.14	0.75	0.88	0.64	0.61	0.59	0.79	0.82	0.81
	Total	6.13	6.05	5.88	5.99	5.91	5.93	6.04	5.98	5.77	5.87
End Members											
	$Mg_3Cr_2Si_3O_{12}$	29.61	31.94	10.42	18.15	0.00	0.00	0.00	0.00	9.56	17.01
	Uvarovite	0.00	0.00	0.00	0.00	9.30	0.00	0.00	0.00	0.00	0.00
	Andradite	5.91	6.63	9.41	3.45	1.54	10.22	0.00	11.47	14.24	8.21
	Grossular	14.25	12.26	3.34	11.18	0.00	0.00	9.77	1.81	0.00	5.61
	Spessartine	0.00	0.00	0.00	0.00	0.00	0.00	0.00	2.20	2.38	0.00
	Almandine	9.78	9.62	12.54	12.25	14.05	0.92	14.84	3.79	2.54	10.43
	Pyrope	40.44	39.56	64.28	54.98	75.11	88.85	75.39	80.73	71.27	58.74

						CL-07-006-195					CL-07-006-208
	Garnet Type	1	9	9	9	5	3	3	5	6	6
Oxide%	**SiO2**	41.48	41.07	42.43	41.89	37.20	26.36	28.07	35.83	36.9	36.41
	TiO2	0.91	0.59	0	0	0.00	0.85	0.77	0	0	0.00
	Al2O3	19.94	20.14	20.03	18.33	21.63	53.96	54.18	20.45	20.81	21.04
	FeOT	7.97	7.71	7.83	5.9	31.65	14.72	14.88	24.07	22.88	22.29
	MnO	0	0	0	0	3.48	0	0	12.95	13.68	18.42
	MgO	21.82	21.96	22.41	21.82	4.55	3.24	2.2	0	1.29	0.94
	CaO	5.23	4.67	4.55	5.4	0.90	0	0	4.82	4.78	0.76
	Cr2O3	2.78	3.19	0	6.8	0.00	0	0	0	0	0.00
	Total	100.58	99.57	99.25	100.14	99.71	99.35	100.11	99.26	100.34	99.75
No. Ions in Formula											
	Si	5.89	5.87	6.12	5.98	5.96	3.91	4.15	5.96	5.95	5.96
	Al	0.11	0.13	0.00	0.02	0.04	2.09	1.85	0.04	0.05	0.04
	Total	6.00	6.00	6.12	6.00	6.00	6.00	6.00	6.00	6.00	6.00
	Al	3.23	3.26	3.41	3.06	4.05	7.36	7.59	3.97	3.91	4.03
	Fe3+	0.37	0.38	0.35	0.19	0.00	0.00	0.00	0.07	0.14	0.01
	Cr	0.31	0.36	0.00	0.77	0.00	0.00	0.00	0.00	0.00	0.00
	Total	3.91	4.00	3.75	4.02	4.05	7.36	7.59	4.04	4.05	4.04
	Mg	4.62	4.68	4.82	4.64	1.09	0.72	0.48	0.00	0.31	0.23
	Fe2+	0.57	0.54	0.60	0.51	4.24	1.83	1.84	3.28	2.95	3.05
	Mn	0.00	0.00	0.00	0.00	0.47	0.00	0.00	1.82	1.87	2.56
	Ca	0.80	0.72	0.70	0.83	0.15	0.00	0.00	0.86	0.83	0.13
	Total	5.99	5.93	6.12	5.98	5.95	2.55	2.32	5.96	5.95	5.96
End Members											
	$Mg_3Cr_2Si_3O_{12}$	0.00	9.00	0.00	19.08	0.00	0.00	0.00	0.00	0.00	0.00
	Uvarovite	7.97	0.00	0.00	0.00	0.00	0.00	0.00	0.00	0.00	0.00
	Andradite	5.32	9.54	9.23	4.82	0.00	0.00	0.00	1.79	3.46	0.20
	Grossular	0.00	2.51	2.26	9.00	2.59	0.00	0.00	12.63	10.42	2.03
	Spessartine	0.00	0.00	0.00	0.00	7.93	0.00	0.00	30.61	31.40	42.85
	Almandine	9.57	9.09	9.78	8.54	71.22	71.82	79.14	54.97	49.51	51.06
	Pyrope	77.14	69.85	78.73	58.57	18.25	28.18	20.86	0.00	5.21	3.85

						CL-07-006-235				CL-07-010-160	
	Garnet Type	5	9	11	11	9	9	9	9	5	
Oxide%	**SiO2**	39.07	43.9	41.49	41.68	41.82	41.1	43.04	41.45	37.21	
	TiO2	0	0	0.97	1.1	0.00	0	0	0	0.00	
	Al2O3	21.22	16.21	16.36	18.9	21.22	17.44	21.23	21.24	21.89	
	FeOT	29.72	9.11	8.84	5.12	7.45	8.66	7.14	8.39	30.85	
	MnO	4.12	0	0.37	0	0.00	0	0	0	3.45	
	MgO	4.26	19.96	20.44	22.57	22.16	20.67	20.27	20.69	5.24	
	CaO	1.06	4.45	5.56	4.67	3.75	5.96	4.41	4.59	1.44	
	Cr2O3	0	4.78	5.21	4.76	2.90	4.87	2.76	2.97	0.00	
	Total	99.53	99.93	99.23	99.34	99.71	99.65	99.61	99.69	99.89	
No. Ions in Formula											
	Si	6.26	6.45	6.05	5.98	5.95	5.98	6.20	5.94	5.89	
	Al	0.00	0.00	0.00	0.02	0.05	0.02	0.00	0.06	0.11	
	Total	6.26	6.45	6.05	6.00	6.00	6.00	6.20	6.00	6.00	
	Al	4.01	2.81	2.81	3.18	3.51	2.97	3.60	3.53	3.97	
	Fe3+	0.00	0.00	0.28	0.06	0.21	0.49	0.00	0.19	0.14	
	Cr	0.00	0.56	0.60	0.54	0.33	0.56	0.31	0.34	0.00	
	Total	4.01	3.36	3.69	3.78	4.05	4.02	3.92	4.06	4.11	
	Mg	1.02	4.37	4.44	4.83	4.70	4.48	4.35	4.42	1.24	
	Fe2+	3.98	1.12	0.80	0.55	0.68	0.57	0.86	0.82	3.95	
	Mn	0.56	0.00	0.05	0.00	0.00	0.00	0.00	0.00	0.46	
	Ca	0.18	0.70	0.87	0.72	0.57	0.93	0.68	0.71	0.24	
	Total	5.74	6.19	6.15	6.10	5.95	5.98	5.89	5.94	5.89	
End Members											
	$Mg_3Cr_2Si_3O_{12}$	0.00	16.51	16.27	14.29	8.06	13.94	8.02	8.30	0.00	0.00
	Uvarovite	0.00	0.00	0.00	0.00	0.00	0.00	0.00	0.00	0.00	0.00
	Andradite	0.00	0.00	7.56	1.61	5.14	12.10	0.00	4.69	0.00	3.34
	Grossular	3.17	11.31	6.55	10.16	4.46	3.44	11.55	7.18	94.16	0.81
	Spessartine	9.74	0.00	0.74	0.00	0.00	0.00	0.00	0.00	0.00	7.85
	Almandine	69.37	18.08	12.98	9.08	11.40	9.49	14.60	13.73	5.84	67.01
	Pyrope	17.72	54.09	55.90	64.86	70.93	61.03	65.83	66.11	0.00	20.99

								CL-07-010-169			
	Garnet Type	5	5	9	9	5	5	5	5	9	1
Oxide%	**SiO2**	36.77	35.95	39.29	41.12	36.34	36.35	34.95	36.47	40	40.78
	TiO2	0	0	0	0	0	0	0.00	0	0	0.59
	Al2O3	21.62	21.71	18.31	16.98	22.07	22.02	22.08	22.29	21.48	21.33
	FeOT	30.43	36.01	6.96	6.42	30.14	30.29	34.46	32.62	8.04	8.68
	MnO	3.36	2.22	0	0	3.04	3.1	2.70	2.88	0	0.29
	MgO	5.5	3.46	22.88	21.17	6.06	5.83	4.37	4.33	23.03	22.1
	CaO	1.75	0.89	5.63	6.35	1.95	1.88	1.72	1.74	4.26	4.61
	Cr2O3	0	0	7.1	8.52	0	0	0.00	0	1.89	1.67
	Total	99.53	100.13	99.96	100.55	99.49	99.58	99.87	100.33	99.4	100.05
No. Ions in Formula											
	Si	5.85	5.77	5.59	5.90	5.74	5.76	5.57	5.79	5.69	5.77
	Al	0.15	0.23	0.41	0.10	0.26	0.24	0.43	0.21	0.31	0.23
	Total	6.00	6.00	6.00	6.00	6.00	6.00	6.00	6.00	6.00	6.00
	Al	3.90	3.88	2.66	2.76	3.85	3.87	3.71	3.96	3.30	3.33
	Fe3+	0.25	0.35	0.83	0.37	0.41	0.37	0.72	0.25	0.80	0.59
	Cr	0.00	0.00	0.80	0.97	0.00	0.00	0.00	0.00	0.21	0.19
	Total	4.15	4.23	4.29	4.10	4.26	4.24	4.43	4.21	4.31	4.10
	Mg	1.30	0.83	4.85	4.52	1.43	1.38	1.04	1.02	4.89	4.66
	Fe2+	3.79	4.49	0.83	0.40	3.58	3.65	3.87	4.08	0.16	0.44
	Mn	0.45	0.30	0.00	0.00	0.41	0.42	0.36	0.39	0.00	0.03
	Ca	0.30	0.15	0.86	0.98	0.33	0.32	0.29	0.30	0.65	0.70
	Total	5.85	5.77	6.54	5.90	5.74	5.76	5.57	5.79	5.69	5.83
End Members											
	$Mg_3Cr_2Si_3O_{12}$	0.00	0.00	18.63	23.53	0.00	0.00	0.00	0.00	4.94	0.00
	Uvarovite	0.00	0.00	0.00	0.00	0.00	0.00	0.00	0.00	0.00	4.55
	Andradite	5.10	2.65	13.13	9.12	5.75	5.54	5.27	5.11	11.41	7.43
	Grossular	0.00	0.00	0.00	7.43	0.00	0.00	0.00	0.00	0.00	0.00
	Spessartine	7.74	5.23	0.00	0.00	7.09	7.22	6.54	6.69	0.00	0.60
	Almandine	64.86	77.77	12.66	6.71	62.31	63.33	69.54	70.50	2.76	7.51
	Pyrope	22.30	14.35	55.58	53.22	24.86	23.91	18.64	17.70	80.89	79.92

				CL-07-010-188							
	Garnet Type	5	5	5	6	1	1	5	9	5	5
Oxide%	**SiO2**	36.82	37.43	34.95	37.44	41.3	40.63	37.16	41.34	35.68	36.41
	TiO2	0	0	0.00	0	0.75	0.69	0	0	0	0
	Al2O3	20.74	21.88	20.03	18.87	19.85	19.23	20.35	17.76	21.07	21.32
	FeOT	31.53	32.78	35.82	13.24	8.65	6.81	35.29	7.09	35.98	35.09
	MnO	4.56	2.39	3.95	27.33	0	0	1.84	0	1.43	1.72
	MgO	4.26	4.21	1.91	0.79	22.5	22.39	3.6	21.48	4.76	4.99
	CaO	2.49	1.42	1.08	1.97	4.05	4.97	1.02	5.58	0.92	0.92
	Cr2O3	0	0	0.00	0	2.67	3.58	0	5.9	0	0
	Total	100.02	99.91	97.59	99.86	99.95	98.55	99.28	99.65	99.58	100.34
No. Ions in Formula											
	Si	5.86	5.96	5.83	6.16	5.87	5.85	6.03	5.97	5.71	5.78
	Al	0.14	0.04	0.17	0.00	0.13	0.15	0.00	0.03	0.29	0.22
	Total	6.00	6.00	6.00	6.16	6.00	6.00	6.03	6.00	6.00	6.00
	Al	3.75	4.07	3.77	3.66	3.20	3.12	3.89	2.99	3.69	3.77
	Fe3+	0.39	0.00	0.39	0.01	0.46	0.47	0.06	0.37	0.59	0.45
	Cr	0.00	0.00	0.00	0.00	0.30	0.41	0.00	0.67	0.00	0.00
	Total	4.14	4.07	4.17	3.67	3.97	4.00	3.95	4.03	4.29	4.22
	Mg	1.01	1.00	0.48	0.19	4.77	4.81	0.87	4.62	1.14	1.18
	Fe2+	3.81	4.37	4.61	1.81	0.57	0.35	4.73	0.48	4.23	4.21
	Mn	0.61	0.32	0.56	3.81	0.00	0.00	0.25	0.00	0.19	0.23
	Ca	0.42	0.24	0.19	0.35	0.62	0.77	0.18	0.86	0.16	0.16
	Total	5.86	5.93	5.83	6.16	5.95	5.93	6.03	5.97	5.71	5.78
End Members											
	$Mg_3Cr_2Si_3O_{12}$	0.00	0.00	0.00	0.00	0.00	0.00	0.00	16.69	0.00	0.00
	Uvarovite	0.00	0.00	0.00	0.00	7.57	10.21	0.00	0.00	0.00	0.00
	Andradite	7.25	0.00	3.31	0.32	2.79	2.74	1.53	9.26	2.76	2.71
	Grossular	0.00	4.09	0.00	5.32	0.00	0.00	1.41	5.20	0.00	0.00
	Spessartine	10.49	5.44	9.57	61.83	0.00	0.00	4.19	0.00	3.39	4.00
	Almandine	65.02	73.62	78.97	29.38	9.52	5.95	78.42	8.08	73.96	72.86
	Pyrope	17.25	16.85	8.15	3.15	80.12	81.11	14.44	60.77	19.89	20.43

		CL-07-010-197					CL-07-010-221				
	Garnet Type	5	5	5	5	5	5	9	9	5	5
Oxide%	**SiO2**	36.00	35.74	38.96	36.65	34.27	36.20	41.83	41.24	38.87	36.33
	TiO2	0.00	0	0	0	0	0.00	0	0.69	0	0
	Al2O3	21.23	20.9	20.51	21.81	19.99	21.31	22.3	22.95	20.95	20.97
	FeOT	35.55	35.87	31.35	32.36	38.44	27.10	8.87	7.97	25.02	33.78
	MnO	2.06	2.4	2.3	3.42	2.46	4.62	0	0	4.56	2.62
	MgO	4.48	3.13	4.94	4.57	3.38	4.22	20.78	22.53	2.79	4.36
	CaO	0.00	1.17	0	1.13	1.43	5.73	3.73	3.96	7.2	1.39
	Cr2O3	0.00	0	0	0	0	0.00	1.43	0	0	0
	Total	99.56	99.29	99.78	99.43	99.59	99.38	99.69	99.87	99.6	99.81
No. Ions in Formula											
	Si	5.81	5.82	6.32	5.84	5.56	5.77	6.00	5.82	6.21	5.84
	Al	0.19	0.18	0.00	0.16	0.44	0.23	0.00	0.18	0.00	0.16
	Total	6.00	6.00	6.32	6.00	6.00	6.00	6.00	6.00	6.21	6.00
	Al	3.84	3.82	3.92	3.94	3.38	3.78	3.76	3.64	3.94	3.82
	Fe3+	0.35	0.36	0.00	0.21	1.06	0.45	0.08	0.39	0.00	0.34
	Cr	0.00	0.00	0.00	0.00	0.00	0.00	0.16	0.00	0.00	0.00
	Total	4.19	4.18	3.92	4.16	4.44	4.23	4.00	4.03	3.94	4.16
	Mg	1.08	0.76	1.19	1.09	0.82	1.00	4.44	4.74	0.66	1.05
	Fe2+	4.45	4.52	4.25	4.10	4.16	3.17	0.98	0.56	3.34	4.20
	Mn	0.28	0.33	0.32	0.46	0.34	0.62	0.00	0.00	0.62	0.36
	Ca	0.00	0.20	0.00	0.19	0.25	0.98	0.57	0.60	1.23	0.24
	Total	5.81	5.82	5.76	5.84	5.56	5.77	6.00	5.90	5.85	5.84
End Members											
	$Mg_3Cr_2Si_3O_{12}$	0.00	0.00	0.00	0.00	0.00	0.00	4.05	0.00	0.00	0.00
	Uvarovite	0.00	0.00	0.00	0.00	0.00	0.00	0.00	0.00	0.00	0.00
	Andradite	0.00	3.51	0.00	3.30	4.47	10.60	2.01	9.58	0.00	4.10
	Grossular	0.00	0.00	0.00	0.00	0.00	6.36	7.54	0.58	21.04	0.00
	Spessartine	4.85	5.69	5.48	7.90	6.08	10.81	0.00	0.00	10.54	6.11
	Almandine	76.60	77.75	73.79	70.20	74.75	54.85	16.39	9.41	57.08	71.90
	Pyrope	18.55	13.06	20.73	18.59	14.70	17.38	70.01	80.43	11.34	17.89

		CL-07-010-224							CL-07-010-233		
	Garnet Type	9	5	9	9	9	1	5	1	5	5
Oxide%	**SiO2**	41.47	35.37	40.53	42.16	41.6	41.03	36.63	41.41	37.12	34.87
	TiO2	0	0.00	0	0	0	0.91	0	0.86	0	0
	Al2O3	18.32	21.70	20.93	21.34	19.14	19.52	19.33	23.26	22.03	21.91
	FeOT	6.22	32.56	7	7.47	7.52	8.66	34.96	12.76	33.96	33.46
	MnO	0.62	2.92	0	0	0	0.35	1.14	0	1.57	4.64
	MgO	23.25	4.10	22	21.54	22.6	21.05	5.33	17.55	4.78	3.63
	CaO	4.89	2.94	4.9	4.51	5.28	4.93	0	3.19	0	1.24
	Cr2O3	4.96	0.00	4.32	0	2.12	2.42	0	0	0	0
	Total	100	99.63	99.8	99.6	99.56	98.87	99.69	99.61	99.91	99.7
No. Ions in Formula											
	Si	5.89	5.66	5.76	6.10	5.97	5.92	6.01	6.04	5.94	5.62
	Al	0.11	0.34	0.24	0.00	0.03	0.08	0.00	0.00	0.06	0.38
	Total	6.00	6.00	6.00	6.10	6.00	6.00	6.01	6.04	6.00	6.00
	Al	2.96	3.76	3.27	3.64	3.21	3.24	3.74	4.00	4.10	3.77
	Fe3+	0.59	0.58	0.48	0.15	0.58	0.36	0.25	0.00	0.00	0.61
	Cr	0.56	0.00	0.49	0.00	0.24	0.28	0.00	0.00	0.00	0.00
	Total	4.11	4.34	4.24	3.79	4.03	3.88	3.99	4.00	4.10	4.38
	Mg	4.92	0.98	4.66	4.65	4.84	4.53	1.30	3.81	1.14	0.87
	Fe2+	0.15	3.78	0.35	0.76	0.32	0.69	4.55	1.56	4.55	3.90
	Mn	0.07	0.40	0.00	0.00	0.00	0.04	0.16	0.00	0.21	0.63
	Ca	0.74	0.50	0.75	0.70	0.81	0.76	0.00	0.50	0.00	0.21
	Total	5.89	5.66	5.76	6.10	5.97	6.02	6.01	5.87	5.90	5.62
End Members											
	$Mg_3Cr_2Si_3O_{12}$	13.56	0.00	11.46	0.00	5.97	0.00	0.00	0.00	0.00	0.00
	Uvarovite	0.00	0.00	0.00	0.00	0.00	7.12	0.00	0.00	0.00	0.00
	Andradite	12.63	8.91	11.31	3.93	13.60	5.54	0.00	0.00	0.00	3.81
	Grossular	0.00	0.00	1.64	7.53	0.00	0.00	0.00	8.49	0.00	0.00
	Spessartine	1.27	6.99	0.00	0.00	0.00	0.71	2.64	0.00	3.61	11.27
	Almandine	2.52	66.82	6.13	12.38	5.42	11.40	75.67	26.51	77.06	69.40
	Pyrope	70.01	17.28	69.45	76.16	75.01	75.22	21.69	65.00	19.33	15.52

CL-07-010-245

	Garnet Type	9	5	5	5	11	9	9	3	4	5
Oxide%	**SiO2**	43.36	36.39	36.41	34.48	40.83	35.54	41.9	27.7	35.67	37.60
	TiO2	0	0	0	0	0.51	0	0	0	0	0.00
	Al2O3	23.05	22.71	21.82	22.5	18.31	19.95	15.48	54.92	19.54	20.99
	FeOT	7.03	34.07	33.5	34.78	7.11	13.24	9.36	14.58	8.78	32.60
	MnO	0	2.76	3.25	3.53	0	28.01	0	0	33.56	2.75
	MgO	19.87	3.63	3.98	3.54	21.31	1.41	19.47	2.17	0	5.69
	CaO	3.47	0	0.7	0.78	5.86	0.68	6.55	0	0	0.00
	Cr2O3	3.1	0	0	0	5.88	0	5.43	0	0	0.00
	Total	99.67	99.9	99.85	99.52	100.03	98.44	99.46	100.11	99.51	100.29
No. Ions in Formula											
	Si	6.18	5.86	5.85	5.56	5.86	5.88	6.19	4.11	6.04	5.99
	Al	0.00	0.14	0.15	0.44	0.14	0.12	0.00	1.89	0.00	0.01
	Total	6.18	6.00	6.00	6.00	6.00	6.00	6.19	6.00	6.04	6.00
	Al	3.87	4.17	3.98	3.84	2.96	3.77	2.70	7.71	3.90	3.93
	Fe3+	0.00	0.00	0.17	0.60	0.40	0.35	0.29	0.00	0.02	0.08
	Cr	0.35	0.00	0.00	0.00	0.67	0.00	0.63	0.00	0.00	0.00
	Total	4.22	4.17	4.15	4.44	4.03	4.12	3.62	7.71	3.92	4.01
	Mg	4.22	0.87	0.95	0.85	4.56	0.35	4.29	0.48	0.00	1.35
	Fe2+	0.84	4.59	4.33	4.09	0.45	1.49	0.87	1.81	1.23	4.27
	Mn	0.00	0.38	0.44	0.48	0.00	3.93	0.00	0.00	4.81	0.37
	Ca	0.53	0.00	0.12	0.13	0.90	0.12	1.04	0.00	0.00	0.00
	Total	5.59	5.83	5.85	5.56	5.92	5.88	6.19	2.29	6.04	5.99
End Members											
	$Mg_3Cr_2Si_3O_{12}$	8.27	0.00	0.00	0.00	16.57	0.00	17.52	0.00	0.00	0.00
	Uvarovite	0.00	0.00	0.00	0.00	0.00	0.00	0.00	0.00	0.00	0.00
	Andradite	0.00	0.00	2.06	2.42	9.90	2.05	8.04	0.00	0.00	0.00
	Grossular	9.48	0.00	0.00	0.00	5.33	0.00	8.71	0.00	0.00	0.00
	Spessartine	0.00	6.45	7.56	8.67	0.00	66.76	0.00	0.00	79.69	6.20
	Almandine	14.99	78.62	74.08	73.60	7.69	25.28	13.98	79.03	20.31	71.25
	Pyrope	67.25	14.93	16.29	15.30	60.50	5.91	51.75	20.97	0.00	22.56

		CL-07-010-255					CL-07-010-264				
	Garnet Type	1	9	2	5	5	9	9	2	2	5
Oxide%	**SiO2**	41.73	41.34	41.96	36.98	37.12	41.85	41.76	41.77	42.05	36.96
	TiO2	0.70	0	0.73	0	0	0	0.00	0	0.78	0
	Al2O3	19.77	20.37	20.29	20.51	20.8	18.64	20.37	21.27	19.96	20.31
	FeOT	8.16	8.31	7.98	33.65	33.69	7.35	7.58	7.85	8.52	25.63
	MnO	0.00	0	0	1.65	1.68	0	0.00	0	0.3	7.94
	MgO	22.61	21.06	22.41	5.14	4.83	21.61	21.58	21.83	21.64	3.82
	CaO	4.57	5.09	4.57	0.98	0.9	5.09	5.00	4.27	4.52	4.45
	Cr2O3	2.12	2.96	2.02	0	0	4.31	3.28	1.6	2.03	0
	Total	99.91	99.77	99.95	99.29	99.21	99.52	99.49	99.75	99.79	99.11
No. Ions in Formula											
	Si	5.93	5.93	5.94	5.95	5.98	6.03	5.95	5.98	5.99	5.94
	Al	0.07	0.07	0.06	0.05	0.02	0.00	0.05	0.02	0.01	0.06
	Total	6.00	6.00	6.00	6.00	6.00	6.03	6.00	6.00	6.00	6.00
	Al	3.24	3.38	3.33	3.84	3.92	3.17	3.38	3.57	3.35	3.79
	Fe3+	0.45	0.35	0.35	0.20	0.10	0.28	0.30	0.27	0.26	0.27
	Cr	0.24	0.34	0.23	0.00	0.00	0.49	0.37	0.18	0.23	0.00
	Total	3.92	4.07	3.90	4.05	4.02	3.94	4.05	4.02	3.84	4.06
	Mg	4.79	4.51	4.73	1.23	1.16	4.64	4.59	4.66	4.60	0.92
	Fe2+	0.52	0.64	0.60	4.32	4.43	0.60	0.60	0.67	0.75	3.18
	Mn	0.00	0.00	0.00	0.22	0.23	0.00	0.00	0.00	0.04	1.08
	Ca	0.70	0.78	0.69	0.17	0.16	0.79	0.76	0.65	0.69	0.77
	Total	6.00	5.93	6.02	5.95	5.98	6.03	5.95	5.98	6.08	5.94
End Members											
	$Mg_3Cr_2Si_3O_{12}$	0.00	8.26	0.00	0.00	0.00	12.46	9.14	0.00	0.00	0.00
	Uvarovite	6.07	0.00	5.79	0.00	0.00	0.00	0.00	4.50	5.96	0.00
	Andradite	5.52	8.67	5.73	2.84	2.57	7.19	7.42	6.45	5.40	6.59
	Grossular	0.00	4.52	0.00	0.00	0.03	5.85	5.41	0.00	0.00	6.31
	Spessartine	0.00	0.00	0.00	3.78	3.83	0.00	0.00	0.00	0.60	18.20
	Almandine	8.65	10.87	9.89	72.66	74.17	9.99	10.14	11.14	12.39	53.49
	Pyrope	79.76	67.68	78.59	20.72	19.40	64.51	67.90	77.91	75.66	15.41

CL-07-014-233

	Garnet Type	9	9	5	5	2	2	2	5	2	1
Oxide%	**SiO2**	40.6	41.38	35.56	35.86	42.06	41.86	40.59	34.62	41.53	40.78
	TiO2	0	0	0	0	0.8	0.76	0	0	1.19	1.03
	Al2O3	20.88	16.93	21.93	21.87	20.86	21.04	21.92	21.59	19.91	20.16
	FeOT	10.53	7.49	35.21	35.24	7.81	8.37	8.05	35.91	8.46	7.61
	MnO	0	0.36	2.33	2.24	0	0	0.46	3.76	0	0.3
	MgO	20.79	20.26	3.4	3.57	21.41	21.98	21.73	2.87	22.55	21.92
	CaO	4.84	6.44	1.21	0.86	4.87	4.73	4.8	0.73	4.14	4.9
	Cr2O3	3.03	7.34	0	0	1.88	1.9	2.97	0	2.24	2.48
	Total	99.98	100.28	99.95	99.76	99.85	100.63	100.52	99.66	99.87	99.18
No. Ions in Formula											
	Si	5.77	5.97	5.74	5.78	5.99	5.90	5.73	5.63	5.89	5.83
	Al	0.23	0.03	0.26	0.22	0.01	0.10	0.27	0.37	0.11	0.17
	Total	6.00	6.00	6.00	6.00	6.00	6.00	6.00	6.00	6.00	6.00
	Al	3.27	2.86	3.91	3.94	3.49	3.39	3.37	3.77	3.22	3.23
	Fe3+	0.62	0.33	0.36	0.28	0.14	0.34	0.57	0.60	0.38	0.43
	Cr	0.34	0.84	0.00	0.00	0.21	0.21	0.33	0.00	0.25	0.28
	Total	4.23	4.03	4.26	4.22	3.84	3.94	4.27	4.37	3.85	3.94
	Mg	4.40	4.36	0.82	0.86	4.54	4.62	4.57	0.70	4.77	4.68
	Fe2+	0.63	0.57	4.39	4.47	0.79	0.65	0.38	4.29	0.62	0.48
	Mn	0.00	0.04	0.32	0.31	0.00	0.00	0.05	0.52	0.00	0.04
	Ca	0.74	1.00	0.21	0.15	0.74	0.71	0.73	0.13	0.63	0.75
	Total	5.77	5.97	5.74	5.78	6.07	5.98	5.73	5.63	6.02	5.95
End Members											
	$Mg_3Cr_2Si_3O_{12}$	8.05	20.82	0.00	0.00	0.00	0.00	0.00	0.00	0.00	0.00
	Uvarovite	0.00	0.00	0.00	0.00	5.51	5.37	7.75	0.00	6.52	7.11
	Andradite	12.77	8.22	3.65	2.57	3.72	6.57	4.92	2.26	3.94	5.52
	Grossular	0.00	8.46	0.00	0.00	3.00	0.00	0.00	0.00	0.00	0.00
	Spessartine	0.00	0.74	5.55	5.29	0.00	0.00	0.96	9.20	0.00	0.61
	Almandine	10.89	9.60	76.55	77.30	12.96	10.84	6.56	76.18	10.31	8.12
	Pyrope	68.29	52.17	14.25	14.84	74.81	77.22	79.80	12.36	79.23	78.63

		CL-07-014-245									CL-07-014-257
	Garnet Type	5	5	9	9	5	1	5	5	9	9
Oxide%	**SiO2**	36.33	37.08	42.92	41.79	37.85	41.9	36.38	36.61	40.55	42.85
	TiO2	0	0	0	0.29	0	0.88	0	0	0.66	0.00
	Al2O3	21.47	20.4	21.41	20.77	20.62	19.98	21.03	21.06	23.36	19.08
	FeOT	33.27	34.01	5.77	6.82	33.86	8.17	34.78	35.64	10.28	7.79
	MnO	2.1	3.03	0	0.79	2.96	0	2.98	2.01	0	0.00
	MgO	4.56	4.19	21.37	21.27	3.11	20.52	3.49	3.39	19.12	19.83
	CaO	0.87	0.82	4.61	4.77	0.85	5.15	0.83	0.85	5.13	4.49
	Cr2O3	0	0	3.31	3.47	0	2.66	0	0	0	5.33
	Total	98.64	99.78	99.95	99.97	99.38	99.41	99.44	99.67	99.58	99.78
No. Ions in Formula											
	Si	5.87	5.98	6.11	5.95	6.15	6.03	5.89	5.92	5.84	6.21
	Al	0.13	0.02	0.00	0.05	0.00	0.00	0.11	0.08	0.16	0.00
	Total	6.00	6.00	6.11	6.00	6.15	6.03	6.00	6.00	6.00	6.21
	Al	3.96	3.85	3.59	3.43	3.95	3.39	3.90	3.94	3.80	3.26
	Fe3+	0.16	0.17	0.00	0.17	0.00	0.05	0.21	0.14	0.22	0.00
	Cr	0.00	0.00	0.37	0.39	0.00	0.30	0.00	0.00	0.00	0.61
	Total	4.13	4.02	3.97	3.99	3.95	3.75	4.11	4.08	4.02	3.87
	Mg	1.10	1.01	4.53	4.51	0.75	4.40	0.84	0.82	4.10	4.28
	Fe2+	4.34	4.41	0.69	0.64	4.60	0.93	4.49	4.68	1.01	0.94
	Mn	0.29	0.41	0.00	0.10	0.41	0.00	0.41	0.28	0.00	0.00
	Ca	0.15	0.14	0.70	0.73	0.15	0.79	0.14	0.15	0.79	0.70
	Total	5.87	5.98	5.93	5.98	5.91	6.13	5.89	5.92	5.91	5.92
End Members											
	$Mg_3Cr_2Si_3O_{12}$	0.00	0.00	9.40	9.78	0.00	0.00	0.00	0.00	0.00	15.78
	Uvarovite	0.00	0.00	0.00	0.00	0.00	8.08	0.00	0.00	0.00	0.00
	Andradite	2.57	2.37	0.00	4.22	0.00	1.45	2.44	2.49	5.55	0.00
	Grossular	0.00	0.00	11.87	7.95	2.50	3.43	0.00	0.00	7.85	11.77
	Spessartine	4.90	6.92	0.00	1.59	6.89	0.00	6.94	4.65	0.00	0.00
	Almandine	73.83	73.86	11.59	10.76	77.86	15.17	76.32	79.06	17.17	15.93
	Pyrope	18.71	16.84	67.14	65.69	12.75	71.87	14.30	13.80	69.44	56.52

									CL-07-014-260		
	Garnet Type	3	5	5	11	9	5	5	5	9	5
Oxide%	**SiO2**	38.81	37.58	37.63	40.67	41.67	38.64	37.44	34.95	39.74	36.1
	TiO2	0	0	0	0.98	0	0	0	0.00	0	0
	Al2O3	21.68	20.74	20.53	17.48	20.91	20.92	21	21.99	21.7	22.42
	FeOT	18.11	34.52	34.51	8.49	8.15	34.09	35.06	29.94	7.91	36.17
	MnO	12.41	0.67	0.64	0	0	1.72	0.68	2.71	0	1.69
	MgO	6.27	4.93	5.01	19.76	21.28	3.37	4.24	3.78	22.25	3.44
	CaO	2.76	1.48	1.56	5.68	4.42	1.08	1.51	6.23	4.05	0
	Cr2O3	0	0	0	6.23	2.49	0	0	0.00	2.43	0
	Total	99.84	99.88	99.71	99.96	99.99	99.66	100.14	99.83	99.29	99.65
No. Ions in Formula											
	Si	6.07	5.99	6.00	5.94	5.98	6.22	5.99	5.56	5.71	5.81
	Al	0.00	0.01	0.00	0.06	0.02	0.00	0.01	0.44	0.29	0.19
	Total	6.07	6.00	6.00	6.00	6.00	6.22	6.00	6.00	6.00	6.00
	Al	4.00	3.88	3.86	2.95	3.51	3.97	3.95	3.69	3.38	4.07
	Fe3+	0.00	0.13	0.15	0.18	0.23	0.00	0.06	0.75	0.63	0.11
	Cr	0.00	0.00	0.00	0.72	0.28	0.00	0.00	0.00	0.28	0.00
	Total	4.00	4.01	4.00	3.85	4.02	3.97	4.01	4.44	4.29	4.19
	Mg	1.46	1.17	1.19	4.30	4.55	0.81	1.01	0.90	4.77	0.83
	Fe2+	2.37	4.47	4.46	0.86	0.75	4.59	4.63	3.24	0.32	4.76
	Mn	1.64	0.09	0.09	0.00	0.00	0.23	0.09	0.37	0.00	0.23
	Ca	0.46	0.25	0.27	0.89	0.68	0.19	0.26	1.06	0.62	0.00
	Total	5.94	5.99	6.00	6.05	5.98	5.82	5.99	5.56	5.71	5.81
End Members											
	$Mg_3Cr_2Si_3O_{12}$	0.00	0.00	0.00	18.70	7.02	0.00	0.00	0.00	6.43	0.00
	Uvarovite	0.00	0.00	0.00	0.00	0.00	0.00	0.00	0.00	0.00	0.00
	Andradite	0.00	3.15	3.64	4.69	5.72	0.00	1.58	16.85	10.92	0.00
	Grossular	7.79	1.07	0.80	10.01	5.65	3.20	2.74	2.25	0.00	0.00
	Spessartine	27.69	1.51	1.44	0.00	0.00	4.03	1.54	6.57	0.00	3.97
	Almandine	39.90	74.71	74.27	14.16	12.51	78.87	77.26	58.21	5.62	81.83
	Pyrope	24.62	19.56	19.85	52.44	69.11	13.90	16.88	16.12	77.03	14.20

					CL-07-014-269				CL-07-014-273		
	Garnet Type	5	9	11	5	5	5	9	5	5	5
Oxide%	**SiO2**	36.75	40.17	40.4	36.28	37.35	36.23	41.74	36.94	36.53	36.87
	TiO2	0	0	0.56	0.00	0	0	0	0.00	0	0
	Al2O3	22.16	17.42	17.7	21.65	22.59	21.78	19.6	20.89	21.21	21.41
	FeOT	32.93	7.56	7.93	34.19	33.65	35.4	5.97	33.93	28.14	29.11
	MnO	2.63	0	0.45	2.96	1.98	1.77	0	2.38	4.55	4.44
	MgO	4.29	19.4	19.78	3.42	4.02	3.81	23.51	4.19	2.67	3.21
	CaO	0.77	5.82	6.02	1.61	0	0.68	4.71	0.76	7.03	4.7
	Cr2O3	0	7.77	7.55	0.00	0	0	5.41	0.00	0	0
	Total	99.65	99.2	100.41	99.96	99.31	99.76	99.9	99.90	100.15	99.97
No. Ions in Formula											
	Si	5.89	5.93	5.84	5.82	5.99	5.83	5.85	5.97	5.82	5.90
	Al	0.11	0.07	0.16	0.18	0.01	0.17	0.15	0.03	0.18	0.10
	Total	6.00	6.00	6.00	6.00	6.00	6.00	6.00	6.00	6.00	6.00
	Al	4.07	2.97	2.86	3.92	4.26	3.96	3.08	3.95	3.80	3.93
	Fe3+	0.04	0.19	0.31	0.26	0.00	0.21	0.47	0.08	0.38	0.17
	Cr	0.00	0.91	0.86	0.00	0.00	0.00	0.60	0.00	0.00	0.00
	Total	4.11	4.07	4.03	4.18	4.26	4.17	4.15	4.03	4.18	4.10
	Mg	1.02	4.27	4.27	0.82	0.96	0.91	4.91	1.01	0.63	0.77
	Fe2+	4.37	0.74	0.65	4.32	4.51	4.56	0.23	4.50	3.37	3.72
	Mn	0.36	0.00	0.06	0.40	0.27	0.24	0.00	0.33	0.61	0.60
	Ca	0.13	0.92	0.93	0.28	0.00	0.12	0.71	0.13	1.20	0.81
	Total	5.89	5.93	5.91	5.82	5.74	5.83	5.85	5.97	5.82	5.90
End Members											
	$Mg_3Cr_2Si_3O_{12}$	0.00	22.31	21.41	0.00	0.00	0.00	14.43	0.00	0.00	0.00
	Uvarovite	0.00	0.00	0.00	0.00	0.00	0.00	0.00	0.00	0.00	0.00
	Andradite	0.93	4.75	7.63	4.76	0.00	2.01	11.29	2.06	9.04	4.12
	Grossular	1.32	10.77	8.17	0.00	0.00	0.00	0.80	0.15	11.58	9.54
	Spessartine	6.06	0.00	0.93	6.91	4.68	4.14	0.00	5.46	10.55	10.20
	Almandine	74.29	12.48	11.03	74.28	78.58	78.17	3.95	75.43	57.93	63.16
	Pyrope	17.40	49.68	50.82	14.05	16.73	15.68	69.53	16.91	10.90	12.98

	Garnet Type	9	9	5	5
Oxide%	**SiO2**	40.72	41.02	35.85	36.88
	TiO2	0	0	0	0
	Al2O3	20.65	20.36	21.45	21.62
	FeOT	7.34	7.4	34.87	34.02
	MnO	0	0.45	1.92	2.54
	MgO	21.18	21.4	4.05	3.99
	CaO	5.04	4.99	1.1	0.9
	Cr2O3	4.66	4.59	0	0
	Total	99.6	100.2	99.61	99.97
No. Ions in Formula					
	Si	5.82	5.84	5.79	5.91
	Al	0.18	0.16	0.21	0.09
	Total	6.00	6.00	6.00	6.00
	Al	3.31	3.25	3.87	3.99
	Fe3+	0.34	0.40	0.35	0.10
	Cr	0.53	0.52	0.00	0.00
	Total	4.18	4.16	4.21	4.09
	Mg	4.52	4.54	0.97	0.95
	Fe2+	0.54	0.48	4.36	4.46
	Mn	0.00	0.05	0.26	0.34
	Ca	0.77	0.76	0.19	0.15
	Total	5.82	5.84	5.79	5.91
End Members					
	$Mg_3Cr_2Si_3O_{12}$	12.62	12.40	0.00	0.00
	Uvarovite	0.00	0.00	0.00	0.00
	Andradite	8.19	9.56	3.29	2.49
	Grossular	5.07	3.48	0.00	0.13
	Spessartine	0.00	0.93	4.54	5.83
	Almandine	9.20	8.27	75.34	75.42
	Pyrope	64.91	65.37	16.84	16.13

Appendix D-9 Ilmenite

Ilmenite		CL-06-003-158										
								CL-06-003-173	CL-06-003-182			
Oxide%												
	SiO2	0	0	0	0	0	1.86	0	1.02	0	0	0
	TiO2	50.25	50	50.43	51.48	51.66	60.84	51.04	57.28	51.13	49.93	14.74
	Al2O3	0	0	0	0	0	0	0	0	0	0	0
	FeOT	48.73	45.03	44.9	41.53	39.1	34.56	31.77	33.03	43.63	48.13	77.43
	MnO	1.28	0	0.63	0.65	0	0	0	5.78	0	0	0
	MgO	0	2.59	2.87	4.44	6.91	0.84	12.39	0	2.69	0	0
	Cr2O3	0	0	0	0	0	0	2.46	0	0	0	0
	CaO	0	0	0	0	0	0	0	0	0	0	0
	Total	99.34	99.07	99.25	98.41	98.81	99.04	97.22	97.99	98.35	97.96	93.2
Convert to Oxide %												
	SiO2	0	0	0	0	0	1.86	0	1.02	0	0	0
	TiO2	50.25	50	50.43	51.48	51.66	60.84	51.04	57.28	51.13	49.93	14.74
	Al2O3	0	0	0	0	0	0	0	0	0	0	0
	FeO2+	43.9	40.35	39.6	37.73	34.14	34.56	23.81	33.03	41.19	44.91	13.26
	FeO3+	5.37	5.2	6.03	4.23	5.51	0	8.85	0	2.71	2.58	71.31
	MnO	1.28	0	0.63	0.65	0	0	0	5.78	0	0	0
	MgO	0	2.59	2.87	4.44	6.91	0.84	12.39	0	2.69	0	0
	Cr2O3	0	0	0	0	0	0	2.46	0	0	0	0
	CaO	0	0	0	0	0	0	0	0	0	0	0
	Total	100.8	98.14	99.56	98.52	98.22	98.1	98.55	97.11	97.72	97.42	99.31
End Members												
	FeTiO3	5.21	4.94	5.72	4	5.07	0	7.98	0	2.58	3.46	70.77
	MgTiO3	0	9.76	10.79	16.65	25.18	4.15	44.29	0	10.16	0	0
	Fe2O3	94.79	85.29	83.49	79.35	69.76	95.85	47.73	100	87.25	96.54	29.23

		CL-06-003-186					CL-06-003-219					
Oxide%												
	SiO2	0.00	0.00	0.00	0.00	0.00	0.00	0.00	0.00	0.00	0.36	0.00
	TiO2	46.90	46.29	36.00	38.05	50.68	51.82	45.27	44.84	57.55	54.99	49.69
	Al2O3	0.00	0.00	0.00	0.53	0.00	0.00	0.00	0.00	0.00	0.00	0.00
	FeOT	49.84	50.04	35.69	35.18	46.57	44.89	51.12	50.21	37.52	39.03	45.37
	MnO	2.40	1.55	0.00	0.00	0.00	1.77	0.00	0.69	2.98	3.04	2.56
	MgO	0.00	0.00	13.26	13.38	1.15	0.00	0.00	1.17	0.00	0.00	0.00
	Cr2O3	0.00	0.00	11.95	11.99	0.00	0.00	0.00	0.00	0.00	0.00	0.00
	CaO	0.00	0.00	0.00	0.00	0.00	0.00	0.00	0.00	0.00	0.00	0.00
	Total	98.98	97.90	98.82	99.12	99.01	99.09	98.80	97.25	98.19	97.74	97.84
Convert to Oxide %												
	SiO2	0.00	0.00	0.00	0.00	0.00	0.00	0.00	0.00	0.00	0.36	0.00
	TiO2	46.90	46.29	36.00	38.05	50.68	51.82	45.27	44.84	57.55	54.99	49.69
	Al2O3	0.00	0.00	0.00	0.53	0.00	0.00	0.00	0.00	0.00	0.00	0.00
	FeO2+	39.75	40.07	8.73	27.59	43.53	44.82	40.72	37.55			42.10
	FeO3+	11.21	11.08	29.96	11.99	3.37	0.08	11.56	14.07			3.63
	MnO	2.40	1.55	0.00	0.00	0.00	1.77	0.00	0.69	2.98	3.04	2.56
	MgO	0.00	0.00	13.26	13.38	1.15	0.00	0.00	1.17	0.00	0.00	0.00
	Cr2O3	0.00	0.00	11.95	11.99	0.00	0.00	0.00	0.00	0.00	0.00	0.00
	CaO	0.00	0.00	0.00	0.00	0.00	0.00	0.00	0.00	0.00	0.00	0.00
	Total	100.26	98.99	99.9	101.89	98.74	98.49	97.55	98.32	60.53	58.39	97.98
End Members												
	FeTiO3	11.26	11.07	29.4	26.62	3.22	0.08	11.33	13.78	0	0	3.74
	MgTiO3	0	0	51.56	51.16	4.35	0	0	4.54	0	0	0
	Fe2O3	88.74	88.93	19.03	22.21	92.42	99.92	88.67	81.68	100	100	96.26

		CL-06-003-222			CL-06-003-236				CL-07-006-195		
Oxide%											
SiO2	0.00	0.00	0.00	0.00	0.00	0.00	0.00	0.00	0.00	0.00	0.00
TiO2	51.06	48.08	48.57	48.43	52.43	51.71	47.43	50.68	52.09	57.29	46.81
Al2O3	0.00	0.00	0.00	0.00	0.00	0.00	0.00	0.00	0.00	0.00	0.00
FeOT	27.23	49.95	46.97	46.75	37.42	37.38	48.44	48.45	35.78	39.28	46.94
MnO	0.00	0.00	0.93	2.69	4.83	5.48	2.31	0.39	10.07	0.82	2.33
MgO	13.32	0.00	1.26	0.00	4.08	4.04	0.00	0.00	0.00	1.03	1.66
Cr2O3	5.97	0.00	0.00	0.00	0.00	0.00	0.00	0.00	0.00	0.00	0.00
CaO	0.00	0.00	0.00	0.00	0.00	0.00	0.00	0.00	0.00	0.00	0.00
Total	97.78	98.54	99.30	98.72	98.70	98.69	98.19	99.50	99.13	99.22	99.14
Convert to Oxide %											
SiO2	0	0.00	0.00	0.00	0.00	0.00	0.00	0.00	0.00	0.00	0.00
TiO2	51.06	48.08	48.57	48.43	52.43	51.71	47.43	50.68	52.09	57.29	46.81
Al2O3	0	0.00	0.00	0.00	0.00	0.00	0.00	0.00	0.00	0.00	0.00
FeO2+	22.17	43.89	40.50	40.84	34.99	33.75	40.32	45.19	35.78	39.28	36.78
FeO3+	5.63	6.73	7.19	6.58	2.70	4.03	9.02	3.62	0.00	0.00	11.29
MnO	0	0.00	0.93	2.69	4.83	5.48	2.31	0.39	10.07	0.82	2.33
MgO	13.32	0.00	1.26	0.00	4.08	4.04	0.00	0.00	0.00	1.03	1.66
Cr2O3	5.97	0.00	0.00	0.00	0.00	0.00	0.00	0.00	0.00	0.00	0.00
CaO	0	0.00	0.00	0.00	0.00	0.00	0.00	0.00	0.00	0.00	0.00
Total	98.15	98.70	98.45	98.54	99.03	99.01	99.08	99.88	97.94	98.42	98.87
End Members											
FeTiO3	5.23	6.46	7.04	6.76	2.8	4.24	9.15	3.48	0	0	11.33
MgTiO3	49.02	0	4.89	0	16.73	16.84	0	0	0	4.47	6.6
Fe2O3	45.75	96.54	88.07	93.24	80.47	78.92	90.85	96.52	100	95.53	82.06

CL-07-006-208

Oxide%											
SiO2	0.00	0.00	0.00	0.52	1.76	0.00	0.00	0.00	0.00	0.00	0.00
TiO2	48.62	59.23	54.55	61.10	60.51	49.68	51.33	51.08	53.66	50.16	50.53
Al2O3	0.00	0.00	0.28	0.00	0.00	0.00	0.00	0.00	0.00	0.00	0.00
FeOT	45.94	36.23	41.45	34.80	34.84	43.98	45.98	46.35	40.89	45.88	46.69
MnO	0.00	2.08	1.98	0.62	0.77	2.65	0.91	0.84	4.05	0.79	0.00
MgO	3.70	0.00	0.00	0.87	0.81	0.00	0.00	0.00	0.00	0.89	0.00
Cr2O3	0.00	0.00	0.00	0.00	0.00	0.00	0.00	0.00	0.00	0.00	0.00
CaO	0.00	0.00	0.00	0.00	0.00	0.00	0.00	0.00	0.00	0.00	0.00
Total	98.50	99.12	99.24	99.65	99.23	96.58	98.45	98.39	98.35	98.48	98.69
Convert to Oxide %											
SiO2	0	0	0	0.52	1.76	0.00	0.00	0.00	0.00	0.00	0.00
TiO2	48.62	59.23	54.55	61.1	60.51	49.68	51.33	51.08	53.66	50.16	50.53
Al2O3	0	0	0.28	0	0	0.00	0.00	0.00	0.00	0.00	0.00
FeO2+	37.13	36.23	41.45	34.8	34.84	42.00	45.25	45.09	40.89	45.88	45.45
FeO3+	9.79	0	0	0	0	2.20	0.81	1.40	0.00	0.00	1.38
MnO	0	2.08	1.98	0.62	0.77	2.65	0.91	0.84	4.05	0.79	0.00
MgO	3.7	0	0	0.87	0.81	0.00	0.00	0.00	0.00	0.89	0.00
Cr2O3	0	0	0	0	0	0.00	0.00	0.00	0.00	0.00	0.00
CaO	0	0	0	0	0	0.00	0.00	0.00	0.00	0.00	0.00
Total	99.24	97.54	98.26	97.91	98.69	96.53	98.30	98.41	98.60	97.72	97.36
End Members											
FeTiO3	9.15	0	0	0	0	2.3	0.8	1.37	0	0	1.35
MgTiO3	13.71	0	0	4.27	4.26	0	0	0	0	3.74	0
Fe2O3	77.14	100	100	95.73	95.74	97.7	99.2	98.63	100	96.26	98.65

			CL-07-006-235						CL-07-010-160			
Oxide%												
	SiO2	0.30	1.46	0.00	0.59	0.00	0.00	0.00	0.00	0.39	0.70	0.00
	TiO2	48.48	63.54	62.09	61.06	51.57	49.32	48.90	48.57	54.73	60.39	58.58
	Al2O3	0.00	0.00	0.00	0.00	0.00	0.00	0.00	0.00	0.00	0.00	0.00
	FeOT	46.26	32.08	35.67	36.11	44.87	47.38	48.20	42.60	31.35	31.49	35.45
	MnO	1.84	1.21	0.00	0.41	1.85	1.46	1.07	0.45	0.45	1.27	1.64
	MgO	0.00	0.00	0.00	0.00	0.00	0.00	0.00	4.73	0.93	0.38	0.87
	Cr2O3	0.00	0.00	0.00	0.00	0.00	0.00	0.00	0.00	0.00	0.00	0.00
	CaO	0.00	0.00	0.00	0.00	0.00	0.00	0.00	0.00	0.00	0.00	0.00
	Total	97.24	99.34	98.12	98.61	98.64	98.33	98.58	96.71	88.19	94.48	98.20
Convert to Oxide %												
	SiO2	0.3	1.46	0.00	0.59	0.00	0.00	0.00	0.00	0.39	0.70	0.00
	TiO2	48.48	63.54	62.09	61.06	51.57	49.32	48.90	48.57	54.73	60.39	58.58
	Al2O3	0	0.00	0.00	0.00	0.00	0.00	0.00	0.00	0.00	0.00	0.00
	FeO2+	46.26	32.08	35.67	36.11	44.51	42.88	42.90	34.79	31.35	31.49	35.45
	FeO3+		0.00	0.00	0.00	0.40	5.00	5.89	8.68	0.00	0.00	0.00
	MnO	1.84	1.21	0.00	0.41	1.85	1.46	1.07	0.45	0.45	1.27	1.64
	MgO	0	0.00	0.00	0.00	0.00	0.00	0.00	4.73	0.93	0.38	0.87
	Cr2O3	0	0.00	0.00	0.00	0.00	0.00	0.00	0.00	0.00	0.00	0.00
	CaO	0	0.00	0.00	0.00	0.00	0.00	0.00	0.00	0.00	0.00	0.00
	Total	96.88	98.29	97.76	98.17	98.33	98.66	98.76	97.22	87.85	94.23	96.54
End Members												
	FeTiO3	0	0	0	0	0.4	4.98	5.82	8.28	0	0	0
	MgTiO3	0	0	0	0	0	0	0	17.9	5.02	2.11	4.19
	Fe2O3	100	100	100	100	99.6	95.02	94.18	73.82	94.98	97.89	95.81

		CL-07-010-169		CL-07-010-188				CL-07-010-197			
Oxide%											
	SiO2	0.00	0.00	1.39	0.00	0.00	0.00	0.29	0.00	0.81	0.00
	TiO2	51.30	52.80	55.64	59.01	55.44	52.24	51.82	50.68	57.32	48.21
	Al2O3	0.00	0.00	0.00	0.00	0.00	0.00	0.00	0.00	0.00	0.00
	FeOT	42.72	31.45	38.09	33.63	28.80	44.85	45.41	43.78	34.46	46.31
	MnO	2.34	0.00	2.91	0.52	0.00	1.27	1.18	0.66	2.27	3.92
	MgO	0.00	13.03	0.00	0.58	14.30	0.00	0.00	3.03	0.62	0.00
	Cr2O3	0.00	0.00	0.00	0.00	0.00	0.00	0.00	0.00	0.00	0.00
	CaO	0.00	0.00	0.00	0.00	0.00	0.00	0.00	0.00	0.00	0.00
	Total	98.08	98.20	98.71	94.35	99.60	98.84	99.21	99.14	95.82	98.34
Convert to Oxide %											
	SiO2	0.00	0.00	1.39	0.00	0.00	0.00	0.29	0.00	0.81	0.00
	TiO2	51.30	52.80	55.64	59.01	55.44	52.24	51.82	50.68	57.32	48.21
	Al2O3	0.00	0.00	0.00	0.00	0.00	0.00	0.00	0.00	0.00	0.00
	FeO2+	42.72	24.25	38.09	24.36	28.80	44.85	22.71	39.51	34.46	39.39
	FeO3+	0.00	8.00	0.00	4.94	0.00	0.00	25.23	4.74		7.69
	MnO	2.34	0.00	2.91	0.52	0.00	1.27	1.18	0.66	2.27	3.92
	MgO	0.00	13.03	0.00	0.58	14.30	0.00	0.00	3.03	0.62	0.00
	Cr2O3	0.00	0.00	0.00	0.00	0.00	0.00	0.00	0.00	0.00	0.00
	CaO	0.00	0.00	0.00	0.00	0.00	0.00	0.00	0.00	0.00	0.00
	Total	96.36	98.08	98.03	89.41	98.54	98.36	101.23	98.62	95.48	99.21
End Members											
	FeTiO3	0	7.05	0	4.27	0	0	0	4.54	0	8.07
	MgTiO3	0	45.48	0	48.96	0	0	0	11.48	3.11	0
	Fe2O3	100	47.47	100	46.78	100	100	100	83.98	96.89	91.93

		CL-07-010-221				CL-07-010-224				CL-07-010-233		
Oxide%												
	SiO2	0.00	1.26	4.50	0.00	0.00	0.00	0.00	0.00	0.00	0.00	0.00
	TiO2	46.35	58.93	59.78	51.00	53.32	49.98	22.13	43.09	49.17	53.12	51.27
	Al2O3	0.00	0.00	0.00	1.22	0.00	0.00	1.17	0.00	0.00	0.00	0.00
	FeOT	49.32	33.30	30.09	27.51	27.94	35.87	58.42	42.76	38.31	39.92	42.31
	MnO	0.72	0.55	2.52	0.50	0.00	0.00	0.00	0.00	0.00	0.00	0.64
	MgO	0.00	0.75	0.00	13.22	14.19	11.10	14.84	9.42	9.60	3.89	4.50
	Cr2O3	0.00	0.00	0.00	2.44	1.80	1.09	0.00	2.95	0.00	0.00	0.00
	CaO	0.00	0.00	0.00	0.00	0.00	0.00	0.00	0.00	0.00	0.00	0.00
	Total	96.97	95.17	99.21	96.04	99.14	98.25	98.86	98.81	98.69	96.96	98.99
Convert to Oxide %												
	SiO2	0.00	1.26	4.50	0.00	0.00	0.00	1.26	4.50	0.00	0	0
	TiO2	46.35	58.93	59.78	51.00	53.32	46.35	58.93	59.78	51.00	53.12	51.27
	Al2O3	0.00	0.00	0.00	1.22	0.00	0.00	0.00	0.00	1.22	0	0
	FeO2+	24.66	16.65	15.05	13.76	13.97	40.96	33.30	30.09	21.78	39.92	37.44
	FeO3+	27.40	18.50	16.72	15.29	15.52	9.29	0.00	0.00	6.36		5.41
	MnO	0.72	0.55	2.52	0.50	0.00	0.72	0.55	2.52	0.50	0	0.64
	MgO	0.00	0.75	0.00	13.22	14.19	0.00	0.75	0.00	13.22	3.89	4.5
	Cr2O3	0.00	0.00	0.00	2.44	1.80	0.00	0.00	0.00	2.44	0	0
	CaO	0.00	0.00	0.00	0.00	0.00	0.00	0.00	0.00	0.00	0	0
	Total	99.13	96.64	98.56	97.42	98.80	97.32	94.79	96.89	96.52	96.93	99.26
End Members												
	FeTiO3	9.26	0	0	5.94	5.23	10.65	21.17	11.25	12	0	5.08
	MgTiO3	0	3.86	0	48.88	50	39.34	34.17	34.36	34.62	14.8	16.75
	Fe2O3	90.74	96.14	100	45.18	44.76	50.01	44.66	54.4	53.38	85.2	78.16

		CL-07-010-245						CL-07-010-255			
Oxide%											
SiO2	0.00	0.00	1.38	0.00	0.00	0.00	0.00	0.00	0.00	0.00	0.00
TiO2	35.54	50.82	50.58	50.49	49.77	49.13	48.67	51.35	50.90	55.39	49.07
Al2O3	0.00	0.00	0.00	0.00	0.00	0.00	0.00	1.52	0.00	0.00	0.00
FeOT	57.67	46.63	43.51	47.72	46.64	46.23	46.31	24.61	41.80	24.16	45.58
MnO	2.43	0.00	2.03	0.00	1.82	2.25	1.40	0.00	4.95	0.00	0.00
MgO	0.00	0.00	0.94	0.00	0.00	0.00	1.64	15.21	0.00	18.54	3.55
Cr2O3	0.00	0.00	0.00	0.00	0.00	0.00	0.00	5.02	0.00	0.00	0.00
CaO	0.00	0.00	0.00	0.00	0.00	0.00	0.00	0.00	0.00	0.00	0.00
Total	97.21	98.64	98.91	98.49	98.37	98.19	98.62	98.60	98.55	99.75	99.56
Convert to Oxide %											
SiO2	0	0.00	1.38	0.00	0.00	0.00	0.00	0.00	0.00	0	0
TiO2	35.54	50.82	50.58	50.49	49.77	49.13	48.67	51.35	50.90	55.39	49.07
Al2O3	0	0.00	0.00	0.00	0.00	0.00	0.00	1.52	0.00	0	0
FeO2+	29.51	45.71	41.76	45.41	42.92	41.91	39.43	19.06	40.77	16.75	37.8
FeO3+	31.3	1.02	1.94	2.56	4.13	4.80	7.64	6.17	1.15	8.24	8.64
MnO	2.43	0.00	0.03	0.00	0.03	0.03	0.02	0.00	4.95	0	0
MgO	0	0.00	0.02	0.00	0.00	0.00	0.04	15.21	0.00	18.54	3.55
Cr2O3	0	0.00	0.00	0.00	0.00	0.00	0.00	5.02	0.00	0	0
CaO	0	0.00	0.00	0.00	0.00	0.00	0.00	0.00	0.00	0	0
Total	98.78	97.55	95.71	98.46	96.85	95.87	95.80	98.33	97.77	98.92	99.06
End Members											
FeTiO3	32.31	1	1.97	2.48	4.15	4.9	7.51	5.67	1.25	6.92	8.1
MgTiO3	0	0	3.78	0	0	0	6.39	55.4	0	61.77	13.18
Fe2O3	67.69	99	94.24	97.52	95.85	95.1	86.1	38.93	98.75	31.3	78.72

					CL-07-010-264						CL-07-014	CL-07-014-245
Oxide%												
	SiO2	0.00	0.00	0.39	1.34	1.26	2.45	1.97	2.09	0.00	0.00	0.00
	TiO2	47.18	52.92	51.75	62.61	60.99	56.65	67.09	66.62	60.64	52.50	50.11
	Al2O3	0.00	0.00	0.00	0.00	0.00	0.41	0.00	0.86	0.00	0.00	0.00
	FeOT	45.12	40.29	40.13	32.92	32.67	36.55	29.30	27.35	35.98	40.92	46.08
	MnO	0.42	5.12	4.55	2.20	1.58	0.39	0.00	0.55	0.83	0.65	0.67
	MgO	3.34	0.00	0.00	0.00	0.36	0.93	0.00	0.49	0.00	5.34	0.00
	Cr2O3	0.34	0.00	0.00	0.00	0.00	0.39	0.00	0.00	0.00	0.00	0.00
	CaO	0.00	0.00	0.00	0.00	0.00	0.00	0.00	0.00	0.00	0.00	0.00
	Total	96.66	98.99	97.01	99.19	97.63	97.92	98.58	98.13	98.15	99.49	97.44
Convert to Oxide %												
	SiO2	0	0	0.39	1.34	1.26	2.45	1.97	2.09	0.00	0.00	0.00
	TiO2	47.18	52.92	51.75	62.61	60.99	56.65	67.09	66.62	60.64	52.50	50.11
	Al2O3	0	0	0	0.00	0.00	0.41	0.00	0.86	0.00	0.00	0.00
	FeO2+	36.05	40.29	40.13	32.92	32.67	36.55	29.30	27.35	35.98	37.04	44.39
	FeO3+	10.08	0	0	0.00	0.00	0.00	0.00	0.00	0.00	4.31	1.87
	MnO	0.42	5.12	4.55	2.20	1.58	0.39	0.00	0.55	0.83	0.65	0.67
	MgO	3.34	0	0	0.00	0.36	0.93	0.00	0.49	0.00	5.34	0.00
	Cr2O3	0.34	0	0	0.00	0.00	0.39	0.00	0.00	0.00	0.00	0.00
	CaO	0	0	0	0.00	0.00	0.00	0.00	0.00	0.00	0.00	0.00
	Total	97.41	98.33	96.82	99.07	96.86	97.77	98.36	97.96	97.45	99.84	97.04
End Members												
	FeTiO3	9.74	0	0	0	0	0	0	0	0	4	1.86
	MgTiO3	12.8	0	0	0	1.93	4.34	0	3.1	0	19.63	0
	Fe2O3	77.46	100	100	100	98.07	95.66	100	96.9	100	76.36	98.14

			CL-07-014-257						CL-07-014-260			
Oxide%												
	SiO2	0.00	2.76	1.15	0.00	0.00	1.11	3.04	0.00	0.00	0.32	1.39
	TiO2	49.94	56.99	57.27	50.96	52.22	60.81	58.03	47.66	47.08	49.26	49.76
	Al2O3	0.00	0.00	0.00	0.00	0.00	0.00	0.00	0.00	0.00	0.00	0.00
	FeOT	45.69	31.94	33.98	43.25	39.91	32.02	31.82	49.16	49.40	45.23	42.45
	MnO	0.70	1.18	1.10	0.75	0.78	2.89	2.93	1.33	1.14	1.62	3.76
	MgO	0.32	1.65	0.60	2.91	5.78	0.63	2.34	0.00	0.00	0.00	0.00
	Cr2O3	0.00	0.00	0.00	0.00	0.00	0.00	0.00	0.00	0.00	0.00	0.00
	CaO	0.00	0.00	0.00	0.00	0.00	0.00	0.00	0.00	0.00	0.00	0.00
	Total	96.90	94.86	94.31	98.23	99.01	98.22	98.49	98.98	98.53	96.77	98.20
Convert to Oxide %												
	SiO2	0.00	2.76	1.15	0.00	0.00	1.11	3.04	0.00	0.00	0.32	1.39
	TiO2	49.94	56.99	57.27	50.96	52.22	60.81	58.03	47.66	47.08	49.26	49.76
	Al2O3	0.00	0.00	0.00	0.00	0.00	0.00	0.00	0.00	0.00	0	0
	FeO2+	43.64	31.94	33.98	39.89	35.87	32.02	31.82	41.52	41.19	42.67	40.95
	FeO3+	2.28	0.00	0.00	3.74	4.49	0.00	0.00	8.49	9.12	2.85	2.78
	MnO	0.70	1.18	1.10	0.75	0.78	2.89	2.93	1.33	1.14	1.62	3.76
	MgO	0.32	1.65	0.60	2.91	5.78	0.63	2.34	0.00	0.00	0	0
	Cr2O3	0.00	0.00	0.00	0.00	0.00	0.00	0.00	0.00	0.00	0	0
	CaO	0.00	0.00	0.00	0.00	0.00	0.00	0.00	0.00	0.00	0	0
	Total	96.88	94.52	94.10	98.25	99.14	97.46	98.16	99.00	98.53	96.72	98.64
End Members												
	FeTiO3	2.27	0	0	3.6	4.19	0	0	8.43	9.06	2.92	2.96
	MgTiO3	1.26	8.43	3.05	11.1	21.39	3.39	11.59	0	0	0	0
	Fe2O3	96.47	91.57	96.95	85.3	74.42	96.61	88.41	91.57	90.94	97.08	97.04

				CL-07-014-269			CL-07-014-273					
Oxide%												
	SiO2	0.86	0.00	0.00	0.45	0.00	0.49	0.57	1.61	0.00	0.00	0.77
	TiO2	50.20	43.80	46.87	46.40	50.05	54.06	60.82	66.04	48.14	47.85	49.28
	Al2O3	0.00	0.00	0.00	0.00	0.00	0.00	0.32	0.00	0.00	0.00	0.00
	FeOT	43.80	53.16	51.00	49.29	45.78	38.62	31.35	27.21	48.83	42.95	44.95
	MnO	2.81	0.00	0.00	0.73	1.67	0.85	1.27	0.00	0.00	1.27	3.32
	MgO	0.49	0.00	0.00	0.34	0.00	0.61	0.00	2.86	0.00	1.78	0.00
	Cr2O3	0.00	0.74	0.00	0.00	0.00	0.00	0.00	0.00	0.00	0.21	0.00
	CaO	0.00	0.00	0.00	0.00	0.00	0.00	0.00	0.85	0.00	0.00	0.00
	Total	98.01	99.39	98.56	97.47	98.52	94.74	94.67	98.34	98.85	97.34	98.25
Convert to Oxide %												
	SiO2	0.86	0	0.00	0.45	0.00	0.49	0.57	1.61	0.00	0	0.77
	TiO2	50.2	43.8	46.87	46.40	50.05	54.06	60.82	66.04	48.14	47.85	49.28
	Al2O3	0	0	0.00	0.00	0.00	0.00	0.32	0.00	0.00	0	0
	FeO2+	41.43	39.4	42.16	40.39	43.33	38.62	31.35	27.21	43.30	38.58	40.96
	FeO3+	2.63	15.3	9.83	9.89	2.73	0.00	0.00	0.00	6.15	4.86	4.43
	MnO	2.81	0	0.00	0.73	1.67	0.85	1.27	0.00	0.00	1.27	3.32
	MgO	0.49	0	0.00	0.34	0.00	0.61	0.00	2.86	0.00	1.78	0
	Cr2O3	0	0.74	0.00	0.00	0.00	0.00	0.00	0.00	0.00	0.21	0
	CaO	0	0	0.00	0.00	0.00	0.00	0.00	0.85	0.00	0	0
	Total	98.42	99.24	98.86	98.20	97.78	94.63	94.33	98.57	97.59	94.55	98.76
End Members												
	FeTiO3	2.72	14.87	9.49	9.8	2.75	0	0	0	6	4.98	4.64
	MgTiO3	2.01	0	0	1.33	0	2.74	0	15.78	0	7.22	0
	Fe2O3	95.27	85.13	90.51	88.37	97.25	97.26	100	84.22	94	87.8	95.36

Appendix D-10 Magnetite

Magnetite	Sample No.:	CL-06-003-186							CL-06-003-205				
	Notes												
Oxide%	**SiO_2**	2.68	3.25	2.17	2.39	2.31	2.60	1.65	1.57	2.04	1.35	1.32	1.33
	TiO_2	0.00	0.00	0.00	0.00	0.00	0.00	0.00	0.00	0.00	0.00	0.00	0.00
	Al_2O_3	0.00	0.00	0.00	0.00	0.00	0.00	0.00	0.00	0.00	0.00	0.00	0.00
	FeO_T	89.04	91.36	90.69	90.91	90.63	88.84	90.70	94.01	92.93	95.34	94.83	90.09
	MnO	1.64	1.00	0.00	0.77	0.00	0.99	1.30	1.17	0.00	0.00	0.00	0.00
	MgO	1.20	0.00	0.00	0.90	0.00	0.64	0.00	0.60	0.00	0.48	0.51	0.00
	CaO	0.00	0.00	0.00	0.00	0.00	0.00	0.00	0.00	0.00	0.00	0.00	0.00
	Cr_2O_3	0.00	0.00	0.00	0.24	0.00	0.00	0.00	0.00	0.00	0.00	0.00	0.00
	Total	94.65	96.25	94.84	95.23	94.05	93.13	94.91	97.46	95.25	97.33	96.87	91.79
Recalculated	**FeO**	31.42	34.96	33.69	32.60	33.89	32.33	31.99	32.34	34.23	33.36	33.11	32.15
	Fe_2O_3	64.03	62.68	63.34	64.80	63.05	62.80	65.25	68.54	65.23	68.88	68.59	64.39
	Total	100.97	101.89	99.20	101.70	99.25	99.36	100.18	104.21	101.50	104.07	103.53	97.87
No. Ions in Formula	**Si**	0.80	0.97	0.67	0.71	0.71	0.79	0.50	0.46	0.61	0.40	0.39	0.42
	Ti	0.00	0.00	0.00	0.00	0.00	0.00	0.00	0.00	0.00	0.00	0.00	0.00
	Al	0.00	0.00	0.00	0.00	0.00	0.00	0.00	0.00	0.00	0.00	0.00	0.00
	Fe^{2+}	7.85	8.72	8.67	8.12	8.71	8.25	8.17	7.91	8.61	8.19	8.17	8.42
	Fe^{3+}	14.40	14.06	14.66	14.52	14.58	14.41	14.99	15.08	14.77	15.21	15.22	15.17
	Mn	0.42	0.25	0.00	0.19	0.00	0.26	0.34	0.29	0.00	0.00	0.00	0.00
	Mg	0.53	0.00	0.00	0.40	0.00	0.29	0.00	0.26	0.00	0.21	0.22	0.00
	Ca	0.00	0.00	0.00	0.00	0.00	0.00	0.00	0.00	0.00	0.00	0.00	0.00
	Cr	0.00	0.00	0.00	0.06	0.00	0.00	0.00	0.00	0.00	0.00	0.00	0.00

Magnetite	Sample No.:		CL-06-003-219				CL-07-010-169					
	Notes											
Oxide%	**SiO_2**	1.16	1.10	0.00	0.00	0.69	1.02	1.27	0.00	1.31	0.00	0.72
	TiO_2	0.00	0.00	0.00	0.00	0.00	0.00	0.00	0.00	0.00	0.00	0.00
	Al_2O_3	0.00	0.00	0.00	0.00	0.00	0.00	0.00	0.00	0.00	0.00	0.00
	FeO_T	88.35	88.61	91.93	88.98	90.78	89.26	91.29	92.93	90.09	94.22	92.64
	MnO	0.47	1.71	0.00	2.35	1.58	1.24	0.75	0.00	1.47	0.00	0.44
	MgO	0.00	1.34	1.09	1.30	0.93	0.00	0.00	0.00	1.13	0.00	0.71
	CaO	0.00	0.00	0.00	0.00	0.00	0.00	0.00	0.00	0.00	0.00	0.00
	Cr_2O_3	0.00	0.00	0.00	0.77	0.00	0.00	0.00	0.00	0.00	0.00	0.00
	Total	90.48	93.15	93.57	94.02	94.33	93.26	94.30	94.70	93.79	94.74	94.72
Recalculated	**FeO**	30.98	28.54	29.35	26.77	29.19	30.54	31.95	30.98	29.78	31.41	30.89
	Fe_2O_3	63.75	66.75	69.55	69.13	68.45	65.25	65.95	68.85	67.02	69.80	68.63
	Total	96.37	99.45	99.99	100.32	100.84	98.06	99.91	99.83	100.71	101.21	101.38
No. Ions in Formula	**Si**	0.37	0.34	0.00	0.00	0.21	0.32	0.39	0.00	0.40	0.00	0.22
	Ti	0.00	0.00	0.00	0.00	0.00	0.00	0.00	0.00	0.00	0.00	0.00
	Al	0.00	0.00	0.00	0.00	0.00	0.00	0.00	0.00	0.00	0.00	0.00
	Fe^{2+}	8.24	7.28	7.50	6.81	7.38	7.99	8.19	8.00	7.51	8.00	7.79
	Fe^{3+}	15.26	15.33	16.00	15.81	15.58	15.36	15.22	16.00	15.21	16.00	15.57
	Mn	0.13	0.44	0.00	0.61	0.40	0.33	0.19	0.00	0.38	0.00	0.11
	Mg	0.00	0.61	0.50	0.59	0.42	0.00	0.00	0.00	0.51	0.00	0.32
	Ca	0.00	0.00	0.00	0.00	0.00	0.00	0.00	0.00	0.00	0.00	0.00
	Cr	0.00	0.00	0.00	0.19	0.00	0.00	0.00	0.00	0.00	0.00	0.00

Magnetite	Sample No.:	CL-07-010-224		CL-07-010-233	CL-07-014-233			CL-07-014-245	
	Notes								
Oxide%	SiO_2	1.92	1.77	1.16	1.06	0.88	0.99	0.40	0.00
	TiO_2	0.00	0.00	0.00	0.00	0.00	0.00	0.00	0.00
	Al_2O_3	0.00	0.00	0.52	0.00	0.00	0.00	0.00	0.00
	FeO_T	89.20	93.09	91.64	91.00	91.34	88.71	90.06	90.22
	MnO	1.23	0.00	0.00	1.42	1.51	1.57	0.00	0.00
	MgO	1.50	0.00	0.00	0.00	0.79	0.47	0.00	0.00
	CaO	0.00	0.00	0.00	0.00	0.00	0.00	0.00	0.00
	Cr_2O_3	0.00	0.00	0.00	0.00	0.00	0.00	0.27	0.00
	Total	95.51	95.13	93.86	93.78	94.26	92.09	90.50	90.61
Recalculated	FeO	30.18	33.85	32.64	31.06	29.89	29.53	30.74	30.07
	Fe_2O_3	65.59	65.83	65.57	66.61	68.29	65.77	65.92	66.84
	Total	100.42	101.45	99.89	100.15	101.36	98.33	97.33	96.91
No. Ions in Formula	Si	0.58	0.53	0.36	0.32	0.26	0.31	0.13	0.00
	Ti	0.00	0.00	0.00	0.00	0.00	0.00	0.00	0.00
	Al	0.00	0.00	0.19	0.00	0.00	0.00	0.00	0.00
	Fe^{2+}	7.59	8.53	8.36	7.96	7.53	7.68	8.13	8.00
	Fe^{3+}	14.85	14.93	15.10	15.35	15.47	15.38	15.68	16.00
	Mn	0.31	0.00	0.00	0.37	0.39	0.41	0.00	0.00
	Mg	0.67	0.00	0.00	0.00	0.35	0.22	0.00	0.00
	Ca	0.00	0.00	0.00	0.00	0.00	0.00	0.00	0.00
	Cr	0.00	0.00	0.00	0.00	0.00	0.00	0.07	0.00